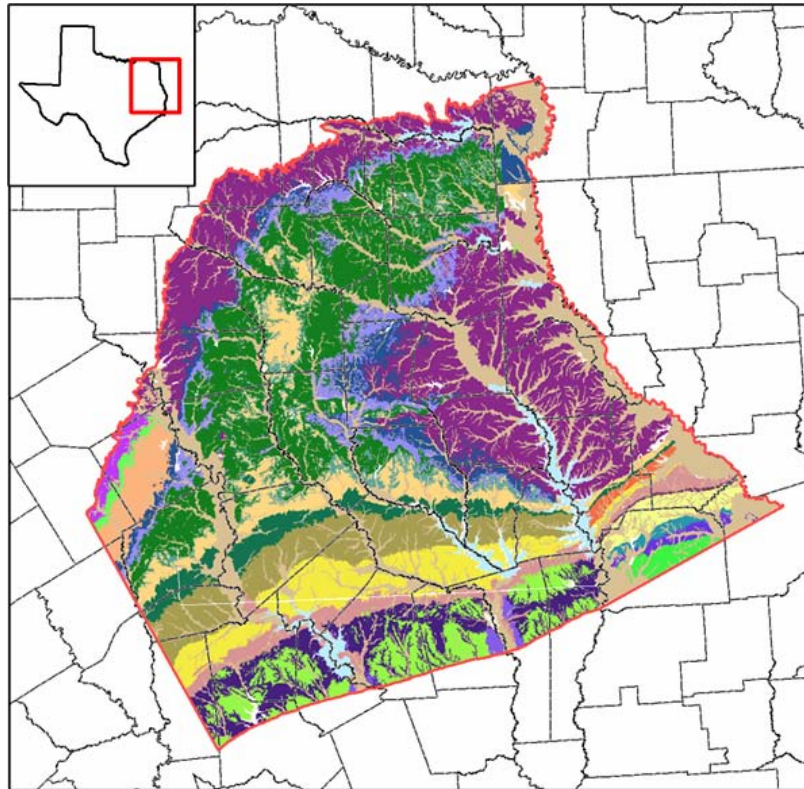


FINAL REPORT

Groundwater Availability Model for the Northern Carrizo-Wilcox Aquifer



Prepared for the:
Texas Water Development Board

Prepared by:
**Dennis Fryar, Rainer Senger,
Neil Deeds, John Pickens
and Toya Jones**



Art J. Whallon, and Kirk E. Dean

PARSONS

January 31, 2003

TABLE OF CONTENTS

ABSTRACT	xiv
1.0 INTRODUCTION.....	1-1
2.0 STUDY AREA.....	2-1
2.1 Physiography and Climate.....	2-10
2.2 Geology	2-19
3.0 PREVIOUS INVESTIGATIONS	3-1
4.0 HYDROGEOLOGIC SETTING	4-1
4.1 Hydrostratigraphy	4-1
4.2 Structure	4-4
4.3 Hydraulic Properties.....	4-22
4.3.1 Processing of the Hydraulic Property Database	4-23
4.3.2 Statistical Analysis of the Hydraulic Property Data	4-23
4.3.3 Spatial Distribution of Hydraulic Property Data	4-24
4.3.4 Relationship between Hydraulic Property and Sand Distribution.....	4-27
4.3.5 Vertical Hydraulic Conductivity.....	4-28
4.3.6 Storativity	4-30
4.4 Water Levels and Regional Groundwater Flow	4-41
4.4.1 Regional Groundwater Flow	4-42
4.4.2 Predevelopment Conditions for the Carrizo Sand and the Wilcox Group....	4-43
4.4.3 Pressure Versus Depth Analysis	4-45
4.4.4 Water-Level Elevations for Model Calibration and Verification.....	4-46
4.4.5 Transient Water Levels	4-48
4.5 Recharge	4-86
4.6 Natural Aquifer Discharge.....	4-92
4.7 Aquifer Discharge Through Pumping	4-102
4.8 Water Quality.....	4-112
5.0 CONCEPTUAL MODEL OF GROUNDWATER FLOW IN THE AQUIFER.....	5-1
6.0 MODEL DESIGN	6-1
6.1 Code and Processor.....	6-1
6.2 Model Layers and Grid.....	6-2
6.3 Boundary Condition Implementation.....	6-5
6.3.1 Lateral Model Boundaries	6-5
6.3.2 Vertical Boundaries	6-6
6.3.3 Surface Water Implementation	6-6
6.3.4 Implementation of Recharge	6-9
6.3.5 Implementation of Pumping Discharge	6-11
6.4 Model Hydraulic Parameters	6-18
6.4.1 Hydraulic Conductivity	6-18
6.4.2 Storativity	6-22

TABLE OF CONTENTS (CONTINUED)

7.0	MODELING APPROACH.....	7-1
7.1	Calibration	7-1
7.2	Calibration Target Uncertainty	7-4
7.3	Sensitivity Analysis.....	7-6
7.4	Predictions	7-6
8.0	STEADY-STATE MODEL.....	8-1
8.1	Calibration	8-1
8.1.1	Calibration Targets.....	8-1
8.1.2	Horizontal and Vertical Hydraulic Conductivities	8-1
8.1.3	Recharge and Groundwater Evapotranspiration.....	8-3
8.1.4	General-Head Boundaries and Stream Conductances	8-3
8.2	Simulation Results	8-14
8.2.1	Hydraulic Heads	8-14
8.2.2	Streams	8-16
8.2.3	Water Budget.....	8-17
8.3	Sensitivity Analysis.....	8-32
9.0	TRANSIENT MODEL.....	9-1
9.1	Calibration	9-1
9.2	Simulation Results	9-5
9.2.1	Hydraulic Heads	9-5
9.2.2	Stream Leakance.....	9-9
9.2.3	Water Budget.....	9-9
9.3	Sensitivity Analysis.....	9-49
10.0	MODEL PREDICTIVE SIMULATIONS.....	10-1
10.1	Drought of Record	10-1
10.2	Predictive Simulation Results	10-8
10.3	Predictive Simulation Water Budget.....	10-34
11.0	LIMITATIONS OF THE MODEL.....	11-1
11.1	Limitations of Supporting Data	11-1
11.2	Limiting Assumptions	11-3
11.3	Limits for Model Applicability.....	11-5
12.0	FUTURE IMPROVEMENTS.....	12-1
12.1	Supporting Data	12-1
12.2	Future Model Improvements	12-2
13.0	CONCLUSIONS.....	13-1
14.0	ACKNOWLEDGEMENTS.....	14-1
15.0	REFERENCES.....	15-1

LIST OF FIGURES

Figure 2.1	Location of the three Carrizo-Wilcox GAMs.	2-4
Figure 2.2	Location of study area showing county boundaries, cities, lakes, and rivers.	2-5
Figure 2.3	Areal extent of the major aquifers in the study area.	2-6
Figure 2.4	Location of Regional Water Planning Groups in the study area.	2-7
Figure 2.5	Location of Groundwater Conservation Districts in the study area.	2-8
Figure 2.6	Map showing the major river basins in the study area.	2-9
Figure 2.7	Ecological regions in the study area.	2-12
Figure 2.8	Topographic map of the study area.	2-13
Figure 2.9	Average pan evaporation rate, in inches per year, in the study area.	2-14
Figure 2.10	Location of precipitation gages in the study area (Period of Record is 1900 to 1999).	2-15
Figure 2.11	Average annual precipitation (1961-1990) over the study area in inches per year (Source: Oregon Climate Service, Oregon State University, PRISM data set).	2-16
Figure 2.12a	Annual precipitation time series for gages in Angelina, Cherokee, Ellis, and Franklin counties (Source: National Climatic DataCenter, Texas Natural Resources Information System).	2-17
Figure 2.12b	Annual precipitation time series for gages in Kaufman, Montgomery, Navarro, and Shelby counties (Source: National Climatic DataCenter, Texas Natural Resources Information System).	2-18
Figure 2.13	Surface geology of the study area.	2-22
Figure 2.14	Generalized stratigraphic section for the Carrizo-Wilcox aquifer in Texas (after Ayers and Lewis, 1985; Hamlin, 1988; Kaiser et al., 1978).	2-23
Figure 2.15a	Structural cross sections A-A' and B-B' showing the major hydrostratigraphic units in the East Texas Basin from Fogg and Kreitler (1982), indicating general groundwater flow patterns. Cross-section locations are shown on Figure 2.13.	2-24
Figure 2.15b	Structural cross section C-C' showing the major hydrostratigraphic units in the East Texas Basin from Fogg and Kreitler (1982), indicating general groundwater flow patterns. Cross-section location is shown on Figure 2.13.	2-25
Figure 3.1	Northern Carrizo-Wilcox GAM boundary with previous modeling study boundaries which have included the Carrizo-Wilcox aquifer.	3-5
Figure 4.1.1	Hydrostratigraphy and model layers.	4-3
Figure 4.2.1	Structural setting of the study area.	4-7
Figure 4.2.2	Structure contour map of the base of the Wilcox Group (CI = 500 ft).	4-8
Figure 4.2.3	Structure contour map of the top of the lower Wilcox (CI = 500 ft).	4-9
Figure 4.2.4	Structure contour map of the top of the middle Wilcox (CI = 500 ft).	4-10
Figure 4.2.5	Structure contour map of the top of the Wilcox Group (CI = 500 ft).	4-11
Figure 4.2.6	Structure contour map of the top of the Carrizo (CI = 500 ft).	4-12

LIST OF FIGURES (CONTINUED)

Figure 4.2.7	Structure contour map of the top of the Reklaw Formation (CI = 500 ft).....	4-13
Figure 4.2.8	Structure contour map of the top of the Queen City (CI = 500 ft).....	4-14
Figure 4.2.9	Thickness map of the lower Wilcox (CI = 100 ft).	4-15
Figure 4.2.10	Thickness map of the middle Wilcox (CI = 100 ft).	4-16
Figure 4.2.11	Thickness map of the upper Wilcox (CI = 100 ft).	4-17
Figure 4.2.12	Thickness map of the Carrizo (CI = 100 ft).....	4-18
Figure 4.2.13	Thickness map of the Reklaw (CI = 100 ft).	4-19
Figure 4.2.14	Thickness map of the Queen City (CI = 100 ft).....	4-20
Figure 4.2.15	Thickness map of formations above the Queen City (CI = 250 ft).....	4-21
Figure 4.3.1	Screening of hydraulic conductivity data.	4-31
Figure 4.3.2	Cumulative distribution function (CDF) curves of hydraulic conductivity for the modeled aquifer units.	4-32
Figure 4.3.3	Variogram for hydraulic conductivity data from the Carrizo Sand.	4-33
Figure 4.3.4	Variogram and kriged map of hydraulic conductivity for the Carrizo Sand.	4-34
Figure 4.3.5	Variogram and kriged map of hydraulic conductivity for the upper Wilcox.....	4-35
Figure 4.3.6	Variogram and kriged map of hydraulic conductivity for the middle Wilcox.....	4-36
Figure 4.3.7	Variogram and kriged map of hydraulic conductivity for the lower Wilcox.....	4-37
Figure 4.3.8	Variogram and kriged map of hydraulic conductivity for the Queen City.	4-38
Figure 4.3.9	Histogram of (a) net-sand thickness for the entire Wilcox Group and (b) maximum sand thickness and hydraulic conductivity (Log K) of the upper Wilcox.	4-39
Figure 4.3.10	Percent sand for the Wilcox Group, based on sand maps by Kaiser et al. (1978) and Fisher and McGowen (1967) (CI = 10 percent).	4-40
Figure 4.4.1	Relationship between the Carrizo Sand and the Wilcox Group in the study area.	4-53
Figure 4.4.2	Water-level measurement locations for the hydrostratigraphic units in the study area.....	4-54
Figure 4.4.3	Groundwater flow lines drawn from the Carrizo-Wilcox potentiometric surface (from Fogg and Kreitler, 1982).....	4-55
Figure 4.4.4	Location and model layer for predevelopment water-level elevation targets.....	4-56
Figure 4.4.5	Water-level measurement locations used for the pressure-depth analysis (for measurements prior to 1950).....	4-57
Figure 4.4.6	Pressure versus depth analysis results (for measurements prior to 1950).	4-58
Figure 4.4.7	Water-level measurement locations used for the pressure-depth analysis (for all measurements).....	4-59
Figure 4.4.8	Pressure versus depth analysis results (for all measurements).	4-60
Figure 4.4.9a	Water-level elevation contours for the Queen City Sand at the start of model calibration (January 1980).....	4-61

LIST OF FIGURES (CONTINUED)

Figure 4.4.9b	Water-level elevation contours for the Carrizo Sand at the start of model calibration (January 1980).....	4-62
Figure 4.4.9c	Water-level elevation contours for the upper Wilcox at the start of model calibration (January 1980).....	4-63
Figure 4.4.9d	Water-level elevation contours for the middle Wilcox at the start of model calibration (January 1980).....	4-64
Figure 4.4.9e	Water-level elevation contours for the lower Wilcox at the start of model calibration (January 1980).....	4-65
Figure 4.4.10a	Water-level elevation contours for the Carrizo Sand at the end of model calibration (December 1989).....	4-66
Figure 4.4.10b	Water-level elevation contours for the upper Wilcox at the end of model calibration (December 1989).....	4-67
Figure 4.4.10c	Water-level elevation contours for the middle Wilcox at the end of model calibration (December 1989).....	4-68
Figure 4.4.10d	Water-level elevation contours for the lower Wilcox at the end of model calibration (December 1989).....	4-69
Figure 4.4.11a	Water-level elevation contours for the Carrizo Sand at the end of model verification (December 1999).....	4-70
Figure 4.4.11b	Water-level elevation contours for the upper Wilcox at the end of model verification (December 1999).....	4-71
Figure 4.4.11c	Water-level elevation contours for the middle Wilcox at the end of model verification (December 1999).....	4-72
Figure 4.4.11d	Water-level elevation contours for the lower Wilcox at the end of model verification (December 1999).....	4-73
Figure 4.4.12	Long-term transient water-level elevations for well 37-36-102 completed to the Carrizo-Wilcox in Nacogdoches County.	4-74
Figure 4.4.13	Model layer for locations with transient water-level data.	4-75
Figure 4.4.14	Example hydrographs for wells located in Nacogdoches and Angelina counties.	4-76
Figure 4.4.15	Example hydrographs for wells in the study area.	4-77
Figure 4.4.16a	Water-level decline in the Carrizo Sand from the start of model calibration (January 1980) to the end of model calibration (December 1989).....	4-78
Figure 4.4.16b	Water-level decline in the Carrizo Sand from the start of model calibration (January 1980) to the end of model verification (December 1999).....	4-79
Figure 4.4.17a	Water-level decline in the upper Wilcox from the start of model calibration (January 1980) to the end of model calibration (December 1989).....	4-80
Figure 4.4.17b	Water-level decline in the upper Wilcox from the start of model calibration (January 1980) to the end of model verification (December 1999).....	4-81
Figure 4.4.18a	Water-level decline in the middle Wilcox from the start of model calibration (January 1980) to the end of model calibration (December 1989).....	4-82

LIST OF FIGURES (CONTINUED)

Figure 4.4.18b	Water-level decline in the middle Wilcox from the start of model calibration (January 1980) to the end of model verification (December 1999).....	4-83
Figure 4.4.19a	Water-level decline in the lower Wilcox from the start of model calibration (January 1980) to the end of model calibration (December 1989).....	4-84
Figure 4.4.19b	Water-level decline in the lower Wilcox from the start of model calibration (January 1980) to the end of model verification (December 1999).....	4-85
Figure 4.5.1	Major reservoirs in the study area.....	4-90
Figure 4.5.2	Hydrographs for select reservoirs in the study area.....	4-91
Figure 4.6.1	Stream gain/loss studies in the study area (after Slade et al., 2002).....	4-100
Figure 4.6.2	Documented spring locations in the study area.....	4-101
Figure 4.7.1	Population density for the Northern Carrizo-Wilcox GAM study area.....	4-108
Figure 4.7.2	Younger (Layer 1) pumpage (AFY), 1990.....	4-109
Figure 4.7.3	Reklaw (Layer 2) pumpage (AFY), 1990.....	4-109
Figure 4.7.4	Carrizo (Layer 3) pumpage (AFY), 1990.....	4-110
Figure 4.7.5	Upper Wilcox (Layer 4) pumpage (AFY), 1990.....	4-110
Figure 4.7.6	Middle Wilcox (Layer 5) pumpage (AFY), 1990.....	4-111
Figure 4.7.7	Lower Wilcox (Layer 6) pumpage (AFY), 1990.....	4-111
Figure 5.1	Conceptual groundwater flow model for the Northern Carrizo-Wilcox GAM.....	5-5
Figure 5.2	Schematic diagram of transient relationships between recharge rates, discharge rates, and withdrawal rates for an unconfined aquifer basin (from Freeze, 1971).....	5-6
Figure 6.2.1	Model grid of the Northern Carrizo-Wilcox GAM.....	6-4
Figure 6.3.1	Layer 1 (Queen City) boundary conditions and active/inactive cells.....	6-12
Figure 6.3.2	Layer 2 (Reklaw) boundary conditions and active/inactive cells.....	6-13
Figure 6.3.3	Layer 3 (Carrizo) boundary conditions and active/inactive cells.....	6-14
Figure 6.3.4	Layer 4 (upper Wilcox) boundary conditions and active/inactive cells.....	6-15
Figure 6.3.5	Layer 5 (middle Wilcox) boundary conditions and active/inactive cells.....	6-16
Figure 6.3.6	Layer 6 (lower Wilcox) boundary conditions and active/inactive cells.....	6-17
Figure 8.1.1	Calibrated horizontal hydraulic conductivity field for Layer 3 (Carrizo).....	8-6
Figure 8.1.2	Calibrated horizontal hydraulic conductivity field for Layer 4 (upper Wilcox).....	8-7
Figure 8.1.3	Calibrated horizontal hydraulic conductivity field for Layer 5 (middle Wilcox).....	8-8
Figure 8.1.4	Calibrated horizontal hydraulic conductivity field for Layer 6 (lower Wilcox).....	8-9
Figure 8.1.5	Calibrated vertical anisotropy (K_h/K_v) field for Layer 2 (Reklaw).....	8-10
Figure 8.1.6	Calibrated recharge distribution for the steady-state model.....	8-11

LIST OF FIGURES (CONTINUED)

Figure 8.1.7	ET extinction depth distribution for the steady-state model.....	8-12
Figure 8.1.8	Calibrated maximum groundwater ET rate distribution for the steady-state model.	8-13
Figure 8.2.1a	Simulated steady-state hydraulic heads and residuals for Layer 1 (Queen City).....	8-21
Figure 8.2.1b	Scatterplot of simulated and measured hydraulic heads for Layer 1 (Queen City).....	8-22
Figure 8.2.2a	Simulated steady-state hydraulic heads and posted residuals for Layer 3 (Carrizo).....	8-23
Figure 8.2.2b	Scatterplot of simulated and measured hydraulic heads for Layer 3 (Carrizo).....	8-24
Figure 8.2.3a	Simulated steady-state hydraulic heads and residuals for Layer 4 (upper Wilcox).	8-25
Figure 8.2.3b	Scatterplot of simulated and measured hydraulic heads for Layer 4 (upper Wilcox).	8-26
Figure 8.2.4a	Simulated steady-state hydraulic heads and residuals for Layer 5 (middle Wilcox).	8-27
Figure 8.2.4b	Scatterplot of simulated and measured hydraulic heads for Layer 5 (middle Wilcox).	8-28
Figure 8.2.5	Simulated steady-state hydraulic heads for Layer 6 (lower Wilcox).....	8-29
Figure 8.2.6	Steady-state model stream gain/loss (negative values denote gaining streams).....	8-30
Figure 8.2.7	Simulated stream gain/loss compared to measurements compiled by Slade et al. (2002) for selected stream segments.	8-31
Figure 8.3.1	Steady-state sensitivity results for Layer 3 (Carrizo) using target locations.	8-35
Figure 8.3.2	Steady-state sensitivity results for Layer 3 (Carrizo) using all active gridblocks.....	8-35
Figure 8.3.3	Steady-state sensitivity results for Layer 1 (Queen City) using all active gridblocks.....	8-36
Figure 8.3.4	Steady-state sensitivity results for Layer 2 (Reklaw) using all active gridblocks.....	8-36
Figure 8.3.5	Steady-state sensitivity results for Layer 4 (upper Wilcox) using all active gridblocks.....	8-37
Figure 8.3.6	Steady-state sensitivity results for Layer 5 (middle Wilcox) using all active gridblocks.....	8-37
Figure 8.3.7	Steady-state sensitivity results for Layer 6 (lower Wilcox) using all active gridblocks.....	8-38
Figure 8.3.8	Steady-state sensitivity results where the vertical hydraulic conductivity of Layer 2 (Reklaw) is varied.	8-38
Figure 8.3.9	Steady-state sensitivity results where streambed conductivity is varied.	8-39
Figure 8.3.10	Steady-state sensitivity results where recharge is varied.	8-39
Figure 9.1.1	Target well locations for the different layers used in the transient calibration.....	9-4

LIST OF FIGURES (CONTINUED)

Figure 9.2.1	Simulated hydraulic head distribution for Layer 1 (Queen City) at the end of the transient model calibration (December 1989).....	9-15
Figure 9.2.2	Simulated and measured hydraulic head distribution for Layer 3 (Carrizo) at the end of the transient model calibration (December 1989).....	9-16
Figure 9.2.3	Simulated and measured hydraulic head distribution for Layer 4 (upper Wilcox) at the end of the transient model calibration (December 1989).....	9-17
Figure 9.2.4	Simulated and measured hydraulic head distribution for Layer 5 (middle Wilcox) at the end of the transient model calibration (December 1989).....	9-18
Figure 9.2.5	Simulated and measured hydraulic head distribution for Layer 6 (lower Wilcox) at the end of the transient model calibration (December 1989).....	9-19
Figure 9.2.6	Residuals at target wells for Layer 3 (Carrizo) at the end of the transient model calibration (December 1989).....	9-20
Figure 9.2.7	Residuals at target wells for Layer 4 (upper Wilcox) at the end of the transient model calibration (December 1989).....	9-21
Figure 9.2.8	Residuals at target wells for Layer 5 (middle Wilcox) at the end of the transient model calibration (December 1989).....	9-22
Figure 9.2.9	Residuals at target wells for Layer 6 (lower Wilcox) at the end of the transient model calibration (December 1989).....	9-23
Figure 9.2.10	Scatterplots of simulated and measured hydraulic heads for the different layers at the end of the transient model calibration (December 1989).....	9-24
Figure 9.2.11	Scatterplots of simulated and measured hydraulic heads for the different layers at the end of the transient model verification (December 1999).....	9-25
Figure 9.2.12	Simulated and measured hydraulic head distribution for Layer 3 (Carrizo) at the end of the transient model verification (December 1999).....	9-26
Figure 9.2.13	Simulated and measured hydraulic head distribution for Layer 4 (upper Wilcox) at the end of the transient model verification (December 1999).....	9-27
Figure 9.2.14	Simulated and measured hydraulic head distribution for Layer 5 (middle Wilcox) at the end of the transient model verification (December 1999).....	9-28
Figure 9.2.15	Simulated and measured hydraulic head distribution for Layer 6 (lower Wilcox) at the end of the transient model verification (December 1999).....	9-29
Figure 9.2.16a	Selected hydrographs of simulated (lines) and measured (points) hydraulic heads in the northern part for Layer 3 (Carrizo).....	9-30
Figure 9.2.16b	Selected hydrographs of simulated (lines) and measured (points) hydraulic heads in the central part for Layer 3 (Carrizo).....	9-31
Figure 9.2.16c	Selected hydrographs of simulated (lines) and measured (points) hydraulic heads in the southern part for Layer 3 (Carrizo).....	9-32

LIST OF FIGURES (CONTINUED)

Figure 9.2.17a	Selected hydrographs of simulated (lines) and measured (points) hydraulic heads in the northern part for Layer 4 (upper Wilcox).	9-33
Figure 9.2.17b	Selected hydrographs of simulated (lines) and measured (points) hydraulic heads in the central part for Layer 4 (upper Wilcox).	9-34
Figure 9.2.17c	Selected hydrographs of simulated (lines) and measured (points) hydraulic heads in the southern part for Layer 4 (upper Wilcox).	9-35
Figure 9.2.17d	Selected hydrographs of simulated (lines) and measured (points) hydraulic heads in the western part for Layer 4 (upper Wilcox).	9-36
Figure 9.2.18a	Selected hydrographs of simulated (lines) and measured (points) hydraulic heads in the northern part for Layer 5 (middle Wilcox).	9-37
Figure 9.2.18b	Selected hydrographs of simulated (lines) and measured (points) hydraulic heads in the central part for Layer 5 (middle Wilcox).	9-38
Figure 9.2.18c	Selected hydrographs of simulated (lines) and measured (points) hydraulic heads in the western part for Layer 5 (middle Wilcox).	9-39
Figure 9.2.19	Selected hydrographs of simulated (lines) and measured (points) hydraulic heads in Layer 6 (lower Wilcox).	9-40
Figure 9.2.20	Average recharge for the transient simulation period (1980-1999).	9-41
Figure 9.2.21	Simulated stream gain/loss for May 1989.	9-42
Figure 9.2.22	Simulated stream gain/loss for November 1989.	9-43
Figure 9.2.23a	Simulated and measured stream flow at gauging station 8032000 on the Neches River.	9-44
Figure 9.2.23b	Simulated and measured stream flow at gauging station 8065000 on the Trinity River.	9-45
Figure 9.2.23c	Simulated and measured stream flow at gauging station 8022040 on the Sabine River.	9-46
Figure 9.2.24	Simulated stream gain/loss compared to measurements compiled by Slade et al. (2002) for selected stream segments.	9-47
Figure 9.2.25	Time history of water budgets for (a) streams and reservoirs, (b) recharge and ET, and (c) pumpage.	9-48
Figure 9.3.1	Transient sensitivity results for Layer 3 (Carrizo) using target locations.	9-52
Figure 9.3.2	Transient sensitivity results for Layer 3 (Carrizo) using all active gridblocks.	9-52
Figure 9.3.3	Transient sensitivity results for Layer 1 (Queen City) using all active gridblocks.	9-53
Figure 9.3.4	Transient sensitivity results for Layer 2 (Reklaw) using all active gridblocks.	9-53
Figure 9.3.5	Transient sensitivity results for Layer 4 (upper Wilcox) using all active gridblocks.	9-54
Figure 9.3.6	Transient sensitivity results for Layer 5 (middle Wilcox) using all active gridblocks.	9-54
Figure 9.3.7	Transient sensitivity results for Layer 6 (lower Wilcox) using all active gridblocks.	9-55
Figure 9.3.8	Transient sensitivity results where the vertical hydraulic conductivity of Layer 2 (Reklaw) is varied.	9-55
Figure 9.3.9	Transient sensitivity results where recharge is varied.	9-56

LIST OF FIGURES (CONTINUED)

Figure 9.3.10	Transient sensitivity results where the horizontal hydraulic conductivity of the Wilcox is varied.....	9-56
Figure 10.1.1	Standard precipitation index (SPI) curves for the Lufkin rain gage (#415424-Angelina Co.) for 1 month, 1 year, 2 year, 3 year time periods.....	10-5
Figure 10.1.2	Standardized precipitation indices for precipitation gages in the region.	10-6
Figure 10.1.3	Standardized precipitation index averaged for all gages in the region from 1950-1960.....	10-7
Figure 10.2.1	Simulated 2000 (a) and 2050 (b) heads surfaces for Layer 1 (Queen City).....	10-11
Figure 10.2.2	Difference between 2000 and 2050 simulated head surfaces for Layer 1 (Queen City).	10-12
Figure 10.2.3	Simulated 2000 (a) and 2050 (b) heads surfaces for Layer 3 (Carrizo).....	10-13
Figure 10.2.4	Difference between 2000 and 2050 simulated head surfaces for Layer 3 (Carrizo).	10-14
Figure 10.2.5	Simulated 2000 (a) and 2050 (b) heads surfaces for Layer 4 (upper Wilcox).	10-15
Figure 10.2.6	Difference between 2000 and 2050 simulated head surfaces for Layer 4 (upper Wilcox).....	10-16
Figure 10.2.7	Simulated 2000 (a) and 2050 (b) heads surfaces for Layer 5 (middle Wilcox).	10-17
Figure 10.2.8	Difference between 2000 and 2050 simulated head surfaces for Layer 5 (middle Wilcox).....	10-18
Figure 10.2.9	Simulated 2000 (a) and 2050 (b) heads surfaces for Layer 6 (lower Wilcox).	10-19
Figure 10.2.10	Difference between 2000 and 2050 simulated head surfaces for Layer 6 (lower Wilcox).....	10-20
Figure 10.2.11	Simulated 2010 head surface (a) and drawdown from 2000 (b), Layer 3 (Carrizo).....	10-21
Figure 10.2.12	Simulated 2010 head surface (a) and drawdown from 2000 (b), Layer 4 (upper Wilcox).....	10-22
Figure 10.2.13	Simulated 2020 head surface (a) and drawdown from 2000 (b), Layer 3 (Carrizo).....	10-23
Figure 10.2.14	Simulated 2020 head surface (a) and drawdown from 2000 (b), Layer 4 (upper Wilcox).....	10-24
Figure 10.2.15	Simulated 2030 head surface (a) and drawdown from 2000 (b), Layer 3 (Carrizo).....	10-25
Figure 10.2.16	Simulated 2030 head surface (a) and drawdown from 2000 (b), Layer 4 (upper Wilcox).....	10-26
Figure 10.2.17	Simulated 2040 head surface (a) and drawdown from 2000 (b), Layer 3 (Carrizo).	10-27
Figure 10.2.18	Simulated 2040 head surface (a) and drawdown from 2000 (b), Layer 4 (upper Wilcox).....	10-28

LIST OF FIGURES (CONTINUED)

Figure 10.2.19	Selected hydrographs from predictive simulation to 2050, Layer 3 (Carrizo).....	10-29
Figure 10.2.20	Selected hydrographs from predictive simulation to 2050, Layer 4 (upper Wilcox).	10-30
Figure 10.2.21	Selected hydrographs from predictive simulation to 2050, Layer 5 (middle Wilcox).	10-31
Figure 10.2.22	Selected hydrographs from predictive simulation to 2050, Layer 6 (lower Wilcox).	10-32
Figure 10.2.23	Simulated difference in head surfaces between the average condition 2050 simulation and the DOR 2050 simulation.	10-33

LIST OF TABLES

Table 2.1	River basins in the Northern Carrizo-Wilcox GAM study area (BEG, 1996).....	2-3
Table 3.1	Previous groundwater models of the Carrizo-Wilcox aquifer in the study area.	3-1
Table 4.2.1	Data sources for layer elevations for the Northern Carrizo-Wilcox GAM.	4-4
Table 4.3.1	Summary statistics for horizontal hydraulic conductivity.	4-24
Table 4.3.2	Summary of literature estimates of Carrizo-Wilcox specific yield.	4-30
Table 4.4.1	Target values for calibration of the steady-state model to predevelopment conditions.	4-50
Table 4.5.1	Review of recharge rates for the Carrizo-Wilcox aquifers in Texas (after Scanlon et al., 2002).	4-88
Table 4.5.2	Characteristics of reservoirs in study area.	4-89
Table 4.6.1	Stream flow gain/loss in the study area (after Slade et al., 2002, Table 1).	4-95
Table 4.6.2	Documented springs in the study area.	4-96
Table 4.7.1	Rate of groundwater withdrawal (AFY) from all model layers of the Carrizo-Wilcox aquifer for counties within the study area.	4-107
Table 8.1.1	Calibrated hydraulic conductivity ranges for the steady-state model.	8-5
Table 8.2.1	Calibration statistics for the steady-state model.	8-19
Table 8.2.2a	Water budget for the steady-state model. All rates reported in acre-ft/yr.	8-20
Table 8.2.2b	Water budget for the steady-state model with values expressed as a percentage of inflow or outflow.	8-20
Table 9.2.1	Calibration statistics for the transient model.	9-11
Table 9.2.2	Calibration statistics for the hydrographs shown in Figures 9.2.16a – 9.2.19.	9-12
Table 9.2.3	Water budget for transient model. All rates reported in acre-ft/yr.	9-14
Table 10.3.1	Water budget for predictive simulations. All rates reported in acre-ft/yr.	10-35

LIST OF FIGURES (CONTINUED)

APPENDICES

Appendix A	Brief Summary of the Development of the Carrizo-Wilcox Aquifer in Each County and List of Reviewed Reports
Appendix B	Standard Operating Procedures (SOPs) for Processing Historical Pumpage Data TWDB Groundwater Availability Modeling (GAM) Projects
Appendix C	Standard Operating Procedures (SOPs) for Processing Predictive Pumpage Data TWDB Groundwater Availability Modeling (GAM) Projects
Appendix D1	Tabulated Groundwater Withdrawal Estimates for the Carrizo-Wilcox for 1980, 1990, 2000, 2010, 2020, 2030, 2040, and 2050
Appendix D2	Post Plots of Groundwater Withdrawal Estimates for the Carrizo-Wilcox for 1980, 1990, 2000, 2010, 2020, 2030, 2040, and 2050
Appendix D3	Carrizo-Wilcox Groundwater Withdrawal Distributions by County
Appendix E	Using SWAT with MODFLOW in a Decoupled Environment
Appendix F	Water Quality
Appendix G	Draft Report Comments and Responses

ABSTRACT

This report documents a three-dimensional groundwater model developed for the northern Carrizo-Wilcox aquifer in northeastern Texas. The model was developed using MODFLOW and consists of six layers which include four layers for the Carrizo-Wilcox aquifer, and additional layers for the overlying Reklaw and Queen City formations. The model incorporates the available information on structure, hydrostratigraphy, hydraulic properties, stream flow, and recharge estimates. The purpose of this model is to provide a tool for making predictions of groundwater availability through 2050 based on current projections of groundwater demands during drought-of-record conditions. The model has been calibrated to predevelopment conditions (prior to significant groundwater withdrawal), which are considered to be at steady state. The steady-state model reproduces the predevelopment aquifer heads well within the estimated head uncertainty. The model was also calibrated to transient aquifer conditions from January 1980 through December 1989, incorporating monthly variations in recharge, streamflow, and pumping. The transient model reproduces aquifer heads within the calibration measures and available estimates of aquifer-stream interaction. The transient-calibrated model was verified by simulating aquifer conditions for the verification period between January 1990 and December 1999, reproducing observed aquifer heads within the calibration measures and available estimates of aquifer-stream interaction. The initial estimates of hydraulic conductivity in the model required some adjustment to better reproduce the observed water-level declines in the confined section of the Carrizo-Wilcox aquifer during the transient period.

The verified model was used to make predictions of aquifer conditions for the next 50 years based upon projected pumping demands as developed by the Regional Water Planning Groups. The predictive modeling indicated noticeable rebound of hydraulic heads in some areas of the confined section even though total pumping showed a gradual increase. This was due to changes in pumping for individual layers in certain areas during the transition from the historical period to the predictive period.

This model provides an integrated tool for the assessment of water management strategies to directly benefit state planners, Regional Water Planning Groups (RWPGs), and Groundwater Conservation Districts (GCDs). The applicability of the model is limited to regional-scale

assessments of groundwater availability (e.g., tens of miles) due to the relatively large grid blocks (1 mile²) over which pumping and hydraulic property data are averaged in the model. In addition to uncertainty in pumping and hydraulic property data, the model is limited to a first-order approach of coupling surface water and groundwater, and does not provide a rigorous solution to surface water flow in the region.

1.0 INTRODUCTION

The Carrizo-Wilcox Aquifer is classified as a major aquifer in Texas (Ashworth and Hopkins, 1995) ranking third in the state for water use (430,000 acre-feet per year [AFY]) in 1997 behind the Gulf Coast aquifer and the Ogallala aquifer (TWDB, 2002). The aquifer extends from the Rio Grande in South Texas to East Texas and continues into Louisiana and Arkansas. The Carrizo-Wilcox aquifer provides water to all or parts of 60 Texas counties with the greatest historical use being in and around the Tyler, Lufkin-Nacogdoches, and Bryan-College Station metropolitan centers and in the Wintergarden region of South Texas (Ashworth and Hopkins, 1995).

The Texas Water Code codified the requirement for the development of a State Water Plan that allows for the development, management, and conservation of water resources and the preparation and response to drought, while maintaining sufficient water available for the citizens of Texas (TWDB, 2002). Senate Bill 1 (SB1) and subsequent legislation directed the TWDB to coordinate the regional water planning process through a process based upon public participation. Also, as a result of SB1, the approach to water planning in the state of Texas has shifted from a water-demand based allocation approach to an availability-based approach.

Groundwater models provide a tool to estimate groundwater availability for various water use strategies and to determine the cumulative effects of increased water use and drought. A groundwater model is a numerical representation of the aquifer system capable of simulating historical and predicting future aquifer conditions. Inherent to the groundwater model, are a set of equations which are developed and applied to describe the physical processes considered to be controlling groundwater flow in the aquifer system. It can be argued that groundwater models are essential to performing complex analyses and in making informed predictions and related decisions (Anderson and Woessner, 1992). As a result, development of Groundwater Availability Models (GAMs) for the major Texas aquifers is integral to the state water planning process as defined in SB1. The purpose of the GAM program is to provide a tool that can be used to develop reliable and timely information on groundwater availability for the citizens of Texas to ensure adequate supplies or recognize inadequate supplies over a 50-year planning period.

The Northern Carrizo-Wilcox GAM has been developed using a modeling protocol which is standard to the groundwater model industry. This protocol includes: (1) the development of a conceptual model for groundwater flow in the aquifer, (2) model design, (3) model calibration, (4) model verification, (5) sensitivity analysis, (6) model prediction, and (7) reporting. The conceptual model is a conceptual description of the physical processes which govern groundwater flow in the aquifer system. We reviewed the available data and reports for the model area in the conceptual model development stage. Model design is the process used to translate the conceptual model into a physical model, in this case a numerical model of groundwater flow. This involved organizing and distributing model parameters, developing a model grid and model boundary conditions, and determining the model integration time scale. Model calibration is the process of modifying model parameters so that observed field measurements (e.g., groundwater levels in wells) can be reproduced. The northern Carrizo-Wilcox model was calibrated to predevelopment conditions (prior to significant resource use) which are considered to be at steady-state and to transient aquifer conditions from 1980 through 1990. Model verification is the process of using the calibrated model to reproduce observed field measurements not used in the calibration to test the model's predictive ability. The model was verified against measured aquifer conditions from 1990 through 1999. Model sensitivity analyses were performed by varying model input parameters for both the steady-state and transient models to offer insight on the uniqueness of the model and on the uncertainty in model parameter estimates. Model predictions were performed to estimate aquifer conditions for the next 50 years based upon projected pumping demands developed by the Regional Water Planning Groups. This report documents the modeling process and results from conceptual model development through predictions (2000 to 2050) according to standard requirements specified by the TWDB in their Request for Qualifications. The model and associated data files are publicly available. These files, along with this report, are available at the TWDB GAM website at <http://www.twdb.state.tx.us/GAM>.

Consistent with state water planning policy, the Northern Carrizo-Wilcox GAM was developed with the support of stakeholders through quarterly stakeholder forums. The purpose of this GAM is to provide a tool for Regional Water Planning Groups, Groundwater Conservation Districts, River Authorities, and state planners for the evaluation of groundwater availability and to support the development of water management strategies and drought

planning. The East Texas Regional Water Planning Group (Region I) plans to meet 59% of their projected water needs by the year 2050 through the use of existing groundwater supplies. The North East Texas Regional Water Planning Group (Region D) plans to meet 25% of their 2050 projected water needs through existing groundwater supplies and an additional 2% through new groundwater resources. The GAM provides a tool for use in assessing the future availability of these supplies.

2.0 STUDY AREA

The Carrizo-Wilcox aquifer is comprised of hydraulically connected sands from the Wilcox Group and the Carrizo Formation of the Claiborne Group (Ashworth and Hopkins, 1995). The Carrizo-Wilcox aquifer extends across Texas from the Rio Grande in the southwest to the Sabine River in the northeast and beyond into Louisiana and Arkansas. The Carrizo-Wilcox aquifer is classified as a major aquifer in Texas providing groundwater resources to all or part of 60 Texas counties (Ashworth and Hopkins, 1995).

Because of its large size, the Carrizo-Wilcox aquifer was divided by the TWDB for modeling purposes into three areas, with each being modeled separately. The three Carrizo-Wilcox GAMs are the Northern Carrizo-Wilcox GAM, the Central Carrizo-Wilcox GAM, and the Southern Carrizo-Wilcox GAM (Figure 2.1). These GAMs have significant overlap areas as shown in Figure 2.1. This study documents the Northern Carrizo-Wilcox GAM. The model area, shown in Figure 2.2, includes all or parts of the following Texas counties: Anderson, Angelina, Bowie, Camp, Cass, Cherokee, Franklin, Freestone, Greg, Grimes, Harrison, Henderson, Hopkins, Houston, Jasper, Leon, Limestone, Madison, Marion, Montgomery, Morris, Nacogdoches, Navarro, Newton, Panola, Polk, Rains, Red River, Robertson, Rusk, Sabine, San Augustine, San Jacinto, Shelby, Smith, Titus, Trinity, Tyler, Upshur, Van Zandt, Walker, and Wood. The model also covers all or part of several parishes in Louisiana, including Caddo, De Soto, Natchitoches, Rapides, Red River, Sabine, and Vernon, and a portion of Miller County in Arkansas.

Groundwater model boundaries typically are defined on the basis of surface or groundwater hydrologic boundaries. Figure 2.3 shows the surface outcrop and downdip subcrop of the major aquifers in the study area. The Northern Carrizo-Wilcox GAM is bounded laterally on the northeast by the Red River in Louisiana and Arkansas, and by the surface water basin divide between the Trinity and Brazos rivers in the southwest. The Trinity-Brazos basin divide serves as the model boundary in the outcrop (presumed groundwater flow divide) and was extended into the subsurface to the down-dip boundary of the model. The upper boundary of the model was defined by the ground surface in the outcrop of the Carrizo-Wilcox aquifer extending south to the extent of the Queen City outcrop. The lower boundary is the base of the Wilcox Group representing the top of the Midway Formation. The down-dip boundary of the Carrizo-

Wilcox aquifer extends past the limits of fresh water to the updip limit of the Wilcox growth fault zone (Bebout et al., 1982).

The study area encompasses parts of five regional water-planning areas (Figure 2.4). These include: (1) the North East Texas Region (Region D), (2) Region C, (3) the East Texas Region (Region I), (4) Region H, and (5) the Brazos Region (Region G). The study area includes all or parts of the following Groundwater Conservation Districts (Figure 2.5): (1) the Anderson County Underground Water Conservation District, (2) the Brazos Valley Groundwater Conservation District (3) the Neches and Trinity Valleys Groundwater Conservation District, (4) the Piney Woods Groundwater Conservation District, (5) the Bluebonnet Groundwater Conservation District, (6) the Lone Star Groundwater Conservation District, (7) the Mid-East Texas Groundwater Conservation District, and (8) the Lake Country Groundwater Conservation District.

The model area intersects five major river basins from west to east: (1) the Brazos, (2) the Trinity, (3) the Neches, (4) the Sabine, and (5) the Red River basins (Figure 2.6). In the model area, the Red River Basin has been further subdivided into the Sulphur River Basin, the Cyprus Creek Basin, and the Red River Basin. The model domain also intersects the San Jacinto River Basin, but only in the downdip portion of the model where there is no direct interaction between streams and the model. Eight river authorities (Angelina-Neches River Authority, Brazos River Authority, the Lower Neches Valley Authority, the Red River Authority, the Sabine River Authority, the San Jacinto River Authority, the Sulphur River Basin Authority, and the Trinity River Authority) are present in the study area.

Rivers and streams in the Northern Carrizo-Wilcox GAM study area are perennial and tend to gain flow from the underlying geology. Table 2.1 provides a listing of the river basins in the study area along with the river length in Texas, the river basin area in Texas, and the number of major reservoirs within the river basin in Texas (BEG, 1976).

Table 2.1 River basins in the Northern Carrizo-Wilcox GAM study area (BEG, 1996)

River Basin	Texas River Length (mi)	Texas River Basin Drainage Area (square miles)	Number of Major Reservoirs
Brazos	840	42,800	19
Trinity	550	17,696	14
Neches	416	10,011	4
Sabine	360	7,426	2
Red	680	30,823	7
San Jacinto	70	5,600	2

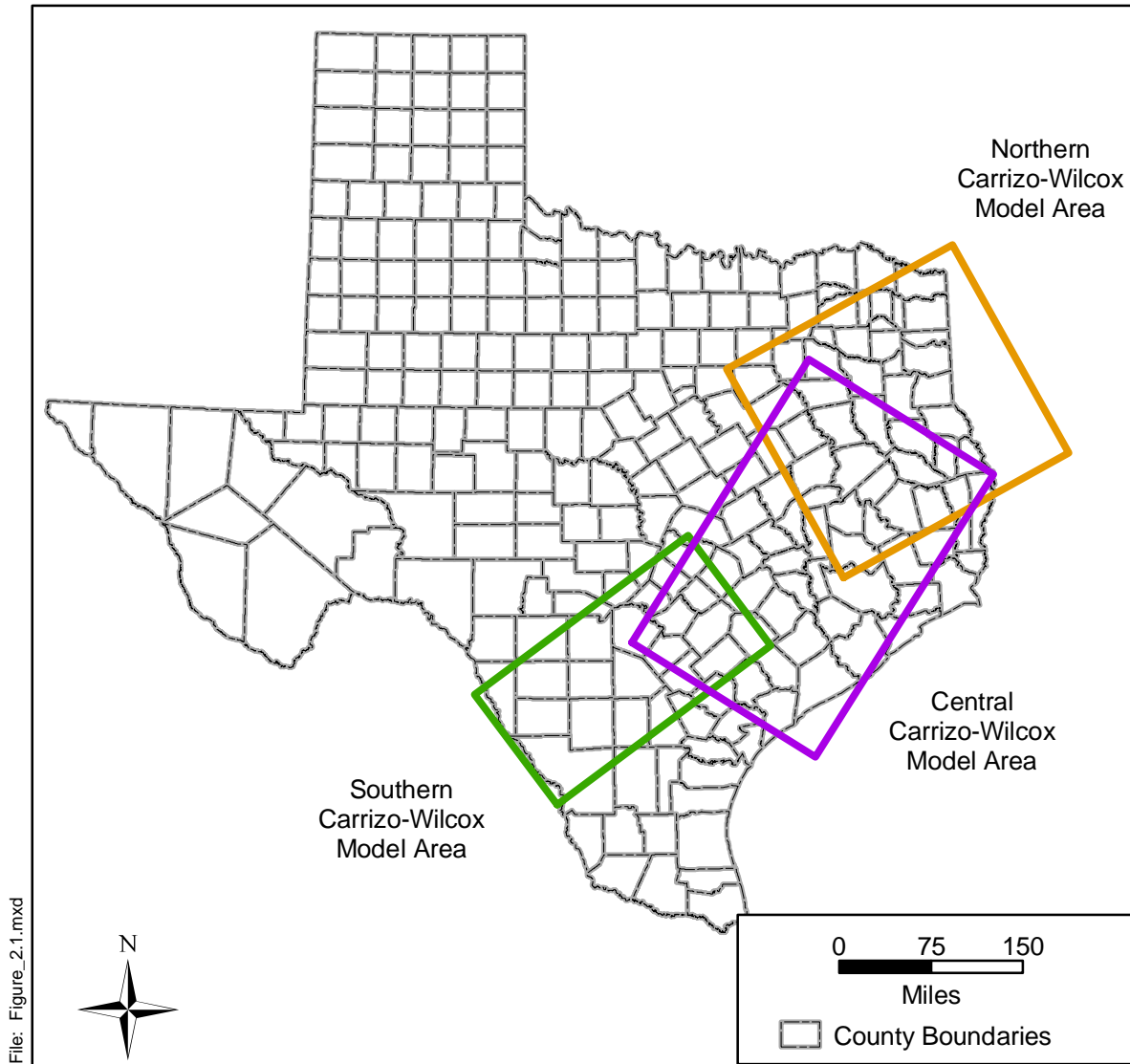
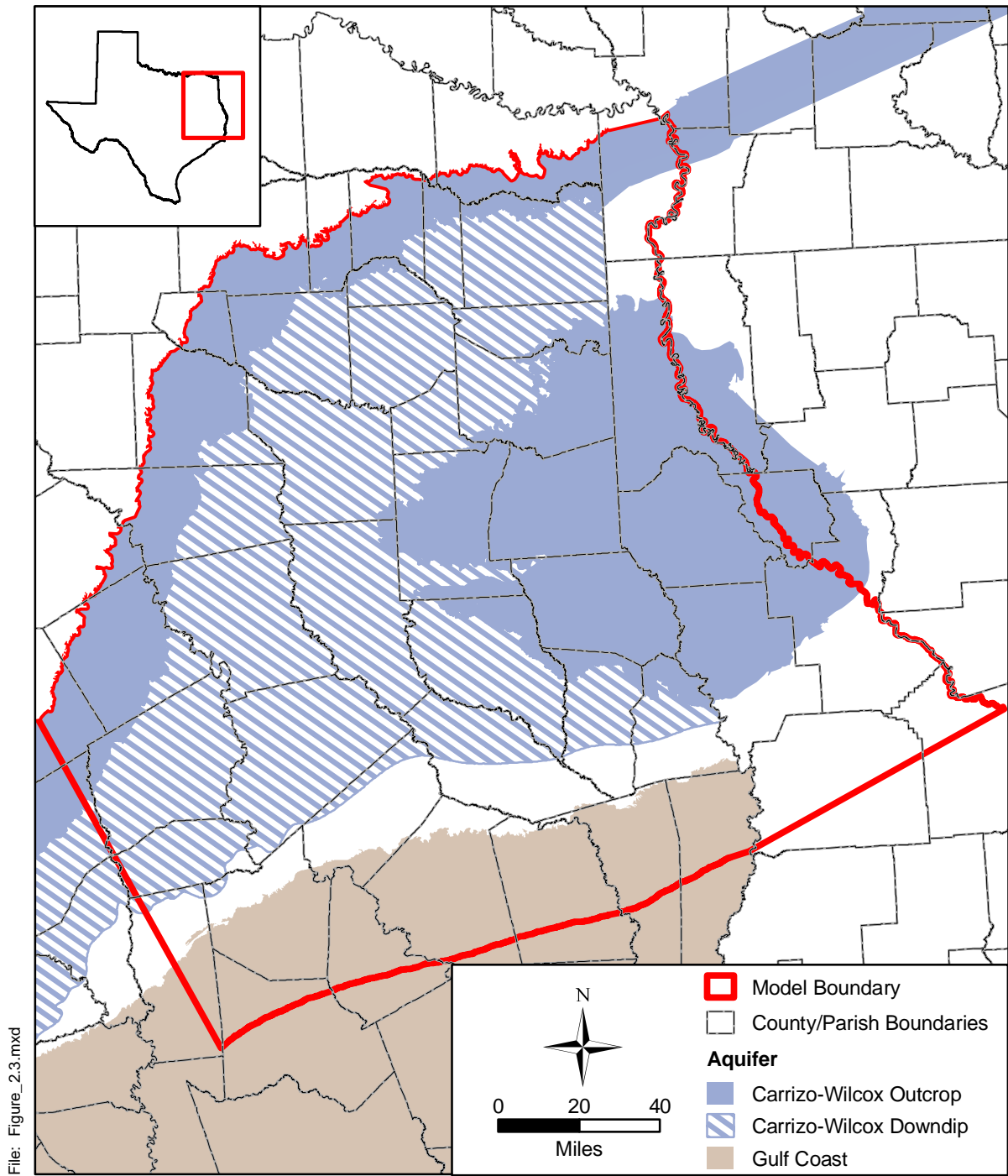


Figure 2.1 Location of the three Carrizo-Wilcox GAMs.



Source: Online: Texas Water Development Board, September 2002, Bureau of Economic Geology

Figure 2.3 Areal extent of the major aquifers in the study area.



Source: Online: Texas Water Development Board, September 2002

Figure 2.4 Location of Regional Water Planning Groups in the study area.

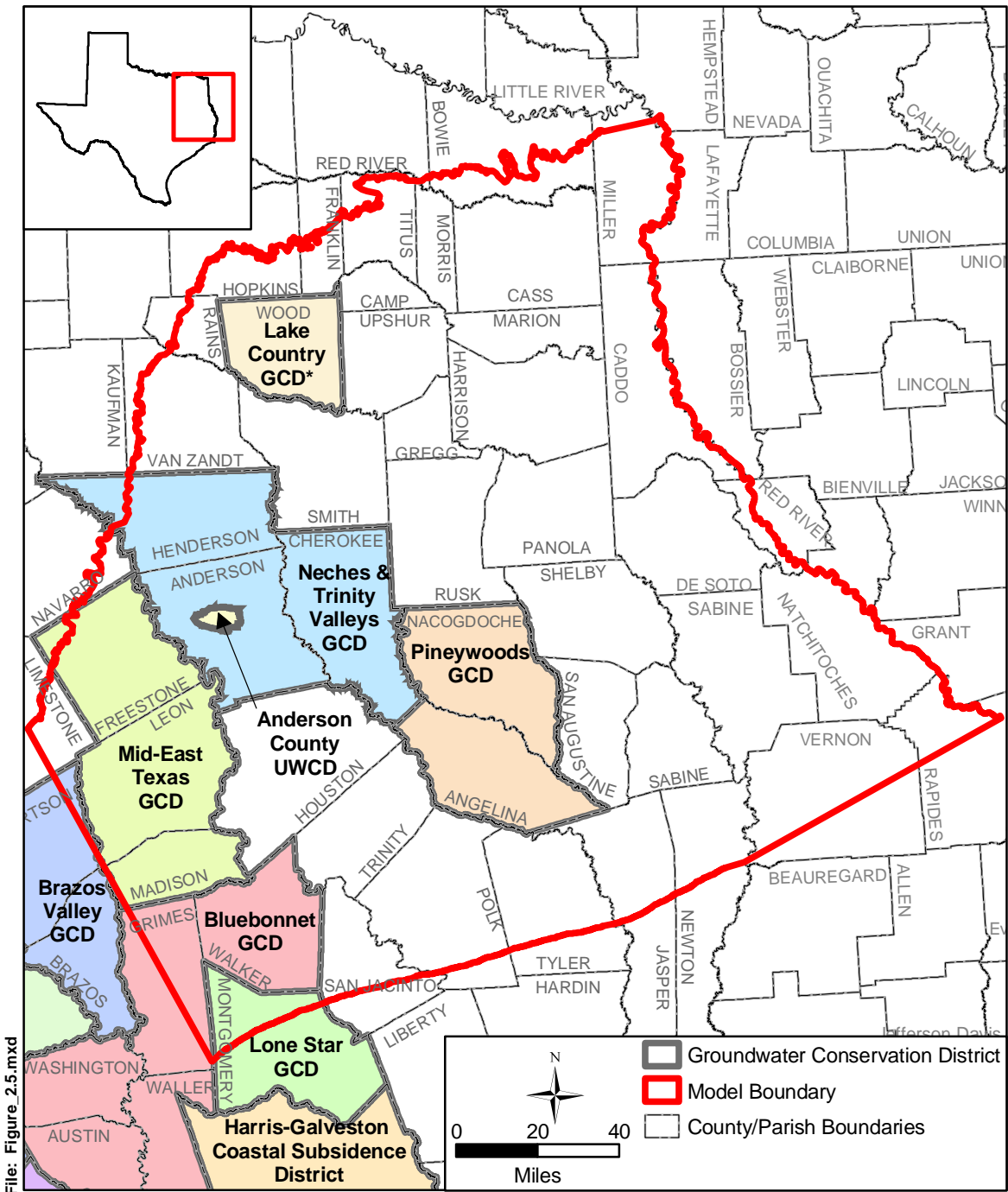


Figure 2.5 Location of Groundwater Conservation Districts in the study area.

2.1 Physiography and Climate

The study area is located in north-central and northeast Texas and extends into far western Louisiana and Miller County, Arkansas. The study area falls within the Gulf Coastal Plains physiographic region. The Gulf Coastal Plains region has been subdivided into several area designations based upon vegetation and topography. In the study area, these include the Piney Woods, the Oak Woods and Prairies, the Blackland Prairie, and the South-Central Plains in Arkansas and Louisiana (Figure 2.7). The Piney Woods, predominant in East Texas, are characterized as hilly with predominantly pine forests, with hardwoods occurring with pine in river valleys. The South-Central Plains region in Arkansas and Louisiana is analogous to the Piney Woods region in East Texas. In the Oak Woods and Prairies region in the western part of the study area, the terrain flattens slightly and the timber changes from pine to predominantly oak. Only small areas of Blackland Prairie extend eastward into the model area.

Figure 2.8 provides a topographic map of the study area. Ground surface elevation varies from greater than 600 feet above sea level on isolated basin divides (ridges) to less than 100 feet above sea level in river valleys and in the southeastern part of the study area. In general, ground surface elevation decreases from the northwestern portion of the study area to the east and south. Superimposed on top of this trend is significant elevation change associated with dissected stream valleys.

The climate in the northern half of the study area is generally mild with an annual average temperature of 65°F (TWDB, 2002, Region D Plan). The mean high temperature for July is 94°F and the mean low temperature for January is 32°F (TWDB, 2002, Region D Plan). In the southern half of the study area, the average maximum temperature in July is approximately 93°F and the average minimum temperature for January is 36°F (TWDB, 2002, Region I Plan). Average annual pan evaporation rates range from 58 inches per year in the western portion of the study area to as low as 38 inches per year in the northeastern portion of the study area (Figure 2.9).

For the study area, historically there have been precipitation data available at approximately 250 stations (Figure 2.10) from 1930 through 2000. The spatial distribution is relatively dense in the model domain across the period of record (Figure 2.10). However, the

number of available gages in any given year is quite variable with a general chronological increase in the number of gages available. Available precipitation gages increase from 25 in 1931 to 50 in 1942 to a high of 92 gages in the late 1960s and early 1970s. Most gages began measuring precipitation in the 1930s or 1940s. The earliest monthly precipitation records in the area extend as far back as 1930. The average period of record in the study area is 41 years and the longest is 69 years through 1999. For the period of record, the average number of gages recording precipitation in a given year is 69.

Based upon the available precipitation records, the average annual precipitation in the study area is 45.6 inches. Historical average annual precipitation varies from a low of 34.4 inches in Frost (Navarro County) to a high of 59.9 in Jasper County. The PRISM (Parameter-elevation Regressions on Independent Slopes Model) precipitation data set developed and presented online by the Oregon Climate Service at Oregon State University¹ provides a good distribution of average annual precipitation across the model area based upon the period of record from 1961 to 1990. Figure 2.11 provides a raster data post plot of average annual precipitation across the model study area. Generally, the average annual precipitation increases from west to east from a low of 36 inches per year in the western part of the study area to a high of 59 inches per year in the far southeast portion of the study area. Figure 2.12 shows annual precipitation recorded at eight representative precipitation gages representative of the model area and located in Angelina, Cherokee, Ellis, Franklin, Kaufman, Montgomery, Navarro, and Shelby counties.

¹ www.ocs.orst.edu/prism/

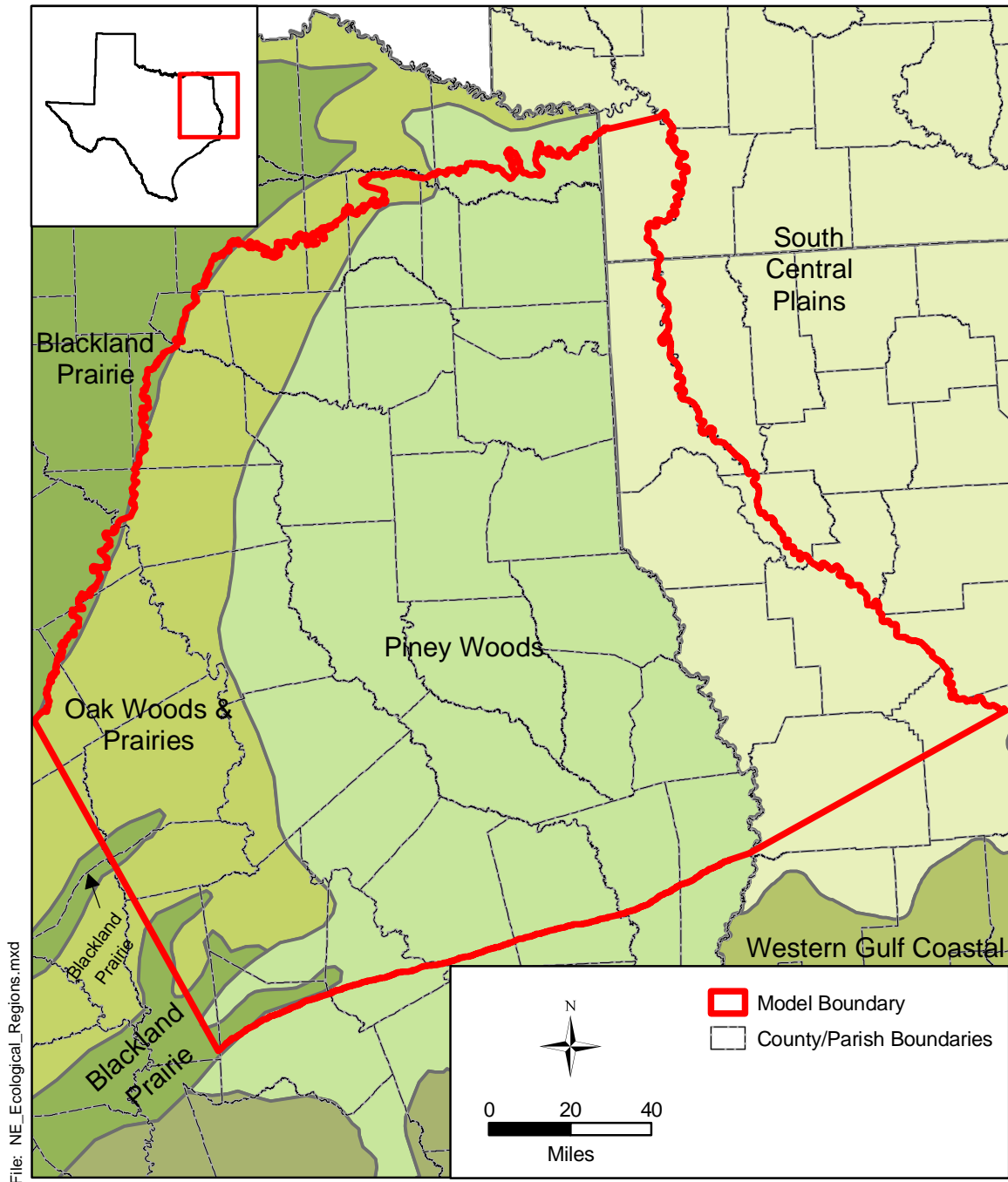


Figure 2.7 Ecological regions in the study area.

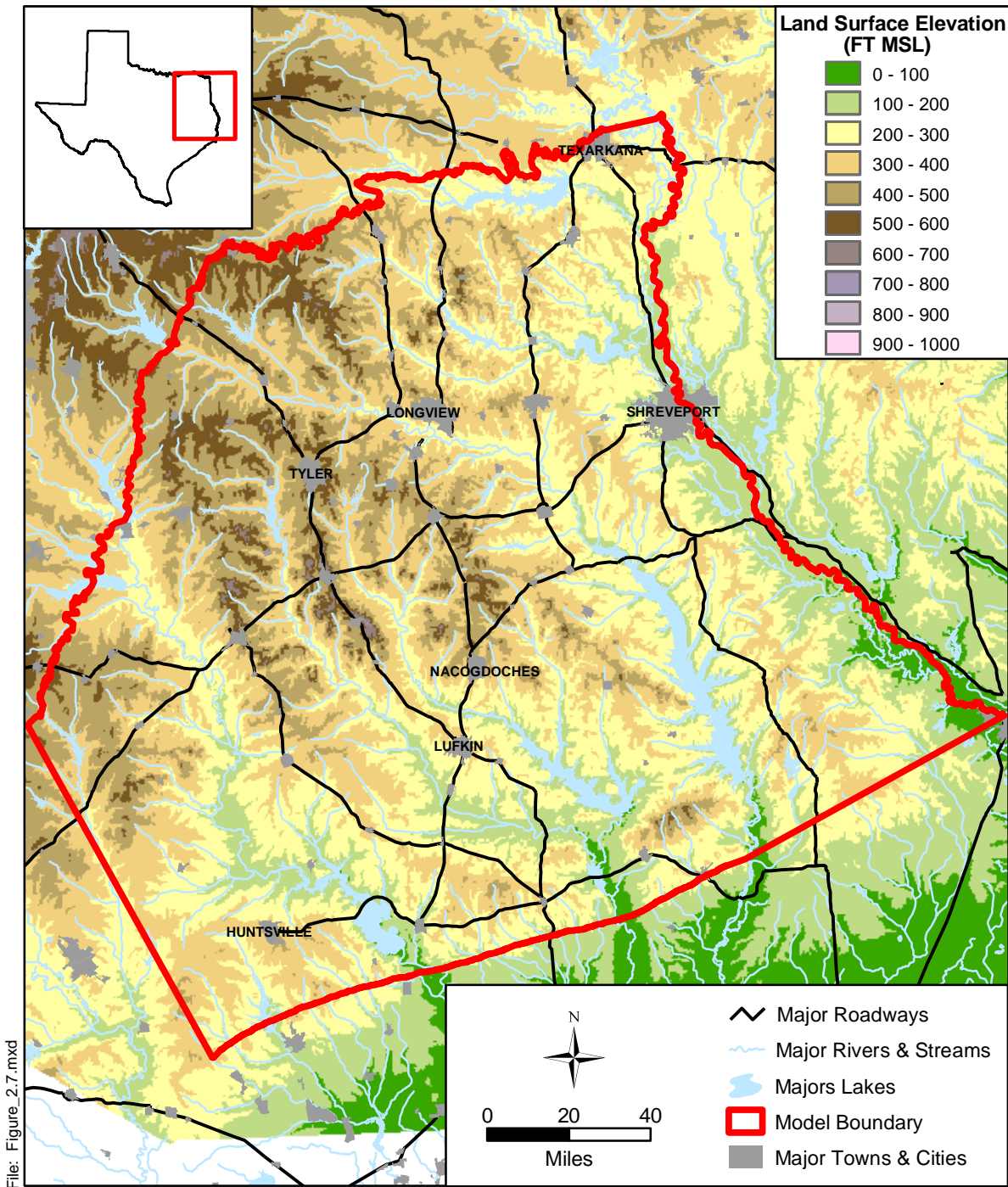
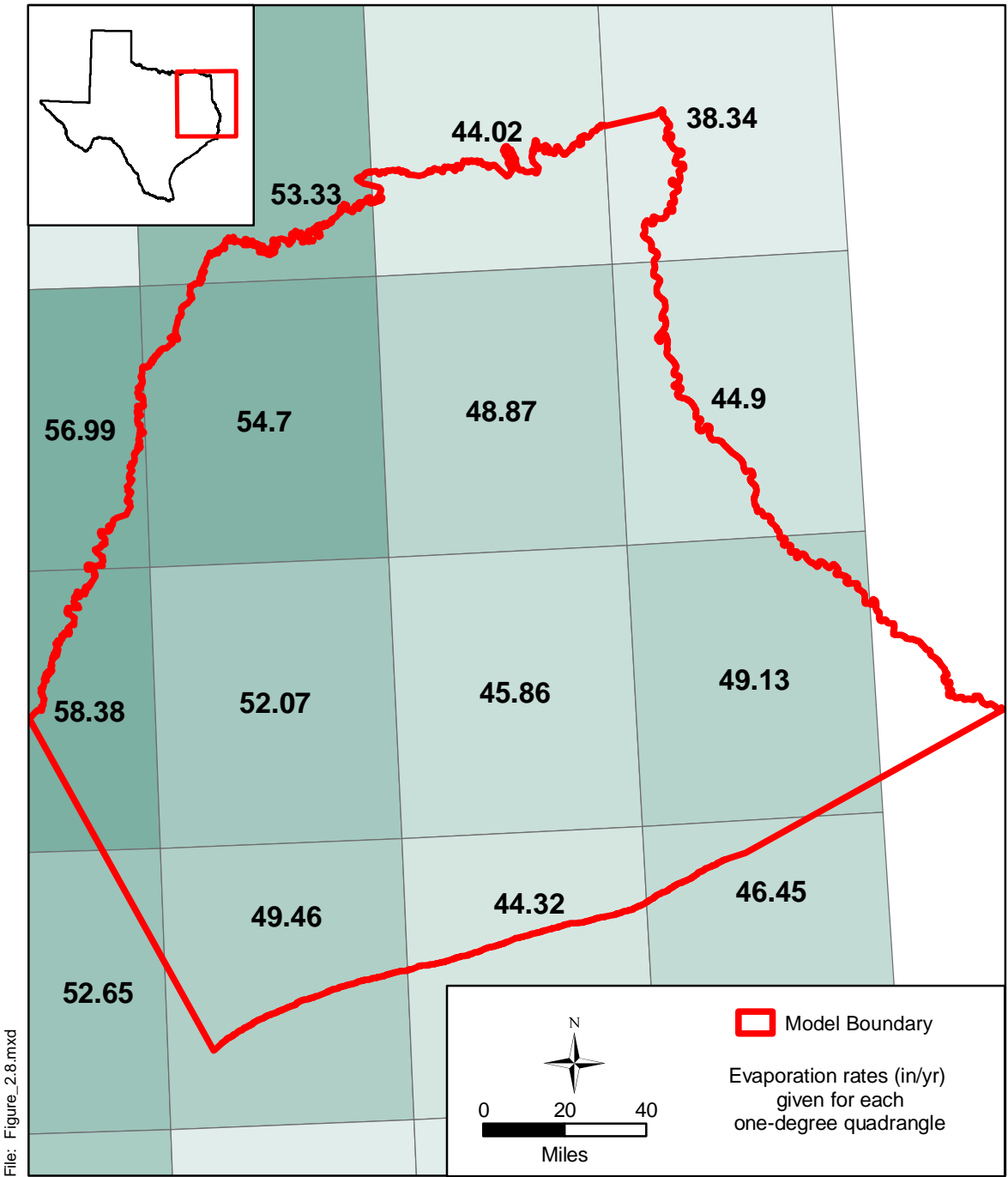


Figure 2.8 Topographic map of the study area.



Source: Online: Texas Water Development Board, September 2002

Figure 2.9 Average pan evaporation rate, in inches per year, in the study area.

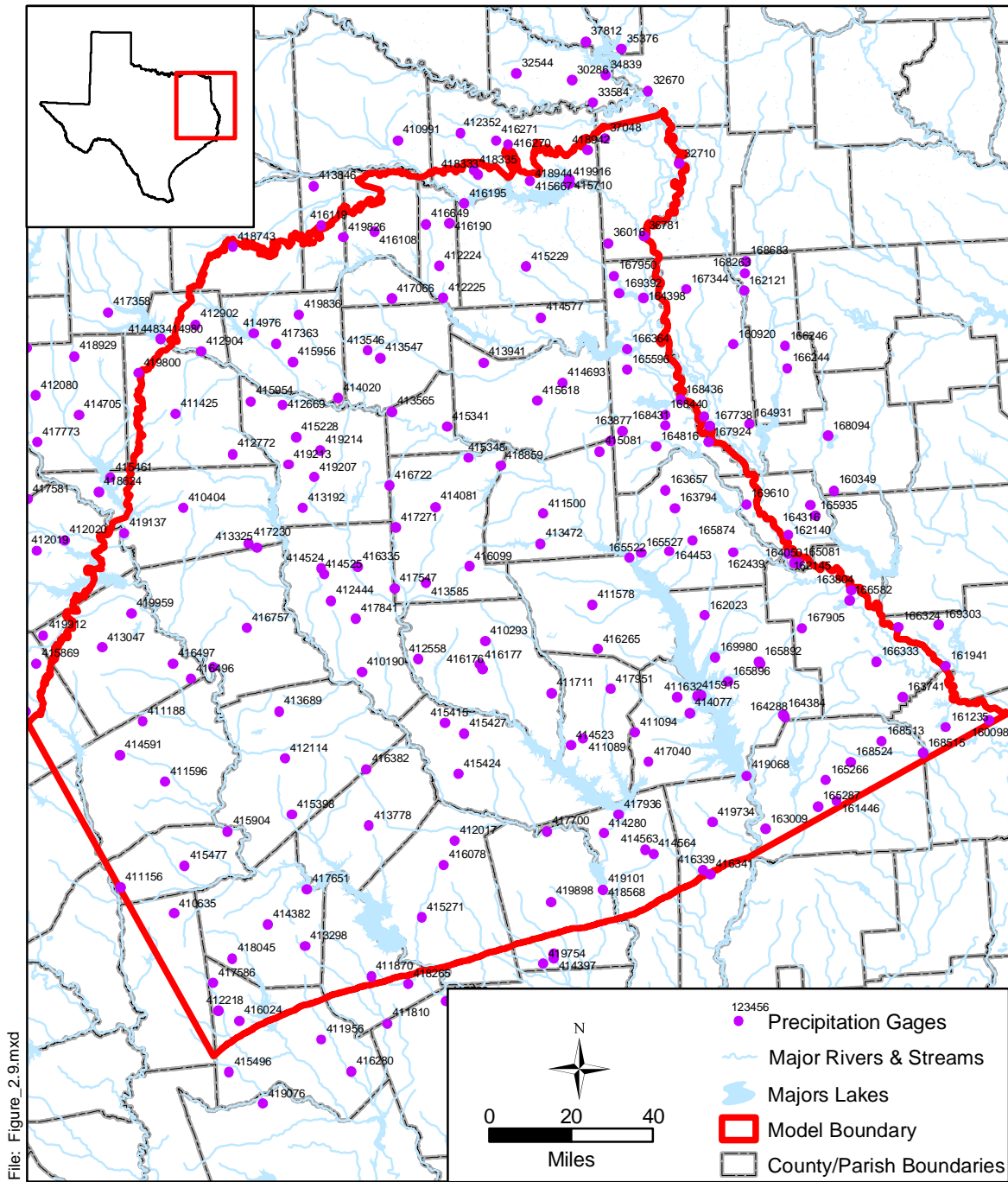


Figure 2.10 Location of precipitation gages in the study area (Period of Record is 1900 to 1999).

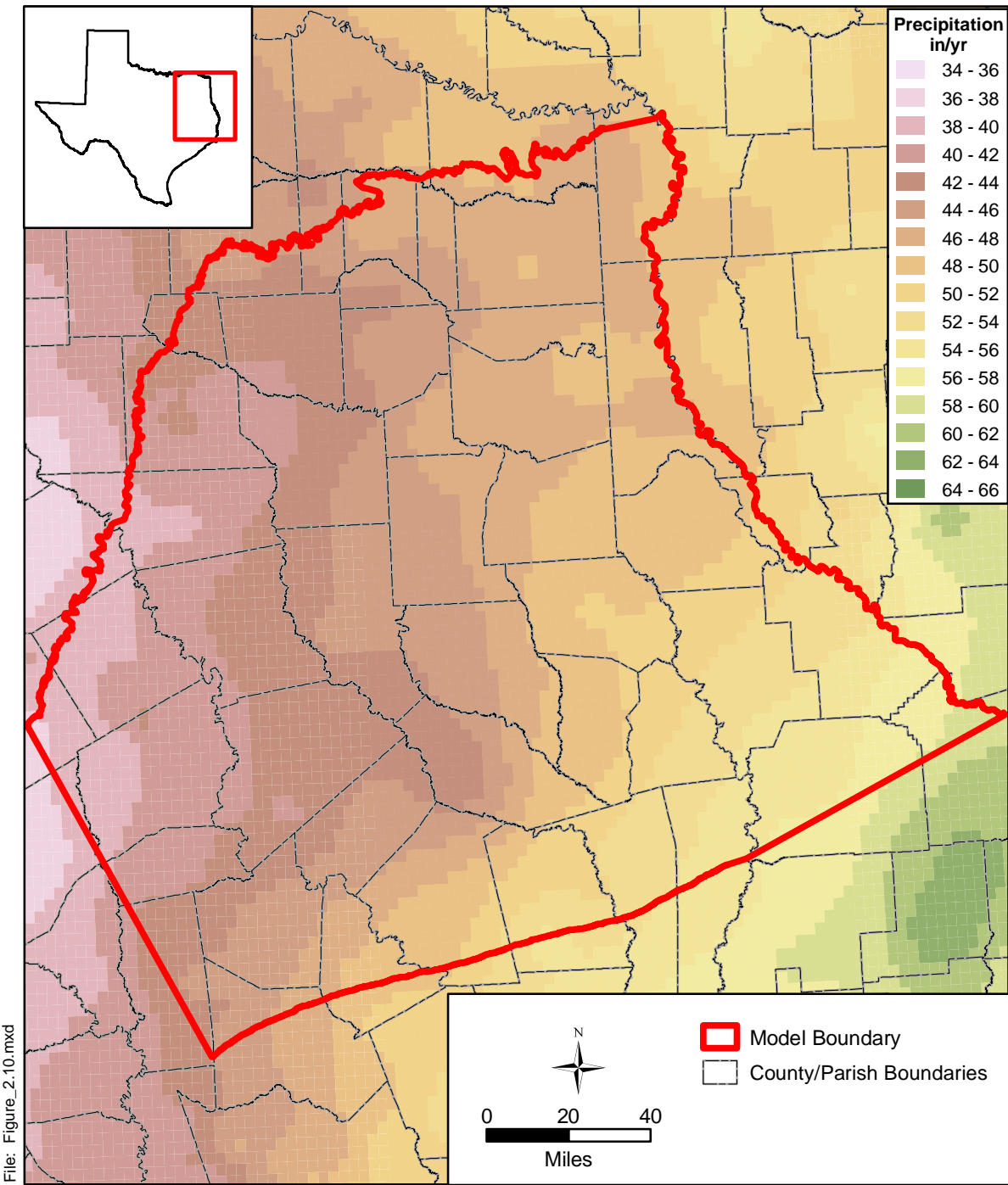


Figure 2.11 Average annual precipitation (1961-1990) over the study area in inches per year (Source: Oregon Climate Service, Oregon State University, PRISM data set).

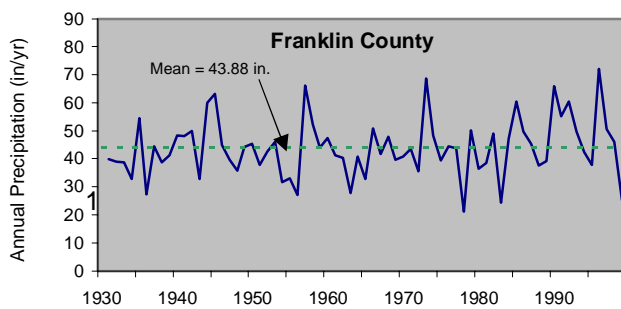
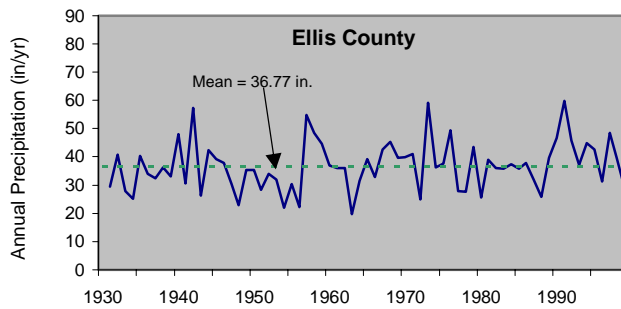
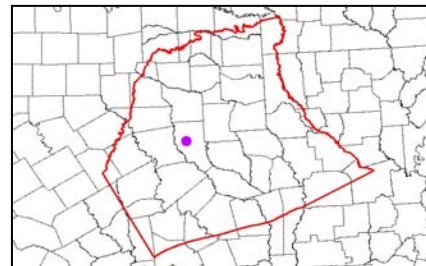
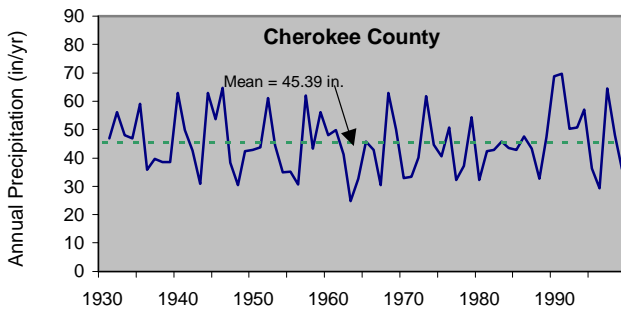
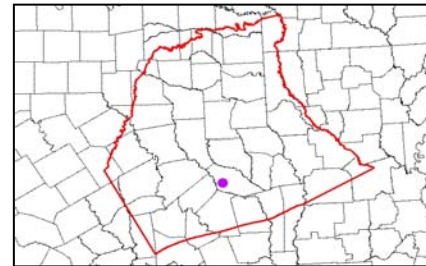
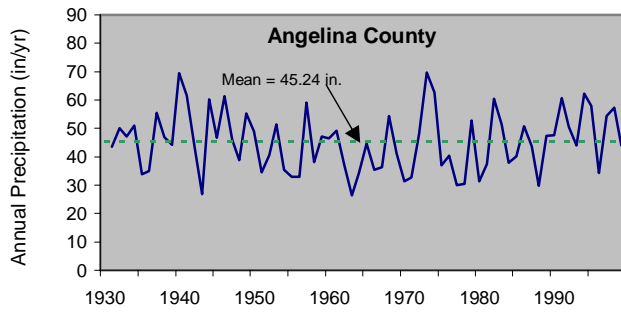


Figure 2.12a Annual precipitation time series for gages in Angelina, Cherokee, Ellis, and Franklin counties (Source: National Climatic DataCenter, Texas Natural Resources Information System).

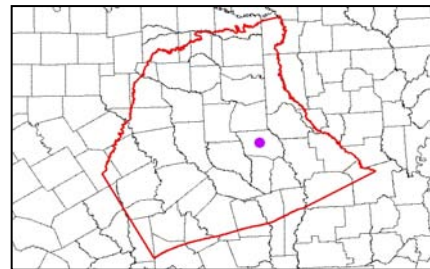
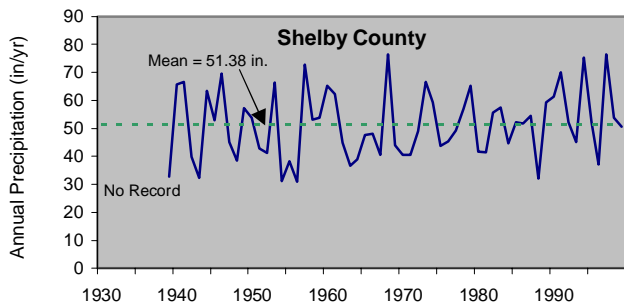
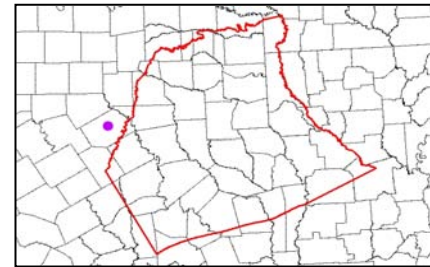
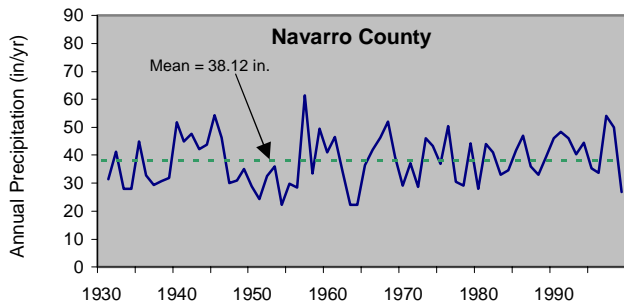
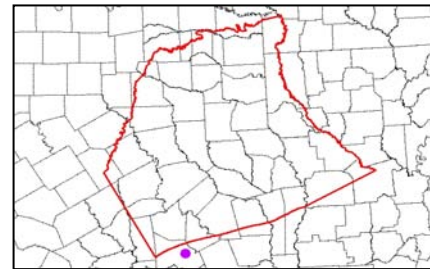
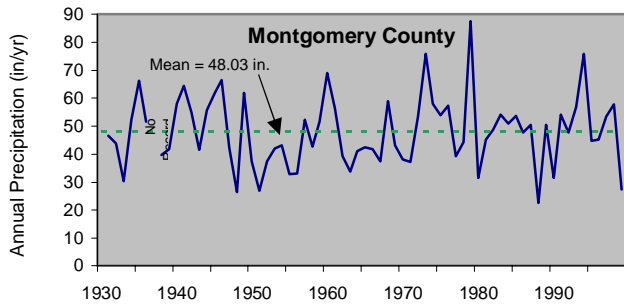
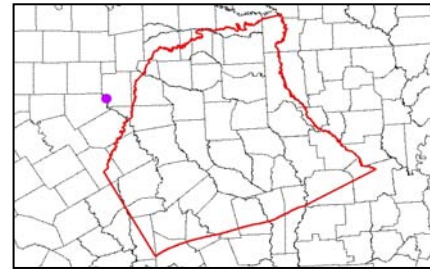
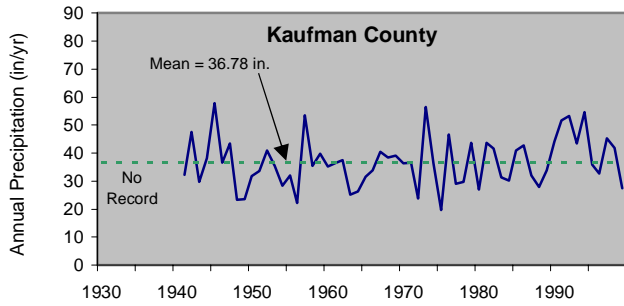


Figure 2.12b Annual precipitation time series for gages in Kaufman, Montgomery, Navarro, and Shelby counties (Source: National Climatic DataCenter, Texas Natural Resources Information System).

2.2 Geology

The sediments that form the aquifers in the study area are part of a gulf-ward thickening wedge of Cenozoic sediments deposited in the East Texas Basin and the Houston Embayment of the Gulf Coast Basin. Deposition has been influenced by regional crust subsidence, episodes of sediment inflow from areas outside of the Gulf Coastal Plain, and eustatic sea-level change (Grubb, 1997). Galloway et al. (1994) characterized Cenozoic sequences in the Gulf Coast with the following three characteristics. Deposition of Cenozoic sequences is characterized as an offlapping progression of successive, basinward thickening wedges. These depositional wedges aggraded the continental platform and prograded the shelf margin and continental slope from the Cretaceous shelf edge to the current Southwest Texas coastline. Deposition occurred along sand-rich, continental margin deltaic depocenters within embayments (Rio Grande, Houston, and Mississippi Embayments) and was modified by growth faults and salt dome development.

The primary Paleogene depositional sequences in ascending stratigraphic order are the lower Wilcox, the upper Wilcox, the Carrizo, the Queen City, the Sparta, the Yegua-Cockfield, the Jackson, and the Vicksburg-Frio (Galloway et al., 1994). Each of these depositional sequences is bounded by marine shales and finer grained sediments representing transgressions (i.e., Reklaw and Weches formations).

Figure 2.13 shows a geologic map of the area showing the Tertiary sediments comprising the aquifers of interest in this study as well as the Quaternary undivided sediments. The Carrizo and Wilcox sediments outcrop along a belt extending along the northern extent of the study area. The Wilcox, and to a lesser degree the Carrizo, also outcrop on the Sabine Uplift in the eastern portion of the model in East Texas and extending eastward into Louisiana. The Queen City and Sparta Sand formations are at ground surface across the majority of the East Texas Basin. South of the Sabine Uplift, the surface geology and outcrop pattern are oriented southwest-northeast coincident with depositional strike, the paleo-shelf, and perpendicular to basin subsidence.

Figure 2.14 shows a representative stratigraphic section for the Carrizo-Wilcox aquifer in Texas. The Carrizo-Wilcox aquifer extends from south Texas northeastward through East Texas into Arkansas and Louisiana. The aquifer consists of fluvial-deltaic sediments of the upper Paleocene and lower Eocene Wilcox Group and Carrizo Sand. The aquifer is underlain by

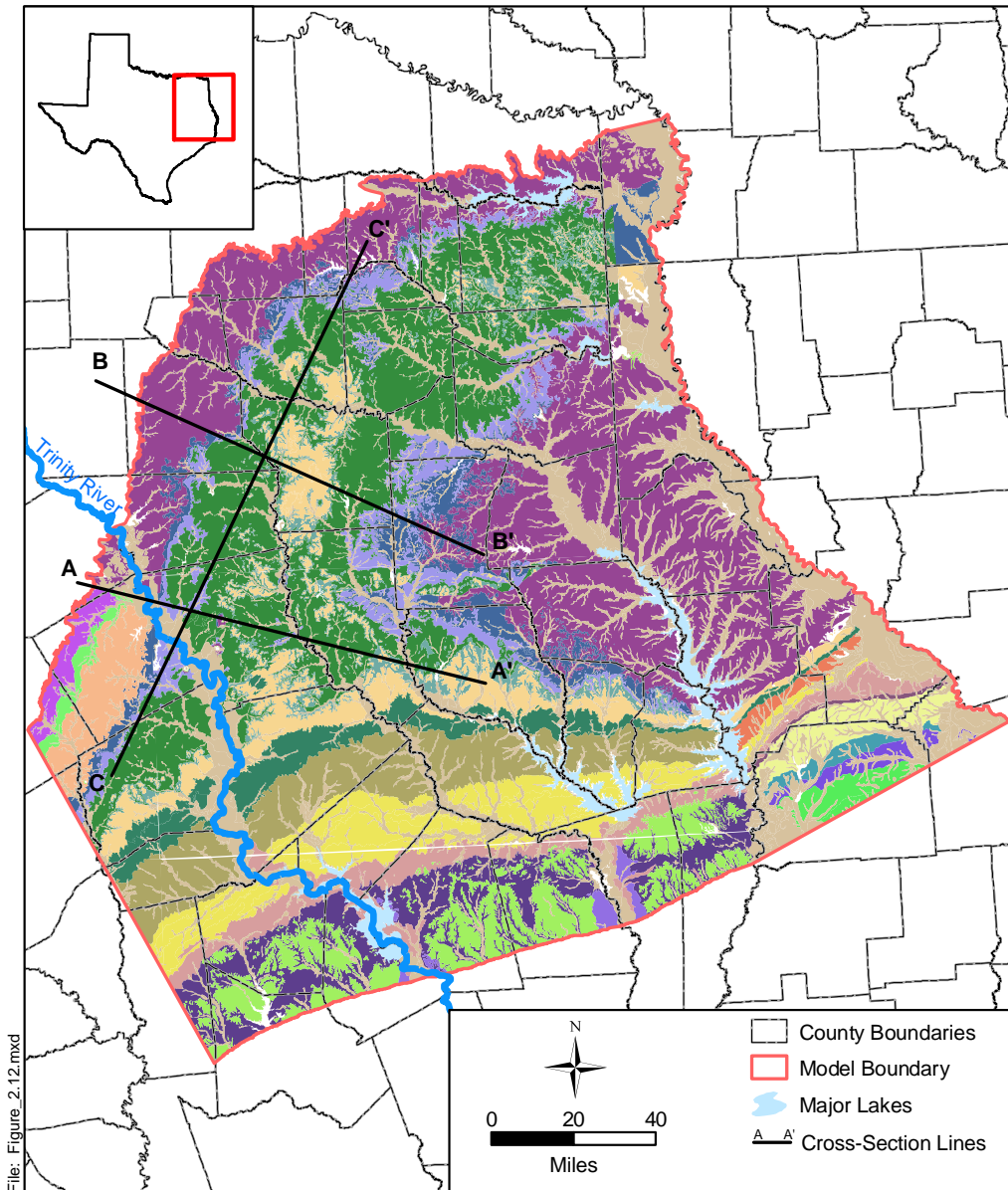
marine deposits of the Midway Group and overlain by the Reklaw Formation, representing a semi-confining unit between the Carrizo Sand and the shallow aquifer of the Queen City Formation.

The complexity of the hydrostratigraphy in the East-Texas Basin is shown in a set of cross-sections by Fogg and Kreitler (1982) together with the inferred groundwater flow patterns (Figure 2.15). The traces of the different sections are indicated in Figure 2.13.

In the western portion of the study area, the Wilcox Group is subdivided into the Hooper, the Simsboro, and the Calvert Bluff formations, corresponding to deltaic, fluvial, and fluvial-deltaic facies, respectively, which occur throughout east-central Texas (Kaiser, 1974). In the Sabine Uplift area, east of the Trinity River, the Simsboro is no longer identifiable and the Wilcox is divided informally into a lower and an upper unit (Kaiser, 1990). The lower Wilcox represents the facies equivalent of the Hooper Formation and the upper Wilcox includes both of the Simsboro and the Calvert Bluff equivalent fluvial and fluvial-deltaic facies, respectively (Kaiser, 1990). The Carrizo Sand unconformably overlies the Wilcox Group and is separated from the Wilcox by a thin regional marine-transgressive unit, which is included as an informal member in the upper Wilcox (Kaiser, 1990). The Carrizo Sand is composed primarily of relatively homogenous fluvial sands and only locally and in the northernmost area contains a significant portion of interbedded muds. The Reklaw Formation consists of variable amounts of mud and sand and is considered the upper confining stratum of the Carrizo-Wilcox aquifer. In the northeastern part the study areas, the Reklaw clays become discontinuous providing a more permeable connection between the Carrizo sand and the overlying Queen City Formation. In Marion and Harrison counties, the combined Wilcox, Carrizo, Reklaw, and Queen City are collectively referred to as the Cypress aquifer (Fogg and Kreitler, 1982). Above, the finer grained Weches Formation separates the Queen City Sand from the overlying Sparta Sand that occurs only locally in the study area.

The Carrizo is a fairly homogeneous sand unit overlying the thicker, more heterogeneous Wilcox Group. The Wilcox Group is a multi-aquifer system composed of fluvial channel sand distributed within the lower permeability interchannel sands and clays. In the study area, the Wilcox Group consists of up to 3,000 ft of interbedded lenticular sands, mud, and lignite. Sand layers constitute about 50 percent of the total Wilcox with thickness ranging from a few feet to

about 200 ft, consisting of fine grained to coarse grained quartz sand with various amounts of silt and clay. Fisher and McGowen (1967) mapped the net-sand distributions of the Wilcox Group in northeast Texas, identifying a dendritic pattern of north-south trending high net-sand channels feeding the principal delta systems of the ancestral Gulf of Mexico. Kaiser et al. (1978) refined the spatial pattern of major sand channels of the fluvial system in the combined Wilcox Group north of Houston, Angelina, and Nacogdoches counties. More recently, Kaiser (1990) mapped maximum sands (single thickest sand) and major sand (any sand of at least 40 ft thickness) to better identify the major continuous channel sands and exclude thinner and less continuous splay and overbank sands. Kaiser's 1990 study area was limited to the area surrounding the Sabine uplift and could not be combined with the earlier net-sand maps of Kaiser et al. (1978). However, the major and maximum sand maps showed similar dendritic patterns as the earlier net-sand maps. For this study, the net-sand map by Kaiser et al. (1978) was combined with the original net-sand map of Fisher and McGowen (1967) covering the southern part of the study area to produce a net-sand map for the entire model area, which is described in detail in Section 4.



West of Trinity River	East of Trinity River	Louisiana
	Quaternary Deposits	Cockfield Formation
	Lisie Formation	Blounts & Castor Creek Member
	Beaumont/Catahoula Formation	Williamson Creek Member
	Fleming Formation	Dough Hills Member
	Jackson Group	Camahan Bayou Member
	Yegua Formation	Lena Member
	Cook Mtn. & Stone City Form.	
	Sparta Formation	
	Weches Formation	
	Queen City Sand	
	Reklaw Formation	
	Carrizo Sand	
	Wilcox Group	
	Midway Group	
Calvert Bluff Formation		
Simsboro Formation		
Hooper Formation		

Figure 2.13 Surface geology of the study area.

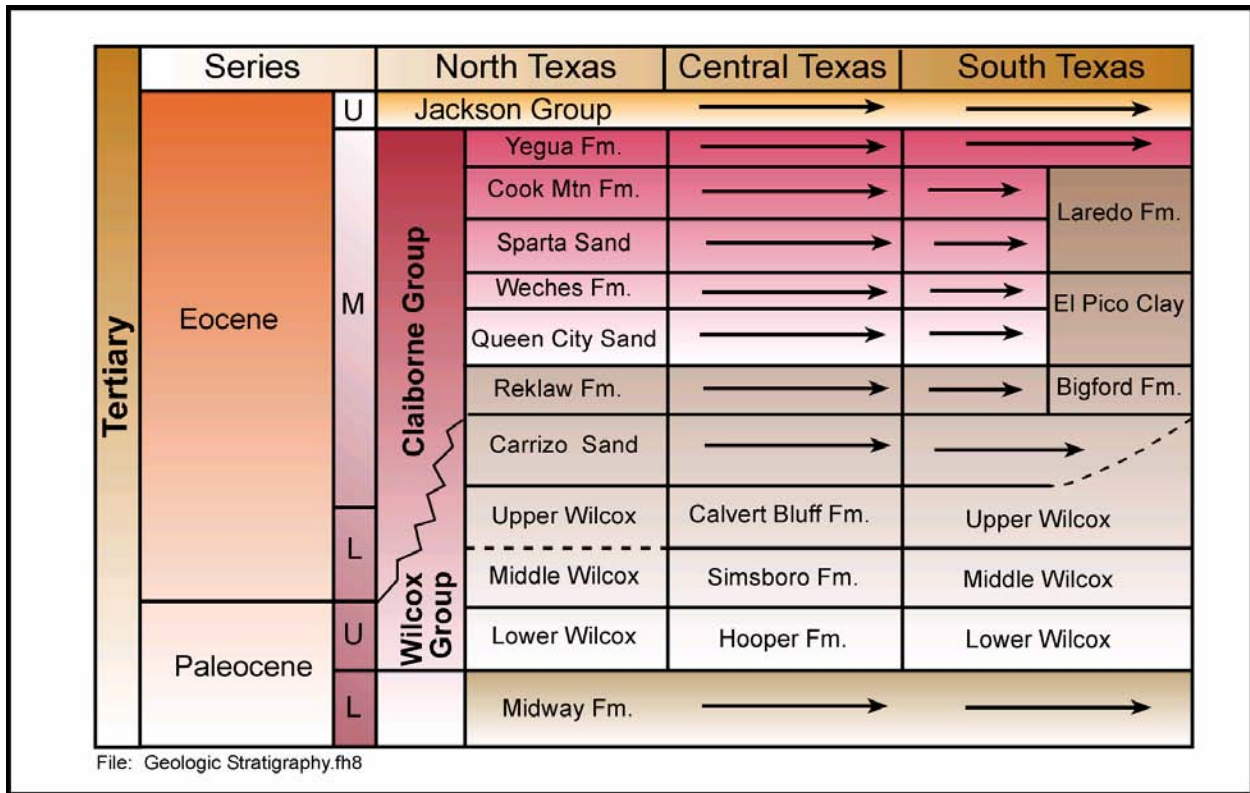


Figure 2.14 Generalized stratigraphic section for the Carrizo-Wilcox aquifer in Texas (after Ayers and Lewis, 1985; Hamlin, 1988; Kaiser et al., 1978).

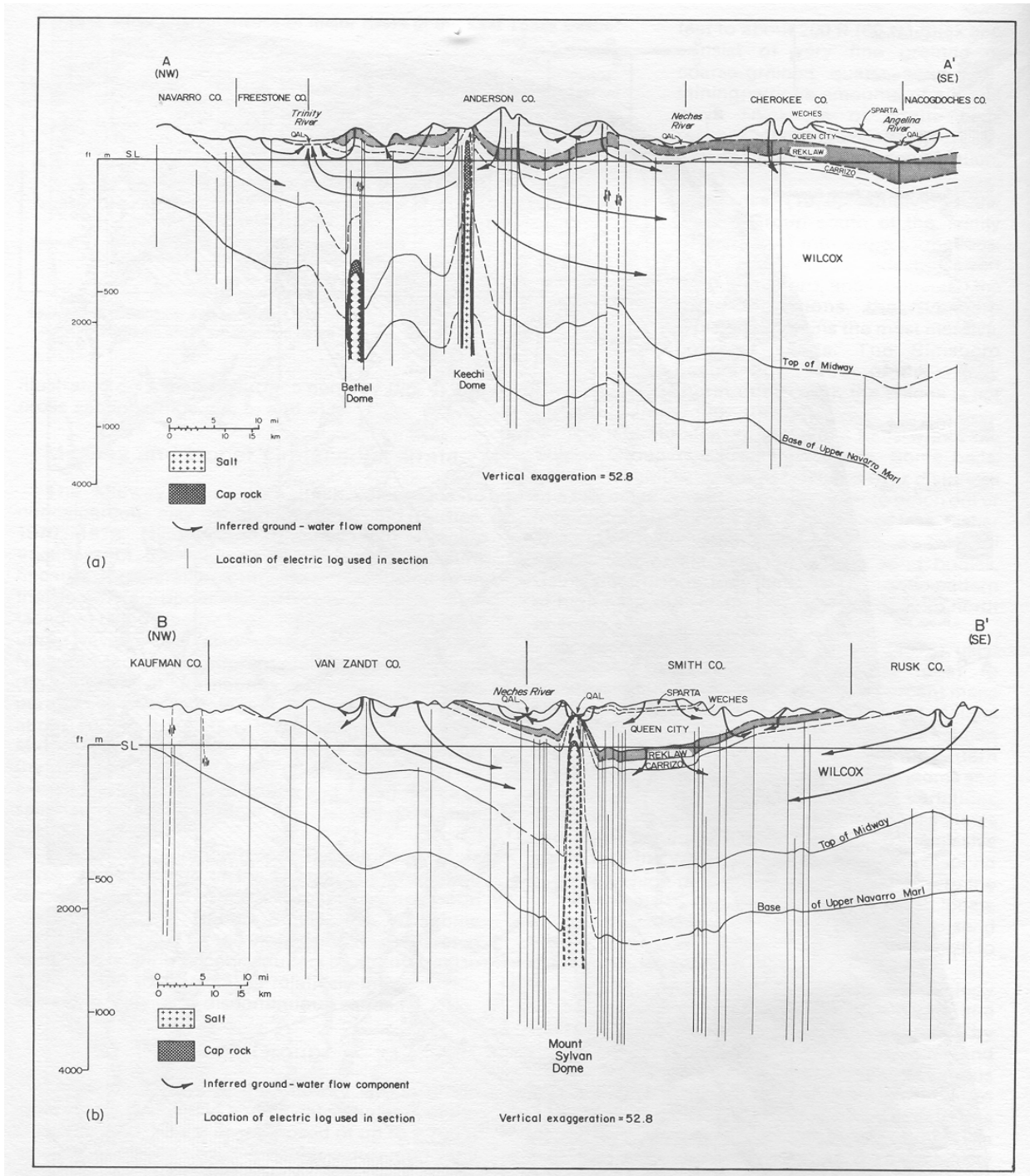


Figure 2.15a Structural cross sections A-A' and B-B' showing the major hydrostratigraphic units in the East Texas Basin from Fogg and Kreitler (1982), indicating general groundwater flow patterns. Cross-section locations are shown on Figure 2.13.

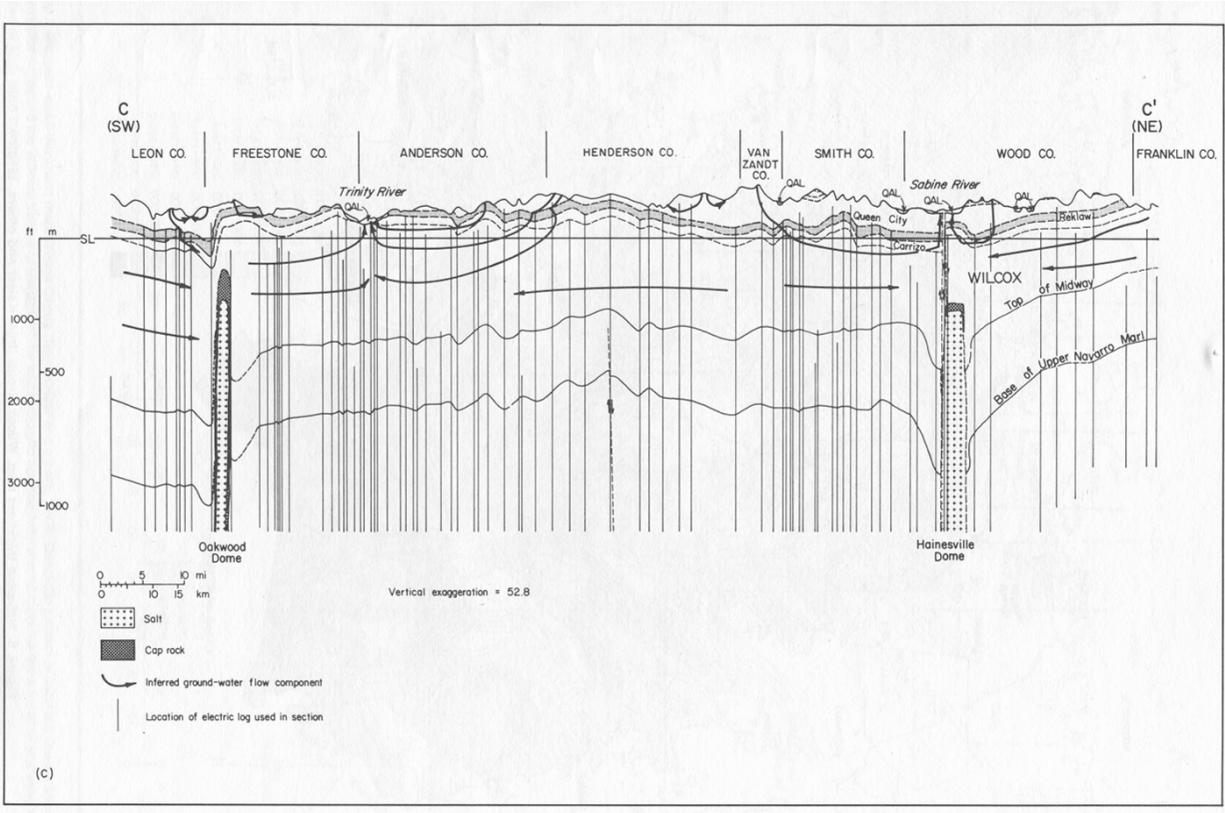


Figure 2.15b Structural cross section C-C' showing the major hydrostratigraphic units in the East Texas Basin from Fogg and Kreitler (1982), indicating general groundwater flow patterns. Cross-section location is shown on Figure 2.13.

3.0 PREVIOUS INVESTIGATIONS

The northern Carrizo-Wilcox aquifer has been studied by many investigators (see Table 3.1) and numerous groundwater bulletins have been prepared by the Texas Water Development Board for the counties in the study area. The East Texas Basin in particular has been the focus of extensive study by the Bureau of Economic Geology when the East Texas salt domes were being considered for their suitability in isolating high-level radioactive waste. Of these, the studies which are most relied on in this report are Kaiser (1974), Kaiser et al. (1978), Fogg and Kreitler (1982), Fogg et al. (1983), and Kaiser (1990).

Table 3.1 Previous groundwater models of the Carrizo-Wilcox aquifer in the study area.

Model	Code	No. of Carrizo-Wilcox Layers	Calibration	Predictive Simulations
Garza (1975)	Unknown	Unknown	Unknown	Unknown
Fogg et al. (1983)	TERZAGI	3	Steady-state	No
Ryder (1988)	Research	2	Steady-state	No
Williamson et al. (1990)	Research	2	Steady-state (1980)	No
Ryder & Ardis (1991)	Research	2	Steady-state (1910) Transient (1910-1982)	Yes
Thorkildsen and Price (1991)	Unknown	Unknown	Unknown	Unknown
TWDB East-Texas Model (unpublished)	MODFLOW	4	Steady-state (1985) Transient	2050
Harden and Assoc. (2000)	MODFLOW	5	Steady-state (1950) Transient (1950 -1998)	50 year

Kaiser (Kaiser, 1974; Kaiser et al., 1978; and Kaiser, 1990) studied the sand geometry and lignite occurrence in the Paleocene-Eocene of East Texas. He investigated the stratigraphy and structure of the Wilcox Group which included the mapping of sand thickness, maximum sand thickness, and sand percent across a large portion of the model study area. Fogg and Kreitler (1982) studied the hydraulics and geochemical facies of the Eocene aquifers of East Texas. They extensively investigated the hydrogeologic setting, aquifer hydraulics, and groundwater chemistry. From a synthesis of this data, they made conclusions regarding aquifer flow and inter-aquifer flow dynamics.

Fogg et al. (1983) developed a detailed three-dimensional groundwater flow model in the area surrounding Oakwood Dome, located in southeast Freestone County and north-central Leon County. This modeling study is briefly discussed below with other groundwater flow models

which have been developed for the Carrizo-Wilcox aquifer in the Northern Carrizo-Wilcox GAM study area. Figure 3.1 shows the model boundaries for the Northern Carrizo-Wilcox GAM as it relates to previous modeling study boundaries. Table 3.1 lists these previous investigations along with some basic model characteristics to provide a basis for the following discussion.

Garza (1975) developed the earliest Carrizo-Wilcox model in the study area evaluating the effects of a proposed reservoir on groundwater conditions in the Carrizo-Wilcox aquifer and Trinity River Alluvium. Fogg et al. (1983) developed a three-dimensional model of the Carrizo-Wilcox aquifer in Leon and Freestone counties in the Trinity River Basin. The model used was an integrated finite difference code called TERZAGI. The major contribution of this study was the investigation of methods for developing effective grid block hydraulic conductivities for the heterogeneous stacked channel sequences which typify the Wilcox Group in East Texas. This model also performed a detailed sensitivity analysis to better understand the plausible ranges of vertical and horizontal hydraulic conductivities, vertical to horizontal anisotropy ratios, and the hydraulic conductivity of the Reklaw Formation.

The United States Geological Survey (USGS) has developed super-regional models which incorporate the entire Carrizo-Wilcox aquifer in Texas (Ryder, 1988; Ryder and Ardis, 1991) and in the entire Gulf Coast Region (Williamson et al., 1990) as part of the RASA (Regional Aquifer-System Analysis) studies. Their analyses modeled from the Midway Formation through the Gulf Coast aquifer systems. The Carrizo-Wilcox aquifer was modeled as two layers, generally a lower and middle Wilcox aquifer and an upper Wilcox and Carrizo aquifer. Ryder (1988) reported that the model objectives were to define the hydrogeologic framework and hydraulic characteristics of the Texas coastal plain aquifer systems, delineate the extent of freshwater and density of saline water in the various hydrogeologic units, and describe the regional groundwater flow system. A steady-state calibration to predevelopment conditions was performed using a research code developed by Kuiper (1985).

The entire U.S. Gulf Coast aquifer system above the Midway Formation was modeled by Williamson et al. (1990) using the research code developed by Kuiper (1985). The model consisted of a steady-state calibration to predevelopment conditions, a steady-state calibration to 1980 water-level data, and transient simulations from 1935 to 1980. The model objectives were “to help in the development of quantitative appraisals of the major groundwater systems of the

United States, and to analyze and develop an understanding of the groundwater flow system on a regional scale, and to develop predictive capabilities that will contribute to effective management of the system”.

Ryder and Ardis (1991) extended the work performed by Ryder (1988) and developed another model of the coastal plain aquifers in Texas. The model, developed using the research code developed by Kuiper (1985), was calibrated to both steady-state predevelopment conditions and transient conditions from 1910 to 1982. In addition, transient predictive simulations were performed using the calibrated model. The objectives for the modeling study consisted of (1) defining the hydrogeologic framework and hydraulic characteristics of the aquifer systems, (2) delineating the extent of fresh to slightly saline water in various hydrogeologic units, (3) describing and quantifying the groundwater flow system, (4) analyzing the hydrologic effects of man’s development on the flow system, and (5) assessing the potential of the aquifer systems for further development.

Thorkildsen and Price (1991) modeled the Carrizo-Wilcox aquifer in the northern Carrizo-Wilcox aquifer study area but only model results were documented. R.W. Harden and Associates (2000) developed a Carrizo-Wilcox aquifer model in support of the Brazos Regional Water Plan (Region G). This model was developed using MODFLOW and divided the Carrizo-Wilcox into five layers including the Newby Formation. The purpose of the model was to provide a first-order analysis to confirm Carrizo-Wilcox groundwater availability as it was defined in the Regional Water Planning Group Region G plan. The model was calibrated to steady-state conditions in 1950 and transient conditions from 1950 to 1998 and was used to perform predictive simulations through 2050. The TWDB developed an unpublished model called the East Texas Model in 2000. This model was developed to improve understanding of groundwater availability in East Texas.

Each of these models provides information which is both relevant and useful to the study of groundwater availability in the northern Carrizo-Wilcox aquifer study area. However, many traits of the previous investigations have made development of the current GAM necessary to meet the GAM specifications defined by the TWDB. Specifically, GAM models are expected to (1) be well documented and publicly available, (2) utilize standard modeling tools which are

non-proprietary (MODFLOW), and (3) be calibrated both in steady-state and transiently and capable of adequately simulating a verification period following a calibration period.

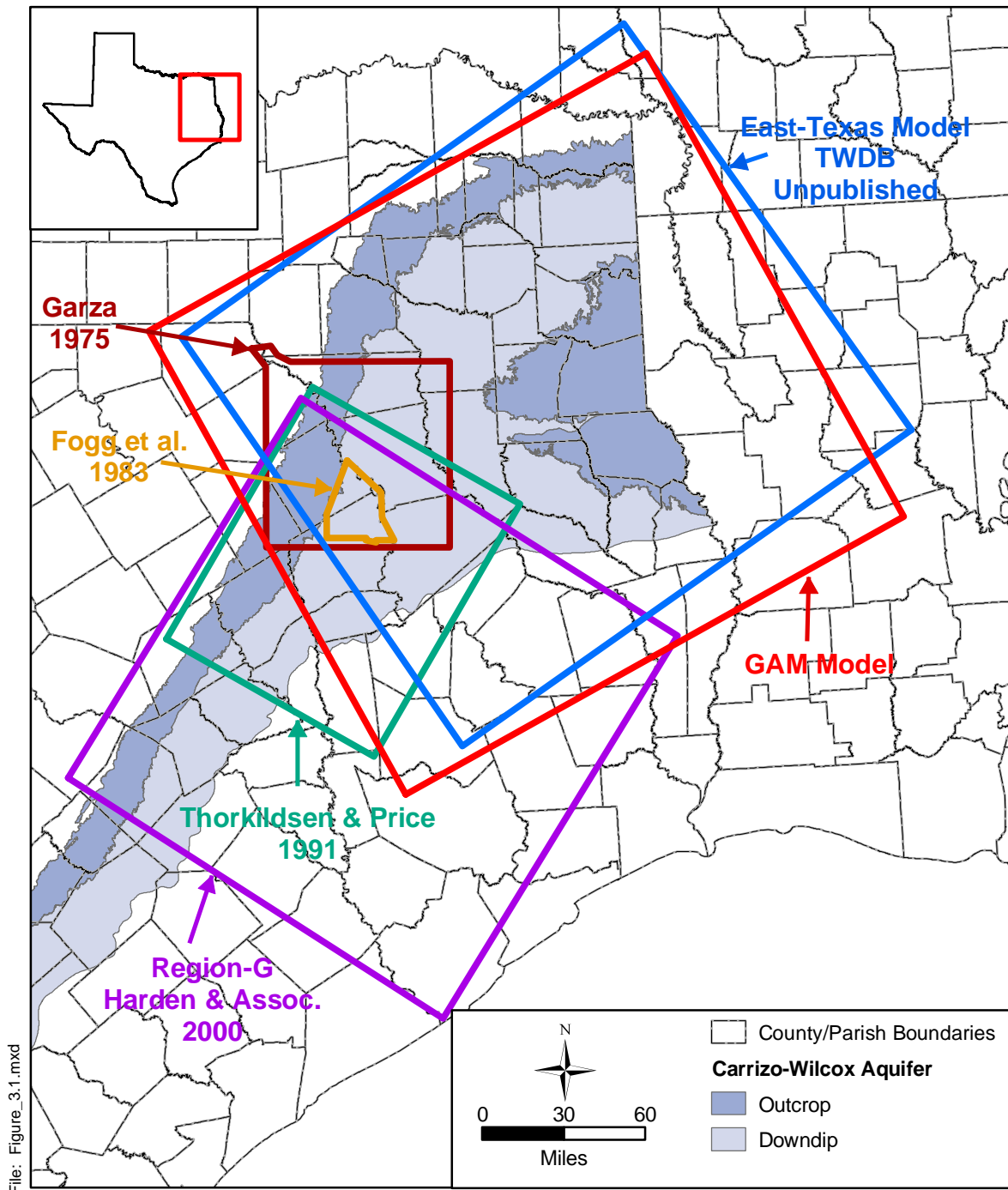


Figure 3.1 Northern Carrizo-Wilcox GAM boundary with previous modeling study boundaries which have included the Carrizo-Wilcox aquifer.

4.0 HYDROGEOLOGIC SETTING

The hydrogeologic setting of the Carrizo-Wilcox aquifer is defined by the hydrostratigraphy, hydraulic properties, structure, regional groundwater flow, surface and groundwater interaction, and recharge and discharge. The characterization of the hydrogeologic setting is based on previous geologic and hydrologic studies in the area and detailed compilation and analyses of structure maps, hydraulic properties, water-level data, spring and stream flow data, and climatic information.

4.1 Hydrostratigraphy

The Carrizo-Wilcox aquifer extends from south Texas northeastward through east Texas into Arkansas and Louisiana. The aquifer consists of fluvial-deltaic sediments of the upper Paleocene and lower Eocene Wilcox Group and Carrizo Sand. The aquifer is bounded below by marine deposits of the Midway Group and above by the Reklaw Formation, representing a semi-confining unit between the Carrizo Sand and the shallow aquifer of the Queen City Formation.

The northern model area extends from the groundwater divide between the Brazos and Trinity rivers to the Red River. In the western portion of the study area, the Wilcox Group is subdivided into the Hooper, Simsboro, and Calvert Bluff formations, corresponding to deltaic, fluvial, and fluvial-deltaic facies, respectively, which occur throughout east-central Texas (Kaiser, 1974). In the Sabine Uplift area, east of the Trinity River, the Simsboro is no longer identifiable and the Wilcox is divided into informal lower and upper units. The lower Wilcox represents the facies equivalent of the Hooper Formation and the upper Wilcox includes both the Simsboro and the Calvert Bluff equivalent fluvial and fluvial-deltaic facies, respectively (Kaiser, 1990). Even though the structure and various sand maps in the Sabine uplift area distinguish only the upper and lower Wilcox (Kaiser, 1990), a predominantly fluvial facies at the bottom and a fluvial-deltaic facies at the top can be identified within the upper Wilcox corresponding to the subdivision of the Wilcox Group in Central Texas as mapped by Ayers and Lewis (1985).

The Carrizo Sand unconformably overlies the Wilcox Group and is separated from it by a thin regional marine-transgressive unit, which is included as an informal member in the upper Wilcox (Kaiser, 1990). The Carrizo Sand is composed primarily of relatively homogenous fluvial sands and only locally and in the northernmost area contains a significant portion of

interbedded muds. The Reklaw Formation consists of variable amounts of mud and sand and is considered the confining strata of the Carrizo-Wilcox aquifer. However, in the northeastern part the clay strata become more discontinuous making the Reklaw probably more pervious to vertical flow between the Carrizo and the overlying Queen City. In Marion and Harrison counties, the combined Wilcox, Carrizo, Reklaw, and Queen City units are referred to as the Cypress aquifer (Fogg and Kreitler, 1982). Above, the Weches Formation separates the Queen City Sand from the overlying Sparta Sand that occurs only locally in the area.

The proposed hydrostratigraphic layers of the Carrizo-Wilcox aquifer for the northern model (Figure 4.1.1) include the main depositional facies of the Wilcox Group and the Carrizo Sand. The Reklaw confining unit is represented by a separate layer, accounting for variations in aquitard thickness and facies change from predominantly clay to mixed clay and sand in the northeastern part of the study area. The Queen City aquifer is represented as the top layer of the model to better define the hydraulic gradient across the confining Reklaw Formation. This allows for evaluating potential leakage between the Carrizo and the shallow Queen City aquifer. Potential recharge through leakage from the Queen City aquifer may be important in case of extensive pumpage in the shallow confined Carrizo aquifer. The top layer has assigned recharge boundary conditions reflecting the shallow water table that follows the topography. Younger formations that lie above the Sparta Sand in the southern part of the model are represented in the model by general head boundary conditions accounting for the hydraulic connection between the Queen City and Sparta aquifers to the shallow water table.

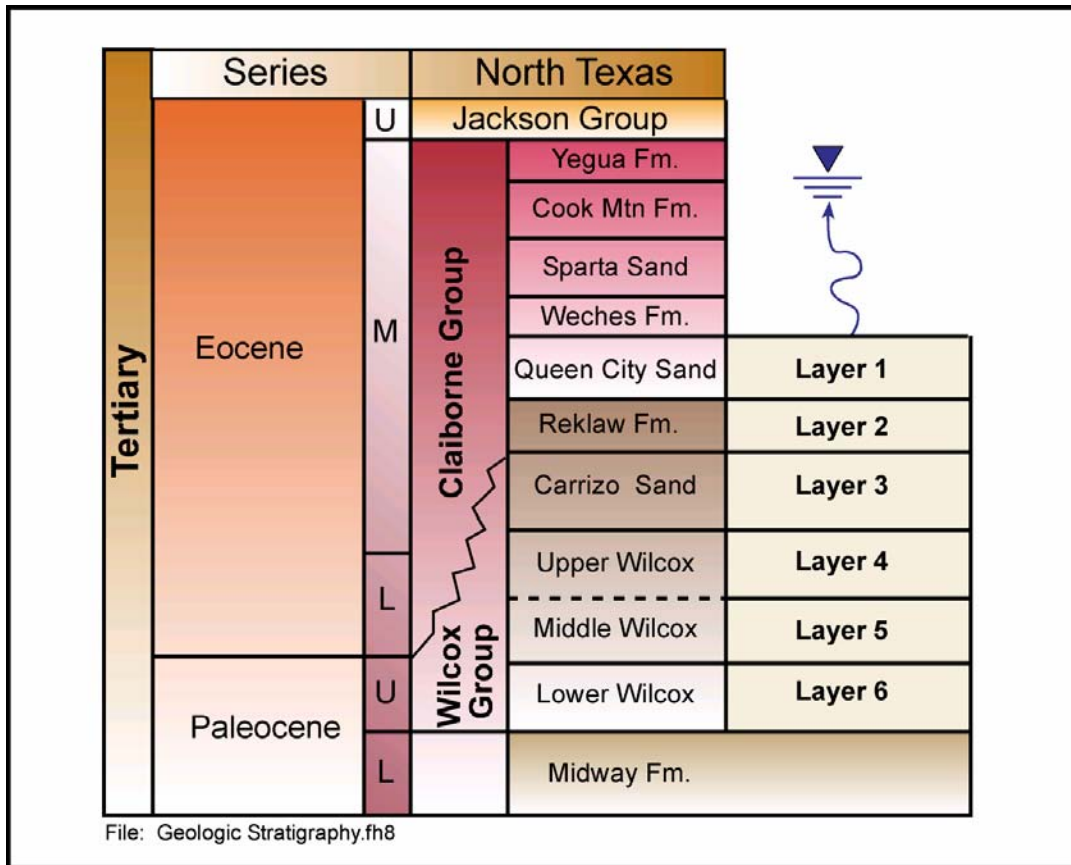


Figure 4.1.1 Hydrostratigraphy and model layers.

4.2 Structure

The geologic structure of the northern Carrizo-Wilcox model is dominated by the East Texas Basin in the north and central model area, the Sabine Uplift in the eastern model area, and the Houston Embayment in the southern portion of the model area (Figure 4.2.1). The structure surfaces of the different hydrostratigraphic units used for the GAM were compiled from different sources, which are summarized in Table 4.2.1.

Table 4.2.1 Data sources for layer elevations for the Northern Carrizo-Wilcox GAM.

Model Layer Boundary	East Texas Model (TWDB, unpublished)	Wilson and Hosman (1988) (USGS RASA)	Kaiser (1990)	Central Carrizo-Wilcox GAM	Surface Elevations (USGS)
Top of Queen City	X				X
Top of Reklaw	X	X		X	X
Top of Carrizo	X	X		X	X
Top of Wilcox	X	X		X	X
Top of Middle Wilcox	X			X	X
Top of Lower Wilcox	X		X	X	X
Base of Wilcox	X	X		X	X

Data Format for the Various Sources:

Data Source	Report Number	Format
East Texas Model TWDB (unpublished)		Text files containing x, y, and elevation.
Wilson and Hosman (1988)	USGS Open-File Report 87-677	Printed tables.
Kaiser (1990)	BEG	Printed tables.
Central Carrizo-Wilcox GAM		Text files containing x, y, and elevation.
USGS DEM (Outcrop Surface Elevations)		DEM files.

The processing of the structure data required several steps. The data from the different sources were digitized and converted to GAM coordinates and merged for the individual structure surfaces. The data were initially kriged to identify problems. Problems were solved through a combination of eliminating data sources, removing data points, and/or defining guide points to constrain the kriging algorithm. The data were kriged again and delimited to the corresponding subcrop areas. The kriged and delimited data were then merged with the outcrop elevation grid, which was developed from U.S. Geological Survey digital elevation model

(DEM) data. The final kriged structure surfaces were then used to calculate layer thicknesses, which were checked (and modified, as appropriate) to insure that layer thicknesses were not less than 20 ft throughout the model.

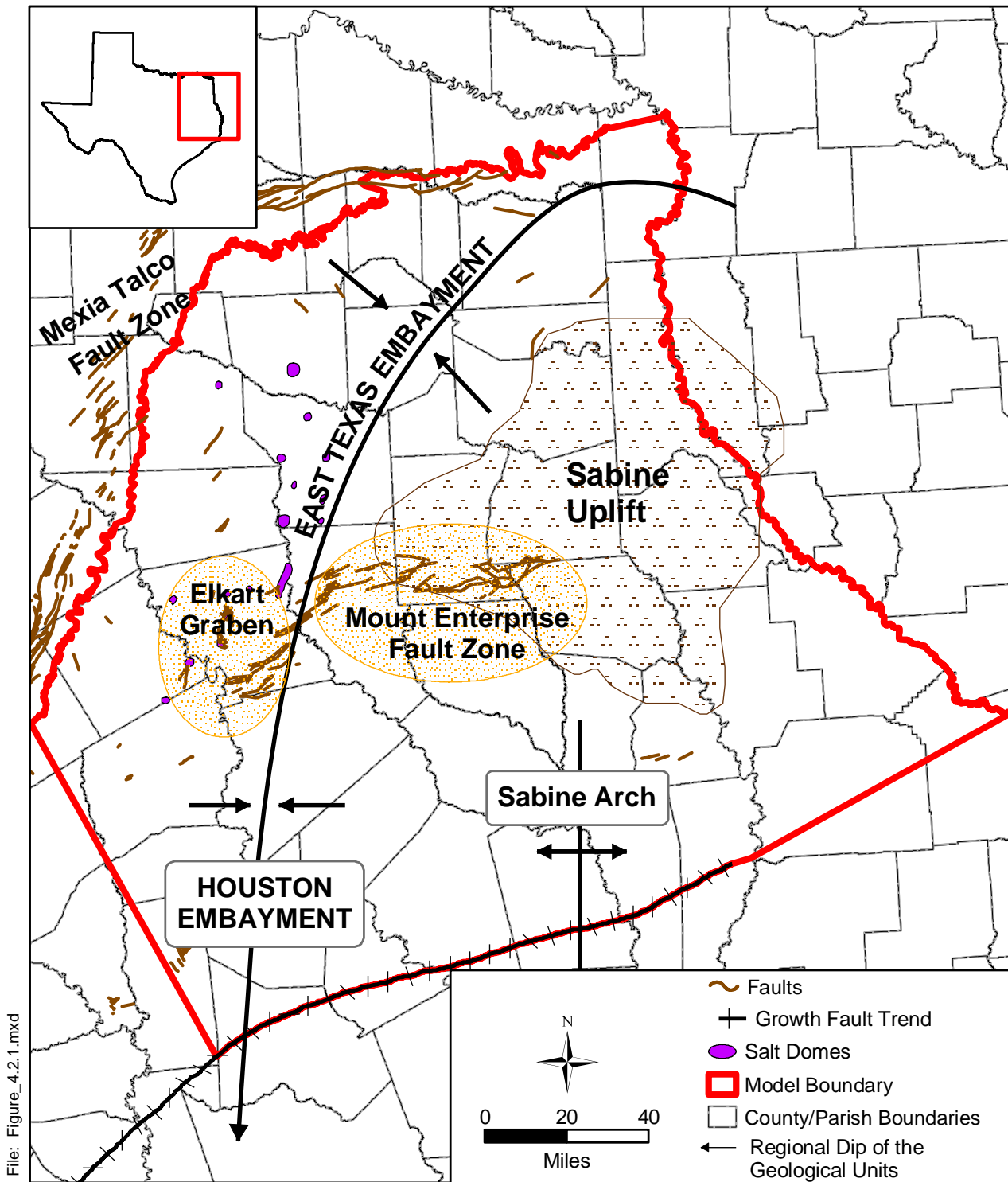
Figures 4.2.2 through 4.2.8 show the structure contour maps of the different hydrostratigraphic units. The structure maps show the data locations and identify the source of the data. The base of the Wilcox dips east and west toward the East Texas Embayment north of the Elkhart - Mount Enterprise Fault Zones. To the south, the strike of the base of the Wilcox is more east-west trending and the surface dips more steeply toward the Houston Embayment (Figure 4.2.2). The top of the lower Wilcox, shown in Figure 4.2.3, shows a similar structure as the base of the Wilcox. Also shown in Figures 4.2.2 and 4.2.3 is a line delineating the northern extent of the lower Wilcox, which extends from south of the Sabine Uplift west-northwest toward the western outcrop of the Wilcox Group. That is, north of the subcrop line the structure surface of the base of the Wilcox and top of the lower Wilcox are the same. As indicated by the different data points, the top of the Hooper Formation identified in east-central Texas correlates with the top of the lower Wilcox northeast of the Trinity River.

The structure at the top of the middle Wilcox extends the top of the Simsboro Formation mapped in central Texas into an arbitrary horizon in the upper Wilcox, which is based on the TWDB's East Texas Model (Figure 4.2.4). The constructed structure of the top of the Wilcox Group (Figure 4.2.5) utilized additional data sources from the USGS RASA study to define the top of the Wilcox in easternmost Texas. The upper Wilcox in the Sabine Uplift area is eroded and its surface corresponds to the land-surface elevation. The top of the Carrizo-Wilcox aquifer is represented by the structure surface, shown in Figure 4.2.6, which combines data from the TWDB's East Texas Model, RASA, and from Ayers and Lewis (1985). The top of the Reklaw Formation, representing the major confining layer of the Carrizo-Wilcox aquifer is shown in Figure 4.2.7. The top layer, represented by the Queen City Formation is shown in Figure 4.2.8, which is based entirely on data from TWDB's East Texas Model.

The thickness maps of the various hydrostratigraphic units are shown in Figures 4.2.9 through 4.2.15, which were constructed based on the elevation difference in the structure contour maps (Figures 4.2.2 through 4.2.8). The thickness of the lower Wilcox decreases to the north, where it was eroded north of an east-west trending line representing the subcrop extent of the

lower Wilcox (Figure 4.2.9). The lower Wilcox thickens rapidly southward into the Houston Embayment. The thickness map of the middle Wilcox extends to the northern outcrop of the Wilcox Group (Figure 4.2.10). In the southwestern part of the area, the middle Wilcox corresponds to the Simsboro Formation of the Central Carrizo-Wilcox GAM area. East of the Trinity River, the top of the middle Wilcox was picked as used in TWDB's East Texas Model. As a result, the thickness map of the middle Wilcox shows a relatively large increase east of the Trinity River. The thickness map of the upper Wilcox (Figure 4.2.11) shows a similar pattern east of the Trinity River. Overall, the upper Wilcox is somewhat thinner than the middle Wilcox. The thickness of the Carrizo is typically 100 to 200 ft or less in the study area (Figure 4.2.12); only to the southwest in the downdip section does the thickness increase significantly. The thickness of the Reklaw Formation in the East-Texas Embayment ranges between less than 40 ft to about 200 ft (Figure 4.2.13) and increases to over 600 ft in the downdip section toward the Houston Embayment. The thickness of the Queen City shows relatively large variations in the East Texas Embayment where the formation crops out (Figure 4.2.14). The Queen City generally decreases in thickness downdip and pinches out toward the southeastern part of the model area. Younger sediments form a wedge above the Queen City, which increases in thickness to more than 6000 ft toward the southern boundary of the study area (Figure 4.2.15).

A number of salt domes and salt pillows affect the structural surfaces of the Wilcox Group in the East-Texas Embayment (Figure 4.2.1). The constructed structure maps did not include salt domes penetrating the Wilcox strata, because of the localized nature of these features. In some cases, the domes caused little uplift and faulting of the surrounding sediments, whereas in other cases they resulted in significant uplift and faulting of strata (Fogg and Kreitler, 1982). The latter caused faulting of aquitards and even exposure of underlying aquifers at the surface (e.g., Keechi Dome in Anderson County as indicated in Figure 2.15a) providing potential points of local recharge to the confined Carrizo-Wilcox aquifer.



File: Figure_4.2.1.mxd

Source: W.R. Kaiser (1990)

Figure 4.2.1 Structural setting of the study area.

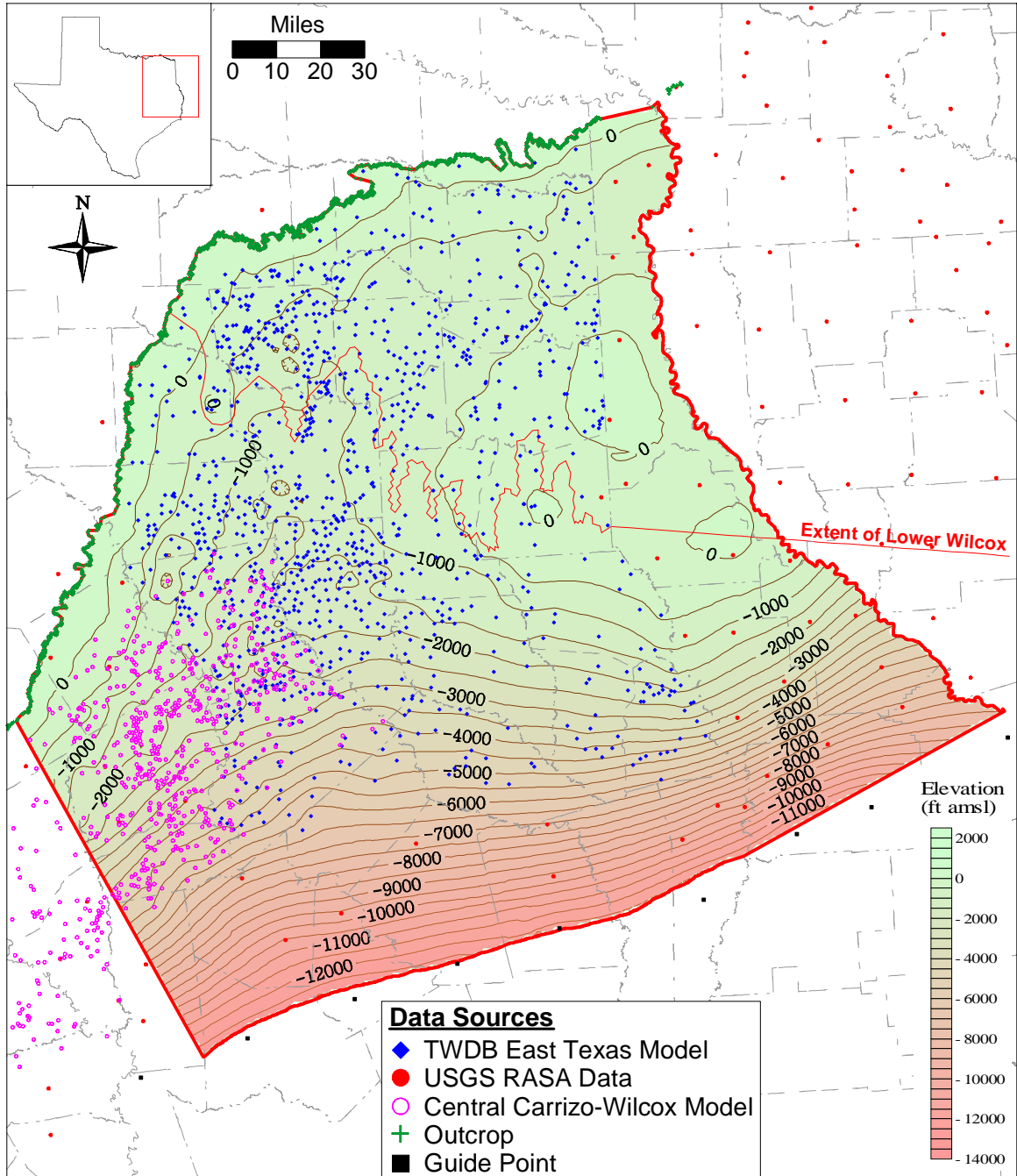


Figure 4.2.2 Structure contour map of the base of the Wilcox Group (CI = 500 ft).

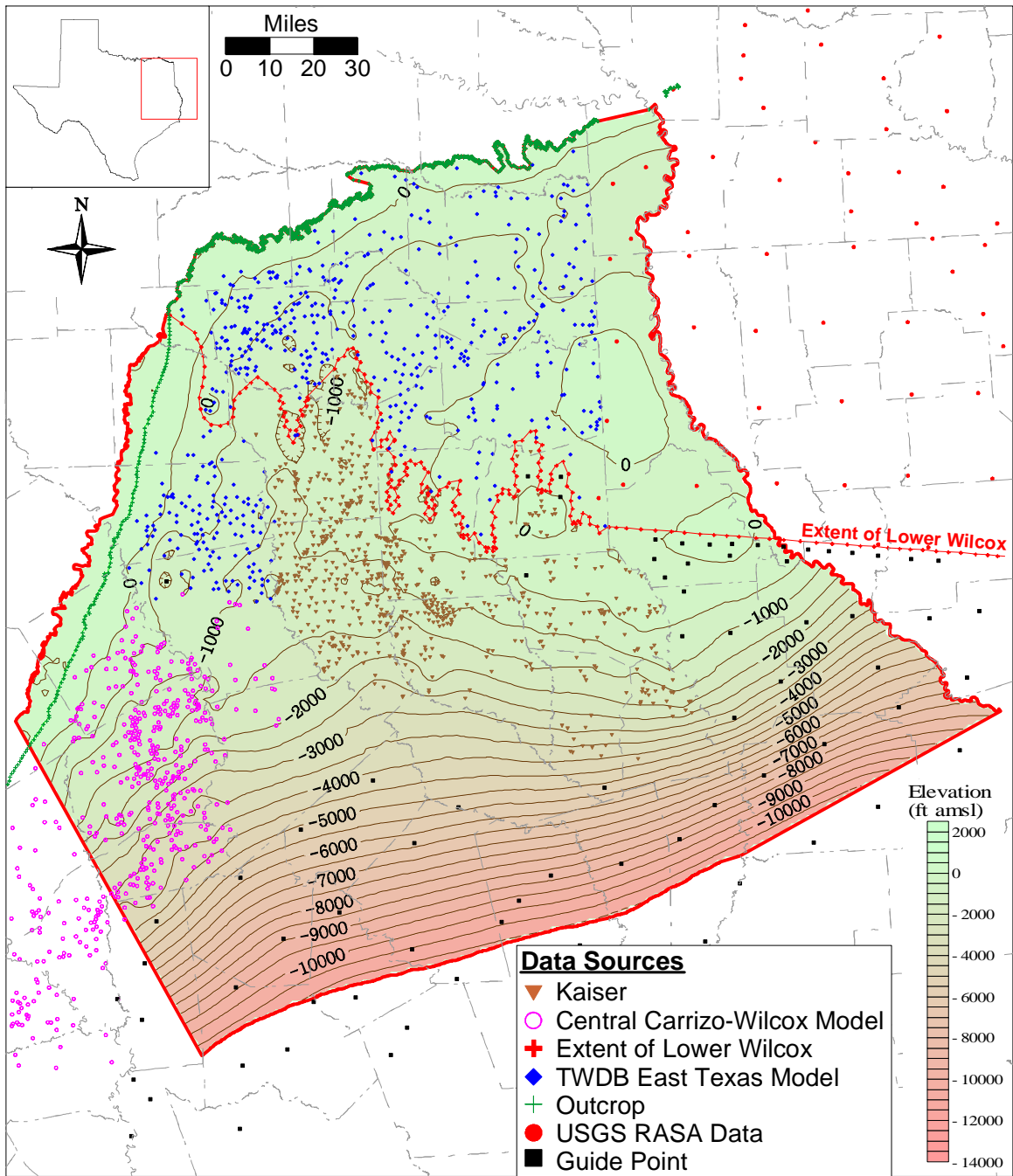


Figure 4.2.3 Structure contour map of the top of the lower Wilcox (CI = 500 ft).

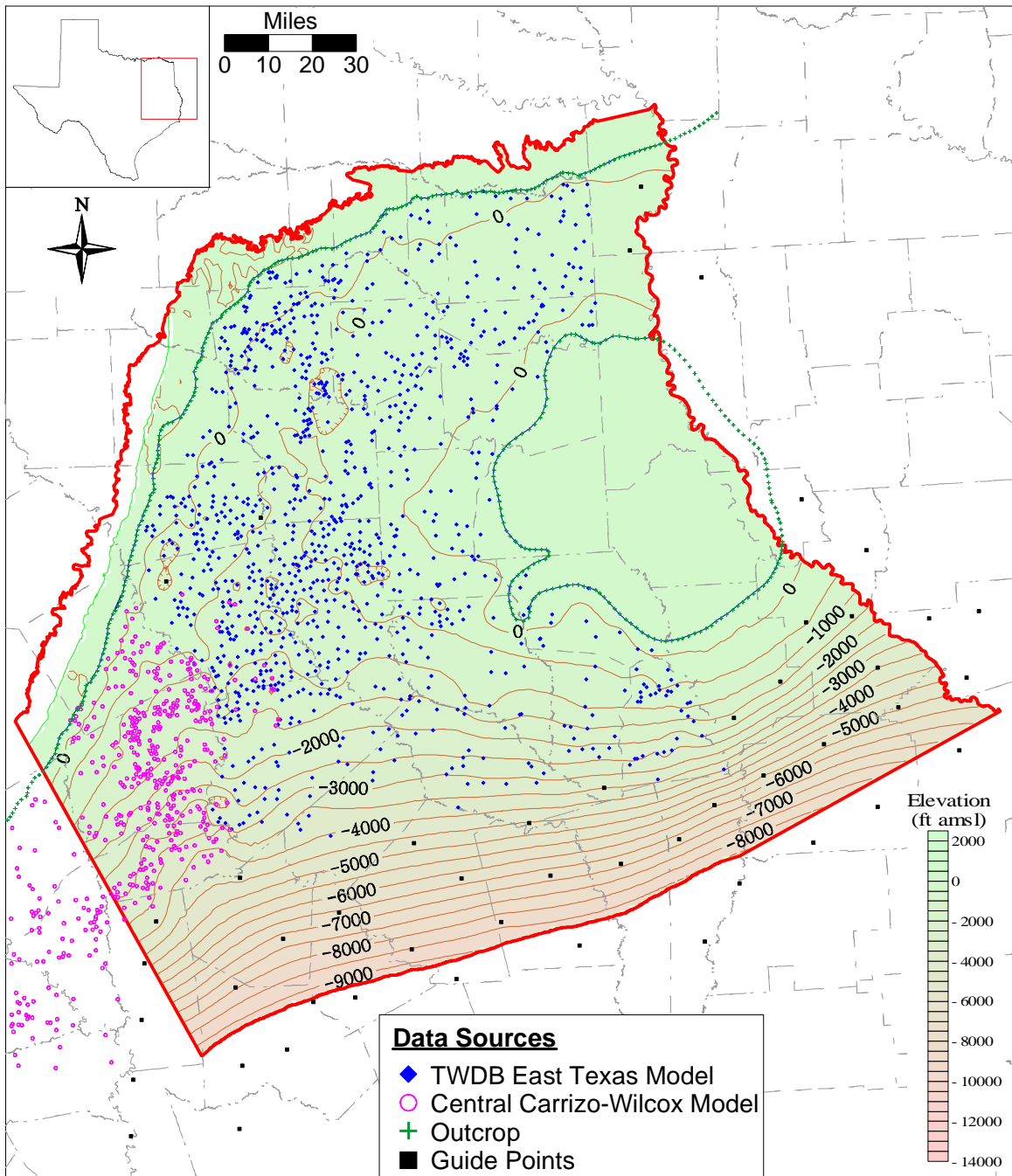


Figure 4.2.4 Structure contour map of the top of the middle Wilcox (CI = 500 ft).

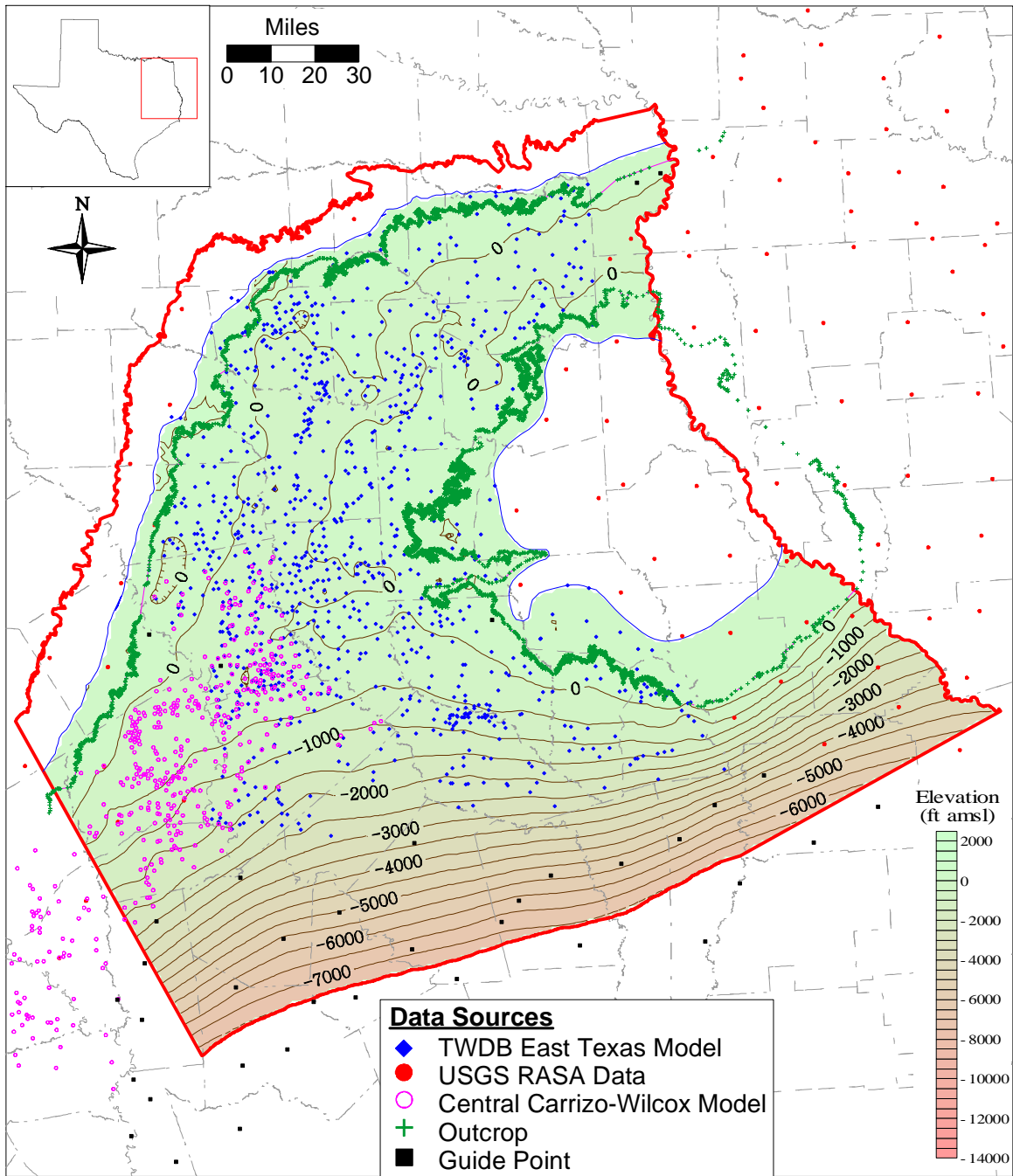


Figure 4.2.5 Structure contour map of the top of the Wilcox Group (CI = 500 ft).

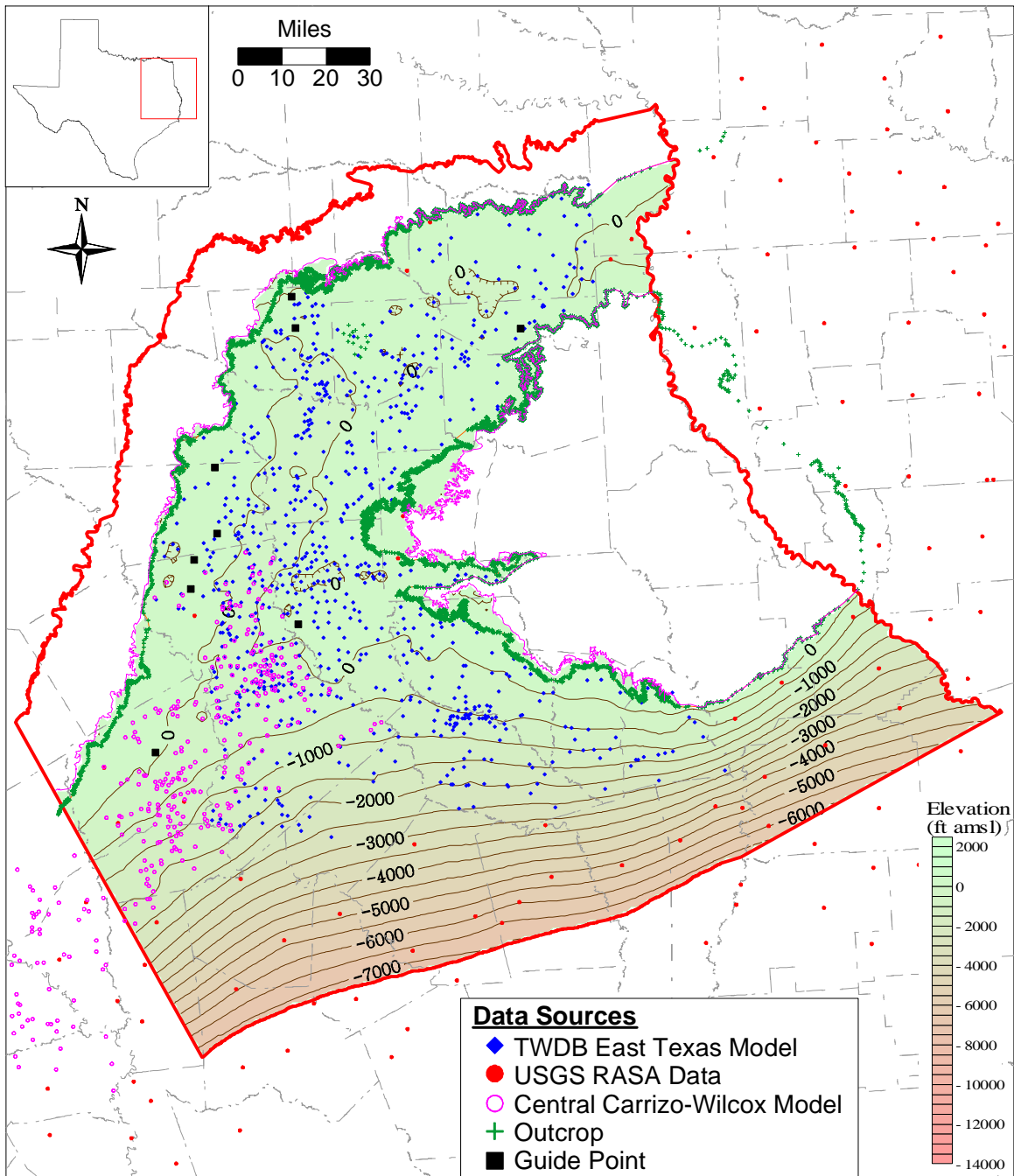


Figure 4.2.6 Structure contour map of the top of the Carrizo (CI = 500 ft).

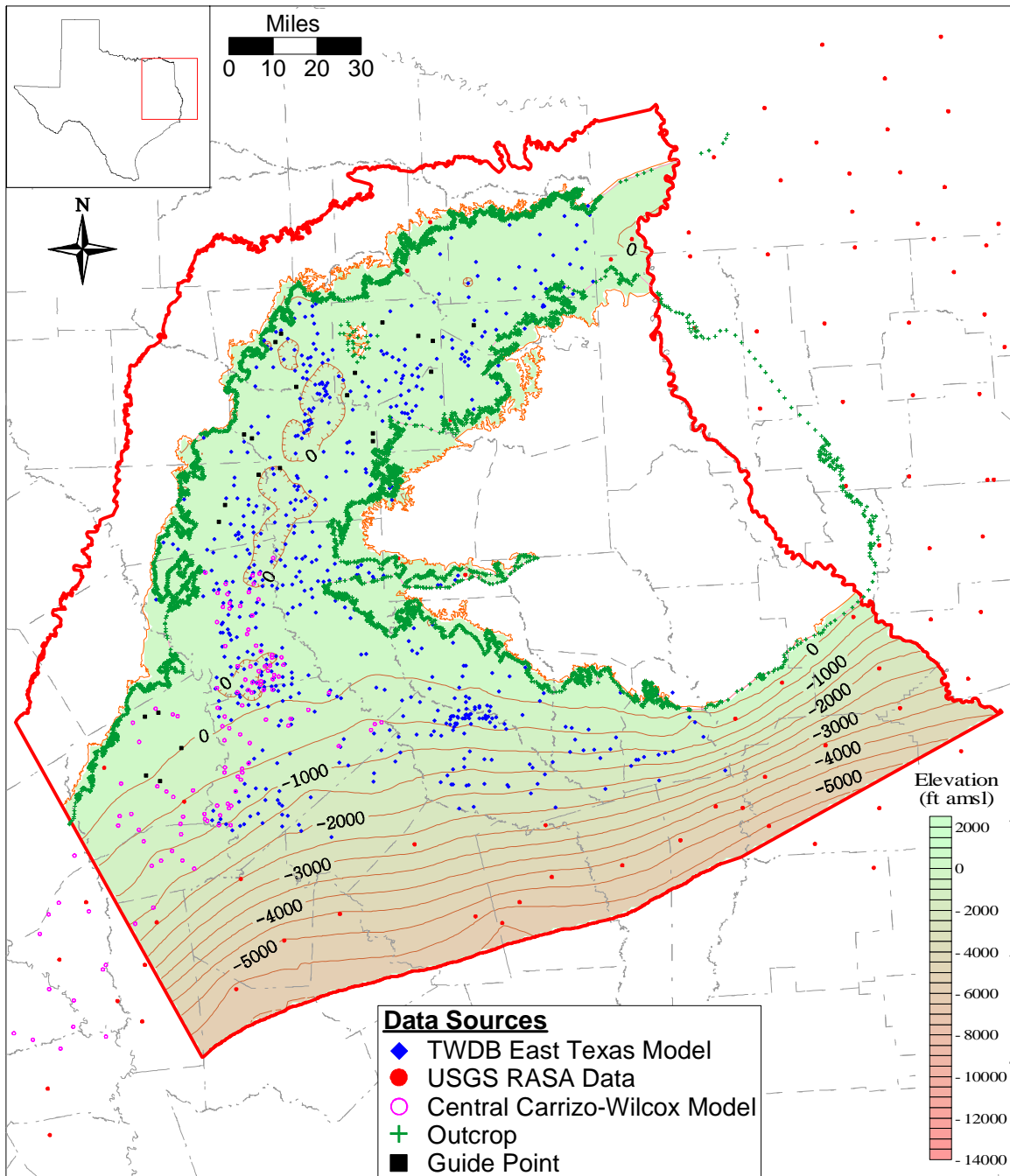


Figure 4.2.7 Structure contour map of the top of the Reklaw Formation (CI = 500 ft).

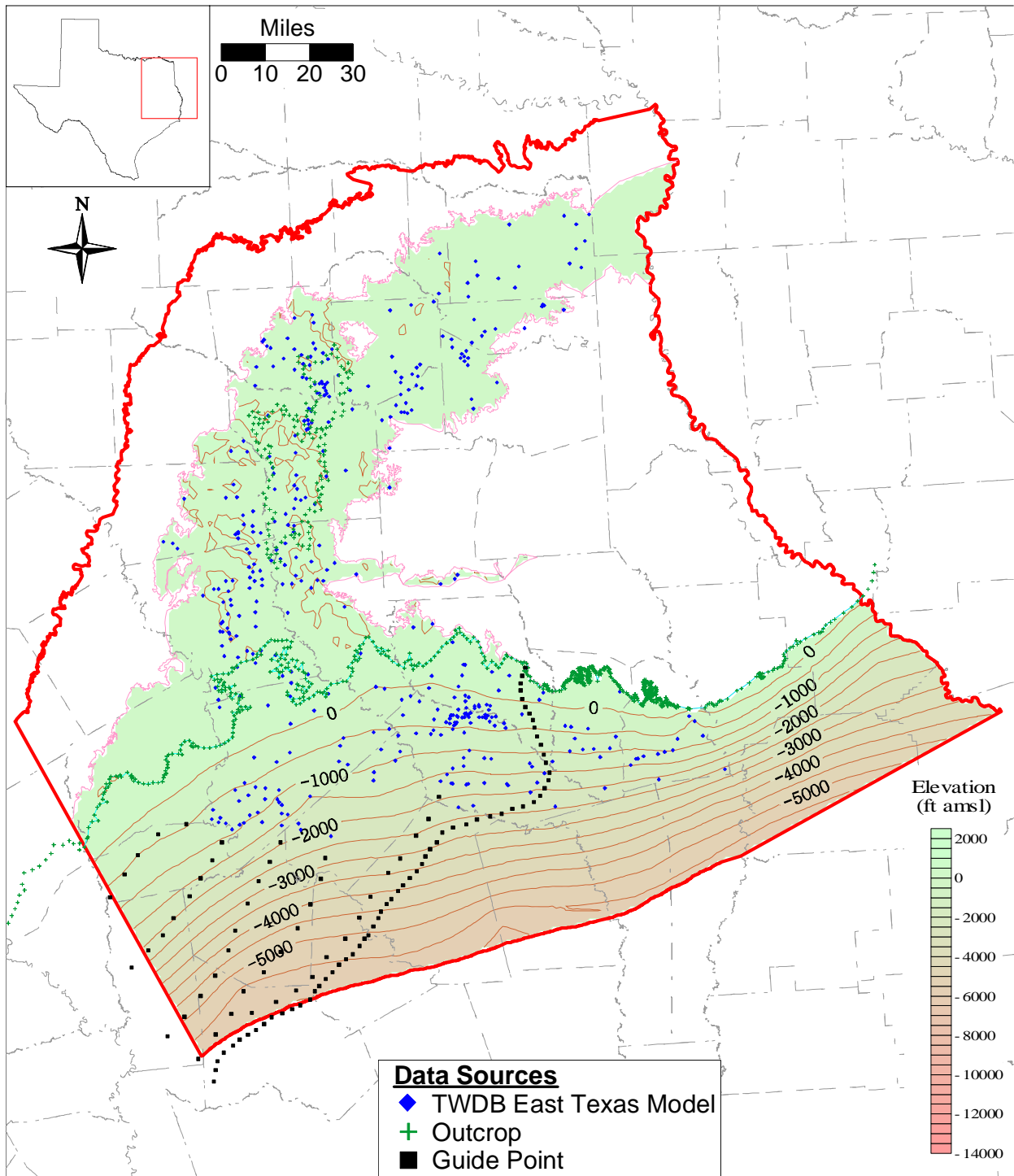


Figure 4.2.8 Structure contour map of the top of the Queen City (CI = 500 ft).

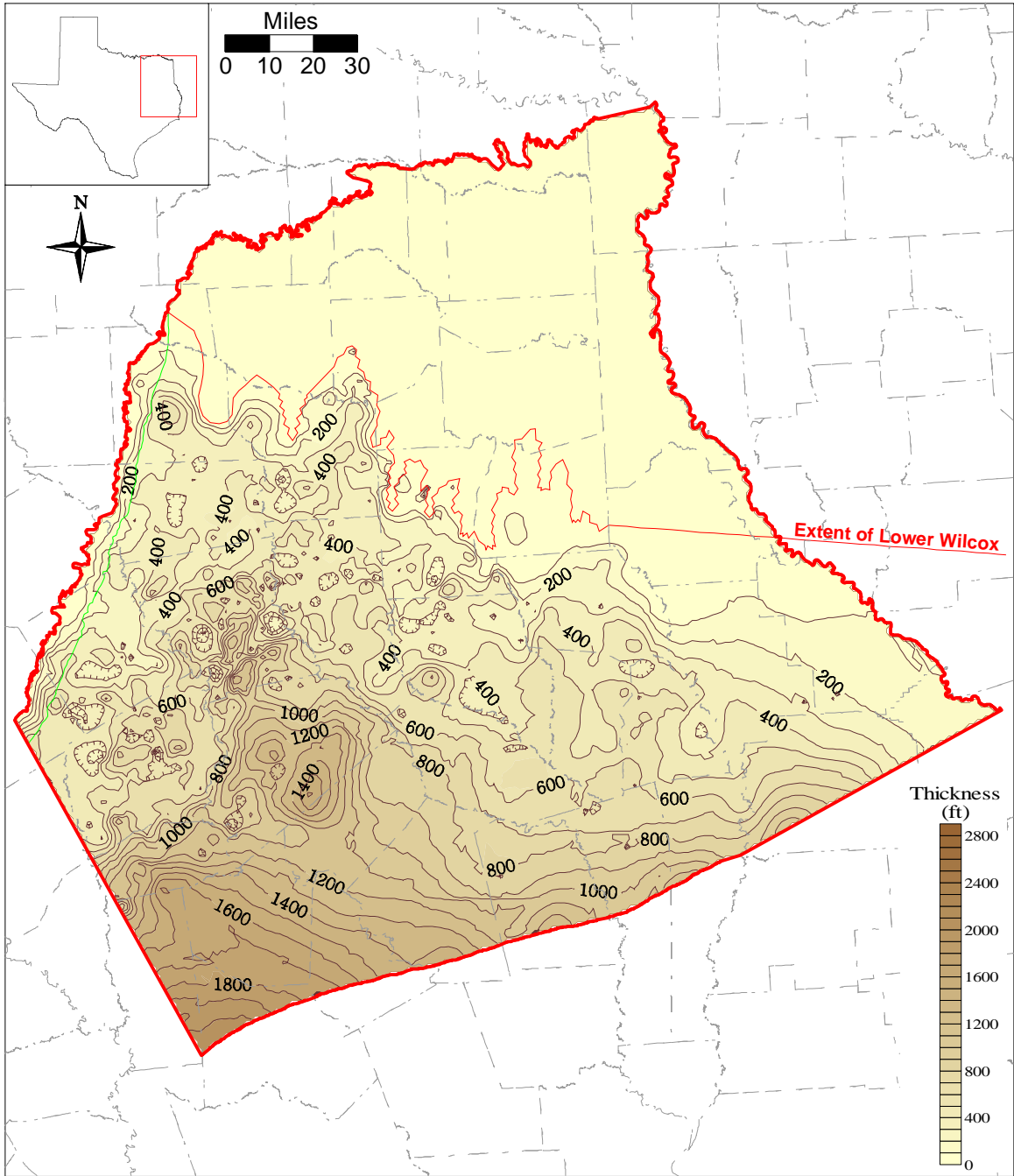


Figure 4.2.9 Thickness map of the lower Wilcox (CI = 100 ft).

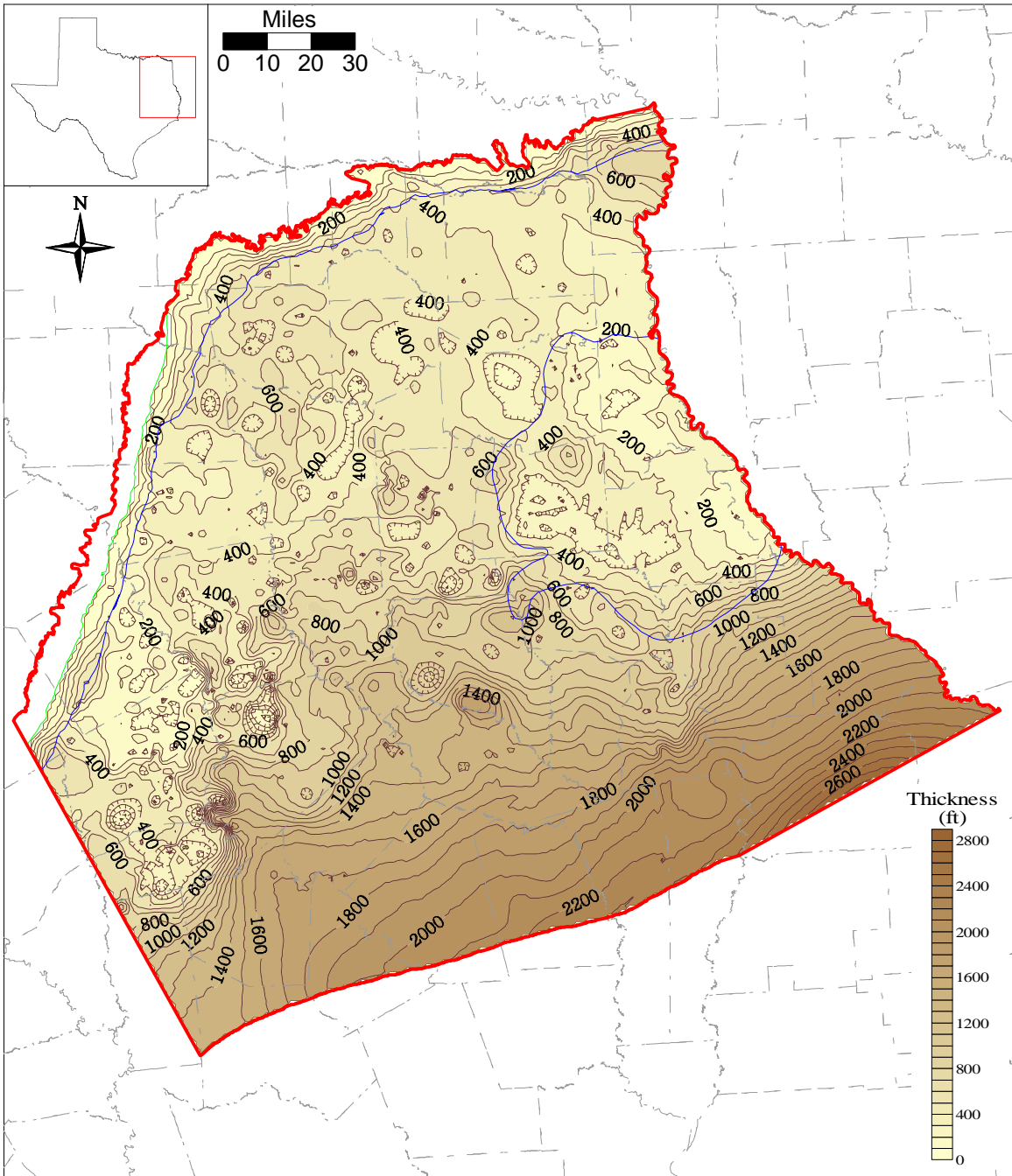


Figure 4.2.10 Thickness map of the middle Wilcox (CI = 100 ft).

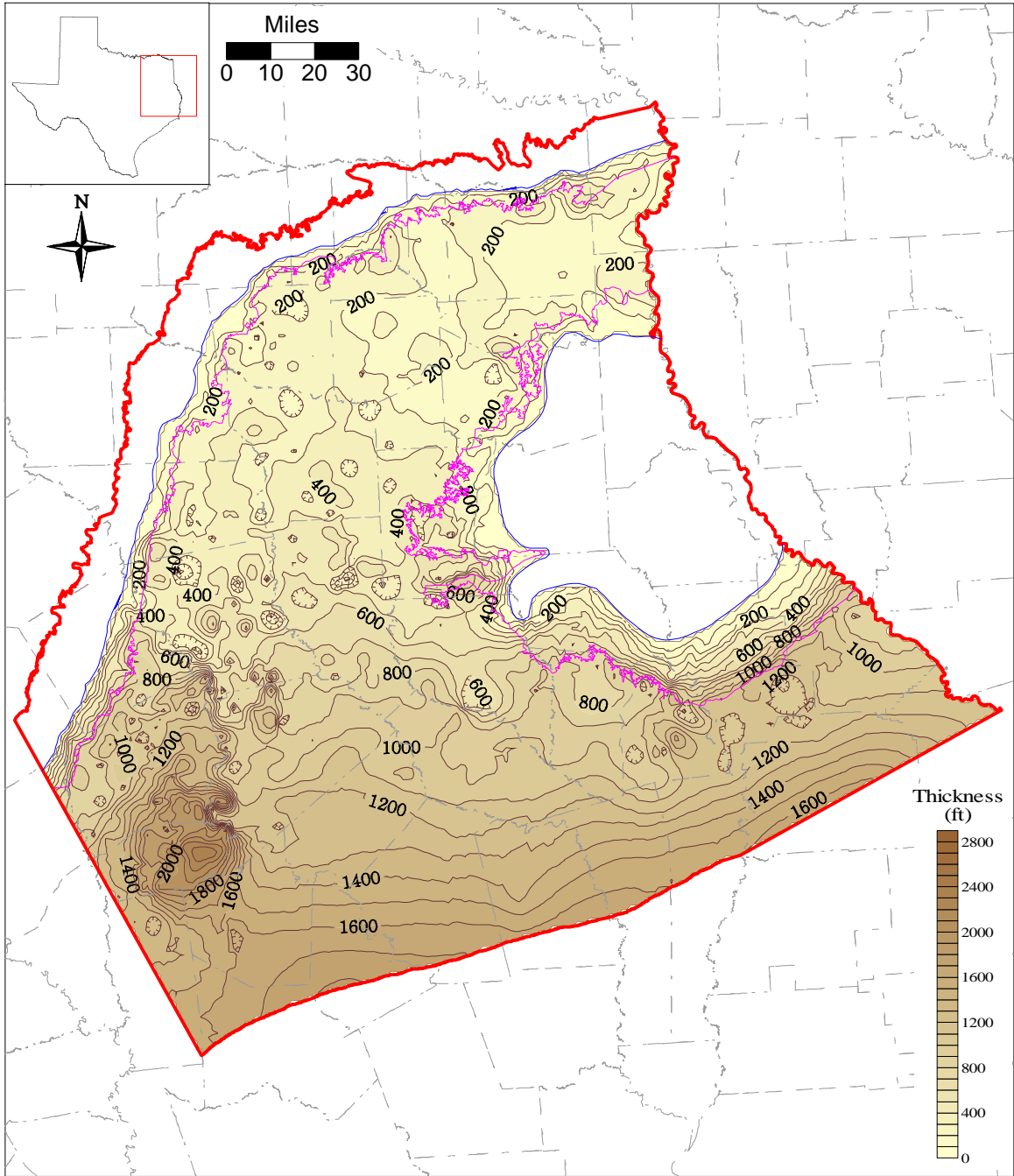


Figure 4.2.11 Thickness map of the upper Wilcox (CI = 100 ft).

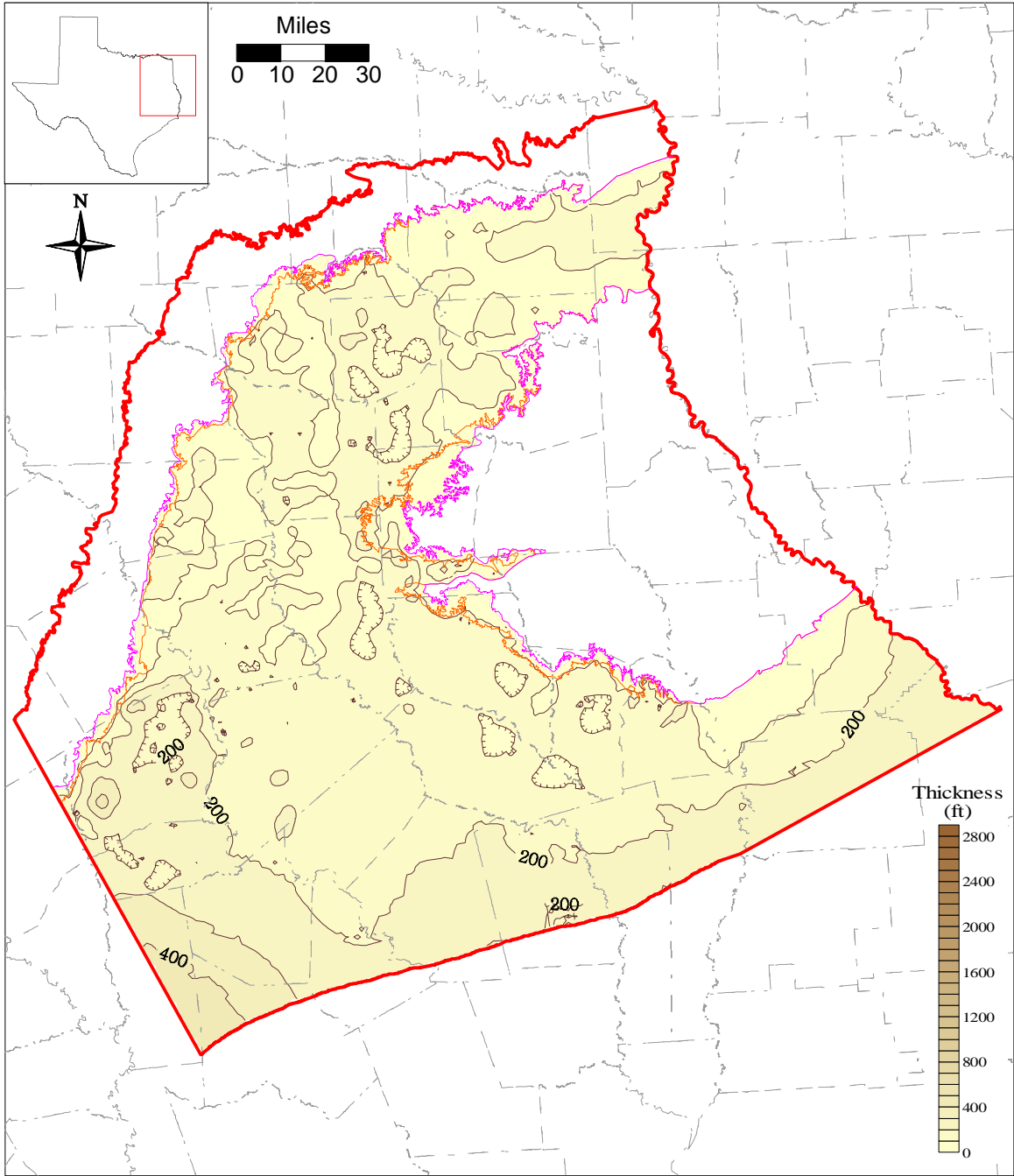


Figure 4.2.12 Thickness map of the Carrizo (CI = 100 ft).

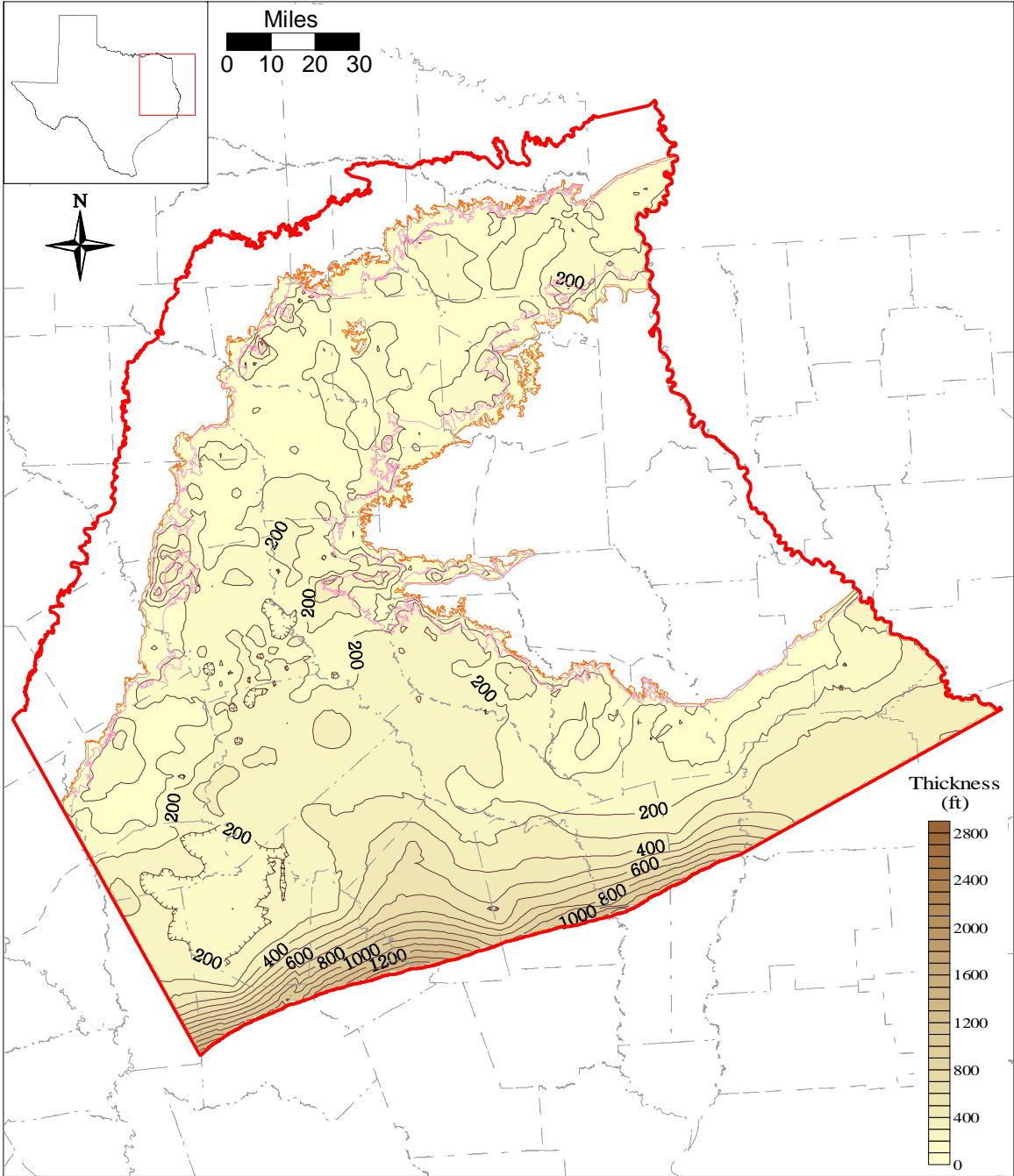


Figure 4.2.13 Thickness map of the Reklaw (CI = 100 ft).

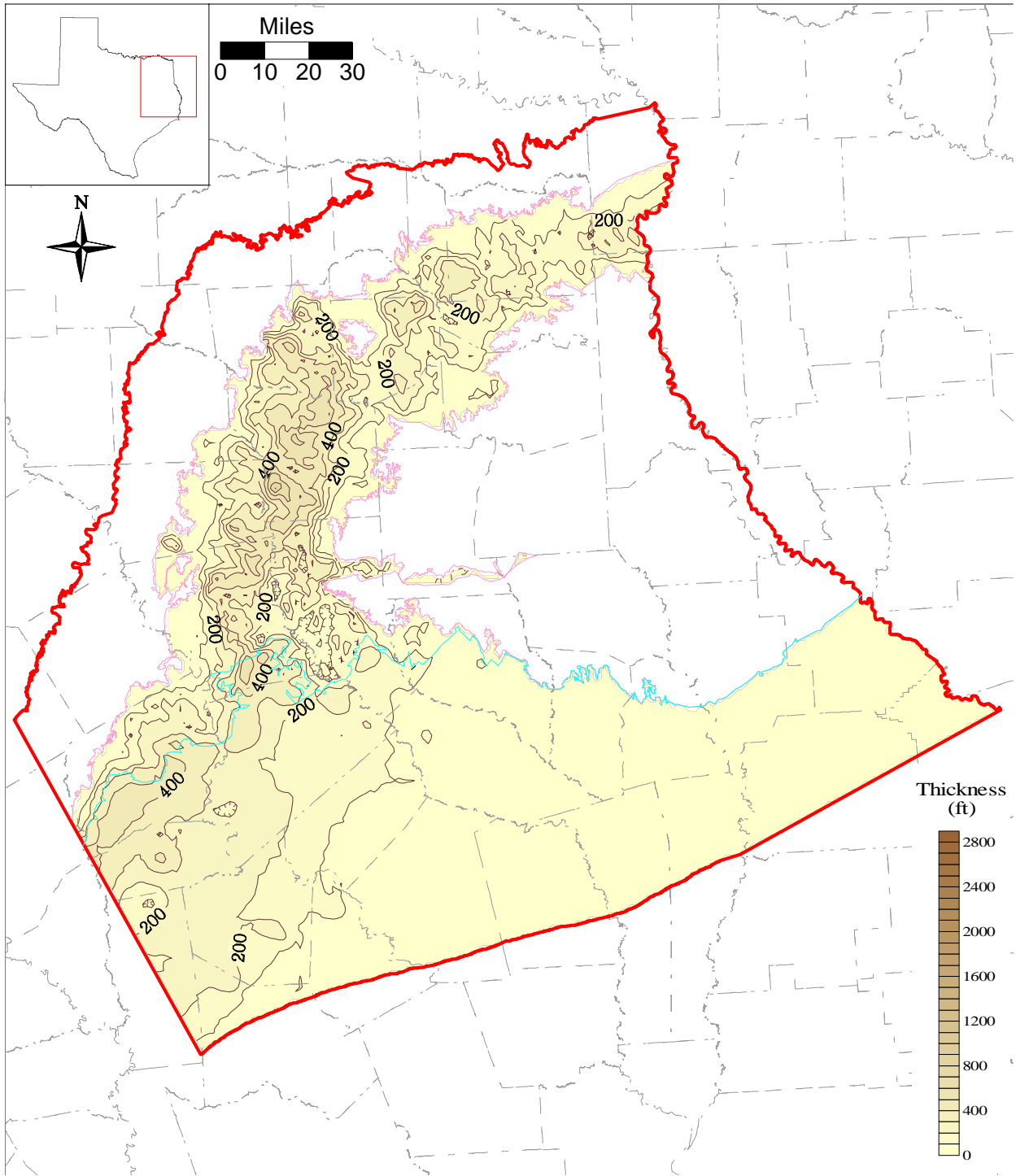


Figure 4.2.14 Thickness map of the Queen City (CI = 100 ft).

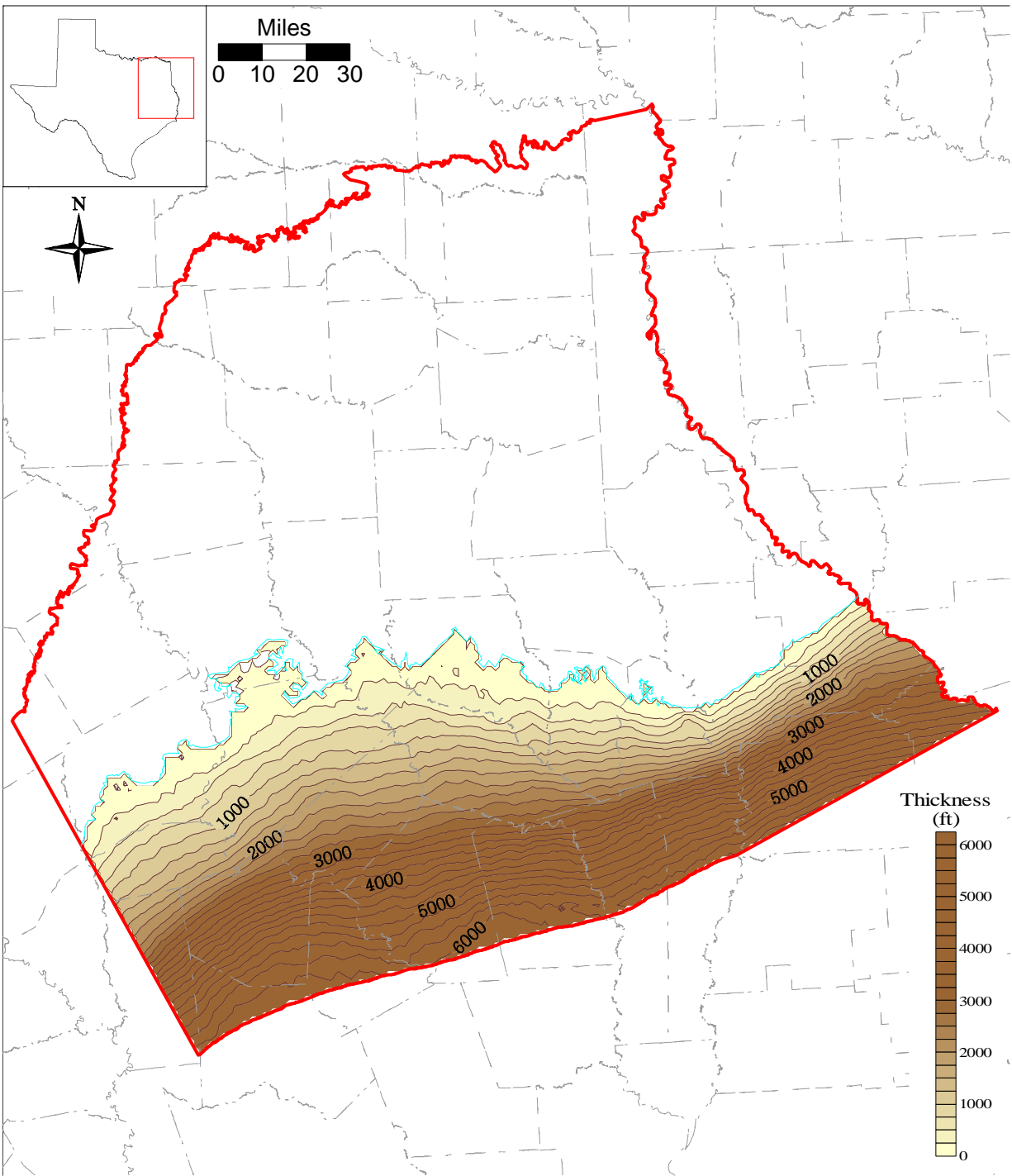


Figure 4.2.15 Thickness map of formations above the Queen City (CI = 250 ft).

4.3 Hydraulic Properties

Information on hydraulic properties of the Carrizo-Wilcox aquifer is based largely on data and sources provided by Mace et al. (2000a). They compiled and statistically analyzed transmissivity, hydraulic conductivity, and storativity data from numerous sources for the entire Carrizo-Wilcox aquifer in Texas. They also analyzed spatial distributions in hydraulic properties in the Carrizo Sands and in the Wilcox Group, suggesting regional trends in kriged transmissivities and hydraulic conductivities. The uneven data coverage and relatively large local-scale variability, expressed in a high nugget in the semivariograms (Mace et al., 2000a), indicate significant uncertainty in the effective hydraulic properties of the aquifer systems. A relationship between hydraulic properties and sand thickness (using sand maps from Bebout et al., 1982) could not be established, even though more detailed local studies did indicate some correlations between different sand facies and hydraulic conductivities (e.g., Payne, 1975; Henry et al., 1980; Fogg, 1986; Thorkildsen and Price, 1991).

The Carrizo aquifer generally consists of fairly homogeneous fluvial sands overlying the multi-aquifer system of the Wilcox Group that is composed of fluvial and deltaic sands distributed among lower permeability interchannel sands and muds. To properly simulate groundwater flow in such a complex depositional environment requires accurate description of both the subsurface arrangement of the various lithofacies (i.e., sand body distributions) and associated hydraulic properties. As pointed out by Fogg (1986), sensitivity of hydraulic head to heterogeneity or interconnectedness of sands in such a complex 3-D aquifer system is relatively low. This results in potential non-unique solutions in model calibrations and concomitant inaccurate representation of simulated groundwater flow patterns. Moreover, hydraulic properties have to be representative for the hydrostratigraphic unit that is implemented as a model layer in the numerical model. That is, both the horizontal and vertical distribution of property measurements is important, which requires information on well locations and screen depths and/or well depths.

The evaluation of the hydraulic property data was done in several steps. Initially, the database from Mace et al. (2000a) was processed in terms of data location relative to the GAM region and to the hydrostratigraphic units. Next, a statistical analysis of the data was performed evaluating potential variations of different data sources and for different aquifer designations. A

geostatistical analysis was then performed characterizing spatial variations of the hydraulic properties. Finally, potential trends in hydraulic properties compared to the depositional trends or sand-body distributions were examined.

4.3.1 Processing of the Hydraulic Property Database

For the Northern Carrizo-Wilcox GAM, the original database from Mace et al. (2000a) was imported into an MS Access Database (file: cw_97_xp.mdb). A new data table that contains a link between the BEG well number and the well location in GAM coordinates was added to the data base (the coordinate conversion from decimal degrees to GAM coordinates was completed in ArcView). A new table (Models) that identified the wells within the northern GAM region was added. This table was created in ArcView by intersecting the GAM outline with the point coverages of the wells. As recommended by Mace et al. (2000a), data from the Texas Railroad Commission (TRRC) and data from slug or bailing tests were excluded in this study, because of a bias toward lower values. Hydraulic conductivity values estimated from well logs were also excluded, as recommended by Mace et al. (2000a), because of a bias toward higher values.

Figure 4.3.1 shows a flow diagram for the screening of hydraulic conductivity data. After discarding the TRRC, well log, slug, and bailing test data, the remaining data were screened for the availability of a horizontal hydraulic conductivity measurement. Some data had a transmissivity measurement, but no estimate of effective thickness (e.g. screen length), and were discarded. If the top and bottom elevation of the well screen was recorded, these were compared to the model layer elevations. The hydraulic conductivity measurement was assigned to the layer that contained the largest fraction of the well screen. If the screen spanned more than three layers, the measurement was discarded. Those data without screen elevation information were checked for the presence of a layer-specific TWBD aquifer code. If this code was available, then the hydraulic conductivity measurement was assigned to that layer. Data marked only with general aquifer codes indicating multiple model layers (e.g. Wilcox Combined or Carrizo-Wilcox) were discarded.

4.3.2 Statistical Analysis of the Hydraulic Property Data

A summary of the statistical analysis of the hydraulic properties for the different hydrostratigraphic units is given in Table 4.3.1. The table summarizes the number of data measurements and the mean and median hydraulic conductivities. The hydraulic conductivities

are summarized by layer with cumulative distribution function (CDF) curves in Figure 4.3.2. These distributions appear to be log-normal. The hydraulic conductivities for the different layers range between 0.1 ft/day to about 800 ft/day.

Table 4.3.1 Summary statistics for horizontal hydraulic conductivity.

Layer	Unit	Count	Median Hydraulic Conductivity (ft/d)	Mean Hydraulic Conductivity (ft/d)
1	Queen City	98	4.1	8.1
2	Reklaw	140	3.9	17.6
3	Carrizo	324	4.8	13.4
4	Upper Wilcox	796	5.1	12.8
5	Middle Wilcox	1126	3.3	8.7
6	Lower Wilcox	332	3.5	7.5

Figure 4.3.2 and Table 4.3.1 indicate that the Reklaw Formation, which is considered the upper confining unit for the Carrizo-Wilcox aquifer, has relatively high horizontal hydraulic conductivity. The Reklaw Formation may contain extensive sand layers within the mud units and pumping is reported from the Reklaw. However, some of the wells that are designated as Reklaw wells by aquifer code or by the structure data are probably completed in the underlying Carrizo Formation or overlying Queen City Formation. Because the Reklaw Formation is relatively thin, small errors in the structure surfaces can result in misplacement of screened intervals. Therefore, the hydraulic conductivities for the Reklaw shown in Table 4.3.1 are not considered representative on a regional basis. For the Reklaw confining unit, the more important hydraulic property is the vertical hydraulic conductivity, which is largely controlled by the hydraulic conductivity of the more continuous muds and shales within the Reklaw.

4.3.3 Spatial Distribution of Hydraulic Property Data

The spatial distribution of hydraulic properties is characterized by variogram analysis to quantify spatial correlation and variability (for detailed background information on geostatistics refer to Isaaks and Srivastavs (1989)). The variogram describes the degree of spatial variability between observation points as a function of distance. Typical hydrogeologic properties show some spatial correlation indicated by low variance for nearby data points that increases with increasing distance to a point where the variance becomes constant which corresponds to the ensemble variance of the entire data set. The variogram quantifies the spatial variability in terms

of the correlation length and variance, and provides information on potential trends in the data. The variogram can also be used as a tool to characterize horizontal anisotropy in the hydraulic conductivity distribution since hydraulic conductivity is a function of direction in an aquifer with horizontal anisotropy. A directional-variogram analysis failed to detect any horizontal anisotropy in the hydraulic conductivity fields for the study area.

Figure 4.3.3 shows a variogram of hydraulic conductivities for the Carrizo Sand in the study area. The variogram indicates a steep increase in variance which levels off for distances greater than about 75,000 ft. A function was fitted to the variogram data (experimental variogram), which shows an intercept of 0.12 at zero distance. The corresponding variance of the intercept is referred to as the “nugget”, indicating the local-scale variability of hydraulic conductivity. The nugget amounts to about half of the total variance of 0.3 of the ensemble data, represented by the “sill”, suggesting potentially large variability of hydraulic conductivity in nearby well locations.

The spatial distribution of the property data is then produced by kriging, which uses the variogram information to estimate property values over the area of interest based on the limited number of data points available. Kriging results in some smoothing of the data by taking a weighted average of nearby measurement points.

The kriged hydraulic conductivity distribution for the Carrizo Sand and corresponding variogram are shown in Figure 4.3.4. The variogram indicates relatively large local-scale variability, even though the Carrizo is considered a relatively homogeneous sand. As indicated on the kriged map of hydraulic conductivity, most of the data are in the northern half of the model areas and have a relatively even distribution. In the deeper section south of the East-Texas Embayment, there is little or no data. Also, south of the Sabine Uplift there are very few data points. The hydraulic conductivities range from less than 1 ft/day to about 30 ft/day with distinct local areas of high conductivities in Anderson, Angelina, Nacogdoches, Rusk, Van Zandt and Henderson counties.

The variogram for hydraulic conductivities of the upper Wilcox shows a correlation length of about 100,000 ft and a significantly higher nugget of about 0.19 compared to a sill of about 0.36 (Figure 4.3.5). Even though the correlation length is greater than that of the Carrizo, the variance is greater suggesting greater heterogeneity. As mentioned in Section 2, the Wilcox

consists of fluvial and fluvial-deltaic sands embedded in muds with an average of 50% sand. The kriged hydraulic conductivities show a relatively even data distribution in the outcrop and updip confined section of the East-Texas Embayment (Figure 4.3.5). Hydraulic conductivities are more uniform ranging between less than 1 ft/day and 10 ft/day.

The middle Wilcox indicates a variogram with a significantly greater correlation length of about 300,000 ft than those in the upper Wilcox and Carrizo (Figure 4.3.6). However, the nugget is relatively high (0.18) compared to the sill (0.3) indicating large local-scale variability. The higher correlation length for the middle Wilcox compared to the upper Wilcox may be associated with predominantly fluvial deposits corresponding to the Simsboro sands in east-central Texas, which are characterized by blocky sands in subsurface geophysical logs (Kaiser, 1990). The kriged map shows a more uneven data distribution focused to the outcrop and shallow confined section within the East-Texas Embayment (Figure 4.3.6). Again, there were no data available for the deeper confined section in the southern part of the area.

The lower Wilcox variogram indicates no spatial correlation with large variability of the variance as a function of distance Figure (4.3.7). The kriged map shows data coverage only in the western part along the outcrop and shallow confined section and few data point in the Sabine Uplift.

Spatial distribution of hydraulic conductivity for the Reklaw confining unit was not explicitly analyzed, because of limited data and uncertainty in the appropriate assignment of the data points to the Reklaw or adjacent aquifer units. A preliminary evaluation of the hydraulic property data for the Queen City aquifer was performed, indicating relatively small correlation length, lower nugget (0.05), and lower sill (0.2) compared to the Carrizo-Wilcox (Figure 4.3.8). The kriged map shows limited data distribution in the northern half of the area and very few data along the southwestern part of the area. For this particular map, the contours were limited to within a certain radius from the nearest observation point. Again, data from the southern part were not available.

In general, the kriged maps of hydraulic conductivities indicate significant variations in hydraulic conductivities. These values represent horizontal permeabilities of sands within the different hydrostratigraphic units, because most wells tend to be completed and tested in sand intervals. In the Carrizo aquifer, which consists typically of 80 to 100% sand the spatial pattern

reflects variability within the sand. The kriged map was extended to the southern model boundary by including false data points to produce a decrease in hydraulic conductivity with depth toward the southern boundary. Such a decrease in hydraulic conductivity with depth is typical in large regional groundwater systems. For the Wilcox, kriging was allowed to extrapolate the contours from data points updip to toward the southern model boundary, indicating a relatively large part of the area that is not constrained by data. Incorporating the hydraulic property information into the numerical model requires an approach that assigns properties where no data are available and produces property values that are representative over the entire layer thickness. This is of particular importance, where the aquifer units consist of significant amounts of muds. In the following section, geologic information is examined for complementing the limited data on hydraulic properties.

4.3.4 Relationship between Hydraulic Property and Sand Distribution

The distribution of sand and muds not only affects the transmissivity of the aquifer but also the groundwater flow. Groundwater tends to flow into more transmissive zones, that consist of well connected sands of relatively high hydraulic conductivity. The hydraulic conductivity data presented in Section 4.3.3 were based on hydraulic tests performed at specific depth intervals which generally do not cover the entire thickness of the aquifer layer. The data are also representative of the sand encountered in the interval rather than an average value over the entire screened section. The kriged hydraulic conductivity maps assume that the sands tested in adjacent wells at different depth intervals are laterally and vertically connected. This is most likely valid for the Carrizo, which is dominantly sand. For the Wilcox Group, which consist of only 50% sand on the average, sand bodies are embedded in a fine grained matrix and may not always be connected. The Wilcox Group is up to 3000 ft thick, allowing for complex vertical stacking of sands within each of the layers. Depositional information has been used to quantify sand-body distribution, indicating that in fluvial systems, sand bodies can be considered connected over a large scale, if sand percent is more than 50 % or even lower (Fogg, 1989).

Sand thicknesses and sand-body distribution are not only important to define the overall transmissivity of the aquifer but can indicate zones of higher permeability. Intuitively, one would expect that sands in the major fluvial channels have generally higher hydraulic conductivities than thinner, more isolated sands. Spatial information on sand distributions could then be used to extrapolate the kriged permeability maps to areas where no hydraulic

conductivity data are available. Mace et al. (2000a) examined generalized net sand maps for upper and lower Wilcox by Bebout et al. (1982) and the corresponding transmissivity values covering the Wilcox Group throughout Texas, but did not find a correlation between sand thickness and transmissivity. However, more local studies did show a relationship between sand thickness or specific channel sands and hydraulic conductivities (Payne, 1975; Fogg, 1986).

For the study area, we examined both the net sand thickness of the entire Wilcox (Kaiser et al., 1978) and maximum sands of the upper Wilcox (Kaiser, 1990) for comparison with hydraulic conductivity values. Maximum sand maps are considered more indicative of the major channel sand, ignoring thinner and less continuous splay and overbank sands. However, the maximum sand maps show only a limited thickness range. Histograms of hydraulic conductivities (log-K) by maximum sand thickness and net-sand thickness (Figure 4.3.9), indicated no clear relationship. The net-sand histograms indicate generally higher median log-K values for thicker sands, but the relationship is not systematic over the different sand thickness intervals. The maximum sand histograms do not indicate a clear trend; in this case, there were only three contour levels. There are certain limitations in the analysis. The sand thickness maps are manually contoured taking into account the depositional model. Furthermore, the hydraulic conductivity data points were assigned to the nearest sand thickness contour.

For this study, the net-sand map was primarily used to estimate the transmissivity of the model layer. The sand maps were not used to extrapolate hydraulic conductivity data into areas where specific data points were not available. However, the sand maps were considered valuable information during model calibration in terms of justifying local modification in hydraulic conductivity values.

As mentioned in section 2.2, the net-sand map from Kaiser et al. (1978) did not cover the entire model area, but agreed reasonably well with the earlier map construction by Fisher and McGowen (1967) for the entire Wilcox Group in Texas. The more detailed map from Kaiser et al. (1978) was combined with the more regional-scale map to construct a net-sand map covering the entire model area. The resulting sand-percent map is shown in Figure 4.3.10.

4.3.5 Vertical Hydraulic Conductivity

Specific data on vertical hydraulic conductivity within the Carrizo-Wilcox aquifer and for the Reklaw confining layer are not available at the scale of this study. Previous modeling studies

of the Carrizo-Wilcox aquifer derived estimates of vertical permeability from model calibration. Stochastic modeling studies of a generic aquifer system consisting of two contrasting hydraulic conductivity facies (channel sands and finer grained interchannel sediments) having various degrees of vertical interconnection indicate effective vertical conductivities ranging between the geometric and harmonic mean conductivities (Fogg, 1989).

A lower bound estimate of vertical conductivity can be calculated as the lowest vertical conductivity value measured in a hydrostratigraphic section, assuming complete lateral continuity of the low-permeability zone. Measurements of hydraulic conductivity typically focus on high-permeability zones with a few core data available for low-permeability muds within the Wilcox Group (Bob Harden, personal communication). In the Region G model developed by Harden and Associates (2000), core estimates of clay hydraulic conductivity were used to represent clay strata within the Carrizo-Wilcox aquifer ($K = 5.35 \times 10^{-6}$ ft/day). The effective vertical conductivity for the different aquifer layers were estimated based on a harmonic mean of the individual proportions of sand, silt, and clay (Harden and Associates, 2000).

Fogg et al. (1983) inferred a maximum reasonable horizontal to vertical permeability ratio K_h/K_v (anisotropy ratio) on the order of 10,000 to 1,000 to reproduce the vertical head gradients within the Carrizo-Wilcox aquifer in a groundwater flow model near the Oakwood salt dome in Freestone and Leon counties. A vertical to horizontal anisotropy ratio of 1,000,000 was considered too low to reproduce the general pressure-depth gradients across the model.

Vertical permeability of the Reklaw confining layer can be considered to be less than that of the Wilcox aquifer, because of more continuous mud units. However, toward the northeast the Reklaw contains more sand layers within the muds, which could increase the effective vertical permeability. Fogg et al. (1983) used a vertical hydraulic conductivity of 2.6×10^{-4} ft/day for the Reklaw in their model, which they considered a maximum value corresponding to that used for the Wilcox. The USGS RASA model for the Texas Gulf Coast aquifer systems reported a vertical hydraulic conductivity of the lower Claiborne confining unit (equivalent to the Reklaw Formation) of 2×10^{-5} ft/day from their calibrated transient model (Ryder and Ardis, 1991), which is lower than the value 1×10^{-4} ft/day calibrated from the steady-state model (Ryder, 1988).

The Carrizo Formation is generally considered to have much lower anisotropy ratios than the Wilcox, because of typically much higher sand content. However, the measured hydraulic

conductivities for the Carrizo in this area range over three orders of magnitude (Figure 4.3.2), indicating the potential range in anisotropy. Previous modeling studies indicated anisotropy ratios (K_h/K_v) of 400 based on steady-state calibration (Ryder, 1988) and 11,500 based on transient model calibration (Ryder and Ardis, 1991).

4.3.6 Storativity

The specific storage of a confined saturated aquifer can be defined as the volume of water that a unit volume of aquifer releases from storage under a unit decline in hydraulic head (Freeze and Cherry, 1979). The storativity is equal to the product of specific storage and aquifer thickness and is dimensionless. For unconfined conditions, the storativity is referred to as the specific yield and is defined as the volume of water an unconfined aquifer releases from storage per unit surface area of aquifer per unit decline in water table (Freeze and Cherry, 1979).

Mace et al. (2000a) compiled 107 estimates of storativity and calculated 64 estimates of specific storage from tests of the Carrizo-Wilcox aquifer where the screen length was known. Storativity ranged in magnitude from 1.0×10^{-6} to 0.1 with a geometric mean equal to 3×10^{-4} . Specific storage ranged from about 1×10^{-7} to 1×10^{-4} 1/m with a geometric mean of 4.6×10^{-6} 1/m. The medians were essentially equal to the geometric mean for both distributions demonstrating the lognormal form of both distributions.

Specific yield estimates provided in Table 4.3.2 originate from aquifer tests and from model calibrated values. The range of specific yield is 0.05 to 0.32. Perhaps the most direct estimate of specific yield is from Duffin and Elder (1979). They performed 20 seismic refraction profiles in the Carrizo Sand outcrop in areas west of Gonzales County (located south of the study area).

Table 4.3.2 Summary of literature estimates of Carrizo-Wilcox specific yield.

Source	Specific Yield	Reference
TWDB Report 210	0.25 (average)	Klemt et al. (1976)
TDWR Report 229	0.16 to 0.32	Duffin and Elder (1979)
TWDB/LCRA model	0.05 to 0.3	Thorkildsen et al. (1989)
TWDB Report 332	0.1 to 0.3	Thorkildsen & Price (1991)
USGS OFR 91-64	0.15	Ryder & Ardis (1991)
BEG RI 256	0.29 (Simsboro)	Dutton (1999)
Region G Model	0.15	Harden & Assoc. (2000)

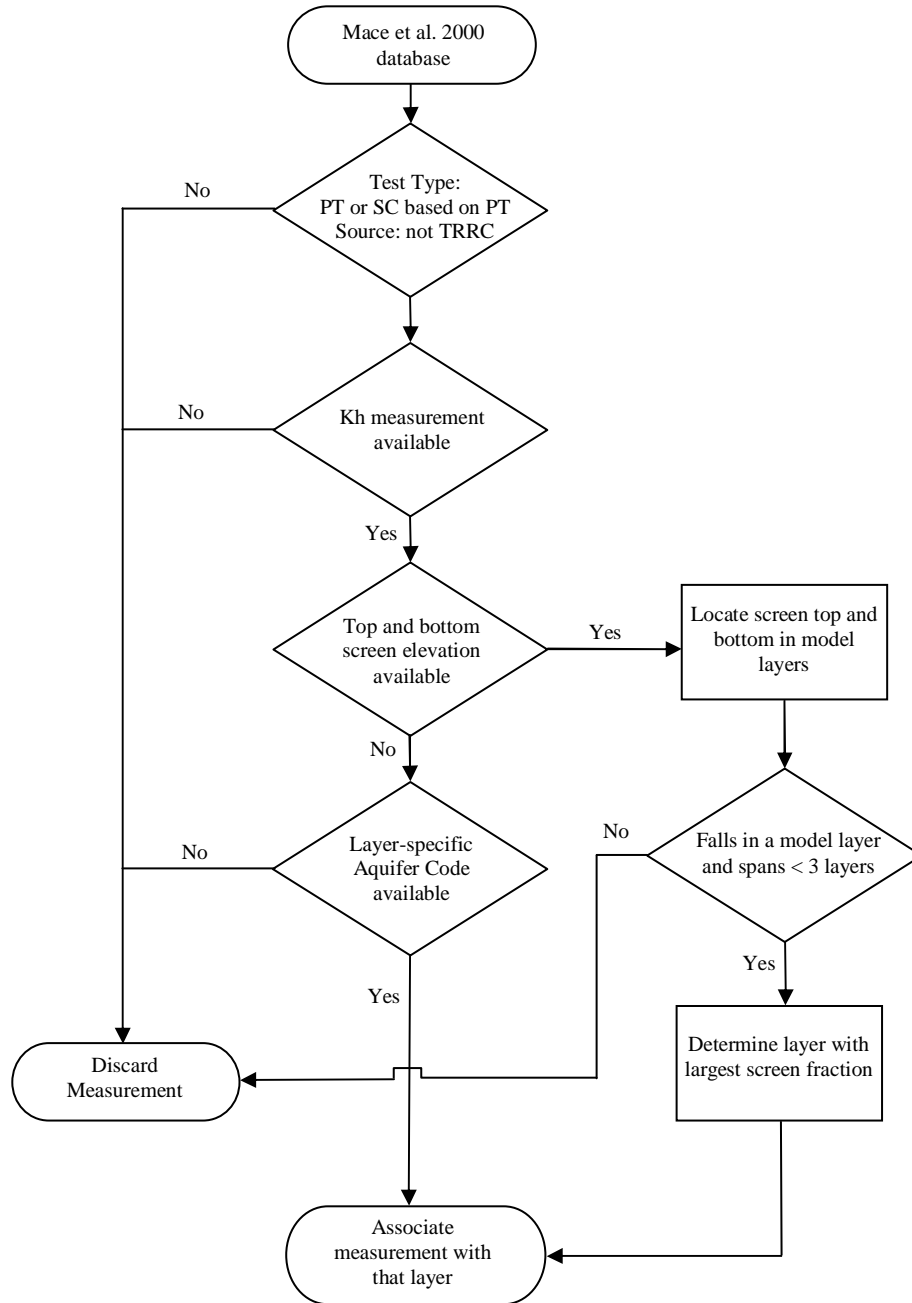


Figure 4.3.1 Screening of hydraulic conductivity data.

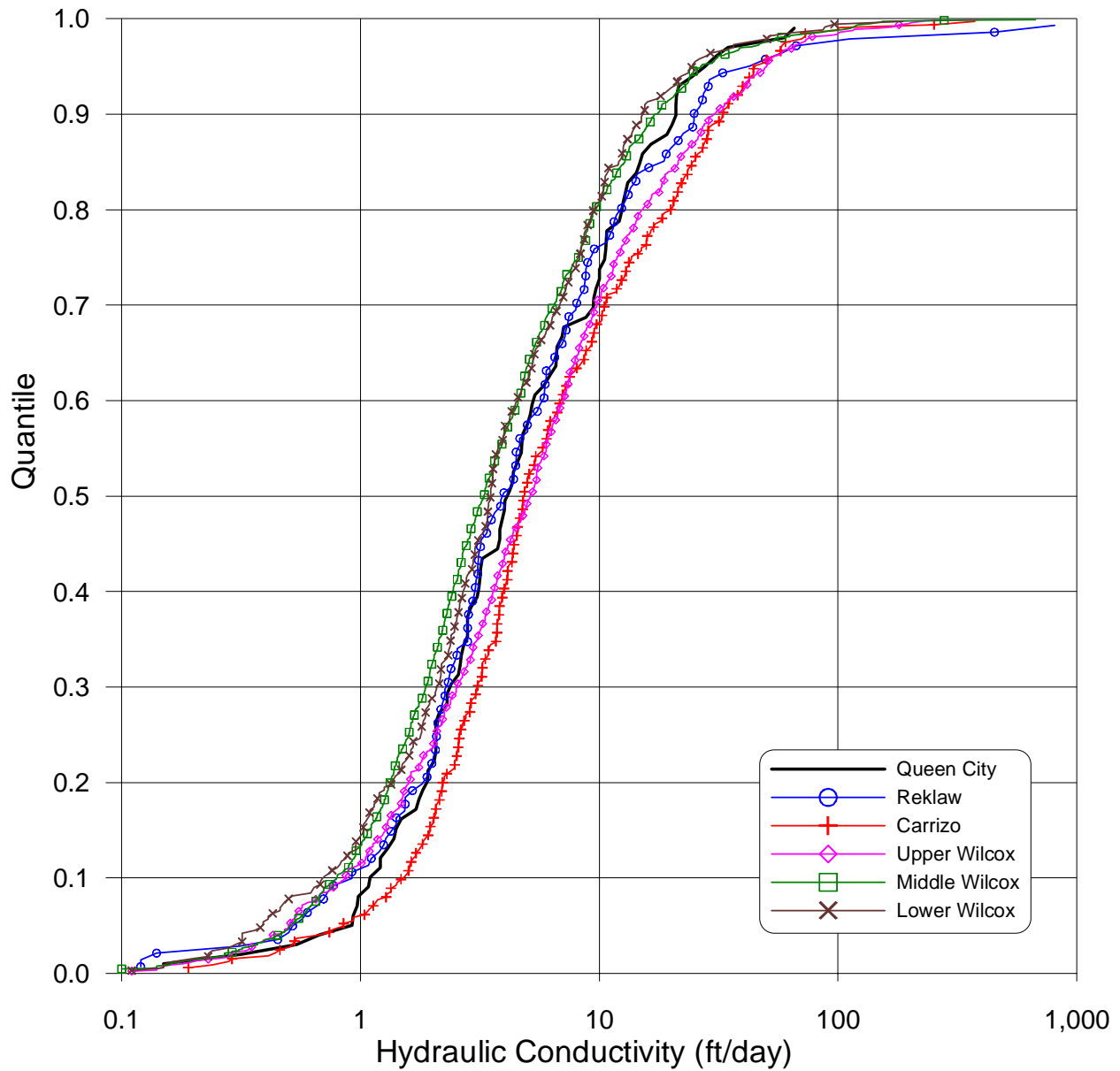


Figure 4.3.2 Cumulative distribution function (CDF) curves of hydraulic conductivity for the modeled aquifer units.

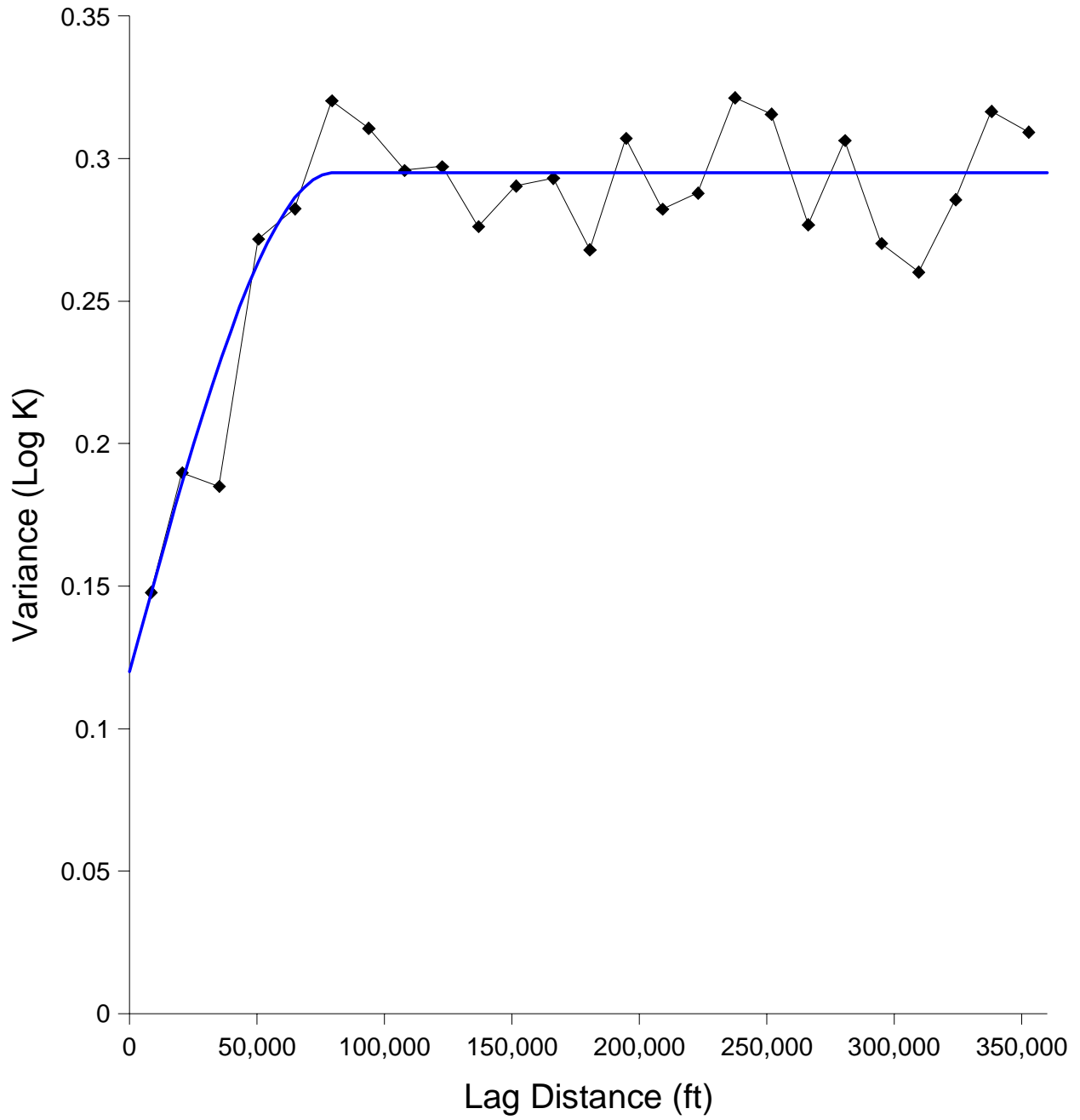


Figure 4.3.3 Variogram for hydraulic conductivity data from the Carrizo Sand.

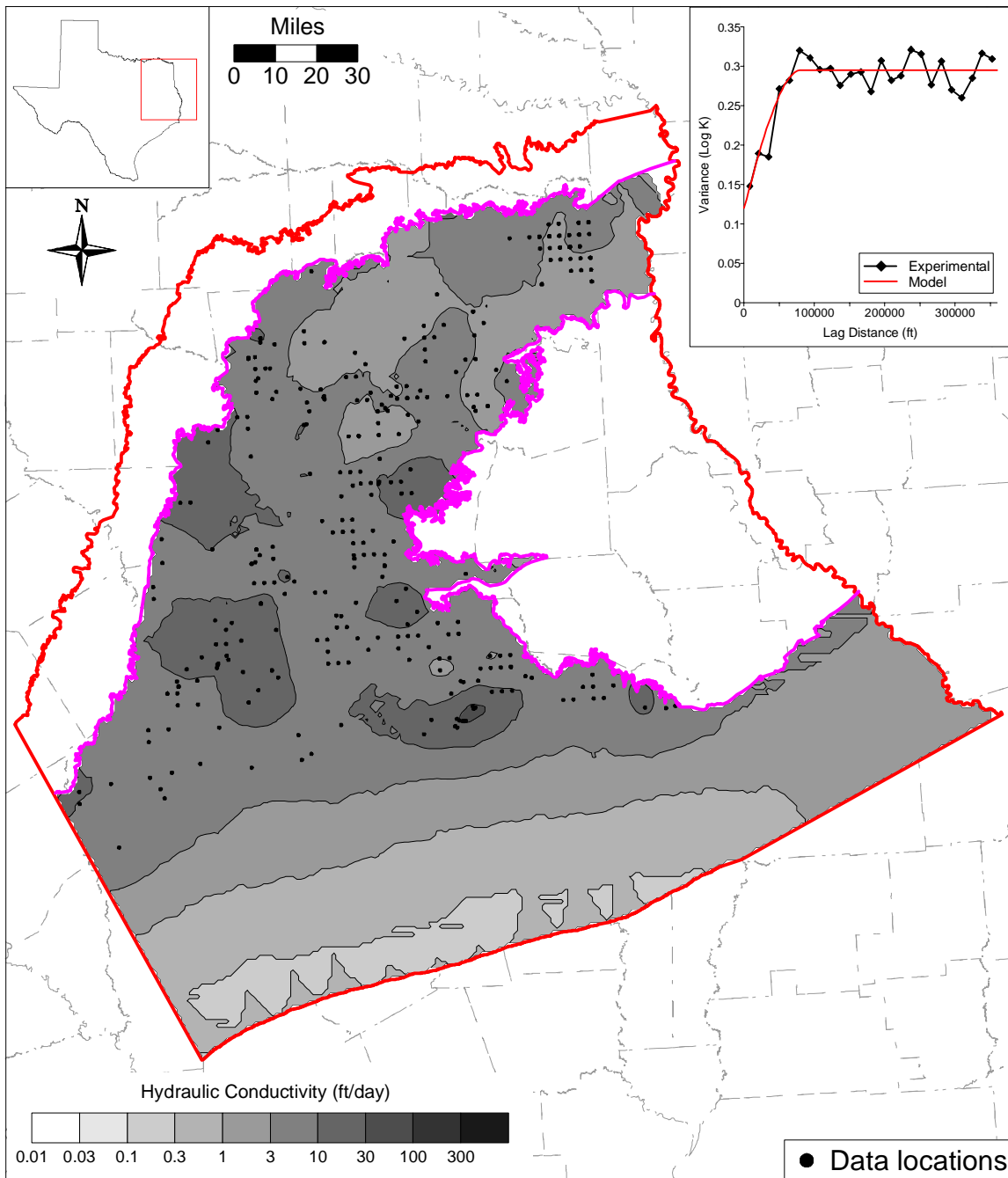


Figure 4.3.4 Variogram and kriged map of hydraulic conductivity for the Carrizo Sand.

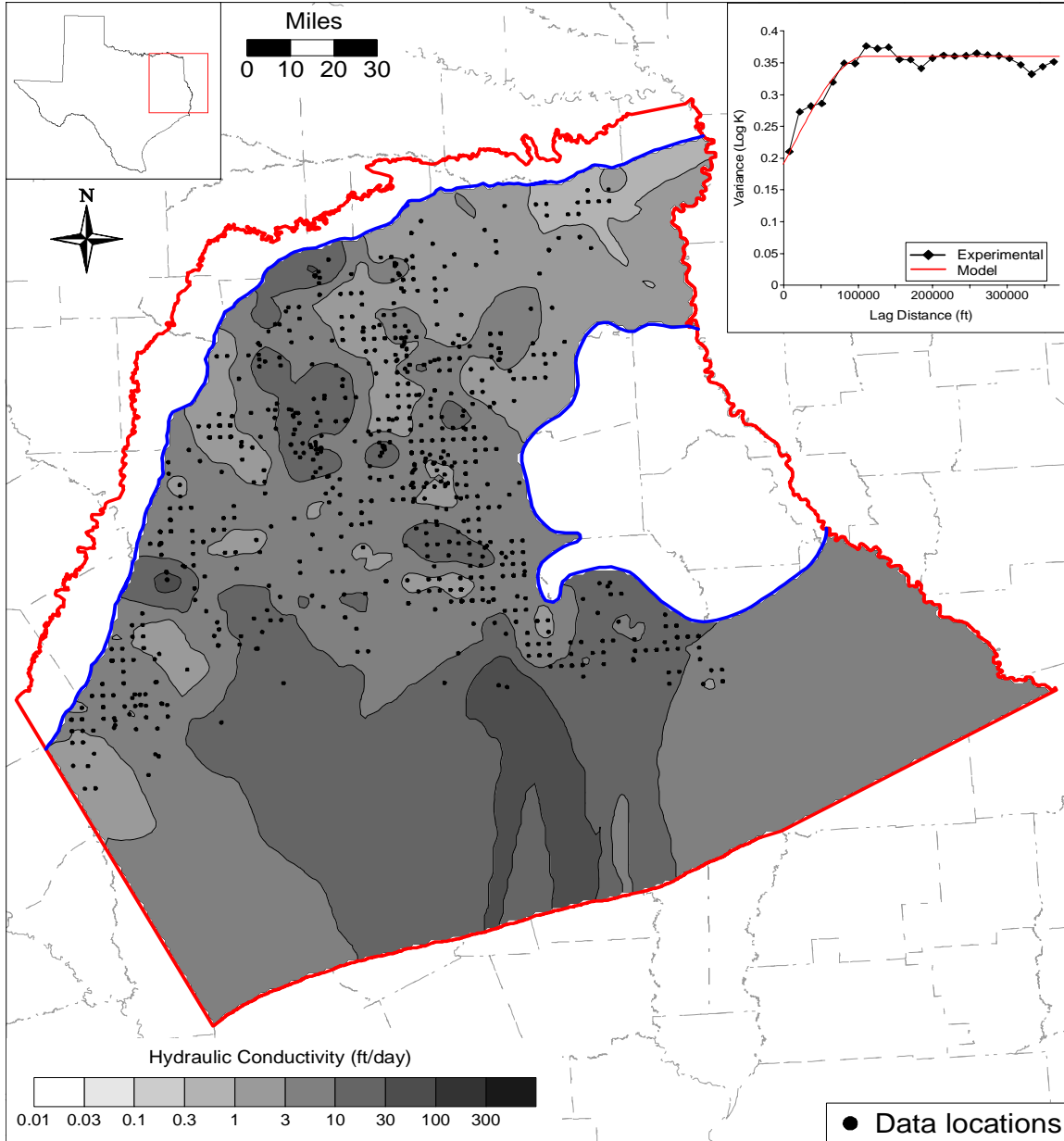


Figure 4.3.5 Variogram and kriged map of hydraulic conductivity for the upper Wilcox.

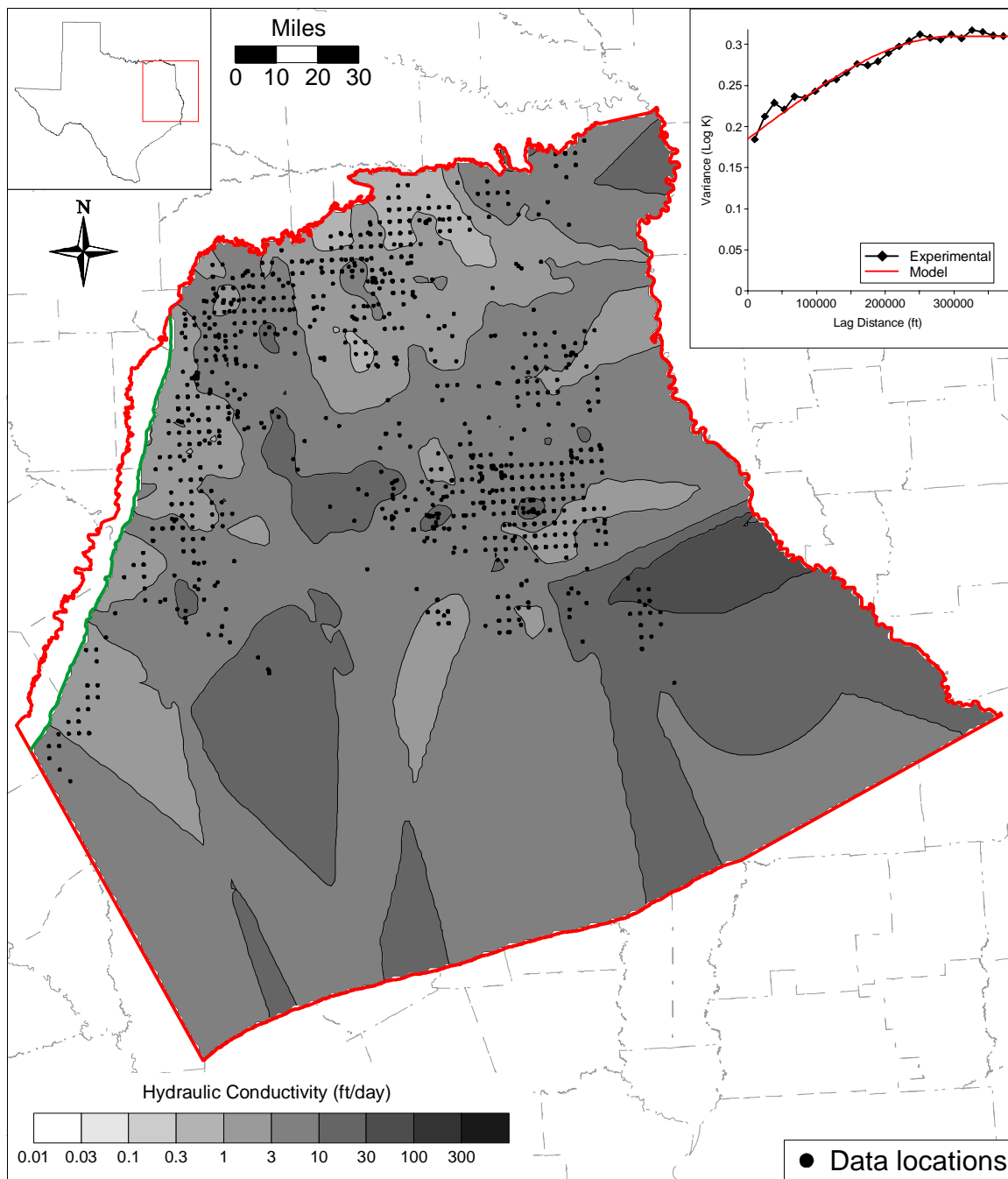


Figure 4.3.6 Variogram and kriged map of hydraulic conductivity for the middle Wilcox.

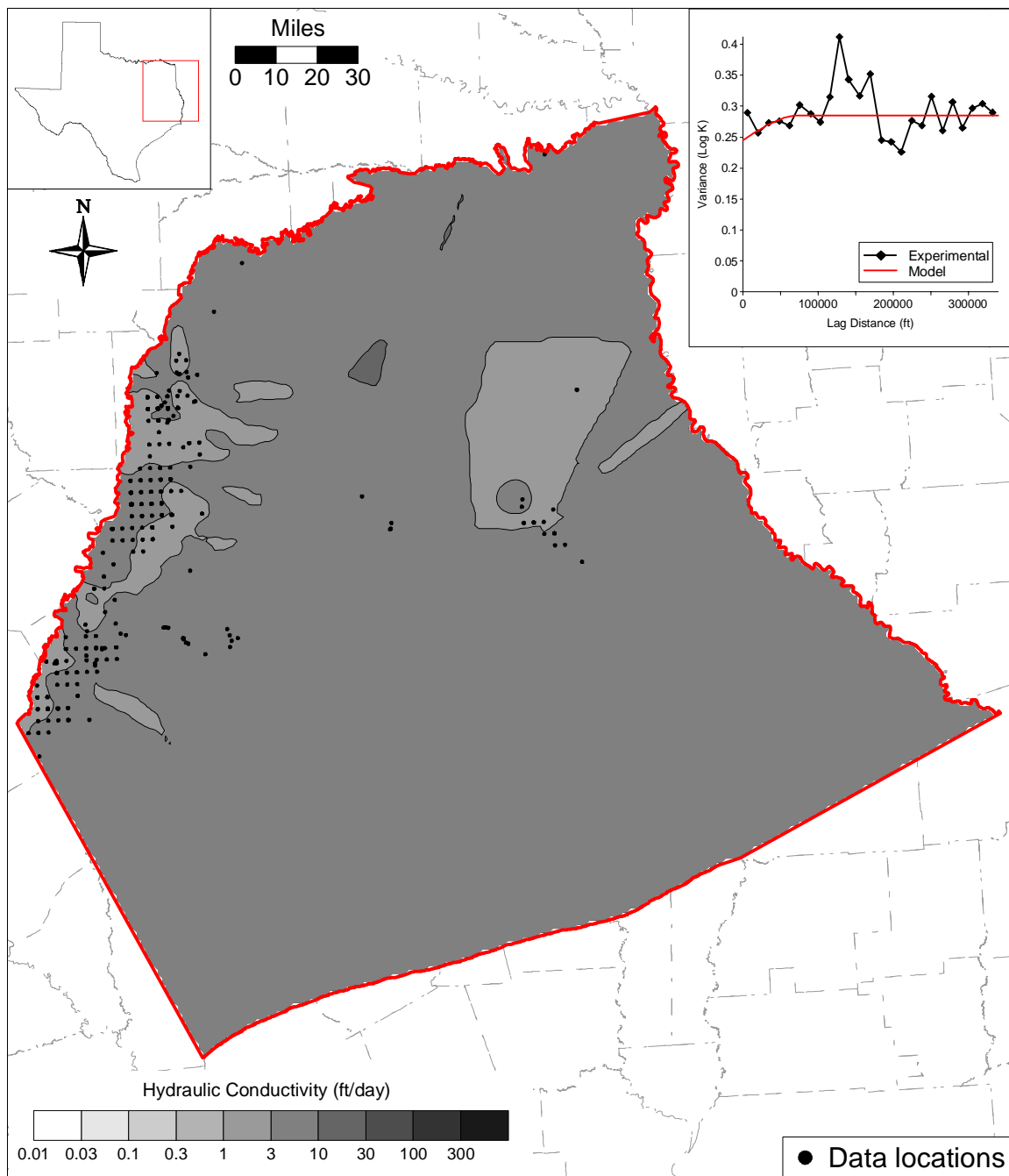


Figure 4.3.7 Variogram and kriged map of hydraulic conductivity for the lower Wilcox.

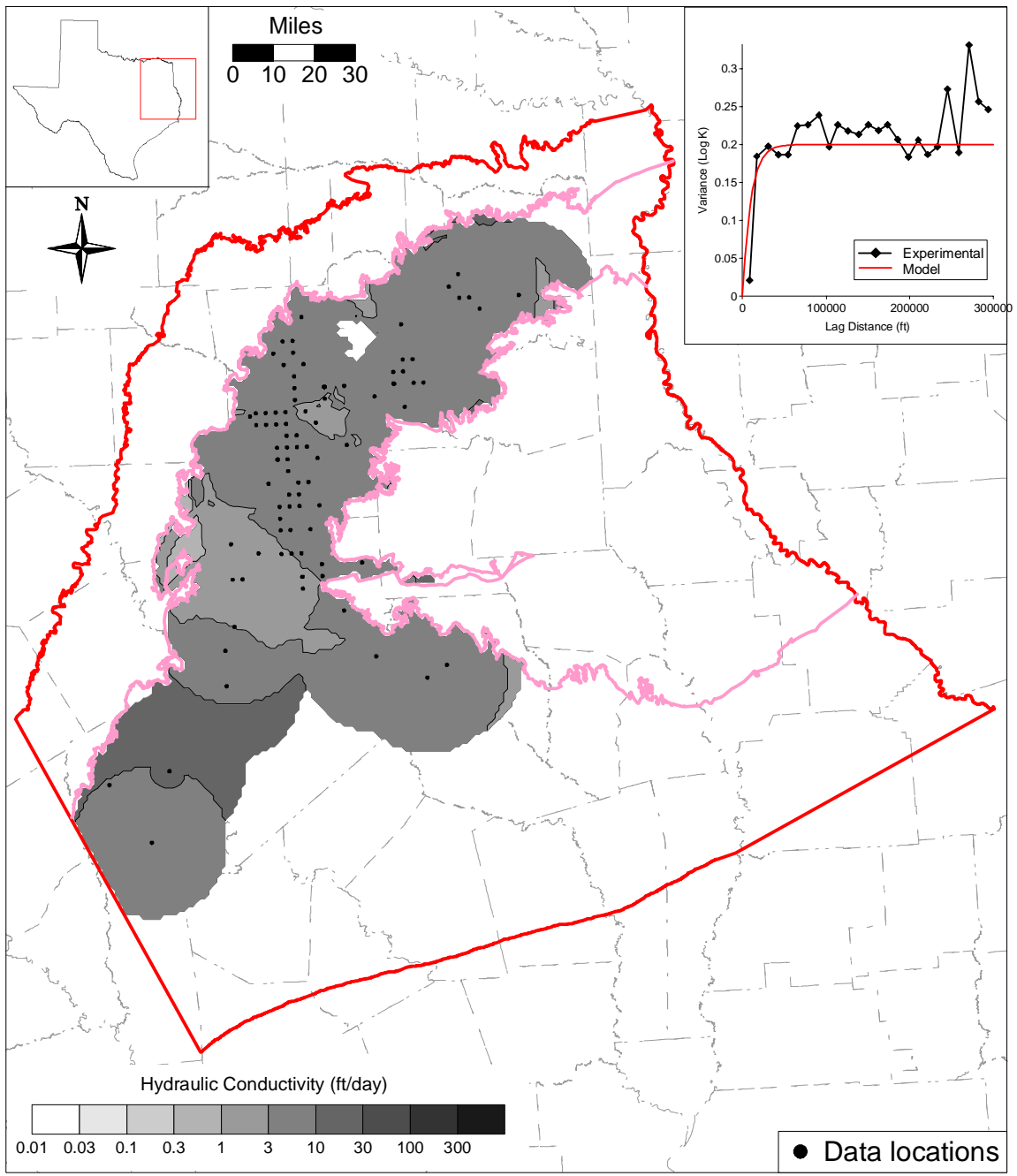
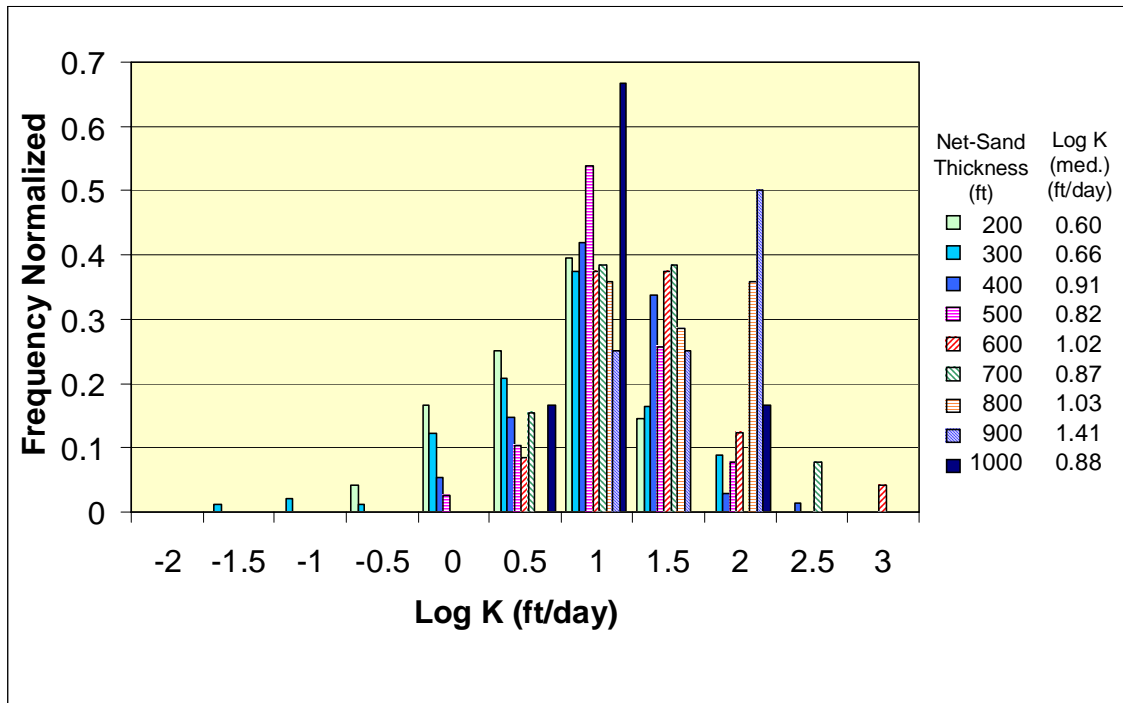
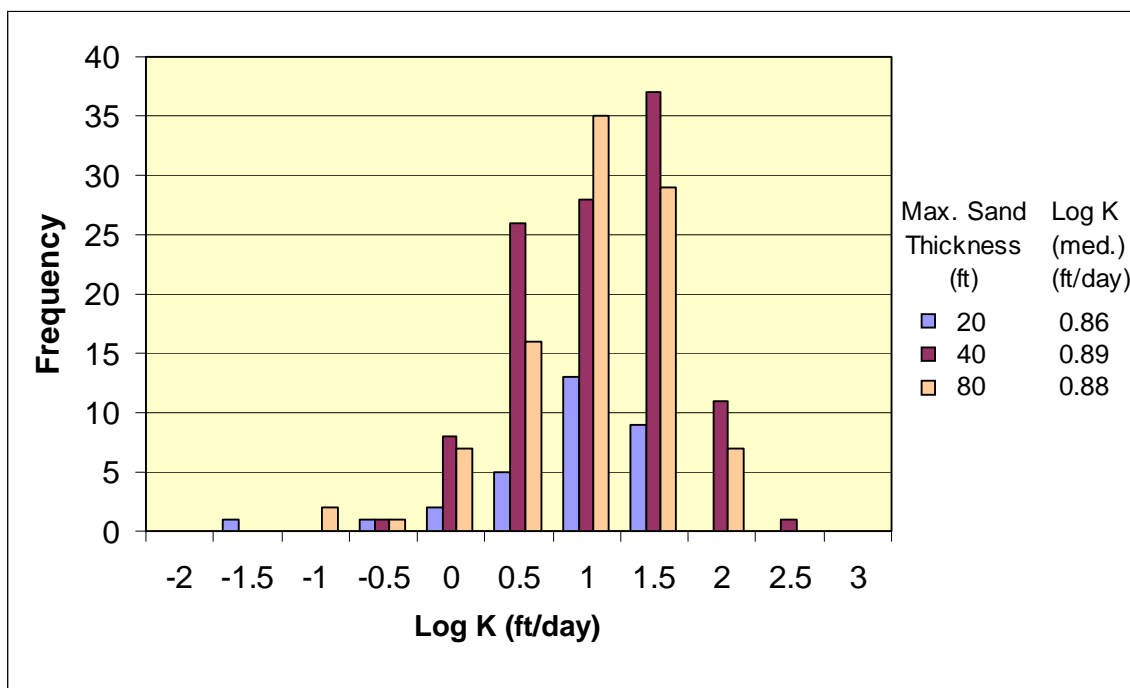


Figure 4.3.8 Variogram and kriged map of hydraulic conductivity for the Queen City.



a.



b.

Figure 4.3.9 Histogram of (a) net-sand thickness for the entire Wilcox Group and (b) maximum sand thickness and hydraulic conductivity (Log K) of the upper Wilcox.

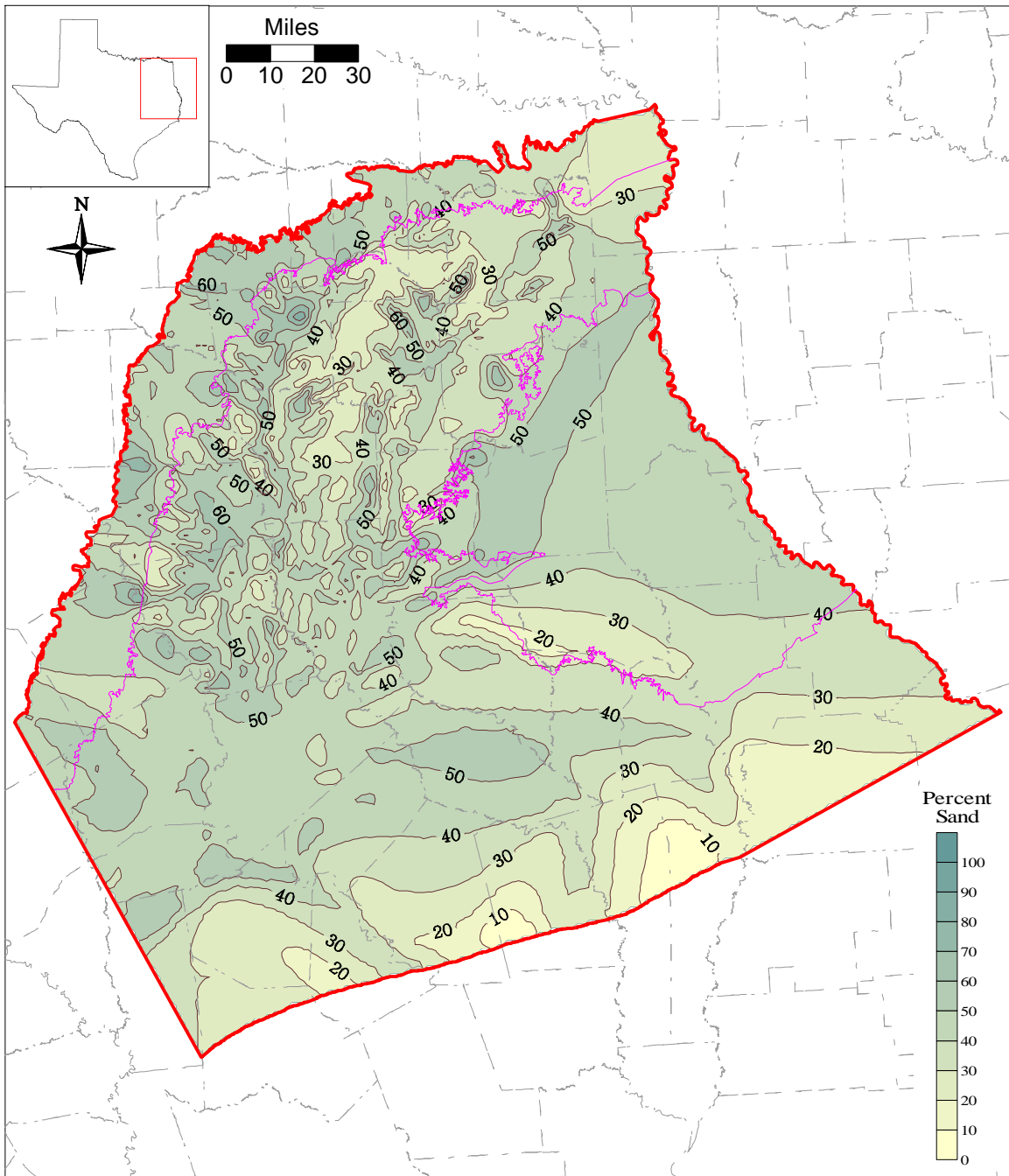


Figure 4.3.10 Percent sand for the Wilcox Group, based on sand maps by Kaiser et al. (1978) and Fisher and McGowen (1967) (CI = 10 percent).

4.4 Water Levels and Regional Groundwater Flow

An extensive literature search was conducted to understand (1) regional groundwater flow in the Carrizo Sand and Wilcox Group prior to extensive development of groundwater resources in the area and (2) the history of groundwater usage from the Carrizo Sand and the Wilcox Group. The literature search included a review of the available county reports, historical USGS reports (predominately water-supply papers), and reports by the various Texas state agencies responsible for water resources (i.e., the Texas Board of Water Engineers, the Texas Water Commission, and the Texas Water Development Board). A summary of all reports reviewed can be found in Appendix A. In addition, water-level data provided by the Texas Water Development Board (TWDB) on their website was used to (1) perform a pressure versus depth analysis, (2) develop water-level elevation contours corresponding to the start time for the transient model (January 1980), the end of the model calibration period (December 1989), and the end of the model verification period (December 1999), and (3) investigate transient water level conditions.

The relationship between the Carrizo Sand and the sands of the Wilcox Group varies across the study area. This variation is graphically presented in Figure 4.4.1. In general, the sands of the Wilcox Group, the Carrizo Sand, the sands of the Reklaw Formation, and the Queen City Sand are hydraulically connected and act as a single aquifer, referred to as the Cypress aquifer, in Cass and Marion counties (Broom, 1971), Camp, Franklin, Morris, and Titus counties (Broom et al., 1965), and Harrison County (Broom and Myers, 1966). The Carrizo Sand and the sands of the Wilcox Group are considered to function as a single aquifer due to their similar properties and hydraulic connection in Wood County (Broom, 1968), Smith County (Dillard, 1963), and Leon County (Peckham, 1965). The sands of the Wilcox Group and the Carrizo Sand are considered a single aquifer in Rains and Van Zandt counties (White, 1973), and San Augustine and Sabine counties (Anders, 1967), with the sands of the Wilcox being the principal source of water. In Upshur and Gregg counties (Broom, 1969), the Carrizo Sand and the sands of the Wilcox Group also act as a single aquifer with the Carrizo Sand being the principal source of water. The Carrizo Sand is missing in Limestone County (Rettman, 1984), and Bowie, Panola, and Shelby counties. The Carrizo Sand and the sands of the Wilcox Group act as separate aquifers in the remaining portions of the study area. The principal aquifer in

Henderson, Freestone, Anderson, and Cherokee counties (William F. Guyton & Associates, 1972), Rusk County (Sandeen, 1987), Caddo Parish, Louisiana (Page and May, 1964), Sabine Parish, Louisiana (Page et al., 1963), and Desoto Parish, Louisiana is the Wilcox aquifer. The principal aquifer in Nacogdoches and Angelina counties (William F. Guyton & Associates, 1970), Houston County (Tarver, 1966), Natchitoches Parish, Louisiana (Newcome et al., 1963), and Miller County, Arkansas (Ludwig, 1972) is the Carrizo Aquifer. Based on data from the TWDB website, the sands of the Wilcox Group are not used as a source of groundwater in Madison County. Neither the Carrizo Sand nor the sands of the Wilcox Group supply groundwater in Trinity County. Only saline water is found in the Carrizo Sand and sands of the Wilcox Group in Grimes County (Baker and Follett, 1974), Walker County (Winslow, 1950), San Jacinto County (Sandeen, 1968), Polk County (Tarver, 1968a), Tyler County (Tarver, 1968b), Montgomery County (Popkin, 1971), and Jasper and Newton counties (Wesselman, 1967). As can be seen from this discussion and Figure 4.4.1, the Carrizo Sand and the sands of the Wilcox Group have a complicated and variable relationship across the study area.

Water-level data for the study area can be found on the TWDB website¹. Water-level data for the Carrizo Sand and Wilcox Group are sparse from about 1929 to the 1950s. Thereafter, the amount of available water-level data increases significantly. Figure 4.4.2 shows well locations at which water-level measurements are available and the hydrologic unit in which each well is completed. These are the data used to investigate water-level elevations for this study.

4.4.1 Regional Groundwater Flow

The discussion on regional groundwater flow in the Carrizo Sand and Wilcox Group provided in this section is taken from Fogg and Kreitler (1982). They studied the hydrochemical facies and groundwater hydraulics of the Eocene aquifers in the East Texas Basin in great detail as part of a research program designed to evaluate the suitability of East Texas salt domes as repositories for high-level nuclear waste.

Water within the Carrizo Sand and the sands of the Wilcox Group is under water-table conditions in the outcrop areas and under artesian conditions down dip of the outcrop. In many areas, artesian pressures within the aquifer were originally sufficient to drive water above ground

¹ rio.twdb.state.tx.us/publications/reports/GroundWaterReports/GWDatabaseReports/GWdatabaserpt.htm

surface. Water still flows to the surface in the valleys of the Trinity and Sabine rivers and some of their tributaries in the artesian portion of the aquifers indicating upward flow in these areas. Flowing wells are not observed along the Neches and Angelina rivers, indicating an absence of an upward component of flow along these rivers.

Groundwater movement within the Carrizo Sand and Wilcox Group is significantly influenced by the topography and by the structure of the units. Topographic highs are present in both outcrop areas, with the eastern outcrop belt at higher elevations than the western outcrop. A structural high, which trends from the northwest to the southeast, is present in Upshur, Gregg, and Smith counties (see Section 2). Topographic lows are found in the stream beds both in the outcrops and in the artesian section of the aquifers. In general, groundwater flows from the topographically and structurally high areas to the topographically and structurally low areas (Figure 4.4.3). Several rivers within the outcrops act as major discharge areas. From north to south, these are the Red River, the Sulphur River, Big Cypress Creek, the Sabine River, Neches River, and the Trinity River (Figure 2.2).

Northeast of the structural divide located in Upshur, Gregg, and Smith counties, groundwater in the artesian portion of the aquifers generally flows northeastward toward the Texas-Louisiana border (see Figure 4.4.3). South of the structural divide, the flow of groundwater is generally to the south. The Sabine River between the structural high to the north and a watershed divide to the south interrupts this latter trend. In this area, groundwater flows to the Sabine River. In addition, groundwater west of the Trinity River flows eastward into the Trinity. The Angelina River appears to have little impact on the flow of groundwater in the Carrizo and Wilcox aquifers. Some groundwater converges towards the Neches River. Strata of the Carrizo Sand and Wilcox Group are displaced by faults in the Elkhart Graben-Mount Enterprise fault system. These faults appear to be a partial barrier to horizontal groundwater flow.

4.4.2 Predevelopment Conditions for the Carrizo Sand and the Wilcox Group

Use of waters from the Carrizo Sand and Wilcox Group began in the late 1800s. Early development predominantly consisted of domestic and stock wells. Precipitation is relatively high over most of this region resulting in little need for irrigation. Consequently, large capacity irrigation wells are not found in the study area. The most significant use was for municipal and

industrial purposes. The cities of Lufkin in Angelina County and Nacogdoches in Nacogdoches County began pumping groundwater from the Carrizo Sand in the 1930s. Heavy industrial pumping by a paper mill (originally the Southland Paper Mills) also occurred in this area. William F. Guyton & Associates (1970) estimated that drawdowns of up to 500 ft have occurred at pumping centers as a result of this municipal and industrial pumpage.

Extensive pumping also began in Upshur, Gregg, Smith, and Rusk counties after discovery of the East Texas Oil Field in 1930-1931. Numerous processes related to the oil industry and the increased population in the area of the oil field created an immediate demand for water. Wells completed to the Carrizo-Wilcox aquifer(s) met these water needs. By the early 1950s, most of the water required by the municipalities in the area near the oil field switched to surface-water sources.

Louisiana began using groundwater from the Carrizo Sand and Wilcox Group as early as 1900. The cities of Shreveport and Bossier City used water from the Wilcox Group for their public supply until they switched to surface water in 1926-1928. Over 60 wells were pumping from the Wilcox Group prior to the first recorded water-level measurements in Louisiana². The Wilcox Group is not used to supply groundwater and very little groundwater is pumped from the Carrizo Sand in Miller County, Arkansas.

Although pumping of the Carrizo Sand and Wilcox Group began early in the 1900s, few water-level data are available prior to 1950 in Texas (TWDB, website) and prior to 1940 in Louisiana (LaDOT, website). A brief description of historical development in each county/parish in the model area can be found in Appendix A. The dates at which wells were first completed to the Carrizo Sand and/or Wilcox Group are also given in the appendix as well as the dates for the first water-level measurements. Based on this information, few of the early water-level measurements available for the Carrizo Sand and Wilcox Group in the study area are considered to be representative of predevelopment conditions. The few data that are considered to represent predevelopment conditions are shown in Figure 4.4.4 and tabulated in Table 4.4.1. Although, these data are insufficient to develop water-level elevation contours corresponding to predevelopment, they were used as point targets in calibration of the steady-state model (see Section 8.1).

² www2.dotd.state.la.us/wells/wells.html

4.4.3 Pressure Versus Depth Analysis

A study of pressure head versus screen-midpoint depth was conducted using wells having both water-level and screen-depth data on the TWDB website. Water-level measurements taken prior to 1950 in Texas counties constituted the data used for the analysis. The goal of the analysis was to evaluate vertical gradients between the hydrostratigraphic units. The locations of the wells used and the unit in which they are completed are given in Figure 4.4.5. This figure shows that little water-level data and screen data are available for times earlier than 1950. All of the wells completed to the Carrizo Sand are located in Nacogdoches, Angelina, or Anderson counties. Wells completed to the Wilcox Group and the Carrizo-Wilcox are scattered throughout the study area.

Figure 4.4.6 shows the pressure-depth analysis results. The screen midpoints for wells completed in the Carrizo Sand range from a depth of about 200 ft to depths greater than 1200 ft. The range in screen midpoints is about 100 to 1700 ft for wells completed in the Wilcox Group. Some data for the combined Carrizo-Wilcox was available for wells with screen depths ranging from about 225 to 1100 ft. A fit through the data for the 28 wells completed in the Carrizo Sand gives a slope of 1.05, indicating a pressure gradient slightly higher than hydrostatic conditions. A fit through the data for the 36 wells completed in the Wilcox Group gives a slope of 0.94, indicating a pressure gradient slightly less than hydrostatic. The difference in slope between the data for the Carrizo Sand and Wilcox Group suggests a lack of communication between these two hydrologic units. For the ten wells completed to the Carrizo and Wilcox, a linear fit through the data yields a slope of 0.96, indicating a pressure gradient slightly less than hydrostatic.

The pressure-depth data show a relatively large scatter between and within the different aquifer units and, considering the large area and uneven distribution (Figure 4.4.5), can mask different flow regimes. Evaluating pressure-depth trends on a county-by-county area indicates significantly different trends for different counties (Figure 4.4.6). Anderson, Angelina, and Rusk counties have slopes less than one, indicating downward flow, whereas Nacogdoches County has a slope greater than one, indicating upward flow. Data from Angelina and Nacogdoches counties are mostly from the Carrizo. The upward flow indicated for Nacogdoches County may be associated with upward flow to the Angelina River. All data points from Angelina County are in the vicinity of the Angelina River (Figure 4.4.5) but the pressure-depth trend indicates significant decline due to pumpage. A similar trend is apparent in Rusk County, which is probably due to

pumpage. Pressure-depth data covers a wide depth range and may reflect different flow regimes within the Wilcox and Carrizo.

Since few data are available prior to 1950, the pressure-depth analysis was repeated using all wells, regardless of time, for which both water-level and screen data could be found on the TWDB website. In all cases, the analysis used the maximum water level measured in each well. The locations of these data points are shown in Figure 4.4.7. Use of more data resulted in greater coverage of the study area. Figure 4.4.8 shows the results of the analysis. For wells completed in the Carrizo Sand, the Carrizo and Wilcox, and the Wilcox Group, use of all available data results in a significant decrease in the slope and correlation, indicating significant depressurization in the aquifers between 1950 and 2000.

4.4.4 Water-Level Elevations for Model Calibration and Verification.

Model calibration considered the time period from January 1, 1980 to December 31, 1989 and model verification considered the time period from January 1, 1990 to December 31, 1999 (see Section 9.1). Water-level data found on the TWDB website were used to develop water-level elevation contours for the start of calibration, the end of calibration, and the end of verification. Initialization of water levels in the transient model utilized the contours for the time corresponding to the start of calibration (January 1980). The contours for the end of calibration and the end of verification aided in assessing the transient model's ability to represent observed conditions.

Water-level data on the TWDB website are not available at regular time intervals in every well. Therefore, the coverage of water-level data for a particular month or even a year is very sparse. For example, water levels were measured in a total of three wells in January, 1980, and in a total of 118 wells during all of 1980. Because this amount of data is not sufficient to develop contours across the entire model area for every geologic unit at the start of model calibration, measured water levels near the date of interest were also used if they met any of the following criteria:

- The water level for a well with a single measurement was used if the date of the measurement fell within ± 3 years of the date of interest;

- For wells with water-level data at times only before or after the date of interest, the closest measurement to the date of interest was used if the measurement date fell within ± 2.5 years of the date of interest;
- For wells with water-level data at dates both before and after the date of interest, the water level at the date of interest was interpolated if (1) both measurement dates were within ± 2.5 years of the date of interest, (2) one measurement was within ± 2.5 years of the date of interest and the total head difference between the two measurements was less than 100 ft; or (3) the total head difference between the two measurements was less than or equal to 20 ft regardless of measurement dates.

Using this method, a total of 1128 water-level measurements were available for constructing water-level elevation maps for the start of calibration (January 1, 1980).

Figures 4.4.9a-e show the water-level elevation contours for the Queen City Sand (layer 1), the Carrizo Sand (layer 3), the upper Wilcox (layer 4), the middle Wilcox (layer 5), and the lower Wilcox (layer 6) at the start of calibration (January 1, 1980). The water-level elevations shown on these contour maps were used as the initial conditions for the transient model. Contours for the Reklaw Formation could not be generated due to a lack of data. To initialize the model, the average of the water-level elevations for the overlying Queen City Sand and underlying Carrizo Sand were used for the Reklaw Formation.

Note that artificial points were used to construct the contours for the Carrizo Sand, upper Wilcox, and middle Wilcox. These points helped define the cone of drawdown (both laterally and vertically) created by municipal pumpage for the cities of Nacogdoches (Nacogdoches County) and Lufkin (Angelina County) because observed data are not available south of this drawdown center. An artificial point located in southeastern Wood County was used to vertically extend to the middle Wilcox a drawdown observed in the upper Wilcox. These artificial points were needed due to a lack of data in the vicinity of locations known to experience drawdown.

Figures 4.4.10a-d show the water-level elevation contours for the Carrizo Sand, upper Wilcox, middle Wilcox, and lower Wilcox at the end of model calibration (December 31, 1989). An estimated water level in the middle Wilcox was used to vertically extend the drawdown observed in the Carrizo Sand and upper Wilcox caused by municipal pumpage by the cities of

Nacogdoches and Lufkin. This estimated point was needed because of a lack of data in an area known to be experiencing drawdown. Figures 4.4.11a-d show the water-level elevation contours for the same units at the end of model verification (December 31, 1999). An estimated water level in the upper and middle Wilcox was used to vertically extend the drawdown observed in the Carrizo Sand caused by municipal pumpage for the cities of Nacogdoches and Lufkin. These estimated points were needed due to a lack of data in areas know to be experiencing drawdown.

4.4.5 Transient Water Levels

Historically, the greatest water-level declines in the Carrizo Sand and Wilcox Group have occurred as a result of municipal pumpage by the cites of Nacogdoches (Nacogdoches County) and Lufkin (Angelina County) and industrial pumpage at a paper mill (formerly the Southland Paper Mill) located on the Nacogdoches-Angelina County border. This municipal and industrial pumping began in the 1930s and continues to the present. Figure 4.4.12 shows the transient water-level record for a well located near the paper mill and completed in the Carrizo Sand and upper Wilcox. The water level in this well decreased 300 ft between May 1947 and November 1985. From 1985 to 1992, the water level increased about 60 ft. In addition to causing large water-level declines in individual wells, this pumping appears to have also affected a large lateral area based on the limited data available south of the pumping center.

Figure 4.4.13 shows the locations for which transient water-level data (hydrographs) are available for the last 20 (1980-1999) years based on data on the TWDB website. Also shown on this figure is either the model layer in which the midpoint of the well screen is located or, where screen data are not available, the model layer in which the bottom of the well is located. Few transient data were available for wells located in the vicinity of the pumpage in Nacogdoches and Angelina counties between January 1980 and December 1999. Wells north of the center in Nacogdoches County for which transient data are available show either no change or an increase in water-level elevations over this period. The water level in several wells increased significantly, such as the 100-ft rise observed in well 37-27-201 (Figure 4.4.14). Most wells south of this area in Angelina County, on the other hand, show declines in water-level elevations over this 20-year period. The water level in well 37-35-703 declined over 150 ft (see Figure 4.4.14).

In general, water levels in the artesian portions of the Carrizo Sand and Wilcox Group in the study area have remained constant or declined over the last 20 years (1980-1999). The amount of decline has varied from county to county and from well location to well location within a county. The largest declines have been observed in Anderson and Smith counties. In the last 20 years, the water level in well 34-61-501, completed to the Carrizo Sand in Anderson County, has declined over 90 ft, and the water level in well 34-38-805, completed to the Carrizo Sand in Smith County, has declined over 175 ft (Figure 4.4.15). In addition to northern Nacogdoches County, significant water-level increases have also been observed in wells located in Cass and Titus counties. The water level in well 35-07-902, completed in the Carrizo Sand in Cass County, and well 16-49-703, completed in the Wilcox Group in Titus County, have risen over 60 ft in the past 20 years (Figure 4.4.15).

In general, water levels in wells located in the Sabine Uplift on the eastern side of the study area have remained relatively constant (less than ± 15 -ft change) over the last 20 years based on the transient data available on the TWDB website. In contrast, many wells located in the outcrop on the western edge of the study area have recorded decreasing water levels since 1980. For example, the water level in well 39-15-802, completed to the Wilcox Group in Freestone County, has declined over 50 ft in the last 20 years (see Figure 4.4.15).

The changes in water levels between the start of the transient model calibration (January 1980) and the end of model calibration (December 1989) and between the start of model calibration (January 1980) and the end of model verification (December 1999) are illustrated in Figure 4.4.16a-b for the Carrizo Sand, Figure 4.4.17a-b for the upper Wilcox, Figure 4.4.18a-b for the middle Wilcox, and Figure 4.4.19a-b for the lower Wilcox. These figures show a large decline in water levels in the southern portion of the active model area. Water levels in this region, however, are not well known due to a lack of data. A region of large and continual decline is also observed in the Carrizo Sand, and the upper and middle Wilcox in Smith, Upshur, Wood, Van Zandt, and Henderson counties. Based on Figure 4.4.17a-b, water levels in the upper Wilcox have risen in Cass County. This increase is consistent with the transient water-level data available for wells in this county. Declines in water level observed over one time period but not the other, most likely are the result of variability in available data.

Table 4.4.1 Target values for calibration of the steady-state model to predevelopment conditions.

Well Number	County/Parish	Observed Water-Level Elevation (ft)	Target Water Level Elevation ^(a) (ft)	Model Layer	Source of Observed Water Level
3457801	Anderson	350	274	4	TWDB (website)
3801202	Anderson	427	362	3	TWDB (website)
3735705	Angelina	269	269	3	TWDB (website)
CD- 150	Caddo	344	323	5	LaDOT (website)
CD- 160	Caddo	340	325	5	LaDOT (website)
CD- 271	Caddo	252	156	5	LaDOT (website)
CD- 409	Caddo	335	275	5	LaDOT (website)
CD- 413	Caddo	297	277	5	LaDOT (website)
CD- 418	Caddo	354	325	5	LaDOT (website)
CD- 684	Caddo	337	339	5	LaDOT (website)
1653103	Cass	355	308	4	TWDB (website)
3464305	Cherokee	402	386	3	TWDB (website)
DS- 101	DeSoto	344	235	5	LaDOT (website)
DS- 199	DeSoto	340	310	5	LaDOT (website)
DS- 216	DeSoto	252	316	5	LaDOT (website)
DS- 218	DeSoto	335	197	5	LaDOT (website)
DS- 227	DeSoto	297	339	5	LaDOT (website)
DS- 234	DeSoto	354	299	5	LaDOT (website)
DS- 246	DeSoto	337	238	5	LaDOT (website)
DS- 247	DeSoto	344	298	5	LaDOT (website)
DS- 261	DeSoto	303	313	5	LaDOT (website)
DS- 267	DeSoto	301	291	5	LaDOT (website)
DS- 289	DeSoto	340	248	5	LaDOT (website)
DS- 303	DeSoto	252	300	5	LaDOT (website)
DS- 305	DeSoto	335	251	5	LaDOT (website)
DS- 307	DeSoto	297	247	5	LaDOT (website)
DS- 308	DeSoto	354	287	5	LaDOT (website)
DS- 309	DeSoto	337	285	5	LaDOT (website)
DS- 85	DeSoto	341	304	5	LaDOT (website)
DS-181	DeSoto	303	272	5	LaDOT (website)
1755407	Franklin	493	492	5	TWDB (website)
3406309	Franklin	539	503	3	TWDB (website)
3923703	Freestone	516	477	5	TWDB (website)
3923704	Freestone	522	482	5	TWDB (website)
3924603	Freestone	474	465	3	TWDB (website)
3931410	Freestone	497	490	5	TWDB (website)

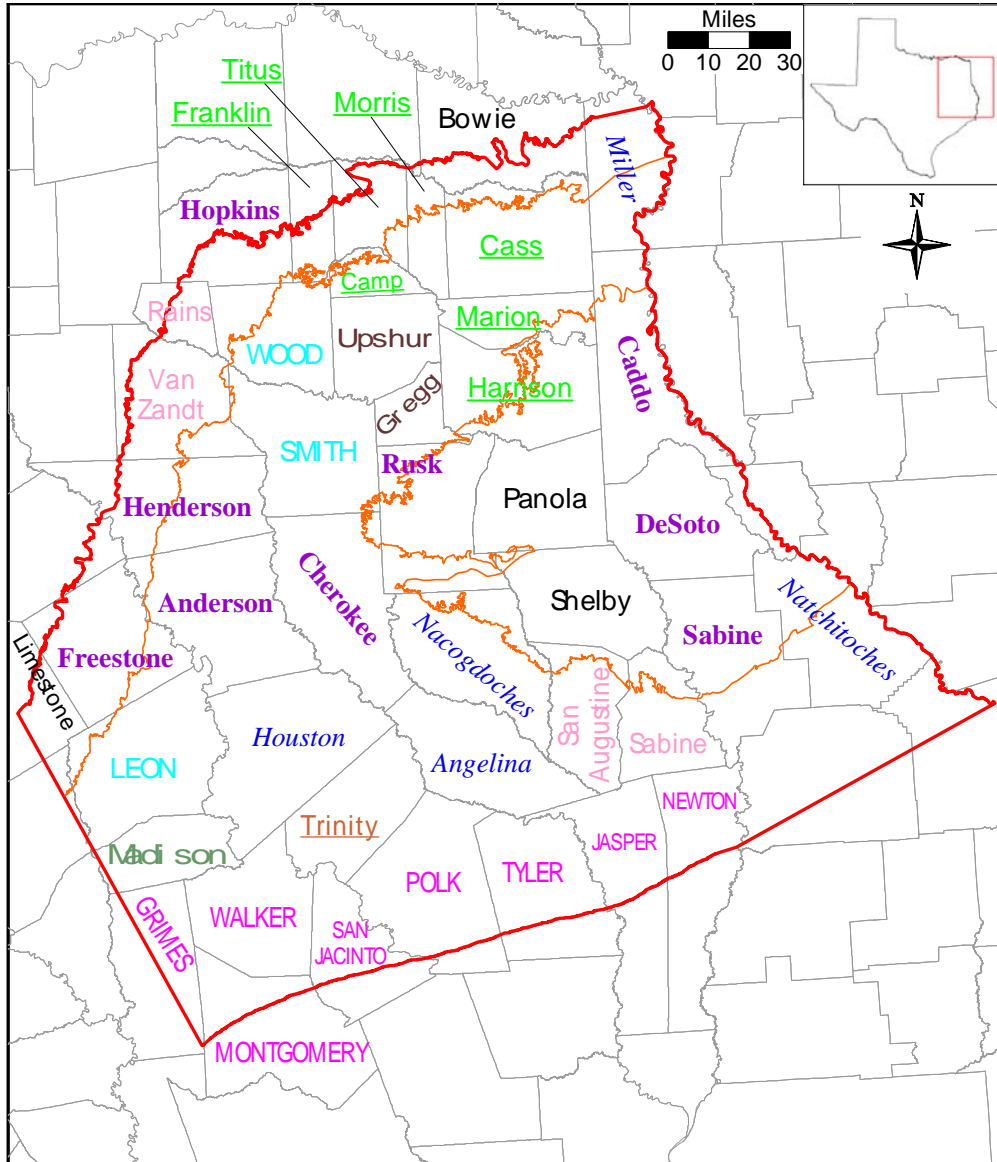
Table 4.4.1 (continued)

Well Number	County/Parish	Observed Water-Level Elevation (ft)	Target Water Level Elevation ^(a) (ft)	Model Layer	Source of Observed Water Level
3932208	Freestone	453	438	3	TWDB (website)
3533911	Gregg	300	300	5	TWDB (website)
3534403	Gregg	291	291	5	TWDB (website)
3529301	Harrison	362	328	3	TWDB (website)
3530501	Harrison	367	385	4	TWDB (website)
3531708	Harrison	366	375	5	TWDB (website)
3537301	Harrison	390	334	4	TWDB (website)
3539201	Harrison	361	345	5	TWDB (website)
3539604	Harrison	376	352	5	TWDB (website)
604	Henderson	437	437	5	Duessen (1914)
3441203	Henderson	478	497	5	TWDB (website)
3441903	Henderson	468	444	4	TWDB (website)
1759603	Hopkins	522	498	5	TWDB (website)
1761301	Hopkins	521	518	5	TWDB (website)
3837102	Houston	332	332	3	TWDB (website)
727	Leon	304	304	5	Duessen (1914)
3843101	Leon	262	262	3	TWDB (website)
3939703	Leon	454	435	4	TWDB (website)
3946301	Leon	428	400	4	TWDB (website)
3857701	Madison	286	286	3	TWDB (website)
3711504	Nacogdoches	470	433	3	TWDB (website)
3712301	Nacogdoches	481	437	4	TWDB (website)
3712501	Nacogdoches	474	425	3	TWDB (website)
3712906	Nacogdoches	477	394	3	TWDB (website)
NA- 114	Natchitoches	375	258	5	LaDOT (website)
852	Panola	320	308	5	Duessen (1914)
3547501	Panola	347	354	5	TWDB (website)
3552301	Panola	316	336	5	TWDB (website)
3555301	Panola	305	300	5	TWDB (website)
3563701	Panola	296	295	5	TWDB (website)
3564101	Panola	280	232	5	TWDB (website)
3564201	Panola	280	269	5	TWDB (website)
3704301	Panola	380	347	4	TWDB (website)
3403703	Rains	513	487	5	TWDB (website)
3541202	Rusk	384	384	4	TWDB (website)
3541509	Rusk	370	370	4	TWDB (website)
3543903	Rusk	430	369	4	TWDB (website)
3544503	Rusk	348	296	4	TWDB (website)

Table 4.4.1 (continued)

Well Number	County/Parish	Observed Water-Level Elevation (ft)	Target Water Level Elevation ^(a) (ft)	Model Layer	Source of Observed Water Level
3544701	Rusk	364	350	4	TWDB (website)
3550601	Rusk	447	454	4	TWDB (website)
3550701	Rusk	435	431	4	TWDB (website)
3550911	Rusk	443	458	4	TWDB (website)
3551903	Rusk	405	353	4	TWDB (website)
3558401	Rusk	436	408	4	TWDB (website)
3559603	Rusk	420	437	4	TWDB (website)
3559701	Rusk	421	416	4	TWDB (website)
3560102	Rusk	382	361	4	TWDB (website)
3702801	Rusk	422	422	5	TWDB (website)
3703301	Rusk	446	446	4	TWDB (website)
3703901	Rusk	482	451	4	TWDB (website)
3704201	Rusk	458	420	4	TWDB (website)
3711201	Rusk	548	414	4	TWDB (website)
SA- 148	Sabine	357	312	5	LaDOT (website)
SA- 164	Sabine	331	285	5	LaDOT (website)
SA- 178	Sabine	264	243	5	LaDOT (website)
SA- 203	Sabine	359	330	4	LaDOT (website)
SA- 231	Sabine	278	287	4	LaDOT (website)
3732111	San Augustine	464	360	3	TWDB (website)
3617802	Shelby	293	265	4	TWDB (website)
3705101	Shelby	424	377	4	TWDB (website)
3714501	Shelby	401	389	4	TWDB (website)
3723601	Shelby	422	326	4	TWDB (website)
953	Smith	436	436	3	Duessen (1914)
957	Smith	399	399	5	Duessen (1914)
3428807	Smith	482	457	3	TWDB (website)
3445803	Smith	377	377	3	TWDB (website)
3549405	Smith	438	438	5	TWDB (website)
1649212	Titus	466	399	5	TWDB (website)
3416703	Upshur	450	450	4	TWDB (website)
3426901	Van Zandt	580	522	4	TWDB (website)
3433902	Van Zandt	572	564	5	TWDB (website)
3434101	Van Zandt	588	574	5	TWDB (website)
3435101	Van Zandt	599	570	3	TWDB (website)

^(a) Target values were determined using the reported depth to water and the ground-surface elevation for the 1 mi x 1 mi model grid block containing the well. Often, the average ground-surface elevation assigned to the model grid block differed significantly from the ground-surface elevation at the well.



Cypress Aquifer

CARRIZO-WILCOX AQUIFER
 Carrizo-Wilcox Aquifer; Carrizo principal source

Carrizo-Wilcox Aquifer; Wilcox principal source

**Separate Carrizo Aquifer and Wilcox Aquifer;
 Wilcox Aquifer is most important**

*Separate Carrizo Aquifer and Wilcox Aquifer;
 Carrizo Aquifer is most productive*

Wilcox Aquifer only

Carrizo Sand and Wilcox Group not used to supply groundwater

SALINE WATER ONLY IN THE CARRIZO SAND AND WILCOX GROUP

Carrizo Aquifer only

Figure 4.4.1 Relationship between the Carrizo Sand and the Wilcox Group in the study area.

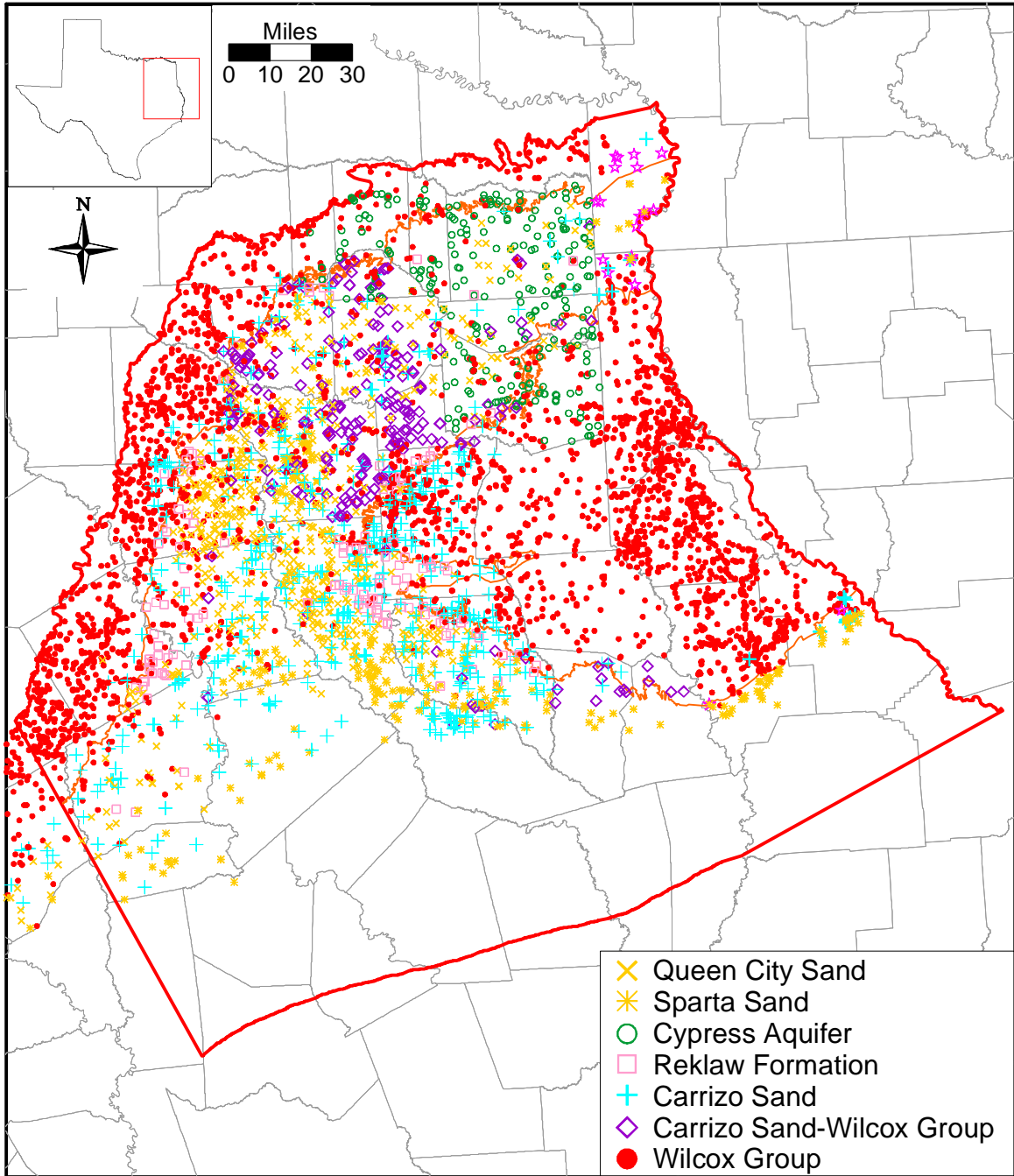


Figure 4.4.2 Water-level measurement locations for the hydrostratigraphic units in the study area.

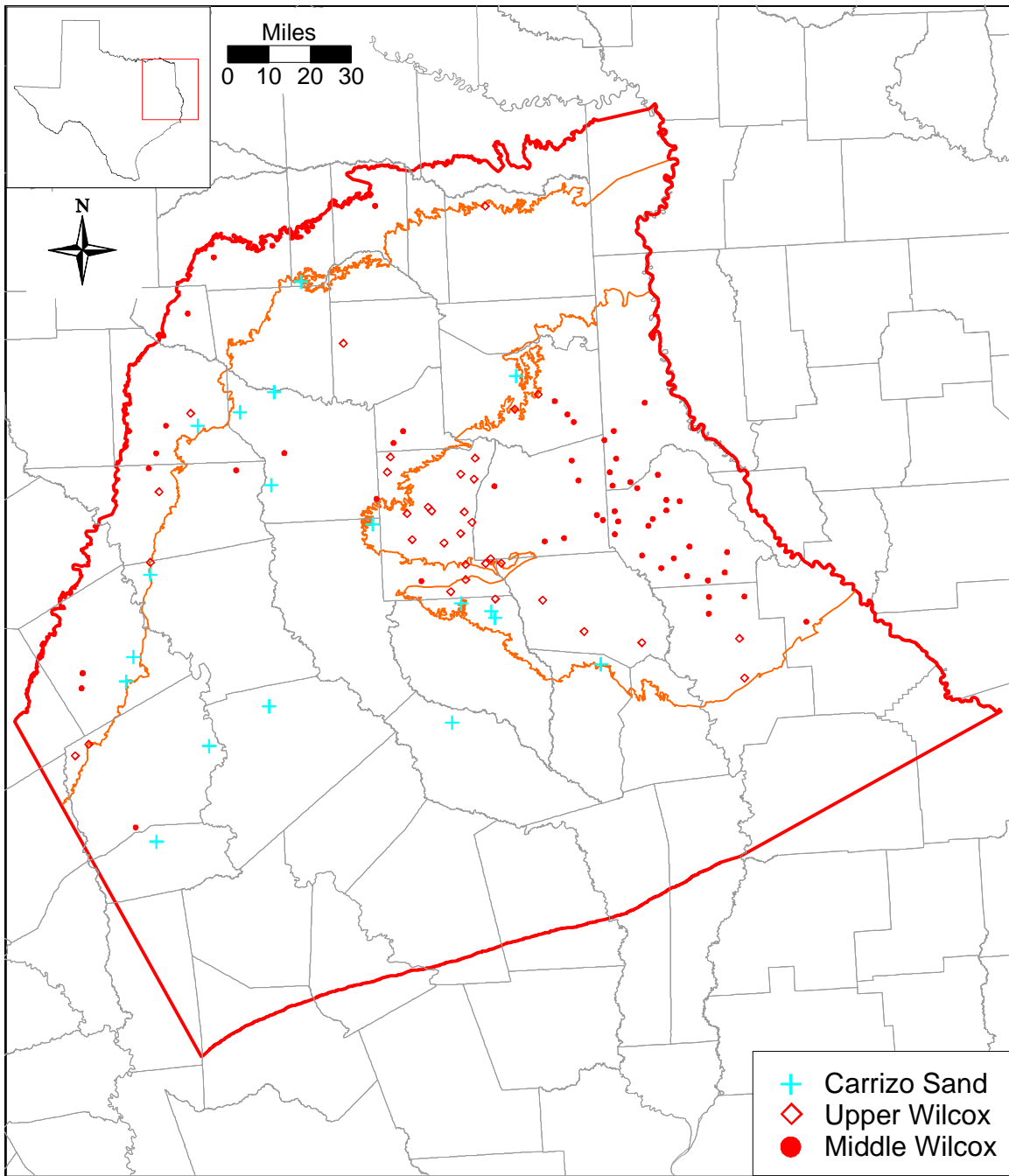


Figure 4.4.4 Location and model layer for predevelopment water-level elevation targets.

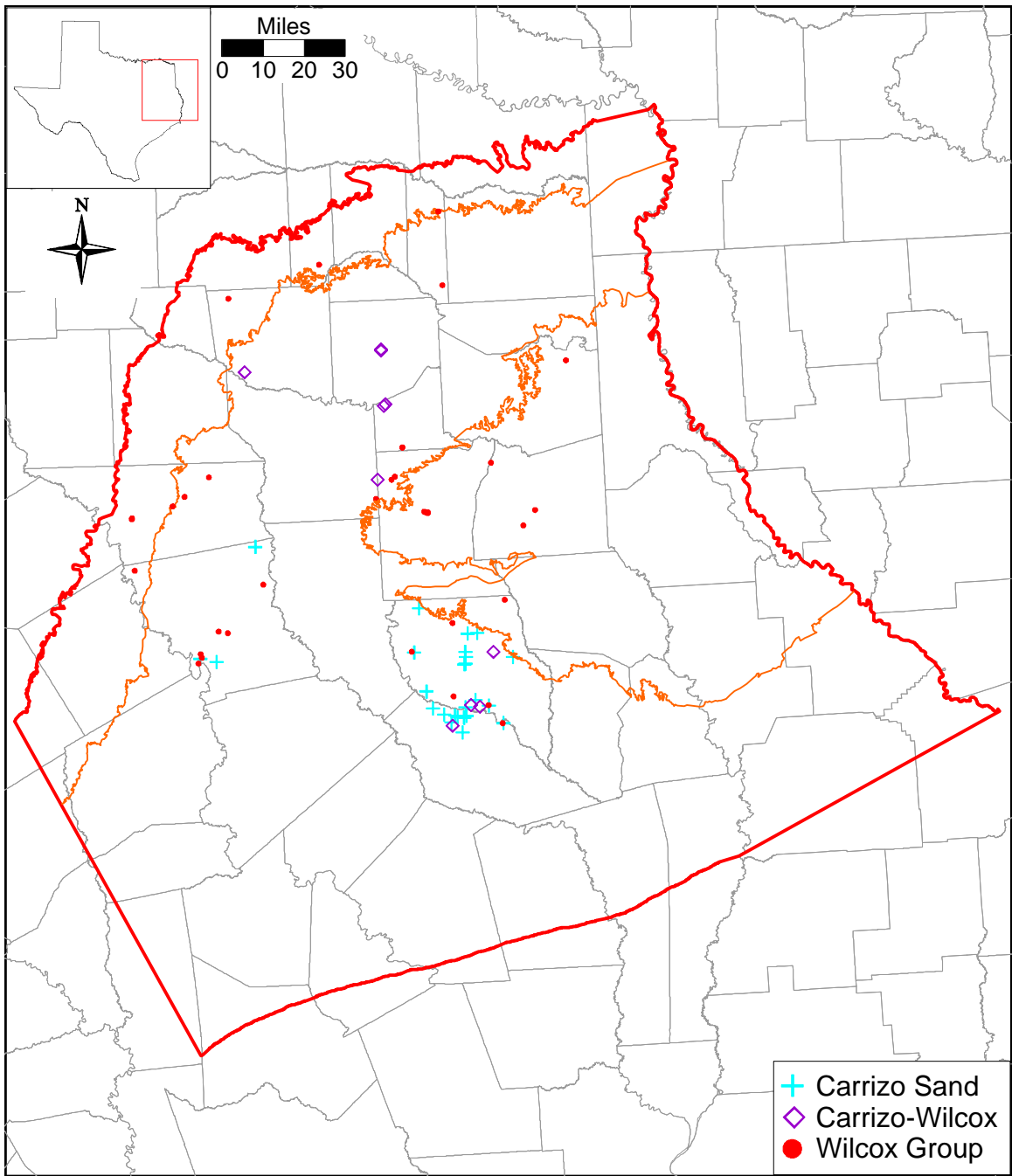


Figure 4.4.5 Water-level measurement locations used for the pressure-depth analysis (for measurements prior to 1950).

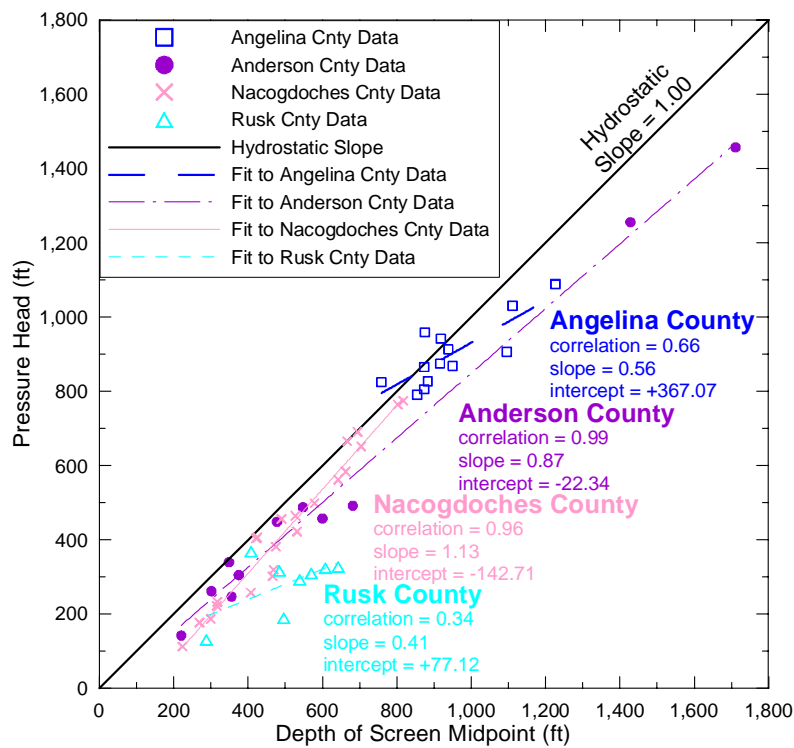
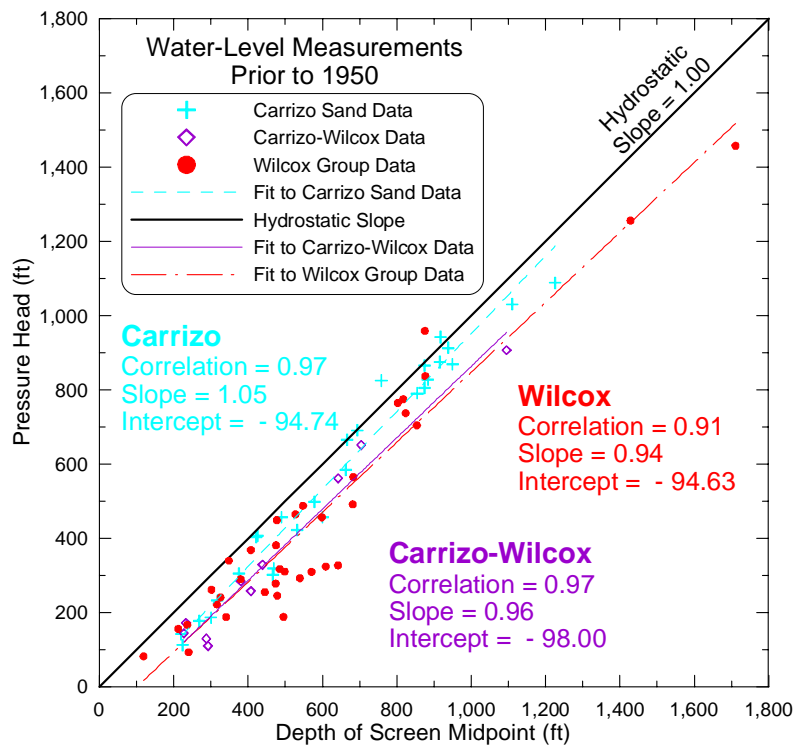


Figure 4.4.6 Pressure versus depth analysis results (for measurements prior to 1950).

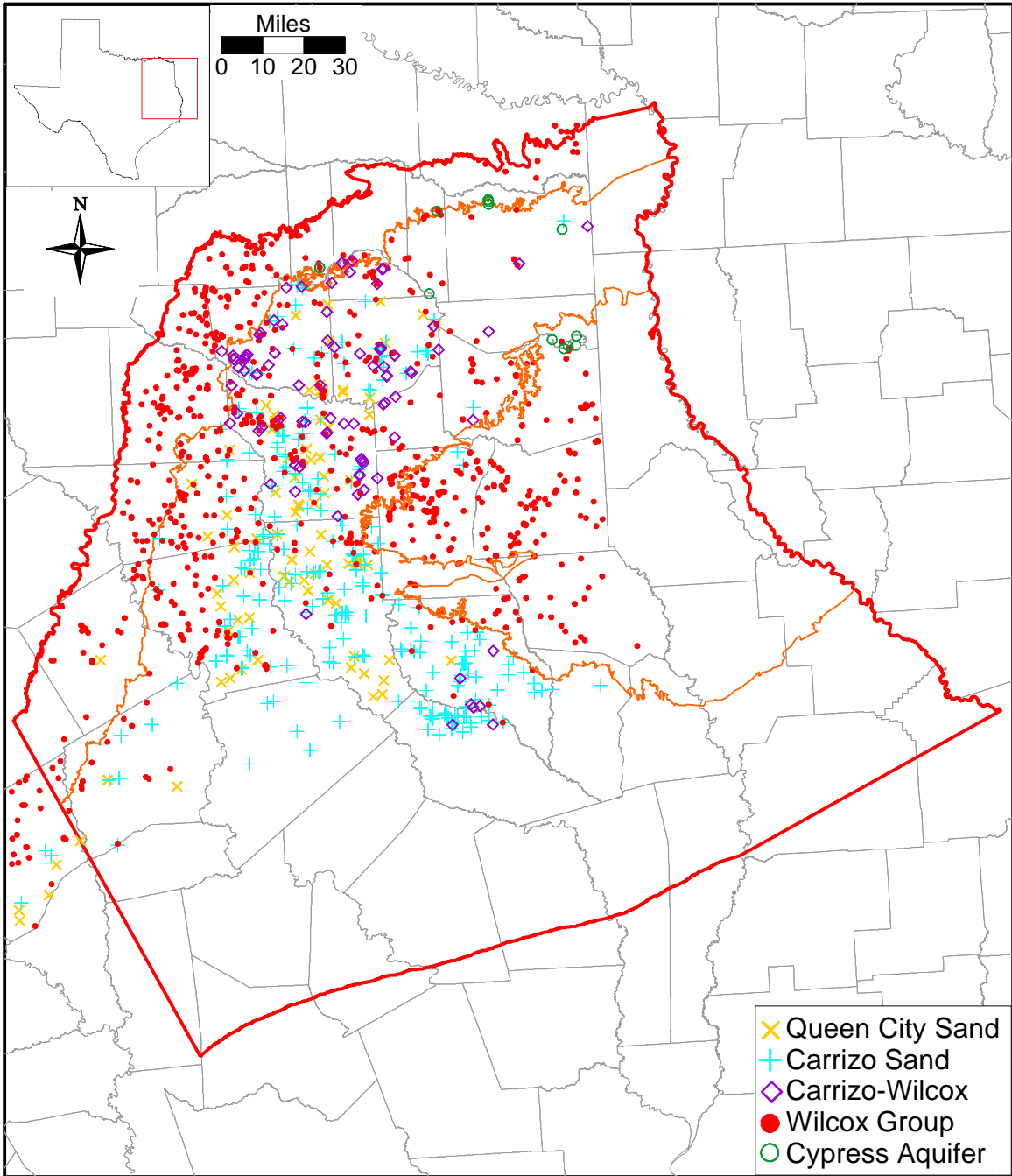


Figure 4.4.7 Water-level measurement locations used for the pressure-depth analysis (for all measurements).

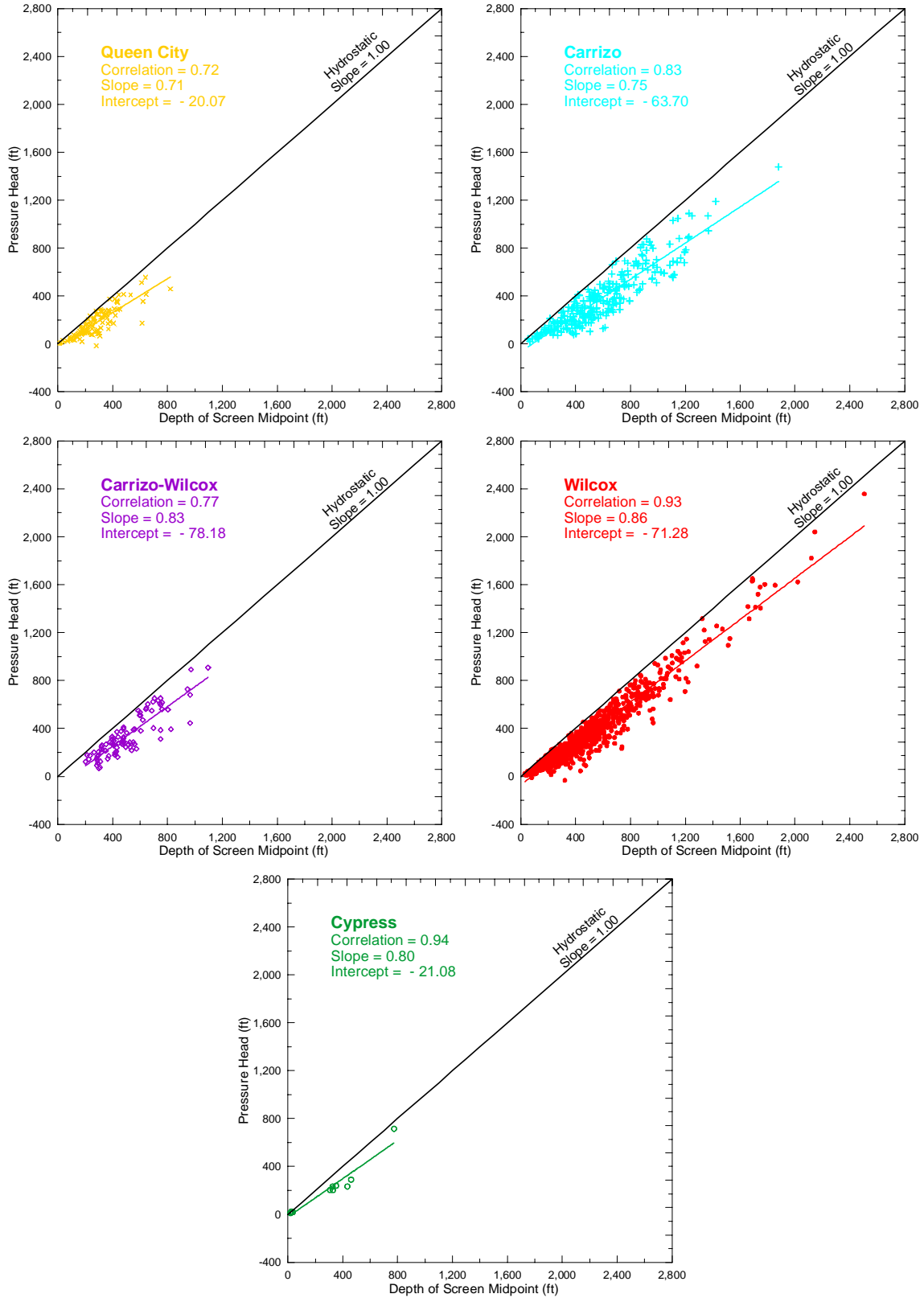


Figure 4.4.8 Pressure versus depth analysis results (for all measurements).

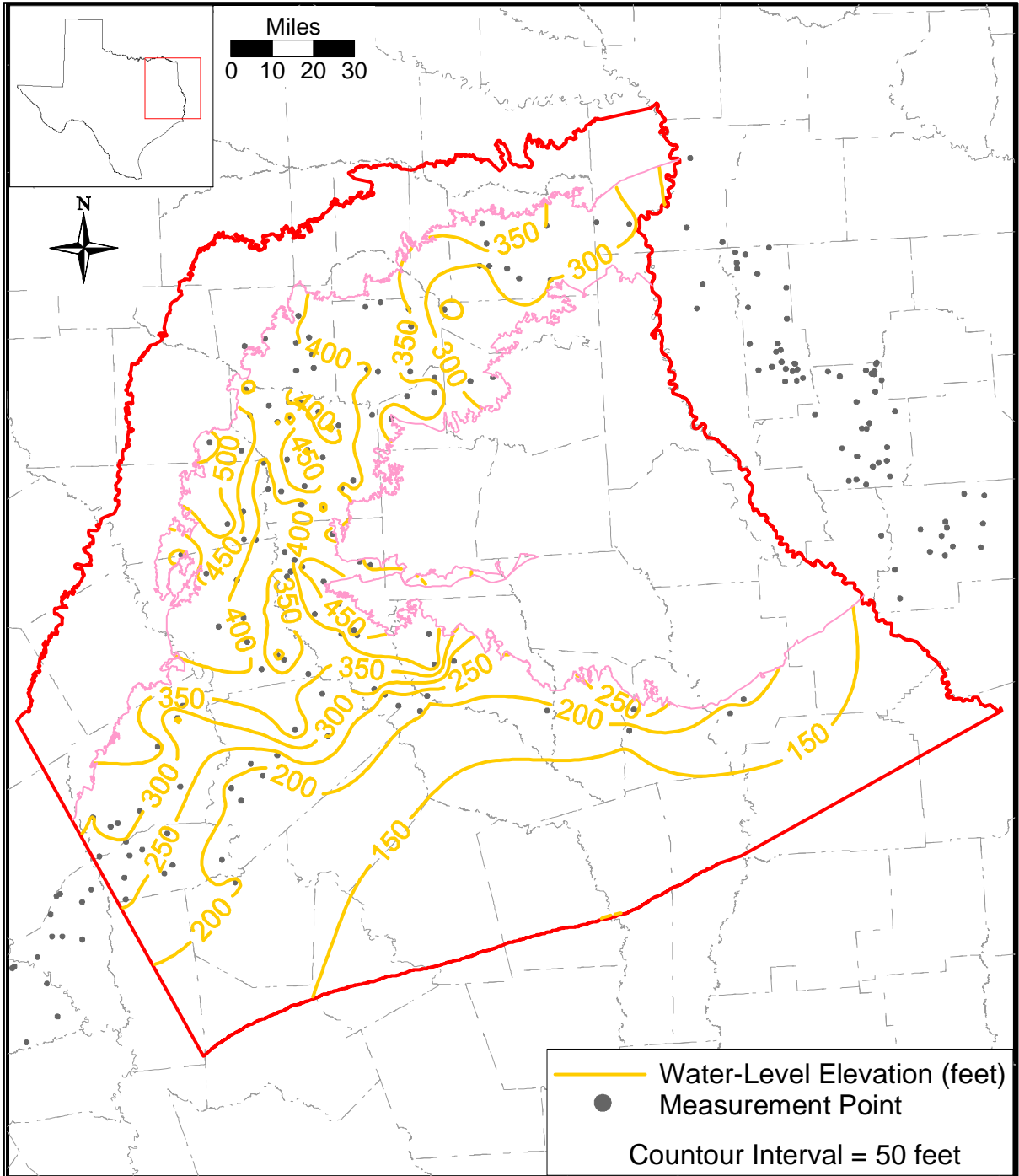


Figure 4.4.9a Water-level elevation contours for the Queen City Sand at the start of model calibration (January 1980).

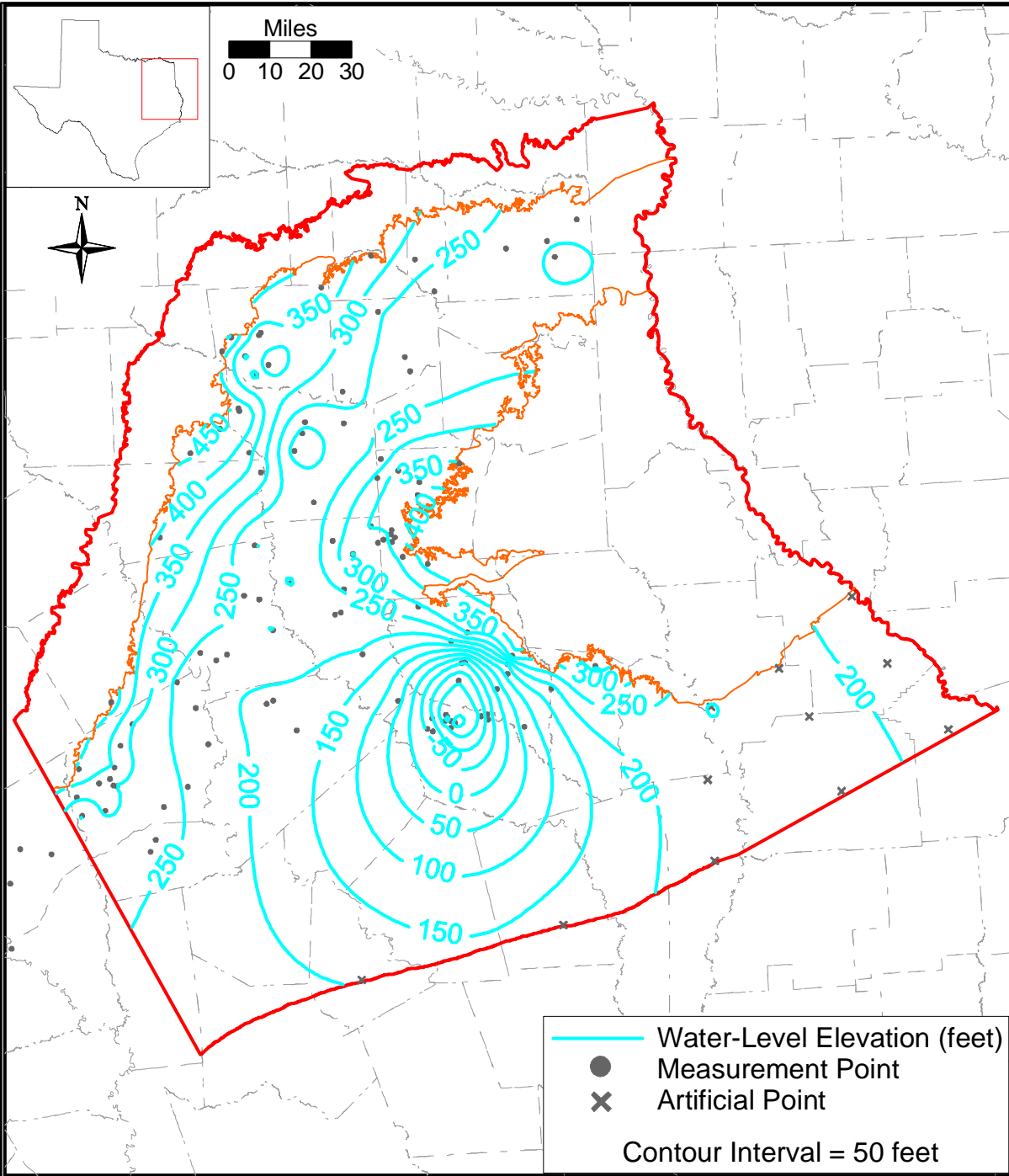


Figure 4.4.9b Water-level elevation contours for the Carrizo Sand at the start of model calibration (January 1980).

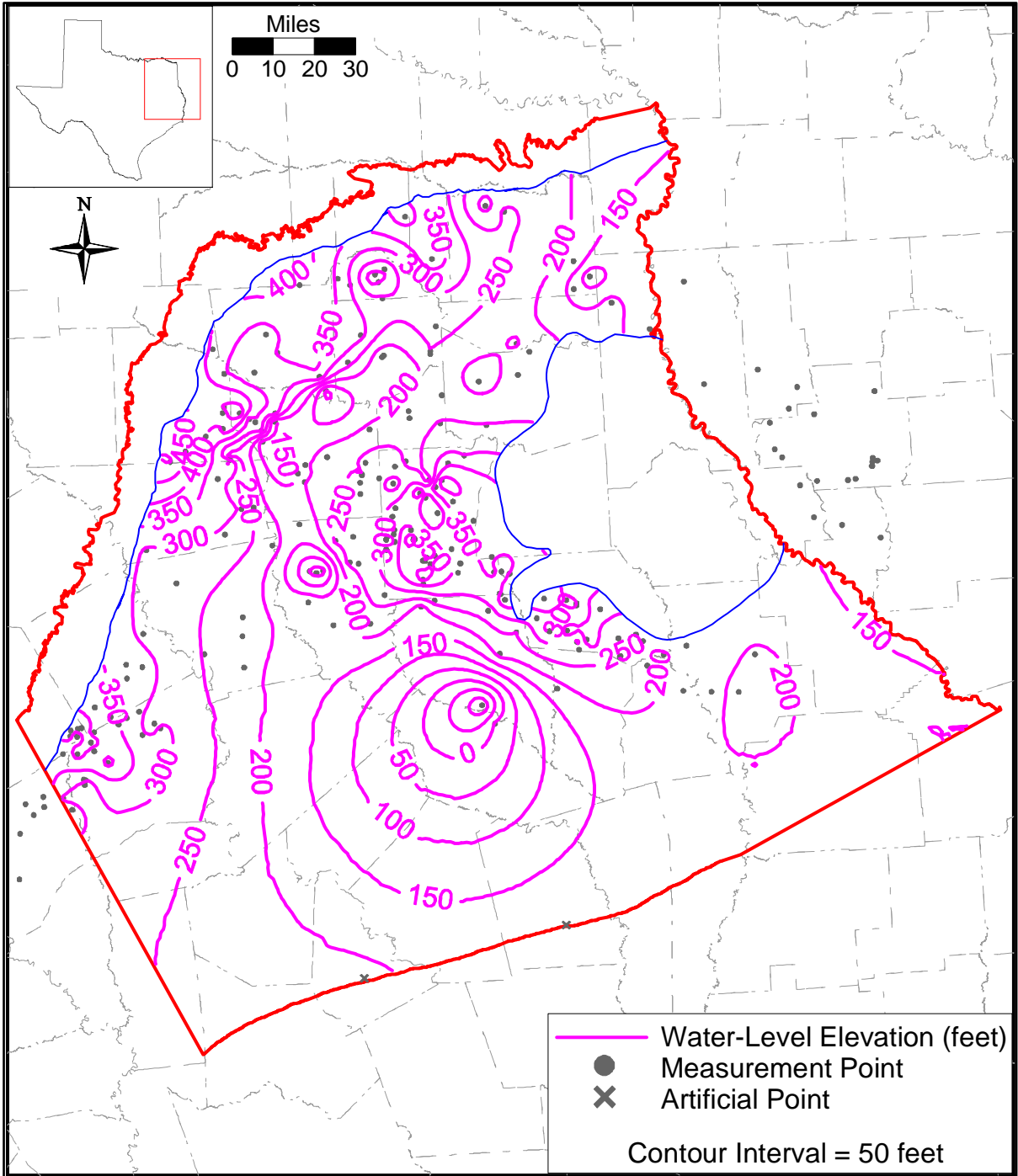


Figure 4.4.9c Water-level elevation contours for the upper Wilcox at the start of model calibration (January 1980).

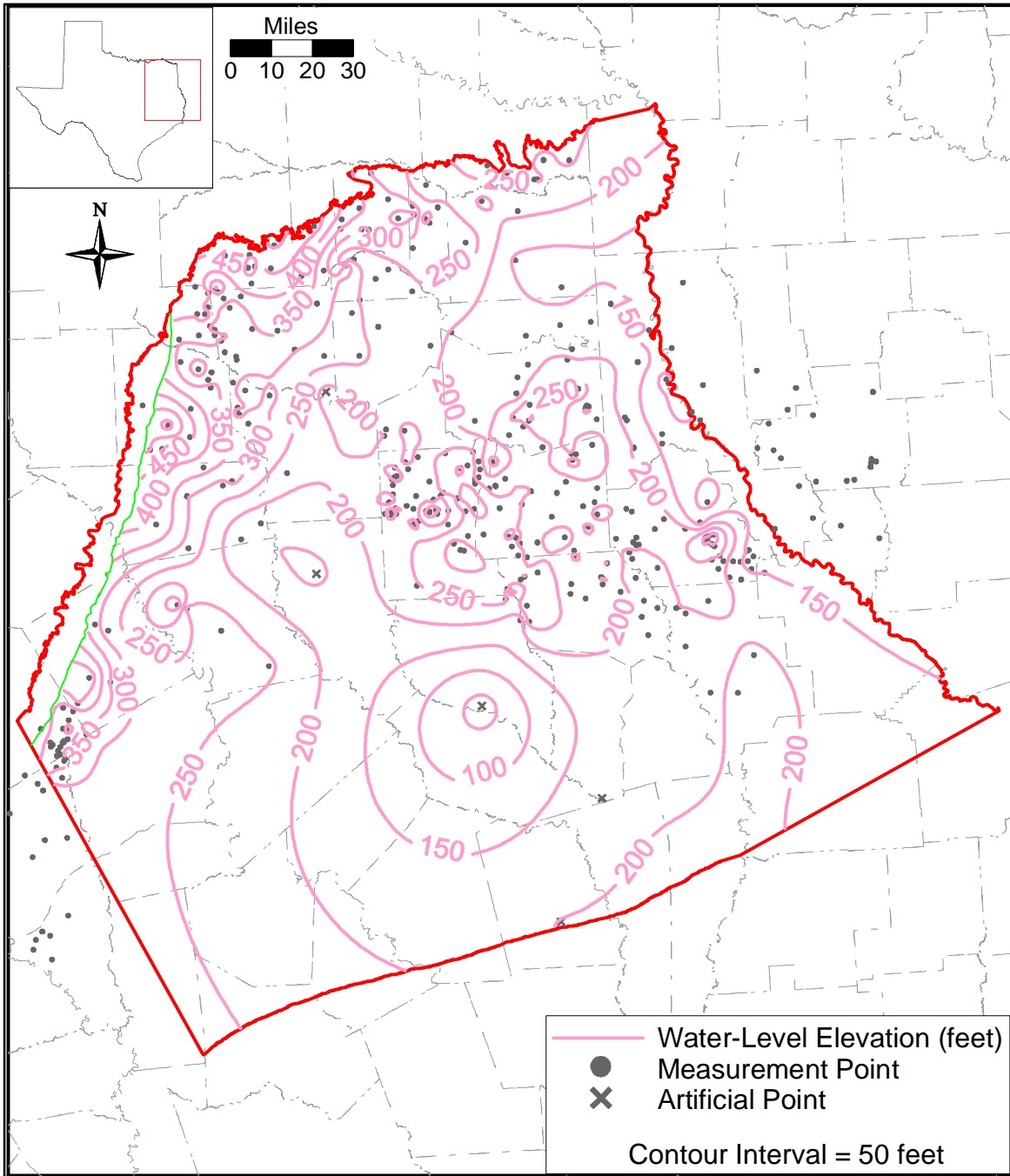


Figure 4.4.9d Water-level elevation contours for the middle Wilcox at the start of model calibration (January 1980).

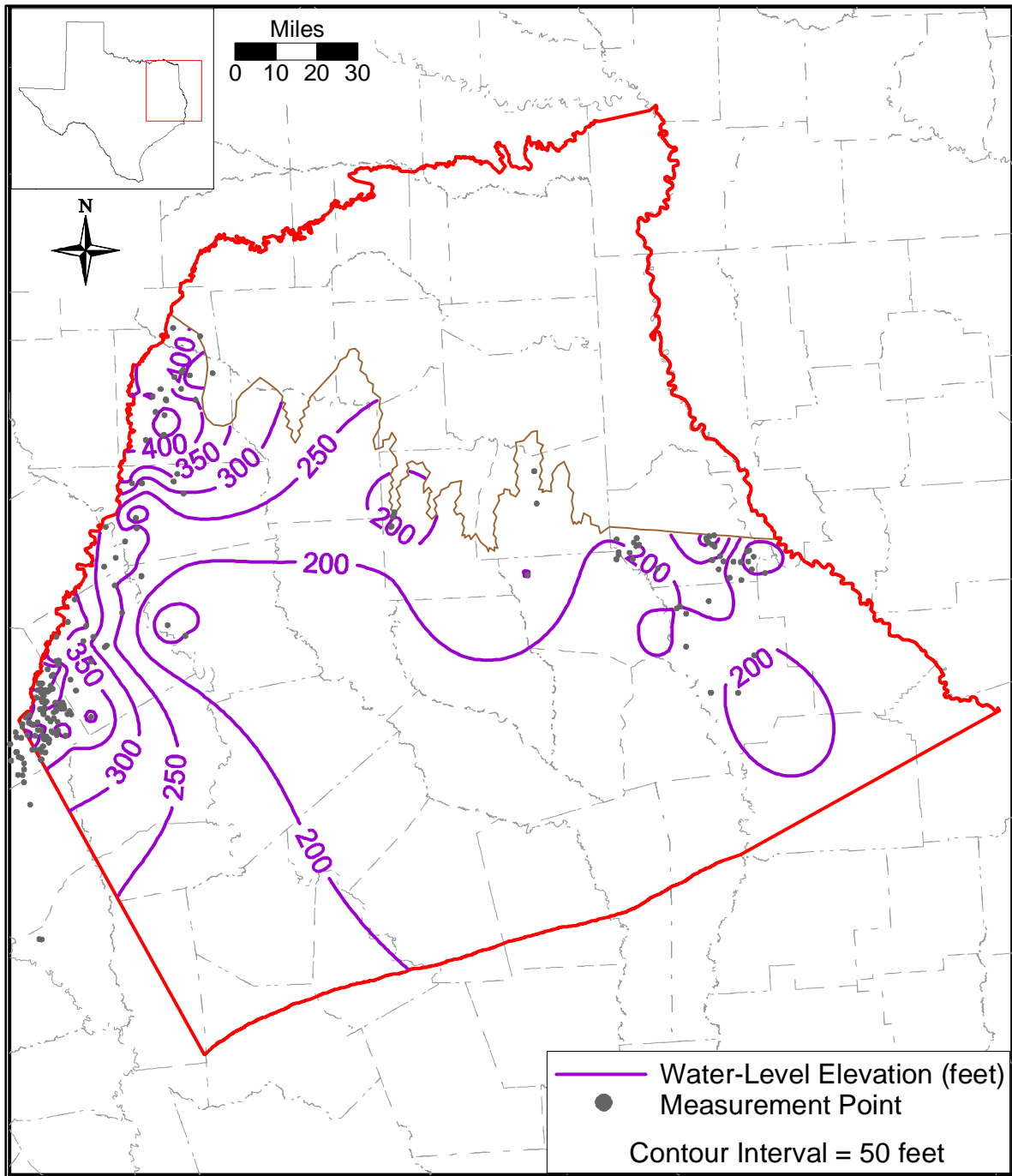


Figure 4.4.9e Water-level elevation contours for the lower Wilcox at the start of model calibration (January 1980).

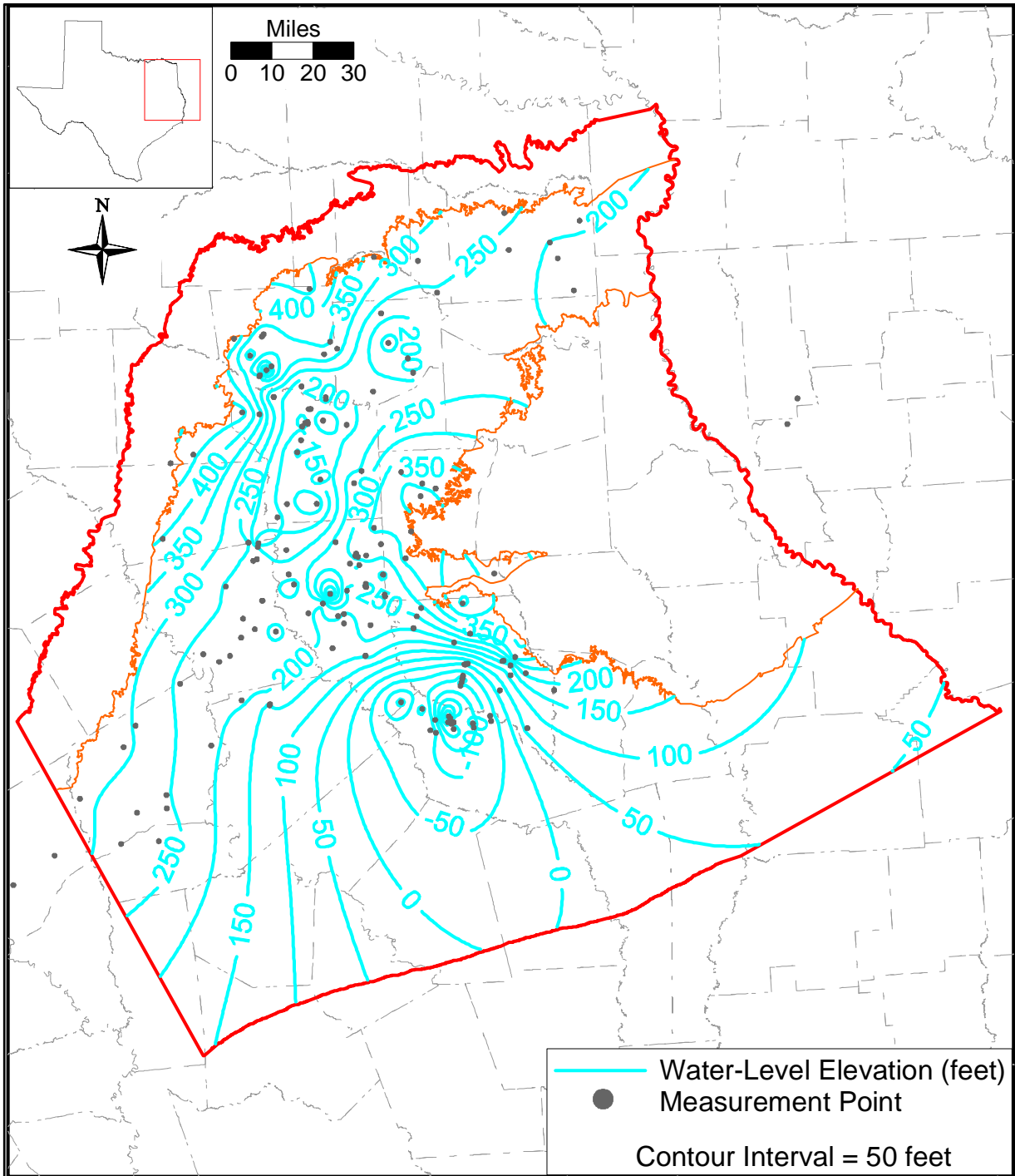


Figure 4.4.10a Water-level elevation contours for the Carrizo Sand at the end of model calibration (December 1989).

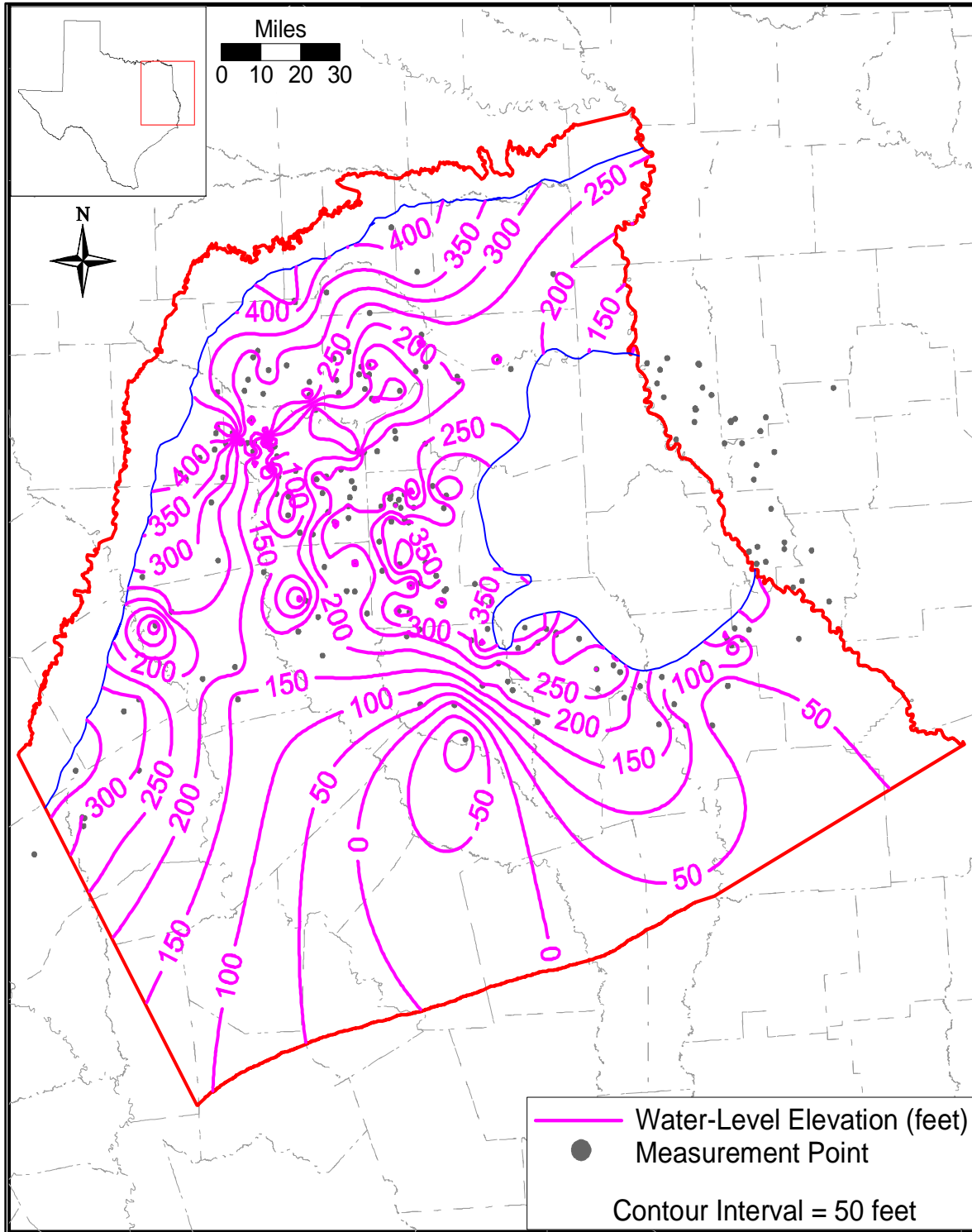


Figure 4.4.10b Water-level elevation contours for the upper Wilcox at the end of model calibration (December 1989).

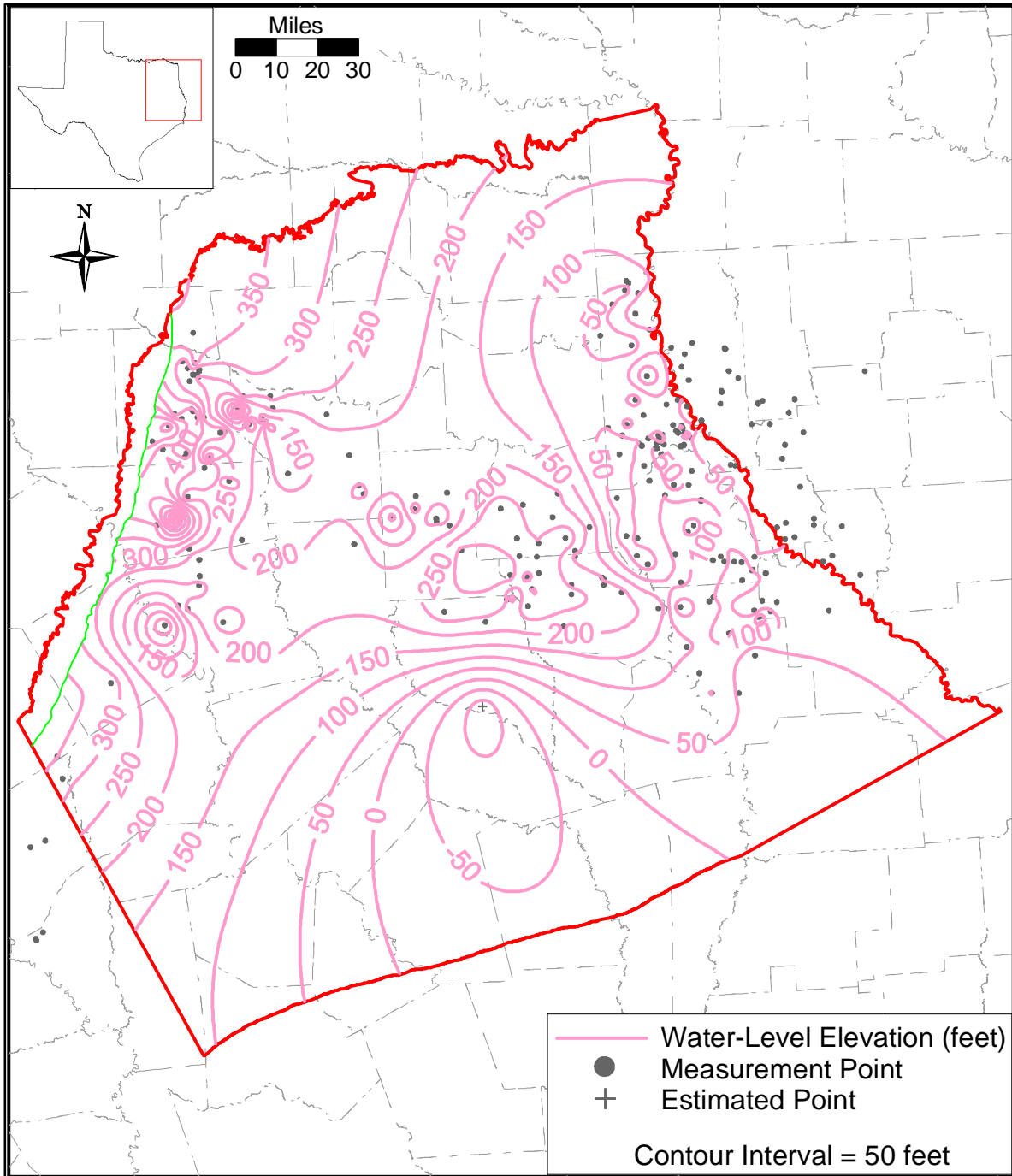


Figure 4.4.10c Water-level elevation contours for the middle Wilcox at the end of model calibration (December 1989).

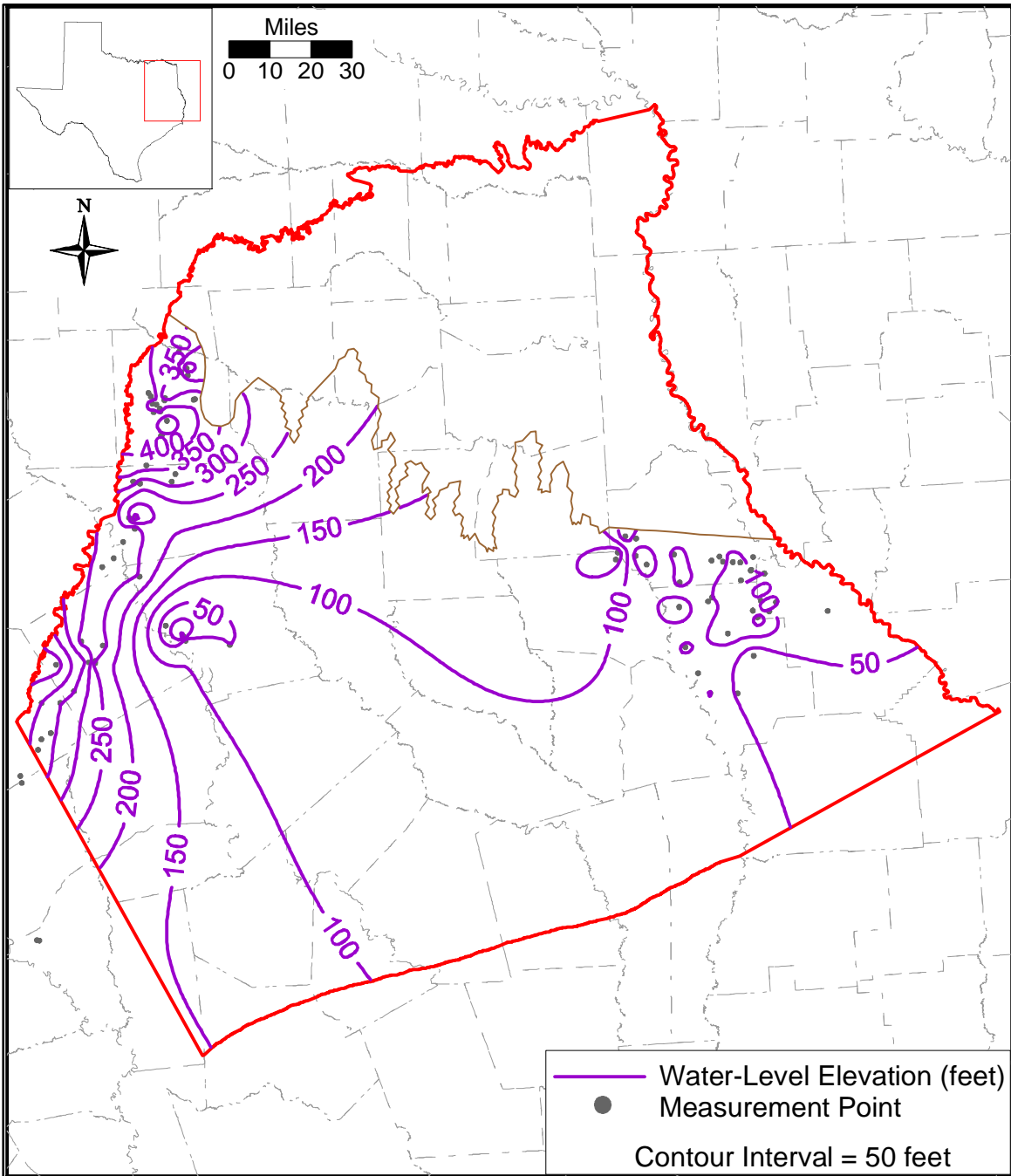


Figure 4.4.10d Water-level elevation contours for the lower Wilcox at the end of model calibration (December 1989).

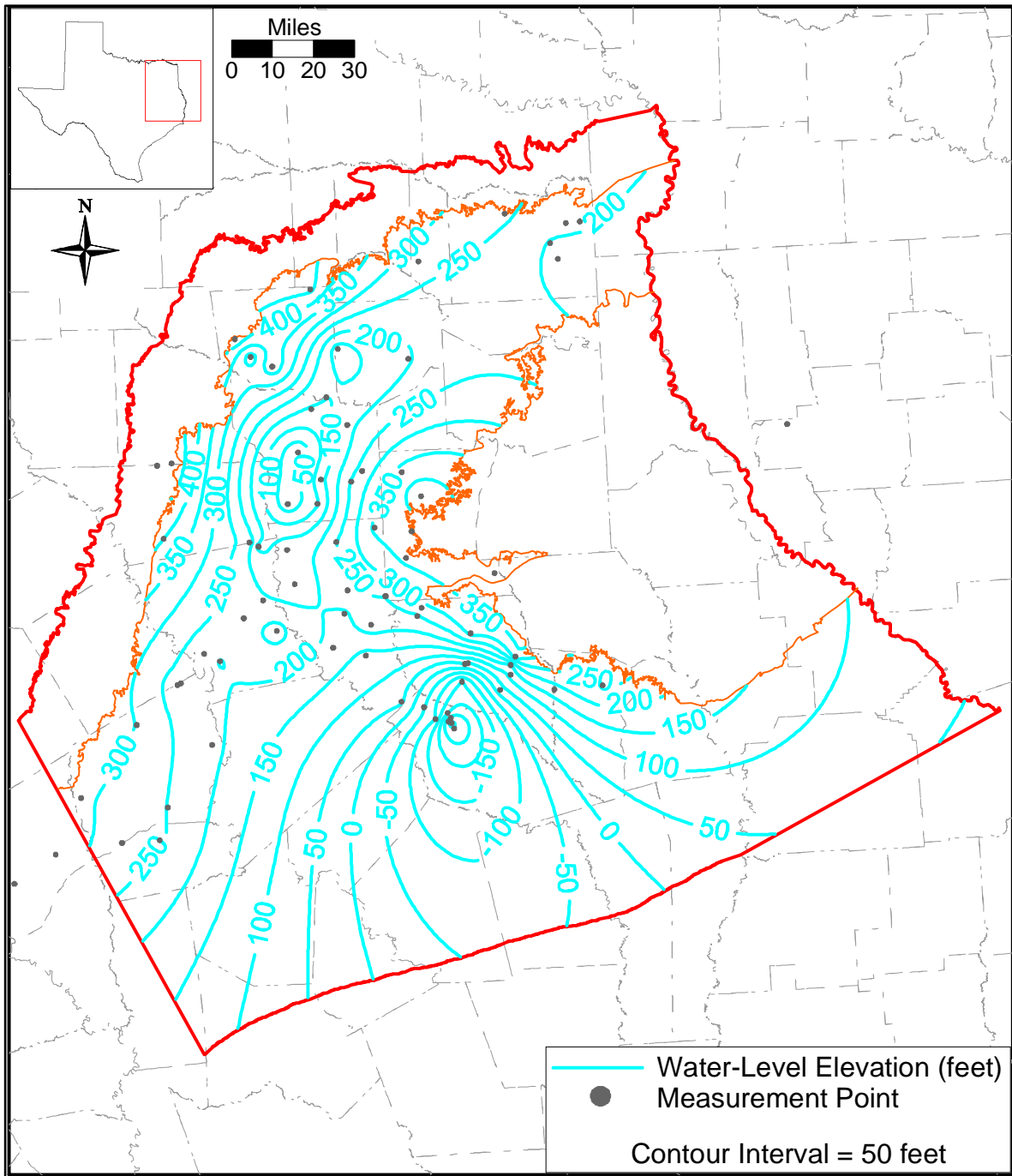


Figure 4.4.11a Water-level elevation contours for the Carrizo Sand at the end of model verification (December 1999).

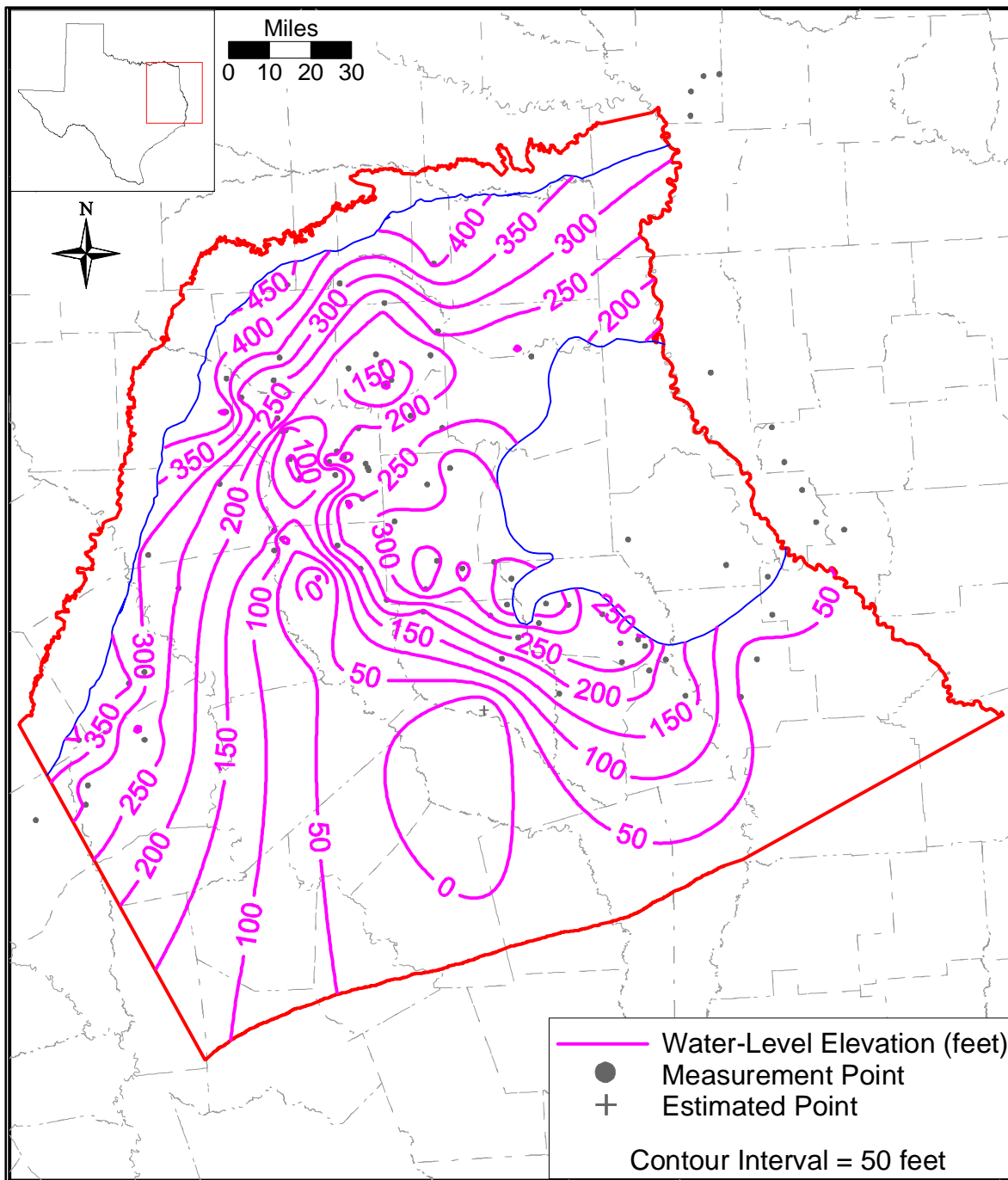


Figure 4.4.11b Water-level elevation contours for the upper Wilcox at the end of model verification (December 1999).

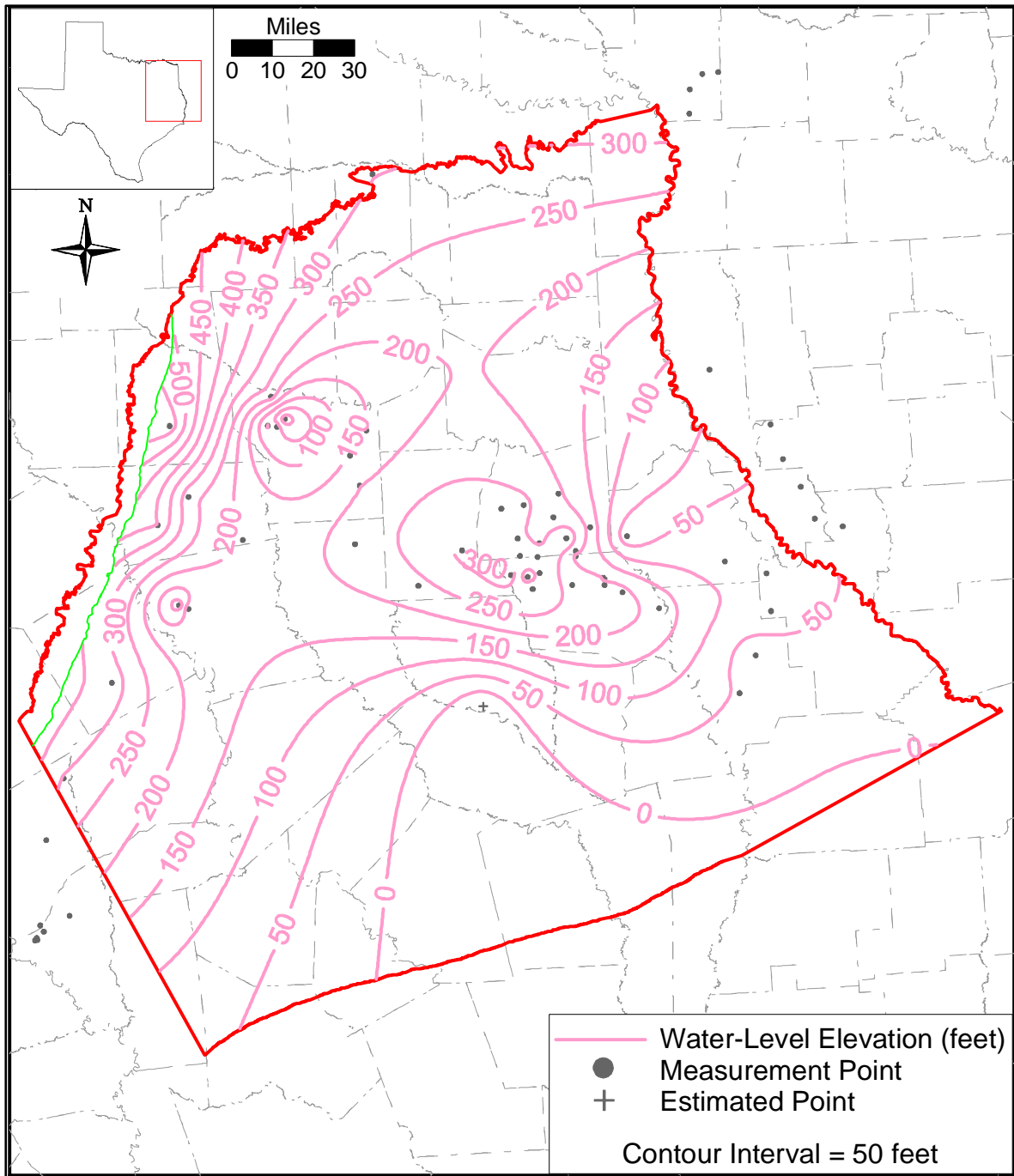


Figure 4.4.11c Water-level elevation contours for the middle Wilcox at the end of model verification (December 1999).

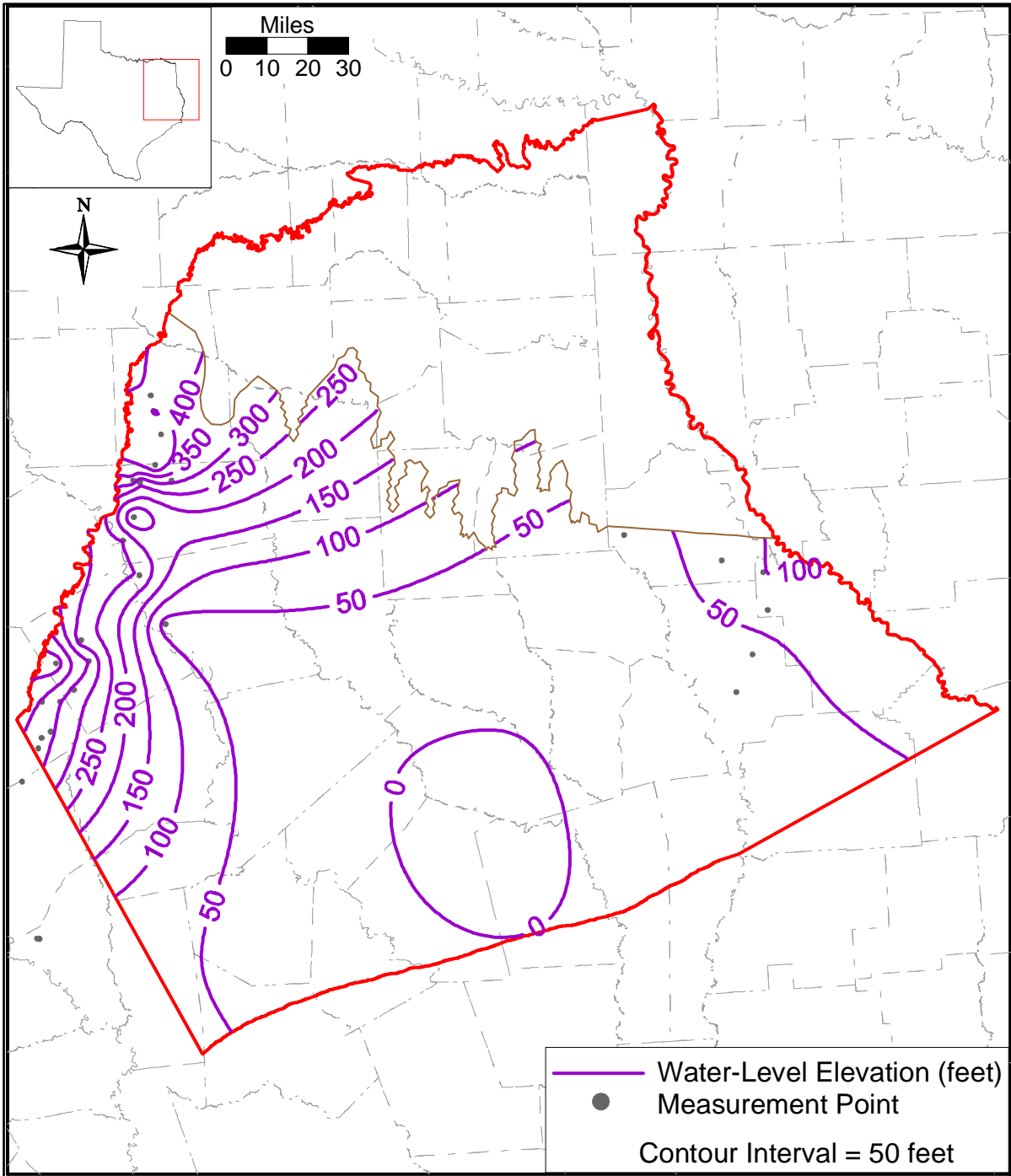


Figure 4.4.11d Water-level elevation contours for the lower Wilcox at the end of model verification (December 1999).

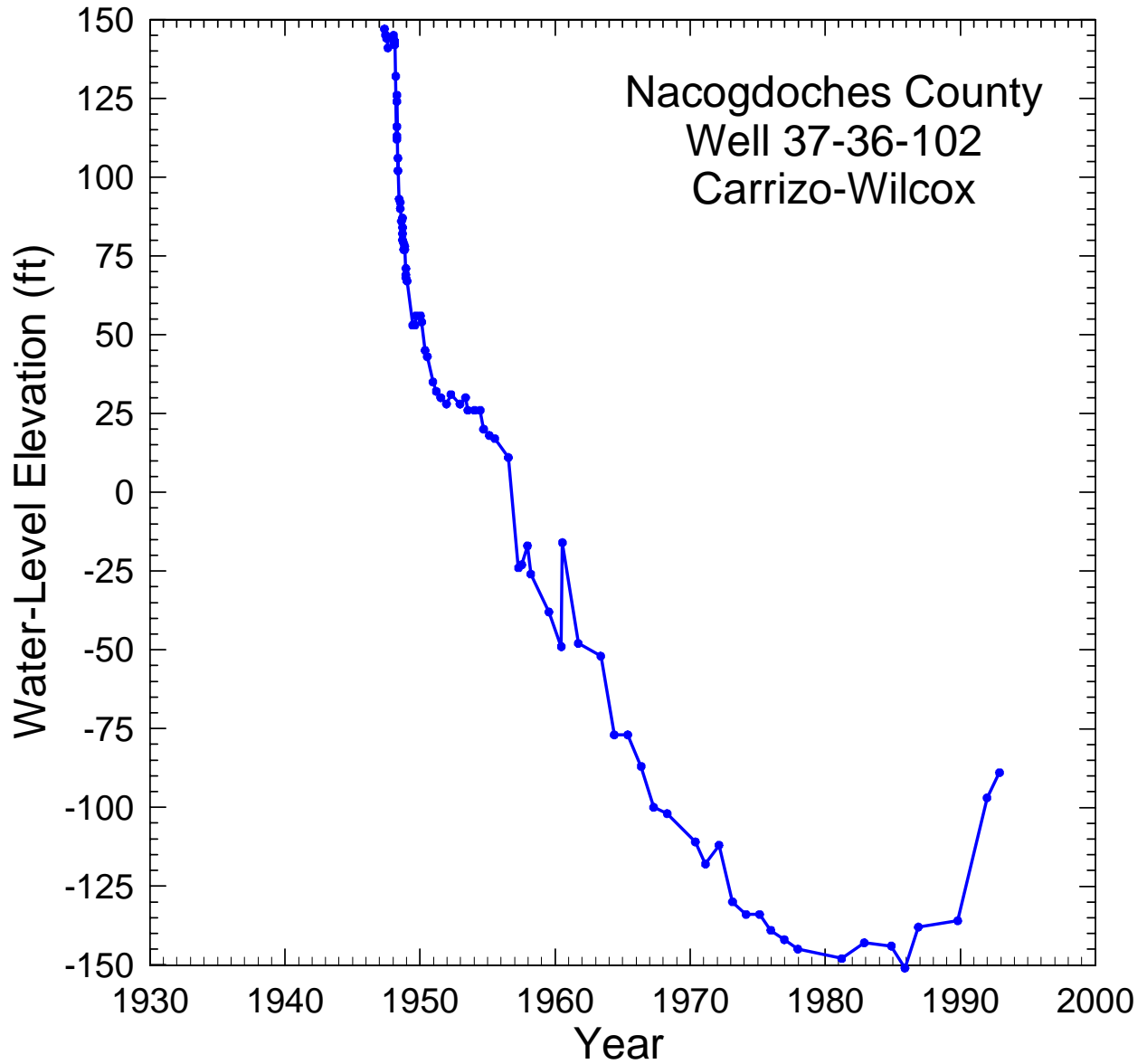


Figure 4.4.12 Long-term transient water-level elevations for well 37-36-102 completed to the Carrizo-Wilcox in Nacogdoches County.

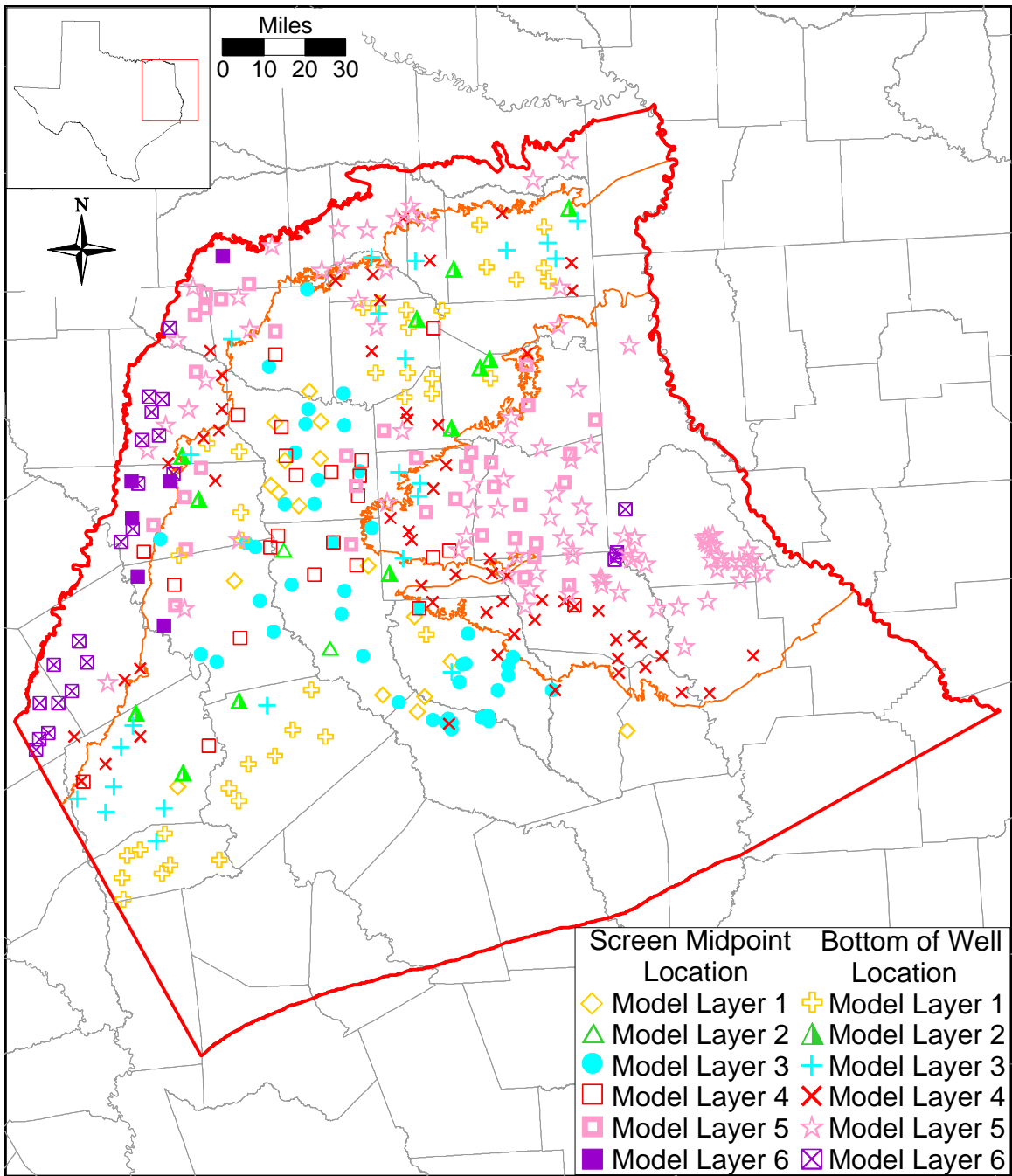


Figure 4.4.13 Model layer for locations with transient water-level data.

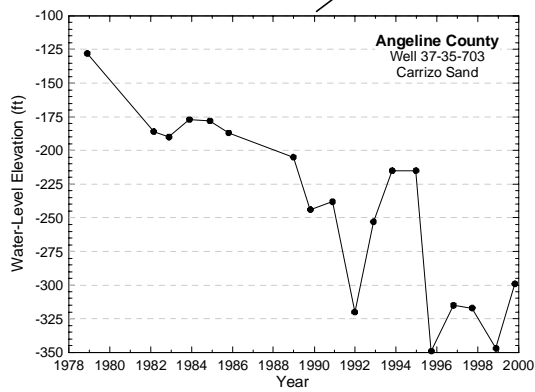
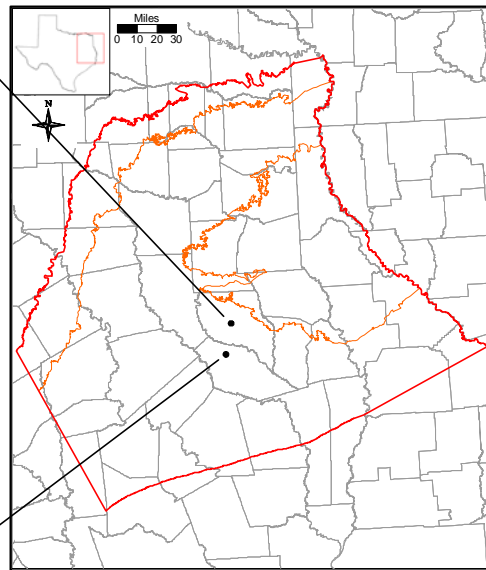
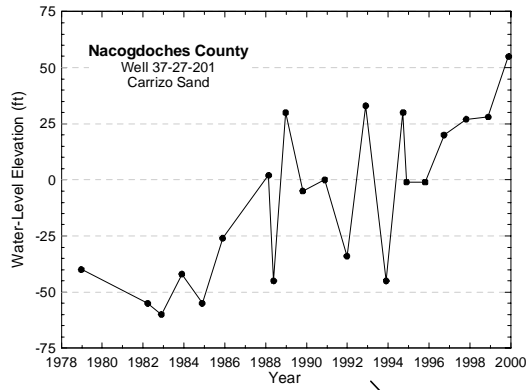


Figure 4.4.14 Example hydrographs for wells located in Nacogdoches and Angelina counties.

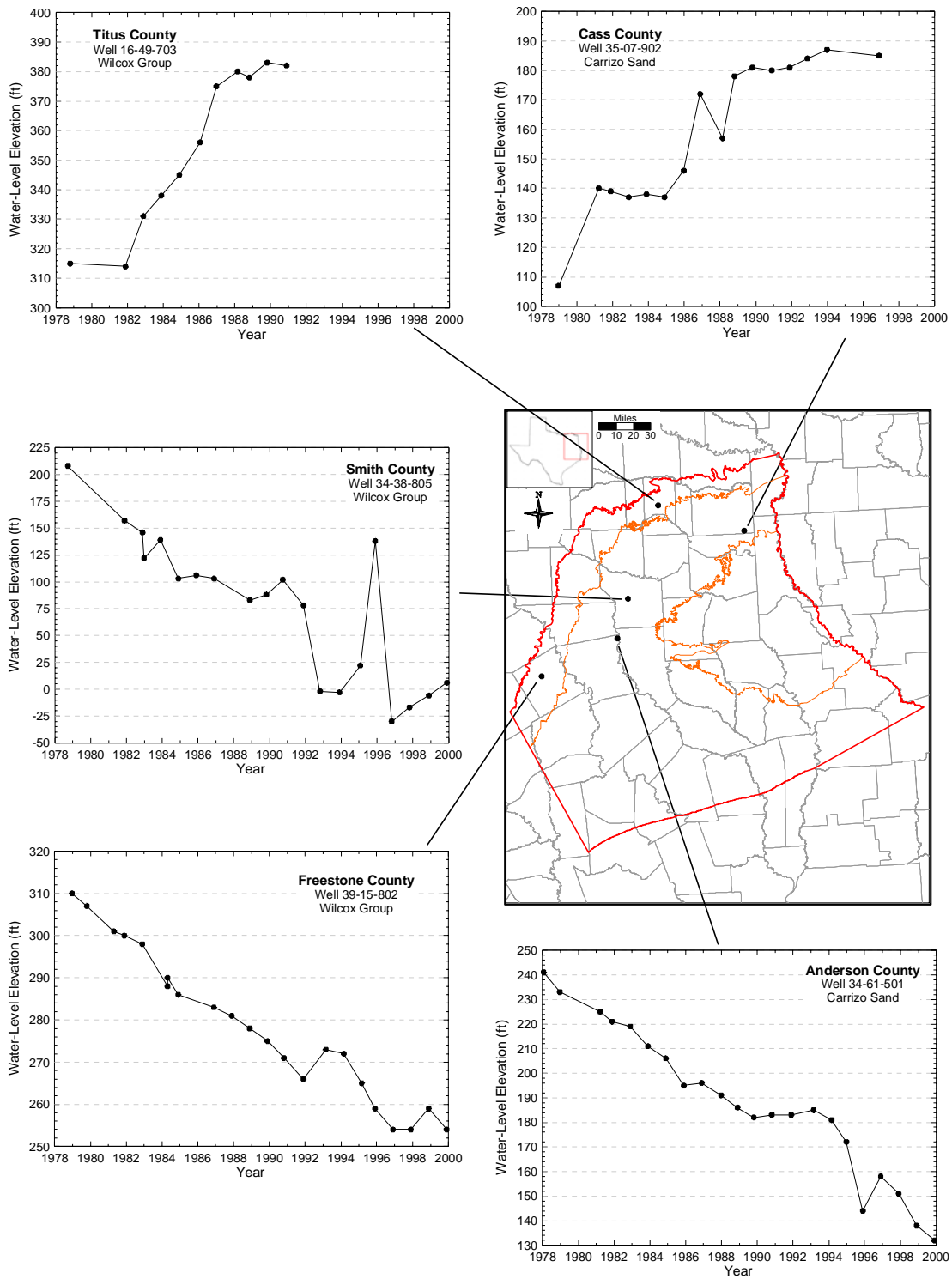


Figure 4.4.15 Example hydrographs for wells in the study area.

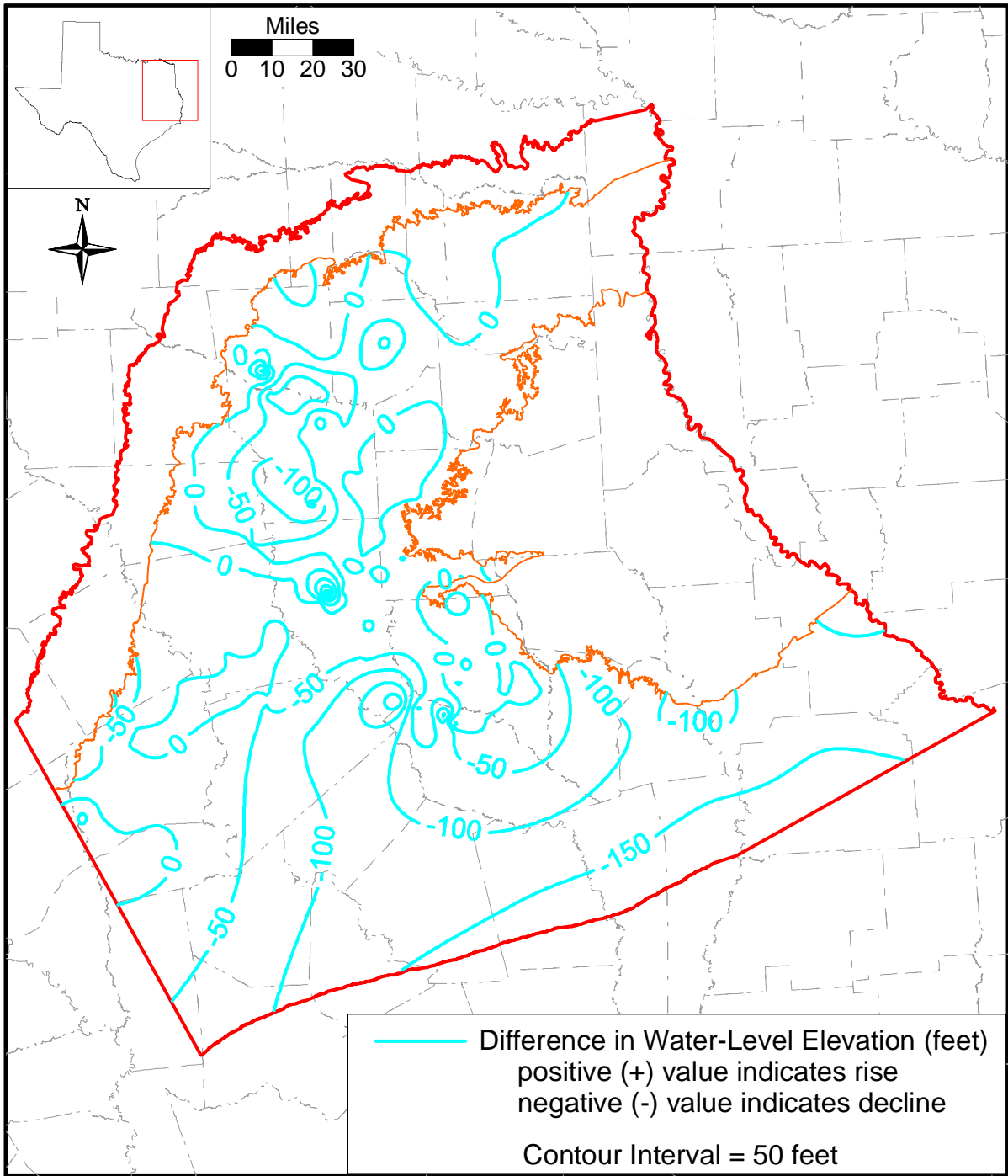


Figure 4.4.16a Water-level decline in the Carrizo Sand from the start of model calibration (January 1980) to the end of model calibration (December 1989).

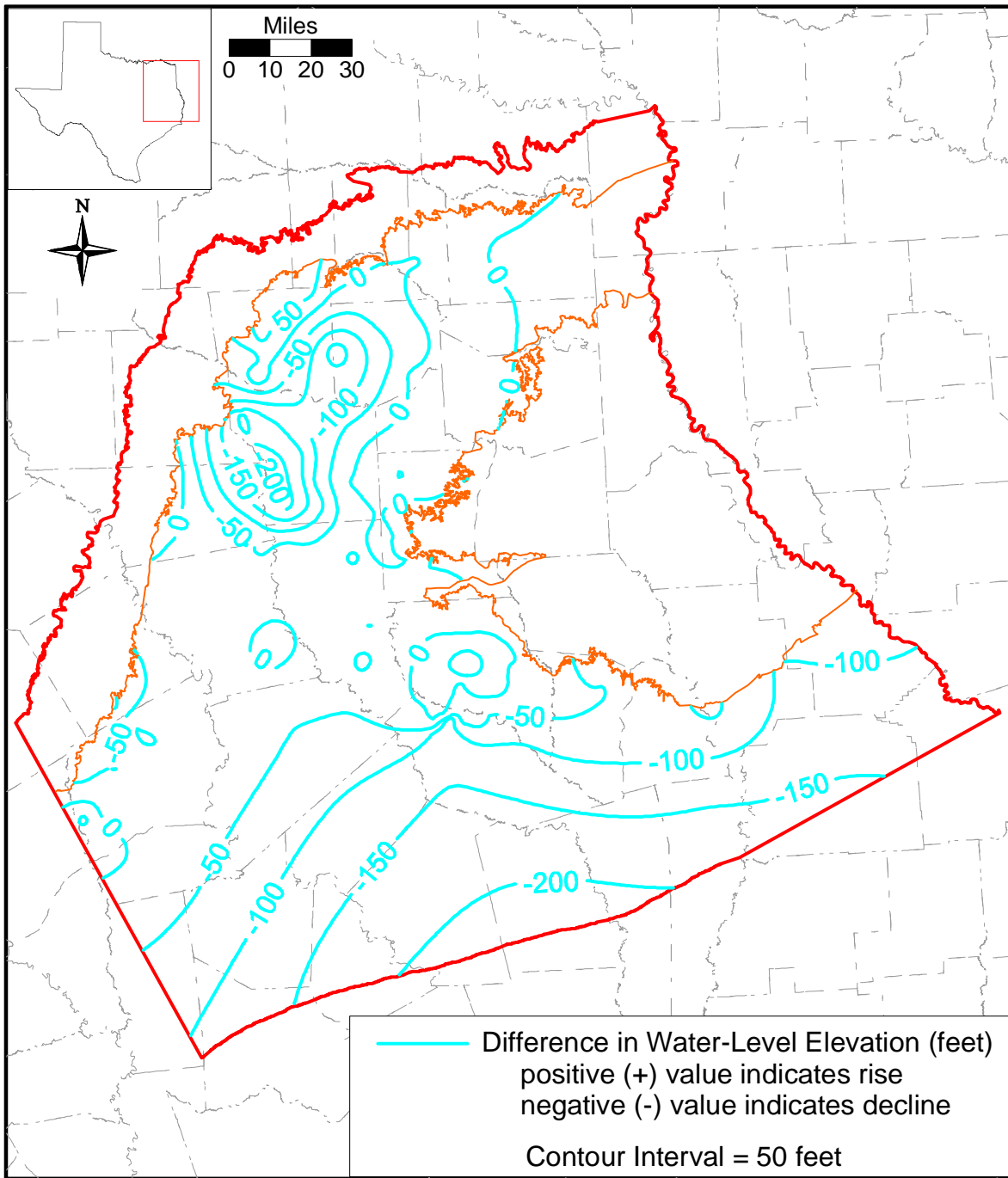


Figure 4.4.16b Water-level decline in the Carrizo Sand from the start of model calibration (January 1980) to the end of model verification (December 1999).

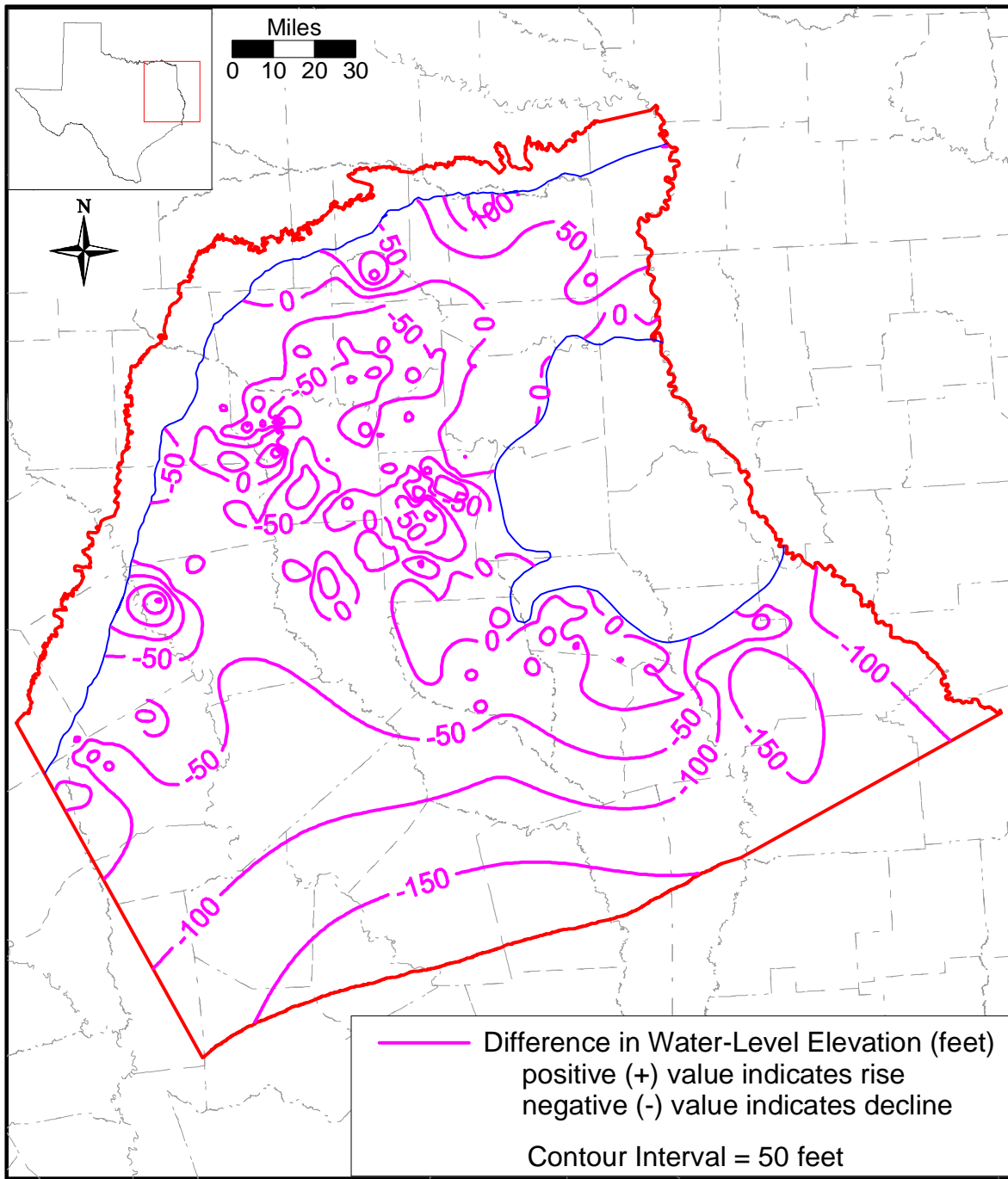


Figure 4.4.17a Water-level decline in the upper Wilcox from the start of model calibration (January 1980) to the end of model calibration (December 1989).

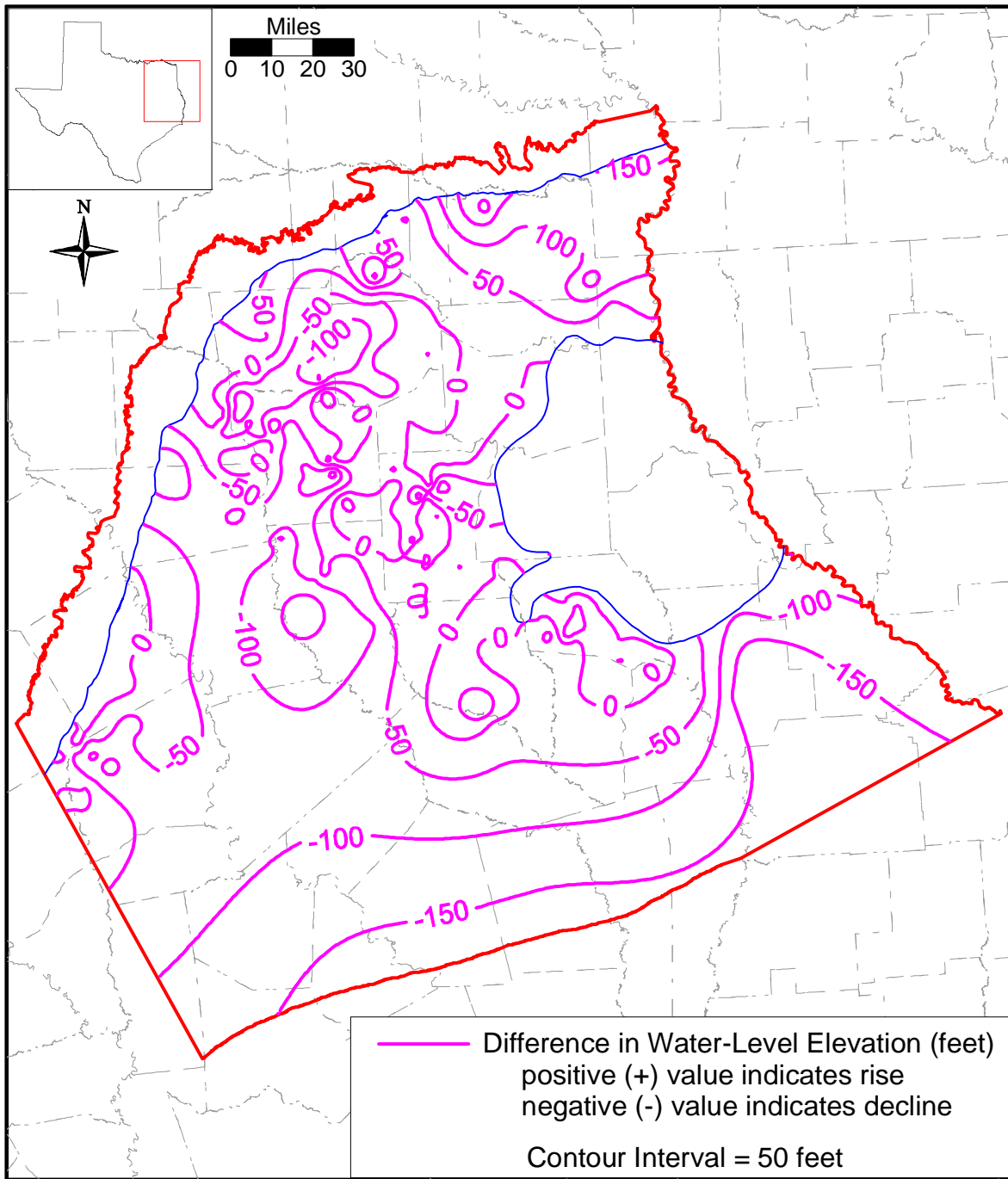


Figure 4.4.17b Water-level decline in the upper Wilcox from the start of model calibration (January 1980) to the end of model verification (December 1999).

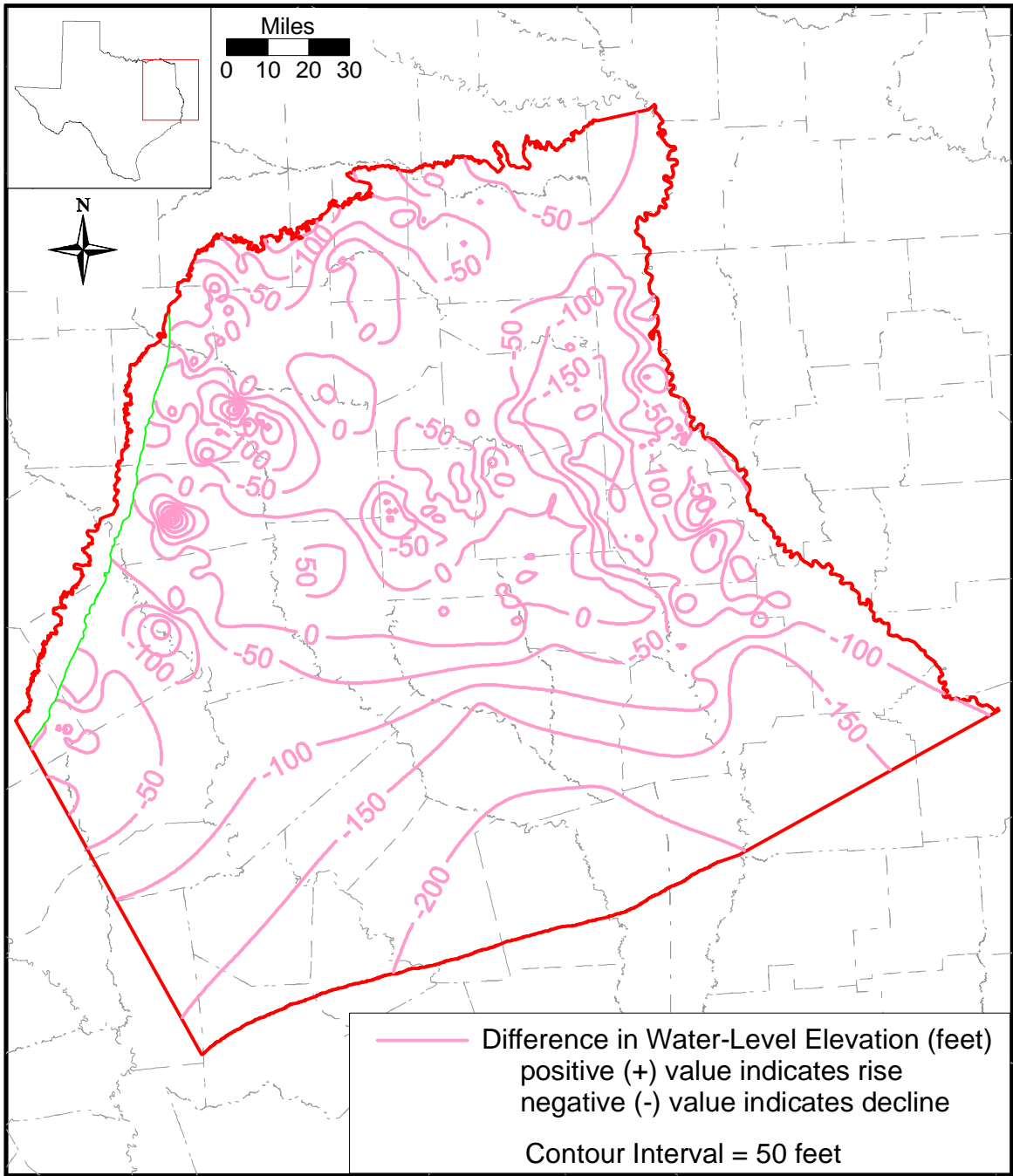


Figure 4.4.18a Water-level decline in the middle Wilcox from the start of model calibration (January 1980) to the end of model calibration (December 1989).

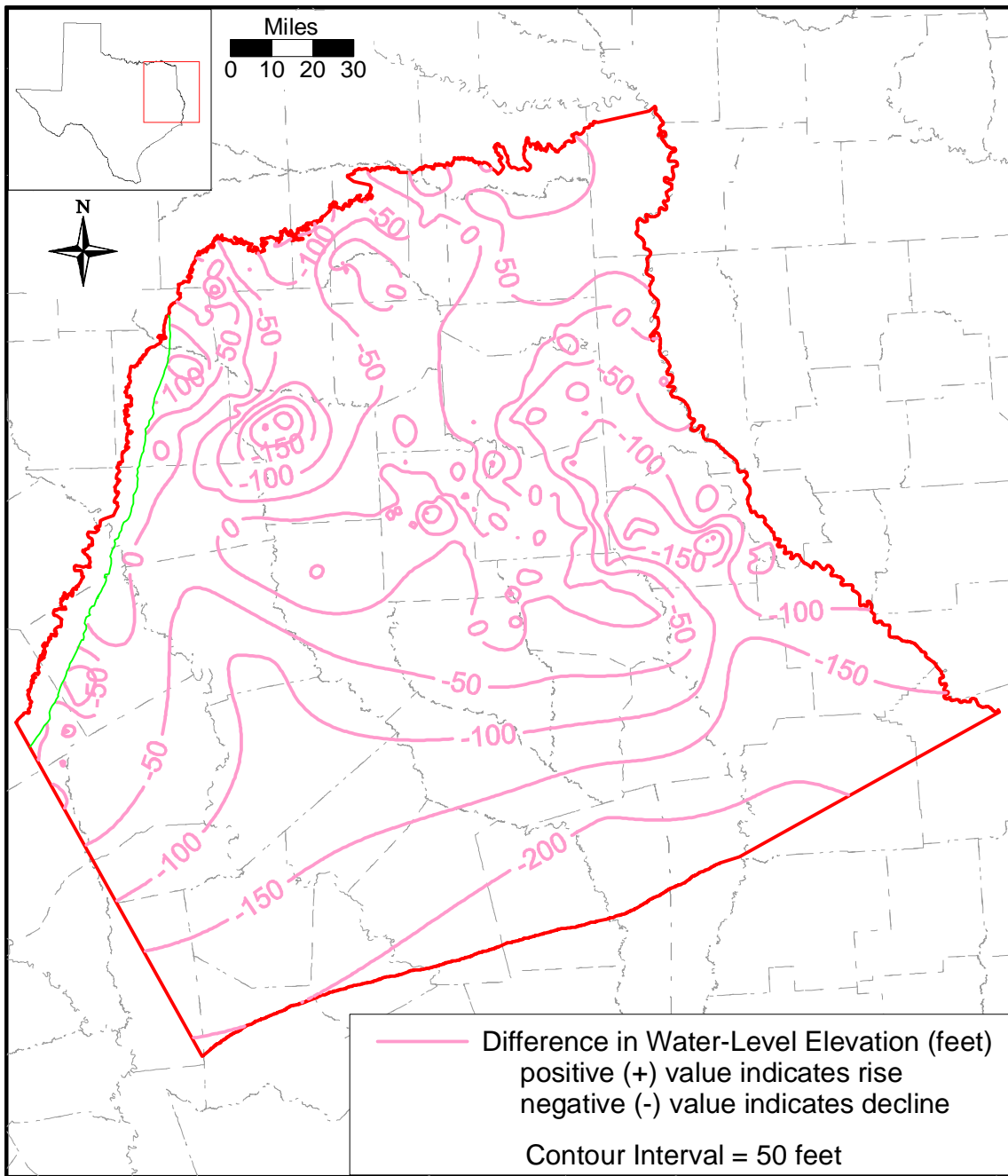


Figure 4.4.18b Water-level decline in the middle Wilcox from the start of model calibration (January 1980) to the end of model verification (December 1999).

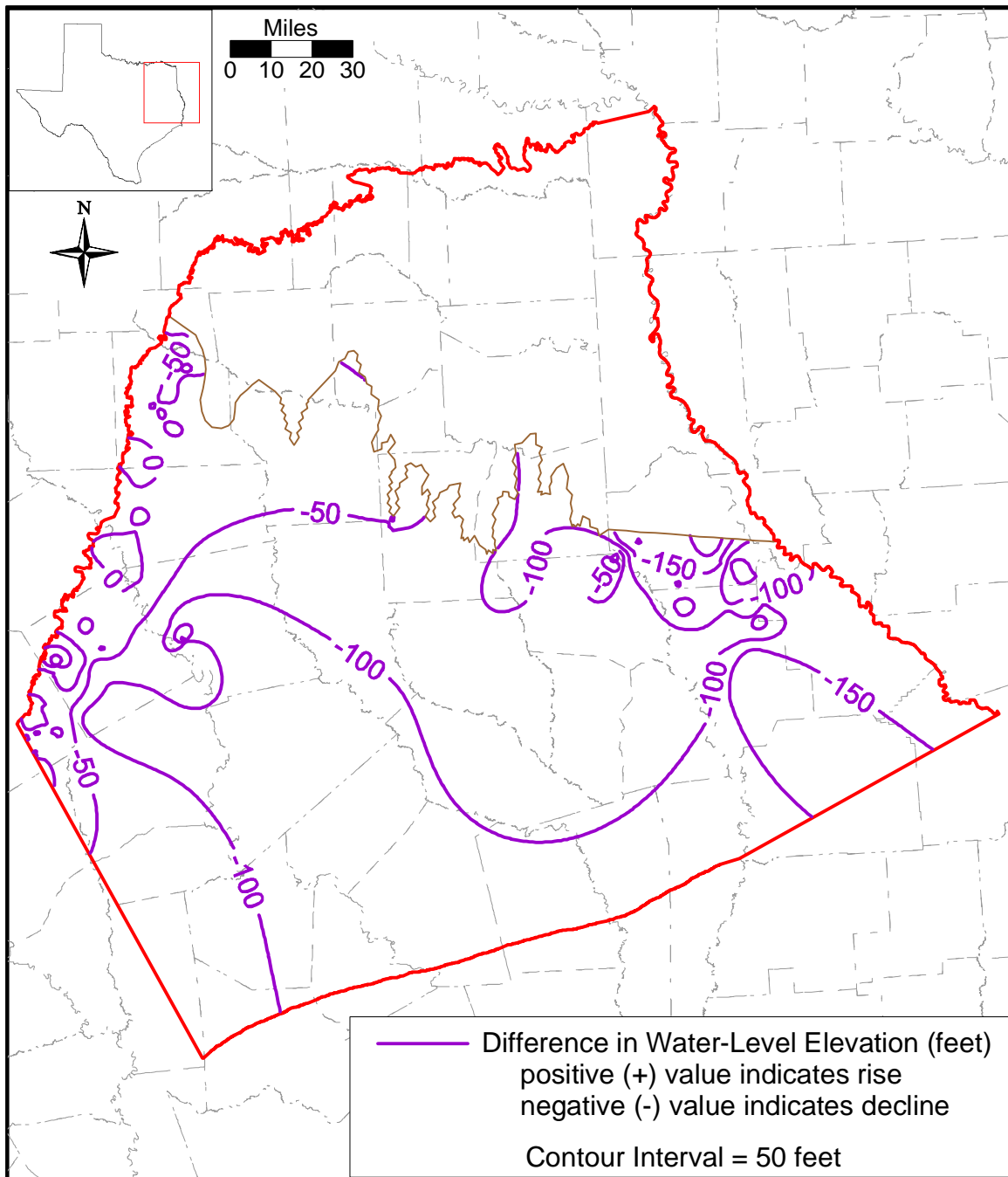


Figure 4.4.19a Water-level decline in the lower Wilcox from the start of model calibration (January 1980) to the end of model calibration (December 1989).

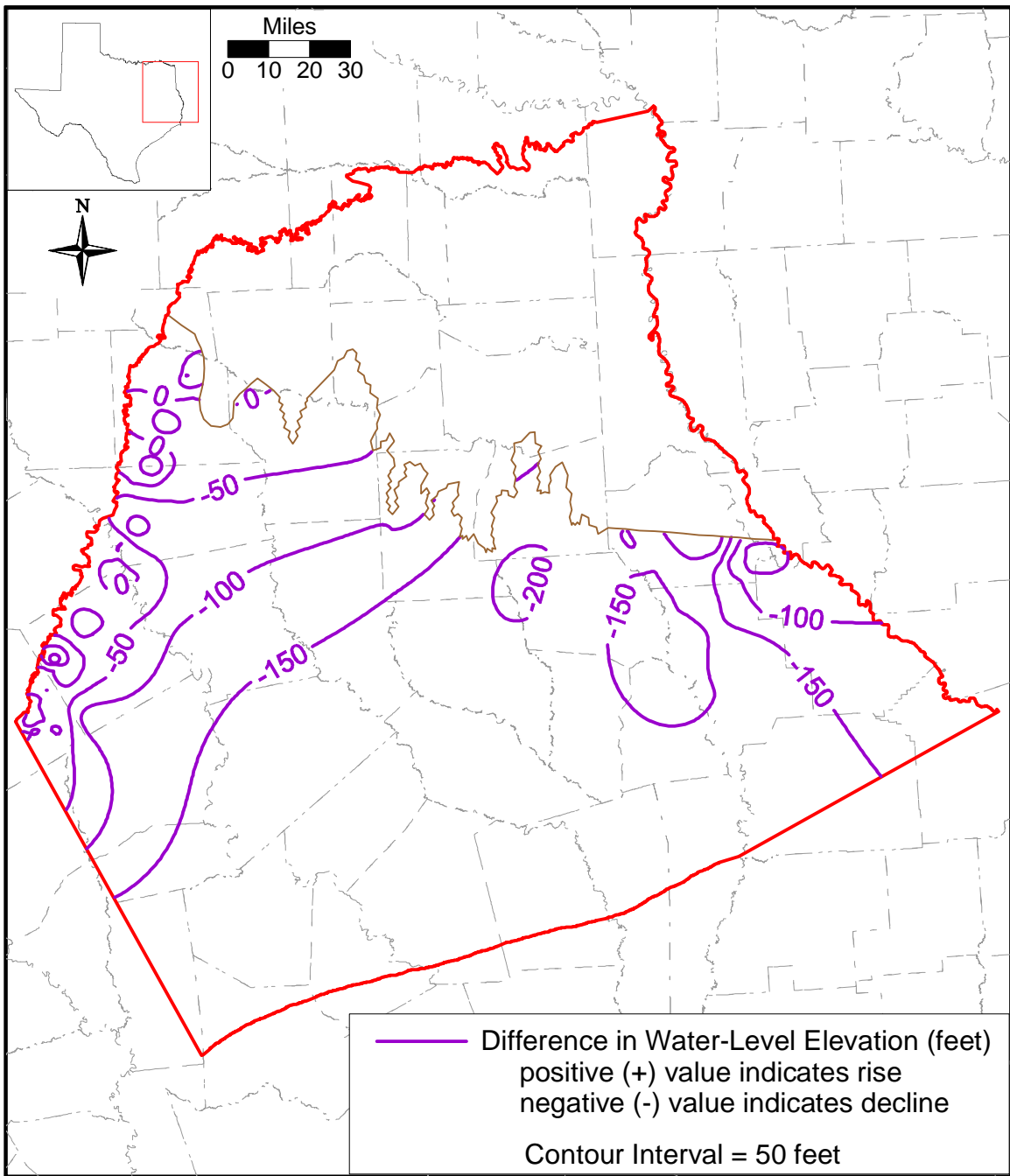


Figure 4.4.19b Water-level decline in the lower Wilcox from the start of model calibration (January 1980) to the end of model verification (December 1999).

4.5 Recharge

Recharge can be defined as water which enters the saturated zone at the water table (Freeze, 1969). Potential sources for recharge to the water table include precipitation, stream or reservoir leakage, or irrigation return flow. In the Northern Carrizo-Wilcox GAM area, recharge is conceptualized to occur as diffuse recharge in the inter-stream areas. Focused recharge may also occur in the vicinity of reservoirs and streams. However, the interaction between groundwater and surface water is determined by the degree of connection between the surface water and the groundwater. In arid areas with relatively thick unsaturated zones, surface water bodies typically lose water. In humid areas, such as the Northern Carrizo-Wilcox GAM study area, surface water bodies are more typically gaining (Scanlon et al., 2002). Any infiltration that does occur in river valleys is much more prone to being rejected by interflow to nearby surface water bodies. The great majority of the infiltration, or shallow recharge, that does occur in the outcrop is discharged through baseflow in streams or is lost to evapotranspiration in lower elevation areas where the water table is shallow (Scanlon et al., 2002).

The cleaner and more massive sands of the Carrizo and Simsboro formations have commonly been assumed to be the preferentially recharged hydrostratigraphic units in the Carrizo-Wilcox aquifer system in central and eastern Texas. This is likely the result of the formations' increased ability to move water away from the water table (Freeze, 1969) relative to other hydrostratigraphic units adjacent to and within the Carrizo-Wilcox. However, recharge has been demonstrated to be a complex function of precipitation rate and volume, soil type, water level and soil moisture, topography, and evapotranspiration (ET) (Freeze, 1969). Because of its large outcrop area and relatively high sand content, the Wilcox Group also has a good potential for diffuse recharge in the study area. When recharge rates exceed the saturated hydraulic conductivity of the underlying soils and aquifer, then the transmission capability of the underlying formation becomes a limiting factor. These conditions may be expected to occur in local areas of focused recharge or in times of exceedingly high precipitation rates.

Because precipitation, ET, and soil moisture vary as a function of time, recharge is also expected to vary as a function of time. Recharge will be highest in times of significant rainfall when soil moisture content is high. In drier times, redistribution and ET may effectively prevent significant recharge.

Several investigators have studied recharge in the Carrizo-Wilcox aquifer in Texas. These studies have been summarized by Scanlon et al. (2002) and are reproduced in Table 4.5.1. Those studies in Table 4.5.1 which are limited to the Northern Carrizo-Wilcox GAM study area are grouped as the top fifteen table entries because of their direct relevance to this study. For all studies reported by Scanlon et al. (2002), recharge rates range from a low of 0.1 inches estimated for Rains and Van Zandt counties (White, 1973) using a Darcy's Law approach to a high of 5.8 inches per year in Atascosa County (Opfel and Elder, 1978), southwest of the study area, using neutron probe measurements in the vadose zone. The range specific to the study area is similar in magnitude ranging from a low of 0.1 inches per year as described above to a high of 5 inches per year (Carrizo & Simsboro) based upon groundwater modeling in Region G (Harden & Associates, 2000). It is worth noting that the two highest reported values of recharge in the model area originate from modeling studies. This is problematic in that steady-state models are sensitive to recharge but are extremely non-unique. Transient models improve model parameter constrains and are less non-unique. However, transient models of the Carrizo-Wilcox are not extremely sensitive to recharge.

There was only one natural lake in the study area, Caddo Lake, which was drained in the 1870s and later impounded in 1914. There are 40 reservoirs with surface areas greater than ½ square mile in the study area that occur in the outcrop of the Carrizo-Wilcox or the Queen City aquifers (Figure 4.5.1). Table 4.5.2 lists the names, owners, and year completed of these reservoirs.

There are several reservoirs in the study area that intersect one or more of the active Carrizo-Wilcox aquifer outcrop grid cells in the GAM area. Figure 4.5.2 shows the lake stage elevations of three of the reservoirs for the historical simulation period from 1980 to 1999. Because they are located in outcrop areas, these reservoirs provide potential areas of focused recharge to the underlying aquifers. Figure 4.5.2 shows that the reservoirs generally have stages that do not vary greatly over the time period of interest.

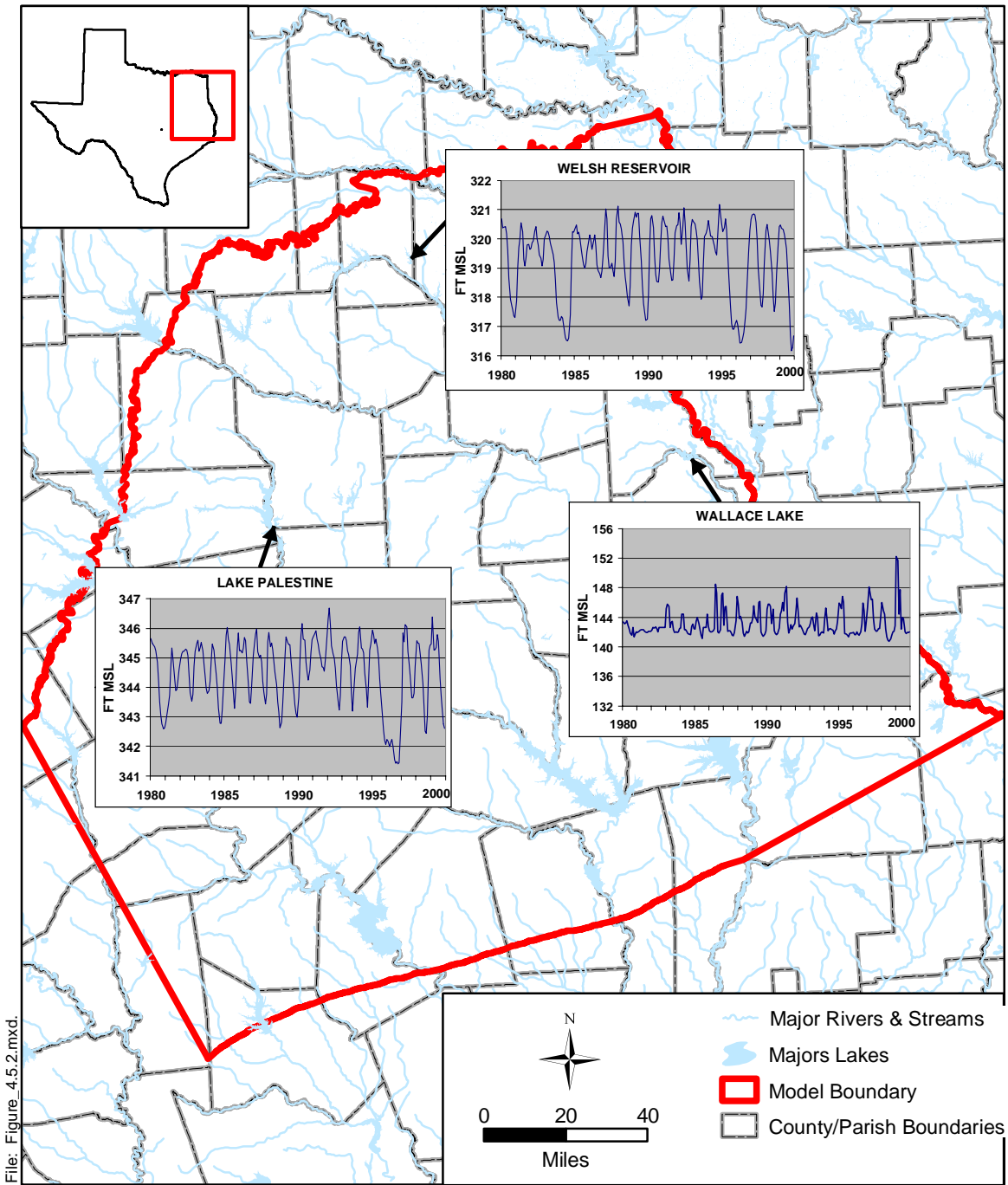
Table 4.5.1 Review of recharge rates for the Carrizo-Wilcox aquifers in Texas (after Scanlon et al., 2002).

Major Aquifer	Location (County/Area)	Aquifer	Recharge rate (mm/yr)	Recharge rate (in/yr)	Total recharge (af/yr)	Reference	Technique
Carrizo Wilcox	Sabine, San Augustine	undifferentiated	50.8	2.0		Anders, 1967	Darcy's Law
	Sabine, San Augustine	undifferentiated	25.4	1.0		Anders, 1967	baseflow discharge
	Camp, Franklin, Morris, Titus	Carrizo Wilcox			12,000	Broom et al., 1965	baseflow discharge
	Harrison	Cypress	7.9	0.3	15,000	Broom and Myers, 1966	Darcy's Law
	Harrison	Cypress	7.9	0.3	40,000	Broom and Myers, 1966	baseflow discharge
	Wood	Carrizo	12.7	0.5	3,000	Broom, 1968	Darcy's Law
	Freestone	Calvert Bluff sands	100			Dutton, 1990	soil water budget
	Bastrop, Lee, Milam	Simsboro, Carrizo	51-102	2.0-4.0		Dutton, 1999	groundwater modeling
	Bastrop	Carrizo, Wilcox sand	38	1.5		Follett, 1970	Darcy's Law
	Bastrop, Lee, Milam, Robertson, Falls, Limestone, Freestone, Navarro	Carrizo, Simsboro	76-127	3.0-5.0		Harden and Associates, 2000	groundwater modeling
	Bastrop, Lee, Milam, Robertson, Falls, Limestone, Freestone, Navarro	Calvert Bluff, Hooper	12.7	0.5		Harden and Associates, 2000	groundwater modeling
	Rusk	Carrizo	<25.4	<1.0		Sandeen, 1987	Darcy's Law
	Navarro	Carrizo Wilcox	12.7	0.5		Thompson, 1972	estimate
	Caldwell, Bastrop, Lee, Milam, Robertson, Limestone, Freestone	undifferentiated	25.4	1.0		Thorkildsen and Price, 1991	groundwater modeling
	Rains, Van Zandt	Carrizo Wilcox	3	0.1	5,000	White, 1973	Darcy's Law
	Atascosa, Frio	Carrizo sand	45.7			Alexander and White, 1966	¹⁴ C, Darcy's Law
	Winter Garden area	undifferentiated	5-127			LBG-Guyton & Assoc. and HDR, 1998	modeling, water budget
	Bexar	Hooper, Simsboro, Calvert Bluff	45.7			HDR Engineering, 2000	groundwater modeling
	Winter Garden area	undifferentiated			100,000	Klemm et al., 1976	groundwater modeling
	Bastrop, Lee, Fayette	undifferentiated	25.4	1.0		Thorkildsen et al., 1989	groundwater modeling
Atascosa, Bexar, Dimmit, Frio, Gonzales, Guadalupe, Medina, Uvalde, Wilson, Zavala	undifferentiated			25,000	Turner et al., 1960	Darcy's Law	

Table 4.5.2 Characteristics of reservoirs in study area.

Reservoir	Reservoir Name	Owner	Date Impounded
1	Black Bayou Lake	State of Louisiana	1955
2	Brandy Branch Cooling Pond	Southwestern Electric Power Company	1983
3	Caddo Lake	Caddo Levee District	1914
4	Cedar Creek Reservoir	Tarrant County WCID #1	1965
5	Clear Lake	*	*
6	Cross Lake	City of Shreveport	1925
7	Eastman Lakes	*	*
8	Ellison Creek Reservoir	Lone Star Steel Company	1943
9	Fairfield Lake	Texas Utilities Generating Company	1969
10	Forest Grove Reservoir	Texas Utilities Generating Company	1980
11	Johnson Creek Reservoir	Southwestern Electric Power Company	1961
12	Lake Athens	Athens Municipal Water Authority	1962
13	Lake Bob Sandlin	Titus County FWSD #1	1977
14	Lake Cherokee	Cherokee Water Company	1948
15	Lake Cypress Springs	Franklin County Water District & T.W.D.B.	1970
16	Lake Fork Reservoir	Sabine River Authority	1979
17	Lake Gladewater	City of Gladewater	1952
18	Lake Hawkins	Wood County	1962
19	Lake Holbrook	Wood County	1962
20	Lake Jacksonville	City of Jacksonville	1957
21	Lake Limestone	Brazos River Authority	1978
22	Lake Monticello	Texas Utilities Generating Company	1972
23	Lake Murvaul	Panola County GWSD #1	1957
24	Lake Nacogdoches	City of Nacogdoches	1976
25	Lake O' the Pines	U.S. Army Corps of Engineers	1957
26	Lake Palestine	Upper Neches River Authority	1962
27	Lake Quitman	Wood County	1962
28	Lake Striker	Angelina-Nacogdoches WCID #1	1957
29	Lake Tyler/Lake Tyler East	City of Tyler	1966
30	Lake Winnsboro	Wood County	1962
31	Martin Lake	Texas Utilities Generating Company	1974
32	Pinkston Reservoir	City of Center	1977
33	Richland-Chambers Reservoir	Tarrant County WCID #1	1987
34	Sibley Lake	State of Louisiana	1962
35	Smithport Lake	State of Louisiana	*
36	Toledo Bend Reservoir	Sabine River Authority	1966
37	Trinidad Lake	*	1925
38	Wallace Lake	U.S. Army Corps of Engineers	1946
39	Welsh Reservoir	Southwestern Electric Power Company	1975
40	Wright Patman Lake	U.S. Army Corps of Engineers	1956

*Information unavailable



File: Figure_4.5.2.mxd.

Source: Upper Neches River Authority (2001), Southwestern Electric Power Co. (2001), U.S. Army Corps of Engineers (2001)

Figure 4.5.2 Hydrographs for select reservoirs in the study area.

4.6 Natural Aquifer Discharge

Under steady-state conditions representative of predevelopment conditions, groundwater flow in the aquifer is elevation driven from the inter-stream higher elevation outcrops to the lower elevation stream valleys and to a lesser degree the confined sections of the aquifer. In the predevelopment condition, recharge occurring as a result of diffuse and focused recharge will be balanced by discharge in stream valleys and springs, and through cross-formational flow. Under predevelopment conditions, it is expected that most streams in the study area were gaining streams. Thorkildsen et al. (1989) reported that the Colorado River and its major tributaries received a significant portion of their natural discharge from the Carrizo-Wilcox aquifer. Dutton (1999) reports that Carrizo-Wilcox discharge supplies some baseflow to both the Colorado and Brazos rivers.

There has been a large number of stream gain/loss studies performed in the Carrizo-Wilcox in Texas. Slade et al. (2002) summarized the results of 366 gain/loss studies involving 249 unique reaches of streams throughout Texas since 1918. They documented 12 individual gain/loss studies in the model area with 9 in the Carrizo-Wilcox outcrop. Studies have been performed on the Sabine River, Bowles Creek (Nueces River Basin), Grays, Little Cypress, and Sugar creeks (Red River Basin), and Lake Fork Creek (Sabine River Basin), and Big and Little Elkhart creeks (Trinity River Basin). Figure 4.6.1 shows the locations and survey numbers of the gain/loss studies in the model area. Table 4.6.1 provides the characteristics of the gain/loss studies reported by Slade et al. (2002). The survey numbers in Figure 4.6.1 correspond to the survey numbers in Table 4.6.1.

Three studies were performed on the Sabine River (surveys 345, 346, and 347). Surveys 345 and 346 were performed in August and September of 1981 and both indicate gaining river base flow conditions with average gains of 592 and 3,847 acre feet per year per mile of stream, respectively. Survey 347 was performed along a 268-mile stretch of the Sabine in September of 1963. The survey average gain for the Sabine River was 564 acre feet per year per mile. Surveys 243, 244, 245, and 249 were performed in 1964 in tributary creeks to the Red River. Average gain/loss estimates range from a slightly losing -6.5 acre feet per year per mile to gaining 431 acre feet per year per mile. Survey 249 was likely performed in the Queen City outcrop. In 1942, a 6.5-mile length of Bowles Creek (Neches River Basin) was surveyed and

found to be gaining 335 acre feet per year per mile. The only strongly losing survey was performed on Lake Fork Creek (Sabine River Basin) in August and September of 1981. This survey (No. 342) estimated an average loss of -1,177 acre feet per year per mile over a 1.6 mile stretch of stream. This estimate appears anomalous. The available gain/loss surveys are consistent with our assumption that most major rivers and streams in the study area are gaining from the Carrizo-Wilcox aquifer in the outcrop.

Discharge also occurs in areas where the water table intersects the surface at springs or weeps. These springs usually occur in topographically low areas in river valleys or in areas of the outcrop where hydrogeologic conditions preferentially reject recharge. We performed a literature survey of springs with location and flow rate data available for the model domain (Figure 4.6.2). Sixty-seven documented springs were identified in the study area. Each spring is numbered and the number corresponds to the spring information provided in Table 4.6.2. The available measured spring flow rates range from less than 0.01 cubic feet per second (<7 acre feet per year) to a high of 3.4 cubic feet per second (2,462 acre feet per year) measured at Elkhart Creek Springs (No. 8) and originating from the Sparta Sand (Brune, 1975). The only two springs originating from the Carrizo-Wilcox which could potentially be significant for this scale model are #16 Roher Springs (No. 23) and spring number 50. Roher Springs flowed at an average rate of 0.5 cubic feet per second (362 acre feet per year) based upon one measurement in 1979 and one in 1995. Spring number 50 located on the county line between Nacogdoches and Rusk counties flowed at 0.5 cubic feet per second (362 acre feet per year) in 1942. The number of flowing springs in the study area is a product of the humid climate, the dissected topography in the model area, and the gently dipping aquifers, all of which contribute to a large percent of rejected recharge which contributes to runoff in the East Texas Basin.

Cross-formational flow is also a natural mechanism for discharge of groundwater from the Carrizo-Wilcox aquifer. Fogg and Kreitler (1982) and Fogg et al. (1983) documented that in the East Texas Basin, flow across the Reklaw is generally downward from the unconfined Queen City to the Carrizo. However, in the vicinity of the Trinity and Sabine rivers, hydraulic heads are reversed with the Carrizo-Wilcox discharging through upward leakage across the Reklaw. Estimates of these fluxes are lacking but Fogg et al. (1983) concluded that leakage across the Reklaw must be significant because of the effect of topography seen in large portions of the confined Carrizo aquifer. South of the East Texas Basin and the Sabine Uplift, the Carrizo-

Wilcox aquifer system begins to dip and thicken significantly into the Houston Embayment. Cross formational flow in this portion of the model area is expected to be from the Carrizo to the Reklaw. With development of the Carrizo-Wilcox aquifer system, the natural balance of recharge and cross-formational flow will change.

Table 4.6.1 Stream flow gain/loss in the study area (after Slade et al., 2002, Table 1).

Streamflow study no.	Major river basin	Stream name	Reach identification	Date of study	Reach length (river)	Total no. of measurement sites	No. of measurement sites on main	Major aquifer outcrop(s) intersected by reach	Total gain or loss (-) in reach	Gain or loss per mile (cfs/mile)	Gain or loss per mile (AFY/mile)
139	Neches	West Fk Bowles Cr - [Bowles Cr]	west of Old London to near Carlisle	10/28/1942	6.5	11	6	Carrizo-Wilcox	3.0	0.462	334.7
243	Red River	Grays Cr	2.6 mi north of Marshall to FM 1997	6/13/1964	3.3	9	2	Carrizo-Wilcox	-0.03	-0.009	-6.5
244	Red River	Little Cypress Cr	SH 155 to FM 134	6/10-13/1964	49.1	35	10	Carrizo-Wilcox	6.52	0.133	96.4
245	Red River	Little Cypress Cr	northeast of Gilmer to near Jefferson	1/2-3/1964	40.5	7	7	Carrizo-Wilcox	24.09	0.595	431.1
249	Red River	Sugar Cr	FM 1403 to SH 154	6/10-11/1964	0.8	3	2	--	0.15	0.188	136.2
342	Sabine	Lake Fk Cr	SH 182 to US 80	8/31-9/1/1981	1.6	3	3	Carrizo-Wilcox	-2.6	-1.625	-1177.3
345	Sabine	Sabine R	FM 1804 to FM 2517	9/22-24/1981	156.4	11	10	Carrizo-Wilcox	127.8	0.817	591.9
346	Sabine	Sabine R	Wills Point (08017410) to Smith-Upshur Co line at county road crossing	8/31-9/2/1981	80.5	8	6	Carrizo-Wilcox	427.42	5.31	3846.9
347	Sabine	Sabine R	northeast of Carthage to Ruliff (08030500)	9/4-5/1963	268	98	30	Carrizo-Wilcox, Gulf Coast	208.72	0.779	564.4
364	Trinity	Big Elkhart Cr	northwest of Grapeland to mouth	9/15-16/1965	25.7	9	7	--	5.18	0.202	146.3
365	Trinity	Little Elkhart Cr	south of Grapeland to mouth	9/16/1965	17.5	11	5	--	-1.59	-0.091	-65.9
366	Trinity	Trinity R	Riverside to Liberty	11/4-8/1952	133.5	21	5	Gulf Coast	37.16	0.278	201.4

Table 4.6.2 Documented springs in the study area.

ID	Spring	Aquifer	Flow Rate LPS	Flow Rate GPM	Flow Rate CFS	Date of Measurement	Measurement	Historical Information	SOURCE
1	#11 Dalby Springs	Wilcox Sand	1.70	26.95	0.06	1/1/1892	1 of 2		Brune, 1975
1	#11 Dalby Springs	Wilcox Sand	0.06	0.95	0.00	1/1/1976	2 of 2		Brune, 1975
2	#12 Hughes Springs/Chalybeate Springs	Wilcox Sand	0.32	5.07	0.01	1/1/1976			Brune, 1975
3	#2 Thrasher Springs	Queen City Sand	0.30	4.76	0.01	1/15/1976			Brune, 1975
4	#5 Castalian Springs	Queen City Sands	0.32	5.07	0.01	7/12/1936	1 of 2		Brune, 1975
4	#5 Castalian Springs	Queen City Sands	0.03	0.48	0.00	11/1/1979	2 of 2		Brune, 1975
5	#10 Hynson, Marshall, Noonday Camp, Iron Springs	Queen City	0.13	2.06	0.00	1/28/1942	1 of 3	Over 100 Springs	Brune, 1975
5	#10 Hynson, Marshall, Noonday Camp, Iron Springs	Queen City	0.13	2.06	0.00	1/27/1967	3 of 3	Over 100 Springs	Brune, 1975
5	#10 Hynson, Marshall, Noonday Camp, Iron Springs	Queen City	0.06	0.95	0.00	7/21/1964	2 of 3	Over 100 Springs	Brune, 1975
6	#6 Coushatta Springs	Wilcox Sand	3.20	50.73	0.11	1/25/1976			Brune, 1975
7	#2 Sulphur Springs	Wilcox Sand	3.60	57.07	0.13	12/20/1997		1841 Over 100 springs reported	Brune, 1975
8	Elkart Creek Springs	Sparta Sand	96.28	1526.03	3.40	9/15/1965			Brune, 1975
9	Hays Branch Springs	Sparta Sand	50.97	807.90	1.80	9/16/1965			Brune, 1975
10	Caney Creek Springs	Sparta Sand	48.14	763.01	1.70	9/16/1965			Brune, 1975
11	Boiling Spring	Sparta Sand	0.32	5.00	0.01	1/1/1963			Brune, 1975
12	#14 Shawnee Mineral/Nacogdoches Springs	Sparta	2.90	45.97	0.10	1/1/1978			Brune, 1975
13	#24 White and Red Springs	Wilcox Sand	0.06	0.95	0.00	1/1/1978	2 of 2		Brune, 1975
13	#24 White and Red Springs	Wilcox Sand		1.00		10/1/1936	1 of 2		Brune, 1975
14	#3 Sulphur Springs	Carrizo Sand	0.13	2.06	0.00	1/1/1976			Brune, 1975
15	#4 Hughes Springs	Carrizo Sand	0.32	5.07	0.01	1/1/1937	1 of 2		Brune, 1975
15	#4 Hughes Springs	Carrizo Sand	0.15	2.38	0.01	1/1/1976	2 of 2		Brune, 1975
16	#9 National Forest Springs	Wilcox Sand	0.32	5.07	0.01	1/1/1937	1 of 2		Brune, 1975

Table 4.6.2 (continued)

ID	Spring	Aquifer	Flow Rate LPS	Flow Rate GPM	Flow Rate CFS	Date of Measurement	Measurement	Historical Information	SOURCE
16	#9 National Forest Springs	Wilcox Sand	0.32	5.07	0.01	1/1/1976	2 of 2		Brune, 1975
17	#11 Headache Springs	Weches Sand	0.35	5.55	0.01	11/2/1979			Brune, 1975
18	#3 Neff Springs	Spart Sand	-					1947 "Moderately large" flow. 1979 dry	Brune, 1975
19	#4 Arms Factory Spring	Spart Sand	0.20	3.17	0.01	10/30/1979		A "bold" spring when first discovered	Brune, 1975
20	#5 Tyler Springs	Sparta Sand	1.70	26.95	0.06	10/30/1970	2 of 2		Brune, 1975
20	#5 Tyler Springs	Sparta Sand	0.63	9.99	0.02	7/6/1936	1 of 2		Brune, 1975
21	#6 Camp Ford & Pine Springs	Sparta Sand	0.08	1.27	0.00	10/30/1979		during Civil War described as "large" spring	Brune, 1975
22	#7 Cousins Springs	Sparta Sand	1.30	20.61	0.05	10/30/1979		Finest spring in area when found	Brune, 1975
23	#16 Roher Springs	Carrizo Sand	17.00	269.48	0.60	9/27/1979	1 of 2		Brune, 1975
23	#16 Roher Springs	Carrizo Sand	11.67	185.00	0.41	9/6/1995	2 of 2		TWDB well database
24	Peacock Spring	Sparta & Queen City	3.15	50.00	0.11			Estimated flow 50 gpm. Known as Peacock Spring.	TWDB well database
25	Palmer Spring	Sparta & Queen City	0.03	0.50	0.00			Estimated flow 1/2 gpm. Known as Palmer Spring.	TWDB well database
26	Dumas Spring	Carrizo & Wilcox, Undifferentiated	6.31	100.00	0.22			Estimated flow 100 gpm. Known as Dumas Spring.	TWDB well database
27	Library Spring	Queen City Sand	0.06	1.00	0.00			Called Library Spring. Flows 1 gal. per minute	TWDB well database
28	Spring	CARRIZO SAND	0.14	2.20	0.00	1/1/1978		Spring encased in wooden box. Reported discharge 2.2 gal/min, 1978 (Gunnar Brune).	TWDB well database
29	Spring	Carrizo Sand	0.13	2.00	0.00	10/19/1936		Spring, estimated flow 2 gal/min 10-19-36.	TWDB well database
30	Spring	Queen City Sand	14.38	228.00	0.51	11/17/1978	1 of 2	Spring. Deussen (1914) reported "large flow." Reported discharge 228 gal/min 1-11-78 (Gunner Brune). Measured discharge 8.5 gal/min and measured temp. 13.8 degrees C. on 7-14-81.	TWDB well database

Table 4.6.2 (continued)

ID	Spring	Aquifer	Flow Rate LPS	Flow Rate GPM	Flow Rate CFS	Date of Measurement	Measurement	Historical Information	SOURCE
30	Spring	Queen City Sand	0.54	8.50	0.02	7/14/1981	2 of 2	Spring. Deussen (1914) reported "large flow." Reported discharge 228 gal/min 1-11-78 (Gunner Brune). Measured discharge 8.5 gal/min and measured temp. 13.8 degrees C. on 7-14-81.	TWDB well database
31	Spring	Reklaw Formation	0.63	10.00	0.02			Spring. Deussen (1914) reported "large flow;" Gunnar Brune (1978) reported 10 gal/min.	TWDB well database
32	Spring	Carrizo & Wilcox, Undifferentiated	2.84	45.00	0.10	1/1/1942		Reported discharge 40 to 50 gpm in 1942. Unable to locate spring in 1964.	TWDB well database
33	King's Spring	Jackson Group	1.26	20.00	0.04	5/15/1947		King's Spring. Estimated flow 20 gpm, May 15, 1947.	TWDB well database
34	Moffitt Springs	Jackson Group	15.77	250.00	0.56	4/13/1994		Moffitt Springs. Reported flow 250 GPM April 13, 1994.	TWDB well database
35	Spring	Cypress	0.03	0.50	0.00	7/1/1964			County Reports
36	Spring	Cypress	0.06	1.00	0.00	8/1/1964			County Reports
37	Spring	Cypress	0.32	5.00	0.01	1/1/1968			County Reports
38	Spring	Cypress	1.26	20.00	0.04	10/1/1967			County Reports
39	Spring	Cypress	0.95	15.00	0.03	10/1/1959			County Reports
40	Spring	Cypress	0.13	2.00	0.00	10/1/1959			County Reports
41	Spring	Cypress	0.19	3.00	0.01	6/1/1963			County Reports
42	Spring	Cypress	1.58	25.00	0.06	7/1/1963			County Reports
43	Spring	Cypress	0.32	5.00	0.01	3/1/1942			County Reports
44	Spring	Cypress	0.41	6.50	0.01	4/1/1963			County Reports
45	Spring	Cypress	0.06	1.00	0.00	5/1/1963			County Reports
46	Spring	Cypress	0.25	4.00	0.01	4/1/1963			County Reports
47	Spring	Carrizo-Wilcox	0.32	5.00	0.01	1/1/1942			County Reports

Table 4.6.2 (continued)

ID	Spring	Aquifer	Flow Rate LPS	Flow Rate GPM	Flow Rate CFS	Date of Measurement	Measurement	Historical Information	SOURCE
48	Spring	Carrizo-Wilcox	0.44	7.00	0.02	1/1/1942			County Reports
49	Spring	Carrizo	0.06	1.00	0.00	1/1/1936			County Reports
50	Spring	Carrizo	14.20	225.00	0.50	3/1/1942			County Reports
51	Spring	Carrizo	0.22	3.50	0.01	1/1/1963			County Reports
53	Spring	Carrizo	0.13	2.00	0.00	1/1/1936			County Reports
54	Spring	Carrizo	0.06	1.00	0.00	1/1/1936			County Reports
55	Boykin Spring	Catahoula Sandstone	8.50	134.73	0.30	2/20/1978			GNIS, Brune (1981)
56	Blue Spring	Yegua Sand	0.18	2.85	0.01	1/1/1978			GNIS, Brune (1981)
57	Harris Spring	Whitsett Sand	0.57	9.03	0.02	3/19/1978			GNIS, Brune (1981)
58	Doggett Spring	Wilcox Sand	0.65	10.30	0.02	1/1/1976			GNIS, Brune (1981)
59	Beauchamps Springs	Weches Sand	1.10	17.44	0.04	10/31/1979			GNIS, Brune (1981)
60	Red Springs		0.65	10.30	0.02	10/31/1979			GNIS, Brune (1981)
61	Walnut Springs		seep	seep	seep	10/31/1979		1960's known as "very fine spring"	GNIS, Brune (1981)
62	Barton Springs							Once furnished water for a sawmill & gin	GNIS, Brune (1981)
63	Cary Martin Springs	Queen City	0.35	5.55	0.01	1/1/1978		Formerly Wolf Springs	GNIS, Brune (1981)
64	Lee Springs	Queen City	7.60	120.46	0.27	1/21/1978		Includes Couch & Joe's Spring	GNIS, Brune (1981)
65	Bowles Springs	Queen City	1.30	20.61	0.05	11/6/1979			GNIS, Brune (1981)
66	Myrtle Spring	Reklaw Formation	4.70	74.50	0.17	11/4/1979		a.k.a. Myrill Springs	GNIS, Brune (1981)
67	Roseborough Springs	Wilcox Sand	1.40	22.19	0.05	1/1/1976		Here 7 springs formerly flowed, although most must be pumped by now	GNIS, Brune (1981)

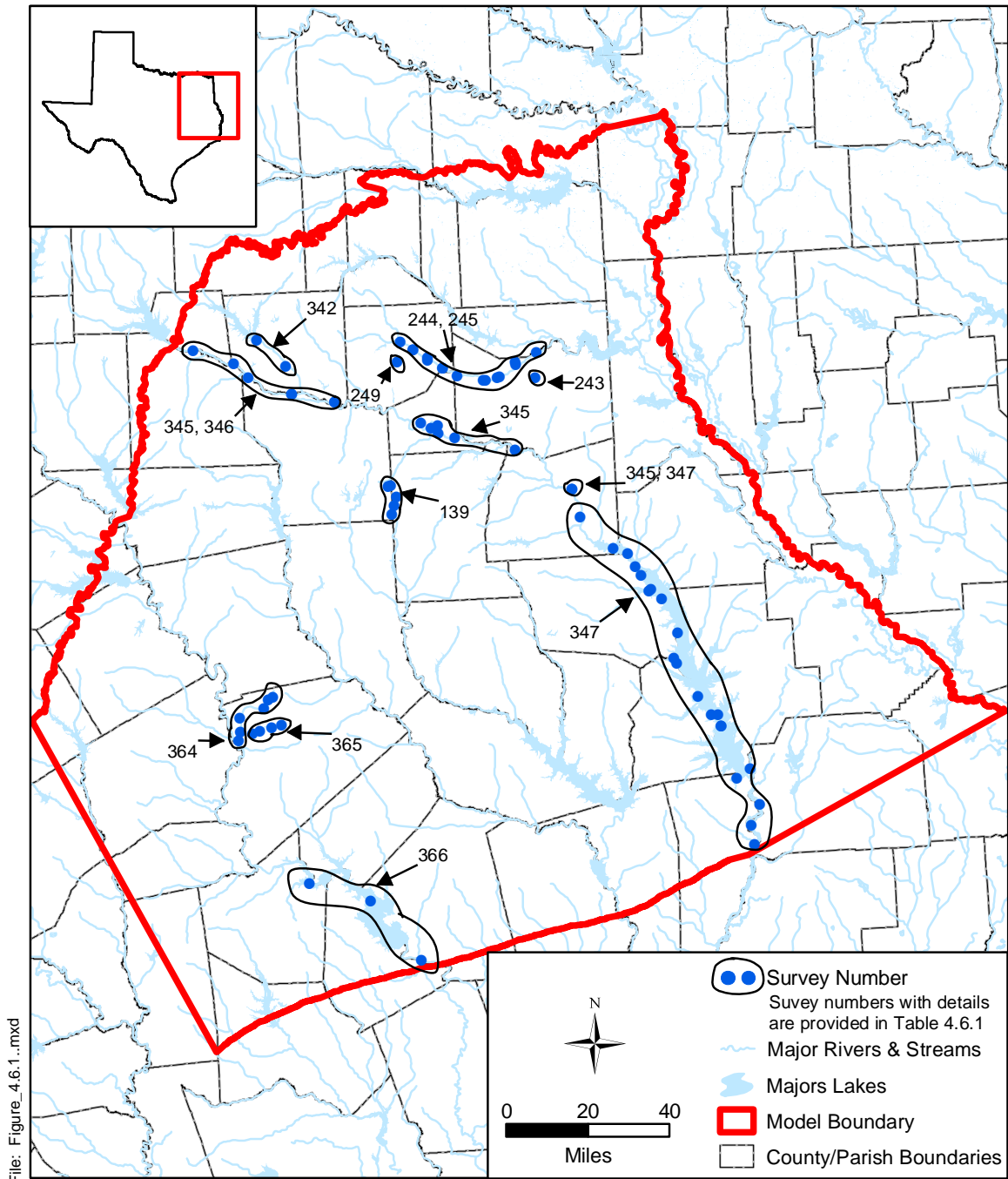


Figure 4.6.1 Stream gain/loss studies in the study area (after Slade et al., 2002).

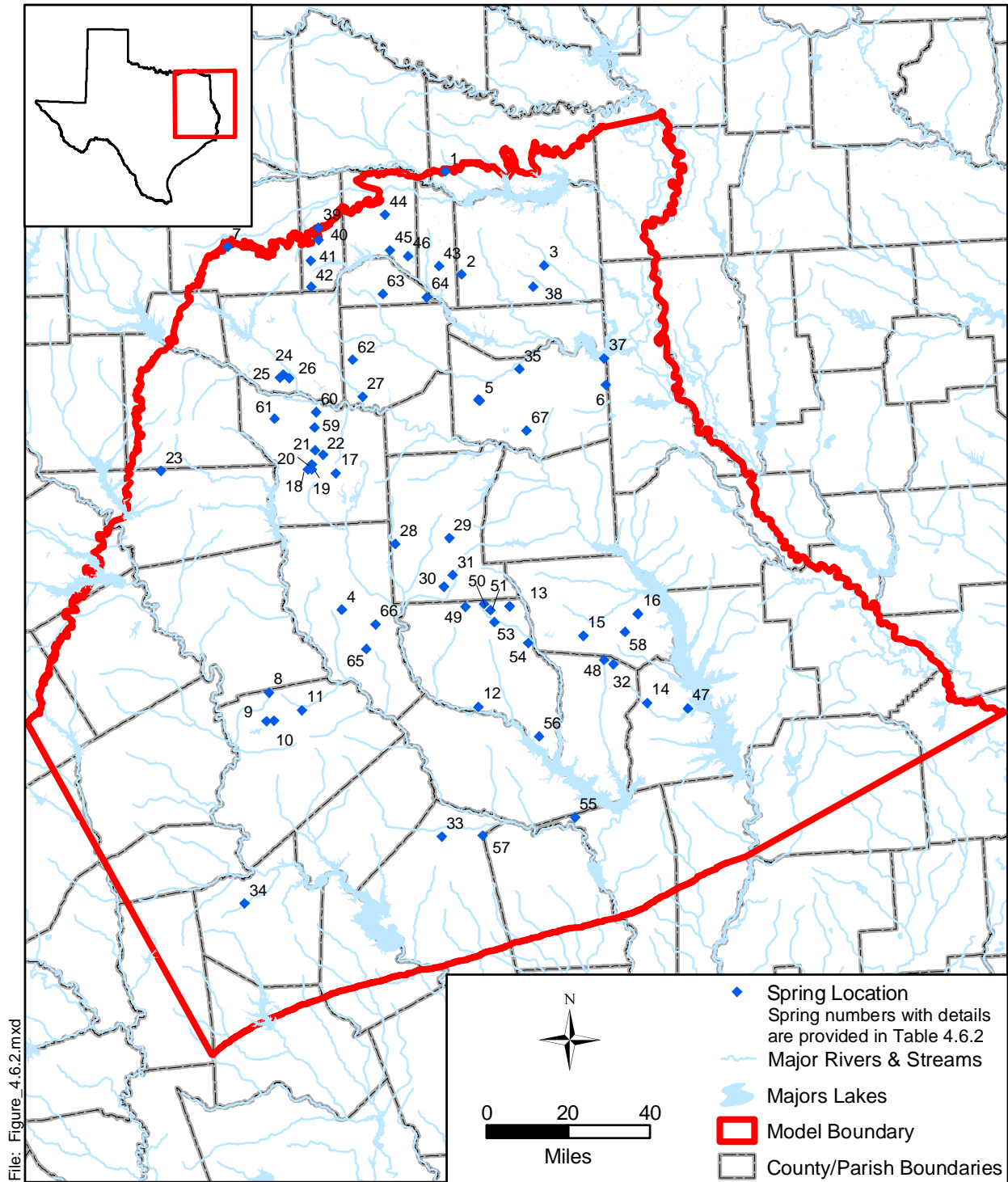


Figure 4.6.2 Documented spring locations in the study area.

4.7 Aquifer Discharge Through Pumping

Pumping discharge from the model required estimations for both the historical modeling period (1980 to 1999) and for the predictive period (2000 to 2050). Historical estimates of groundwater pumpage from the Carrizo-Wilcox aquifer were based on the water use survey database provided by the Texas Water Development Board. The seven water use categories utilized were municipal (MUN), manufacturing (MFG), power generation (PWR), mining (MIN), livestock (STK), irrigation (IRR), and county-other (C-O), which consists primarily of unreported domestic water use. The methodology used to distribute those pumpage estimates is described briefly below, and in detail in the “Standard Operating Procedure for Processing Historical Pumpage Data”, Appendix B to this report.

Municipal, manufacturing, mining, and power pumpage estimates were actual monthly water use records reported by the water user, which were available for 1980 through 1999. In cases where only the total annual pumpage was reported, the average monthly distribution of annual pumpage for the same water use category in the same county-basin, or an adjacent county-basin, was used. A county-basin is a geographic unit created by the intersection of county and river basin boundaries. For example, a county partly crossed by two river basins comprises two county-basins.

The water use survey also included historical annual pumpage estimates for livestock, irrigation, and county-other water use for the years 1980 and 1984 through 1997 for each county-basin. Annual pumpage estimates for the years 1981, 1982, 1983, 1998, and 1999 were developed by linear regression based on significant relationships between reported pumpage and (1) average annual temperature, (2) total annual rainfall measured at the nearest weather station, and (3) the year, for each water use category.

The monthly distribution of county-other water use was assumed to be similar to that of municipal use. The average monthly distribution of municipal water use for a given year within the same (if possible) or an adjacent county-basin was used to estimate how much of the annual total county-other usage was pumped in each month.

Annual livestock water use was distributed uniformly across all twelve months. While this may not accurately reflect seasonality of livestock use, it was not expected to have much impact because livestock is a relatively minor use in the study area.

The procedures for temporal distribution of annual irrigation water use differed for rice and non-rice crops. For rice, monthly irrigation pump electricity consumption use records were used to indicate how much water was pumped in each month for rice irrigation. For non-rice crops, annual irrigation water use was distributed among months using predicted monthly water deficits, based on the rainfall deficit and crop evapotranspiration estimates for each Texas Crop Reporting District, using the approach of Borrelli et al. (1998).

Reported historical pumpage for municipal, manufacturing, mining, and power water uses were matched to the specific wells from which it was pumped to identify the location in the aquifer from which it was drawn (latitude, longitude, and depth below mean sea level) based on the well's reported properties. The well properties were obtained by compiling data from the TWDB's state well database, the Texas Commission on Environmental Quality's Public Water System database, the U.S. Geological Survey's National Water Information System, the TWDB's follow up survey with water users, and various other minor sources as described in the "Standard Operating Procedure for Processing Historical Pumpage Data", Appendix B to this report. When more than one well was associated with a given water user, groundwater withdrawals were divided evenly among those wells.

Livestock pumpage totals within each county-basin were distributed uniformly over the rangeland within the county-basin, based on land use maps, using the categories "herbaceous rangeland", "shrub and brush rangeland", and "mixed rangeland". Vertical assignment of livestock pumpage to model flow layers was performed by interpolating an average well depth and screened interval for all Carrizo-Wilcox livestock watering wells in the TWDB state well database, using the inverse distance method to enhance the influence of nearby wells.

County-other pumpage was distributed within each county-basin based on population density (Figure 4.7.1), after excluding urban areas which would generally be served by municipal water suppliers, using the 1990 federal block-level census data for the years 1980-1990, and the 2000 census data for the years 1991-1999. Vertical assignment of county-other pumpage to model flow layers was performed by interpolating an average well depth and screened interval

for all Carrizo-Wilcox county-other wells in the TWDB state well database, using the inverse distance method to enhance the influence of nearby wells.

Irrigation pumpage within each county-basin was spatially distributed across the land use categories “row crops”, “orchard/vineyard”, and “small grains”. However, the pumpage was not uniformly distributed across these land uses, but weighted based on proximity to irrigated farms mapped from the irrigated farmlands surveys performed in 1989 and 1994 by the Natural Resource Conservation Service of the U.S. Department of Agriculture. The 1989 irrigation survey was used for pumpage between 1980 and 1989, while the 1994 survey was used for pumpage from 1990 to 1999. Further details of the procedure are available in the “Standard Operating Procedure for Processing Historical Pumpage Data”, Appendix B to this report. Vertical assignment of irrigation pumpage to model flow layers was performed by interpolating an average well depth and screened interval for all Carrizo-Wilcox irrigation wells in the TWDB state well database, using the inverse distance method to enhance the influence of nearby wells.

In the northern Carrizo-Wilcox aquifer, groundwater pumpage estimates for portions of the model domain in Arkansas were derived from data provided by the Arkansas Soil & Water Conservation Commission. The U.S. Geological Survey provided groundwater pumpage estimates for Louisiana.

Predicted groundwater pumpage from the Carrizo-Wilcox aquifer for the period 2000 through 2050 was estimated based on projected water demand reported by Regional Water Planning Groups as part of Senate Bill 1 planning (TWDB, 2002). The methodology used to distribute pumpage estimates is described briefly here, and in detail in the “Standard Operating Procedure for Processing Predictive Pumpage Data”, Appendix C to this report. The RWPG water demand projections were available for the years 2000, 2010, 2020, 2030, 2040, and 2050; intervening year projections were developed by linear interpolation. In some cases, the RWPGs identified new well field locations for developing new water supplies. In such instances, the specific locations of the future well fields were used to spatially distribute the groundwater pumpage forecasts. However, in the absence of any data indicating otherwise, it was assumed that the most recent past spatial distribution of groundwater pumpage represented the best available estimate of the locations of future groundwater withdrawals.

Predicted municipal water use totals for each public water supplier were matched to the same wells used for that water user in 1999. Similarly for manufacturing, mining, and power generation, predicted future water pumpage totals by county-basin were distributed among the same wells and locations used by those water users in 1999. Irrigation, county-other, and livestock pumpage estimates for each county-basin from 2000 to 2050 also utilized the same spatial distribution within county-basins as was used in 1999.

Estimates of projected Arkansas and Louisiana groundwater pumpage for 2000 through 2050 were not available. Municipal and County-Other pumpage totals for future years were predicted by multiplying the per capita consumption for the period 1995 to 1999 by the projected future county/parish populations, which were supplied by the state demographers. Predicted future pumpage for other water use categories in Louisiana and Arkansas was not projected. Instead we assumed that pumpage in future years would equal the average pumpage for the period 1995 to 1999.

Groundwater withdrawal estimates from the Carrizo-Wilcox aquifer for the years 1980 and 1990, and predictions for 2000, 2010, 2020, 2030, 2040, and 2050 in those counties, or portions of counties, within the model area are provided in Tables D1.1 through D1.12 in Appendix D1. It should be noted that these estimates are the sums of model grid cells. Because the 1 square mile grid cells often cross county boundaries, and are added to that county total in which the center of the grid cell occurs, these county-level estimates are not exact. County-level estimates also may not match the original TWDB estimate because a portion of the county occurred outside the model domain or in inactive model cells, because the location of groundwater withdrawal could not be identified, or because the groundwater was found to have been pumped from a different aquifer based on well depth information.

Based on this analysis, approximately 132,000 acre-feet of groundwater were withdrawn from the modeled portion of the Carrizo-Wilcox aquifer in 1980 (Table 4.7.1). The amount of groundwater withdrawn increased by approximately 18% to roughly 155,000 acre-feet by 1990. Based upon the regional water plans, it is estimated that approximately 167,000 acre-feet were withdrawn in 2000. Groundwater withdrawals from the aquifers in the model area are expected to remain near the year 2000 level through 2050, when the projected groundwater withdrawal will be approximately 170,000 acre-feet.

Figures 4.7.2 through 4.7.7 show the pumping demands for the year 1990 for the six model layers. From these figures it appears that the Queen City (Layer 1) is pumped in significant quantities in the study area. The Carrizo and upper Wilcox (Layers 3 and 4) are produced primarily from the confined section of the aquifers in the East Texas Basin. In contrast, the middle Wilcox and the lower Wilcox (Layers 5 and 6) are predominantly used in the unconfined (outcrop) portion of the aquifers.

In most cases, the largest withdrawals from the Carrizo-Wilcox aquifer are for municipal and industrial purposes, and are found in counties with substantial urban areas, such as Angelina and Smith counties. Groundwater withdrawal from the Carrizo-Wilcox for irrigation purposes can also be substantial, as in Robertson County after 1990.

Appendix D2 provides post plots for the pumping distribution in AFY for each model layer for years 1980, 1990, 2000, and 2050. Appendix D3 provides total pumping distributions in AFY by year from 1980 through 2050 organized by county.

Figures 4.7.2 and 4.7.3 indicate pumpage from both the Queen City (Layer 1) and the Reklaw (Layer 2). Due to uncertainty in allocating pumpage from reported or inferred well interval depths to the different model layers, it is considered reasonable to assume that most of the estimated pumpage from the Reklaw is actually from the Carrizo Formation. Consequently, 90% of the estimated pumpage in the Reklaw was moved to the Carrizo (Layer 3). Similarly, relatively large amounts of pumpage are shown for the Queen City in Smith County (Figure 4.7.2), though TWDB Report 327 indicates that most of the groundwater pumpage in Smith County is from the Carrizo-Wilcox aquifer. As a result, 80% of the estimated Queen City pumpage in Smith and northern Cherokee counties was moved to the Carrizo (Layer 3). The model could not reproduce the observed drawdowns without reallocating pumpage from the Queen City to the Carrizo, even though the vertical permeability of the Reklaw was explicitly decreased in this area.

Table 4.7.1 Rate of groundwater withdrawal (AFY) from all model layers of the Carrizo-Wilcox aquifer for counties within the study area.

County	1980	1990	2000	2010	2020	2030	2040	2050
Anderson	3,493	4,701	6,740	6,788	6,772	6,816	6,783	6,908
Angelina	22,523	20,190	17,807	16,174	15,077	16,112	16,994	18,678
Bienville, LA	0	0	669	669	669	669	669	669
Bossier, LA	128	75	1,728	1,825	1,917	2,003	2,085	2,162
Bowie	1,924	2,191	867	1,945	1,946	1,948	1,952	1,957
Caddo, LA	5,023	3,806	3,979	4,078	4,278	4,582	4,989	5,499
Camp	1,397	1,711	1,542	1,837	1,862	1,892	1,913	1,931
Cass	3,903	4,297	1,291	1,439	1,138	1,140	1,185	1,175
Cherokee	7,093	7,790	8,713	4,321	4,445	4,584	4,844	5,077
De Soto, LA	1,905	1,380	231	231	231	231	231	231
Franklin	1,107	1,335	2,032	1,940	1,894	1,837	1,867	1,925
Freestone	2,408	3,337	3,020	3,039	3,027	3,053	3,084	3,107
Gregg	2,817	2,363	2,191	2,440	2,441	2,537	2,625	2,708
Grimes	383	733	742	777	816	864	869	967
Harrison	3,649	4,492	3,488	3,672	4,023	4,148	4,246	4,314
Henderson	4,135	5,662	5,170	4,922	4,918	4,822	4,807	4,991
Hopkins	2,132	2,978	1,812	2,044	2,042	2,092	2,193	2,246
Houston	1,912	1,781	1,440	1,466	1,468	1,475	1,484	1,488
Leon	2,034	2,988	5,905	5,619	5,197	5,234	5,339	5,540
Limestone	368	1,177	8,477	9,177	9,214	9,284	9,360	9,453
Madison	890	1,111	1,733	1,687	1,648	1,609	1,551	1,500
Marion	922	1,043	777	782	803	834	864	916
Miller, AR	26	8,780	7,185	7,188	7,190	7,190	7,193	7,195
Morris	1,945	7,821	718	721	705	699	682	674
Nacogdoches	8,698	9,624	7,139	6,908	7,133	7,115	7,864	8,382
Natchitoches, LA	1,121	1,018	1,784	1,824	1,884	1,956	2,043	2,148
Navarro	67	115	12	12	12	12	12	12
Panola	3,487	4,638	3,877	3,579	3,261	4,152	4,178	4,148
Rains	387	618	368	389	408	276	293	311
Red River, LA	24	99	932	957	1,011	1,093	1,204	1,345
Robertson	382	265	14,506	14,181	14,027	13,687	13,379	13,080
Rusk	7,238	7,912	8,973	7,925	7,620	7,637	7,598	7,740
Sabine, LA	961	1,141	1,842	1,977	2,122	2,281	2,452	2,635
Sabine, TX	792	1,045	1,025	1,094	1,158	1,272	1,340	1,369
San Augustine	6,609	4,996	557	555	550	557	556	560
Shelby	2,982	3,182	3,429	3,896	3,239	3,252	4,118	4,723
Smith	11,548	12,026	18,184	19,196	20,800	11,774	12,706	11,094
Titus	1,500	1,895	3,193	3,369	3,378	3,489	3,550	3,594
Trinity	1,819	1,816	0	0	0	0	0	0
Upshur	3,580	4,043	3,227	3,424	3,427	3,483	3,152	3,531
Van Zandt	4,556	5,053	4,604	4,868	6,030	5,921	6,261	6,535
Wood	4,101	4,153	5,723	6,104	6,401	6,789	7,114	7,692
Grand Total	131,969	155,381	167,632	165,039	166,182	160,401	165,629	170,210

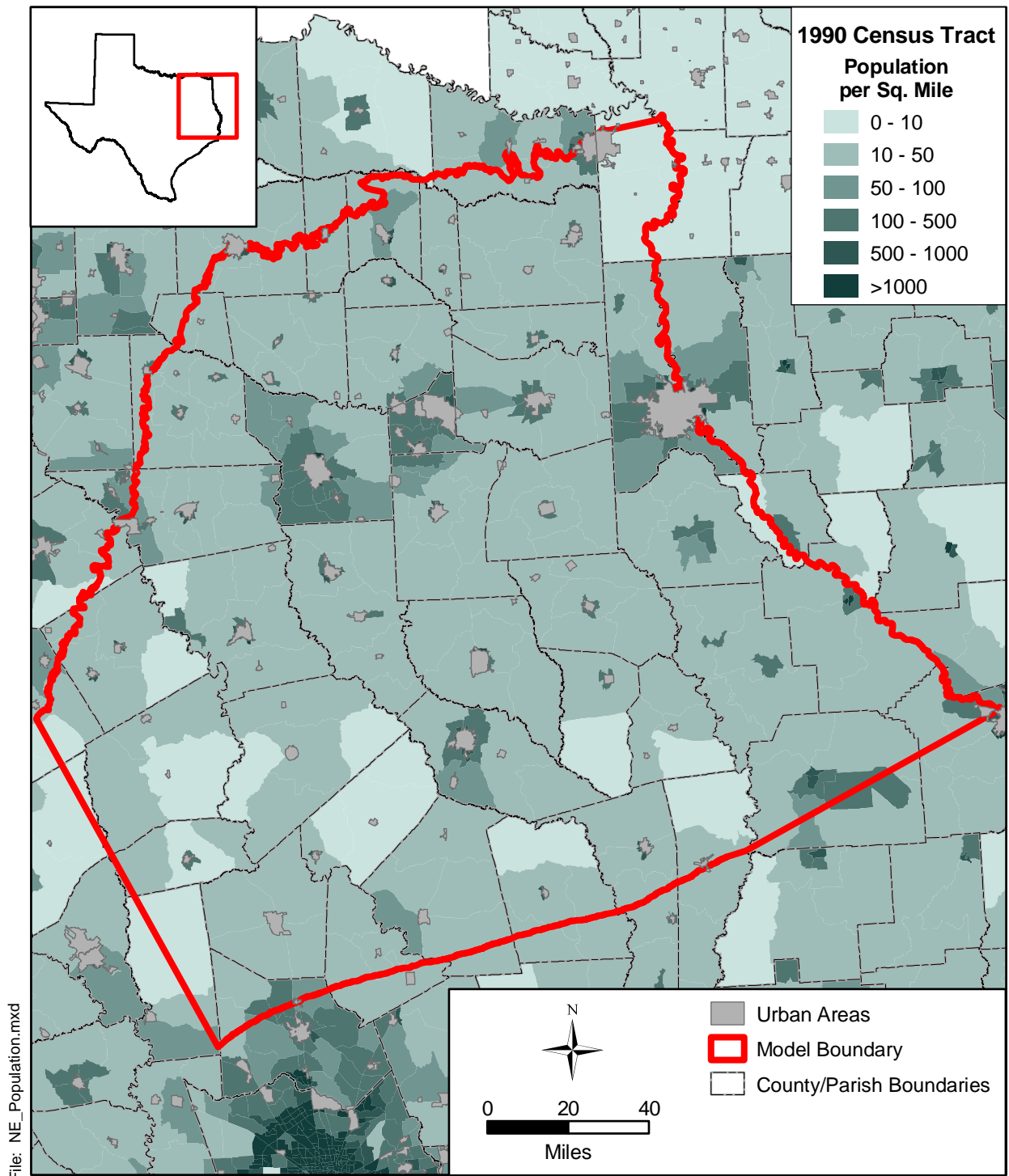


Figure 4.7.1 Population density for the Northern Carrizo-Wilcox GAM study area.

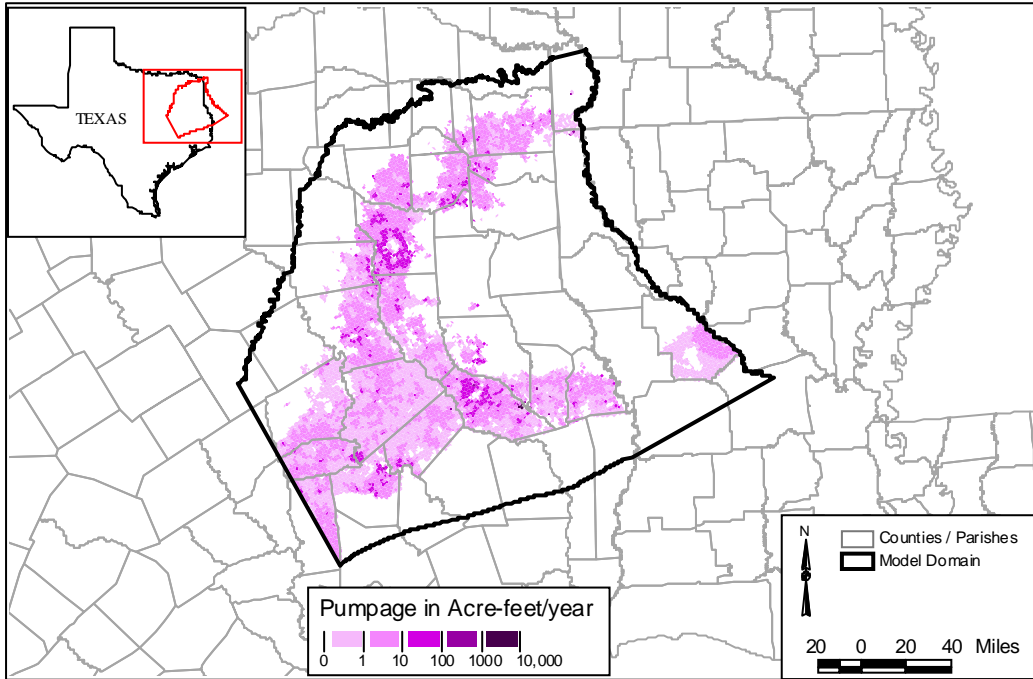


Figure 4.7.2 Younger (Layer 1) pumpage (AFY), 1990.

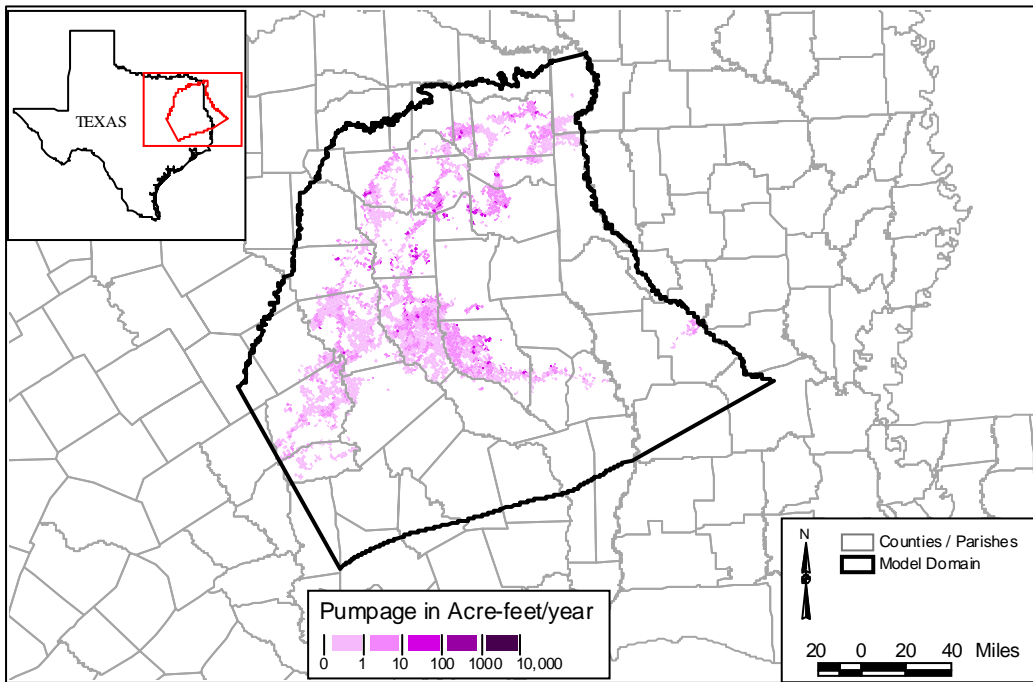


Figure 4.7.3 Reklaw (Layer 2) pumpage (AFY), 1990.

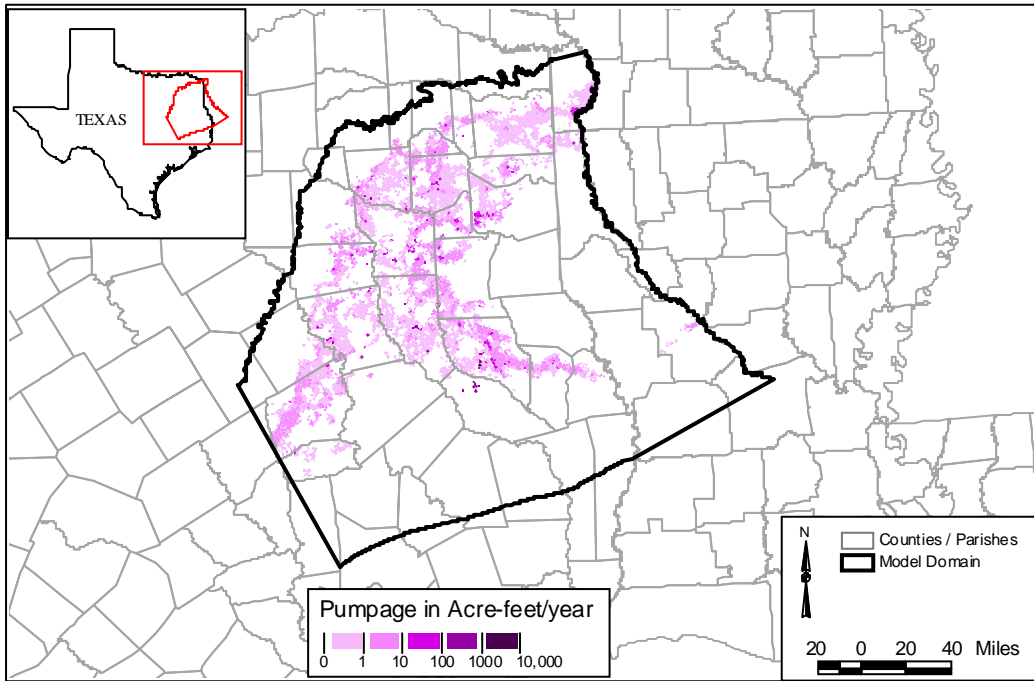


Figure 4.7.4 Carrizo (Layer 3) pumpage (AFY), 1990.

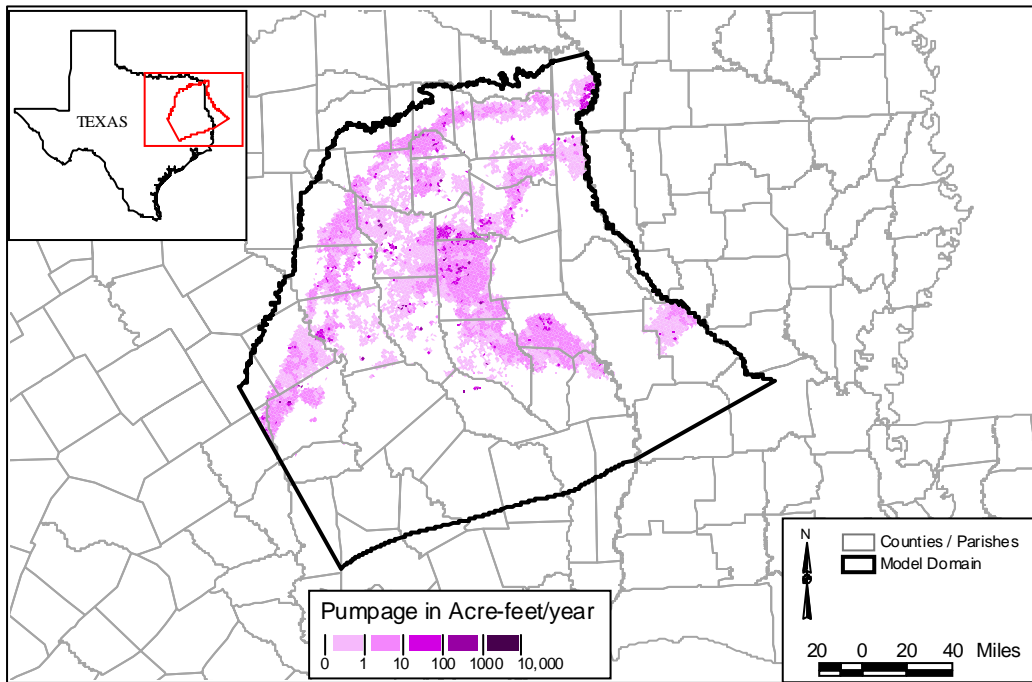


Figure 4.7.5 Upper Wilcox (Layer 4) pumpage (AFY), 1990.

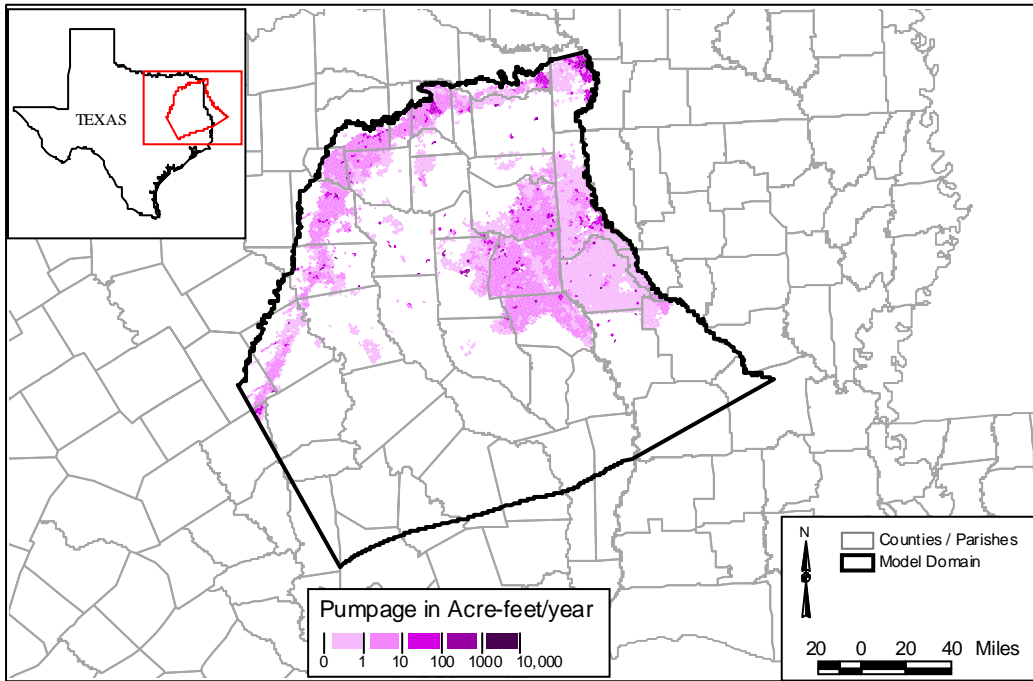


Figure 4.7.6 Middle Wilcox (Layer 5) pumpage (AFY), 1990.

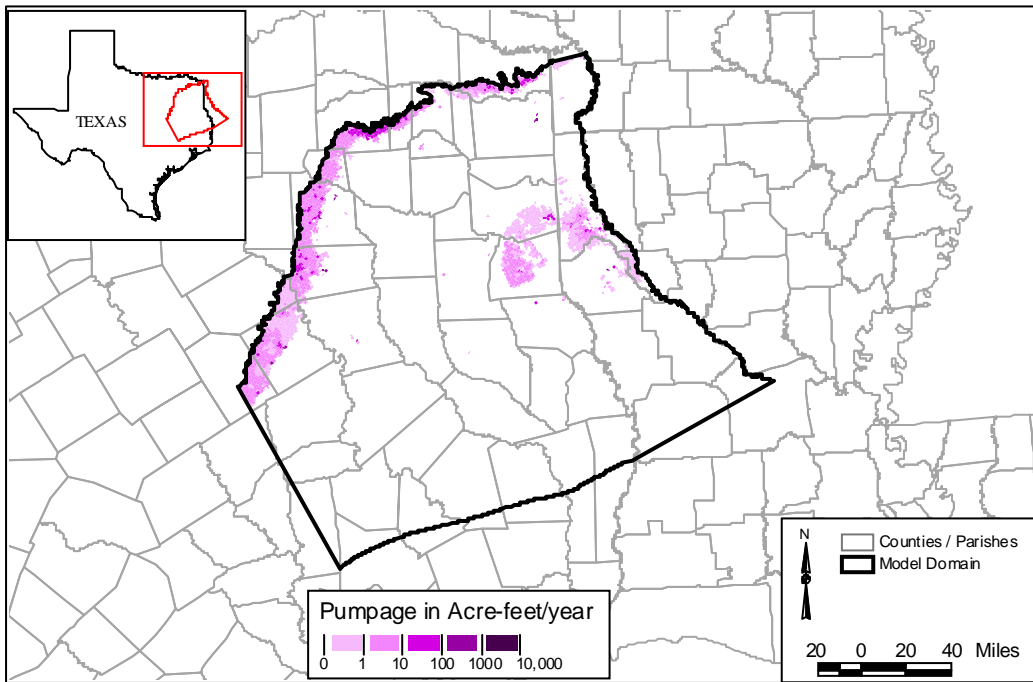


Figure 4.7.7 Lower Wilcox (Layer 6) pumpage (AFY), 1990.

4.8 Water Quality

Water quality data for the northern Carrizo-Wilcox aquifer were examined in terms of drinking water quality, irrigation water quality, and industrial water quality, as described in detail in Appendix F. For the water-quality assessment, available water quality measurements derived from various databases were compared to screening levels for specific constituents (Table F.1 and F.2). Screening levels for drinking water supplies are based on the maximum contaminant levels (MCLs) established in National Primary and Secondary Drinking Water Regulations. Irrigation water quality is evaluated based on the concentrations of specific constituents, such as boron, chloride, and TDS, as well as the salinity hazard, owing to their limited tolerance for crop irrigation. Groundwater suitability for industrial purposes is indicated by the content of dissolved solids, as well as its corrosiveness and tendency to form scale and sediments (Table F.1 and F.2). Table F.1 indicates for each constituent the percent of wells in the Carrizo-Wilcox aquifer exceeding the screening levels, and Table F.2 list the percentage of wells in individual counties exceeding one or more screening levels. The spatial concentration distributions of selected constituents in the northern Carrizo-Wilcox aquifer are shown in Figures F.1 through F.7. Note that these water quality data have been reported to the different state agencies and are typically from operational wells. Wells that were drilled and subsequently abandoned due to insufficient yield or unsuitable water quality are typically not reported and may not be included in the data bases.

5.0 CONCEPTUAL MODEL OF GROUNDWATER FLOW IN THE AQUIFER

The conceptual model for groundwater flow in the Northern Carrizo-Wilcox GAM area is based on the hydrogeologic setting, described in Section 4. The conceptual model is a simplified representation of the hydrogeological features which govern groundwater flow in the aquifer. These include the hydrostratigraphy, hydraulic properties, stresses such as pumping and recharge, and the boundaries. Each of the elements of our conceptual model is described below. The schematic diagram in Figure 5.1 depicts the conceptual hydrogeologic model of groundwater flow in the Carrizo-Wilcox aquifer under predevelopment conditions. With additional pumping as the aquifer is developed, an additional flow component representing discharge from individual layers would be depicted in Figure 5.1.

The conceptual model distinguishes four layers in the Carrizo-Wilcox aquifer, consisting of the lower, middle, and upper Wilcox layers in addition to the Carrizo Sand. These layers tie in with the subdivision of the aquifer in the Central Carrizo-Wilcox GAM. The Carrizo-Wilcox aquifer is overlain by the Reklaw Formation, representing the confining unit in the East Texas Embayment and in the southern part of the study area. The Reklaw Formation separates the major Carrizo-Wilcox aquifer from the shallow, minor Queen City and Sparta aquifers. The Reklaw confining unit and the overlying Queen City aquifer unit are represented as separate layers in the model to account for potential vertical flow across the Reklaw. In the southern part of the study area, where all the layers dip toward the Gulf of Mexico, a wedge of younger sediments overlies the topmost model layer (Queen City aquifer). In this part of the study area, vertical flow between the aquifer and the shallow water table is approximated using general-head boundary conditions.

In addition to identifying the hydrostratigraphic layers of the aquifer, the conceptual model also defines the mechanisms of recharge and discharge, as well as groundwater flow through the aquifer. Recharge occurs mainly in the outcrop areas of the Carrizo-Wilcox layers along the northwestern edge of the East Texas Basin and in the Sabine Uplift area to the east. Similarly, recharge to the shallow Queen City aquifer occurs through infiltration in the outcrop area, which covers the center axis of the East-Texas Embayment (Figure 4.2.1). Additional recharge to the Carrizo-Wilcox aquifer may occur by cross-formational flow from the Queen

City aquifer through the Reklaw confining unit (Figure 5.1). Cross-formational flow between the different layers within the Carrizo-Wilcox aquifer may redistribute groundwater that is recharged in the outcrops into different aquifer layers as a result of variations in hydraulic properties, hydraulic heads, and topography (Figure 5.1).

Most of the precipitation falling on the outcrop runs off into the small creeks, which discharge through major streams out of the model area. In addition to runoff, a significant portion of the precipitation is lost by evapotranspiration (ET), leaving only a small fraction of the precipitation to infiltrate into the subsurface and recharge the aquifer. Diffuse recharge occurs preferentially in topographically higher interstream areas within the outcrops. Focused recharge along streams can occur when the water table in the aquifer is below the stream-level elevation. If stream levels are lower than surrounding groundwater levels, groundwater discharges to the streams resulting in gaining streams. In this case, water levels in the valley are typically close to land surface and some of the shallow groundwater in this area can be lost to evapotranspiration.

Recharge is a complex function of precipitation, soil type, geology, water level and soil moisture, topography, and ET. Precipitation, ET, water-table elevation, and soil moisture vary spatially and temporally, whereas soil type, geology, and topography vary spatially. In addition to natural phenomena, water levels are affected by pumpage and man-made surface-water reservoirs and lakes, which in turn affect recharge. Under undisturbed conditions (e.g., prior to pumping), groundwater recharge is balanced by natural discharge of groundwater. To maintain a state of dynamic equilibrium, groundwater withdrawal by pumping must be balanced by: (1) an increase in recharge, (2) a decrease in natural discharge, (3) a loss of storage, (4) or a combination of these factors. Balancing pumping by increased recharge implies that recharge was rejected prior to the onset of pumpage (Theis, 1940; Domenico and Schwartz, 1990). This occurs primarily in outcrop areas of aquifers where the water table is near land surface.

The onset of pumpage and the concomitant water-level decline induces an increase in recharge, because less water is captured by evapotranspiration as the water table declines below the root zone and vertical gradients in the recharge zone increase. Freeze (1971) showed for an unconfined aquifer that the increase in recharge occurs initially without affecting the natural discharge even though pumpage continues to increase (Fig. 5.2a). After some time, the recharge stabilizes as the increased pumpage is offset by a decrease in the natural discharge (i.e., gaining

streams) leading to induced recharge (i.e., losing streams). With continued increase in pumpage and concomitant decrease in basin discharge, the conditions could become 'unstable', whereby the decrease in natural discharge can no longer feed the increased pumpage (Fig. 5.2b). Water levels decline to a depth below which the maximum recharge rate can no longer be sustained, because of consistently drier conditions in the unsaturated zone and increased evapotranspiration during redistribution (Freeze, 1969). Compared to the hypothetical system described by Freeze (1971), the unconfined-confined system of the Carrizo-Wilcox aquifer will exhibit a more complex response, whereby the water-table response in the outcrop to pumpage in the confined section would be delayed.

Our conceptual model for the northern Carrizo-Wilcox aquifer is considered to represent a stable groundwater basin, as indicated in Figure 5.2a, characterized by a significant rejected recharge potential. This implies that effective recharge during predevelopment conditions is expected to be lower than during current transient conditions subject to pumpage over the last several decades.

Groundwater from the aquifers discharges to local creeks and major streams throughout the area, contributing to the baseflow of the major streams. In addition, discharge from the Carrizo-Wilcox aquifer occurs by cross-formational flow. In the East Texas Basin, the direction of cross-formational flow between the Carrizo and the Queen City depends on topography, and in some areas, pumping stresses. In the southern part of the study area, discharge from the Carrizo-Wilcox occurs through cross-formational flow into the Queen City which, in turn, discharges by vertical flow through the overlying younger formations into stream valleys.

Groundwater flow within the aquifers is controlled by the topography, the structure, and the permeability variation within the different layers. A map showing the inferred groundwater flow pattern in the northern Carrizo-Wilcox aquifer is shown in Figure 4.4.3 (Fogg and Kreitler, 1982). Generally, the Carrizo Sand has the highest average hydraulic conductivity, whereas the Simsboro (middle Wilcox) is considered the main water-producing layer of the Wilcox in the southwestern part of the area, which extends southward into the Central Carrizo-Wilcox GAM. East of the Trinity River, the Simsboro Sand is no longer identified in geophysical logs as a separate lithologic unit, and the large-scale aquifer transmissivity largely depends on sand thickness and connectivity of individual sand bodies.

The vertical boundary along the southern edge of the model corresponds to the updip limit of the growth faults, displacing mainly Wilcox and deeper strata downward toward the Houston Embayment (Figure 5.1). This boundary is represented by a no-flow boundary in the model, representing the stagnant zone associated with the overall downdip gradient of the Carrizo-Wilcox aquifer system and the general updip gradient of the geopressed zone downdip from the fault zone. As a result, discharge from the confined section of the Carrizo-Wilcox aquifer is through upward leakage or through pumpage.

The heterogeneity and structure of the aquifer, particularly the Wilcox, affect the water quality. Sand bodies connected to recharge areas in the outcrop, and sands within the major fluvial channels typically represent pathways for fresh water from the outcrop into the deeper confined section. Fault zones may limit downdip flow of fresh groundwater, as indicated by higher total dissolved solids (TDS) groundwater south the Mount Enterprise fault system (Fogg and Kreitler, 1982). Isolated sands and sands in contact with thick mud units may also have poor water quality due to leakage of saline water from surrounding mud units. Even though delineating high-TDS groundwater is important for water availability determinations, water quality assessment is not an explicit requirement of the current GAM. However, a preliminary characterization of water quality for the Carrizo-Wilcox aquifer is given in Appendix F.

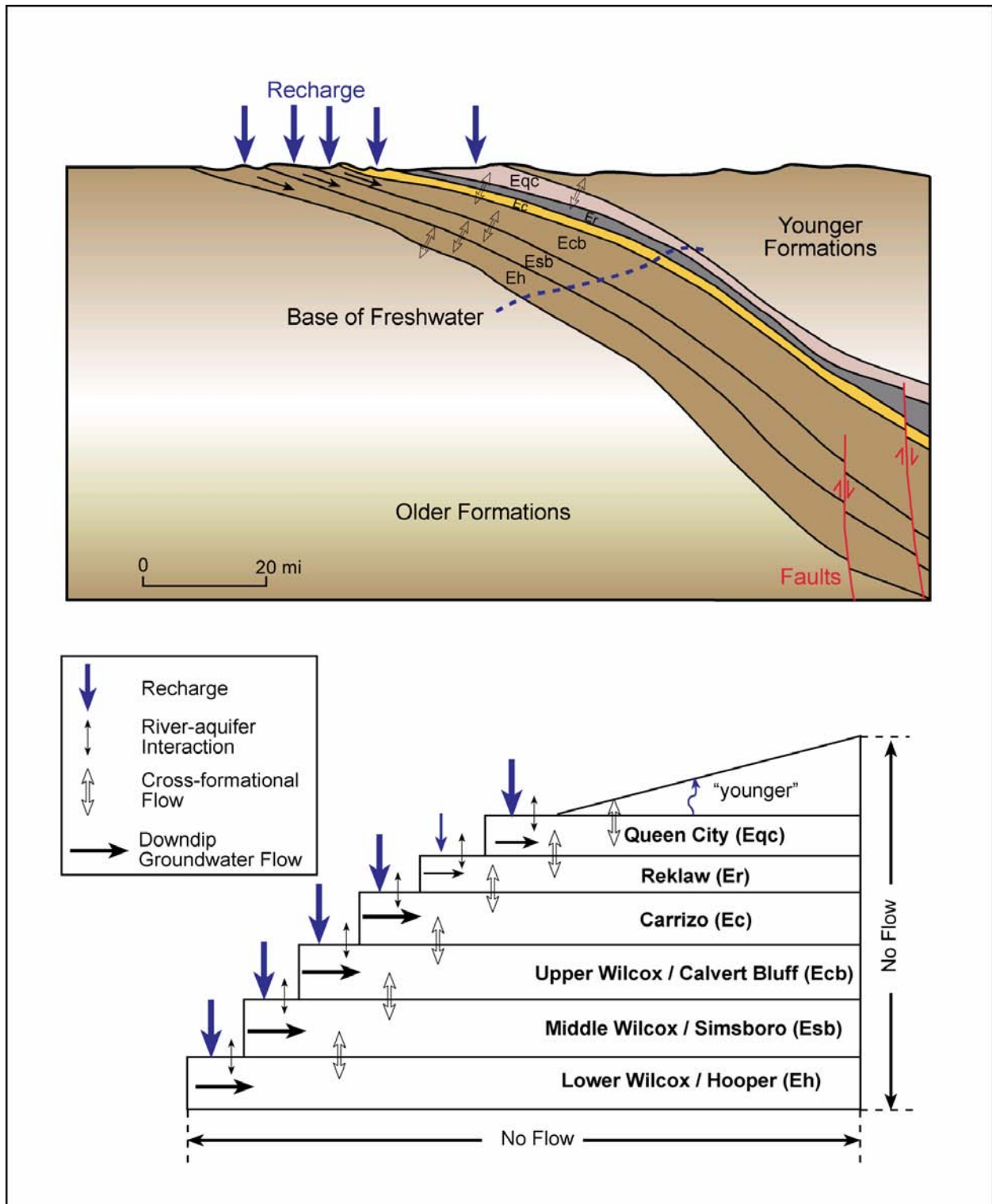


Figure 5.1 Conceptual groundwater flow model for the Northern Carrizo-Wilcox GAM.

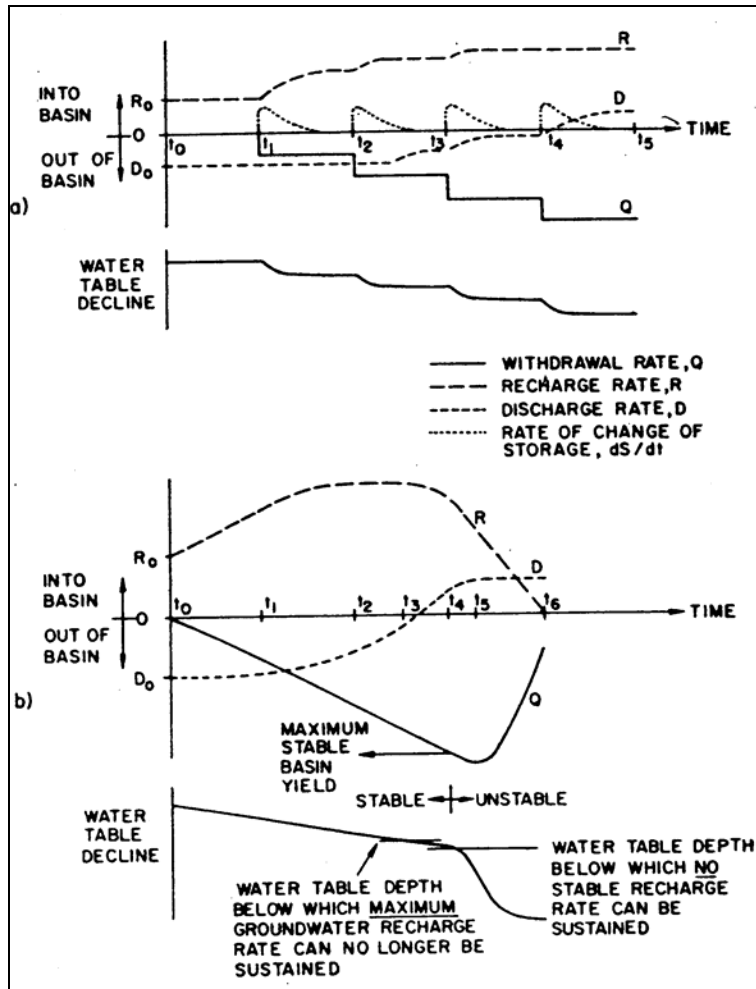


Figure 5.2 Schematic diagram of transient relationships between recharge rates, discharge rates, and withdrawal rates for an unconfined aquifer basin (from Freeze, 1971).

6.0 MODEL DESIGN

Model design represents the process of translating the conceptual model for groundwater flow in the aquifer (Section 5) into a numerical representation which is generally described as the model. The conceptual model for flow defines the required processes and attributes for the code to be used. In addition to selection of the appropriate code, model design includes definition of the model grid and layer structure, the model boundary conditions, and the model hydraulic parameters. Each of these elements of model design and their implementation are described in the remainder of this section.

6.1 Code and Processor

The code selected for the Northern Carrizo-Wilcox GAM and for all GAMs developed by or for the TWDB is MODFLOW-96 (Harbaugh and McDonald, 1996). MODFLOW-96 is a multi-dimensional, finite-difference, block-centered, saturated groundwater flow code which is supported by enhanced boundary condition packages to handle recharge, ET, streams (Prudic, 1988), and reservoirs (Fenske et al., 1996).

The benefits of using MODFLOW for the Northern Carrizo-Wilcox GAM include: (1) MODFLOW incorporates the necessary physics represented in the conceptual model for flow described in Section 5 of this report, (2) MODFLOW is the most widely accepted groundwater flow code in use today, (3) MODFLOW was written and is supported by the USGS and is public domain, (4) MODFLOW is well documented (McDonald and Harbaugh, 1988; Harbaugh and McDonald, 1996), (5) MODFLOW has a large user group, and (6) there are a plethora of graphical user interface programs written for use with MODFLOW.

To the extent possible, we have developed the MODFLOW data sets to be compatible with Processing MODFLOW for Windows (PMWIN) Version 5.3 (Chiang and Kinzelbach, 1998). The size of the GAM and the complexity of our application precludes 100-percent compatibility with PMWIN, as well as many other interfaces.

We have executed the model on x86 compatible (i.e., Pentium or Athlon) computers equipped with the Windows 2000 operating system. MODFLOW is not typically a memory-intensive application in its executable form. However, if any preprocessor (such as PMWIN) is used for this size and complexity of model, at least 256MB of RAM is recommended.

6.2 Model Layers and Grid

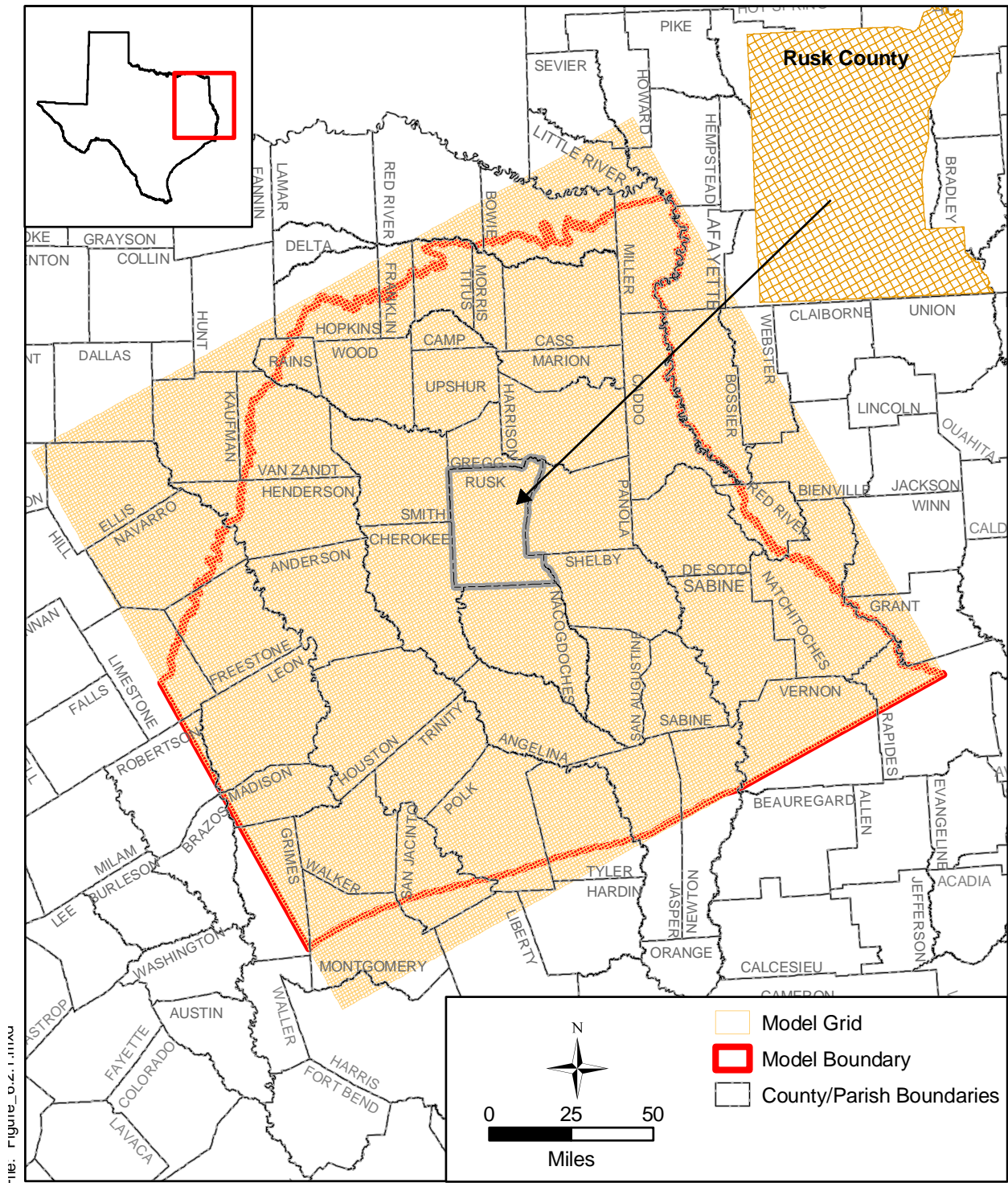
Consistent with the model hydrostratigraphy described in Section 4.1 and the conceptual flow model detailed in Section 5, we have divided the Northern Carrizo-Wilcox GAM into six model layers. MODFLOW-96 numbers layers from top to bottom and this is the order by which each layer will be introduced. Layer 1 is the Queen City Formation which outcrops over a large area of the East Texas Basin (see Figure 2.13). Layer 2 is the Reklaw Formation. Layer 3 is the Carrizo Formation. Layer 4 is the upper Wilcox. Layer 5 is the middle Wilcox and Layer 6 is the lower Wilcox. The lower Wilcox is not present in the northeastern portion of the model area. Where the lower Wilcox is not present, Layer 6 cells are flagged as inactive. The model layers are shown with the corresponding hydrostratigraphic units in Figure 4.1.1.

The Northern Carrizo-Wilcox GAM boundaries are defined on the basis of surface or groundwater hydrologic boundaries. The model area for the Northern Carrizo-Wilcox GAM is bounded laterally by the Red River to the east in Louisiana and Arkansas, and the drainage divide between the Trinity and Brazos rivers to the west. The Trinity-Brazos basin divide serves as the model boundary in the outcrop (presumed groundwater flow divide) and is extended in the subsurface to the downdip boundary of the model. The northern boundary of the model is defined by the updip edge of the Wilcox Group outcrop and the southern boundary by the updip limit of the Wilcox growth fault zone (Bebout et al., 1982). The upper boundary is defined by the ground surface in the outcrop of the Carrizo-Wilcox aquifer extending south to the extent of the Queen City outcrop. South of the Queen City outcrop, the contact between the Queen City and the overlying Weches Formation defines the upper boundary.

MODFLOW-96 requires a rectilinear grid and also requires an equal number of rows for all columns. As a result, the model area is constrained to being a rectangular grid. Typically, one axis of the model grid is aligned parallel to the primary direction of flow (this is to the southeast in the western part of the Northern Carrizo-Wilcox GAM and to the southwest in the Sabine Uplift area). The model area was determined by imposing the preceding constraints with the additional constraint of minimizing the number of model grid cells. The model grid origin is located at GAM Coordinates 19,257,000 ft north and 6,295,000 ft east, with the x-axis rotated positive 29.11°. The GAM standard requires that grid cells be square of a uniform dimension of 1 mile (area of 1 square mile). The model has 210 columns and 195 rows for a total of

40,950 grid cells per layer. As discussed below, not all of these grid cells are active in the model. Figure 6.2.1 shows the entire model grid. Included on this figure is an inset with an enlargement of Rusk County to show the model grid at the county scale.

We defined the active area of each model layer by intersecting the layer grid with the geologic map and the growth fault boundaries to the south. Cells extending past the outcrop or downdip of the growth fault boundary were defined as inactive in the IBOUND array. If a cell was 50% or more in the outcrop, it was defined as active. Cells east of the Red River on the eastern boundary of the model were also made inactive on the assumption that the Red River is a regional sink for the aquifer being modeled. After clipping the layers to their proper dimensions, Layers 1 through 6 had the following number of grid cells respectively, 18799, 20523, 21463, 24844, 30001, and 22312. The total number of active grid cells in the model grid is 137942.



file: figure_6.2.1.tif

Figure 6.2.1 Model grid of the Northern Carrizo-Wilcox GAM.

6.3 Boundary Condition Implementation

A boundary condition can be defined as a constraint put on the active model grid to characterize the interaction between the active simulation grid domain and the surrounding environment. There are generally three types of boundary conditions; specified head (First Type or Dirichlet), specified flow (Second Type or Neumann), and head-dependent flow (Third Type or Cauchy). The no-flow boundary condition is a special case of the specified flow boundary condition.

Boundaries can be defined as being time independent or time dependent. An example of a time dependent boundary might be a pumping flow boundary or a reservoir stage elevation. Because many boundaries require time dependent (transient) specification, the stress periods used by MODFLOW must be specified. A stress period in MODFLOW defines the time period over which boundary and model stresses remain constant. Each stress period may have a number of computational time steps which are some fraction of the stress period. For this model, the stress periods have been set at one month. Therefore, all transient boundaries in the model cannot change over a period of less than one month.

Boundaries requiring specification include: layer lateral and vertical boundaries, surface water boundaries, recharge boundaries, and discharge boundaries caused by pumping. Lateral and vertical boundaries will be a combination of specified flow (no-flow, Second Type) or head-dependent flow boundaries (general-head boundaries, Third Type). Surface water boundaries are head-dependent flow boundaries (Third Type). Recharge is a specified flow boundary (Second Type). Evapotranspiration (ET) is a head-dependent flow boundary (Third Type). Pumping discharge is a specified flow boundary (Second Type).

Figures 6.3.1 through 6.3.6 show the active and inactive grid cells along with the model boundary conditions for each of the six model layers, respectively. Implementation of the boundary conditions for the Northern Carrizo-Wilcox GAM is described below.

6.3.1 Lateral Model Boundaries

The lateral model boundaries have been defined to occur on the northeast at the Red River and to the southwest along the drainage divide between the Brazos and Trinity rivers. Both of these boundaries are assumed to be no-flow boundaries (Second Type). From a review

of the predevelopment hydraulic head map, we concluded that the southwestern boundary is coincident with the groundwater flow direction and reasonably mimics a no-flow boundary. A no-flow boundary was also assumed for the northeastern model boundary assuming that there is insignificant underflow of the Red River in the model area.

The applicability of no-flow boundaries was investigated further for the simulated historical period (1980 through 1999). A no-flow boundary was maintained at the Red River during the transient and predictive model periods (1980-2050). For the southwestern model boundary, water levels were reviewed for the period from 1980 through 1999. Water levels were found to be reasonably constant given the scale of the model with head decrease observed from a few feet to up to 30 feet. Because specification of boundary heads across the model boundary is inherently uncertain, and because head decreases along the boundary are within the model head error, the southwestern boundary was maintained as a no-flow boundary throughout the transient historical simulation period. If pumping is at least balanced on both sides of the no-flow boundary, the assumed boundary is conservative. The representativeness of this boundary could not be meaningfully investigated for the predictive simulation period (2000-2050).

6.3.2 Vertical Boundaries

The model has a no-flow boundary on the bottom of Layer 6 (the lower Wilcox) representing the marine shales of the Midway Formation. The upper model boundary is the free-water surface calculated in the outcrops of Layers 1 through 6. In the downdip portions of the model where younger sediments overlie the Queen City, these sediments are represented by a general-head boundary condition (Third Type). The initial vertical conductances of the general-head boundaries were calculated based on a harmonic average of the hydraulic conductivities of the overlying units, which were taken from Williamson et al. (1990). Their hydraulic conductivity data were used because they were determined through calibration of a regional model. The hydraulic heads associated with the upper general-head boundary condition were set equal to the water table that was estimated using the regression equations of Williams and Williamson (1989).

6.3.3 Surface Water Implementation

Surface water acts as a head-dependent flow (Third Type) boundary condition for the top boundary of the active model grid cells (outcrop). The stream package (Prudic, 1988) and

reservoir package (Fenske et al., 1996) are head-dependent flow boundary conditions that offer a first-order approximation of surface water/groundwater interaction. The stream-routing package allows for stream-related recharge to be rejected during gaining conditions and for stream-related recharge to be induced during losing conditions. When pumping affects water levels near stream/aquifer connections, recharge will be included through stream loss.

The stream-routing package requires designation of segments and reaches. A reach is the smallest division of the stream network and is comprised of an individual grid cell. A segment is a collection of reaches which are contiguous and do not have contributing or diverting tributaries. In MODFLOW, physical properties must be defined describing the hydraulic connection (conductance) between the stream and the aquifer. Stream flow rates are defined at the beginning of each segment for each stress period.

INTERA developed a GIS-based method for developing the reach and segment data coverages for MODFLOW. Figures 6.3.1 through 6.3.6 show the model grid cells which contain stream reaches in the model domain. Required physical properties of the reaches including stream width, bed thickness, and roughness are taken from the EPA River Reach data set (<http://www.epa.gov/region02/gis/atlas/rf1.htm>). The hydraulic conductivity used to define the hydraulic conductance between the aquifer and the stream was set at the hydraulic conductivity of the underlying formation. Hibbs and Sharp (1991) studied the hydraulic connection between the Colorado River and the alluvium and Carrizo-Wilcox aquifer near a Bastrop well field. They concluded that the connection between the river and the aquifer was very good and did not see hydraulic evidence for a low permeability river bed. Our initial approach was to keep the hydraulic conductivity of the stream bed high and relatively constant and allow the stream width taken from the EPA River Reach data set (RF1) to control the streambed conductance.

The stream-routing package also requires specification of stream flow rate for each starting reach at each stress period. For predevelopment conditions, and for the historical period, no representative stream gage data exist for the majority of the stream segments. To handle this for the pre-development simulation, we used mean flow rates from the EPA RF1 data set to specify the flow rate entering each model segment. The EPA RF1 data set contains mean flow rates estimated along the entire stream and coinciding with all of the modeled stream segments.

For the transient simulations, stream flows are based on historical records. However, because the stream gage coverage is sparse, stream flow rates required estimation at the majority of stream segments. The approach we employed to develop ungaged stream segment flow rates has the following assumptions: (1) gages in close proximity behave similarly, (2) the RF1 average stream segment stream flow estimates are accurate, (3) a gage's distribution of monthly stream flow is lognormal, and (4) the standard deviation of the log of monthly flow rate at an ungaged location is equal to the standard deviation of the log of monthly flow rate at a nearby ungaged location. We have checked assumptions 1 through 3 and have found they generally do hold for the model region. Assumption 4 cannot be definitively established in the current domain, due to lack of data for cross validation.

To calculate the ungaged stream segment flow rates at each monthly stress period, we first constructed the monthly distribution of log flow rate at our gaged stream locations and calculated the standard deviation of that distribution. From the EPA RF1 data set we have the mean flow rates for all segments. If for stress period one the gaged monthly stream flow was equal to the 75th percentile of the distribution, we would use the mean flow rate from the EPA RF1 data set with the standard deviation taken from the actual gaged flow distribution to estimate the 75th percentile flow rate at the ungaged segment. This technique maintains the proper magnitude of flows at ungaged locations as constrained by the EPA RF1 mean flow estimates while superposing the flow variability based upon the nearest gaged data.

The MODFLOW reservoir package (Fenske et al., 1996) has been used to model reservoirs and lakes. The properties required for specification for reservoirs includes the hydraulic conductance between the lake and the aquifer and the reservoir stage as a function of stress period. Because reservoirs are in river valleys, the reservoir package must be integrated with the stream-routing package. This is done by starting a new segment at the downstream side of each reservoir. Similar to the streams, the hydraulic conductivity used to estimate the reservoir/aquifer hydraulic conductance was initially set equal to the hydraulic conductivity of the underlying material. INTERA developed lake stage records by reviewing records in the literature and by contacting various river authorities in the study area. These stage histories are provided in the data model delivered with this modeling report. Forty reservoirs were modeled in the Northern Carrizo-Wilcox GAM (see Figure 4.5.1).

Spring discharge records were reviewed for application in the Northern Carrizo-Wilcox GAM as drain boundary conditions (Type 3). However, as discussed in Section 4 of this report, there are no significant springs still flowing in the model area that are not being handled by stream reach cells, which provide a sufficiently similar boundary condition.

6.3.4 Implementation of Recharge

Because an evaluation of groundwater availability is largely dependent upon recharge (Freeze, 1971), it is an important model input parameter warranting careful examination and meaningful implementation. In typical model applications, recharge is either homogeneously defined as a percentage of the yearly average precipitation or calibrated as an unknown parameter. Unfortunately, recharge and hydraulic conductivity can be correlated parameters preventing independent estimation when using only head data constraints. Another compounding problem is that recharge is a complex function of precipitation rate and volume, soil type, water level and soil moisture, topography, and ET (Freeze, 1969). Precipitation, ET, water-table elevation, and soil moisture are areally and temporally variable. Soil type, geology, and topography are spatially variable. For the GAM, recharge requires specification for steady-state conditions, for transient conditions from 1980 until 2000, for the transient drought of record, and for average conditions. Reliable tools for specification of recharge at the watershed scale, or the regional model scale (1000s of square miles for the GAMs) do not currently exist.

As a tractable approach to dealing with recharge at the scale of this model, we have used SWAT (Soil Water Assessment Tool) to estimate diffuse recharge rates. SWAT was developed for the USDA Agricultural Research Service by the Blacklands Research Center in Temple, Texas. SWAT is a public-domain model. The SWAT Website where downloads and code-specific documentation can be found is <http://www.brc.tamus.edu/swat/>. SWAT provides a GIS-driven, watershed scale tool to estimate regional soil water balances, incorporating soils data (USDA/NRCS STATSGO) with the USGS Multi-Resolution Land Characteristics (MRLC) data. SWAT uses standard techniques to track water after it reaches the ground as precipitation. SWAT uses the SCS Curve Number Method (accounting for antecedent moisture conditions) to partition precipitation into runoff and infiltration. Infiltrating water either increases the soil moisture, is lost through ET, or continues down to the water table. We used the Hargreaves Method for estimating Potential ET because it only requires estimates of monthly mean minimum and maximum temperatures which are available for the study area. Average daily net

radiation is available within SWAT for month and degrees of latitude. The Hargreaves method is considered accurate for simulation periods that are equal to, or larger than, one month. This is consistent with one month stress periods and the assumptions underlying the NRCS curve-number method for estimating runoff. The potential ET is converted to an actual ET based on the vegetation size and type (determines maximum ET) and soil water availability (determines actual ET).

SWAT is used in an uncoupled mode to estimate several model inputs for MODFLOW. Consistent with the transient MODFLOW stress periods of one month, SWAT is also simulated with one month stress periods using daily data (time steps). SWAT was simulated for the time period from 1975 through 1999 to coincide with the calibration and transient model simulation periods.

For each MODFLOW stress period, SWAT calculates: (1) the recharge rate for the recharge package, (2) the ET max for the ET package, and (3) the extinction depth for the ET package. The SWAT estimate of shallow recharge is used as a recharge flux in MODFLOW. SWAT accounts for ET which may occur in the vadose zone. However, in our method of application, SWAT does not account for groundwater transpiration. To account for groundwater ET, the “surplus” ET from SWAT (ET potential – ET actual) was applied as ET max in the ET package in MODFLOW. For each month simulated, SWAT calculates a rooting depth representative of the season, vegetative cover, and soil type. This rooting depth is passed through to MODFLOW as the extinction depth required by the MODFLOW ET Package. As a result, ET from groundwater will occur when the water table (as simulated by MODFLOW) is above the extinction depth and there is surplus ET potential for that particular stress period. Appendix E provides a more detailed explanation of our use of SWAT in an uncoupled mode with MODFLOW.

For the predevelopment model, the SWAT estimates for recharge were averaged values taken from the 1975 to 1999 simulation. The ET max estimates were also averaged for this same time period for input into the MODFLOW ET package. The maximum extinction depth for each cell was used for input into the MODFLOW ET package. In the transient simulation, recharge varies as a function of time with a monthly stress period.

SWAT was also used for implementing recharge in the predictive simulation period (2000-2050). Average recharge conditions (1975-1999) were used for each predictive simulation period. Recharge was varied seasonally in the predictive simulations based upon monthly average recharge (1975 - 1999). Predictive simulations end with a drought-of-record. Recharge conditions for the drought-of-record were developed running SWAT through the drought-of-record climatic conditions. A discussion of the drought-of-record is given in the predictive simulation Section 10.

6.3.5 Implementation of Pumping Discharge

Pumping discharge is not considered in the predevelopment model because the model is meant to be representative of times prior to significant resource use. However, pumping discharge is the primary stress on the model during the historical (1980 - 1999) and the predictive (2000-2050) model periods. Pumping discharge is a cell dependent specified flow boundary.

The procedural techniques that we used in estimating and allocating pumping are provided as Appendices B and C. For details on how the historical or predictive pumping was derived, the reader is referred to those appendices. Once the pumping had been estimated for each of the seven user groups (municipal, manufacturing, power generation, mining, livestock, irrigation, and county-other), it was summed across all user groups for a given model cell (row, column) and a given model layer. This process was repeated for all active model cells in the model domain for each transient stress period. As discussed above, the stress period used in the transient simulations is one month. Therefore, the MODFLOW well-package data set has a specified flow boundary condition for each month of simulation, for each active grid cell within which pumping is occurring.

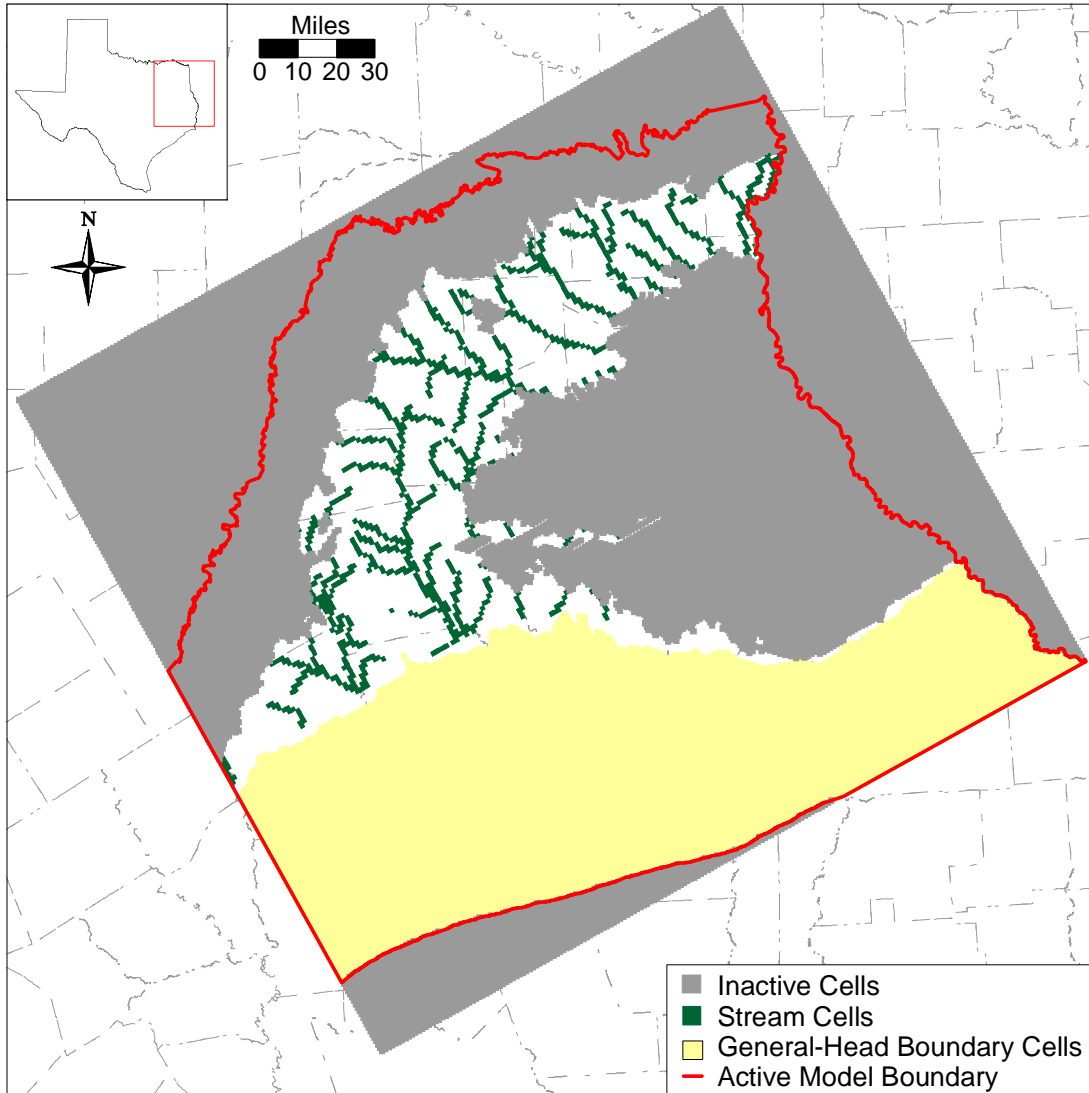


Figure 6.3.1 Layer 1 (Queen City) boundary conditions and active/inactive cells.

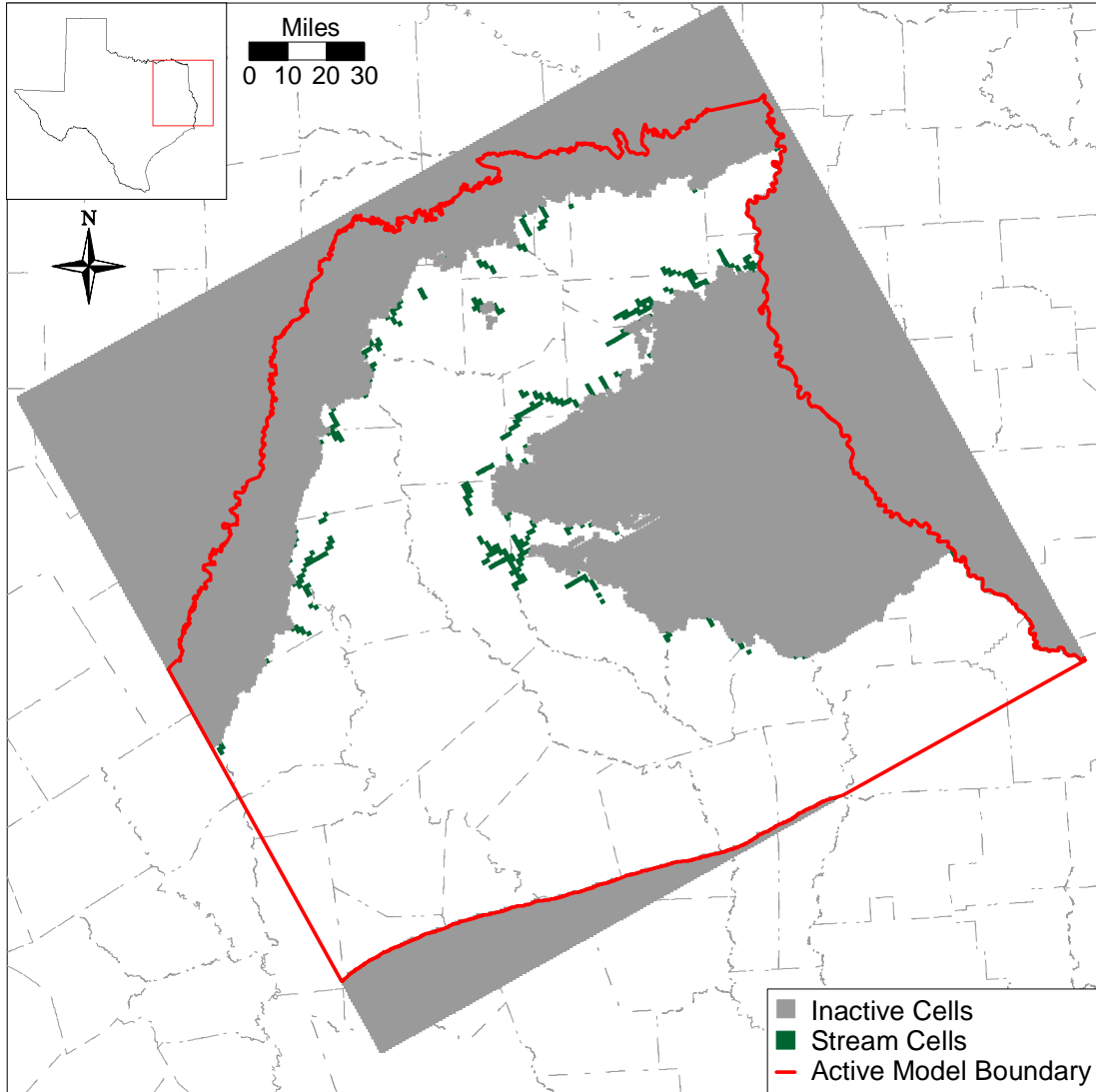


Figure 6.3.2 Layer 2 (Reklaw) boundary conditions and active/inactive cells.

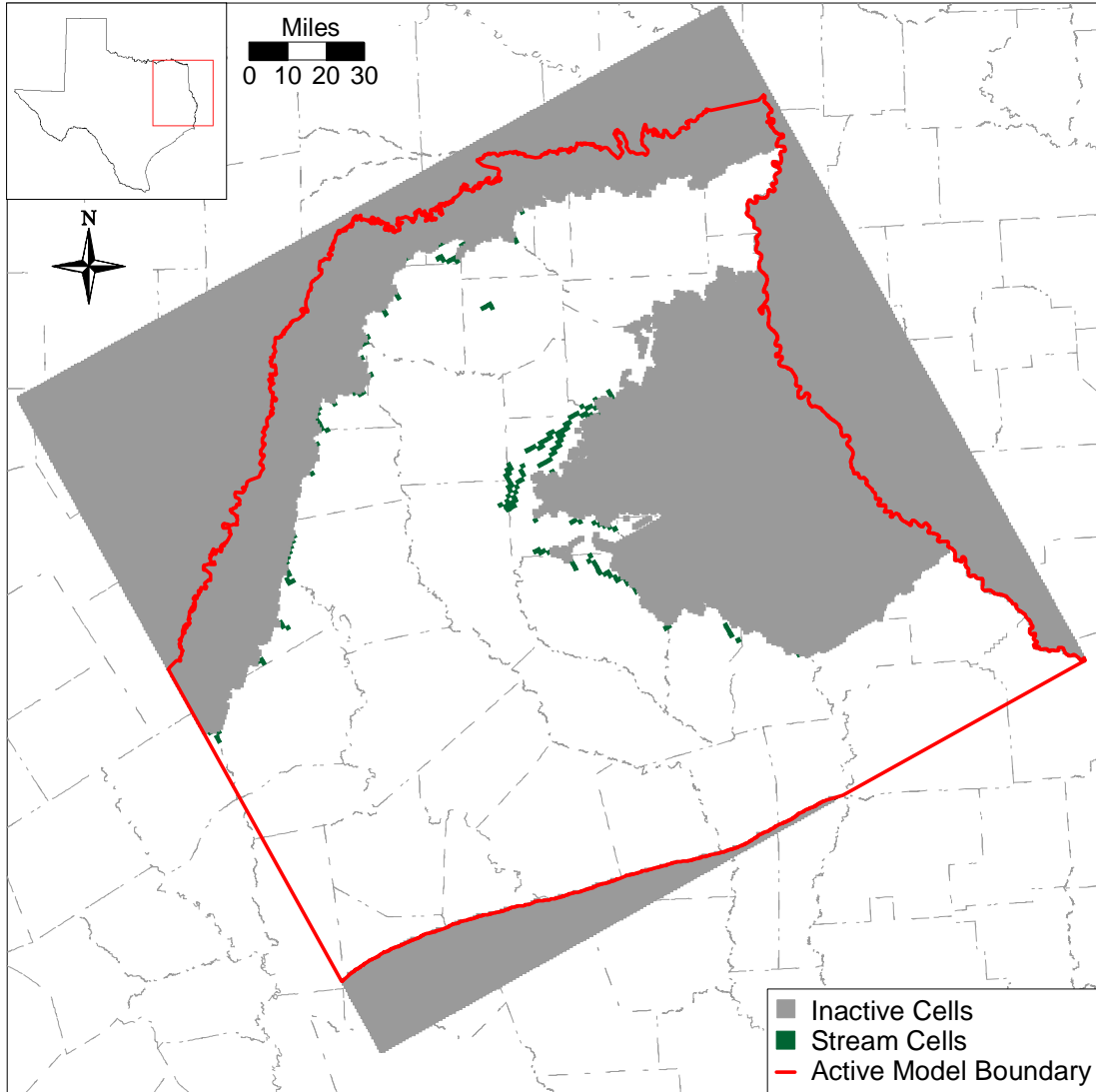


Figure 6.3.3 Layer 3 (Carrizo) boundary conditions and active/inactive cells.

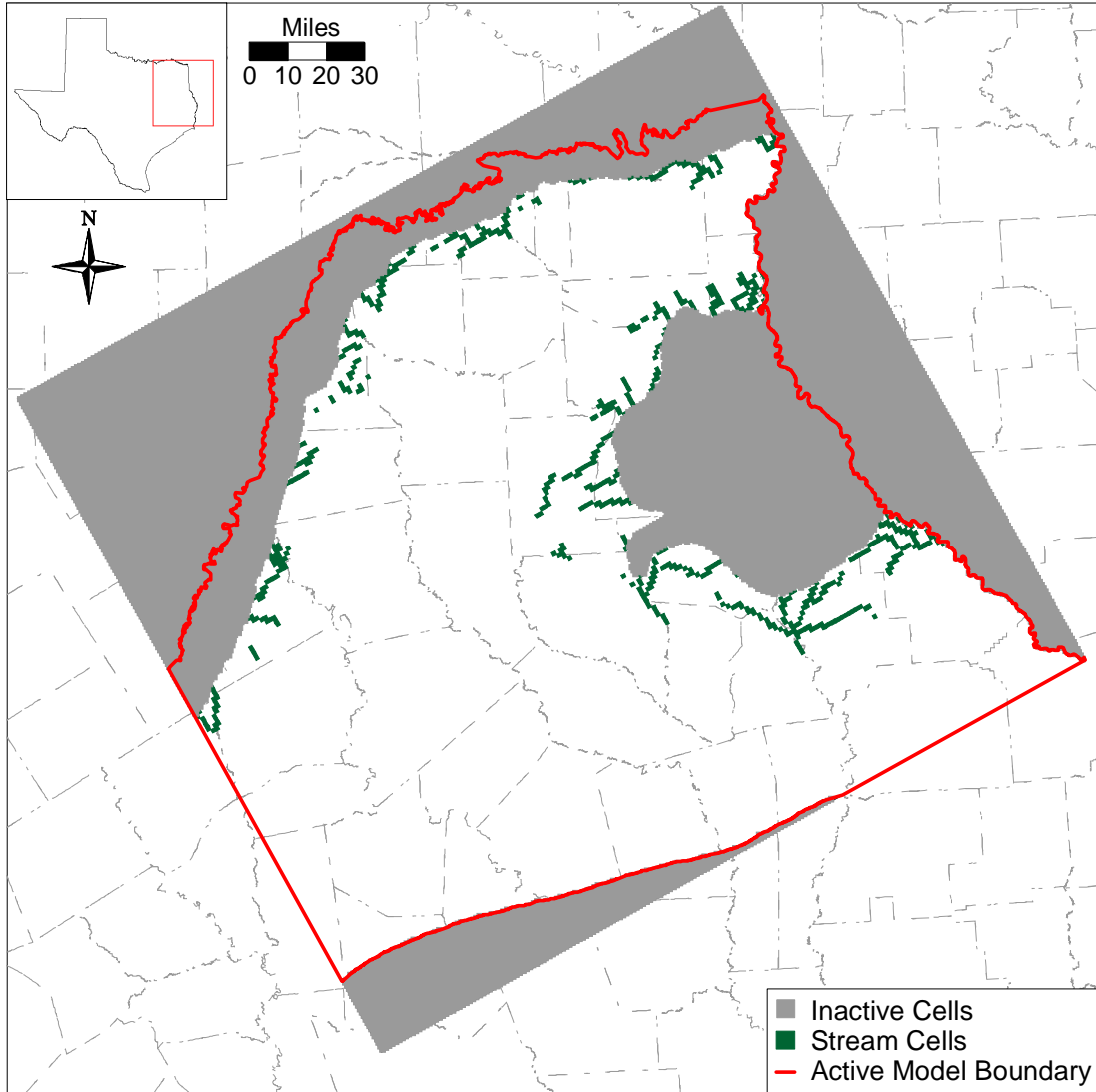


Figure 6.3.4 Layer 4 (upper Wilcox) boundary conditions and active/inactive cells.

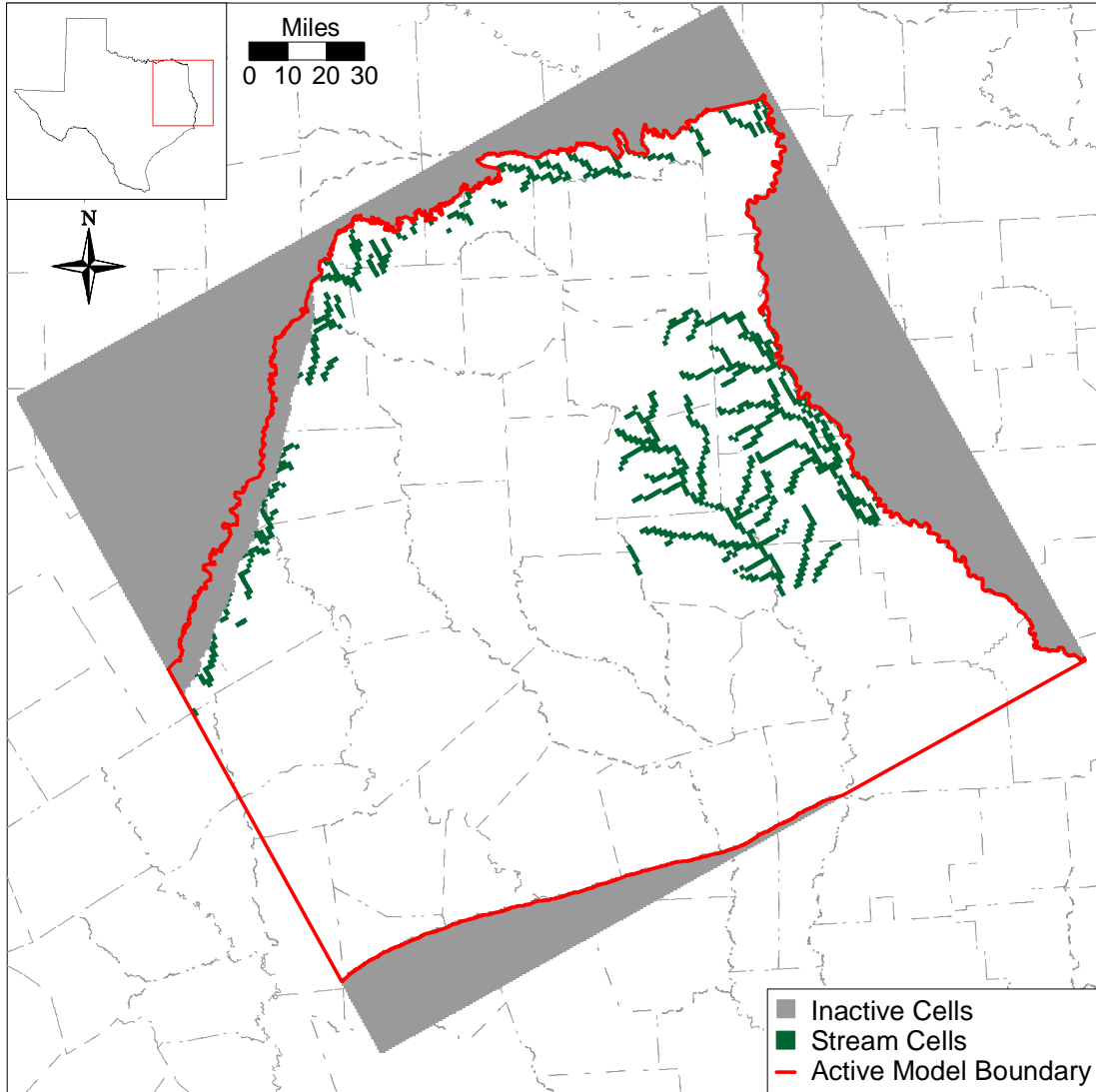


Figure 6.3.5 Layer 5 (middle Wilcox) boundary conditions and active/inactive cells.

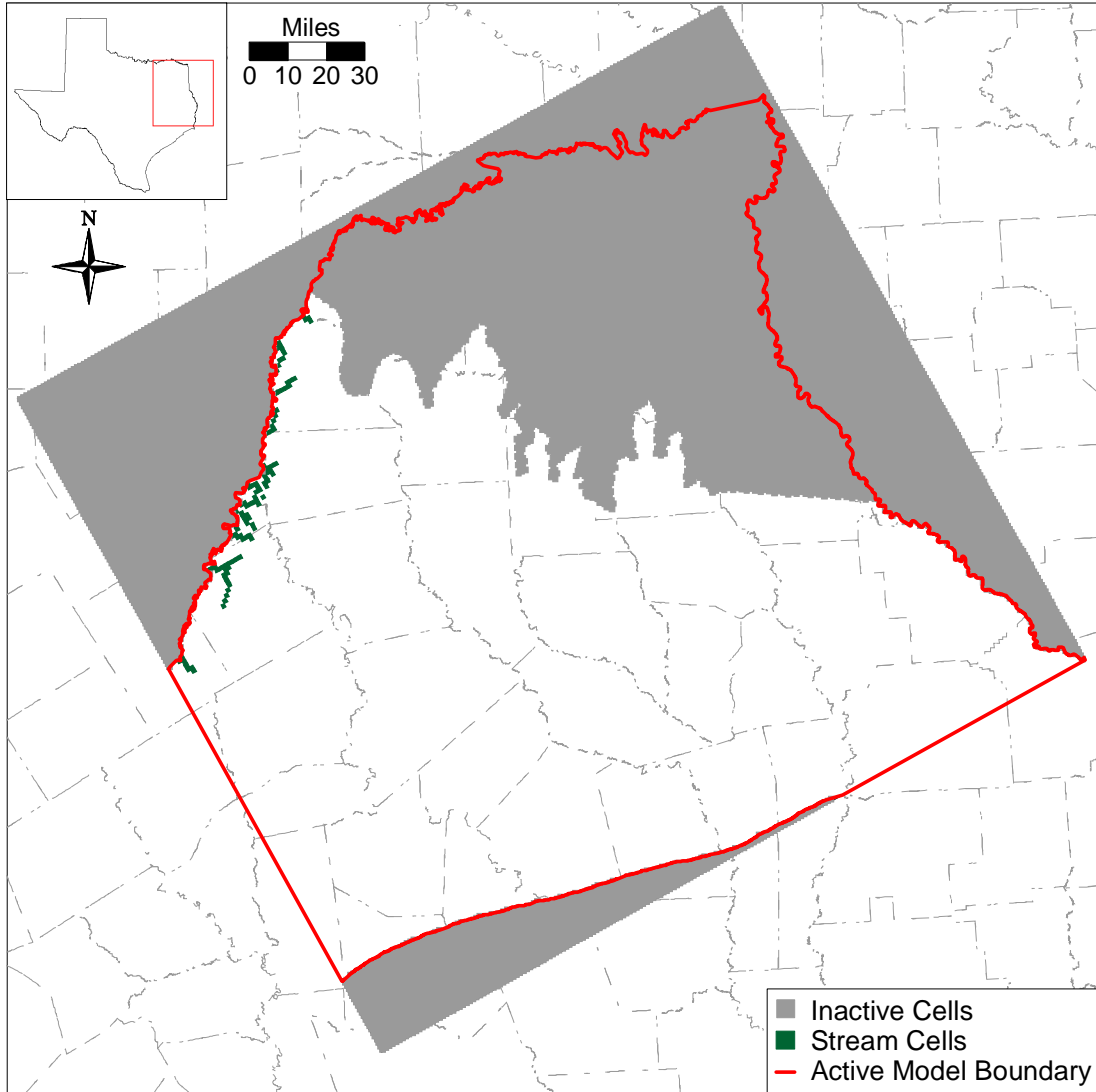


Figure 6.3.6 Layer 6 (lower Wilcox) boundary conditions and active/inactive cells.

6.4 Model Hydraulic Parameters

For the steady-state model, the primary parameter to be estimated and distributed across the model grid is hydraulic conductivity. For the transient model, we must add the storage coefficient. The method used for distributing hydraulic conductivity and storage in the model domain is described in the following.

6.4.1 Hydraulic Conductivity

In the GAM, model properties are constant within a given grid block which is one square mile in area and varies in thickness from a minimum of 20 feet to hundreds of feet. The challenge in constructing a regional model at this scale is in the development of an accurate “effective” hydraulic conductivity that is representative of the grid block scale accounting for the different lithologies present in each grid cell. The effective hydraulic conductivity depends on the geometry, individual hydraulic conductivity, and the correlation scale relative to the grid scale and simulation scale of the various lithologies present in the grid cell (Freeze, 1975).

There have been many investigations on estimating an average effective hydraulic conductivity given assumptions for flow dimension, layer geometry, and correlation scales (Warren and Price, 1961; Gutjahr et al., 1978; Fogg, 1989). For one-dimensional flow in lithologies combined in parallel (i.e., layered), the appropriate effective hydraulic conductivity would be the weighted arithmetic mean. For one-dimensional flow in lithologies combined in series, the effective hydraulic conductivity is the harmonic mean. Hydraulic conductivity has been found to be a log-normally distributed parameter. In two-dimensional uniform flow, assuming that the hydraulic conductivity is log-normally distributed and randomly juxtaposed, the effective hydraulic conductivity is exactly the geometric mean (deMarsily, 1986). Fogg (1989) has studied effective hydraulic conductivity for a model of the Carrizo-Wilcox aquifer in Freestone and Anderson counties in East Texas. His study concluded that for the case when the individual lithologic layers vary in dimension from smaller and larger than the model grid scale, the effective hydraulic conductivity in the horizontal dimension is between the geometric mean and the arithmetic mean. In the vertical dimension, he found that the effective hydraulic conductivity should vary from the geometric to the harmonic mean.

In Section 4.3, we discussed the distribution of hydraulic conductivities available for the Carrizo-Wilcox aquifer in Mace et al. (2000a). Hydraulic parameterization of coastal plain

sediments is often correlated to sand body thickness, geometry, and depositional facies (e.g., Payne, 1975; Henry et al., 1980; Fogg, 1986; Thorkildsen and Price, 1991). From the analysis provided in Section 4.3 of this report, hydraulic conductivity has been distributed within the model regions where data were available. Likewise, sand thickness and sand fraction (%) distributions for the modeled aquifers were developed where data were available. However, as discussed earlier in Section 4.3, a clear correlation between sand thickness (sand fraction) and hydraulic conductivity could not be established. Similarly, variograms in different directions showed little difference, indicating a lack of horizontal anisotropy in hydraulic conductivity. Only the sand-thickness trends of the major fluvial channels (Figure 4.3.10) provide some degree of horizontal anisotropy in the spatial distribution of the transmissivity of the aquifer layer.

There are two key assumptions that underlie the method which we used to estimate horizontal and vertical hydraulic conductivity. First, it was assumed that the available transmissivity data, or interpreted hydraulic conductivity data, are representative of the higher permeability strata encountered in the borehole. The higher permeability strata were also assumed to be dominated by a sand lithology. Second, it was assumed that the measured hydraulic conductivities are representative of horizontal hydraulic conductivity, not vertical hydraulic conductivity. Vertical hydraulic conductivity data at a scale representative of this model were not available. Based upon these assumptions, the method we used to distribute horizontal and vertical hydraulic conductivity is discussed below.

In the model we used our geostatistical analysis (kriging) presented in Section 4.3 as the initial sand hydraulic conductivities for a given block. In areas lacking hydraulic conductivity measurements, we used depositional models, lithofacies zones, and sparse hydraulic data to estimate hydraulic conductivity within zones. Data tends to be biased towards the outcrop and shallow subcrop. Previous investigators have found, both theoretically and empirically, that the hydraulic conductivity of unconsolidated sediments decreases with depth (Helm, 1976; Prudic, 1991). This is thought to be a result of sediment compaction with increased overburden pressure. In the Texas Gulf Coastal Plain, this could also be a result of low-energy depositional environments toward the coast. Regardless, we considered the decreasing of hydraulic conductivity as a function of overburden when data were not available.

With the sand hydraulic conductivity estimated at the grid scale by kriging, we used the sand fraction to estimate an effective horizontal hydraulic conductivity adjusted for the percent of the formation that is not sand (i.e., silt or clay), given by:

$$K_h(\text{effective}) = K_{\text{sand}} \cdot (b_{\text{net-sand}} / b_{\text{layer}}) \quad (6.1)$$

where $K_h(\text{effective})$ is the effective grid block horizontal hydraulic conductivity, K_{sand} is the hydraulic conductivity of the sand as interpreted from hydraulic test data and interpolated to the grid scale, $b_{\text{net-sand}}$ is the net-sand thickness in feet in a given layer, and b_{layer} is the total layer thickness. This equation assumes horizontal flow and also assumes that the horizontal hydraulic conductivity of the non-sand lithologies is unimportant to grid-scale horizontal flow relative to the sands. MODFLOW combines total layer thickness (b_{layer}) and $K_h(\text{effective})$ to calculate grid block transmissibilities which govern flow rates within the model. Equation (6.1) above essentially adjusts MODFLOW's calculation of transmissibility to account for the lower permeability strata in the individual layers.

Section 4.3 examined the available data on hydraulic conductivities, indicating that the model layers had varying amounts of available supporting data for assigning effective horizontal hydraulic conductivity to model grid cells in the layer. Queen City data points are concentrated in the central and northern parts of the East-Texas Basin, with only sparse data south of northern Cherokee county. As noted in Section 4.3.3, reasonably good distributions of data points were available for the Carrizo, upper Wilcox, and middle Wilcox (Layers 3, 4, and 5) in the outcrop and East-Texas Basin subcrop. For areas south of the East-Texas Basin and the Sabine Uplift, data were sparse to absent in these layers. For the lower Wilcox (Layer 6), hydraulic conductivity data were almost all within or very near the western outcrop, with a few data points in the East-Texas Basin subcrop and in the Sabine Uplift.

The kriged hydraulic conductivity values for the Wilcox (Layers 3, 4, and 5) were combined with the calculated percent sand map in Figure 4.3.10 using Equation 6.1 to yield effective horizontal hydraulic conductivity fields. Since the sand-percent map is for the entire Wilcox Group, the sand was subdivided into the individual layers according to the following fractions: (a) 37.5% to the upper Wilcox, (b) 37.5% to the middle Wilcox, and (c) 25% to the lower Wilcox. These sand percentages correspond roughly to the average sand percentages between the Hooper, Simsboro, and Calvert Bluff formations west of the Trinity River, which

were explicitly mapped by Ayers and Lewis (1985). The Carrizo (Layer 3) was assumed to be essentially all sand and was therefore not adjusted for sand percent. A percent sand study was not done for the Queen City Formation since it was not the focus of this GAM scope. For the Reklaw confining unit (Layer 2) a constant horizontal hydraulic conductivity of 1 ft/day was used.

In areas where hydraulic conductivity data coverage was sparse or missing, effective hydraulic conductivity was estimated by dividing each layer into large zones of constant effective horizontal hydraulic conductivity, based on “soft” data -- depositional models, lithofacies zones, etc. The properties in these zones could then be scaled during calibration if necessary. In the Queen City (Layer 1) two zones were created, one extending from the downdip edge of the Queen City outcrop to the downdip extent of the Queen City sands (Guevara and Garcia, 1972), and the other extending southward from there to the south edge of the model. For the Carrizo (Layer 3) conductivities were extrapolated south of the data points. The Wilcox (Layers 4, 5, and 6) was zoned in the southern downdip portion according to depositional systems as described by Fisher and McGowen (1967) and Fisher (1969). Initial estimates of hydraulic conductivity for these zones varied from 1.5 ft/day to 3 ft/day. The calibrated conductivity fields with the zonation discussed above are described in Section 8.1.

Vertical hydraulic conductivity is not measurable on a model grid scale and is therefore generally a calibrated parameter. Typical vertical anisotropy ratios (K_h/K_v) are on the order of 1 to 1000 determined from model applications (Anderson and Woessner, 1992). However, Williamson et al. (1990) reported that vertical resistance to flow could be significant in the Gulf Coast Aquifer system in Texas and Louisiana which is composed of similar types of coastal plain sediments as encountered in the Carrizo-Wilcox aquifer. Previous regional modeling studies in the Carrizo-Wilcox aquifer have documented vertical anisotropy ratios as high as 50,000 (Williamson et al., 1990).

Because vertical hydraulic conductivity of an aquifer is expected to be controlled by depositional environment and lithofacies, we used percent sand, maximum sand, depositional environment, lithofacies, and depth of burial in zoning vertical hydraulic conductivity to the degree practical.

6.4.2 Storativity

For unconfined aquifer conditions, a uniform storativity value of 0.20 was assigned to the different layers. Grid cells, which represented outcrop (land surface), are modeled as either confined or unconfined depending upon the elevation of the simulated water table in that grid cell. The confined storativity assigned to outcrop cells was done to account for water ponding on the ground surface and to prevent non-physical heads being computed and used in the equations governing groundwater flow.

For confined aquifer conditions, the storativity was specified as a function of aquifer thickness based upon a constant specific storage of 4.5×10^{-6} 1/ft, representing the average of reported values for the Carrizo-Wilcox aquifer (Mace et al., 2000a). This results in storativities ranging from 2×10^{-4} to 2×10^{-3} in the downdip portions of the Carrizo-Wilcox aquifer.

7.0 MODELING APPROACH

In the context of groundwater modeling, model calibration can be defined as the process of producing an agreement between model simulated water levels and aquifer discharge, and field measured water levels and aquifer discharge through the adjustment of independent variables (typically hydraulic conductivity, storativity, and recharge). Generally accepted practice for groundwater calibration usually includes performance of a sensitivity analysis and, if the model is going to be used for predictive purposes, a verification analysis. A sensitivity analysis entails a systematic variation of the calibrated parameters and stresses and the re-simulation of the aquifer conditions. Those parameters which strongly change the simulated aquifer heads and discharges would be important parameters to the calibration. It is important to note, that the “one-off” standard sensitivity analysis does not estimate parameter uncertainty as limited parameter space is investigated and parameter correlation is not accounted for. A verification analysis is a test to determine if the model is suitable for use as a predictive tool. This is performed by using the model to predict aquifer conditions during a period which was not used in the model calibration. Consistent with the approach outlined above, we calibrated the model, verified the model, performed sensitivity analyses, and performed predictive simulations.

7.1 Calibration

Groundwater models are inherently non-unique, meaning that multiple combinations of hydraulic parameters and aquifer stresses can reproduce measured aquifer water levels. To reduce the impact of non-uniqueness, we employed a method described by Ritchey and Rumbaugh (1996). This method includes (1) calibrating the model using parameter values (i.e., hydraulic conductivity, storativity, recharge) that are consistent with measured values, (2) calibrating to multiple hydrologic conditions, and (3) using multiple calibration performance measures such as hydraulic heads and discharge rate to assess calibration. Each of these elements is discussed below.

We used measured hydraulic conductivity and storativity data to initially estimate our parameters. The analysis of hydraulic parameters in Section 4.3 of this report indicates that there is a large amount of hydraulic conductivity data that is available for use as initial model values. Vertical hydraulic conductivity is not measurable at the model scale and thus cannot be well

constrained. Storativity is a parameter which is not well defined on the scale of the model. However, storativity is estimated from measured specific storage data in combination with the aquifer thickness. Recharge has not been directly measured in the study area and is arguably not measurable at the model scale. As described earlier in the report, we used SWAT to provide an initial estimate of shallow recharge. Adjustment of all model parameters were held to within plausible ranges based upon the available data and relevant literature. Adjustments to aquifer parameters from initial estimates were minimized to the extent possible to meet the calibration criteria. As a general rule, parameters that have few measurements were adjusted preferentially as compared to properties that have a good supporting database.

The model was calibrated over two time periods, one representing steady-state conditions and the other representing transient conditions. Because the confined section of the Carrizo-Wilcox aquifer in northeast Texas has been extensively developed, portions of the aquifer have not been at a steady state over much of the historical record. Therefore, we chose to use “predevelopment” conditions as our steady-state model. Section 4.4.2 describes the process used to estimate aquifer water levels for the steady-state predevelopment model. No pumping stresses were applied to the predevelopment model consistent with the assumption of steady-state conditions prior to significant resource development.

The transient calibration period ran from 1980 through 1989 consistent with the GAM model requirements. The actual transient simulation started in 1975, allowing the model to equilibrate over a 5-year period to the initial hydraulic heads that represent transient conditions during 1980. Section 4.4.4 describes the aquifer water levels and how they were derived to be used for the transient calibration period. Pumping estimates based upon historical records were applied on a monthly time scale in the transient calibration period. Likewise, recharge, stream flow, and reservoir stage were estimated on a monthly time basis and set as input through the transient calibration period. The time period from 1990 until 1999 was used as the verification period to assess the predictive ability of the model. Like the calibration period, transient stresses or boundary conditions were determined on a monthly time step. Unlike the calibration period, parameters were not adjusted in the verification process.

The model was calibrated through a wide range of hydrological conditions. The steady-state predevelopment model represents a period of equilibrium where recharge and aquifer

discharge through streams and cross-formational flow are in balance. Under these conditions, the aquifer rejects the maximum amount of recharge and, as was detailed in Section 5, a minimum amount of recharge is expected under stable basin conditions (Freeze, 1971). The steady-state model is sensitive to recharge. The calibration and verification period (1980 through 1999) represents a significantly different period. By this time, portions of the aquifer have been extensively developed resulting in loss of storage and declining heads. Some of the recharge being rejected under steady-state predevelopment conditions may be captured as a result of losing streams and increased vertical gradients. The calibration and verification periods also help constrain the model parameterization because a wide range of hydrologic conditions are encountered and simulated. The transient model is sensitive to parameters that are not sensitive for the steady-state model.

Calibration requires development of calibration targets and specification of calibration measures. To address the issue of non-uniqueness, it is best to use as many types of calibration targets as possible. The primary type of calibration target is hydraulic head (water level). However, we also used stream flows and gain/loss estimates. Simulated heads were compared to measured heads at specific observation points through time (hydrographs) and head distributions (maps) for select time periods (see Section 4.4) to ensure that model head distributions are consistent with hydrogeologic interpretations and accepted conceptual models for flow within the aquifer.

Stream calibration targets were derived from two types of data. First, we compared model simulated stream flow rates to observed flow rates at key stream gages in the model area. Because stream flow rates exceed aquifer/stream fluxes for local cells, available gain/loss estimates were also used for the major streams crossing the outcrop.

Traditional calibration measures (Anderson and Woessner, 1992) such as the mean error, the mean absolute error, and the root mean square error quantify the average error in the calibration process. The mean error (ME) is the mean of the differences between measured heads (h_m) and simulated heads (h_s):

$$ME = \frac{1}{n} \sum_{i=1}^n (h_m - h_s)_i \quad (7.1)$$

where n is the number of calibration measurements. The mean absolute error (MAE) is the mean of the absolute value of the differences between measured heads (h_m) and simulated heads (h_s):

$$MAE = \frac{1}{n} \sum_{i=1}^n |(h_m - h_s)_i| \quad (7.2)$$

where n is the number of calibration measurements. The root mean square (RMS) error is the average of the squared differences between measured heads (h_m) and simulated heads (h_s):

$$RMS = \left[\frac{1}{n} \sum_{i=1}^n (h_m - h_s)_i^2 \right]^{0.5} \quad (7.3)$$

where n is the number of calibration measurements. The difference between the measured hydraulic head and the simulated hydraulic head is termed a residual.

We used the RMS as the basic measure of calibration for heads. The required calibration criterion for heads is a RMS that is equal to or less than 10 percent of the observed head range in the aquifer being simulated. To provide information on model performance with time, the RMS was calculated for the calibration period (1980-1989) and the verification period (1990-1999). The RMS is useful for describing model error on an average basis but, as a single measure, it does not provide insight into spatial trends in the distribution of the residuals.

An examination of the distribution of residuals is necessary to determine if they are randomly distributed over the model grid and not spatially biased. Post plots of head residuals for each model layer were used to check for spatial bias by indicating the magnitude and direction of mis-match between observed and simulated heads. Simulated head distributions were also compared to the head distributions developed from the field measurements. Finally, scatter plots were used to determine if the head residuals are biased based on the magnitude of the observed head surface.

For streams, the calibration criteria were defined to be within 10% of the measured values where uncertainty in these targets is proven to be acceptable for such a criteria.

7.2 Calibration Target Uncertainty

Calibration targets are uncertain. In order to not “over-calibrate” a model, which is a stated desire for the GAM models, calibration criteria should be defined consistent with the

uncertainty in calibration targets. The primary calibration target in groundwater modeling is hydraulic head. Uncertainty in head measurements can be the result of many factors including, measurement error, scale errors, and various types of averaging errors both spatial and temporal. The calibration criteria for head is a RMS less than or equal to 10% of head variation within the aquifer being modeled. Head differences across the aquifers in the study area are on the order of 400 to 500 feet. This leads to an acceptable RMS of between 40 and 50 feet. We can compare this RMS to an estimate of the head target errors and see what level of calibration the underlying head targets can support.

Measurement errors are typically on the order of tenths of feet, and at the GAM scale can be considered insignificant. However, measuring point elevation errors can be significant. Our analysis of differences between the reported land-surface datum (LSD) and the ground surface elevation as determined from a digital elevation map determined that the average difference was -5 feet with a standard deviation of 28 feet. Add to this error the error in averaging ground surface elevations available on a 30 m grid to a one mile grid, and the resulting errors can average 10 to 20 feet and greatly exceed 70 feet in areas with higher topographic slopes.

Another error is the one caused by combining fluvial deltaic sand channels into single grid blocks representing one simulated head. Horizontal to vertical hydraulic conductivity ratios have been proven to be high in the Coastal Plain aquifers of Texas (Fogg et al., 1983; Williamson et al., 1990). As a result, significant vertical gradients can occur within individual model layers. Vertical gradients near pumping centers are quite large and approach 0.1 (Williamson et al., 1990). This implies that portions of the aquifer can have head variations within a single model layer on the order of 10 to 50 feet. On average, in areas away from large pumping centers, this scale effect is expected to be on the order of 10 to 20 feet. Horizontal gradients relative to the grid scale also account for an additional 1 to 5 feet error with even greater errors near pumping centers. When these errors are added up, the average error in model heads could easily equal our calibration criteria of 40 to 50 feet. The nugget observed on kriged head maps within the modeled aquifers equals from 20 to 30 feet. This nugget captures both uncertainty and variability in the observed heads being rationalized above. Calibrating to RMS values significantly less than 30 feet would constitute over calibration of the model and parameter adjustments to reach that RMS are not supported by the hydraulic head uncertainty.

7.3 Sensitivity Analysis

A sensitivity analysis was performed on the steady-state and transient calibrated models to determine the impact of changes in a calibrated parameter on the predictions of the calibrated model. A standard “one-off” sensitivity analysis was performed. This means that hydraulic parameters or stresses were adjusted from their calibrated “base case” values one by one while all other hydraulic parameters are unperturbed.

7.4 Predictions

Once the model satisfied the calibration criteria for both the calibration and verification periods, the model was used to make predictive simulations. The predictive simulations have different simulation periods. Simulations were run from 1999 to 2010, 2020, 2030, 2040, and 2050. Average climatic conditions were applied for each predictive simulation with the simulation ending with a drought of record. Stream flow rates and recharge were applied with seasonal variation in the average conditions period. Pumping stresses were based upon the Regional Water Plans as described in Section 4.7 and Appendix C.

8.0 STEADY-STATE MODEL

The current section details the calibration of the steady-state model and presents the steady-state model results. This section also describes analyses of model sensitivity to various hydrologic parameters.

8.1 Calibration

This section describes the steady-state calibration targets and calibrated parameters including horizontal and vertical hydraulic conductivity, recharge, ET, stream conductance, and vertical conductance for younger sediments overlying the Queen City Formation.

8.1.1 Calibration Targets

Water-level measurements are needed as targets for steady-state calibration. However, where there is a well, water levels have often been affected by groundwater pumpage. As a result, valid targets for predevelopment conditions were limited, because wells were typically drilled for pumpage. Acceptable predevelopment targets included 18 Carrizo measurements and 91 Wilcox measurements (34 in the upper Wilcox and 57 in the middle Wilcox). A distinction was made between outcrop wells and wells located in the confined section. For wells in the outcrop, the water-level elevation was calculated based on the measured water-level depth using the grid-block averaged elevation from the model. For the confined section, the listed well elevation was used for calculating the water-level elevation. This was done to reduce potential errors induced by averaging ground-surface elevation over a 1-mile by 1-mile grid-block.

8.1.2 Horizontal and Vertical Hydraulic Conductivities

Section 6.4.1 described the determination of initial horizontal and vertical hydraulic conductivities for the model. Figures 8.1.1-8.1.4 show the final calibrated horizontal hydraulic conductivity (K_h) fields for Layer 3 (Carrizo), Layer 4 (upper Wilcox), Layer 5 (middle Wilcox), and Layer 6 (lower Wilcox). Figure 8.1.5 shows the vertical anisotropy ratio field for Layer 2 (Reklaw) for which a uniform horizontal hydraulic conductivity value of 1 ft/day was assumed. We used a hydraulic conductivity map for Layer 1 (Queen City) in the model, but no explicit calibration was performed for Layer 1. The spatial horizontal hydraulic conductivity distribution

for Layer 1, shown in Figure 4.3.8, is considered preliminary. Table 8.1.1 summarizes the calibrated hydraulic conductivity ranges and anisotropy ratios (K_h/K_v) for each layer.

The calibration process for the Northern Carrizo-Wilcox GAM was iterative. We developed an initial steady-state calibration through adjustment of recharge and hydraulic conductivity. Although the initial steady-state calibrated model met the calibration criteria, the subsequent transient model calibration indicated that the vertical hydraulic conductivities were too high. It became necessary to jointly calibrate the steady-state and transient models to achieve a consistent calibration to both steady-state and transient water-level data.

Overall, vertical hydraulic conductivities (K_v) were lowered based on the transient calibration. We then recalibrated the steady-state model through adjustment of recharge, ET (from groundwater), and hydraulic conductivities. Modifications to the initial estimates of horizontal hydraulic conductivity (Section 6.4.1), based on the steady-state calibration, involved increasing conductivities in areas where values were low to a minimum of 2 ft/day for Layer 3 and 1.5 ft/day for Layers 4, 5 and 6. On the other hand, transient calibration required limiting horizontal hydraulic conductivity in selected areas of the Carrizo, upper Wilcox, and middle Wilcox layers. This area encompassed part of Cherokee, Anderson, Henderson, Smith, Wood, Upshur, and Camp counties, where a uniform hydraulic conductivity value of 1 ft/day was assigned to Layers 4 and 5 (Wilcox), and a slightly higher value of 2 ft/day was assigned to Layer 3 (Carrizo). Also, the relatively high hydraulic conductivity area in the southern part of the Sabine Uplift, which was not supported by data, was reduced to values similar to those of surrounding data. For the Queen City (Layer 1), the minimum horizontal hydraulic conductivity value was set to 5 ft/day, mainly because of numerical instabilities along the outcrop edge of the Queen City, where it becomes relatively thin.

Table 8.1.1 shows the final calibrated anisotropy ratios for the steady-state model which were increased by a factor of 10 to 1000 from that of the initial steady-state calibration. Vertical hydraulic conductivity of the Reklaw was set to 1×10^{-5} ft/day and modified in two selected areas (Figure 8.1.5). In central Smith County and the adjacent northern part of Cherokee and Anderson counties, the vertical hydraulic conductivity of Layer 2 (Reklaw) was reduced to 1×10^{-6} ft/day based on transient calibration, to restrict downward flow from the shallow Queen City aquifer which has been induced by steep water-level declines in the Carrizo and upper

Wilcox in Smith County due to pumpage. On the other hand, vertical permeability in eastern Nacogdoches was increased to 1×10^{-4} ft/day based on the transient calibration to allow more cross-formational flow, because simulated water-level declines owing to pumpage exceeded observed declines in the Carrizo Aquifer.

There is no clear geologic or hydrologic information that can be used to support these spatial changes in vertical hydraulic conductivities of the Reklaw. The potential limitations of the steady-state model are discussed in Section 11.

8.1.3 Recharge and Groundwater Evapotranspiration

Recharge was input initially as an averaged distribution from the transient recharge results (Sections 6.3.4). However, this averaged recharge estimate was too high, resulting in numerical instabilities in the steady-state simulation. The low vertical hydraulic conductivities required for transient calibration required a reduction in recharge in the steady-state model. Recharge was selectively reduced by hydrogeologic unit and adjusted locally in case of numerical instabilities, until an acceptable calibration was achieved. The spatial distribution of calibrated recharge is shown in Figure 8.1.6.

Average groundwater ET was input, as provided by the SWAT results, and applied as ET maximum in the model (Section 6.3.4). The maximum rooting depths were taken from the SWAT results and input as the extinction depth (Figure 8.1.7). The ET surface was set to ground surface, so groundwater ET varied linearly starting from a maximum at ground surface and going down to the root depth. The potential ET from groundwater can and did exceed recharge in some circumstances; however, MODFLOW was unable to model this under steady-state conditions. For conditions where groundwater was near the surface and the ET rate exceeded the recharge rate, model convergence was difficult and model mass balances were not acceptable. In order to overcome this problem, we reduced the maximum ET rate (Figure 8.1.8) to 70 percent of the recharge rate on a cell by cell basis. This resulted in acceptable convergence and mass balances.

8.1.4 General-Head Boundaries and Stream Conductances

General-head boundaries (GHBs) were assigned to the confined part of the Queen City in the southern part of the model. The elevations of the GHBs were estimated from the surficial

water table (Section 6.3.2). The initial conductivities of the GHBs were estimated from reported vertical conductivities (Williamson et al., 1990) of the younger sediments overlying the Queen City. Heads in the Queen City formation (Layer 1) indicated limited sensitivity to the conductivity of the GHBs, and are more controlled by recharge in the outcrop and by streambed conductivities. Streambed conductivities were based on the hydraulic conductivities of the underlying formation. The overall conductance varies with the streambed width as specified in the EPA RF1 dataset (Section 6.3.3).

Table 8.1.1 Calibrated hydraulic conductivity ranges for the steady-state model.

	Horizontal Hydraulic Conductivity K_h (ft/d)	Vertical Hydraulic Conductivity K_v (ft/d)	Anisotropy Ratio (K_h/K_v)
Layer 1 (Queen City)	5 – 25	$5 \times 10^{-4} - 2.5 \times 10^{-2}$	1,000-10,000
Layer 2 (Reklaw)	1	$1 \times 10^{-6} - 1 \times 10^{-4}$	10,000 – 1,000,000.
Layer 3 (Carrizo)	2 – 40	$2 \times 10^{-2} - 4 \times 10^{-1}$	100
Layer 4 (upper Wilcox)	1 – 10	$1 \times 10^{-4} - 1 \times 10^{-3}$	10,000
Layer 5 (middle Wilcox)	1 – 10	$1 \times 10^{-4} - 1 \times 10^{-3}$	10,000
Layer 6 (lower Wilcox)	1.5 – 25	$1.5 \times 10^{-4} - 2.5 \times 10^{-3}$	10,000

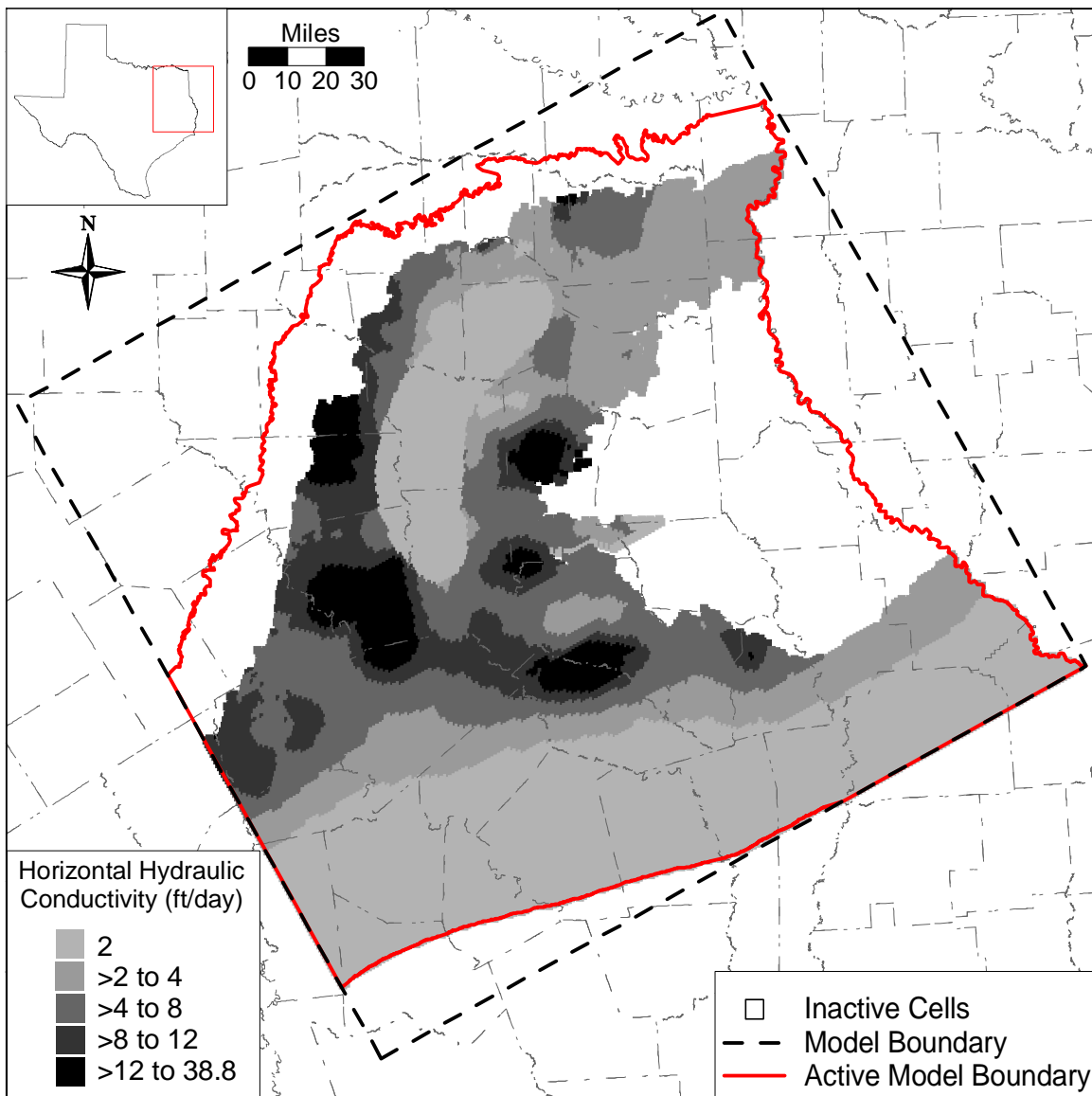


Figure 8.1.1 Calibrated horizontal hydraulic conductivity field for Layer 3 (Carrizo).

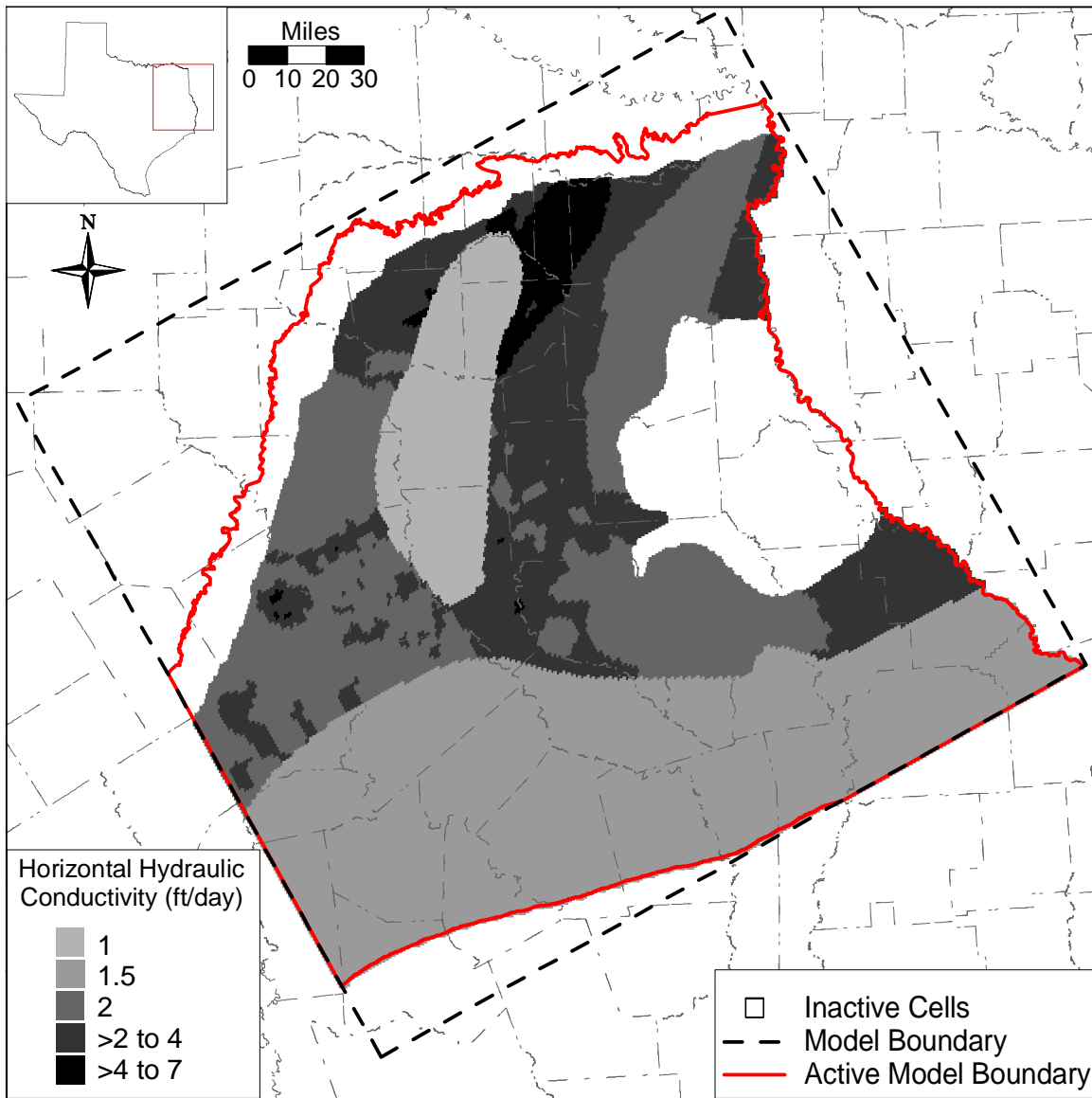


Figure 8.1.2 Calibrated horizontal hydraulic conductivity field for Layer 4 (upper Wilcox).

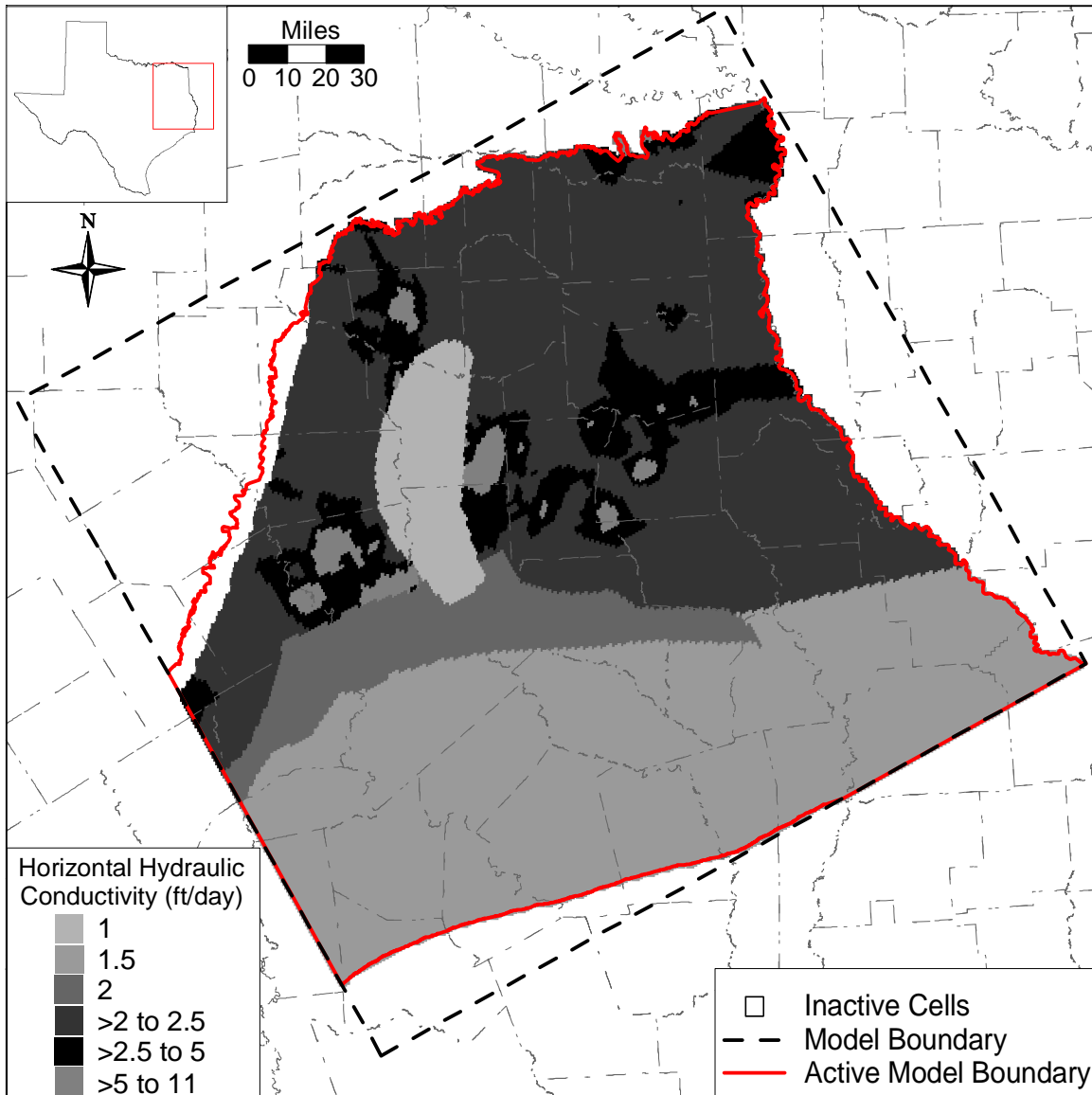


Figure 8.1.3 Calibrated horizontal hydraulic conductivity field for Layer 5 (middle Wilcox).

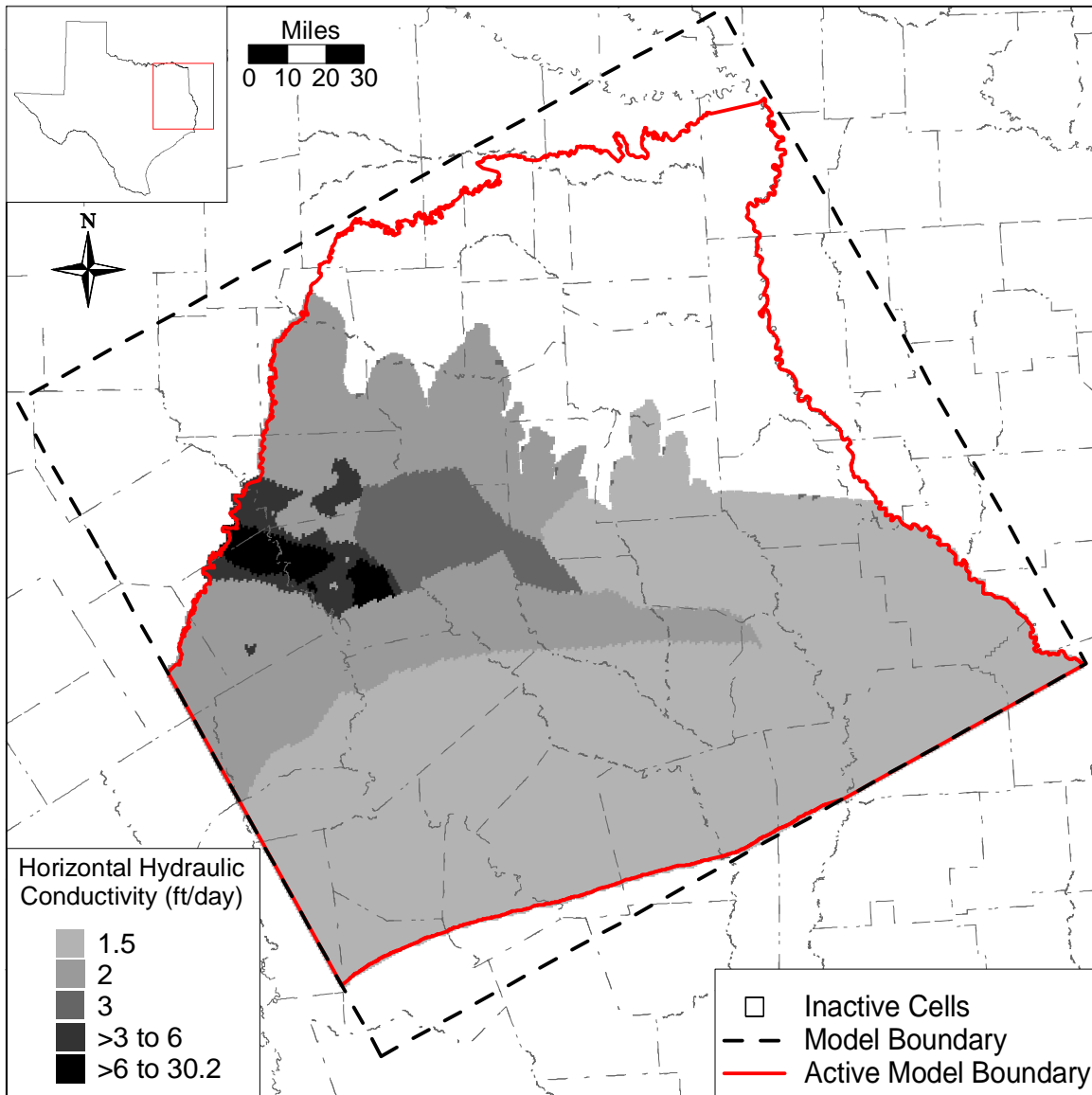


Figure 8.1.4 Calibrated horizontal hydraulic conductivity field for Layer 6 (lower Wilcox).

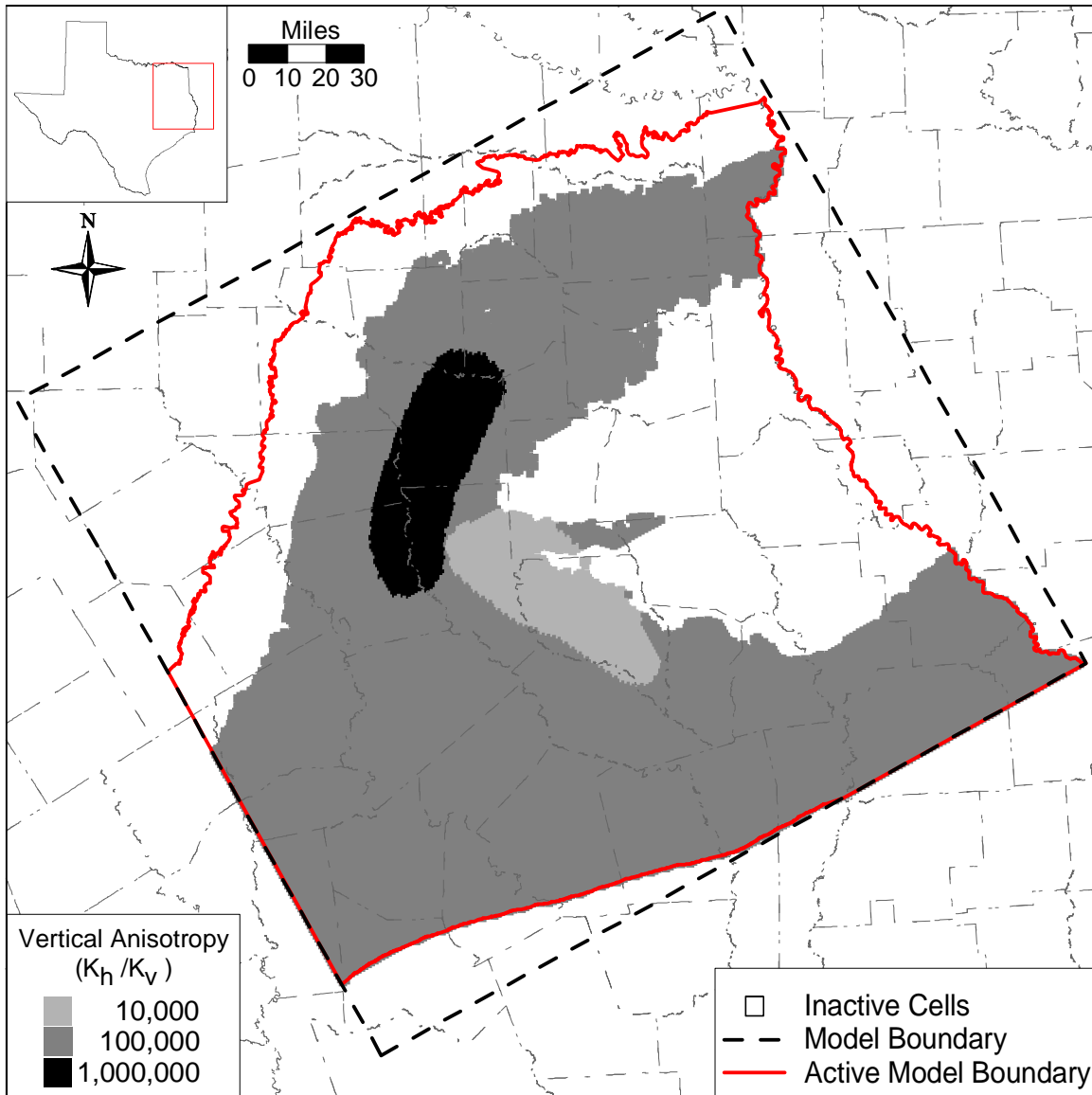


Figure 8.1.5 Calibrated vertical anisotropy (K_h/K_v) field for Layer 2 (Reklaw).

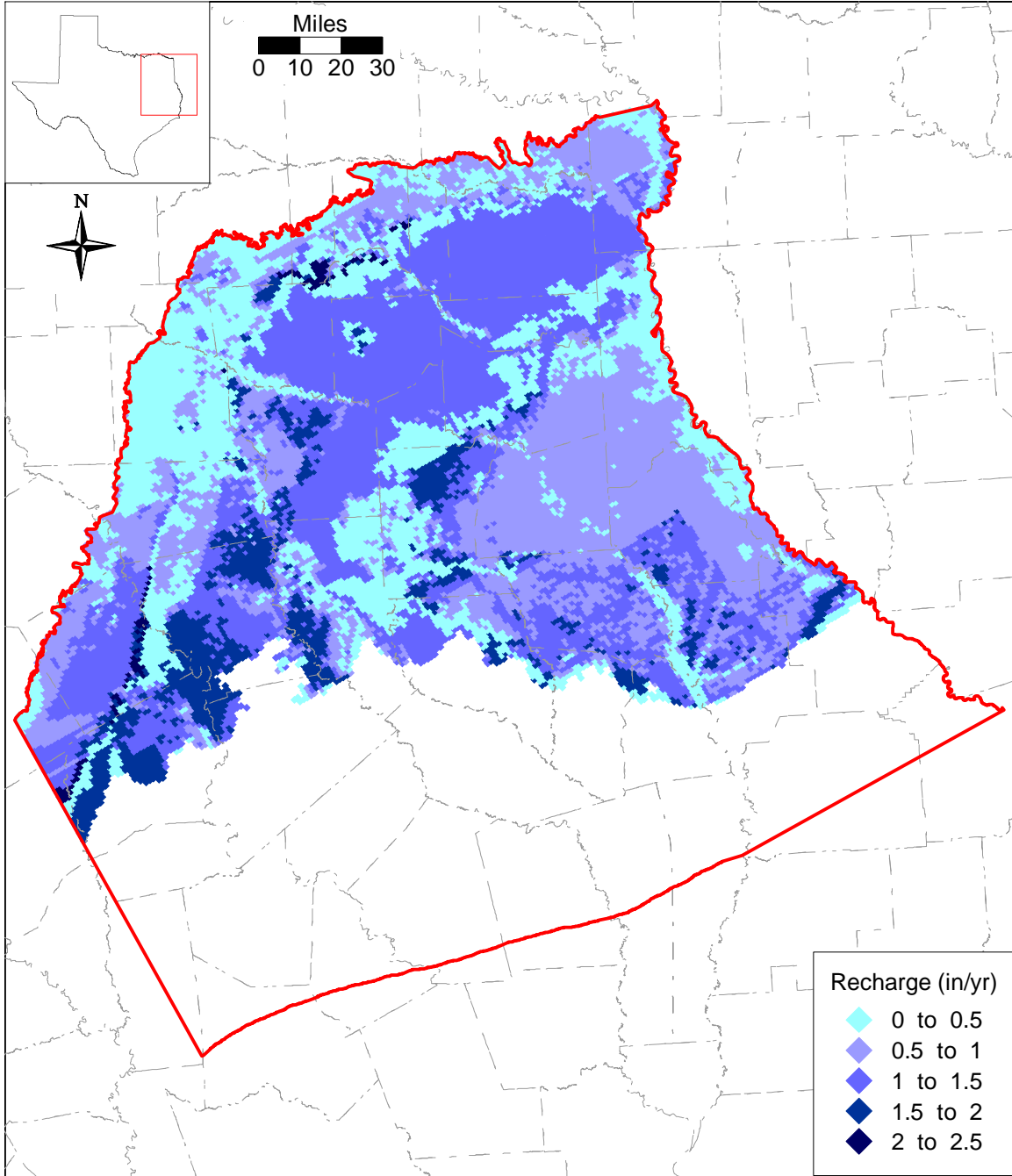


Figure 8.1.6 Calibrated recharge distribution for the steady-state model.

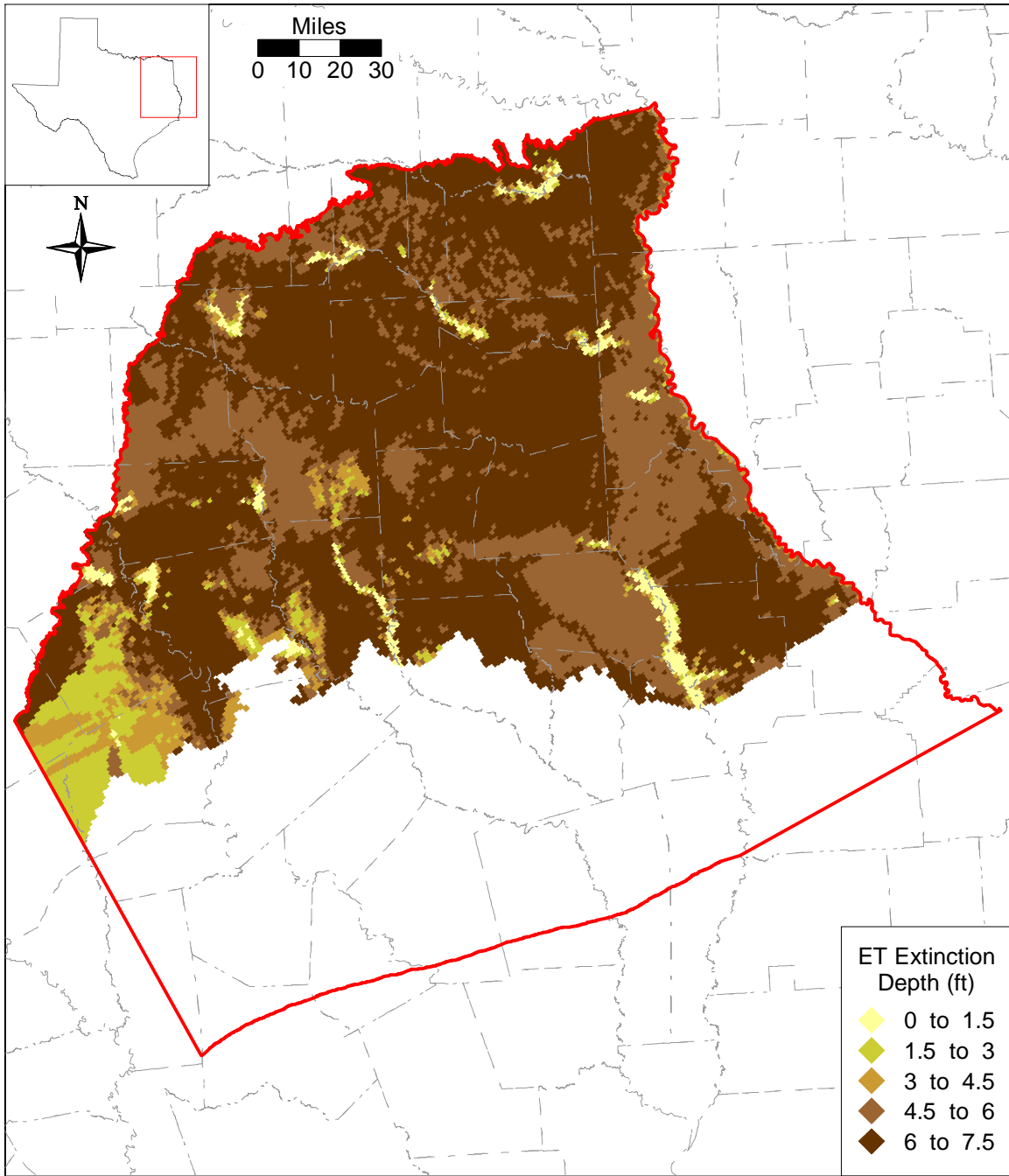


Figure 8.1.7 ET extinction depth distribution for the steady-state model.

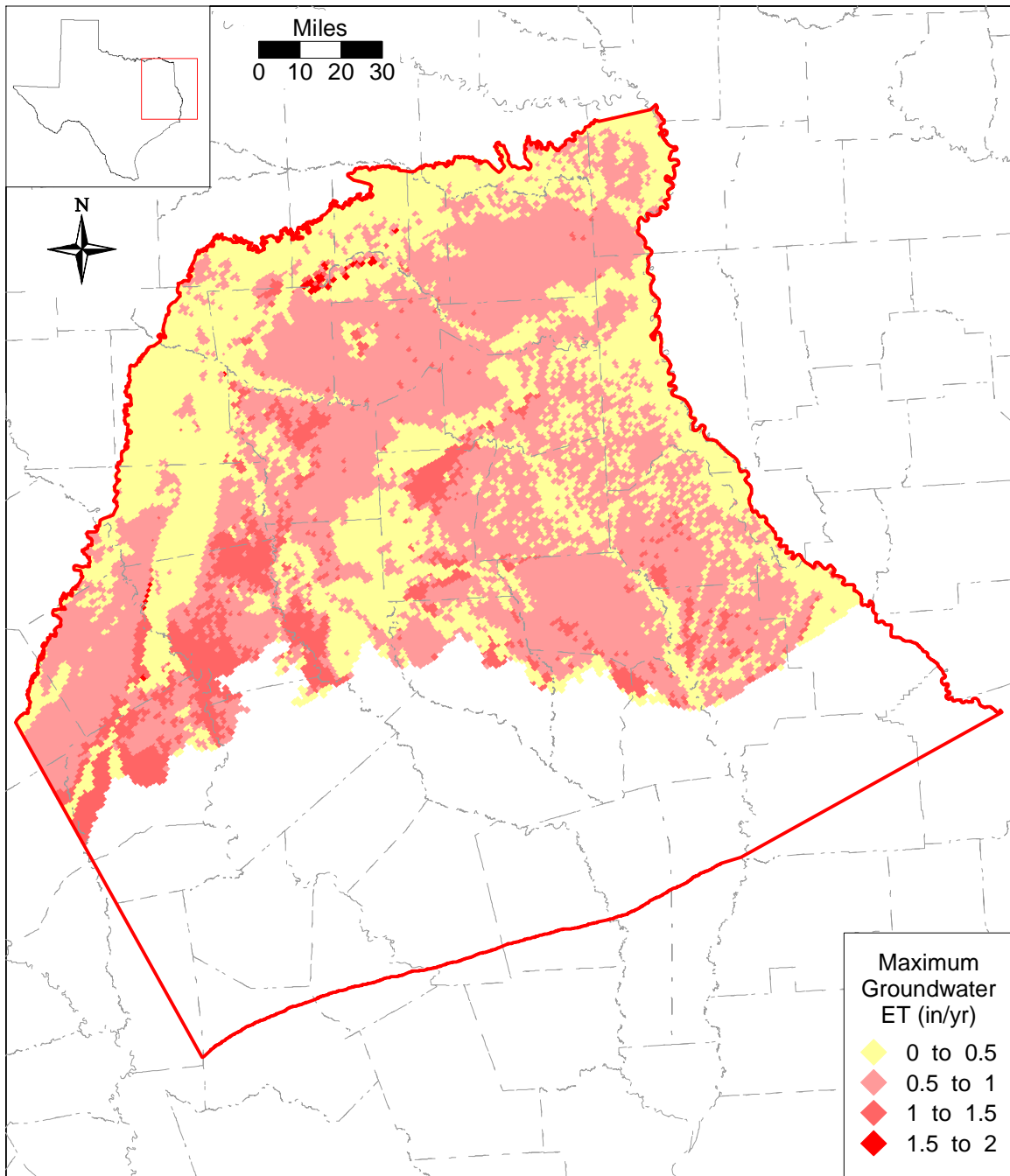


Figure 8.1.8 Calibrated maximum groundwater ET rate distribution for the steady-state model.

8.2 Simulation Results

Calibration of the steady-state model is not unique. Calibrated results can be obtained by numerous combinations of recharge and vertical and horizontal hydraulic conductivities. Overall, the steady-state model is most sensitive to recharge. This is to be expected, since recharge is the primary input source of water for the model.

8.2.1 Hydraulic Heads

Figures 8.2.1-8.2.5 show the head surface results from the calibrated steady-state model, together with the residuals for the target wells in the individual layers. The residuals were calculated from:

$$residual = head_{measured} - head_{simulated} \quad (8.2.1)$$

A positive residual indicates that the model has underpredicted the hydraulic head, while a negative residual indicates overprediction. The calibration statistics for the individual layers are summarized in Table 8.2.1, and the overall mass balance calculated by the steady-state model is given in Tables 8.2.2a and 8.2.2b.

Figure 8.2.1a shows the simulated hydraulic heads for Layer 1 (Queen City) and the corresponding residuals for the target well locations. As mentioned above, the Queen City aquifer was not explicitly calibrated during this GAM phase; however, hydraulic heads in the Queen City were considered important for controlling vertical flow across the Reklaw confining unit. The simulated hydraulic heads for Layer 1 in Figure 8.2.1 compare reasonably well with measured hydraulic heads, reproducing the water table as a reflection of the general topography in the Queen-City outcrop. No effort was made to refine the hydraulic parameters and improve the calibration for Layer 1. The calibration statistics shows an adjusted RMS of 13% for the Queen City, which is considered acceptable for bounding the vertical gradient across the Reklaw confining unit.

The calibration statistics for the Carrizo shows an adjusted RMS of 8% (Table 8.2.1) based on a relatively even distribution of the residuals throughout the confined and unconfined part of the aquifer (Figure 8.2.2a). The scatterplot of simulated and measured hydraulic heads indicates a uniform distribution around the unit-slope line (Figure 8.2.2b). The steady-state

hydraulic head surface shows an approximate west-east groundwater divide from van Zandt County through Smith County to Rusk County. North of this divide the hydraulic gradients in the confined portion of the Carrizo are to the east, indicating groundwater flow to the east toward the Red River in Louisiana. South of the divide, groundwater flow in the confined section is to the south and further downdip to the southeast. The overall head distribution and general flow pattern agrees reasonably well with that shown in Figure 4.4.3 (Fogg and Kreitler, 1982), considering that the simulated heads represent steady-state pre-development conditions and Fogg and Kreitler (1982) included pumpage effects on their constructed potentiometric surface for the entire Carrizo-Wilcox aquifer.

The calibration statistics for Layer 4 (upper Wilcox) indicates a relatively high adjusted RMS of 15%, even though the overall total RMS of 38.5 ft is not significantly greater than that of Layer 5 (Table 8.2.1). This is due to the relatively narrow hydraulic head range of 257 ft, compared to 418 ft for Layer 5. Figure 8.2.3a shows that the calibration data are located mostly in the outcrop in the Sabine Uplift, with some data points along the western outcrop, and with only a few data points in the confined section in Upshur and Rusk counties. The scatterplot of simulated and measured hydraulic heads shows this narrow head range (Figure 8.2.3b), resulting in the relatively large adjusted RMS. Given the potential uncertainty in well-location and associated uncertainty in well elevation and measured water-level elevation, an improvement in the fit was not attempted. Using the greater head range for the entire Wilcox aquifer would decrease the adjusted RMS to 9%. The overall groundwater flow pattern as inferred from the hydraulic head distribution (Figure 8.2.3a) corresponds largely to that of the Carrizo (Figure 8.2.2a).

The calibration statistics for Layer 5 (middle Wilcox) shows an adjusted RMS of 8% (Table 8.2.1). The simulated hydraulic head distribution together with the posted residual in the target wells is shown in Figure 8.2.4a. The residuals are generally low and uniformly distributed in the scatterplot (Figure 8.2.4b), except for a couple of data points in southern van Zandt County, indicating simulated hydraulic heads nearly 100 ft below measured heads of 574 ft. The recharge distribution used in this area is somewhat low compared to the surrounding areas in the outcrop of Layer 5 (Figure 8.1.6), and it is probable that by increasing recharge rates in this area, the difference could be reduced. On the other hand, potential uncertainties in the actual well location could cause a significant change in well elevation in this rather hilly outcrop area. That

is, the measured water levels could be significantly in error. Water-level measurements in a nearby well, used for transient calibration (well 3433801), indicated a water-level elevation of about 505 ft, which is significantly lower than the 574 ft reported for the two steady-state target wells. Furthermore, the water levels in nearby wells in the upper Wilcox and Carrizo agree well with simulated values, indicating little difference in hydraulic heads. As a result, no additional adjustment of recharge in this particular area was attempted to improve the fit. Overall, the adjusted RMS for Layer 5 was 8%, below that of the calibration criteria.

The simulated hydraulic head distribution for Layer 6 is shown in Figure 8.2.5. In the northern part of the area, the lower Wilcox pinches out and no simulated heads are shown. There were no calibration points identified in the lower Wilcox to provide a check of the simulated steady-state hydraulic heads in Layer 6. The simulated heads compare well with those in the overlying layer, showing somewhat higher hydraulic heads in the deeper confined section, which indicates upward flow from Layer 6, as one would expect.

Some cells went dry in the steady-state simulation. Out of 18,679 outcrop cells, 77 cells or less than one present were dry. These dry cells can be indicative of model instability or actual subsurface conditions. Because no obvious discontinuity exists in the outcrop water table, these cells likely are indicative of actual subsurface conditions (i.e., small cell thickness, low water table). The small number of dry cells does not have a significant impact on model results.

8.2.2 Streams

Figure 8.2.6 shows the gain/loss values for the stream reaches in the steady-state model. As would be expected, the larger stream segments are all gaining. Only the upper reaches of tributaries show losing segments. These losses are typically higher in shallow channels at higher overall elevations.

We compared the stream leakances to the stream gain/loss data compiled by Slade et al. (2002). Seven of the nine documented gain/loss studies that fall within the model area and include the Carrizo-Wilcox outcrop were compared to simulated stream leakances. The other two studies were conducted on minor streams that were not included as boundary conditions in the model due to their small size. The seven gain/loss studies used were conducted between 1942 and 1981 and covered reaches of the Sabine River, Little Cyprus Bayou, Bowles Creek, and Lake Fork Creek. Because the steady-state model simulates predevelopment conditions

based on average recharge, ET, and stream flows, stream gain/loss studies conducted under a particular set of conditions may or may not agree with the steady-state results. Figure 8.2.7 shows a cross-plot of the measured gain/loss values and those derived from the model. The data comparison shows a large scatter, though most of the data fall within the same quadrant.

Slade et al. (2002) note that the potential error in stream flow measurements is typically about 5 to 8 percent. Since this error is possible at both ends of a gain/loss subreach, the potential error in gain/loss can equal a significant fraction of the total flow in the subreach. Comparing the available gain/loss values discussed in the previous paragraph to mean stream flows from the EPA River Reach data set shows that almost all of the gain/loss values are less than 5 percent of the mean stream flow. This suggests that the gain/loss values are uncertain and can be used only qualitatively.

8.2.3 Water Budget

Tables 8.2.2a and 8.2.2b summarize the water budget for the model in terms of total volume and as a percentage of total inflow and outflow. The overall mass balance error for the steady-state simulation was 0.04 percent, well under the GAM requirement of one percent. The predominant input source is recharge, which accounts for 93% of the total inflow to the model. Water discharging from the model is mainly through the streams (68%), followed by ET (28%), and the GHBs (4%) in descending order. The total recharge averaged over the entire model region is 0.93 inches/yr.

As discussed above, the recharge for the steady-state model was reduced from the long-term average rate calibrated from the transient model. ET in the steady-state model also had to be reduced in certain location by limiting the ET rates to 70% of the recharge rate. This was done to avoid numerical difficulties in the steady-state MODFLOW simulation. The net recharge to the aquifer (i.e., recharge minus ET) for the steady-state simulation was 0.65 inches/yr. For comparison, the long-term average in the transient model was 0.93 inches/yr, based on the average recharge rate of 2.59 inches/yr. The likelihood of overall higher recharge rates during transient conditions because of water-level declines owing to pumpage was discussed in Section 5. Accordingly, the increased recharge during transient conditions would be equivalent to the rejected recharge during predevelopment conditions. However, the numerical problems encountered during the steady-state MODFLOW simulations required limiting ET to

about 70% of the recharge rate for a given cell. This problem may have some effect on the net recharge estimates for the steady-state model. In general, the estimated recharge rates are within the range reported in the various studies that are summarized in Table 4.5.1.

Table 8.2.1 Calibration statistics for the steady-state model.

Layer	ME (ft)	MAE (ft)	RMS (ft)	Range (ft)	RMS/Range
Layer 1 (Queen City)	-2.14	35.86	45.8	366	0.13
Layer 3 (Carrizo)	-6.10	20.99	25.9	308	0.08
Layer 4 (upper Wilcox)	10.12	32.20	38.5	257	0.15
Layer 5 (middle Wilcox)	12.62	24.56	33.9	418	0.08

ME = mean error

MAE = mean absolute error

RMS = root mean square error

Table 8.2.2a Water budget for the steady-state model. All rates reported in acre-ft/yr.

IN	Layer	GHBs	Recharge	Streams	Top	Bottom
	1	34517	448732	20668		11128
	2		33019	607	17033	13523
	3		65999	268	16198	8234
	4		165194	5292	20542	9816
	5		195020	10741	21359	6027
	6		17475	342	6929	
	Sum	34517	925439	37919	82060	48727
OUT	Layer	GHBs	ET	Streams	Top	Bottom
	1	35018	141058	321909		17033
	2		13264	23588	11128	16198
	3		26492	30132	13523	20542
	4		48854	122327	8234	21359
	5		45437	170685	9816	6929
	6		6017	12667	6027	
	Sum	35018	281123	681309	48727	82060

Table 8.2.2b Water budget for the steady-state model with values expressed as a percentage of inflow or outflow.

IN	Layer	GHBs	Recharge	Streams
	1	3	45	2
	2		3	0
	3		7	0
	4		17	1
	5		20	1
	6		2	0
	Sum	3	93	4
OUT	Layer	GHBs	ET	Streams
	1	4	14	32
	2		1	2
	3		3	3
	4		5	12
	5		5	17
	6		1	1
	Sum	4	28	68

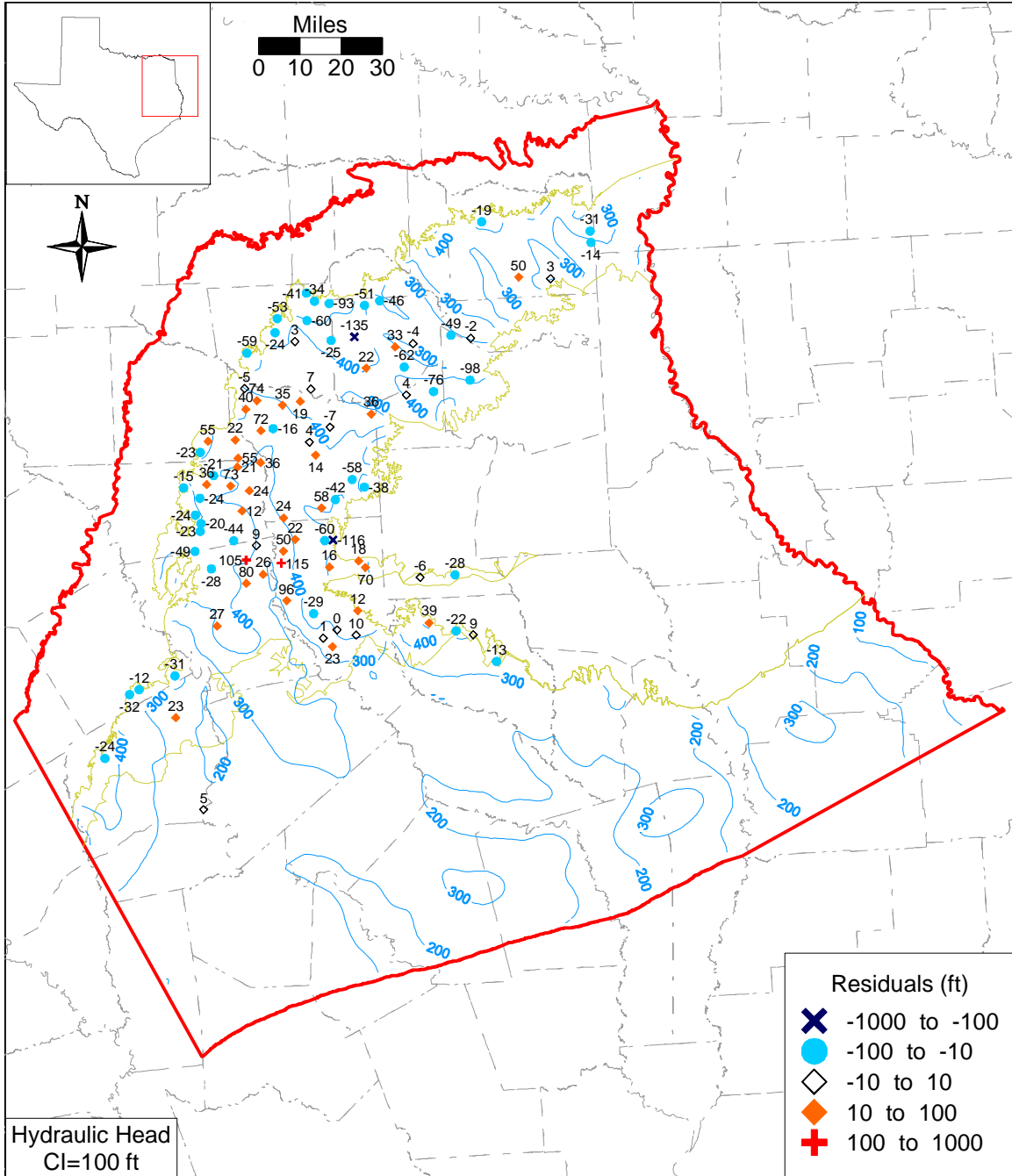


Figure 8.2.1a Simulated steady-state hydraulic heads and residuals for Layer 1 (Queen City).

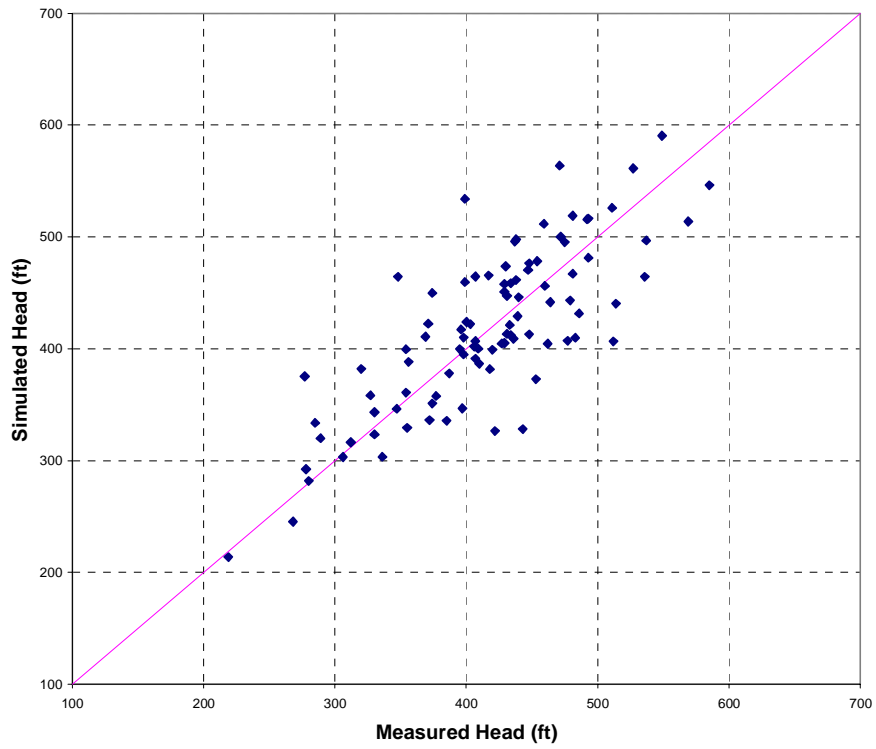


Figure 8.2.1b Scatterplot of simulated and measured hydraulic heads for Layer 1 (Queen City).

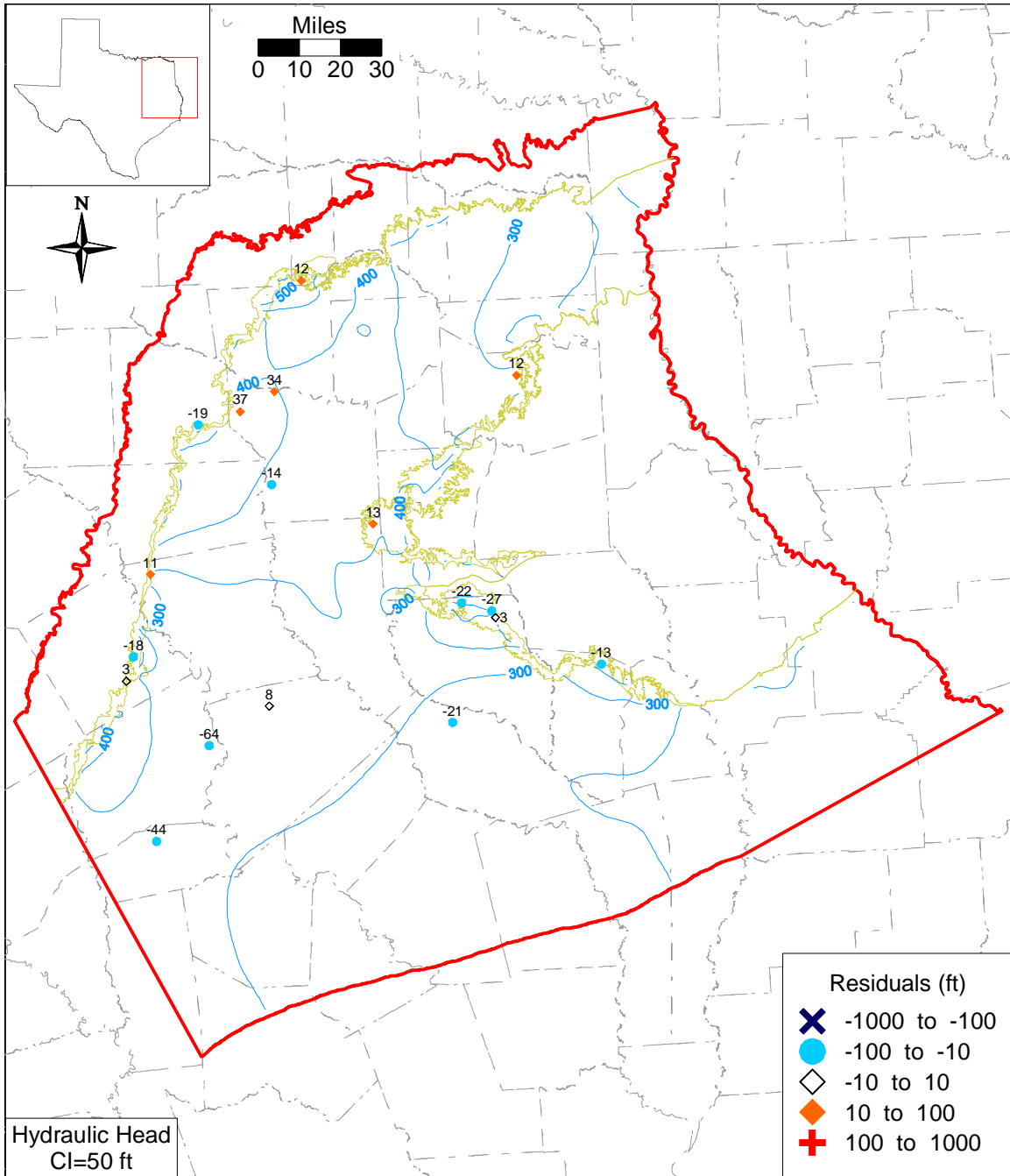


Figure 8.2.2a Simulated steady-state hydraulic heads and posted residuals for Layer 3 (Carrizo).

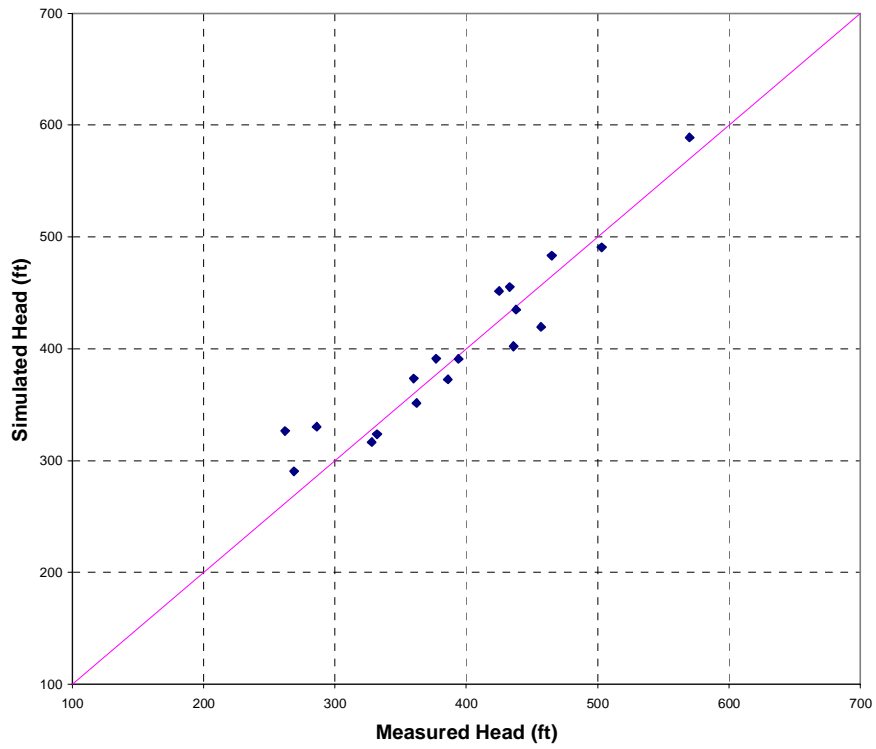


Figure 8.2.2b Scatterplot of simulated and measured hydraulic heads for Layer 3 (Carrizo).

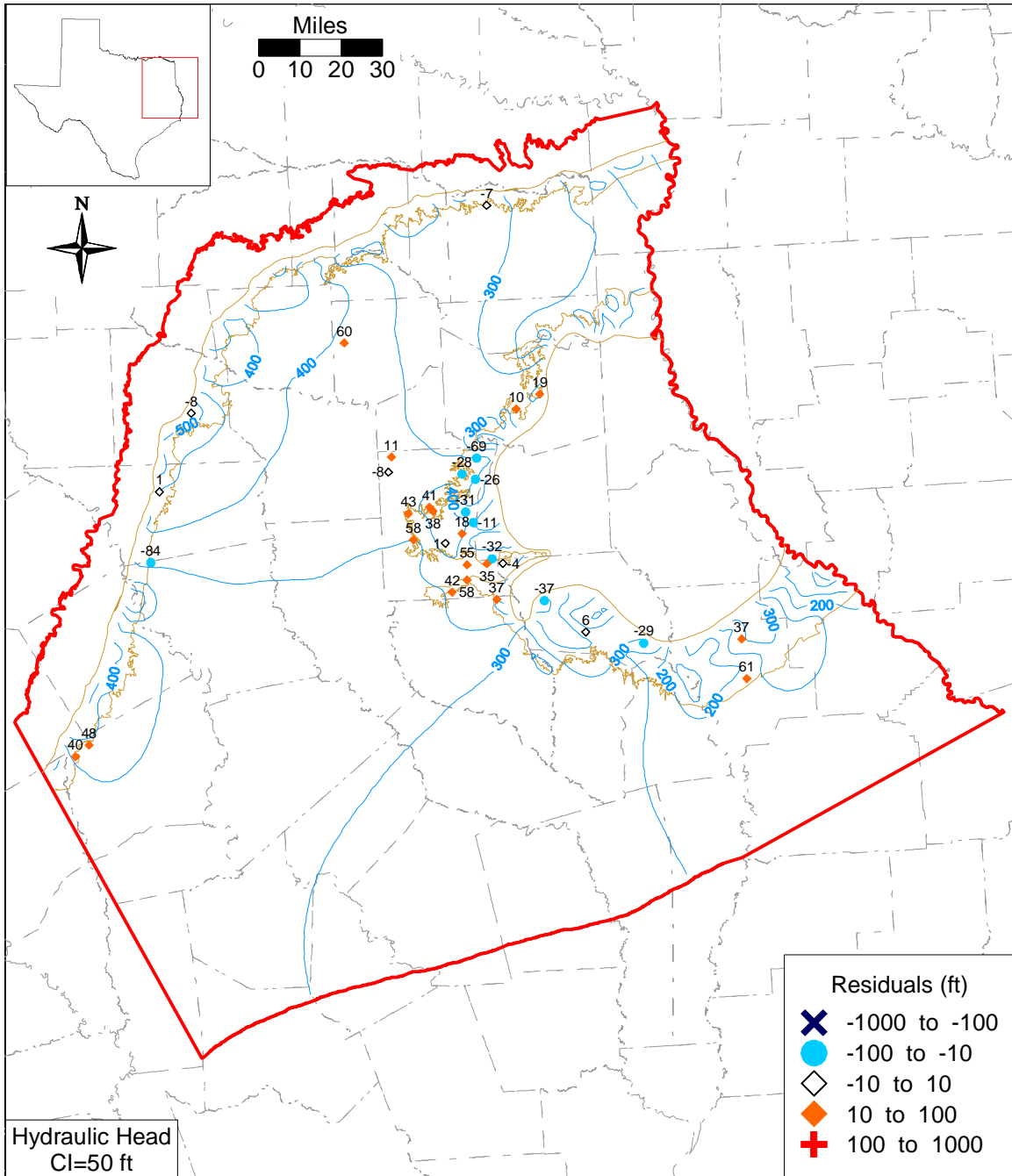


Figure 8.2.3a Simulated steady-state hydraulic heads and residuals for Layer 4 (upper Wilcox).

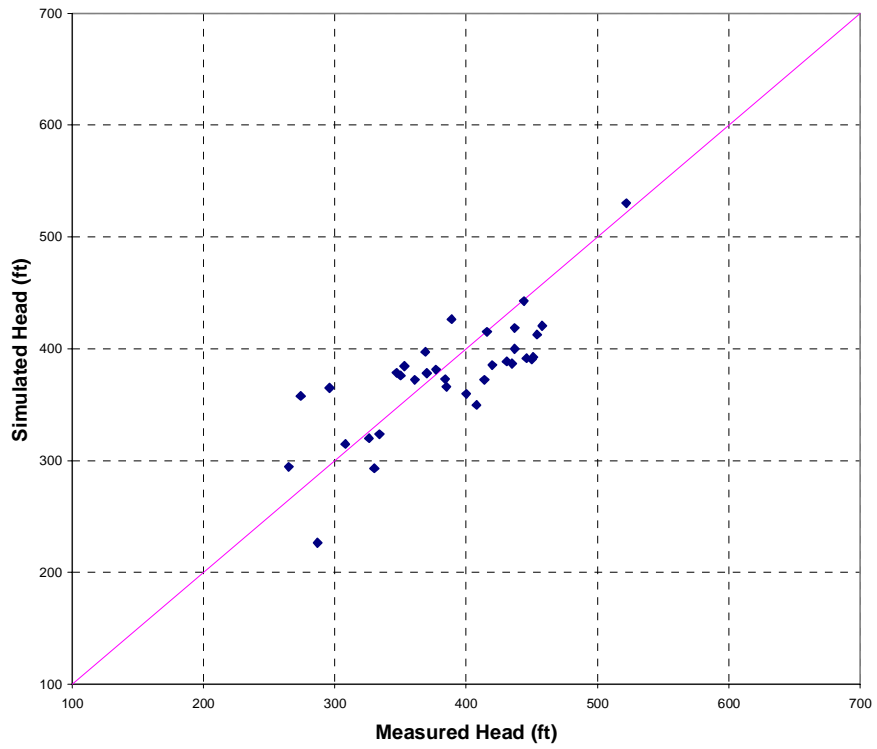


Figure 8.2.3b Scatterplot of simulated and measured hydraulic heads for Layer 4 (upper Wilcox).

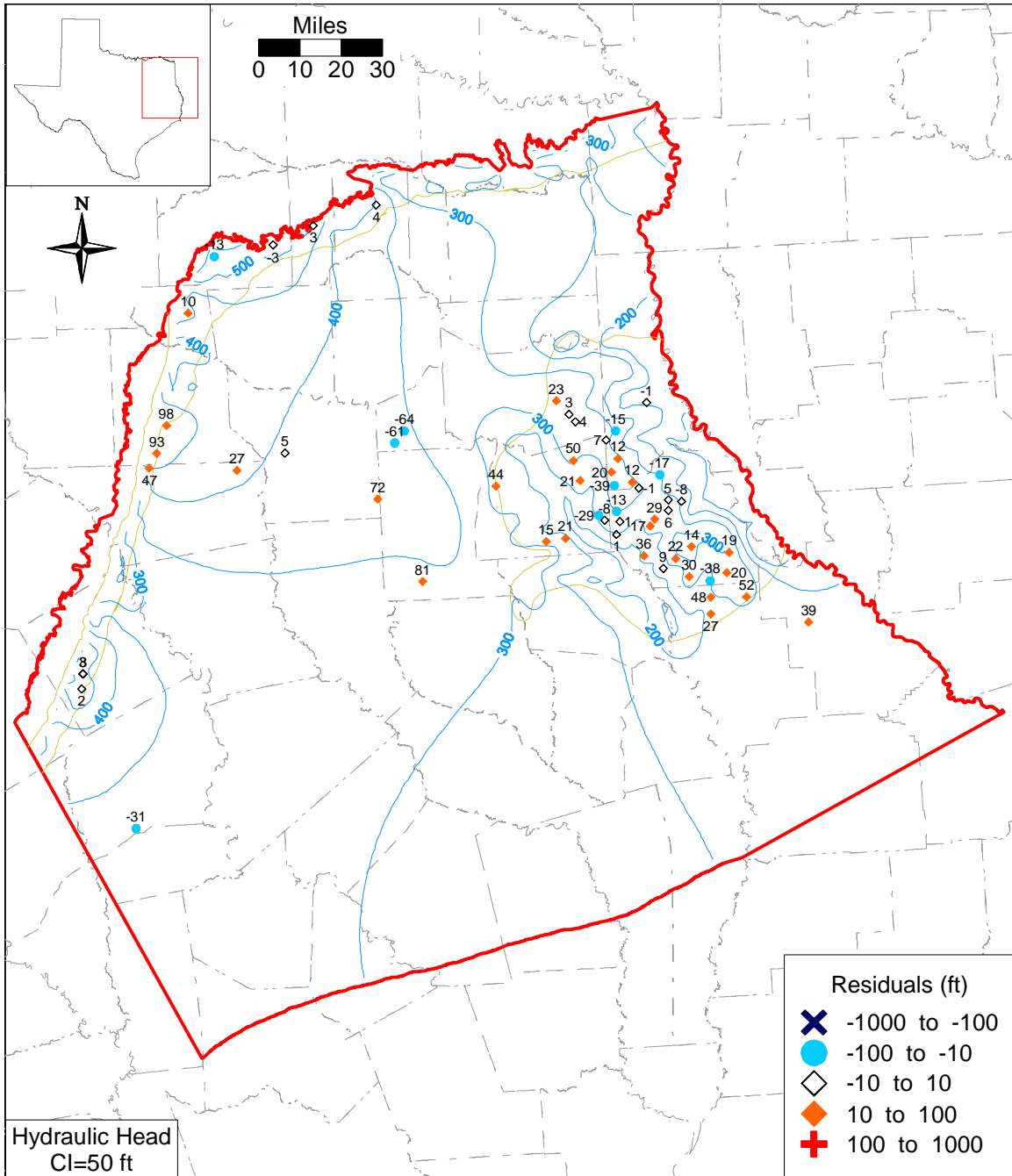


Figure 8.2.4a Simulated steady-state hydraulic heads and residuals for Layer 5 (middle Wilcox).

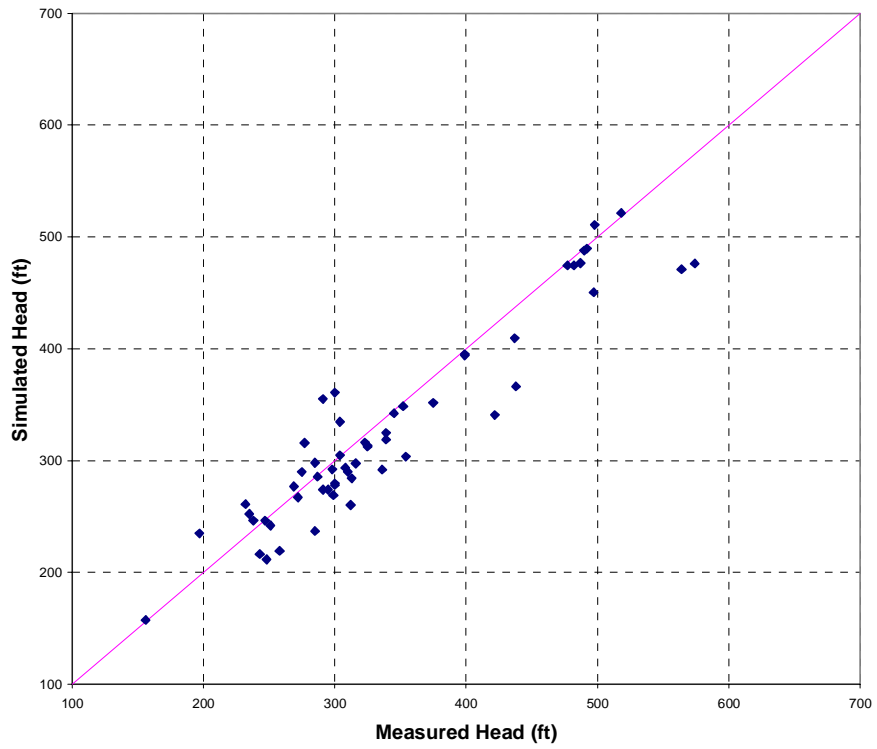


Figure 8.2.4b Scatterplot of simulated and measured hydraulic heads for Layer 5 (middle Wilcox).

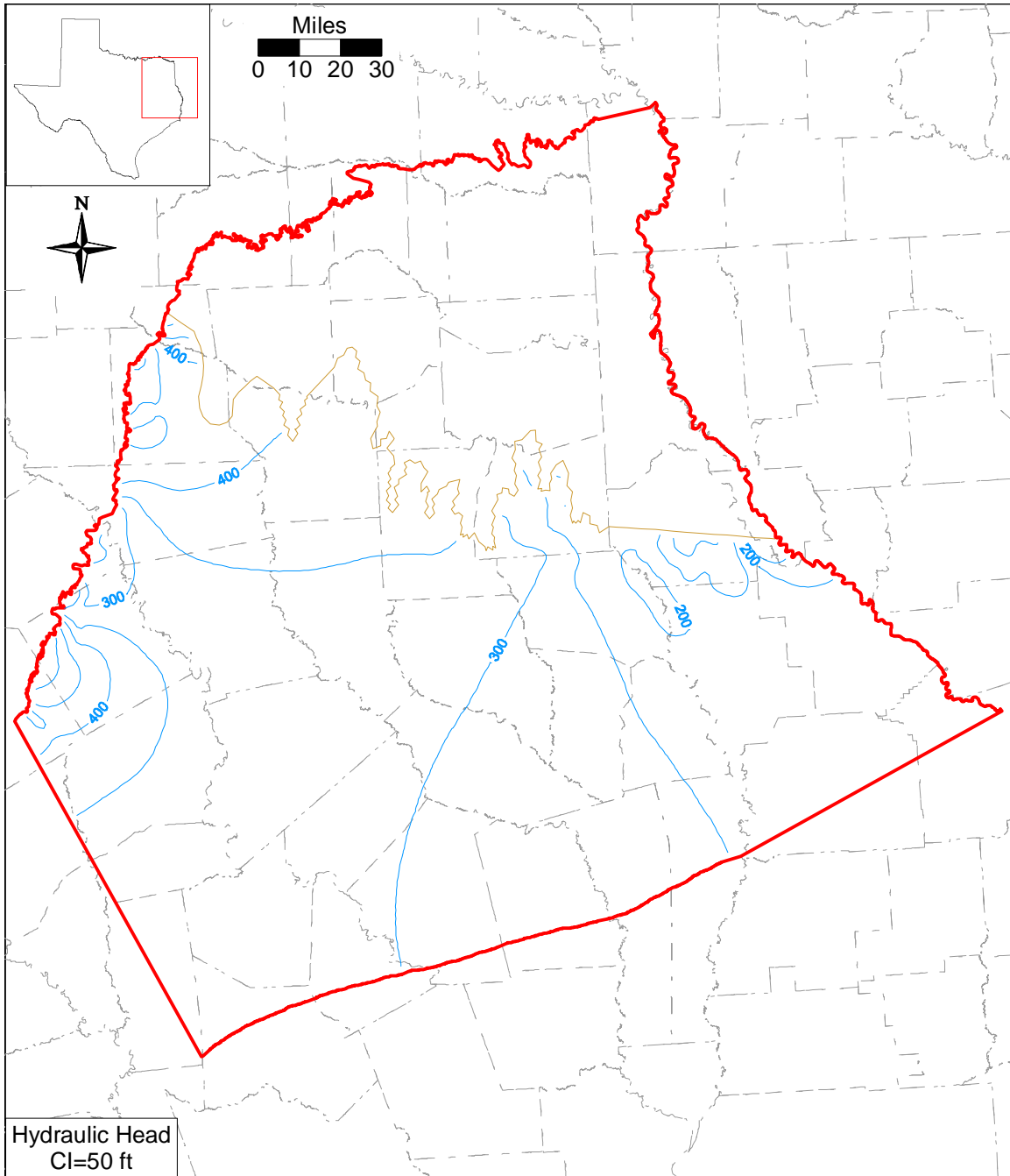


Figure 8.2.5 Simulated steady-state hydraulic heads for Layer 6 (lower Wilcox).

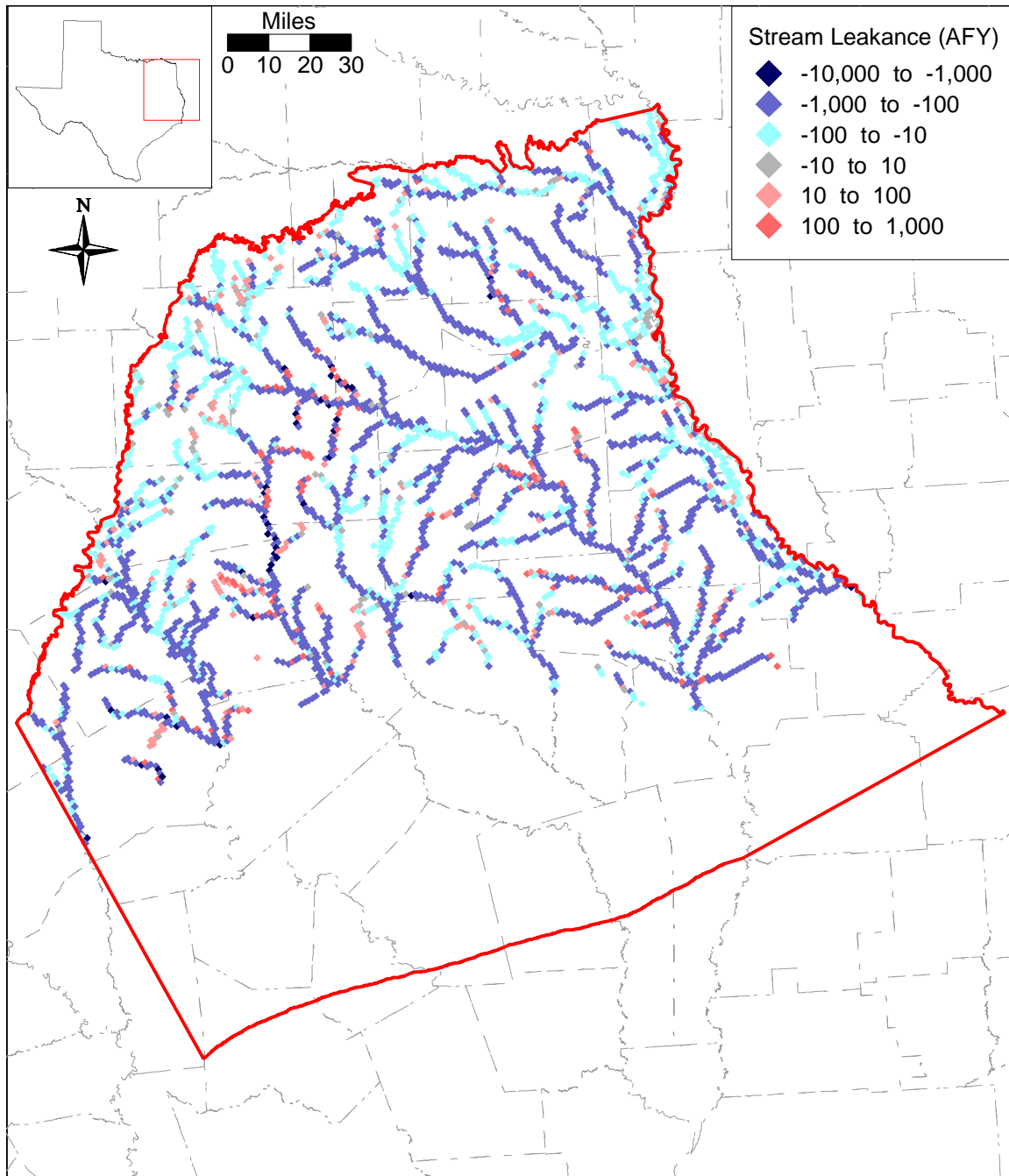


Figure 8.2.6 Steady-state model stream gain/loss (negative values denote gaining streams).

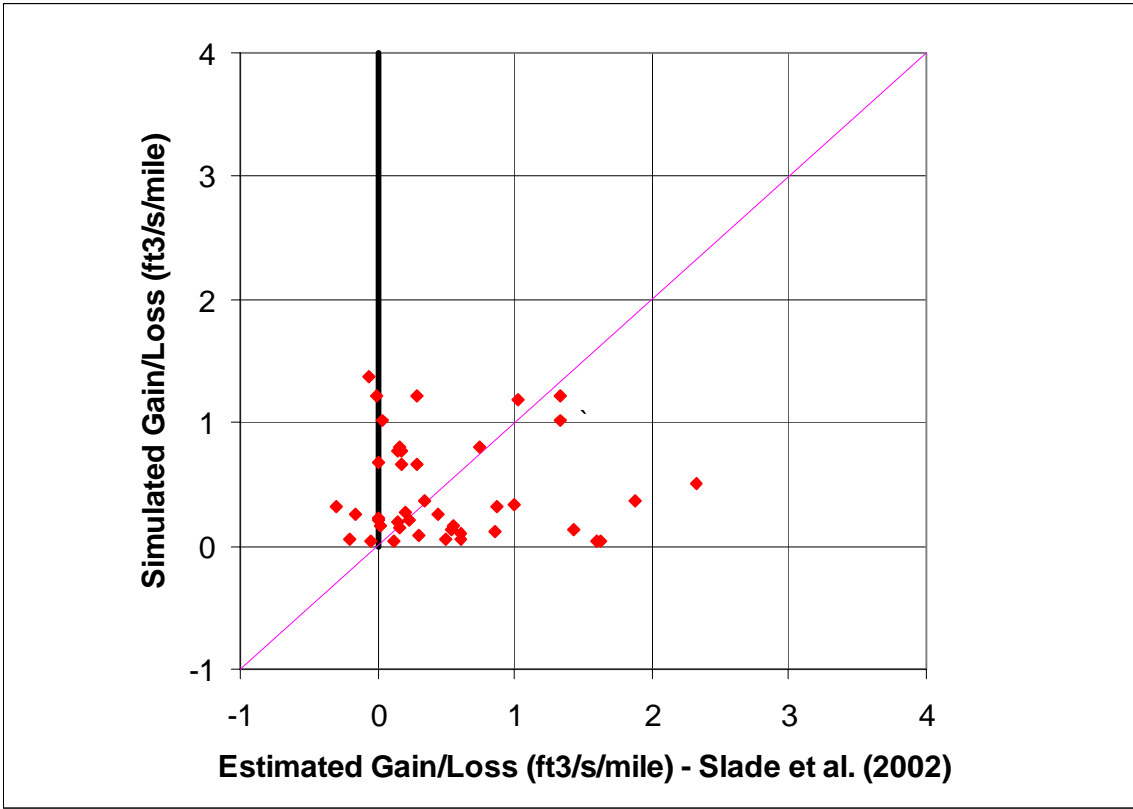


Figure 8.2.7 Simulated stream gain/loss compared to measurements compiled by Slade et al. (2002) for selected stream segments.

8.3 Sensitivity Analysis

A sensitivity analysis was performed on the calibrated steady-state model. A sensitivity analysis provides a means of formally describing the impact of varying specific parameters or groups of parameters on model outputs. In this sensitivity analysis, input parameters were systematically increased and decreased from their calibrated values while the change in head was recorded. Four simulations were completed for each parameter sensitivity, where the input parameters were varied either according to:

$$(\text{new parameter}) = (\text{old parameter}) * \text{factor} \quad (8.3.1)$$

or

$$(\text{new parameter}) = (\text{old parameter}) * 10^{(\text{factor} - 1)} \quad (8.3.2)$$

and the factors were 0.75, 0.9, 1.1, and 1.25. For parameters such as hydraulic conductivity, which are typically thought of as log-varying, equation (8.3.2) was used. Parameters such as recharge were varied linearly using equation (8.3.1). For the output variable, we calculated the mean difference (MD) between the base simulated head and the sensitivity simulated head:

$$MD = \frac{1}{n} \sum_{i=1}^n (h_{sens,i} - h_{cal,i}) \quad (8.3.3)$$

where

$h_{sens,i}$ = sensitivity simulation head at active gridblock i

$h_{cal,i}$ = calibrated simulation head at active gridblock i

n = number of active gridblocks

For the steady-state analysis, we completed seven parameter sensitivities:

1. Horizontal hydraulic conductivity of Layer 3 (K_h -Carrizo)
2. Horizontal hydraulic conductivity of Layers 4 - 6 (K_h -Wilcox)
3. Vertical hydraulic conductivity in Layer 2 (K_v -Reklaw) (leakance between Layers 2 and 3)
4. Vertical hydraulic conductivity in Layers 4-6 (K_v -Wilcox) (leakance between layers 3-4, 4-5, and 5-6)
5. Streambed conductance, model-wide (K -stream)
6. GHB conductance, model-wide (K -GHB)

7. Recharge, model-wide.

Equation 8.3.1 was used for sensitivity 7, and Equation 8.3.2 was used for the other sensitivities.

Figure 8.3.1 shows the results of the sensitivity analyses for the Carrizo (Layer 3) with *MDs* calculated from just the grid blocks where targets were available. In comparison, Figure 8.3.2 shows the corresponding sensitivity results with *MDs* calculated from all active cells in the layer. Note that the two figures indicate similar trends in sensitivities. The relative sensitivity differs somewhat between the two cases for *MDs* that were close to zero. However, the good agreement for the significant *MDs* indicates adequate target coverage. Because of the good agreement between sensitivities calculated using only target cells and those calculated using all active cells, only those sensitivities using all active cells are shown for the remaining sensitivities.

Figure 8.3.1 indicates that the change in head in the Carrizo for the steady-state model is most positively correlated with recharge. Similar *MD* trends are shown in Figures 8.3.3 and 8.3.4 indicating that hydraulic heads in Layer 1 (Queen City) and Layer 2 (Reklaw) are also strongly influenced by recharge. This is to be expected since Layer 1 crops out through most of the model and Layer 2 is in direct contact with Layer 1. Figure 8.3.5 indicates similar sensitivity to recharge for Layer 4 (upper Wilcox). In this case, the horizontal hydraulic conductivity of the Wilcox also shows high *MDs*, characterized by a negative correlation between hydraulic conductivity and head change in Layer 4. Similar sensitivity patterns are shown in Figures 8.3.6 and 8.3.7 for Layer 5 (middle Wilcox) and Layer 6 (lower Wilcox), respectively. Because of the relatively large outcrop area for the Wilcox, particularly in the Sabine Uplift, a decrease in the horizontal hydraulic conductivity of the Wilcox results in an increase in head, because of the more restricted flow of recharged groundwater.

The sensitivity of the vertical hydraulic conductivity of Layer 2 (Reklaw) on hydraulic heads in Layers 1 through 6 shows maximum *MDs* ranging between -2.5 and +3 ft (Figure 8.3.8). The plot indicates that the greatest impact is on Layer 3, followed by Layer 4, Layer 6, and Layer 5. The high impact on Layer 3 is expected because of its close proximity to Layer 2.

Sensitivity to streambed conductance is shown in Figure 8.3.9, indicating a negative correlation for all layers. Lower stream conductivities results in decreased discharge from the layers and concomitantly increased hydraulic heads. Layer 1 (Queen City) shows the lowest *MDs* despite the relatively large outcrop area, where the streams are in contact with the layer. This is probably an artifact caused by the relatively high minimum hydraulic conductivities assigned to the Layer 1 (Queen City). Even though the Carrizo is relatively thin, compared to the Wilcox layers, it shows relatively high *MDs*, suggesting that stream segments in the Queen City above the Reklaw confining unit affect vertical upward leakage from the Carrizo to discharge sites in stream valleys in the Queen City outcrop.

Sensitivity to recharge, shown in Figure 8.3.10, indicates similar trends for all layers, with Layer 4 (upper Wilcox) showing the greatest *MDs*. This can be explained by the relatively large outcrop area of the upper Wilcox, particularly on the Sabine uplift. Layer 1 (Queen City) shows the smallest *MDs* which may be due to the relatively high conductivities, which were artificially increased to avoid numerical problems. Note, for the Northern Carrizo-Wilcox GAM, the Queen City was included as a layer but was not explicitly calibrated. A separate GAM for the Queen City will be developed during the TWDB's next GAM phase.

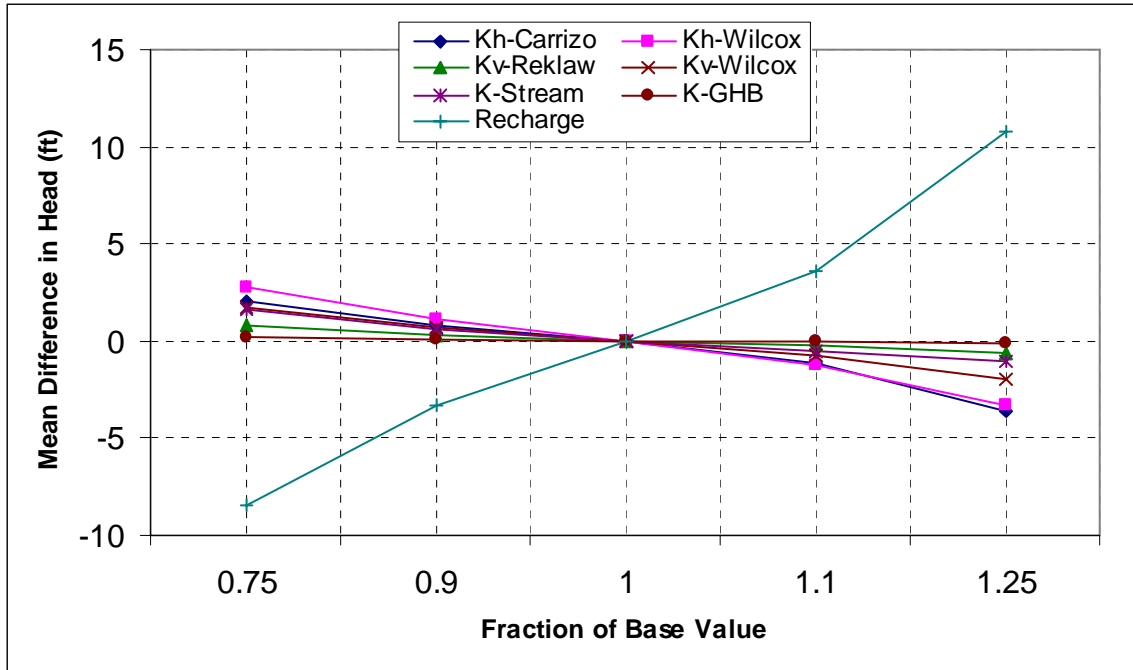


Figure 8.3.1 Steady-state sensitivity results for Layer 3 (Carrizo) using target locations.

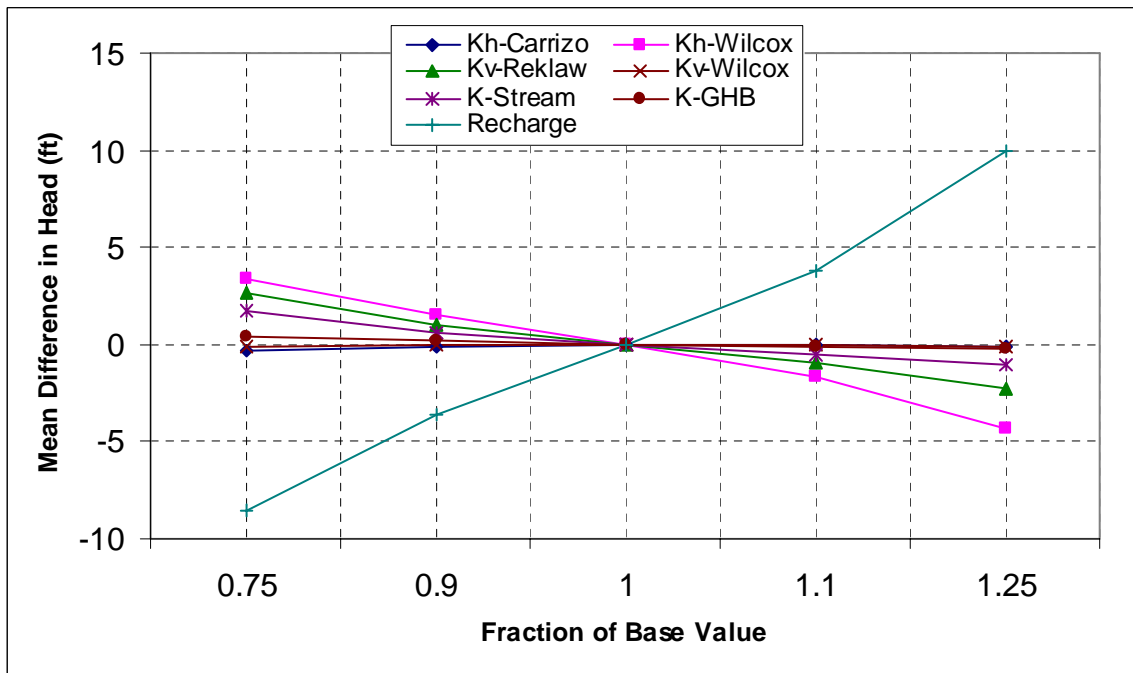


Figure 8.3.2 Steady-state sensitivity results for Layer 3 (Carrizo) using all active gridblocks.

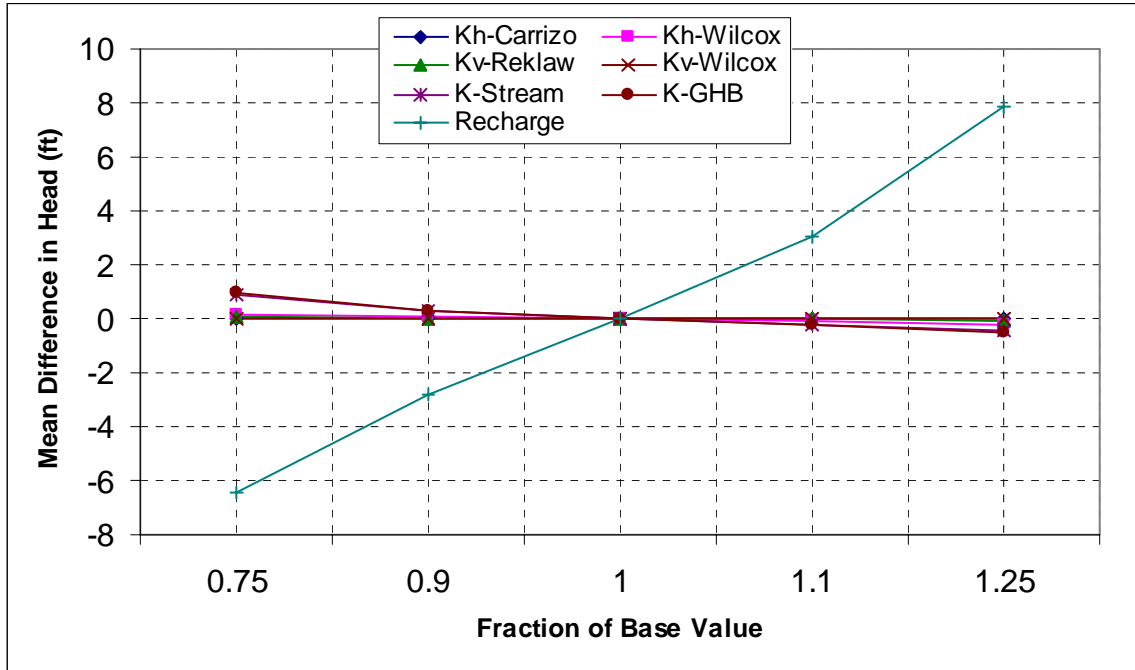


Figure 8.3.3 Steady-state sensitivity results for Layer 1 (Queen City) using all active gridblocks.

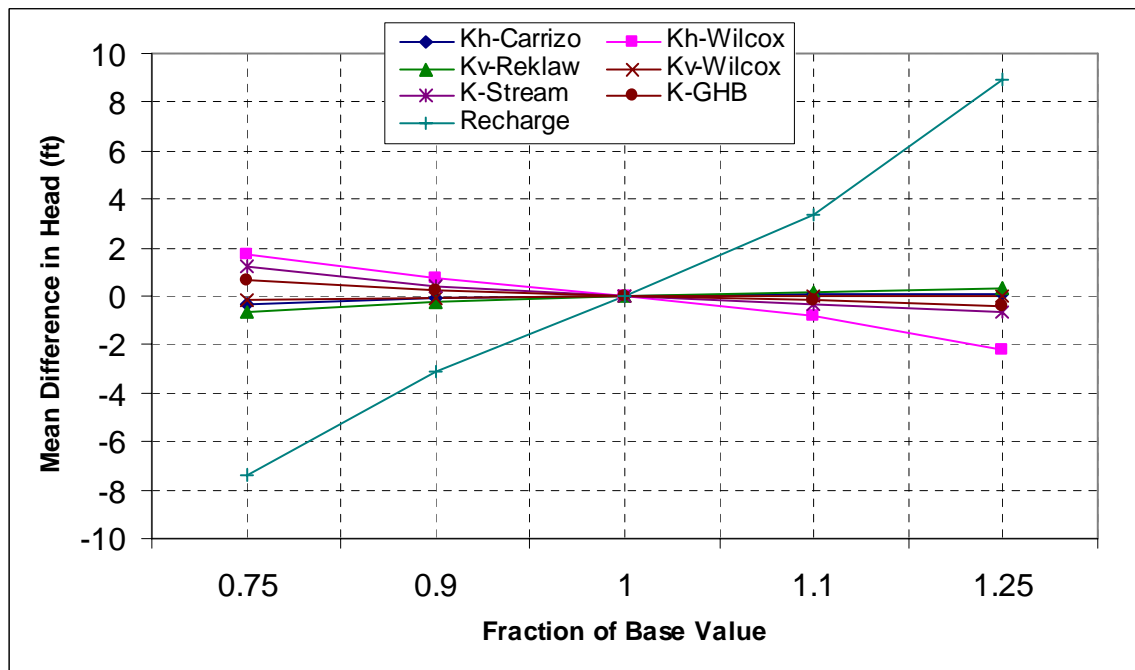


Figure 8.3.4 Steady-state sensitivity results for Layer 2 (Reklaw) using all active gridblocks.

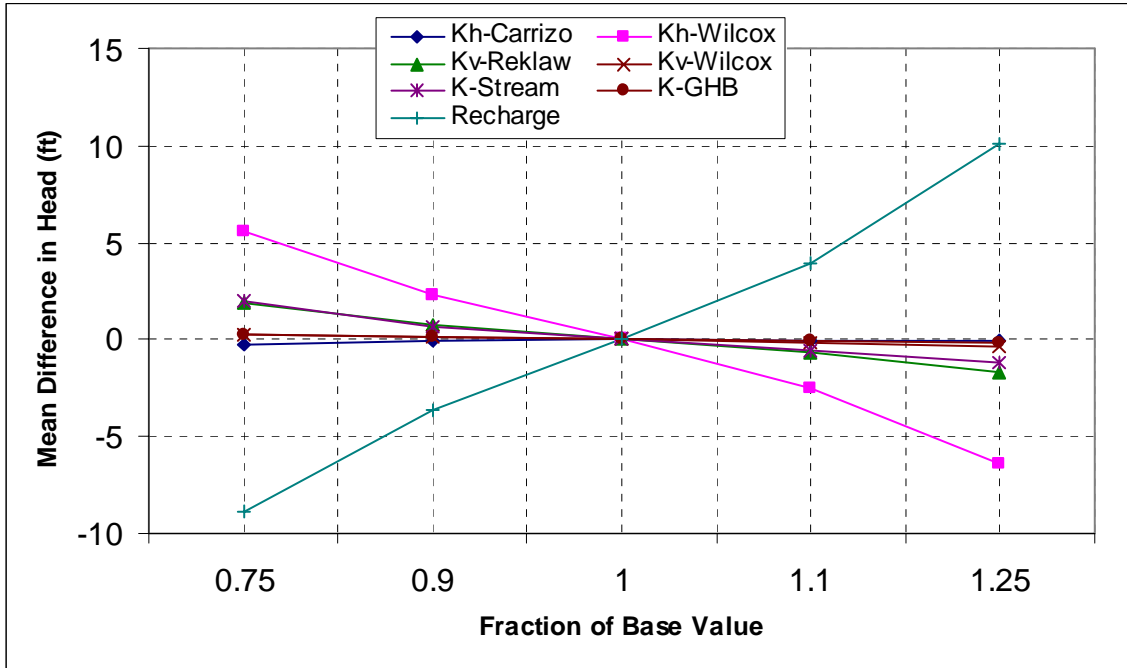


Figure 8.3.5 Steady-state sensitivity results for Layer 4 (upper Wilcox) using all active gridblocks.

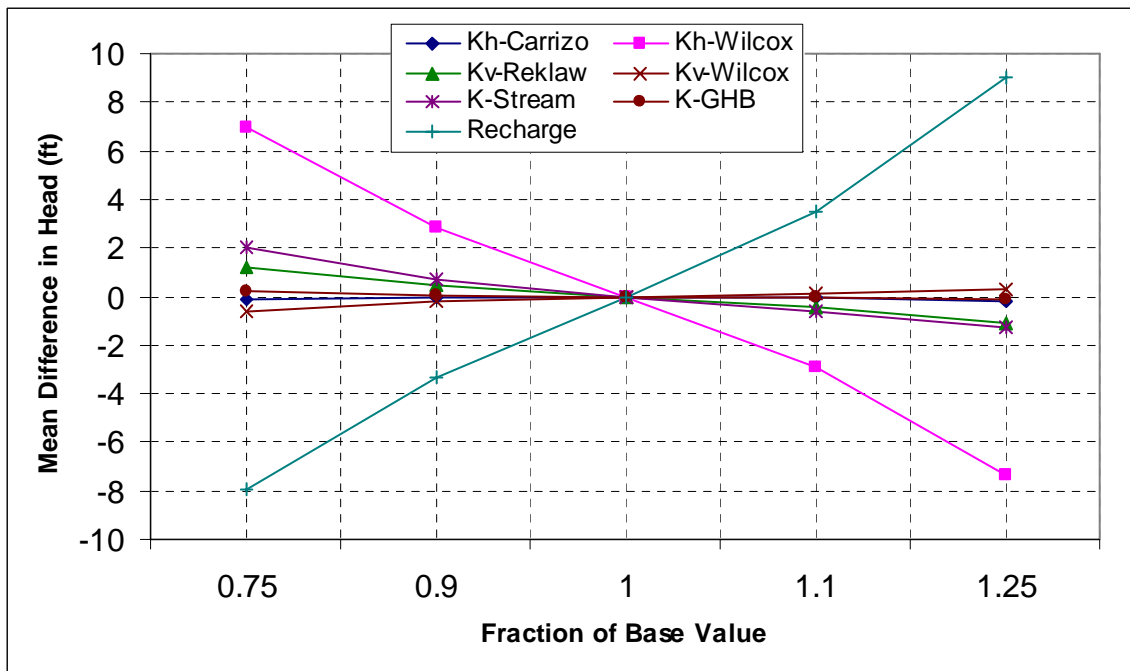


Figure 8.3.6 Steady-state sensitivity results for Layer 5 (middle Wilcox) using all active gridblocks.

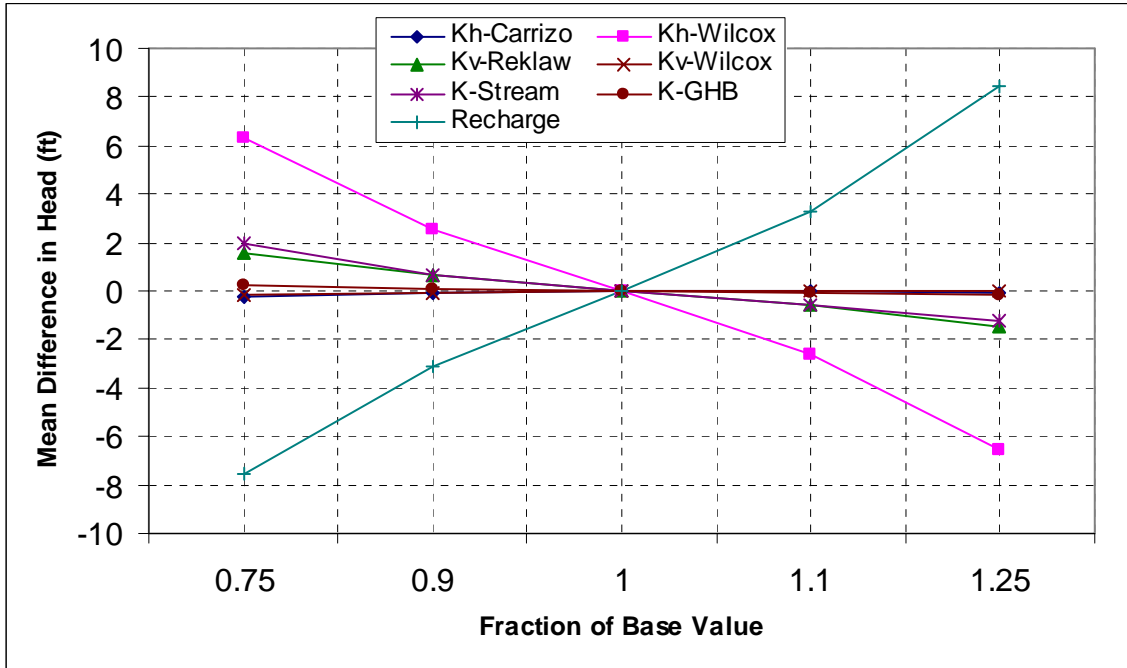


Figure 8.3.7 Steady-state sensitivity results for Layer 6 (lower Wilcox) using all active gridblocks.

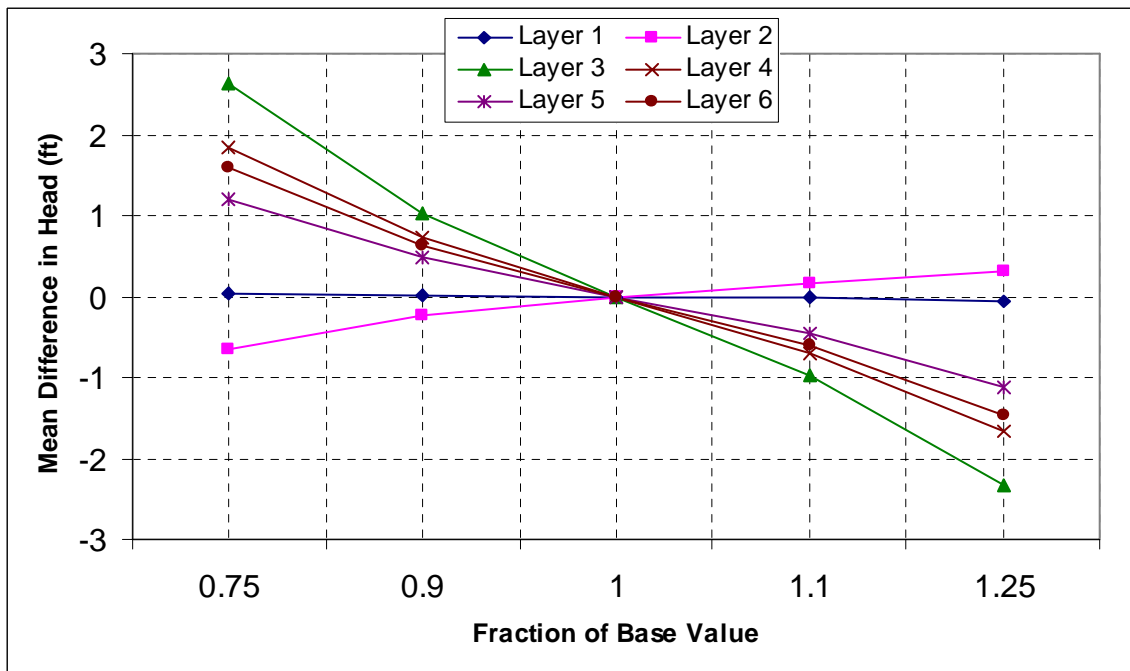


Figure 8.3.8 Steady-state sensitivity results where the vertical hydraulic conductivity of Layer 2 (Reklaw) is varied.

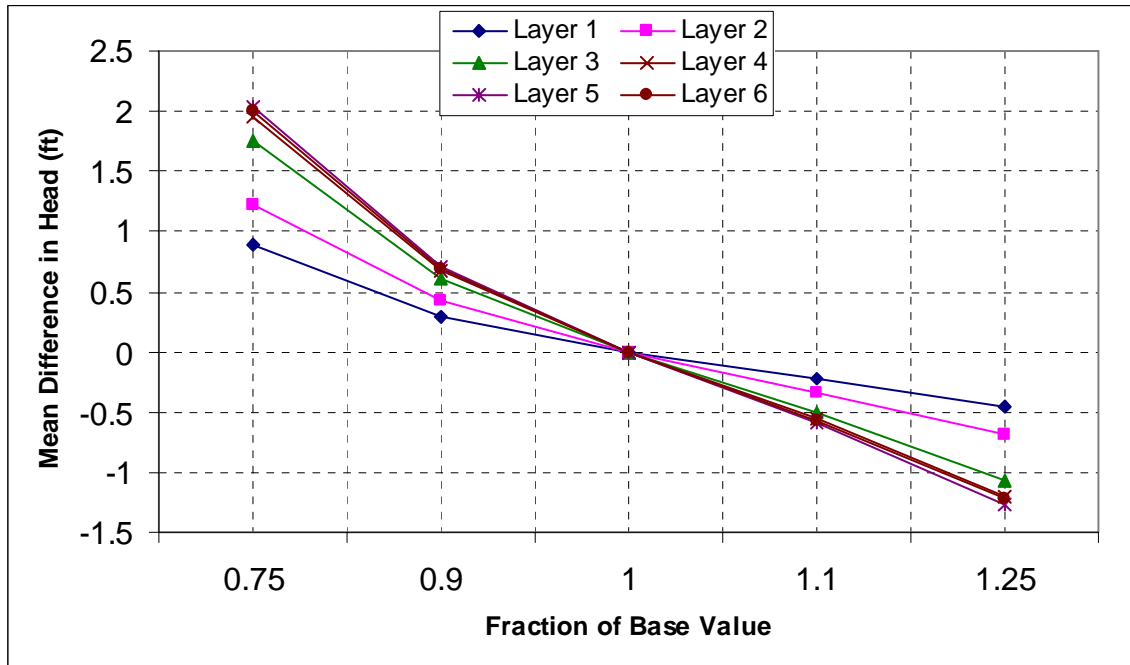


Figure 8.3.9 Steady-state sensitivity results where streambed conductivity is varied.

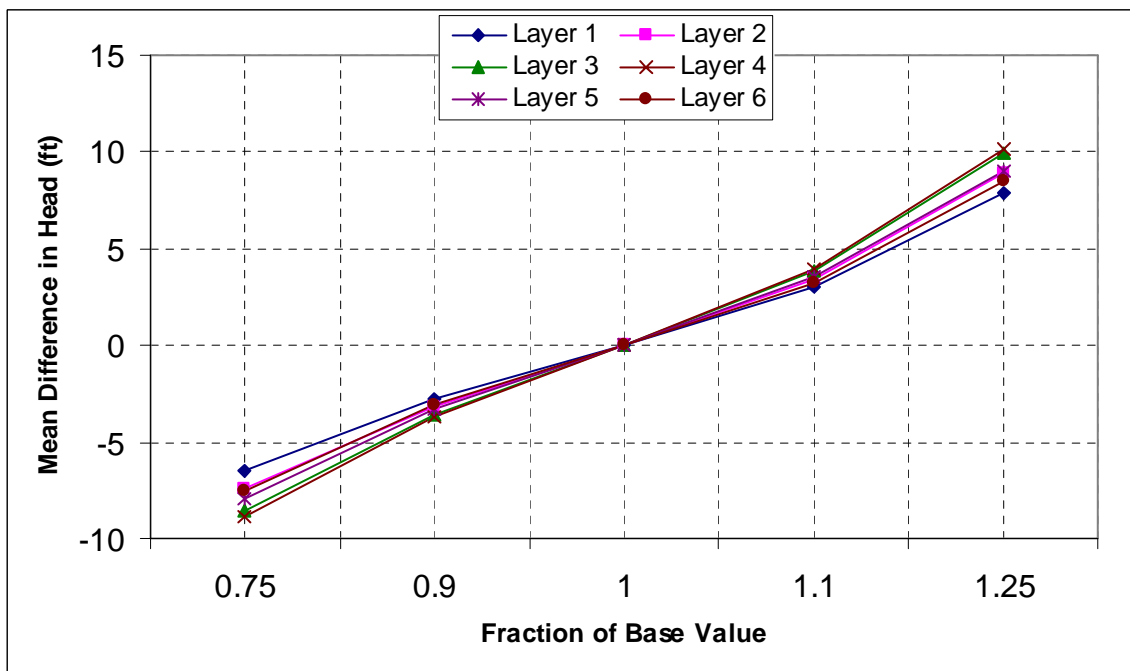


Figure 8.3.10 Steady-state sensitivity results where recharge is varied.

9.0 TRANSIENT MODEL

This section details the calibration and verification of the transient model and presents the transient model results. Section 9.1 describes the salient features of the calibration approach, and Section 9.2 presents the results of the transient calibration and verification together with the examination of residuals, hydrographs, and stream flow. A formal sensitivity analysis with the calibrated transient model can be found in Section 9.3.

9.1 Calibration

All properties or parameters common with the steady-state model were identical in the transient model. Section 8.1 contains the discussion of hydraulic properties in the steady-state model. A discussion of important inputs and new properties (such as storativity) follows. Figure 9.1.1 shows the distribution of calibration targets (head measurements) used for the transient model calibration.

The transient model played an important part in setting vertical anisotropy ratios for the model. We had initially set the anisotropy ratios of Layers 3, and 4 through 6, representing the Carrizo and Wilcox, respectively, to values on the order of 10 to 100; further, the maximum anisotropy for Layer 2 (Reklaw) was 4000. However, during initial transient calibration we found that water was passing between formations so easily that drawdowns could not be maintained at the estimated pumping rates. Water was moving into the Carrizo from storage in the Wilcox and Reklaw layers (or from storage in the Queen City through the Reklaw) due to the cross-formational flow resulting from the initialized drawdown cones, especially in Smith and Nacogdoches counties. We significantly increased the anisotropy ratios (decreased vertical hydraulic conductivity) in Layers 2, 4, 5 and 6 to near the extreme of previous/published values. This increase in anisotropy mitigated the “rebound” effect considerably. The final vertical hydraulic conductivities resulting from the calibrated anisotropy ratios (Table 8.1.1) are within published limits for these formation materials, but are closer to the “pure” material vertical hydraulic conductivity values than we would have anticipated for a regional scale model.

Note that for Smith and surrounding counties, the vertical permeability of the Reklaw (Layer 2) had to be decreased from 1×10^{-5} to 1×10^{-6} ft/day and the horizontal permeability of the Carrizo (Layer 3) and Wilcox (Layers 4 and 5) was limited to a maximum of 2 ft/d and 1 ft/d,

respectively (see Section 8.1.2). Such a reduction was needed even after reallocating 80% of the estimated pumpage from the Queen City to the Carrizo Layer to reproduce the observed drawdown. In contrast, the vertical hydraulic conductivity of Layer 2 had to be increased in Nacogdoches County from 1×10^{-5} to 1×10^{-4} ft/day so that the model did not overpredict the observed drawdown in Nacogdoches and Angelina counties.

Primary and secondary storage (also called storativity and specific yield) are properties in a transient model that are not present in a steady-state model. For specific storage, we used the geometric mean value of 4.5×10^{-6} 1/ft in all layers, based on field data compiled for the Carrizo-Wilcox aquifer by Mace et al. (2000a). This specific storage was then multiplied by layer thickness to provide the storativity at each grid cell. As a result, the variation in storativity corresponds to the variation in thickness of the different layers. Storativity has some effect on amplitude of head variation due to pumping. However, we did not find overall hydrograph trends to be sensitive to storativity, and, therefore, did not make areal changes in storativity during calibration or distinguish between specific storage of sand and mud in the Wilcox.

Because we lacked good targets for stream leakance, we set the streambed conductivity in a first approximation to the same value as the hydraulic conductivity in that particular cell. The streams exchange significant volumes of water with the aquifer, so they are important in the outcrop area. However, in the transient model, the hydrology of the outcrop has little effect on downdip regions during the simulation period, as hydraulic heads in the deeper confined section were mostly unaffected by streams or by recharge.

There are a total of 40 reservoirs in the model area, which played a significant role in the calibration. Initially, the conductivity of the reservoir bed was set to the hydraulic conductivity value of the corresponding layer; however, the value had to be reduced by two orders of magnitude, so that the amount of water passing between the reservoirs and the aquifer was within a reasonable range.

Similar to the steady-state calibration, recharge was critical for the calibration, primarily for hydraulic heads in the outcrop areas, whereas recharge was less sensitive for heads in the confined sections. The initial seasonally varying recharge distribution was reduced to about 33% of the initial SWAT estimates to get acceptable hydraulic heads in the outcrop. The recharge rates at 50% of the SWAT estimates generally yielded heads that were high, whereas recharge

rates at 15% of the SWAT estimates resulted in average recharge rates that were less than ET, and, hence, unacceptable.

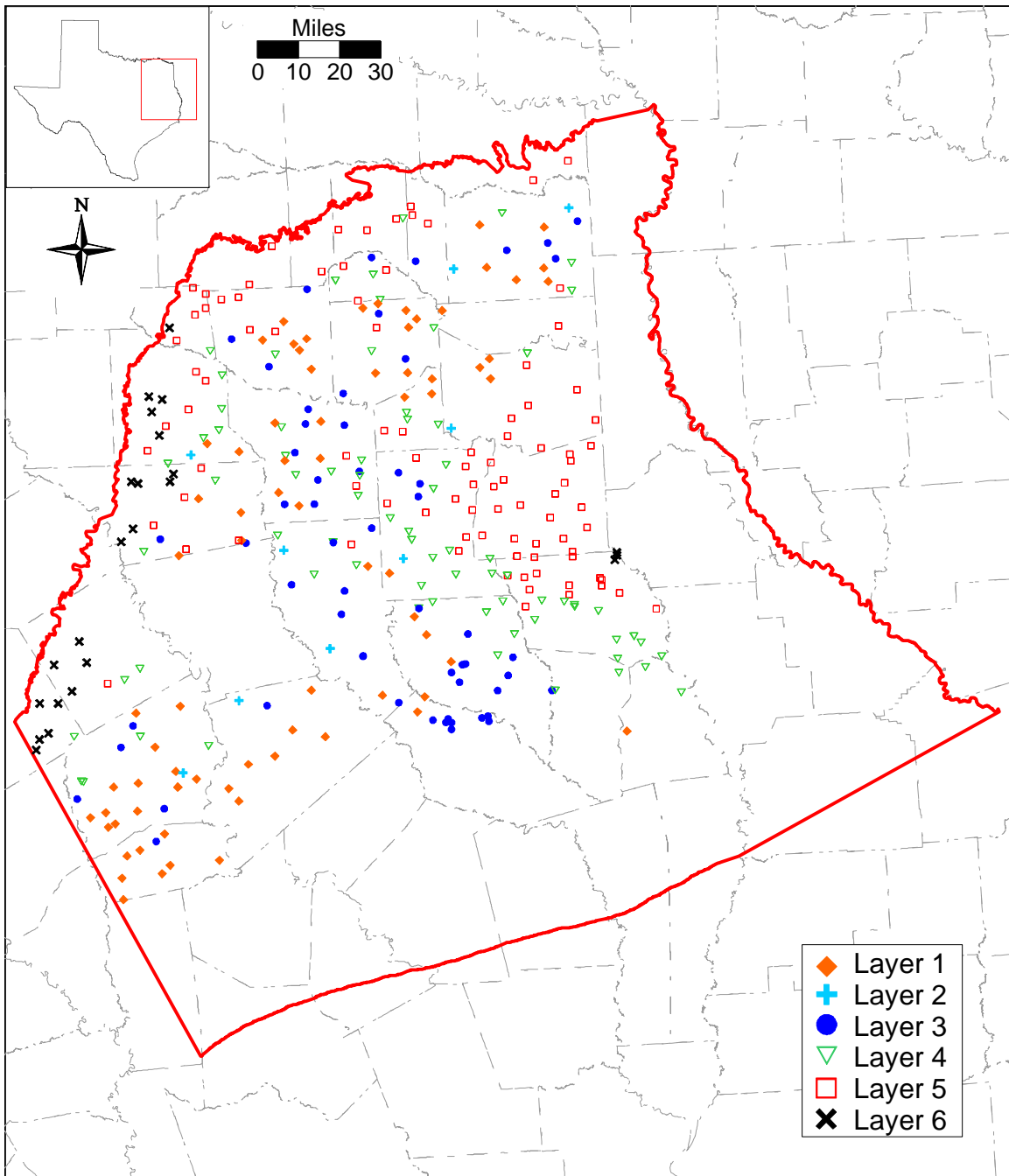


Figure 9.1.1 Target well locations for the different layers used in the transient calibration.

9.2 Simulation Results

Results for the transient model are presented in this section. Simulated hydraulic heads are compared to measured values, and stream leakances and water budgets are discussed.

9.2.1 Hydraulic Heads

The transient modeling is divided into a calibration period (1980 – 1989) and a verification period (1990 – 1999). Results of the calibration period are described first, followed by the performance of the verification period. Table 9.2.1 lists the mean error (ME), mean absolute error (MAE), root mean square error (RMS), range, and RMS/range for all aquifer layers for the calibration and verification periods. Figure 9.2.1 shows the simulated hydraulic-head distribution for Layer 1 (Queen City) at the end of the transient calibration period (December 1989). There was no hydraulic head contour map produced for the Queen City for 1989 as was done for the Carrizo-Wilcox aquifer layers, which are documented in Section 4.4. As mentioned in Section 8 for the steady-state results, the hydraulic head distribution in the Queen City was not explicitly calibrated. Nevertheless, the Queen City was considered relevant for controlling potential vertical flow between the confined Carrizo-Wilcox and the shallow water table aquifer in the study area. The simulated hydraulic heads reflect the overall topography in the Queen City outcrop and simulated heads compared reasonably well with target heads as indicated by the overall calibration statistics (Table 9.2.1).

Figure 9.2.2 shows the simulated and measured hydraulic heads for Layer 3 (Carrizo) at the end of the calibration period (December 1989). The measured head contours correspond to those discussed in Section 4.4 (Figure 4.4.10a), which were based on water-level measurements taken at various times over a five year period between 1987 and 1992. That is, the measured head contour may have significant seasonal variability included and an exact “fit” cannot be expected. Overall, the simulated and measured hydraulic head contours show a good agreement, reproducing the major cones of depression in Nacogdoches and Angelina counties, as well as in Smith County (Figure 9.2.2).

Figures 9.2.3 to 9.2.5 show the simulated and measured hydraulic heads for Layer 4 (upper Wilcox), Layer 5 (middle Wilcox), and Layer 6 (lower Wilcox) at the end of the calibration period (December 1989). Similar to Layer 3, the cones of depression in Layer 4 (upper Wilcox) in Nacogdoches County and in Smith County are reproduced reasonably well.

For the middle and lower Wilcox, there were no specific water-level measurements in Nacogdoches or Angelina counties, but a cone of depression was inferred owing to the close proximity of the pumpage from the overlying layers. In the outcrop and shallow confined section, the simulated head contours agree more closely with the measured heads (Figure 9.2.4). A similar pattern is indicated in Figure 9.2.5 for Layer 6 (lower Wilcox).

Figures 9.2.6 through 9.2.9 show the residuals at the different target well locations for Layers 3, 4, 5, and 6, respectively, at the end of the calibration period (December 1989). A positive residual indicates that the model has underpredicted the hydraulic head, while a negative residual indicates overprediction. The magnitude and spatial distribution of residuals at the target well locations for Layer 3 (Carrizo) indicate a maximum head difference of 151 ft in Smith County (Figure 9.2.6). In general, however, the differences are less than 40 ft. The residuals for Layer 4 (upper Wilcox) (Figure 9.2.7) are generally lower than those in Layer 3 (Figure 9.2.6). Target well locations for Layer 5 (middle Wilcox) are primarily in the Sabine Uplift and the western outcrop area, indicate a relatively even distribution of positive and negative residuals (Figure 9.2.8). For Layer 6 (lower Wilcox), the target wells are mainly in the western outcrop area (Figure 9.2.9).

The goodness-of-fit of the simulated and measured hydraulic heads is presented as scatterplots for Layers 1, 3, 4, 5, and 6 at the end of the calibration period (December 1989) in Figure 9.2.10. The data show mostly uniform scatter around the unit-slope line, indicating no particular trend in the simulated results. A similar distribution is shown for the comparison of the simulated and measured heads at the target wells for Layers 1, 3, 4, 5, and 6 at the end of the verification period (December 1999) in Figure 9.2.11. In general, the goodness-of-fit at the end of the verification period decreases somewhat compared to the calibration period. This is indicated in the calibration statistics in Table 9.2.1, where the adjusted RMS increased slightly for Layers 5 and 6. Overall, the adjusted RMS is significantly below 10%.

The hydraulic head contours based on the simulated heads at the end of the verification period (December 1999) and water-level contours that were discussed in Section 4.4 are shown in Figures 9.2.12 through 9.2.15 for Layers 3, 4, 5, and 6, respectively. Similar to the comparison at the end of the calibration period, the head contours show reasonably good agreement for Layer 3 (Carrizo) and Layer 4 (upper Wilcox), reproducing the cone of depression

in Nacogdoches and Angelina counties and in Smith County. For Layer 5 (middle Wilcox) and Layer 6 (lower Wilcox), the simulated heads in the deeper confined section are generally higher than the kriged head contours.

In the following discussion, selected hydrographs of simulated and measured heads are presented describing the general model response in the different layers. Table 9.2.2 lists the calibration statistics for these hydrographs. All hydrographs in this section are shown on a 100-ft vertical scale for consistency, unless the data range exceeds 100 ft. Figures 9.2.16a – c show hydrographs from Layer 3 (Carrizo). Hydrographs from the northern part indicate relatively little change in water levels through time (Figure 9.2.16a) with simulated water levels falling both above and below the measured heads and trending slightly upward or downward. Similar patterns are shown for hydrographs in the central part of the Carrizo (Figure 9.2.16b). Simulated heads tend to be lower than measured heads and reproduced the overall trend, particularly the observed drawdown in Smith County. Hydrographs in the southern part indicated effects of pumpage, particularly in Nacogdoches and in Angelina counties (Figure 9.2.16c). Simulated heads in wells 37-27-506 (Nacogdoches County) and in 37-36-501 (Angelina County) are noticeably lower than measured heads, whereas simulated heads in well 37-35-703 are significantly higher than measured heads at the end of the verification period (December 1999). As mentioned above, vertical hydraulic conductivity for Layer 2 (Reklaw) was increased from 1×10^{-5} ft/d to 1×10^{-4} ft/d in Nacogdoches County to allow for more vertical leakage to offset the head decline owing to pumpage.

Hydrographs from Layer 4 (upper Wilcox) are shown in Figures 9.2.17a – d. Simulated heads in the northern part (Figure 9.2.17a) show reasonably good agreement in Wood County and Van Zandt County, whereas the observed water-level decline could not be reproduced in Upshur County. The simulated heads in Cass County are lower than the measured heads, but reproduce the general trend. Hydrographs from the central part indicate relatively good agreement, reproducing the water-level declines in western Smith County and northern Cherokee County (Figure 9.2.17b). In eastern Smith County, however, the simulated heads did not reproduce the downward trend of measured water levels. Simulated heads in Rusk, Gregg, and Harrison counties showed relatively good agreement, though the simulated heads in Harrison County show an upward trend. The hydrograph of well 34-46-511 in Smith County indicates relatively large variability in both measured and simulated heads that indicate significant short-

term water-level declines owing to pumpage (Figure 9.2.17b). Vertical permeability of Layer 2 (Reklaw) was decreased from 1×10^{-5} ft/day to 1×10^{-6} ft/day in the central area in order to maintain the cone of depression observed in Smith and Cherokee counties. Hydrographs from the southern part (Figure 9.2.17c) show relatively small water-level changes and generally good agreement, except in central Nacogdoches County. The simulated heads in well 37-20-902 trend upward, whereas measured water levels show a significant decline. Hydrographs from the western part (Figure 9.2.17d) show both positive and negative offsets in the simulated heads but reproduce the overall trends.

Hydrographs for Layer 5 (middle Wilcox) are shown in Figures 9.2.18a – c. Simulated heads in the northern part indicated a relatively good fit for Morris, Rains, Wood, and Harrison counties (Figure 9.2.18a). Simulated heads in Cass County are higher than the measured heads, but reproduce the general trend, whereas simulated heads in Upshur County trend in an opposite direction from the measured water-level trends. Similar hydrograph patterns are evident in the central part (Figure 9.2.18b), with higher simulated heads in Smith and central Rusk counties, and a flat to upward trend in Shelby County. Simulated heads in the western part indicate significant offsets both positive and negative within the same county (Figure 9.2.18c).

Hydrographs for Layer 6 (lower Wilcox) are shown in Figure 9.2.19. Simulated heads trend upward in Henderson, Limestone, and Freestone counties, whereas measured water levels show a slight decline. The hydrographs in Rains and Van Zandt counties agree reasonably well, whereas Shelby County simulated heads are higher than measured heads. The simulated upward trend in hydraulic heads corresponds to the overall higher heads in the lower Wilcox in the southern part of the model as indicated in the hydraulic head contours in Figure 9.2.15.

The simulated head increase in the southwestern part of Layer 6 (lower Wilcox) suggests potentially too high recharge rates in the outcrop or low hydraulic conductivity in this area. A long-term average recharge distribution over the 25-year transient simulation period is shown in Figure 9.2.20. These SWAT recharge estimates indicate significantly higher recharge rates in the Carrizo-Wilcox outcrop in the southwestern part (e.g., Freestone County) compared to the outcrop area farther north (e.g., Van Zandt County). SWAT recharge estimates are largely controlled by soil type and vegetation cover that are based on the STATSGO soil maps. Any error in these input data can result in errors in the recharge estimates.

9.2.2 Stream Leakance

Figures 9.2.21 and 9.2.22 show the simulated stream leakance indicating the gains and losses along the major streams in the area at two different times, representing relatively dry and wet conditions. The stream leakance during May 1989 indicates predominantly losing stream segments during relatively wet conditions when stream stages are highest (Figure 9.2.21), whereas the plotted stream leakance during November 1989 indicates gaining stream segments (Figure 9.2.22). The different flow conditions are indicated in the individual streamflow gauges. Figure 9.2.23 shows simulated and measured stream flows for specific gauging stations on the Trinity, Neches, and Sabine rivers for the transient simulation period (1980 – 2000). Simulated stream flows follow the seasonal pattern and are typically below the measured flow rates. This is expected because the model does not simulate surface runoff.

We also compared the stream leakances to the stream gain/loss study by Slade et al. (2002). They documented stream flow measurements along a couple of segments of the Sabine River and at one of its tributaries (Lake Fork Creek) over the transient simulation period. Figure 9.2.24 shows a cross-plot of the measured gain/loss and those derived from the model. The data comparison shows a large scatter, though most of the data fall within the same quadrant. Relatively large variability in measured streamflows are indicated by the measured data at the different gaging stations along the river that were measured on the same day. In comparison, simulated stream flows show more gradual changes along the river.

Slade et al. (2002) note that the potential error in stream flow measurements is typically about 5 to 8 percent. Since this error is possible at both ends of a gain/loss subreach, the potential error in gain/loss can equal a significant fraction of the total flow in the subreach. Comparing the available gain/loss values to mean stream flows from the EPA River Reach data set shows that almost all of the gain/loss values are less than 5 percent of the mean stream flow. This suggests that the gain/loss values are uncertain and can be used only qualitatively.

9.2.3 Water Budget

Table 9.2.3 shows the water budget for the transient model totaled for years 1980, 1988 (drought year for the calibration period), 1989 and 1999. The overall mass balance error for the transient simulation was 0.09 percent, well under the GAM requirement of one percent. In the model, the greatest influx of water consistently occurs from recharge, and the greatest outflow of

water is through streams and groundwater ET. Overall outflow from pumpage increased from 117,000 ac-ft/yr in 1980 to 148,000 ac-ft/yr in 1999. Groundwater ET rates show relatively large changes from hot summers (e.g., 1980) to more temperate summers (e.g., 1990). The seasonal variations in totals for stream recharge/discharge, diffuse recharge, groundwater ET, and pumpage over the transient simulation period (1980 – 1999) are summarized in Figure 9.2.25. Peak pumpage during the summer months continuously increased over the years, and total ET exceeds recharge during the summer months.

Table 9.2.1 Calibration statistics for the transient model.

Calibration period (1980-1989)					
	Layer 1	Layer 3	Layer 4	Layer 5	Layer 6
ME	-22.49	4.55	0.53	1.24	-10.03
MAE	31.05	26.10	18.86	23.43	20.28
RMS	40.87	35.14	26.57	31.74	24.70
Range	433	743	491	523	310
RMS/Range	0.094	0.047	0.054	0.061	0.080
Verification period (1990-1999)					
	Layer 1	Layer 3	Layer 4	Layer 5	Layer 6
ME	-20.48	-4.64	-9.67	-5.57	-18.93
MAE	31.40	31.43	23.74	28.71	26.67
RMS	41.08	42.10	34.37	38.44	31.01
Range	459	821	660	523	300
RMS/Range	0.090	0.051	0.052	0.073	0.103

ME = mean error

MAE = mean absolute error

RMS = root mean square error

Table 9.2.2 Calibration statistics for the hydrographs shown in Figures 9.2.16a – 9.2.19.

Well	Layer	Count	ME (ft)	MAE (ft)	RMS (ft)	Figure Number
1658904	3	20	5.57	6.61	8.84	9.2.16a
1663402	3	21	-6.16	8.60	9.80	9.2.16a
3412803	3	19	16.27	16.27	16.45	9.2.16a
3518401	3	18	-23.47	23.47	24.60	9.2.16a
3453604	3	14	0.39	26.45	34.02	9.2.16b
3457301	3	20	21.94	21.94	22.26	9.2.16b
3463503	3	14	-1.38	4.38	5.34	9.2.16b
3464302	3	19	11.49	11.49	11.85	9.2.16b
3550501	3	18	12.10	12.10	12.17	9.2.16b
3719301	3	19	3.47	3.90	4.78	9.2.16c
3727506	3	20	54.17	58.32	61.92	9.2.16c
3735703	3	17	-87.01	87.01	107.99	9.2.16c
3736501	3	14	39.39	39.39	74.66	9.2.16c
3940601	3	19	-32.55	32.55	32.62	9.2.16c
1663902	4	9	27.35	27.35	27.38	9.2.17a
3421302	4	17	10.80	10.80	13.67	9.2.17a
3442108	4	21	4.38	4.38	4.94	9.2.17a
3501803	4	18	-35.02	35.07	40.24	9.2.17a
3446511	4	17	11.71	21.62	27.56	9.2.17b
3448802	4	15	-25.09	25.09	25.81	9.2.17b
3522401	4	17	-8.35	8.35	9.85	9.2.17b
3526706	4	18	-6.50	6.68	9.49	9.2.17b
3549801	4	17	2.34	4.13	4.61	9.2.17b
3806603	4	16	1.23	40.66	54.09	9.2.17b
3617502	4	20	-7.20	7.20	7.31	9.2.17c
3625504	4	17	1.60	2.22	2.59	9.2.17c
3704301	4	17	-6.48	6.48	7.01	9.2.17c
3710302	4	11	-1.07	1.48	1.94	9.2.17c
3714501	4	20	2.20	2.20	2.41	9.2.17c
3720902	4	13	19.68	20.08	24.34	9.2.17c
3932205	4	19	-8.34	10.81	12.60	9.2.17d
3938902	4	23	-14.62	15.04	15.24	9.2.17d
3940906	4	20	-13.60	13.60	14.30	9.2.17d
1650207	5	18	3.72	5.05	6.00	9.2.18a
3403101	5	12	9.28	9.28	9.43	9.2.18a
3413401	5	18	-4.29	5.62	6.46	9.2.18a
3507801	5	18	-46.80	46.80	47.41	9.2.18a
3509403	5	19	-48.70	48.70	51.32	9.2.18a
3531602	5	19	-4.59	4.59	5.56	9.2.18a
3448803	5	13	-33.32	33.32	34.13	9.2.18b
3464403	5	10	4.56	9.13	11.61	9.2.18b
3544103	5	11	0.52	4.99	5.78	9.2.18b
3550801	5	22	-91.32	91.32	94.33	9.2.18b
3553902	5	17	-4.15	4.66	6.32	9.2.18b
3706401	5	20	-11.03	11.09	13.38	9.2.18b

Table 9.2.2 (continued)

Well	Layer	Count	ME (ft)	MAE (ft)	RMS (ft)	Figure Number
3426605	5	11	-30.21	30.21	33.47	9.2.18c
3434101	5	18	44.69	44.69	45.27	9.2.18c
3449810	5	15	45.66	45.66	45.68	9.2.18c
3450306	5	18	-60.04	60.04	60.81	9.2.18c
3410202	6	6	3.18	3.18	3.21	9.2.19
3433302	6	18	7.28	10.22	12.09	9.2.19
3442403	6	17	-18.47	18.87	21.35	9.2.19
3708801	5	15	-10.89	10.89	10.92	9.2.19
3923101	6	15	-37.79	37.79	41.35	9.2.19
3929801	6	23	-9.05	9.05	11.04	9.2.19

Table 9.2.3 Water budget for transient model. All rates reported in acre-ft/yr.

Year	Layer	GHBs	Reservoirs	Wells	ET	Top	Bottom	Recharge	Streams	Storage
1980	1	29,653	-42,758	-6,959	-452,559	0	-30,614	847,222	-410,536	66,529
	2	0	-1,485	-526	-208,546	30,614	-39,195	205,313	-422,217	436,044
	3	0	-2,066	-42,808	-120,840	39,195	-35,608	135,122	-78,963	105,965
	4	0	128,011	-34,789	-237,959	35,608	-29,049	395,803	-248,242	-9,382
	5	0	32,984	-26,829	-178,205	29,049	-14,449	508,713	-181,172	-170,106
	6	0	3,928	-5,257	-36,912	14,449	0	41,101	-36,687	19,378
	Sum	29,653	118,613	-117,169	-1,235,020	148,915	-148,915	2,133,274	-1,377,818	448,429
1988*	1	24,516	-63,754	-8,891	-492,581	0	-30,230	860,053	-477,642	188,513
	2	0	-474	-653	-196,440	30,230	-39,849	188,680	-135,772	154,280
	3	0	-1,550	-46,075	-118,868	39,849	-33,494	91,755	-46,330	114,709
	4	0	-58,974	-42,851	-227,104	33,494	-24,196	309,932	-217,521	227,215
	5	0	-107,645	-37,556	-157,848	24,196	-11,673	453,461	-343,416	180,466
	6	0	2,289	-6,616	-25,541	11,673	0	25,473	-17,468	10,189
	Sum	24,516	-230,109	-142,642	-1,218,383	139,441	-139,441	1,929,354	-1,238,149	875,373
1989	1	24,259	-20,561	-9,386	-176,442	0	-30,289	1,014,412	-316,591	-485,426
	2	0	-1,295	-667	-61,568	30,289	-40,638	267,297	-92,189	-101,228
	3	0	-2,715	-49,773	-43,235	40,638	-34,551	148,618	-36,114	-22,874
	4	0	-30,151	-45,465	-62,292	34,551	-23,327	480,413	-85,660	-268,077
	5	0	-47,297	-31,641	-71,423	23,327	-11,164	587,913	-30,078	-419,660
	6	0	128,949	-6,134	-10,415	11,164	0	48,274	-4,242	-167,597
	Sum	24,259	26,931	-143,066	-425,375	139,969	-139,969	2,546,927	-564,874	-1,464,862
1999	1	21,848	-33,720	-11,772	-385,815	0	-30,673	694,847	-556,026	301,132
	2	0	-515	-775	-121,227	30,673	-42,263	171,875	-117,977	80,206
	3	0	-4,021	-51,789	-55,999	42,263	-30,706	89,235	-45,898	56,908
	4	0	-87,738	-37,766	-108,712	30,706	-22,093	331,665	-192,157	86,089
	5	0	-92,453	-38,875	-104,099	22,093	-9,300	438,221	-317,435	101,827
	6	0	-14,165	-6,847	-17,520	9,300	0	33,520	-24,286	19,998
	Sum	21,848	-232,612	-147,825	-793,372	135,035	-135,035	1,759,363	-1,253,780	646,160

*Drought year for calibration period

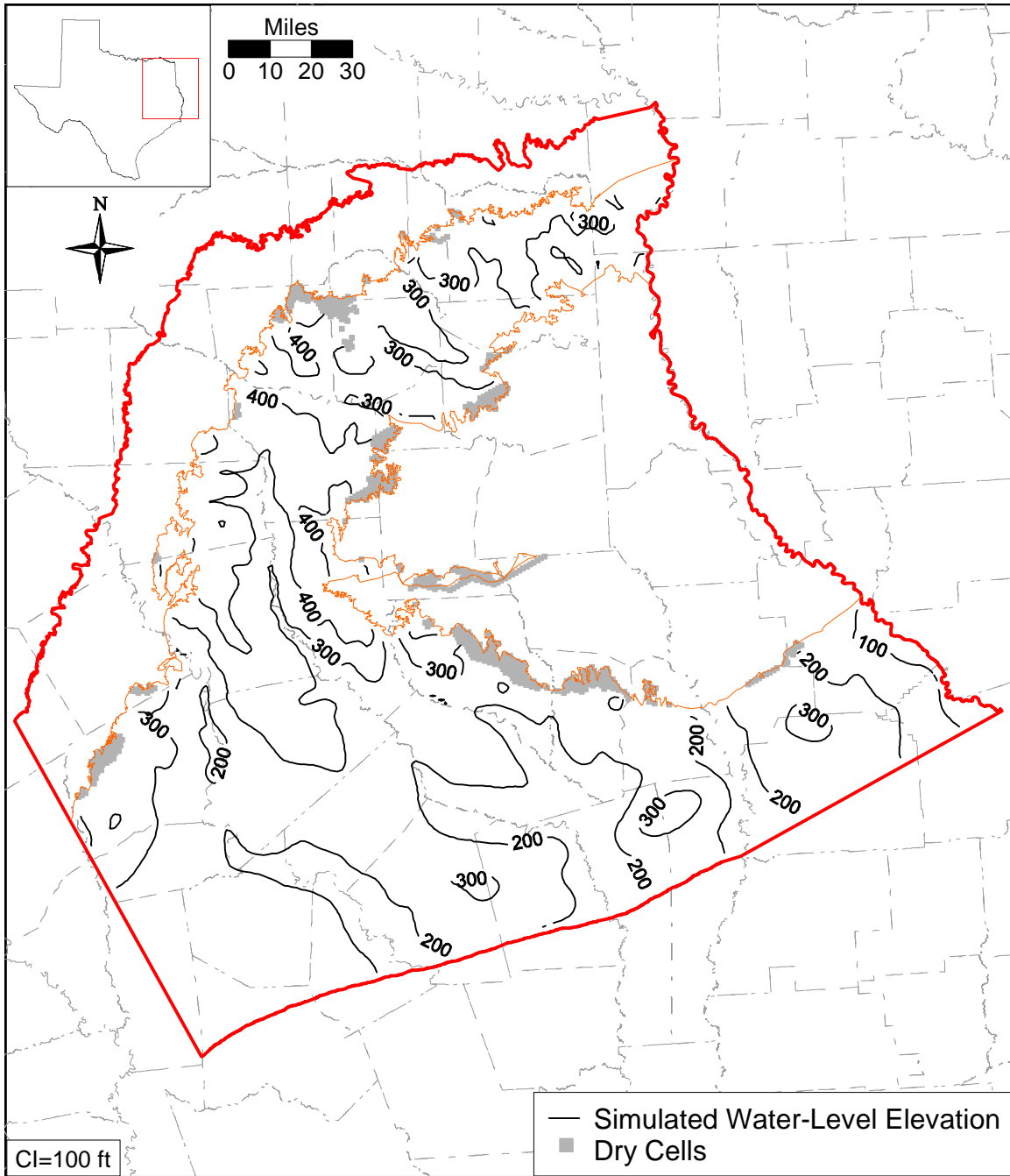


Figure 9.2.1 Simulated hydraulic head distribution for Layer 1 (Queen City) at the end of the transient model calibration (December 1989).

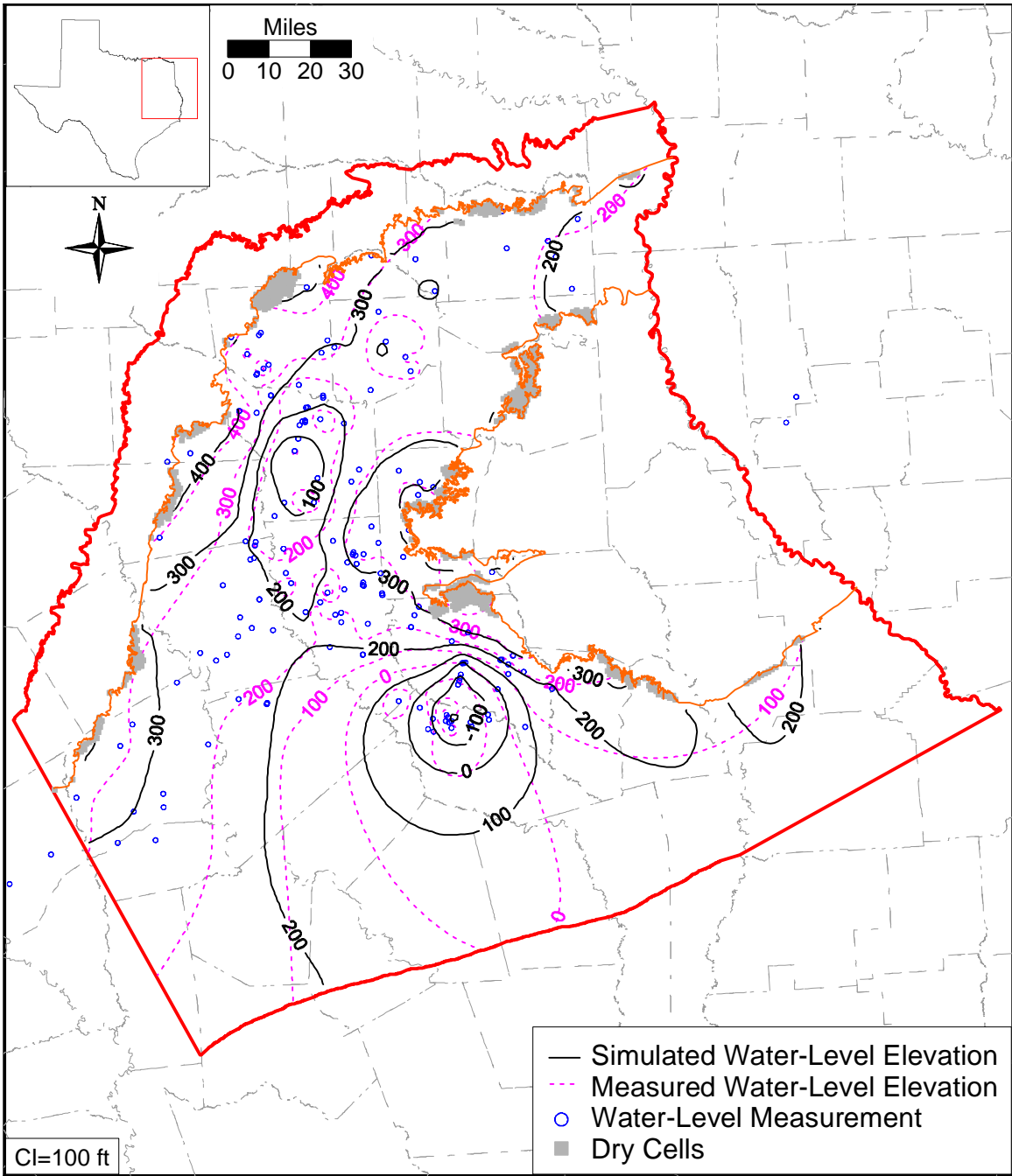


Figure 9.2.2 Simulated and measured hydraulic head distribution for Layer 3 (Carrizo) at the end of the transient model calibration (December 1989).

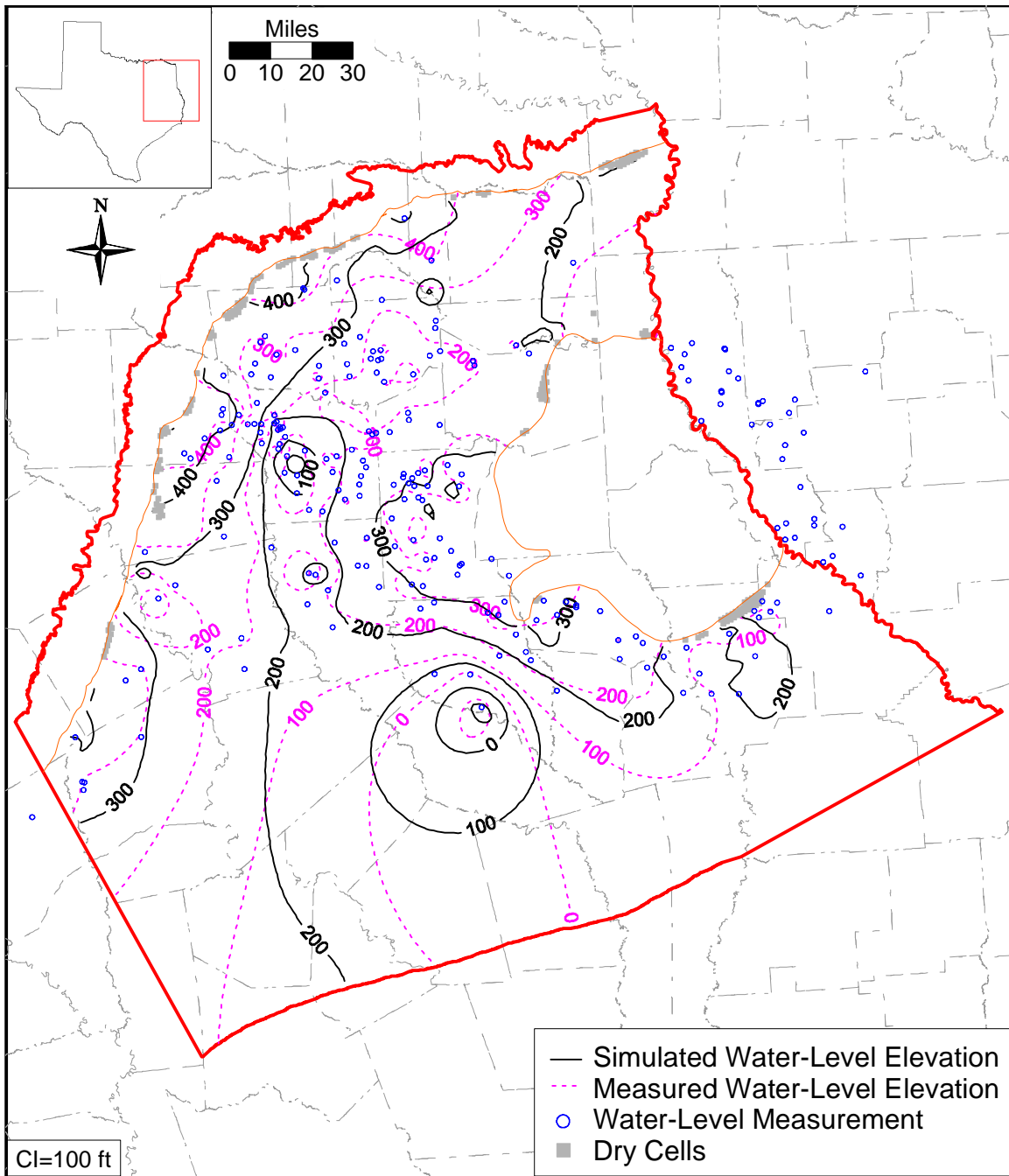


Figure 9.2.3 Simulated and measured hydraulic head distribution for Layer 4 (upper Wilcox) at the end of the transient model calibration (December 1989).

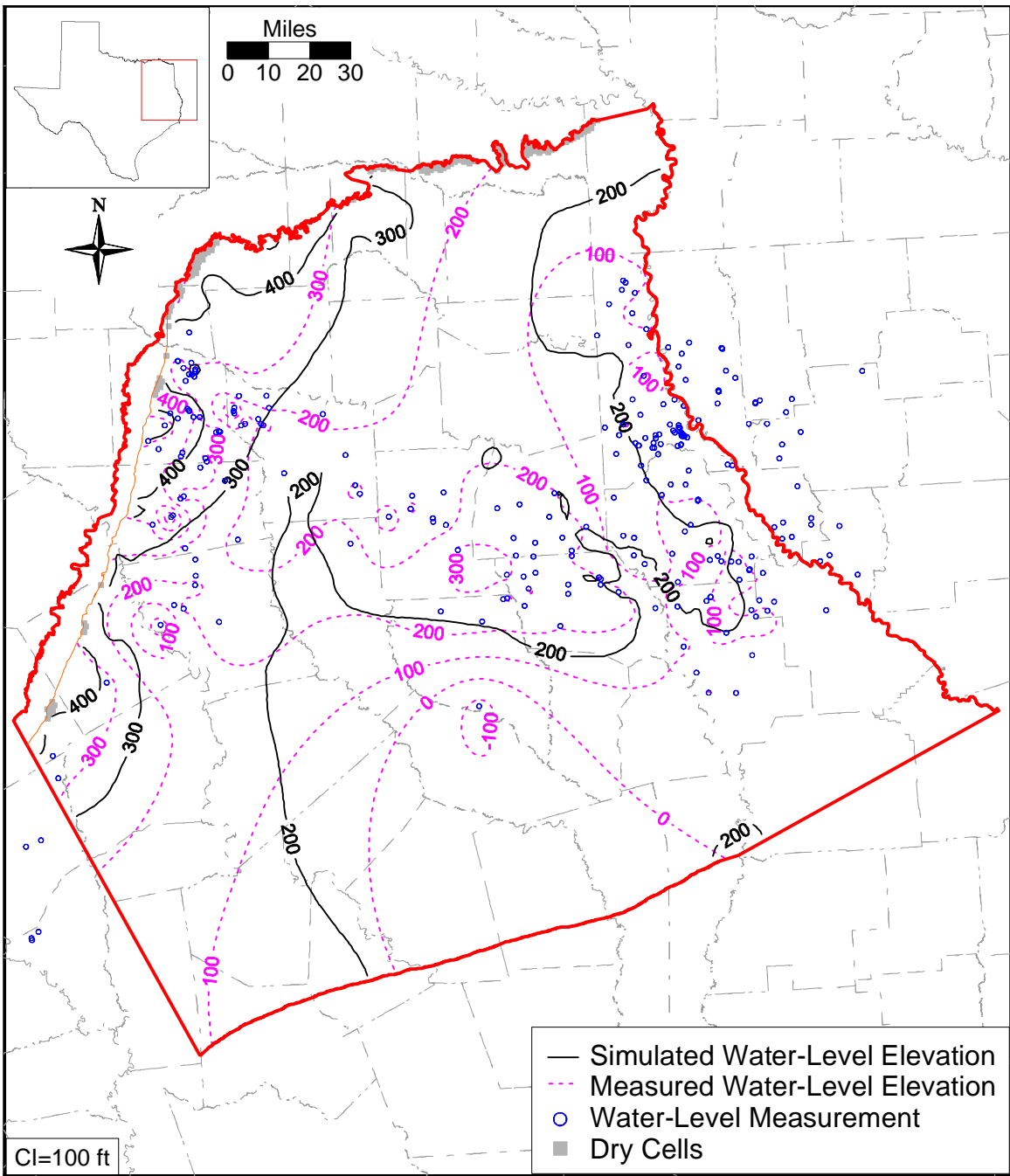


Figure 9.2.4 Simulated and measured hydraulic head distribution for Layer 5 (middle Wilcox) at the end of the transient model calibration (December 1989).

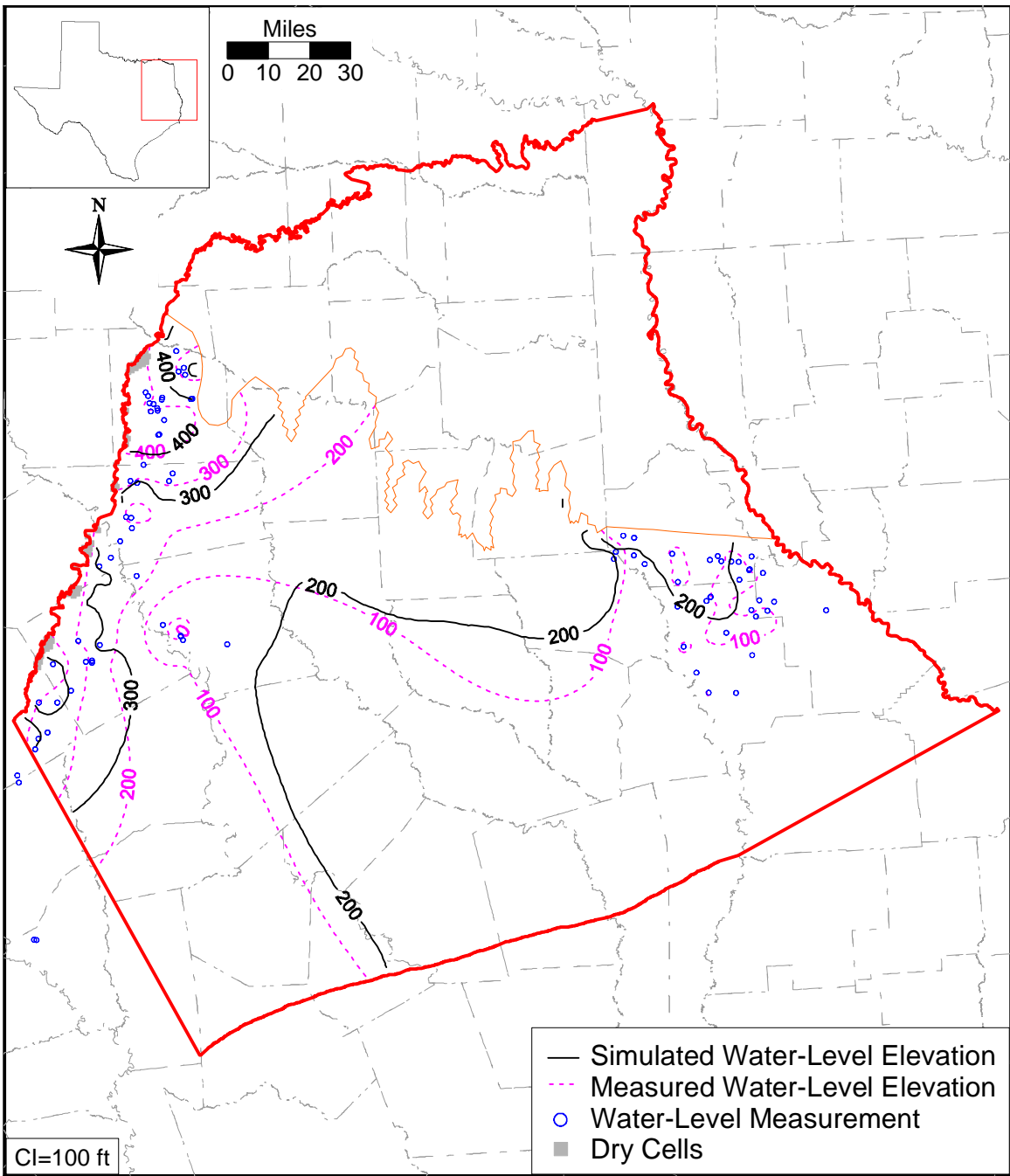


Figure 9.2.5 Simulated and measured hydraulic head distribution for Layer 6 (lower Wilcox) at the end of the transient model calibration (December 1989).

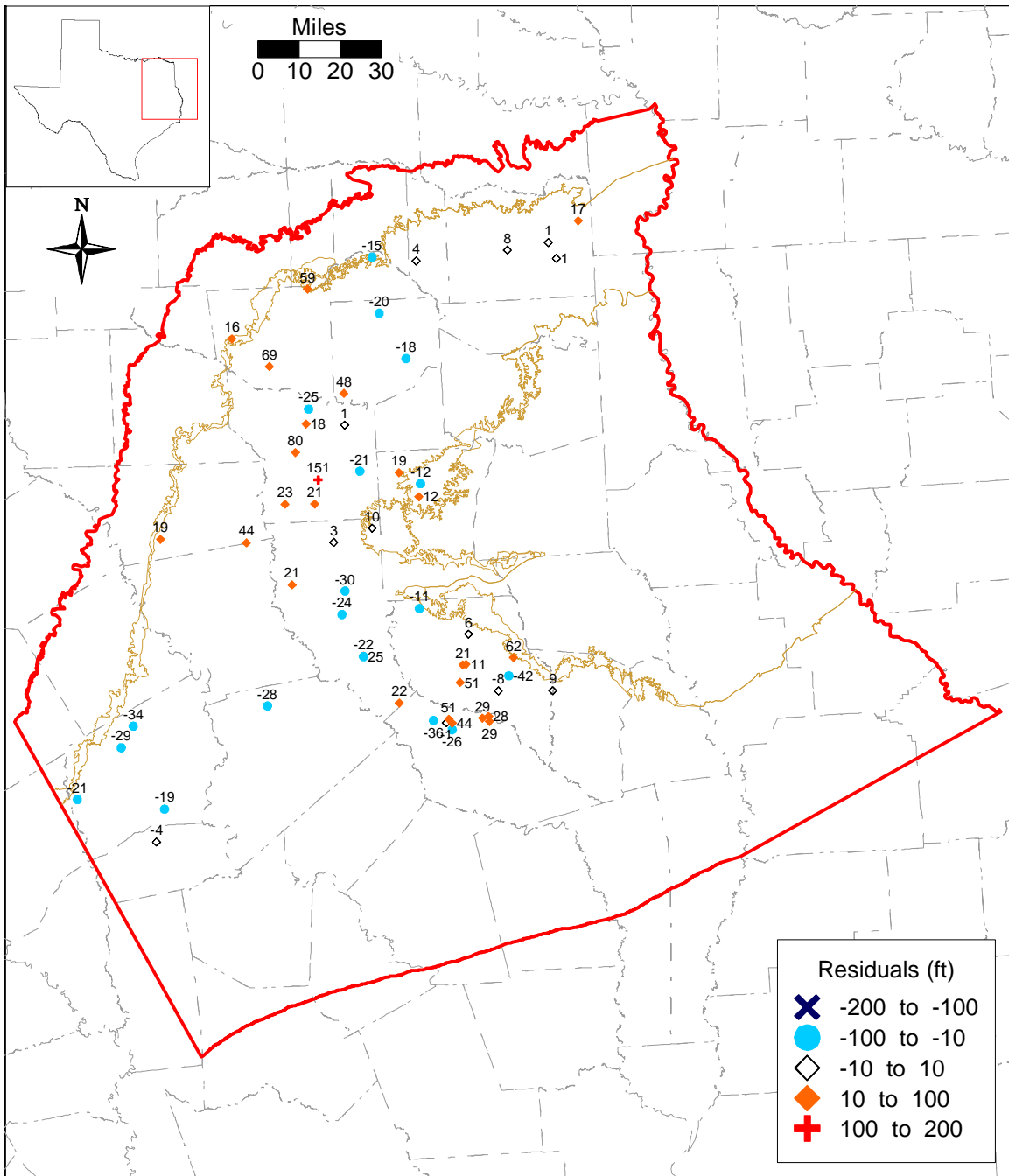


Figure 9.2.6 Residuals at target wells for Layer 3 (Carrizo) at the end of the transient model calibration (December 1989).

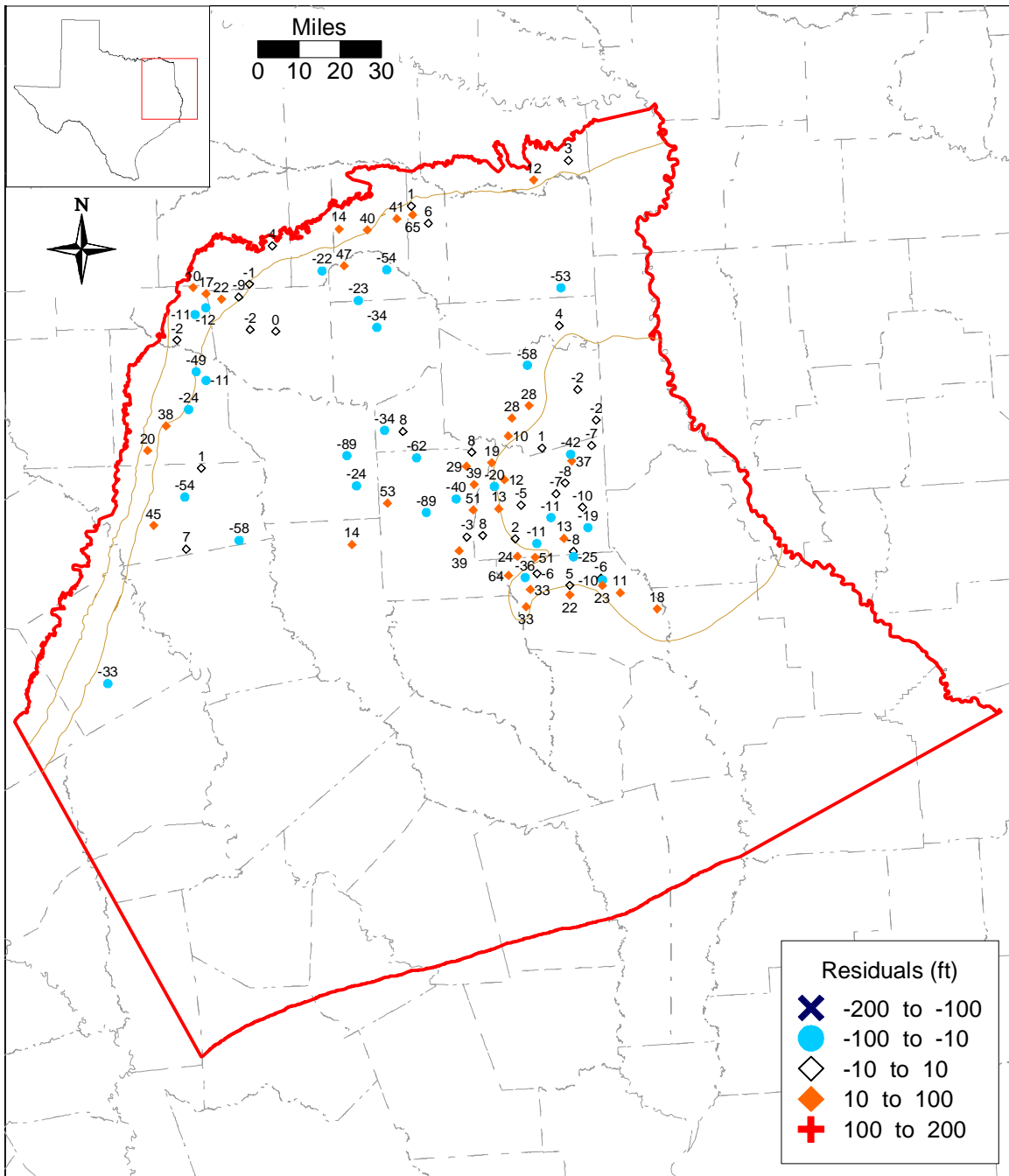


Figure 9.2.8 Residuals at target wells for Layer 5 (middle Wilcox) at the end of the transient model calibration (December 1989).

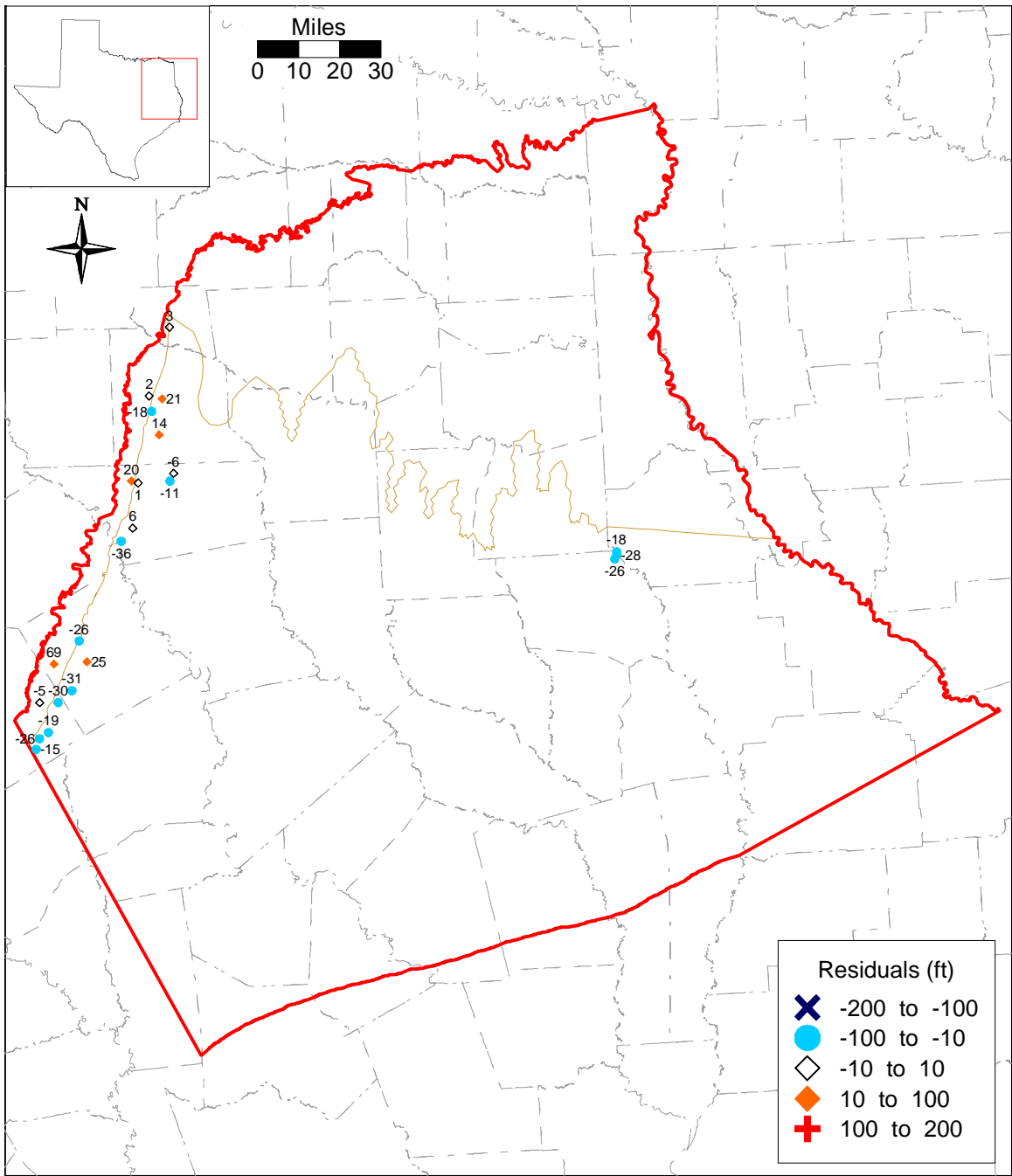


Figure 9.2.9 Residuals at target wells for Layer 6 (lower Wilcox) at the end of the transient model calibration (December 1989).

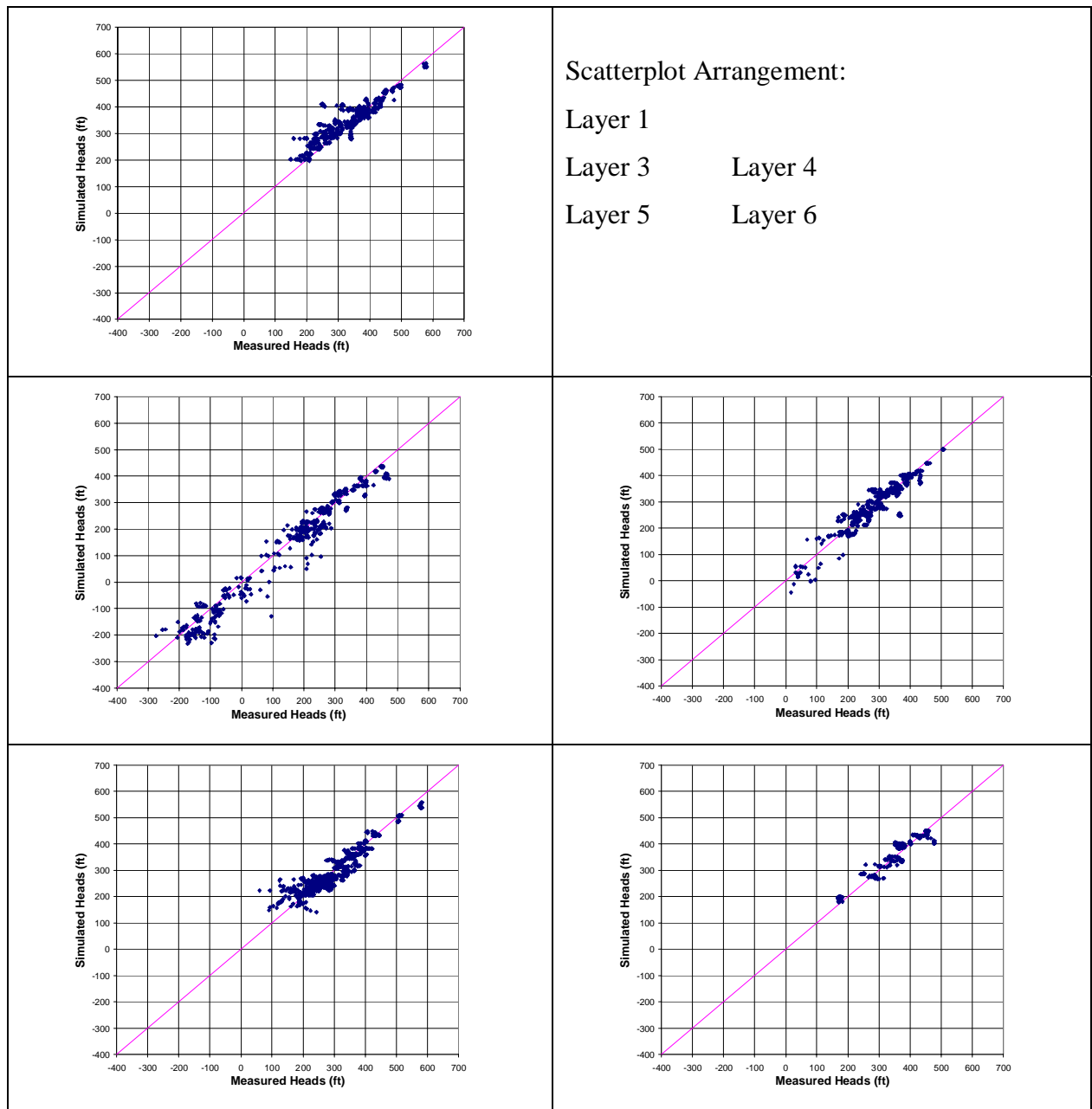


Figure 9.2.10 Scatterplots of simulated and measured hydraulic heads for the different layers at the end of the transient model calibration (December 1989).

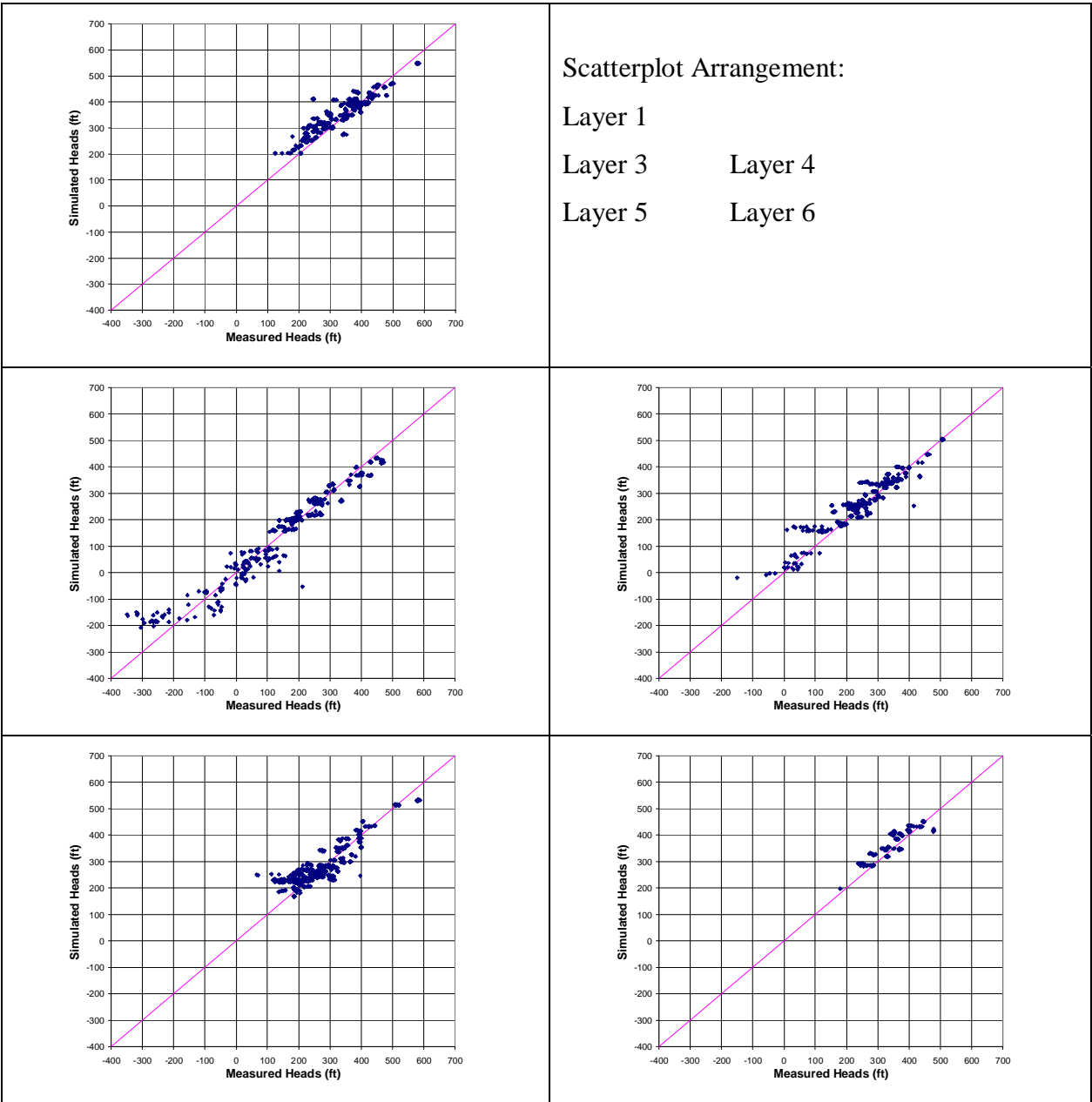


Figure 9.2.11 Scatterplots of simulated and measured hydraulic heads for the different layers at the end of the transient model verification (December 1999).

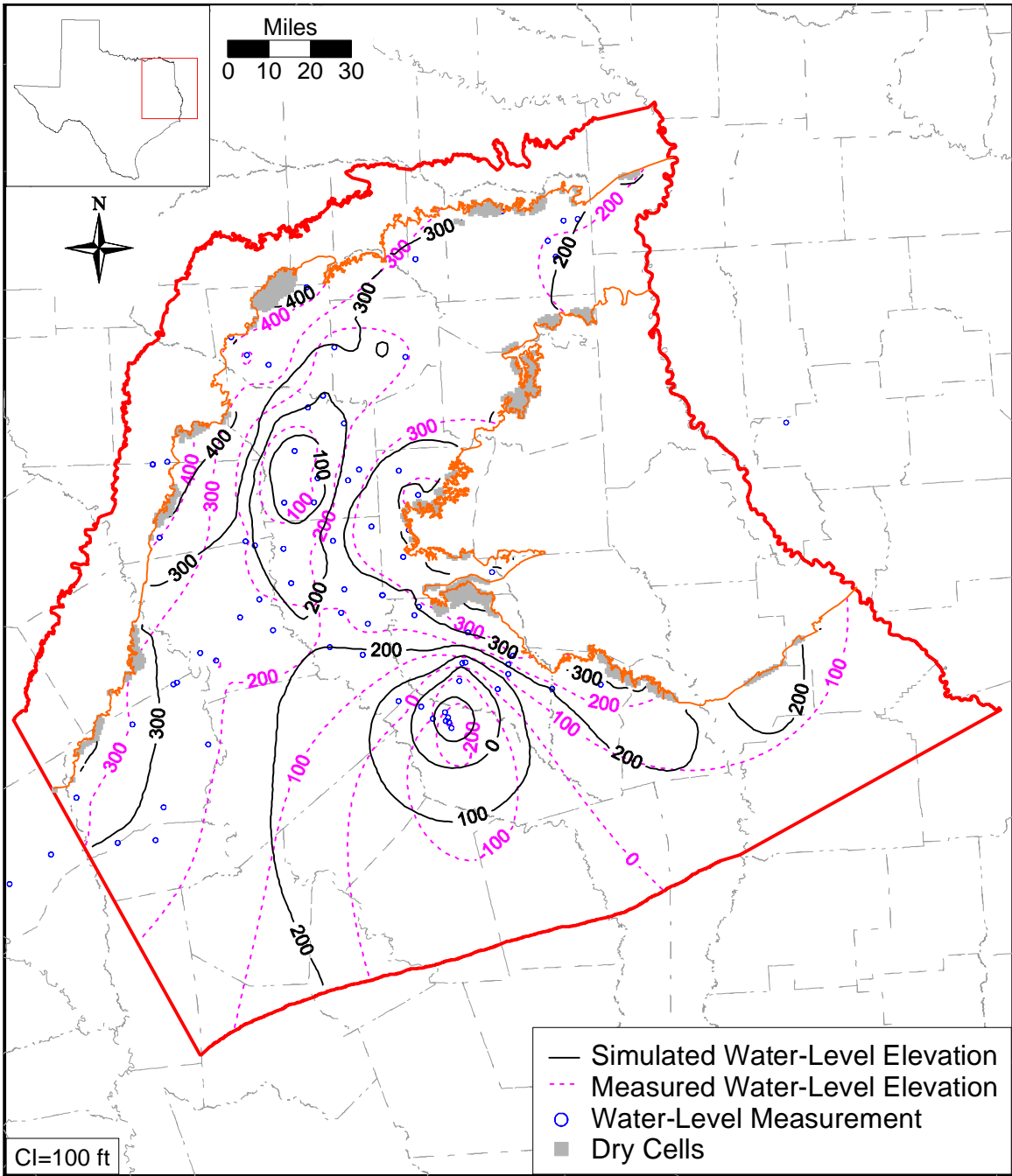


Figure 9.2.12 Simulated and measured hydraulic head distribution for Layer 3 (Carrizo) at the end of the transient model verification (December 1999).

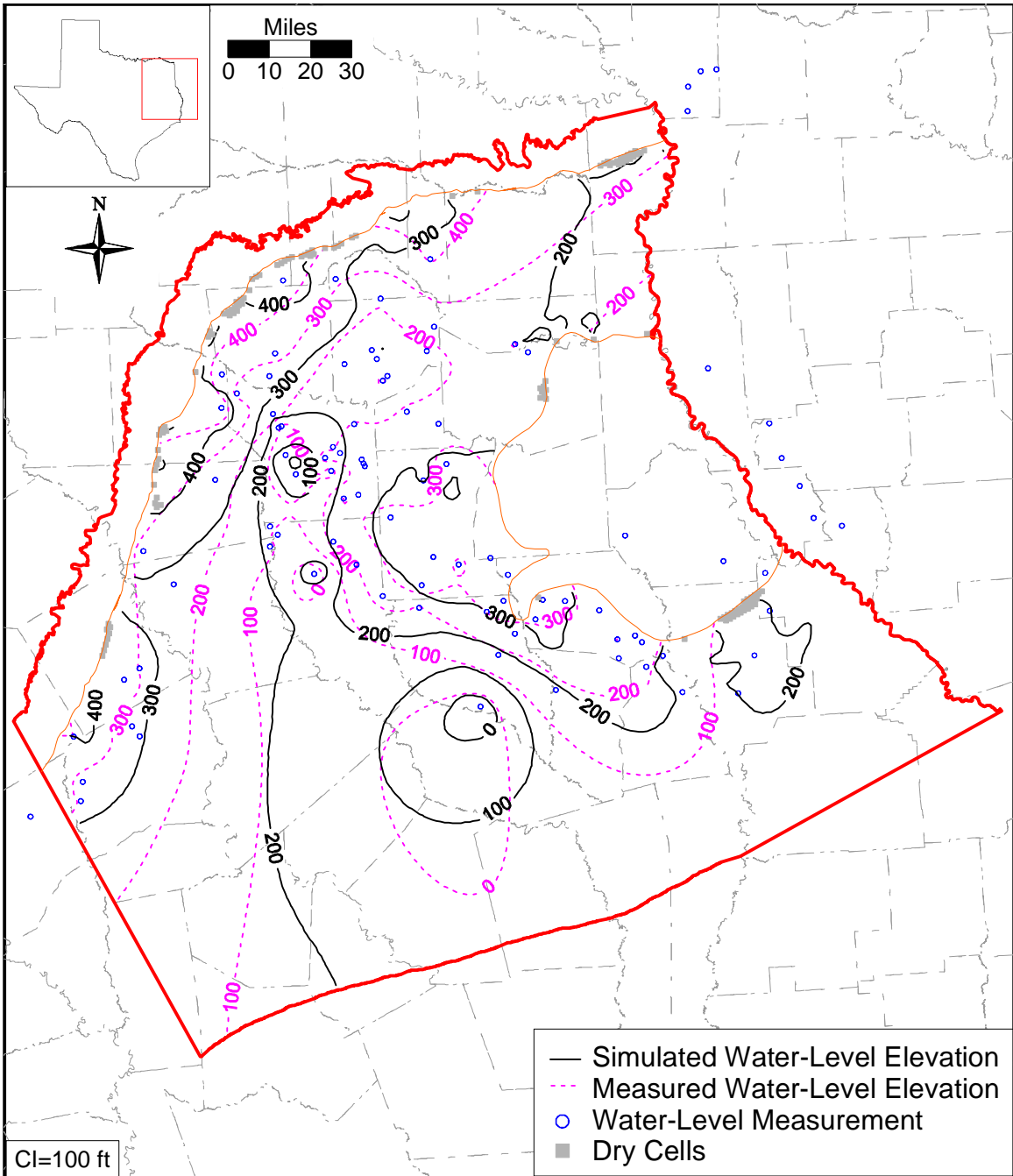


Figure 9.2.13 Simulated and measured hydraulic head distribution for Layer 4 (upper Wilcox) at the end of the transient model verification (December 1999).

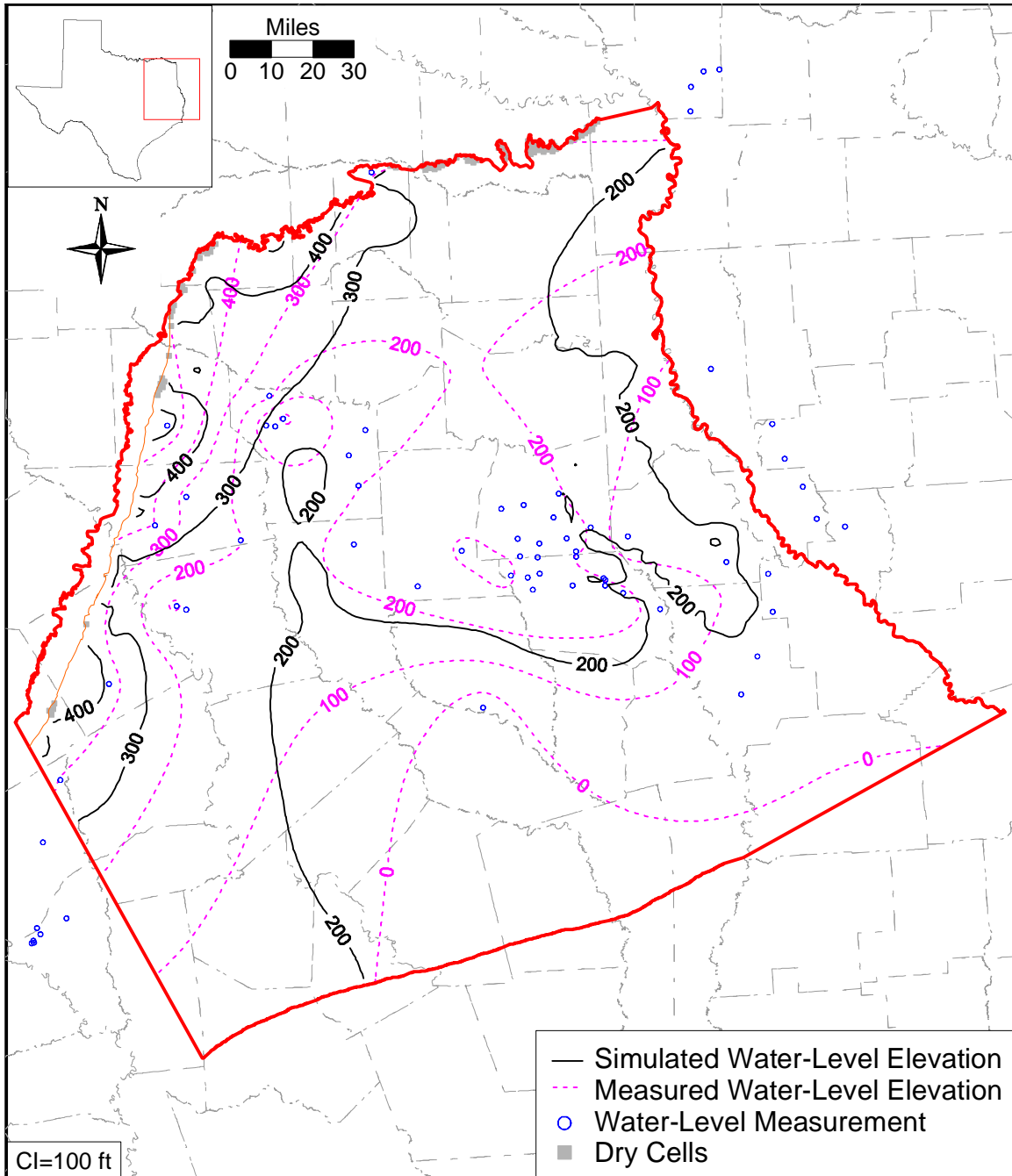


Figure 9.2.14 Simulated and measured hydraulic head distribution for Layer 5 (middle Wilcox) at the end of the transient model verification (December 1999).

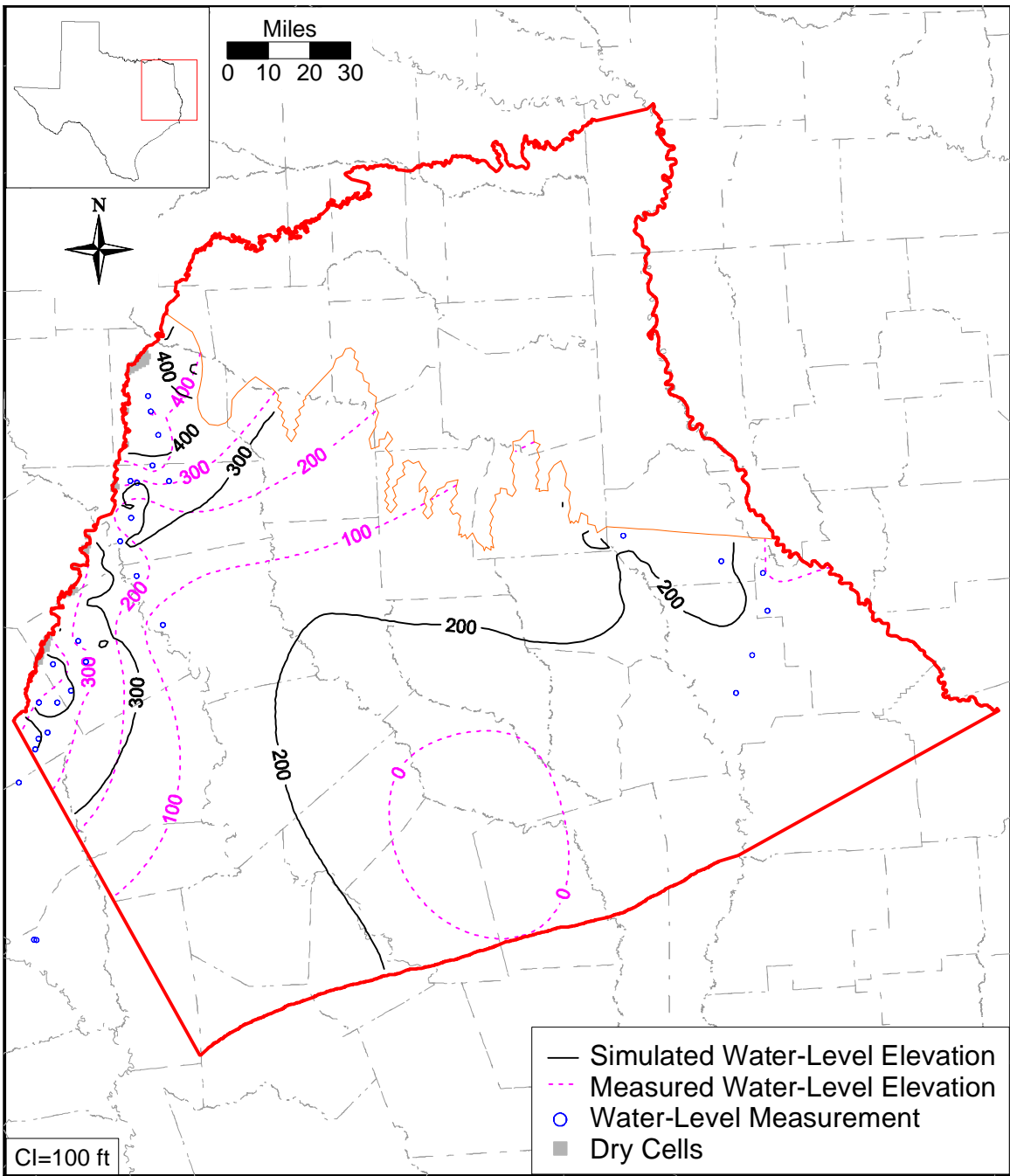


Figure 9.2.15 Simulated and measured hydraulic head distribution for Layer 6 (lower Wilcox) at the end of the transient model verification (December 1999).

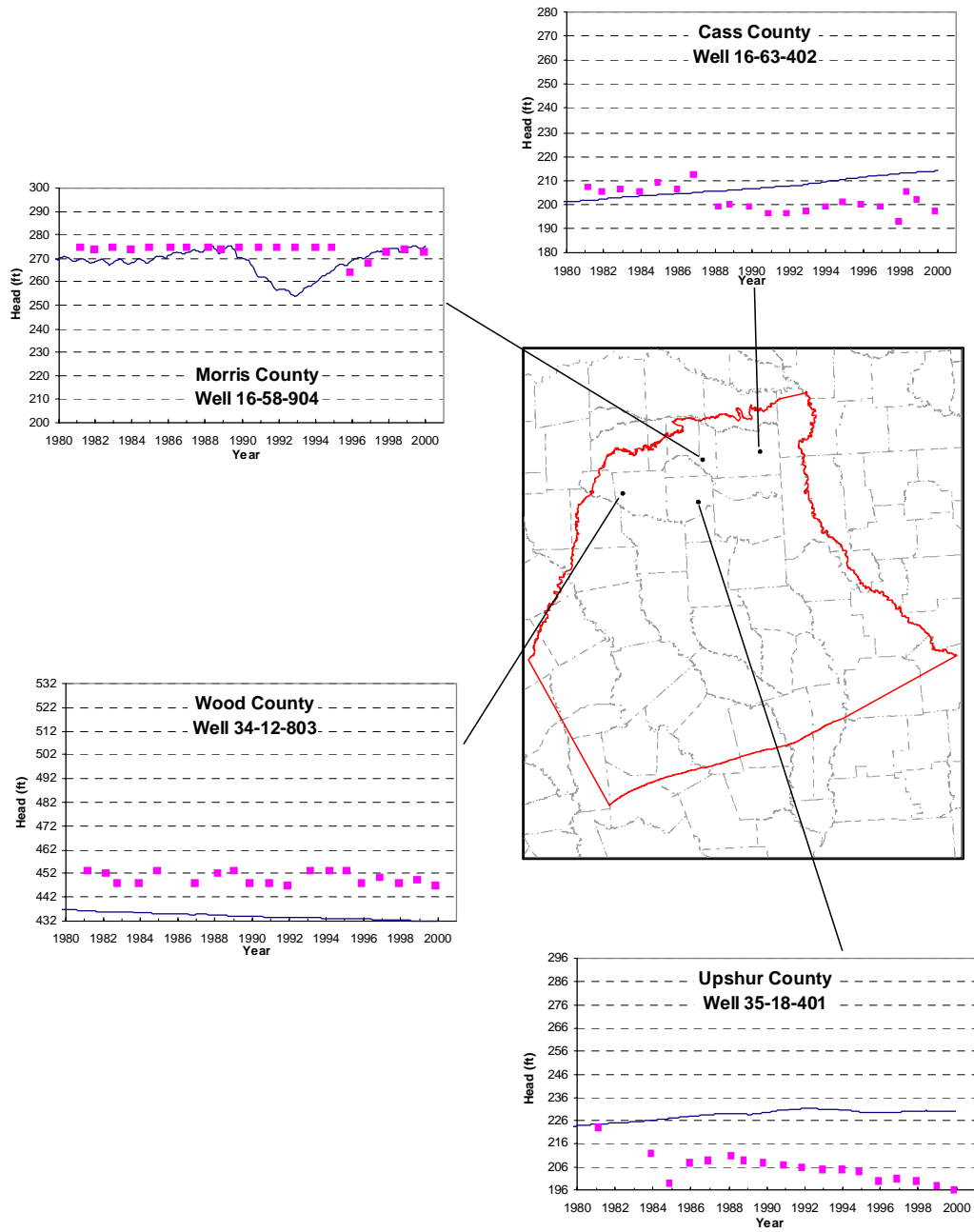


Figure 9.2.16a Selected hydrographs of simulated (lines) and measured (points) hydraulic heads in the northern part for Layer 3 (Carrizo).

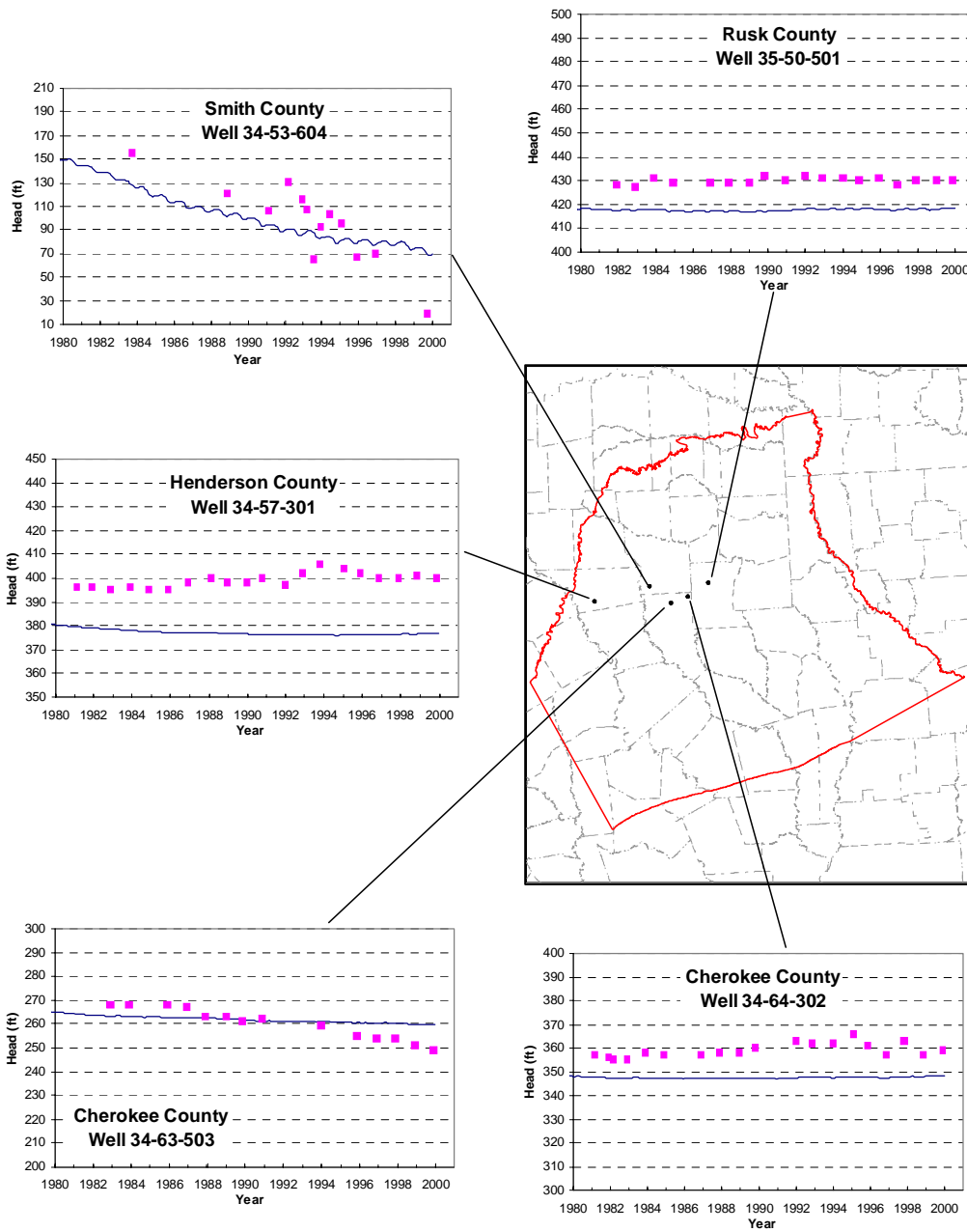


Figure 9.2.16b Selected hydrographs of simulated (lines) and measured (points) hydraulic heads in the central part for Layer 3 (Carrizo).

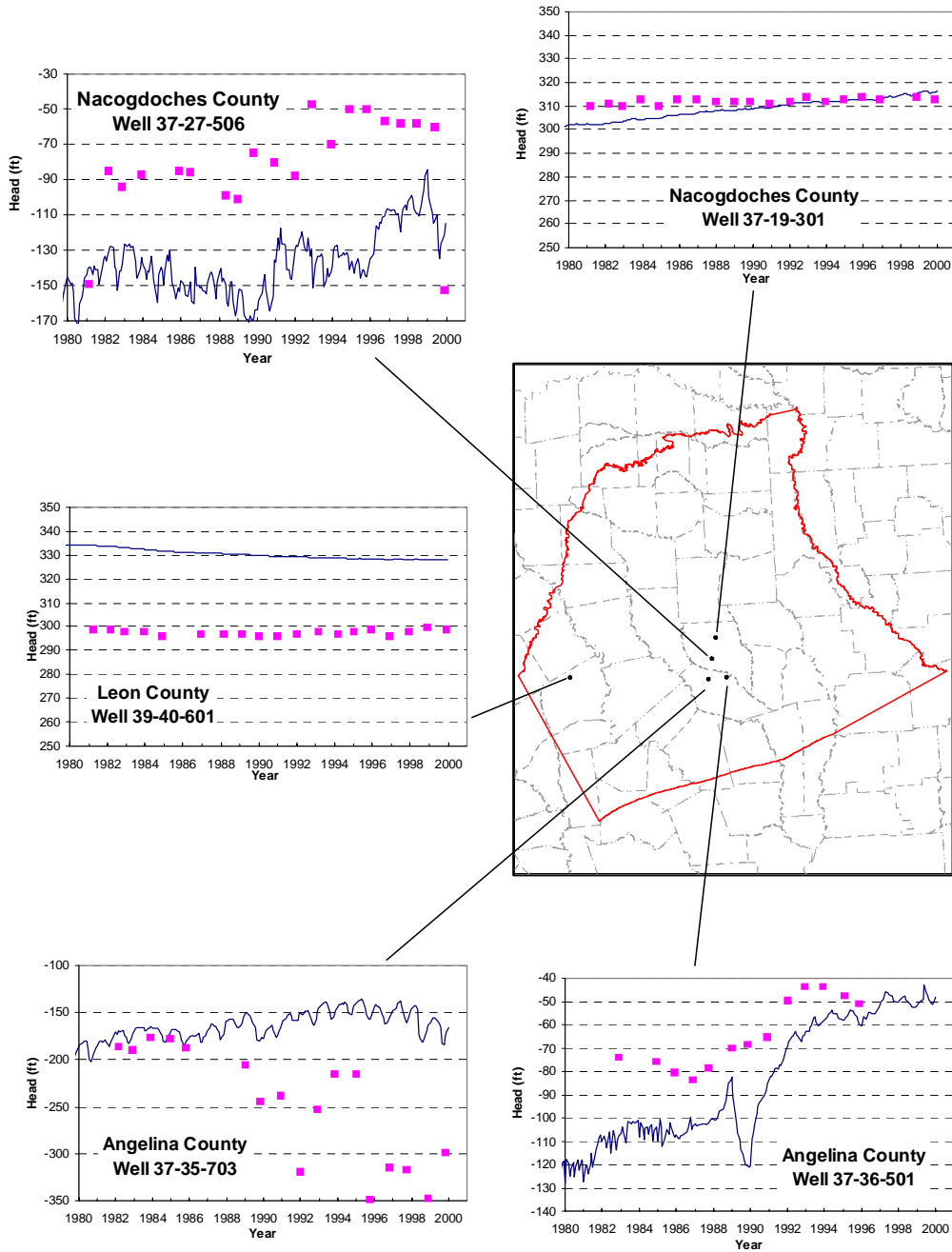


Figure 9.2.16c Selected hydrographs of simulated (lines) and measured (points) hydraulic heads in the southern part for Layer 3 (Carrizo).

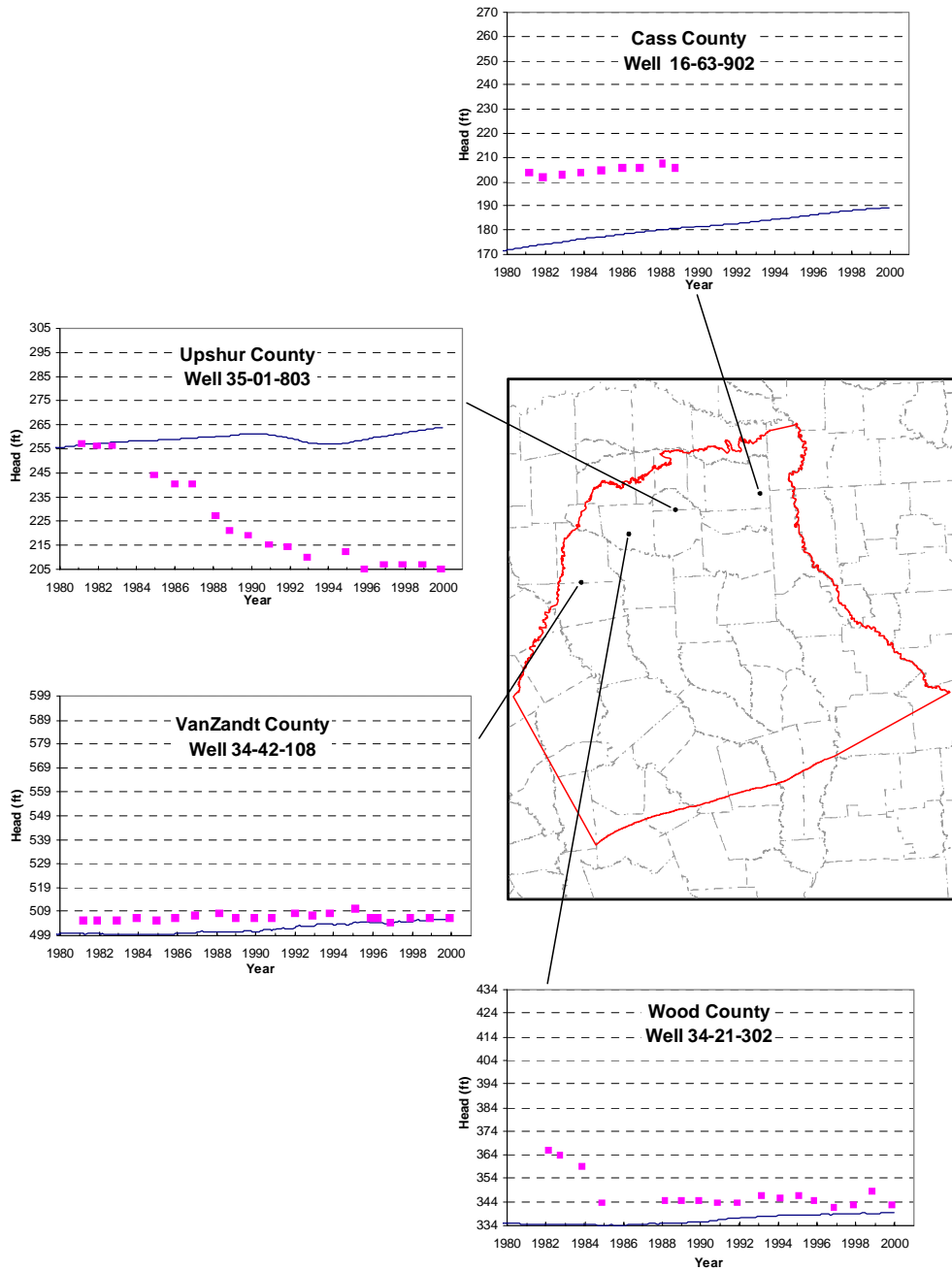


Figure 9.2.17a Selected hydrographs of simulated (lines) and measured (points) hydraulic heads in the northern part for Layer 4 (upper Wilcox).

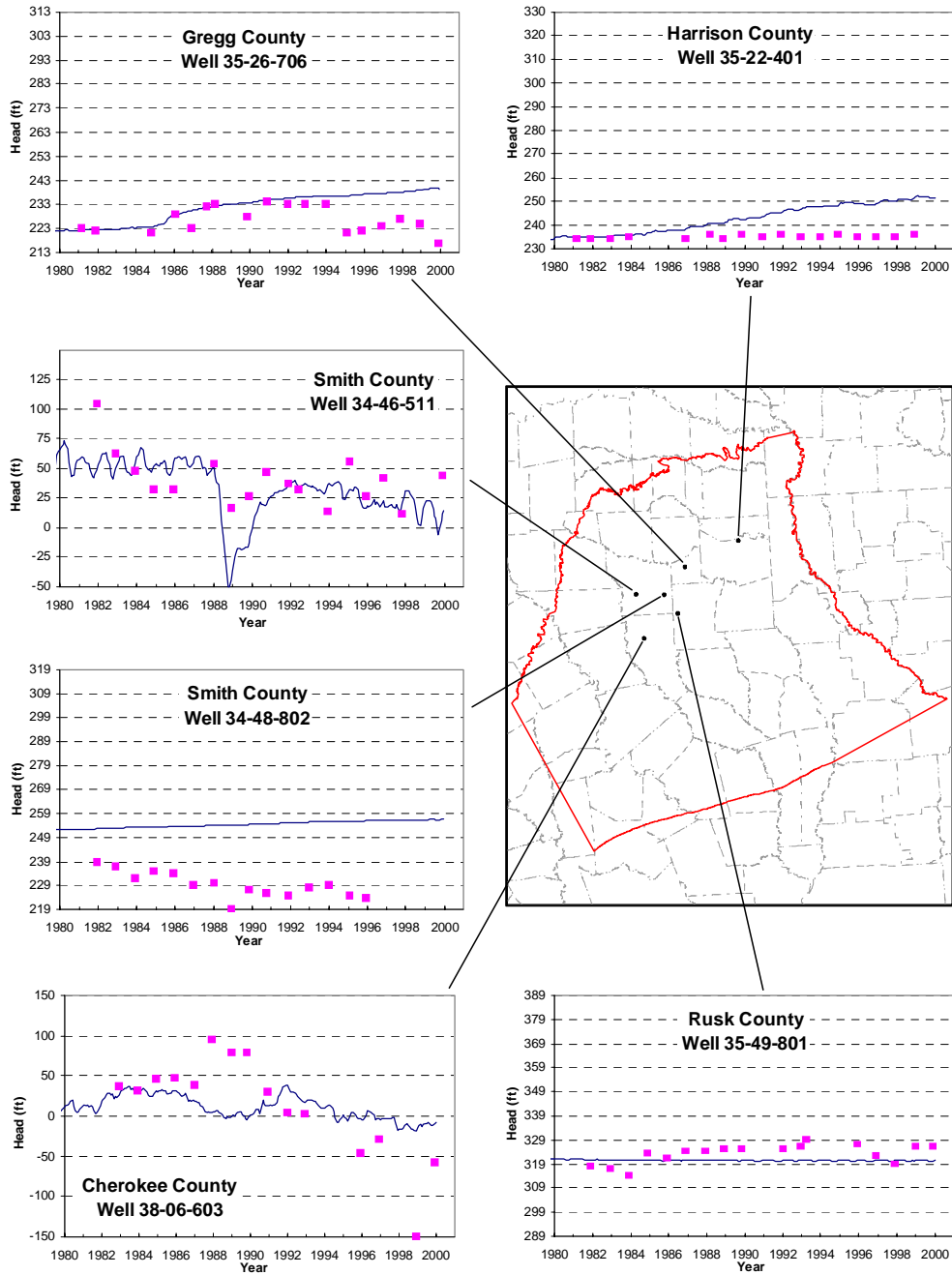


Figure 9.2.17b Selected hydrographs of simulated (lines) and measured (points) hydraulic heads in the central part for Layer 4 (upper Wilcox).

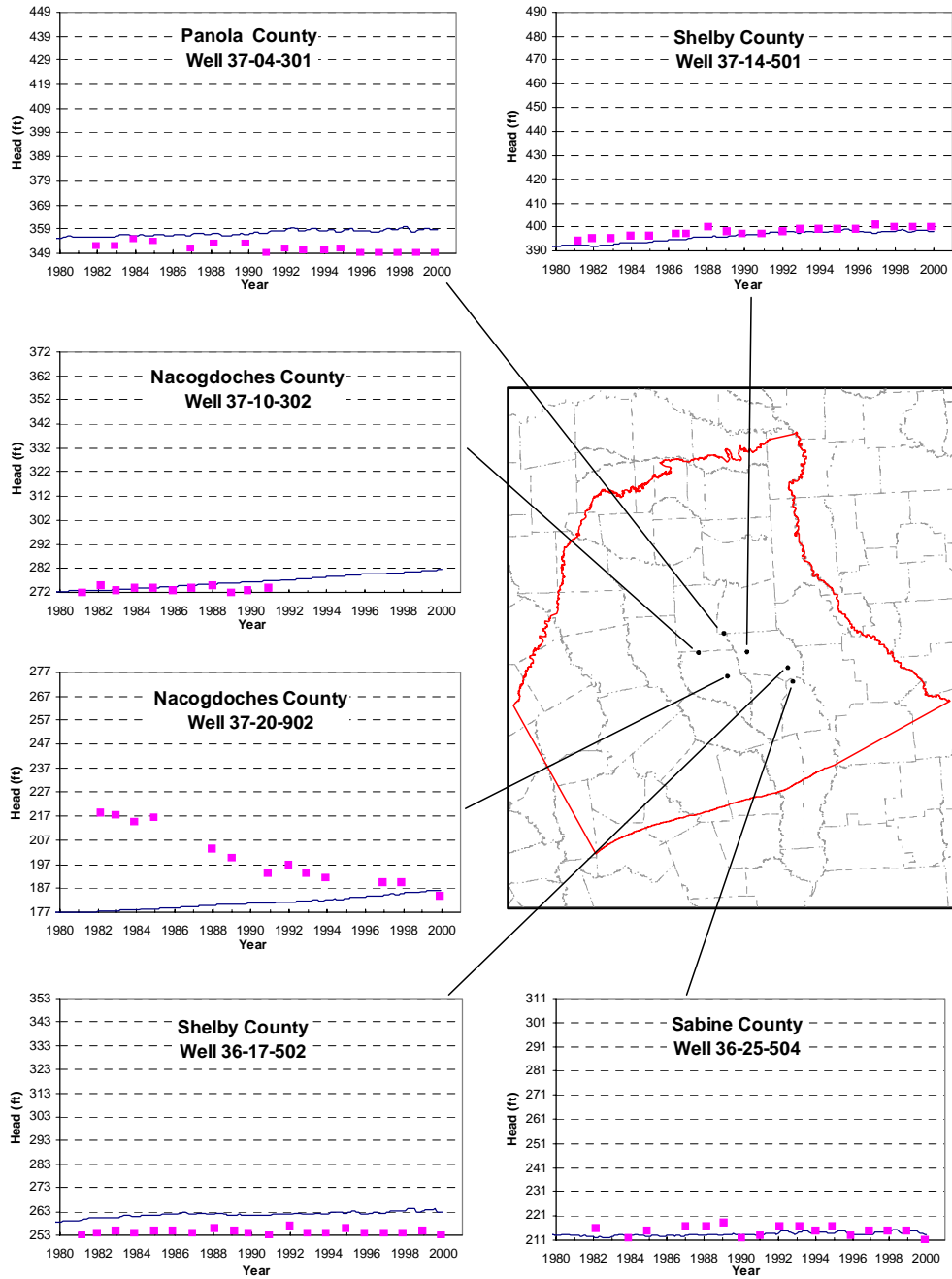


Figure 9.2.17c Selected hydrographs of simulated (lines) and measured (points) hydraulic heads in the southern part for Layer 4 (upper Wilcox).

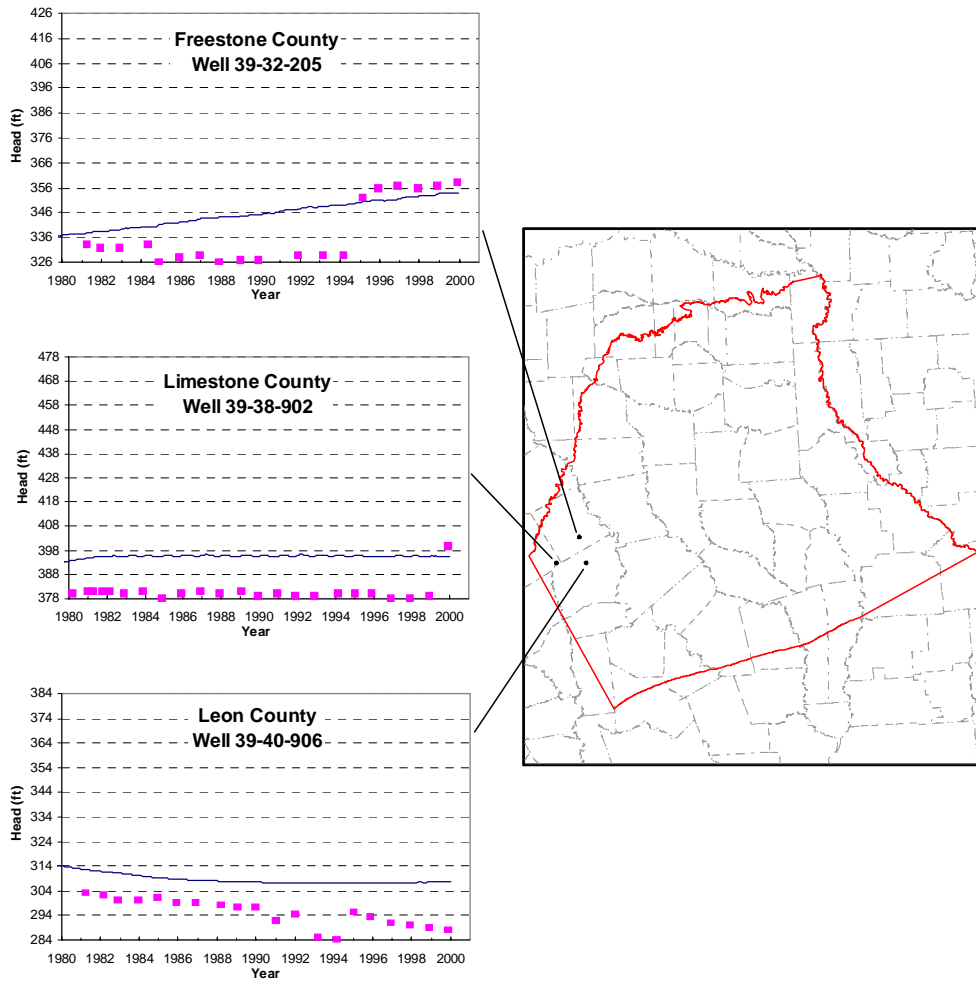


Figure 9.2.17d Selected hydrographs of simulated (lines) and measured (points) hydraulic heads in the western part for Layer 4 (upper Wilcox).

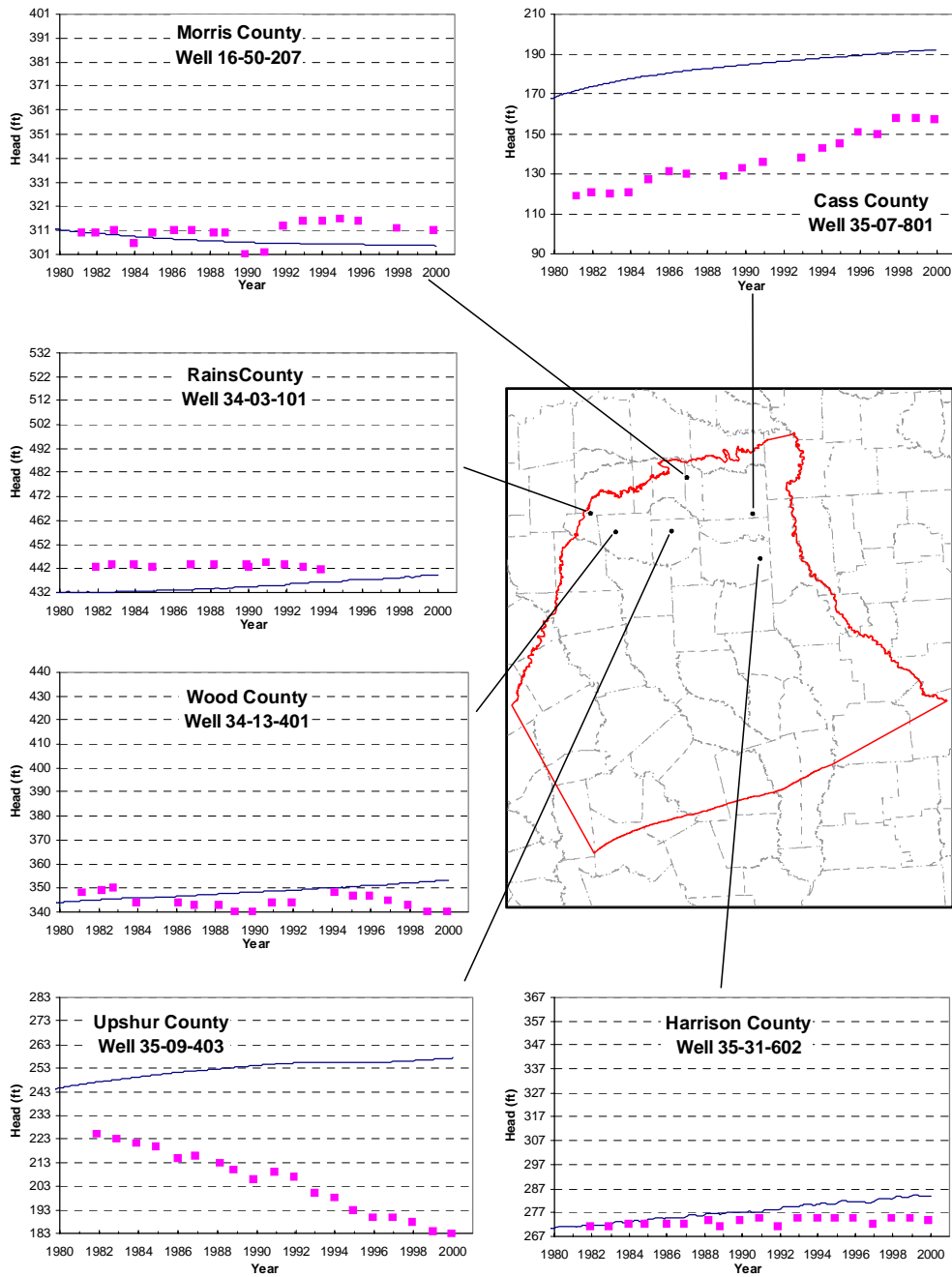


Figure 9.2.18a Selected hydrographs of simulated (lines) and measured (points) hydraulic heads in the northern part for Layer 5 (middle Wilcox).

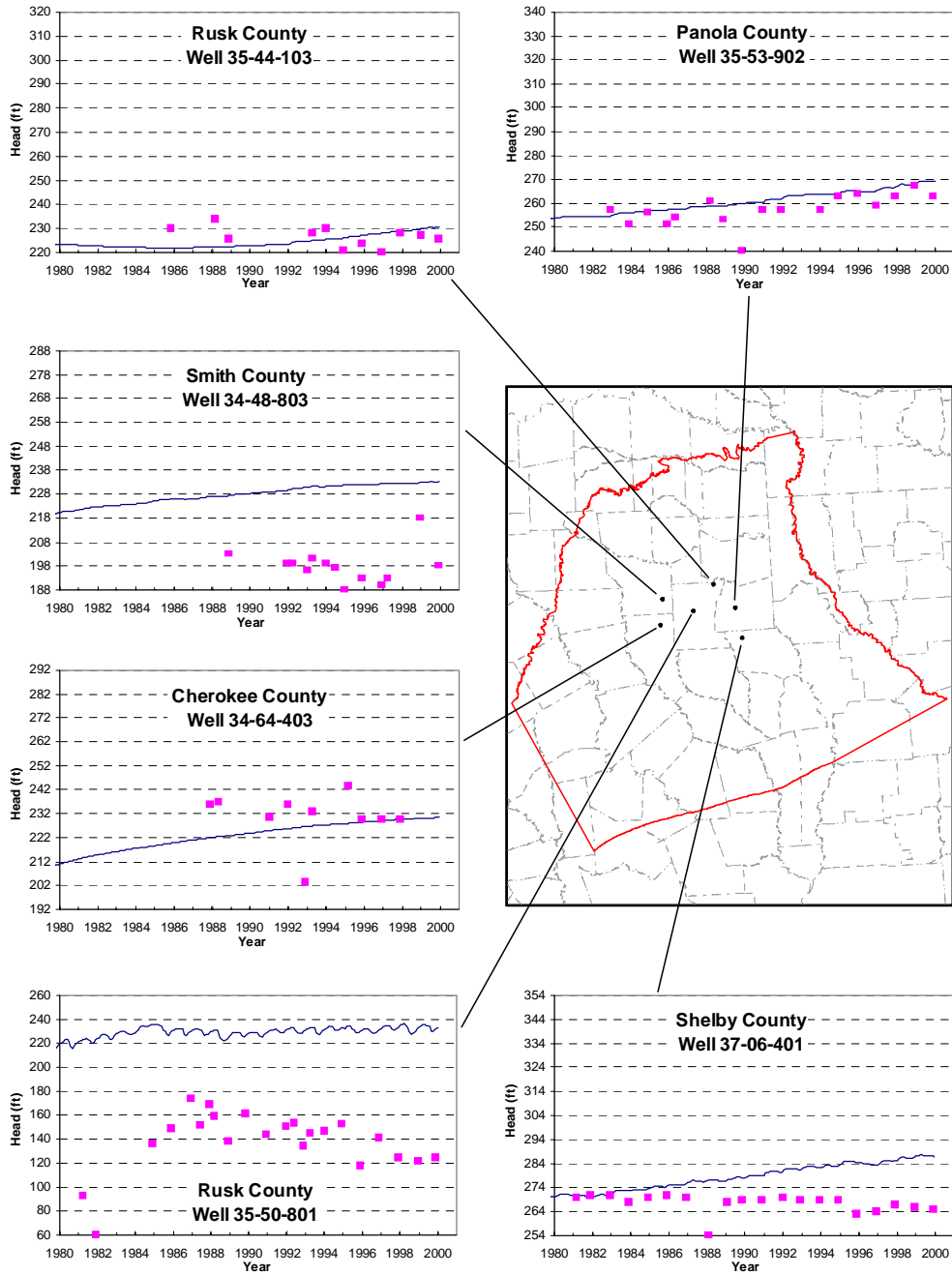


Figure 9.2.18b Selected hydrographs of simulated (lines) and measured (points) hydraulic heads in the central part for Layer 5 (middle Wilcox).

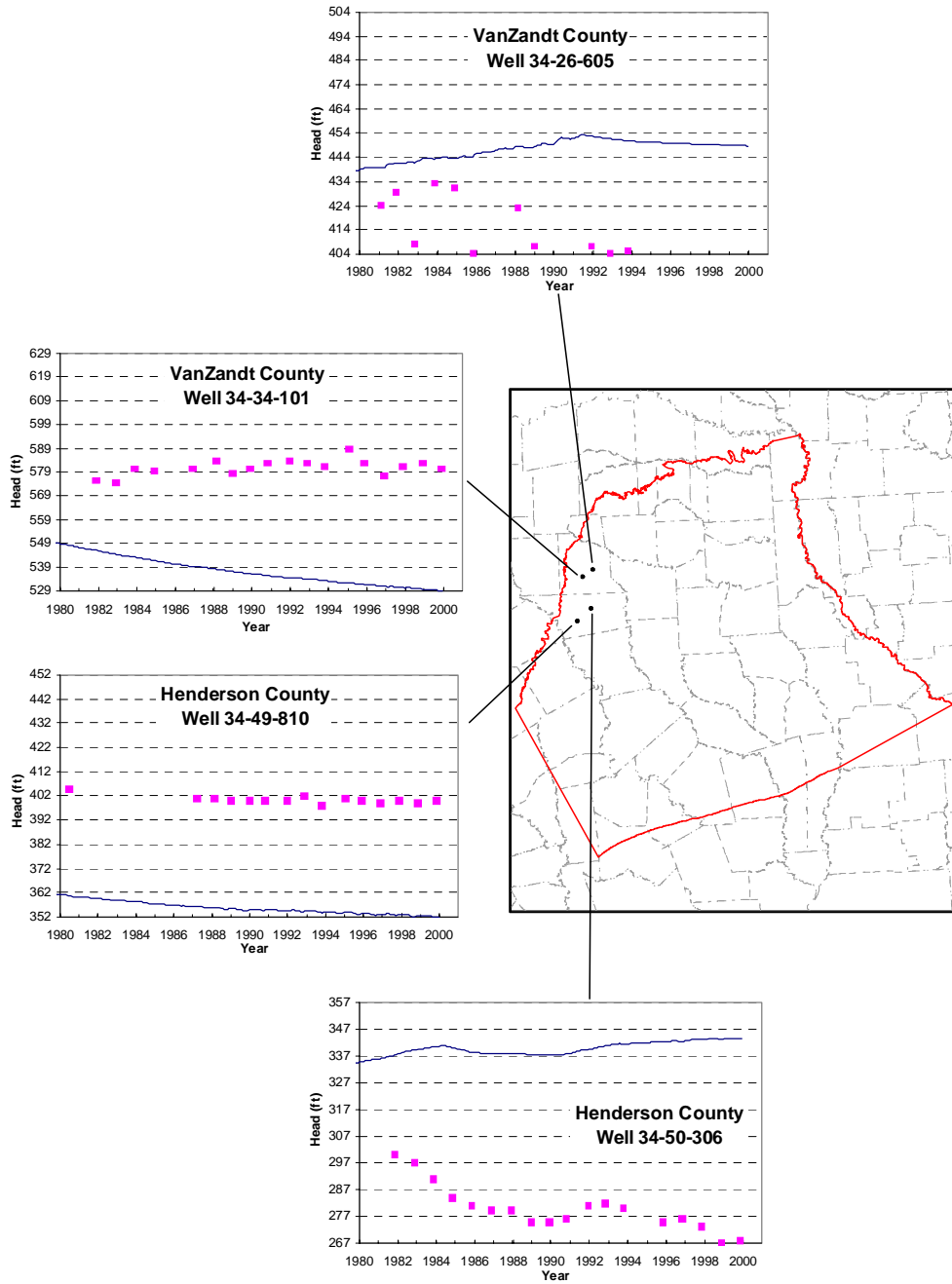


Figure 9.2.18c Selected hydrographs of simulated (lines) and measured (points) hydraulic heads in the western part for Layer 5 (middle Wilcox).

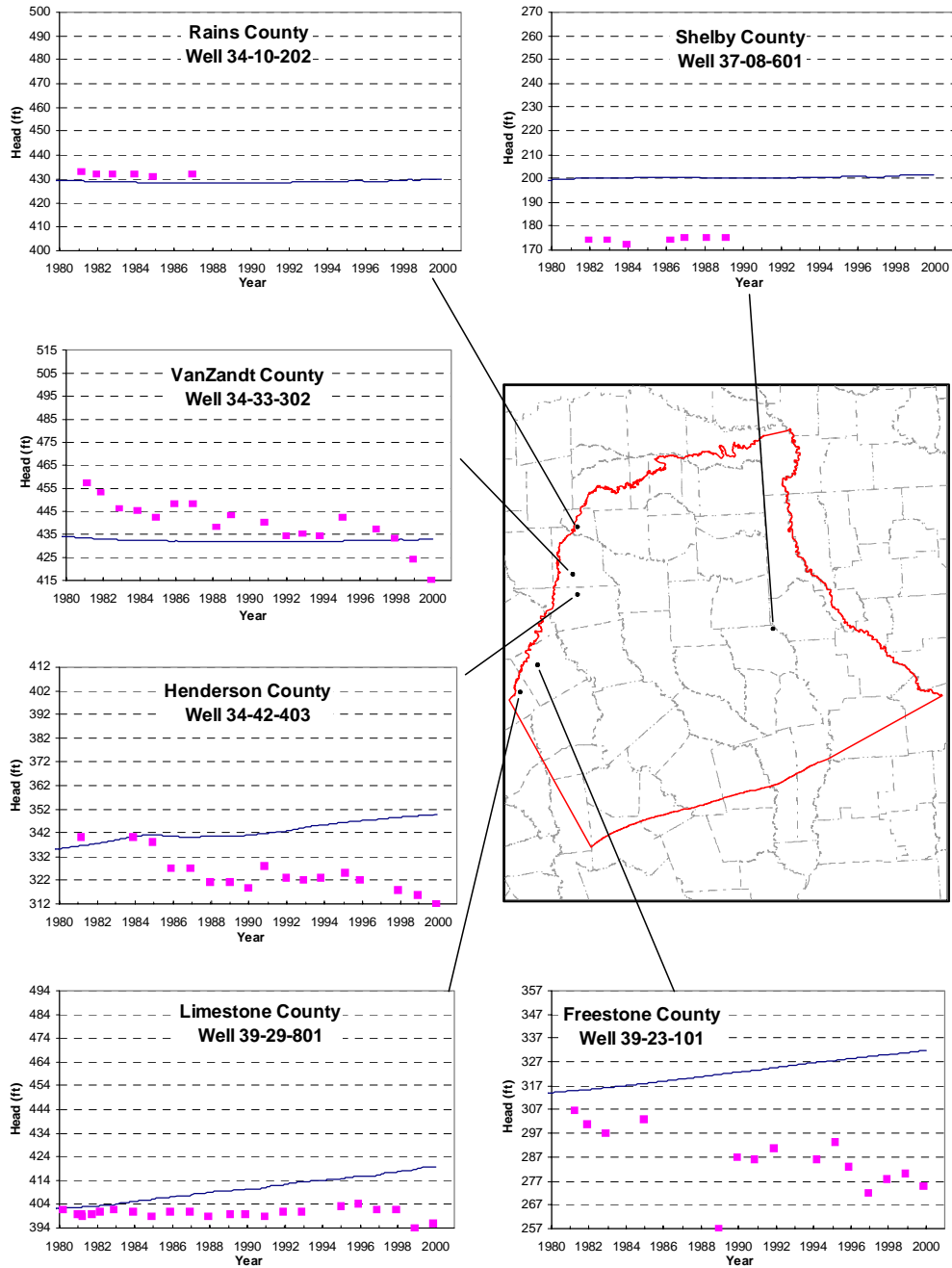


Figure 9.2.19 Selected hydrographs of simulated (lines) and measured (points) hydraulic heads in Layer 6 (lower Wilcox).

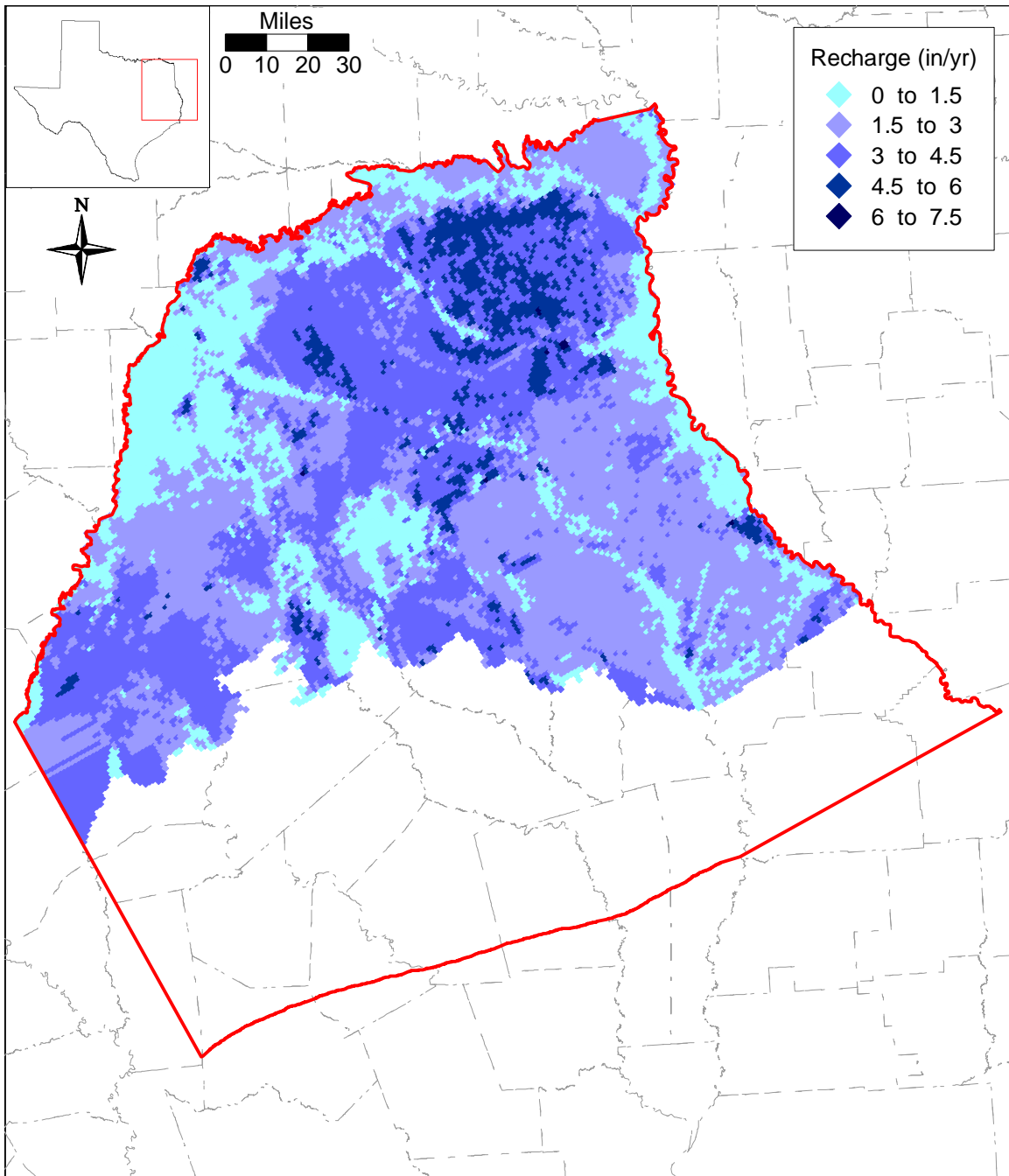


Figure 9.2.20 Average recharge for the transient simulation period (1980-1999).

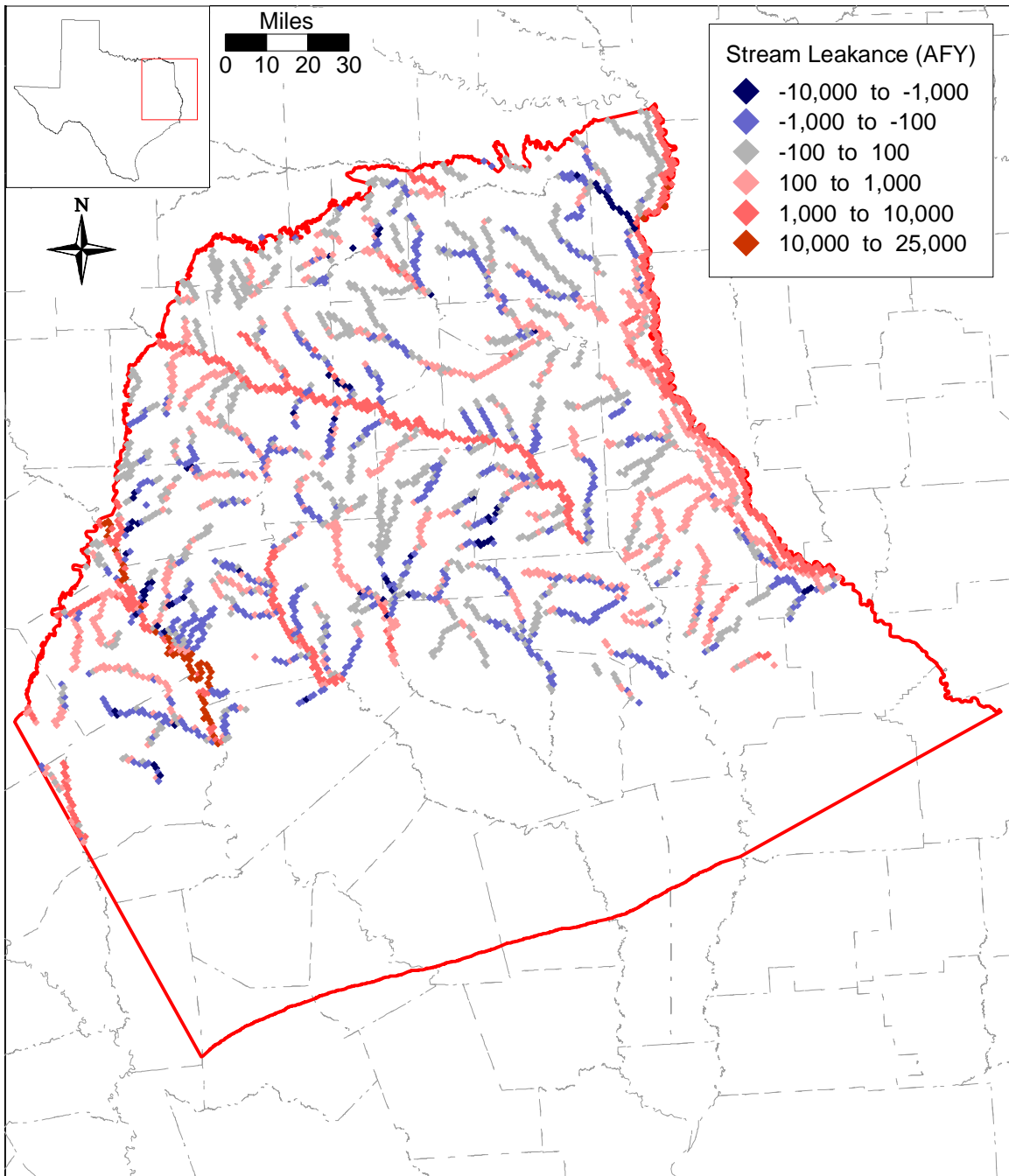


Figure 9.2.21 Simulated stream gain/loss for May 1989.

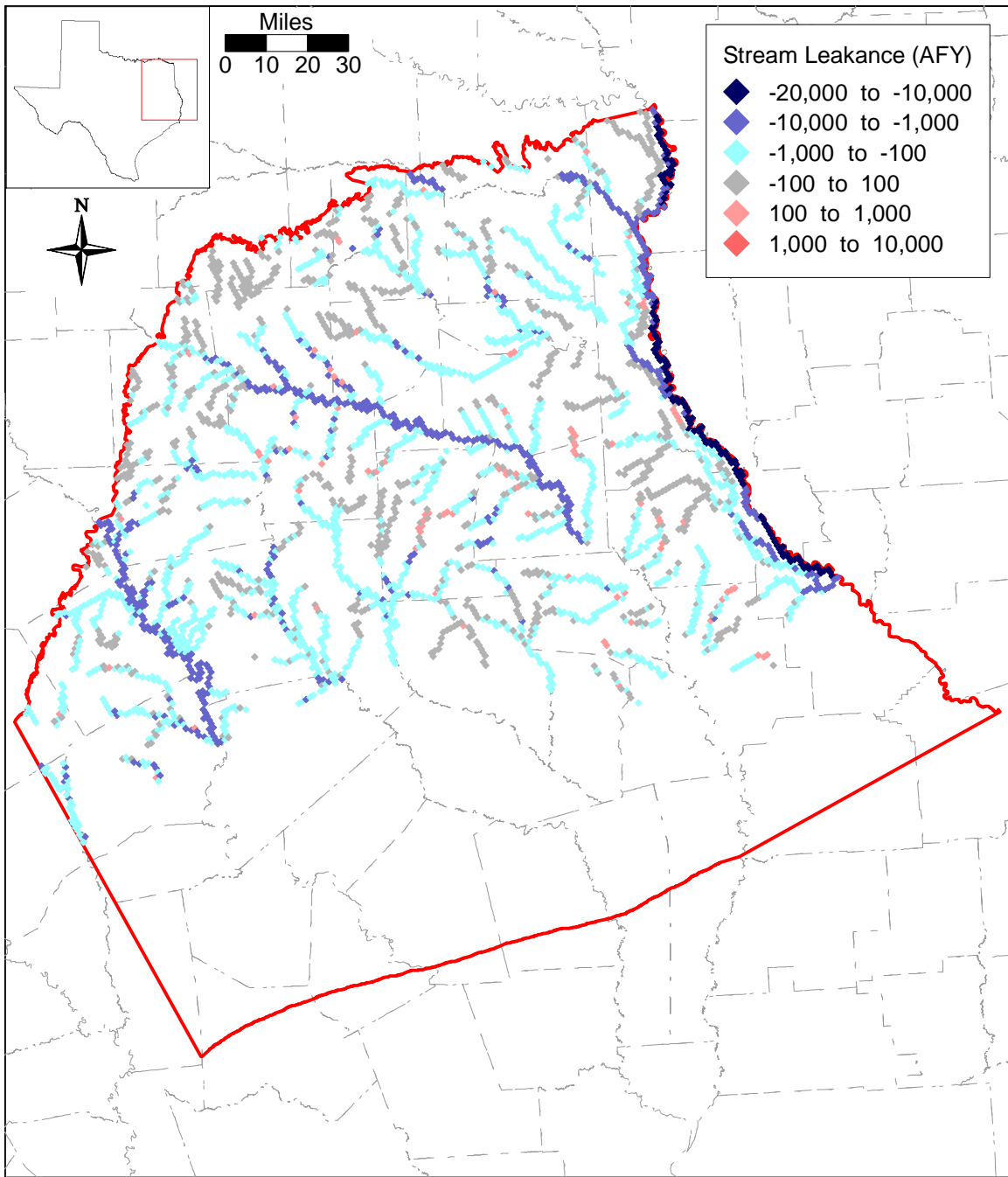


Figure 9.2.22 Simulated stream gain/loss for November 1989.

Comparison of Neches River Gauge 8032000 to Model Predicted Streamflow

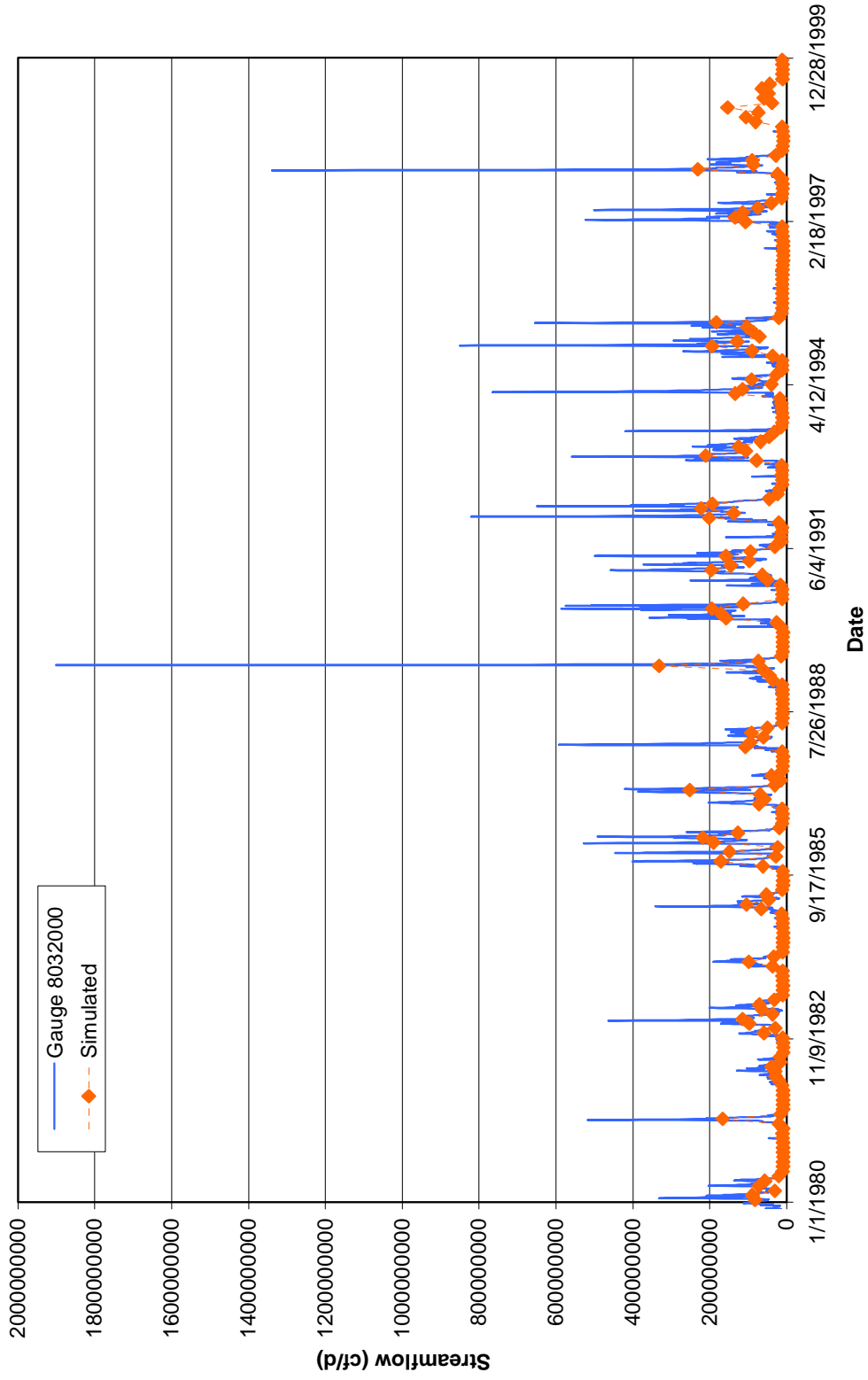


Figure 9.2.23a Simulated and measured stream flow at gauging station 8032000 on the Neches River.

Comparison of Trinity River Gauge 8065000 to Model Predicted Streamflow

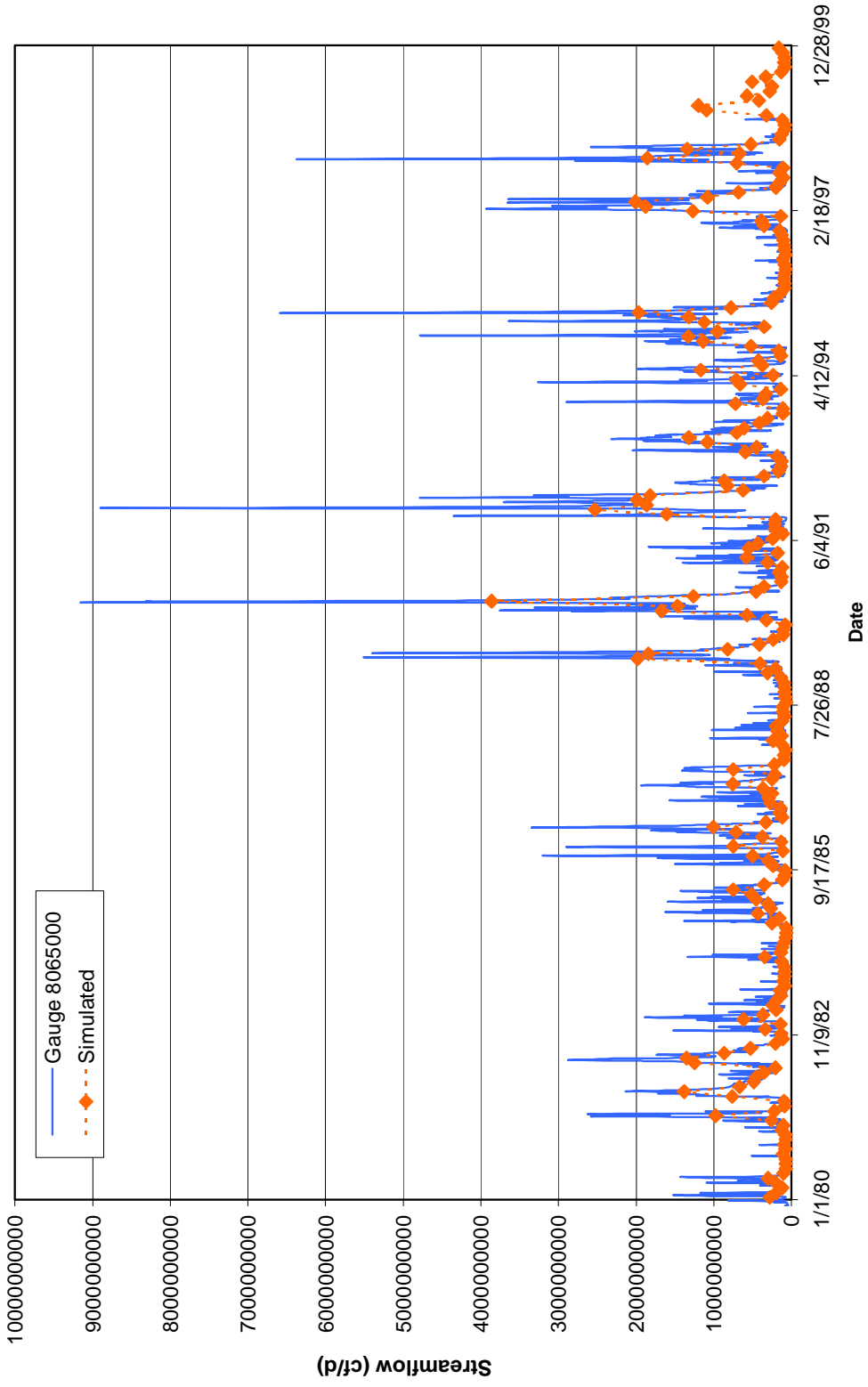
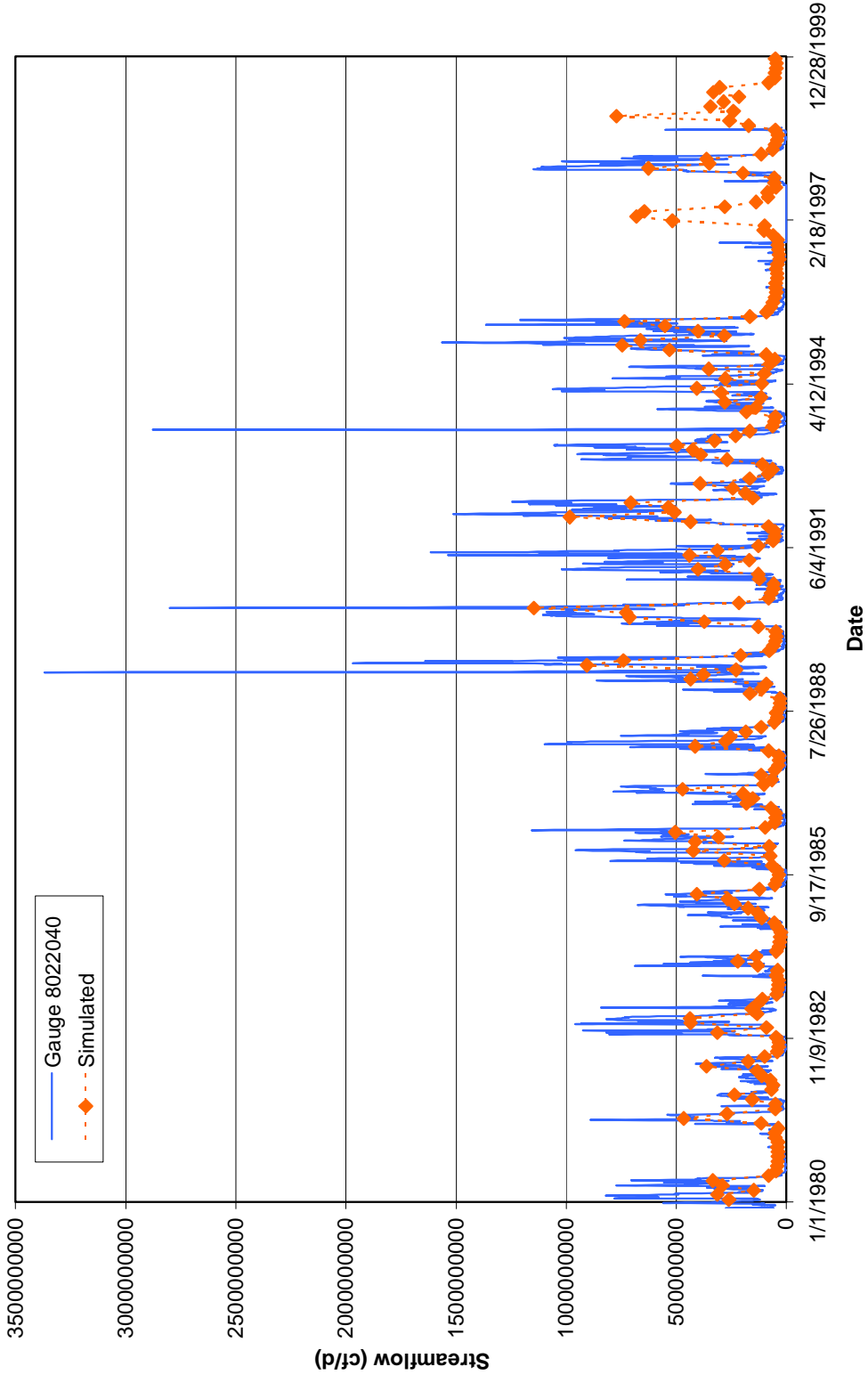


Figure 9.2.23b Simulated and measured stream flow at gauging station 8065000 on the Trinity River.

Comparison of Sabine River Gauge 8022040 to Model Predicted Streamflow



c.

Figure 9.2.23c Simulated and measured stream flow at gauging station 8022040 on the Sabine River.

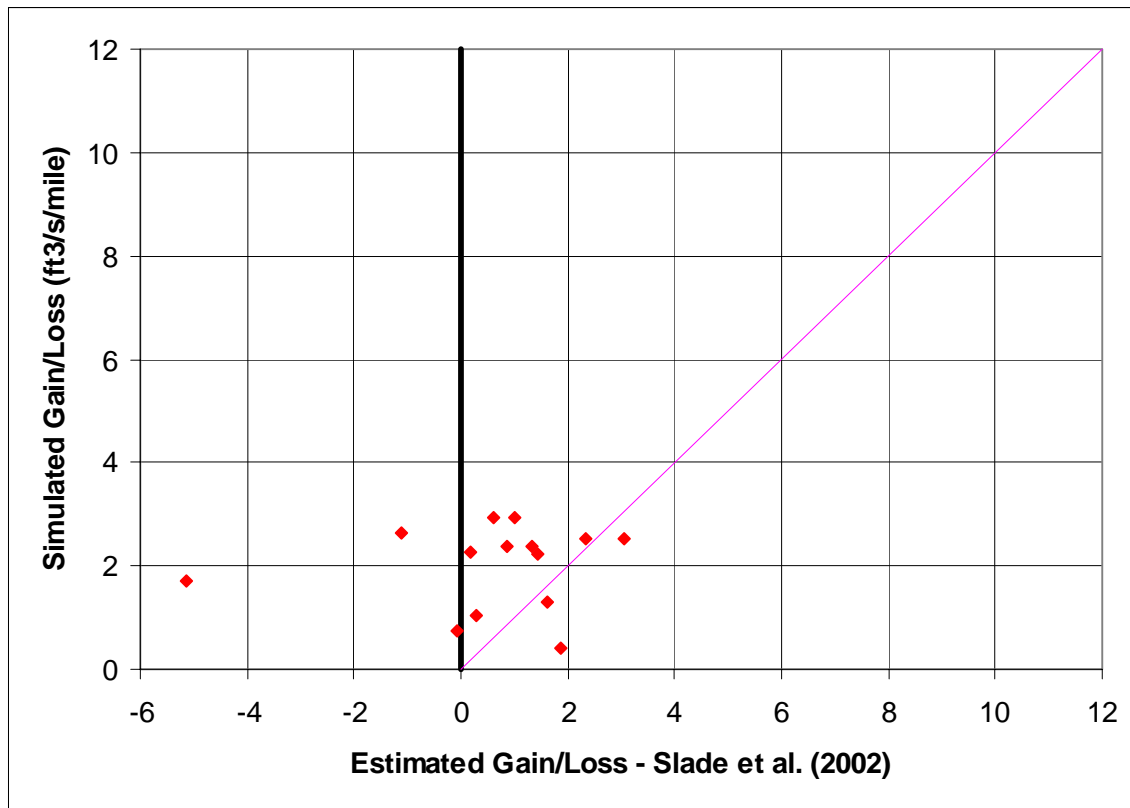
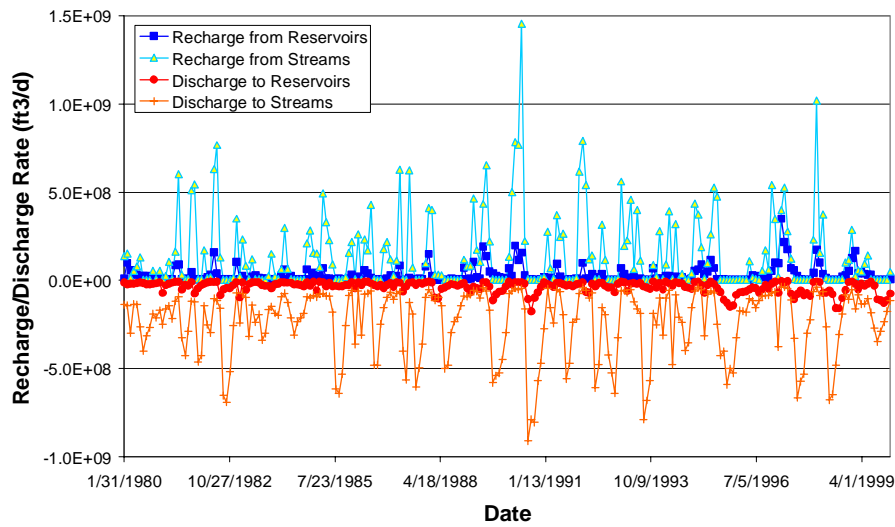
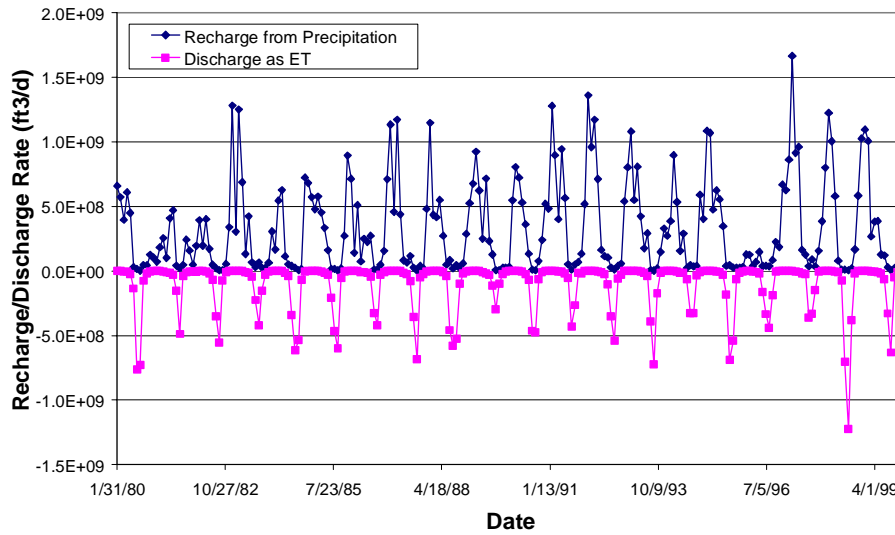


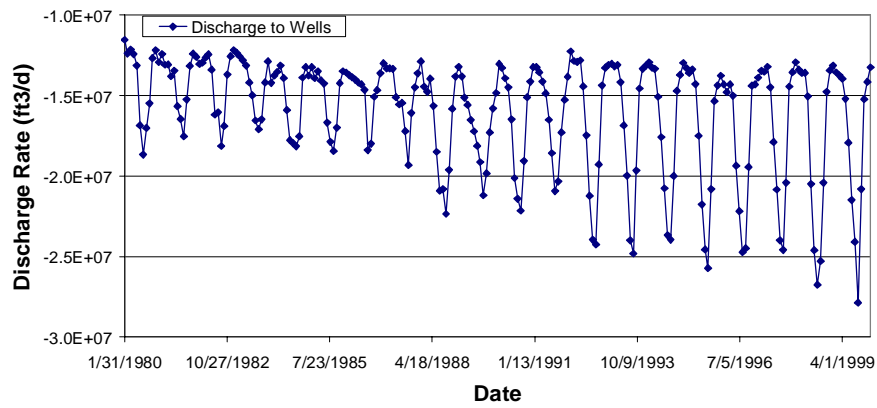
Figure 9.2.24 Simulated stream gain/loss compared to measurements compiled by Slade et al. (2002) for selected stream segments.



a.



b.



c.

Figure 9.2.25 Time history of water budgets for (a) streams and reservoirs, (b) recharge and ET, and (c) pumpage.

9.3 Sensitivity Analysis

Section 8.3 discussed the approach for sensitivity analyses for the steady-state model. The analyses were similar for the transient model, with the addition of several sensitivities. For the transient analysis, we completed 10 parameter sensitivities:

1. Horizontal hydraulic conductivity, Layer 3 (K_h -Carrizo)
2. Horizontal hydraulic conductivity, Layers 4 - 6 (K_h -Wilcox)
3. Vertical hydraulic conductivity in Layer 2 (K_v -Reklaw) (leakance between Layers 2 and 3)
4. Vertical hydraulic conductivity in Layers 4 - 6 (K_v -Wilcox) (leakance between layers 3 - 4, 4 - 5, and 5 - 6)
5. Recharge, model-wide
6. Streambed conductance, model-wide (K-stream)
7. GHB conductance, model-wide (K-GHB)
8. Storativity in Layer 3 (storage-Carrizo)
9. Storativity in Layers 4 - 6 (storage-Wilcox)
10. Pumping rate
11. Reservoir conductivity (K-reservoir)
12. Specific yield, model-wide

Equation 8.3.1 (varying linearly) for parameter variation was used for sensitivities 5, 10, and 12, and Equation 8.3.2 was used for the rest of the sensitivities listed above.

As with the steady-state model, we checked the mean difference between the base simulated head and the sensitivity in simulated head by applying Equation 8.3.3 at all gridblocks and also only at gridblocks where targets were present. Figure 9.3.1 shows the transient sensitivity results for Layer 3 (Carrizo) calculated for the target gridblocks and Figure 9.3.2 shows the transient sensitivity results for Layer 3 calculated at all gridblocks. As with the steady-state model, the order of the first four most important sensitivities is the same between both methods, even though the magnitude of the mean head differences (MD) is significantly different. This is to be expected as the target cells are concentrated in areas of groundwater decline. This indicates an adequate target coverage in this layer.

Figure 9.3.2 shows that the most positively correlated parameter for the Carrizo is horizontal hydraulic conductivity. The most negatively correlated parameter for the Carrizo is pumping. This is an important result, because these parameters were changed very little during calibration (Section 9.1). The third most important parameter is the vertical hydraulic conductivity of the Reklaw. This parameter was adjusted significantly during calibration. In comparison, in the steady-state model recharge was the dominant parameter followed by the horizontal hydraulic conductivity of Layers 4 - 6 (Wilcox), the vertical hydraulic conductivity of Layer 2 (Reklaw), and the horizontal hydraulic conductivity of Layer 3 (Carrizo) having significantly lower sensitivities. In the transient model, heads become more sensitive to the horizontal hydraulic conductivity of Layer 3 (Carrizo), followed by the vertical hydraulic conductivity of Layer 2 (Reklaw), and then by the horizontal hydraulic conductivity of Layers 4 - 6 (Wilcox). This difference is another indication of the importance of calibrating two hydrologic scenarios to improve the uniqueness of the calibrated parameter values.

Figures 9.3.3 through 9.3.7 show the transient sensitivity results for Layers 1, 2, 4, 5, and 6. The results for the Layer 1 (Figure 9.3.3) indicates that recharge and the GHB conductance show the greatest MDs, due to the fact that the Queen City crops out over the northern section and is confined in the southern part overlain by younger sediments, which are represented by a GHB boundary. As one expects, the greatest sensitivity for Layer 2 is the vertical hydraulic conductivity of the Reklaw (Figure 9.3.4.). Layers 4 – 6 show similar sensitivity patterns, except that for Layer 4 the horizontal hydraulic conductivity of the Wilcox shows the greatest MD values (Figure 9.3.5), whereas for Layer 5 and Layer 6, the highest positively correlated MDs are for the vertical hydraulic conductivity of the Wilcox layers followed by the Wilcox horizontal hydraulic conductivity (Figures 9.3.6 and 9.3.7). Note that, for the negatively correlated parameters, the most sensitive parameter is pumpage for Layer 4, whereas for Layers 5 and 6 the most sensitive parameter is the Wilcox storativity followed by pumpage.

Figure 9.3.8 shows the sensitivity results for all layers, where the vertical hydraulic conductivity of the Reklaw is varied. The layer with the greatest MD is Layer 2 followed by Layer 3, indicating that the Carrizo is most hydrologically affected by vertical flow across the Reklaw. Figure 9.3.9 shows the sensitivity results for all layers for variations in recharge. As indicated above, recharge is most important for Layer 1 (Queen City) followed by Layer 5

(middle Wilcox), because of the relatively large outcrop areas, respectively. Note that the maximum mean difference for both of these sensitivities is less than 1 ft. These figures indicate that recharge and specific yield, which should be most important in the outcrop, do not have a large overall effect on the heads in the model. Figure 9.3.10 shows the sensitivities to the Wilcox horizontal hydraulic conductivity on hydraulic heads in the different layers. The results show that Layer 4 (upper Wilcox) shows the greatest MDs followed by Layer 3 (Carrizo). That is, changes in horizontal hydraulic conductivity of the Wilcox layers significantly affect hydraulic heads in the overlying Carrizo.

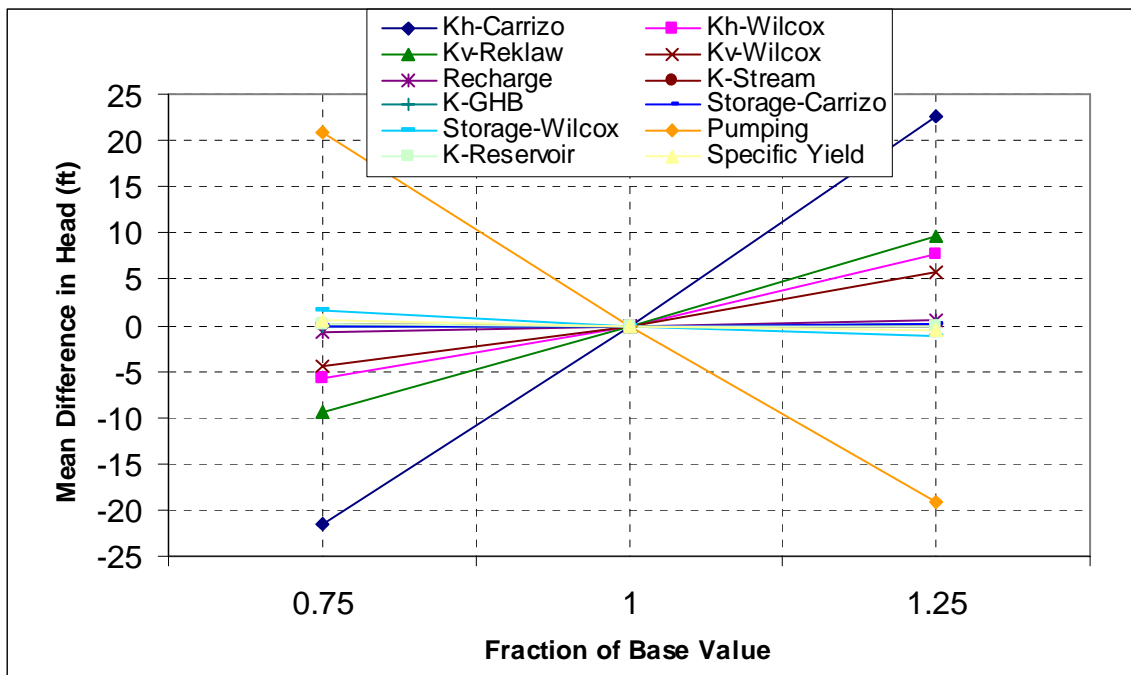


Figure 9.3.1 Transient sensitivity results for Layer 3 (Carrizo) using target locations.

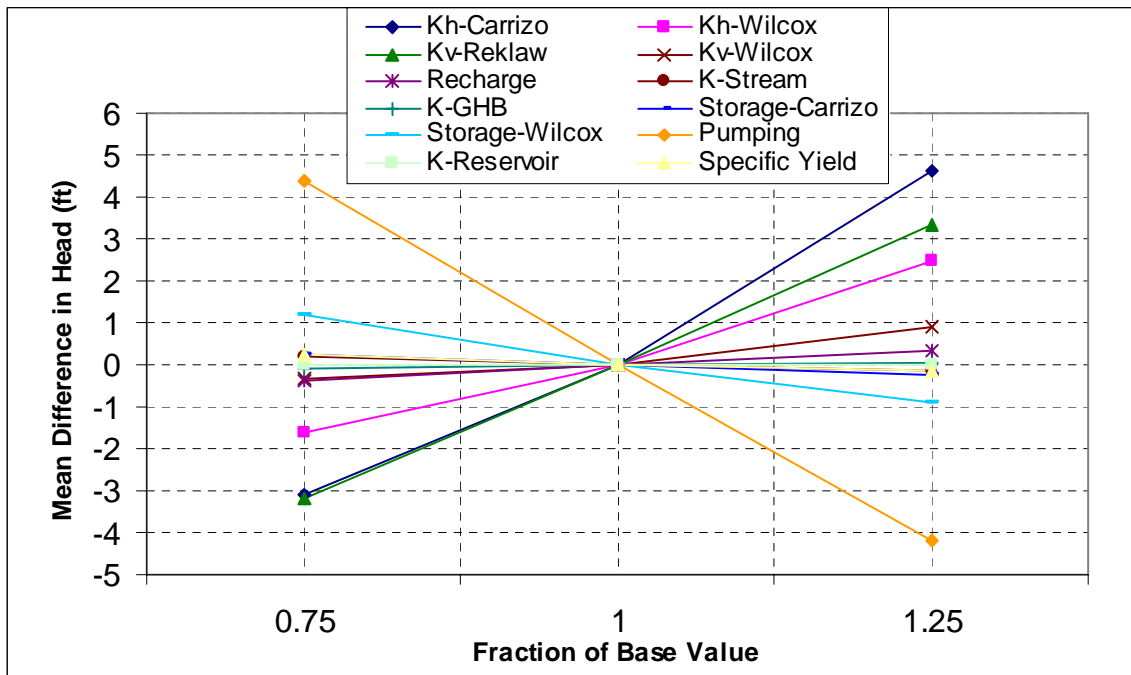


Figure 9.3.2 Transient sensitivity results for Layer 3 (Carrizo) using all active gridblocks.

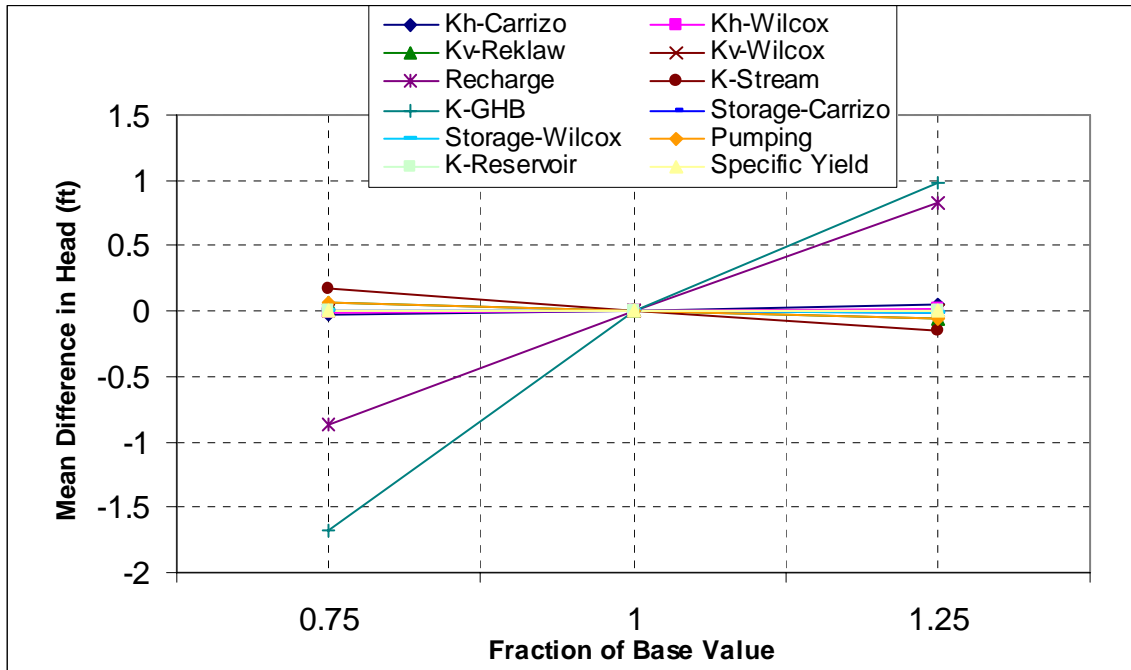


Figure 9.3.3 Transient sensitivity results for Layer 1 (Queen City) using all active gridblocks.

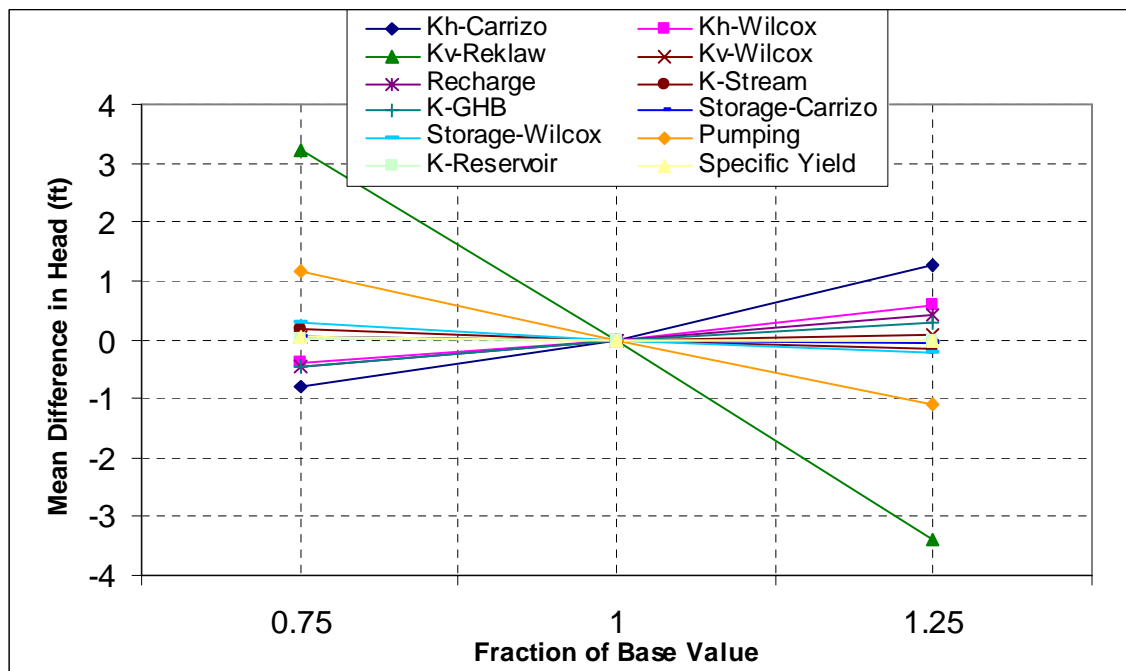


Figure 9.3.4 Transient sensitivity results for Layer 2 (Reklaw) using all active gridblocks.

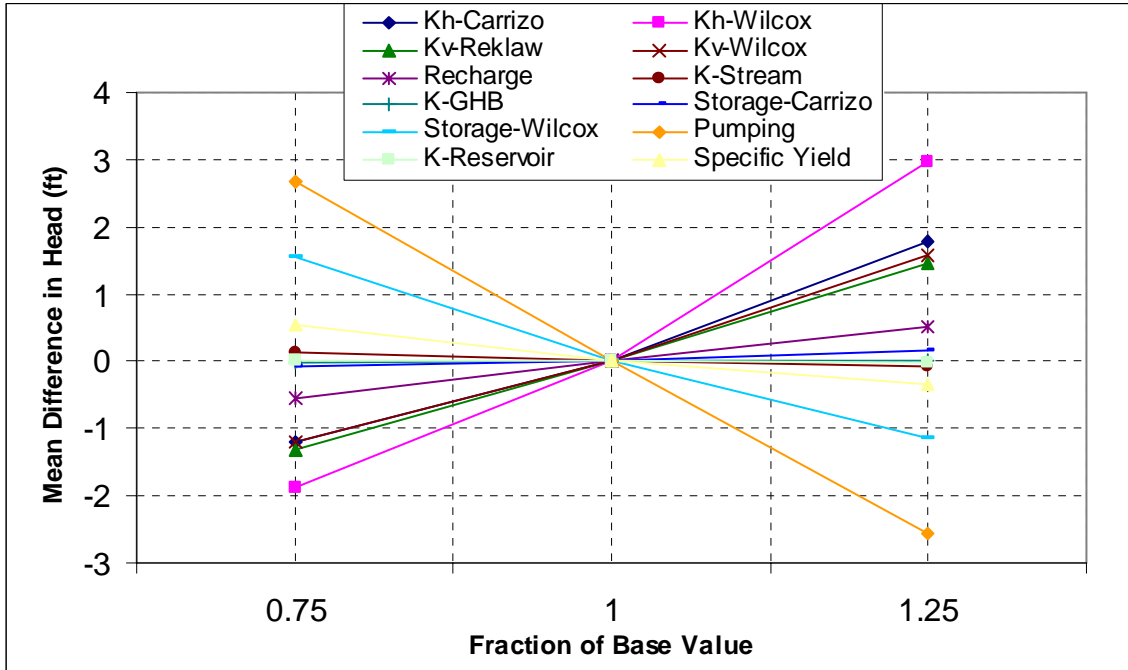


Figure 9.3.5 Transient sensitivity results for Layer 4 (upper Wilcox) using all active gridblocks.

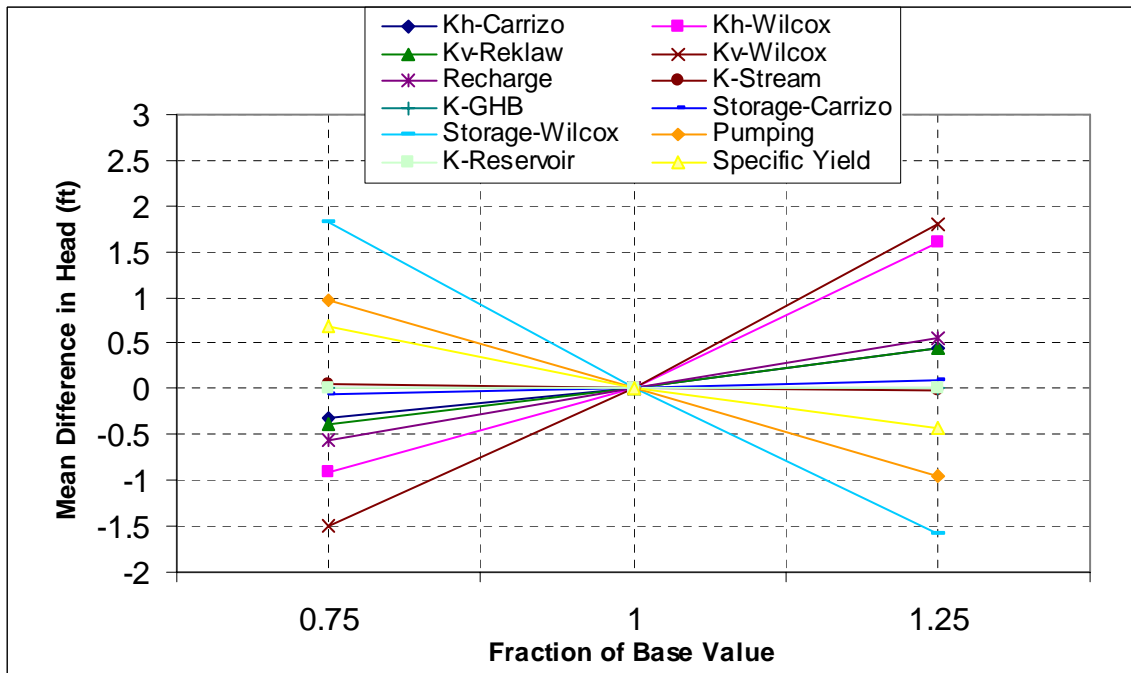


Figure 9.3.6 Transient sensitivity results for Layer 5 (middle Wilcox) using all active gridblocks.

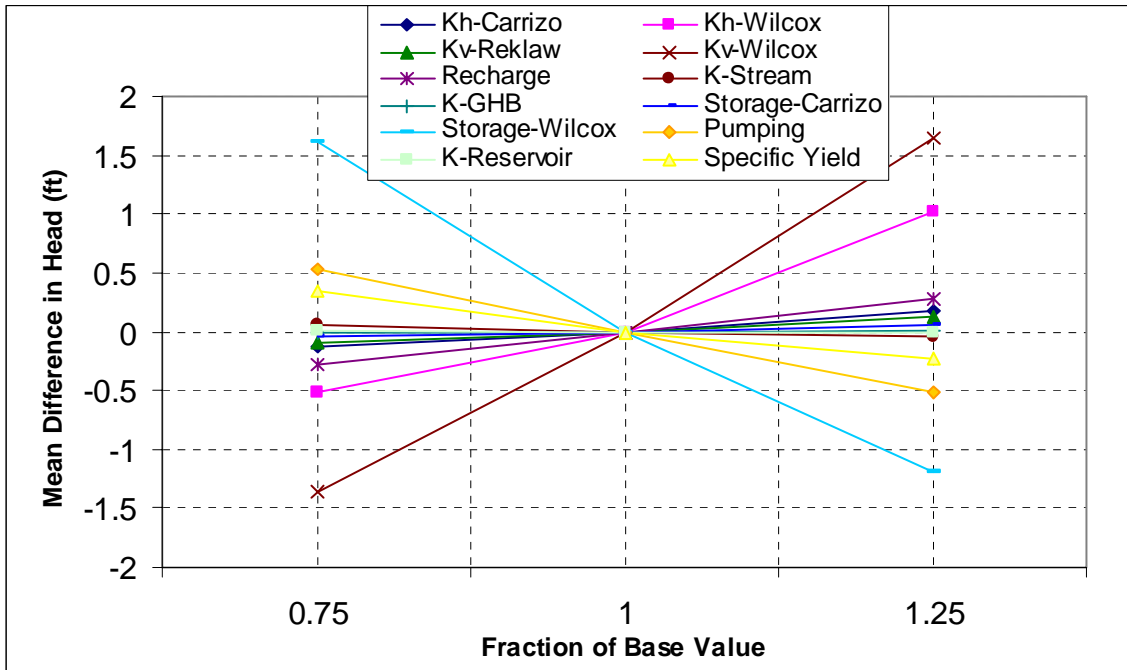


Figure 9.3.7 Transient sensitivity results for Layer 6 (lower Wilcox) using all active gridblocks.

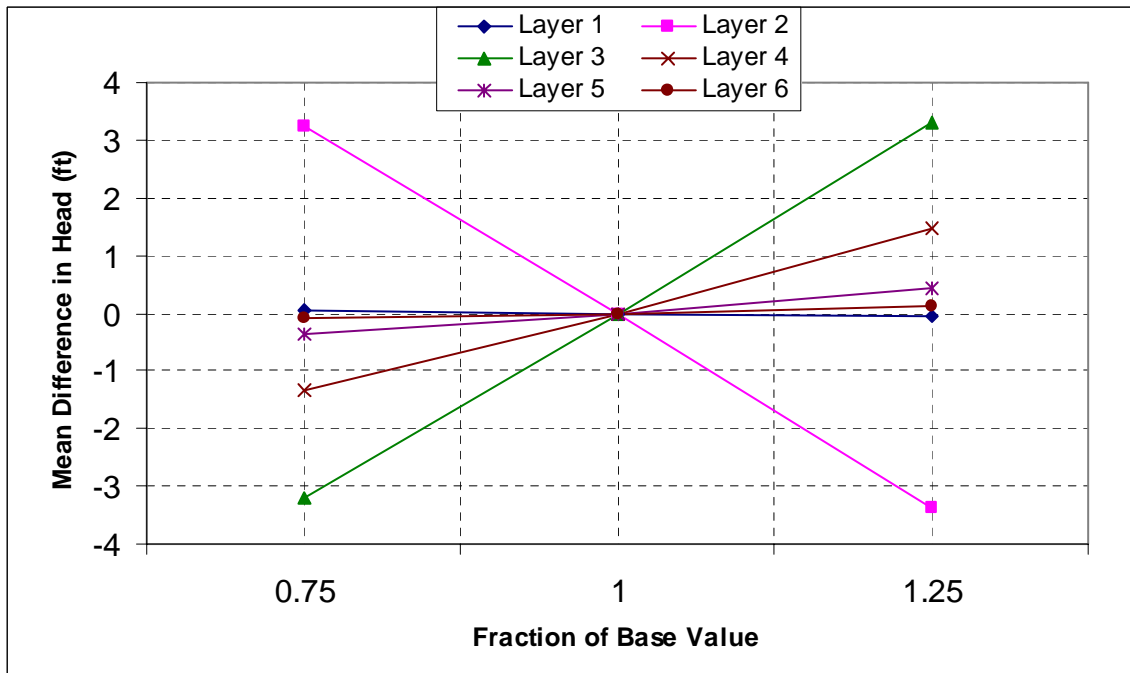


Figure 9.3.8 Transient sensitivity results where the vertical hydraulic conductivity of Layer 2 (Reklaw) is varied.

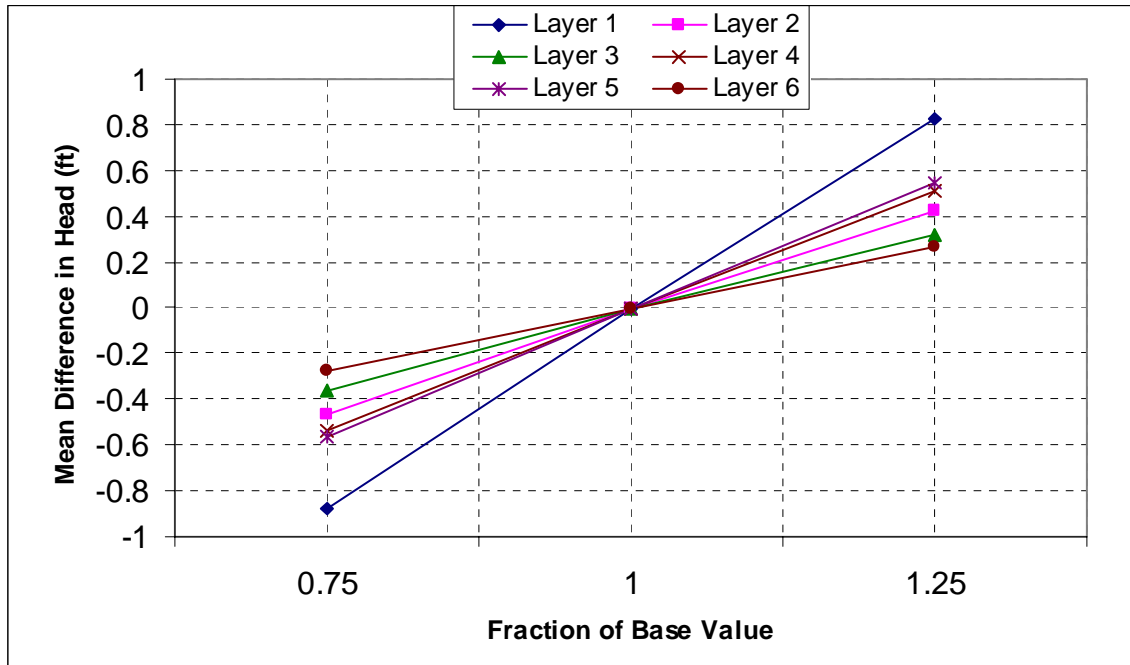


Figure 9.3.9 Transient sensitivity results where recharge is varied.

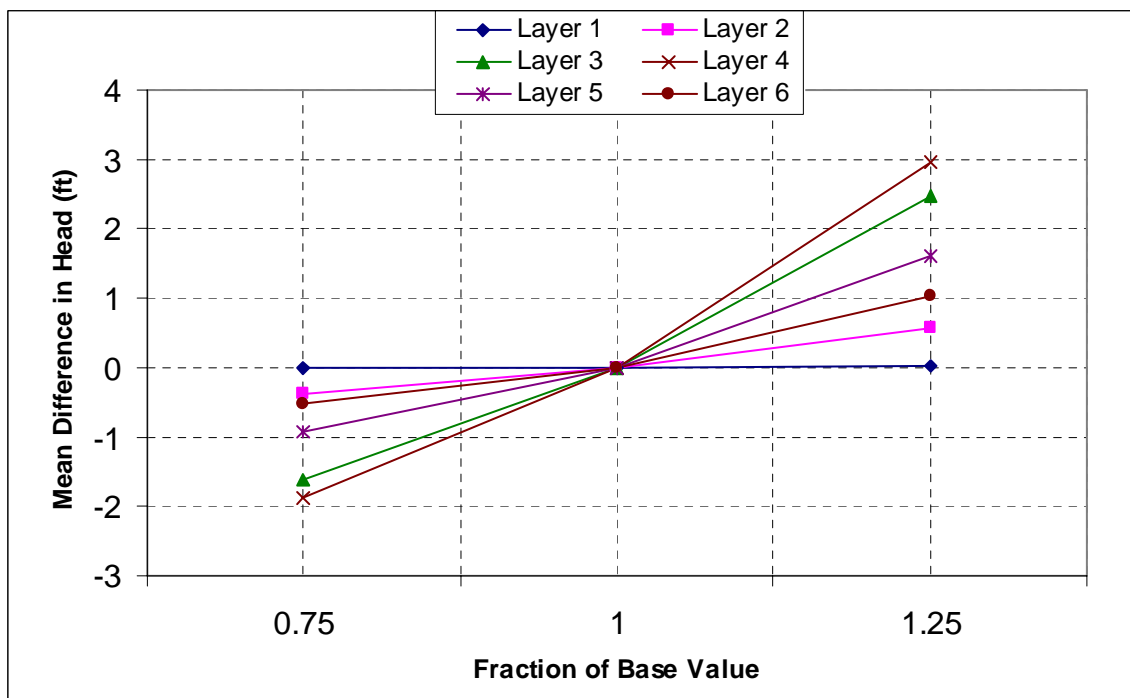


Figure 9.3.10 Transient sensitivity results where the horizontal hydraulic conductivity of the Wilcox is varied.

10.0 MODEL PREDICTIVE SIMULATIONS

The purpose of the GAM is to assess groundwater availability within the modeled northern Carrizo-Wilcox region over a 50-year planning period (2000-2050) using RWPG water-demand projections under drought-of-record (DOR) conditions. The GAM will be used to predict changes in regional groundwater water levels (heads) and fluxes related to baseflow to major streams and rivers, springs, and cross-formational flow. The two most important stresses to be considered in the future predictive modeling period are the same two stresses imposed during the calibration and verification periods; recharge and pumping.

Predictive pumping demands from the RWPGs are used in the predictive mode simulations assuming that the pumping distribution (as determined in Appendix D) for 1999 applies in the future (2000-2050). Predictive simulations assume average recharge conditions for the duration of the prediction ending with DOR conditions. For purposes of this report, average recharge is defined as the average recharge rate applied in the transiently calibrated model from 1975 through 1999.

Six basic predictive model runs are presented and documented: (1) average recharge through 2050, (2) average recharge ending with the DOR in 2010, (3) average recharge ending with the DOR in 2020, (4) average recharge ending with the DOR in 2030, (5) average recharge ending with the DOR in 2040, and (6) average recharge ending with the DOR in 2050.

Development of the predictive model datasets requires determination of the DOR and development of the predictive pumping datasets. The procedure for determining the predictive pumping demands is described in Appendix D. Similar to the model implementation of the historical pumpage data, it was assumed that the predicted pumpage from the Reklaw (Layer 2) is actually from the Carrizo (Layer 3). However, for the model predictive simulations, pumpage from the Queen City was not reallocated to the Carrizo, as was done in the transient model (Chapter 9). The following will discuss the development of the DOR.

10.1 Drought of Record

GAM specifications require that the DOR used for model predictions be representative for the past 100 years and be defined by severity and duration. Drought is considered a normal, recurring climatic event. It is conceptually defined by the National Drought Mitigation Center as

a protracted period of deficient precipitation resulting in extensive damage to crops with loss of yield. Operational definitions of drought are typically used to define the beginning, end, and severity of a drought over a given historical period. Operational definitions typically quantify the departure of precipitation, or some other climatic variable, from average conditions over a defined time window (typically 30 years).

Drought indices are quantitative measures that assimilate raw data into a single value that defines how precipitation has varied from a specific norm. As discussed above, drought is a phenomenon related directly to available moisture from precipitation. Precipitation is the primary variable controlling recharge in the model region. Accordingly, we used precipitation data as the raw data for defining the DOR in the Northern Carrizo-Wilcox GAM region.

In the Northern Carrizo-Wilcox GAM model region, historical precipitation data are available for approximately 250 stations from 1930 to 2000 (Figure 2.10). From Figure 2.10, it is evident that the spatial distribution of precipitation data is relatively dense in the model domain. However, most stations possess incomplete records across the 100-year time frame of interest. Most gages began recording precipitation in the late 1930s through the 1960s. The earliest monthly precipitation records in the area extend as far back as 1930. Approximately 25 precipitation gages have records in 1931 as opposed to only one in 1930.

There are many drought indices available to measure the degree that precipitation has deviated from historical norms. The typical measure is “percent of normal”, calculated by dividing the actual precipitation depth by the normal precipitation depth and multiplying by 100. This calculation could be performed over a range of time scales but is typically annualized. The normal precipitation depth is usually a long-term arithmetic mean. The available precipitation records within the model domain were analyzed to calculate the percent of normal as an indicator of drought. Figure 2.12 shows a select set of long-term annual precipitation records in the model region. Inspection of these time series shows particularly dry periods in 1936, 1948, 1954 through 1956, 1963 through 1964, 1980, and 1988. The two most severe droughts occurred in 1954 through 1956 and 1963 through 1964.

The 1950’s represents a period of historical drought in Texas including the region being modeled. The drought peaked in 1954 and continued through 1956. In 1956, 13 of 75 gages (17%) recorded their period of record low annual precipitation depths. In 1963, 23 of 81 gages

(28%) recorded their period of record low annual precipitation depths. In 1988, 16 of 88 available gages (18%) recorded their period of record low annual precipitation depths. From this analysis, we concluded that the 1963-1964 drought might be the DOR. However, when the average deficit across the model area was considered, it became evident that the DOR was in the 1950s. The average precipitation, as measured in percent of normal averaged across all available gages in the model area, was equal to 84% from 1950 through 1956. The same metric calculated for the drought peak years from 1954 through 1956 was 73% of normal.

The secondary drought index we used to quantify the DOR is the Standardized Precipitation Index (SPI). This index was developed to define precipitation deficits over multiple time scales (McKee et al., 1993). The SPI is calculated based upon the precipitation record for a given location. The long-term precipitation record is fitted to a general probability distribution (typically the Gamma distribution). This distribution is then normally transformed and standardized so that the mean SPI for that location over the time period of interest is equal to zero. When the SPI is equal to zero, it signifies median precipitation conditions for that location based upon the time integration window specified (Edwards and McKee, 1997). Because the index is normalized, comparison of SPI values between locations (i.e., across our model domain), is simplified in that an SPI of -1 represents a similar magnitude deficit for all stations. Monthly precipitation averages are used as the raw data for the SPI calculation. A one-month SPI would represent normalized precipitation data without temporal averaging. The SPI is backward-averaged over some user-specified duration, typically between six months and three years. By lengthening this time integration window, one effectively looks at longer term precipitation trends less subject to short-term variations. Short-term deficit conditions or anomalies are of less concern for predicting groundwater conditions; for this reason, the SPI was calculated for long time periods (1 year, 2 year, and 3 year windows). Figure 10.1.1 shows the SPI for precipitation gage 415424 in Angelina County calculated using one-year, two-year, and three-year averaging windows. Current SPI index maps are available online for the State of Texas for multiple time averaging periods from one month through three years at the following URL: <http://www.txwin.net/Monitoring/Meteorological/Drought/spi.htm>

McKee et al. (1993) defined a classification system for defining drought conditions using the SPI. This classification is taken from (Hayes, 2001) and presented in the table below.

SPI Value	Precipitation Deficit Condition
2.0 and above	Extremely wet
1.5 to 1.99	Very wet
1.0 to 1.49	Moderately wet
-0.99 to 0.99	Near normal
-1.0 to -1.49	Moderately dry
-1.5 to -1.99	Severely dry
-2.0 and less	Extremely dry

McKee et al. (1993) defined a drought event as any time period over which the SPI is continuously negative and reaches a magnitude of -1.0 or less. Figure 10.1.2 plots SPI curves for eight representative long-term precipitation gages in the model area. A two year time window was used for the analysis. Drought occurs most consistently in these gages in the 1950s, 1963-1964, and in the period from 1970 to 1975. Of these time periods, the drought in the 1950s is most consistent among all of the gages. Thus, the SPI analysis corroborates the results of our analysis of percent normals. The DOR is, therefore, considered to have occurred in the 1950s.

With the DOR picked to occur in the 1950s, we next reviewed the monthly data to define the month the DOR began and ended. Records from all of the precipitation stations in the model area were averaged for each month to provide input to an “overall” SPI. Figure 10.1.3 shows the SPI calculated for this average dataset for several time integration windows. The curves from the longer duration (2- and 3-year) integration windows show the most dramatic depression in the range of 1956-1957. These curves drop below -1 at different times, June 1955 and March 1956, respectively, indicating the effect of the backward averaging. The monthly data, which is not temporally averaged, show that the consistently below-normal precipitation driving this drought period began in June 1954, and continued until March 1957, when a wet-dry-wet period occurred, followed by more normal precipitation trends. Therefore, we chose the DOR to have occurred between June 1954 and March 1957 for this model region.

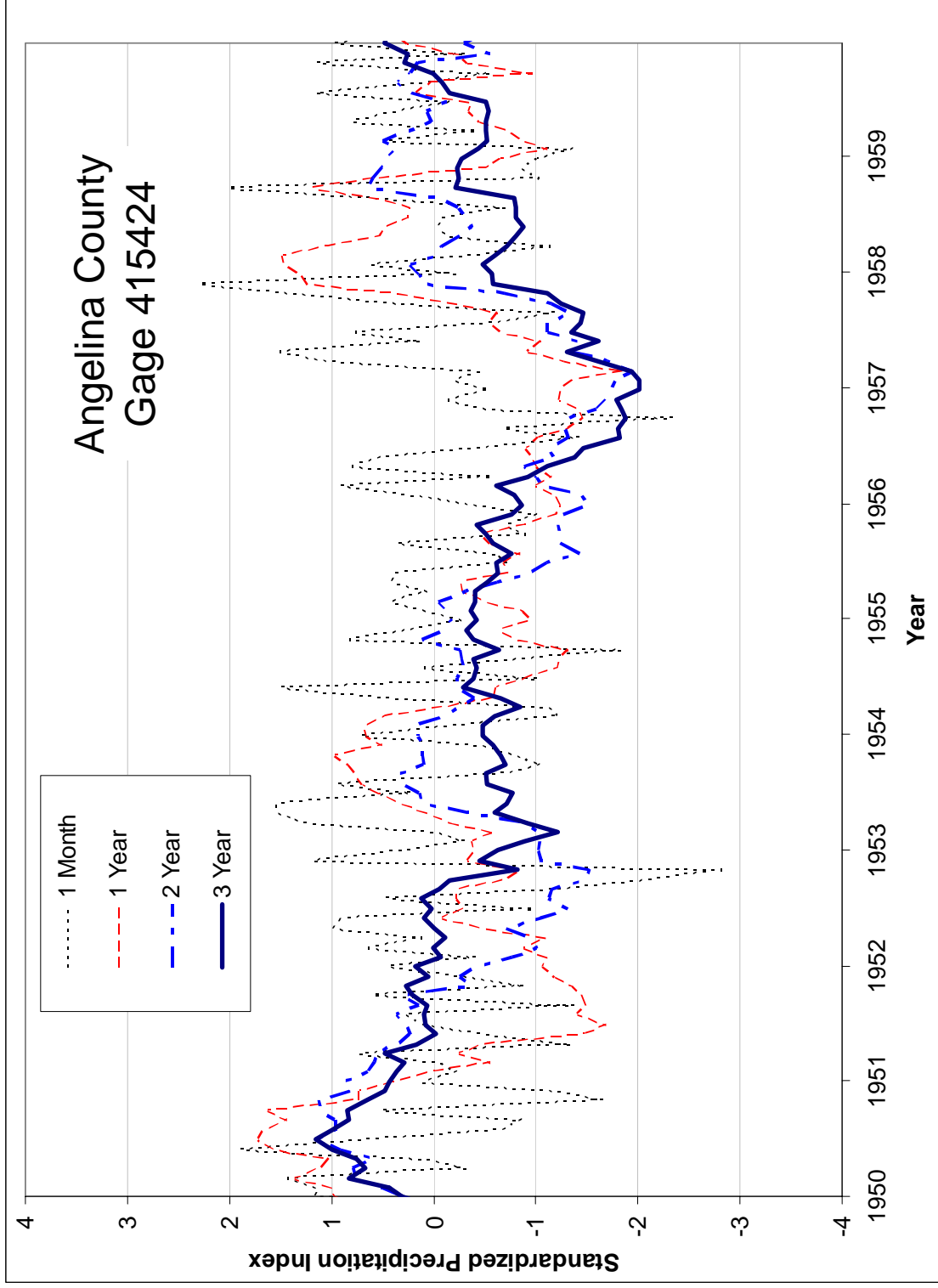


Figure 10.1.1 Standard precipitation index (SPI) curves for the Lufkin rain gage (#415424-Angelina Co.) for 1 month, 1 year, 2 year, 3 year time periods.

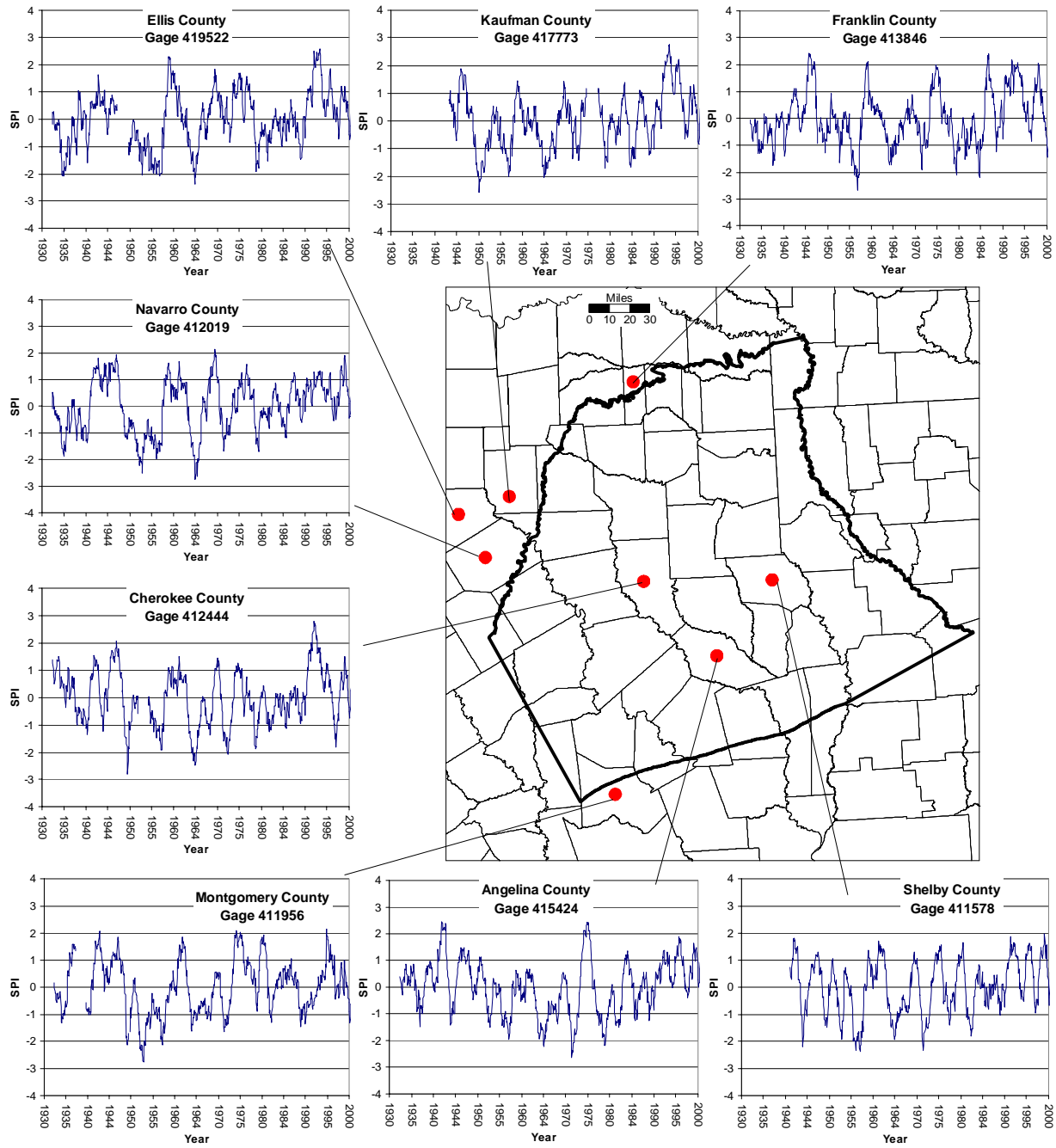


Figure 10.1.2 Standardized precipitation indices for precipitation gages in the region.

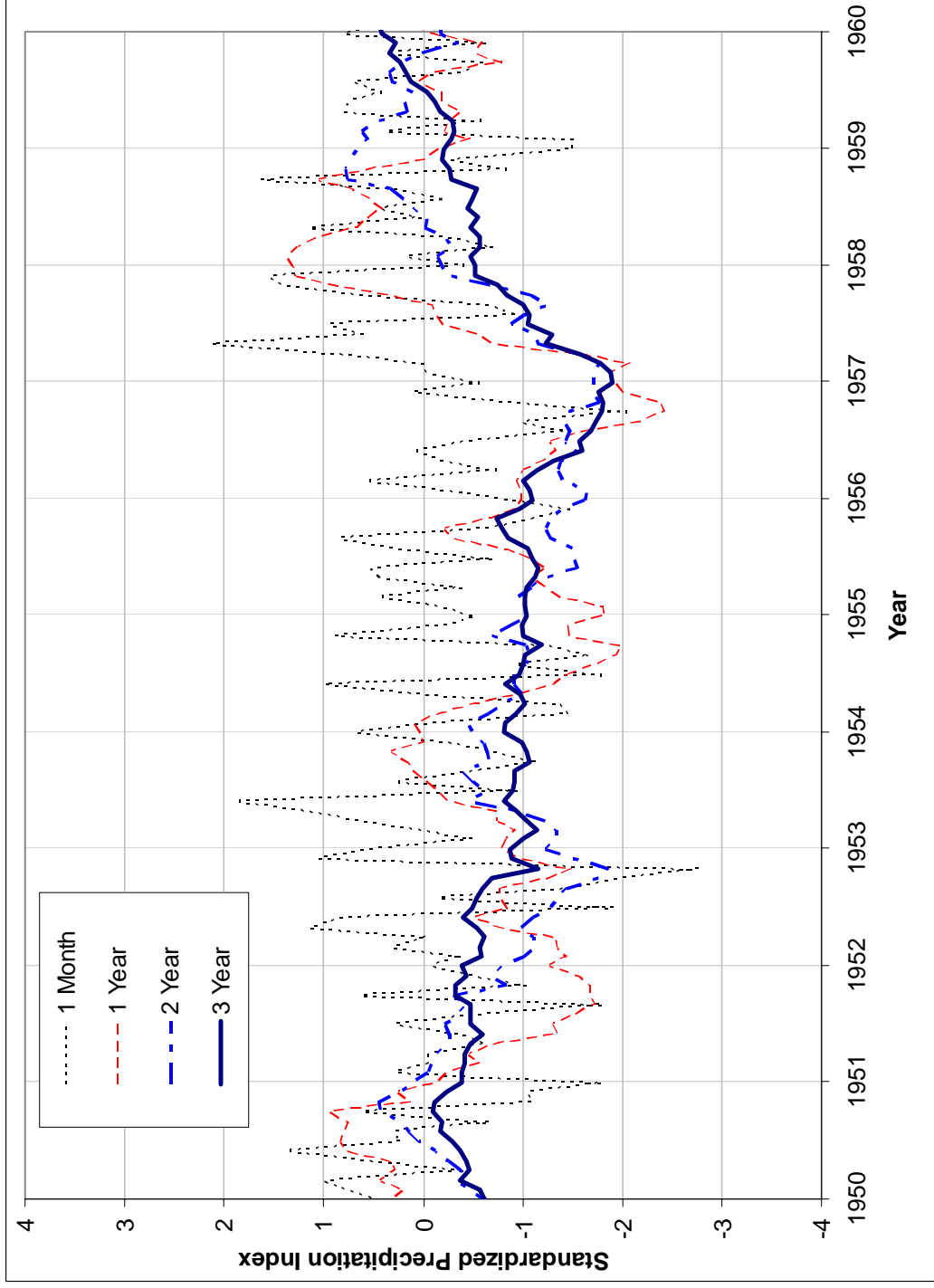


Figure 10.1.3 Standardized precipitation index averaged for all gages in the region from 1950-1960.

10.2 Predictive Simulation Results

In this section, we present the head and drawdown surfaces from the predictive simulation results. We also discussed a comparison between the average recharge condition simulation and the simulation with a DOR.

Figure 10.2.1 shows the simulated 2000 and 2050 head surfaces in Layer 1. The head surfaces show little change, reflecting the general topography in the outcrop and in confined section to the south. Consequently, the head difference plot in Figure 10.2.2 shows head declines typically less than 10 ft, except in Nacogdoches County where heads decline as much as 50 ft. This is probably due to the higher K_v of Layer 2 (Reklaw) assigned to eastern Nacogdoches County, based on the transient calibration. This causes the pumpage induced head decline in the Carrizo-Wilcox to extend into the overlying Queen City aquifer (Layer 1).

Figure 10.2.3 shows the simulated 2000 and 2050 head surfaces in the Carrizo (Layer 3). This figure shows significant rebound of the cone of depression in Angelina and Nacogdoches counties, as well as in Smith County. In these areas, water levels increase by more than 100 ft in Angelina County and about 50 ft in Smith and northern Cherokee County (Figure 10.2.4). In the southwestern part of the model, simulated head declines of about 10 ft are observed, which are due to local pumpage. Note that the southwestern model boundary was assumed to represent a no-flow boundary.

The simulated head surfaces in the upper Wilcox (Layer 4) in 2000 and 2050 indicate some reduction of the cone of depression in Angelina County after 50 years, whereas the withdrawal cone in Smith County remained the same (Figure 10.2.5). This is also shown in Figure 10.2.6, which shows a rebound of up to 100 ft in Angelina County and less than 10 feet in Smith County. Similar to Layer 3, the southwestern part of the model indicates continued water-level declines in Layer 4.

Figure 10.2.7 shows the simulated 2000 and 2050 head surfaces in the middle Wilcox (Layer 5). For the middle Wilcox, the closed contour reflecting the pumpage cone in Angelina and Nacogdoches counties in the overlying upper Wilcox and Carrizo layers has disappeared. However, the cone of depression in Smith County shows noticeably more drawdown. Figure 10.2.8 indicates generally less than 10 ft of rebound in the northern confined section, whereas Smith County shows additional water-level declines of as much as 50 ft. The

southwestern part shows localized water-level decline at or near the outcrop of Layer 5, due to increased pumpage in Freestone and Leon counties.

As discussed below, the rebound of water levels in the Carrizo and upper Wilcox and continued water-level decline in the middle Wilcox is due to the reallocation of the predictive pumpage estimates from the Carrizo to the middle Wilcox layer. In comparison, the head surfaces in the lower Wilcox (Layer 6) for 2000 and 2050 are very similar, indicating relatively little change in water levels of generally less than 10 ft (Figures 10.2.9 and 10.2.10). The southwestern part, again indicates water-level declines of about 10 ft. Note that the pumpage effects in this particular area may be enhanced by its proximity to the no-flow boundary.

In the following discussion, the head surfaces and predicted changes over the 10-year intervals are described. Figure 10.2.11 shows the simulated 2010 heads and the corresponding head change between 2000 and 2010 in Layer 3 (Carrizo). As indicated above, overall heads rebound in the confined section of the Carrizo, particularly in Smith and Angelina counties, due to a redistribution of the increased projected pumpage from different layers, as described in Section 4.7. The simulated 2010 heads in the upper Wilcox (Figure 10.2.12) indicate a maximum of about 10 ft rebound in the confined section.

The changes of the head surface in Layer 3 (Carrizo) between 2000 and 2020 is shown in Figure 10.2.13, indicating a maximum rebound of as much as 100 ft in Angelina County and about 50 ft in Smith and northern Cherokee counties. The corresponding 2020 head surface for Layer 4 (upper Wilcox) indicates relatively small changes of less than 10 ft (Figure 10.2.14).

The 30-yr change in hydraulic heads for Layer 3 (Carrizo) between 2000 and 2030, shown in Figure 10.2.15, indicates increased rebound of more than 100 ft in Angelina County and more than 50 ft in Smith County. The 2030 head surface for Layer 4 (upper Wilcox) maintained the drawdown cone in Smith County and showed about 50 ft rebound in Angelina County (Figure 10.2.16).

The changes of the head surface for Layer 3 between 2000 and 2040 are shown in Figure 10.2.17, which shows more 100 ft rebound in Angelina County and about 50 ft in Smith and northern Cherokee counties. The corresponding head surface for Layer 4 indicates a local increase in the drawdown in west-central Smith County (Figure 10.2.18). The surrounding counties show some rebound with local maxima in Cherokee and Angelina counties.

Selected hydrographs of simulated heads and measured heads in selected target wells for the transient calibration period between 1980 and 1999 with the subsequent 50-yr predictive period between 2000 and 2050 are shown in Figures 10.2.19 through 10.2.22. Layer 3 (Carrizo) indicates drastic water-level rebound at the start of the predictive period (Figure 10.2.19) in Smith and Angelina counties and a smaller rebound in Cherokee County, whereas water levels in Wood County continued to decline. The water levels in Layer 4 (upper Wilcox) indicate continued decline with a recovery period after 2040 in Smith County, whereas water levels in Leon County indicated minor decline during the predictive period (Figure 10.2.20). Hydrographs for Layer 5 (middle Wilcox) indicate continued recovery in Panola County in the Sabine uplift, and a general decline in Van Zandt County during the predictive period (Figure 10.2.21). For Layer 6, the hydrograph in Van Zandt County did not reproduce the decline during the transient calibration-verification period, and simulated heads remained relatively constant during the predictive period (Figure 10.2.22). The hydrograph in Henderson County shows a similar water level decline during the transient period which is not well reproduced in the model, and the subsequent predictive heads indicate a general upward trend.

Figure 10.2.23 shows the difference between the simulated head surface for 2050 with average recharge and the simulated head surface for 2050 with the DOR for the Carrizo (Layer 3), upper Wilcox (Layer 4) and middle Wilcox (Layer 5). In all of these layers there is a maximum head difference of less than 10 ft. All of the simulated head differences are near the outcrop, where recharge will have the most impact. These figures emphasize an important point about the hydrology of this aquifer system. Recharge does not have a significant impact on downdip heads over the timescale of these simulations. One aspect of these simulations that is misleading is that pumping does not increase during the DOR. The DOR only impacts climate data and subsequently, recharge. Therefore, the effect of a DOR will be seen predominantly in the updip and outcrop areas.

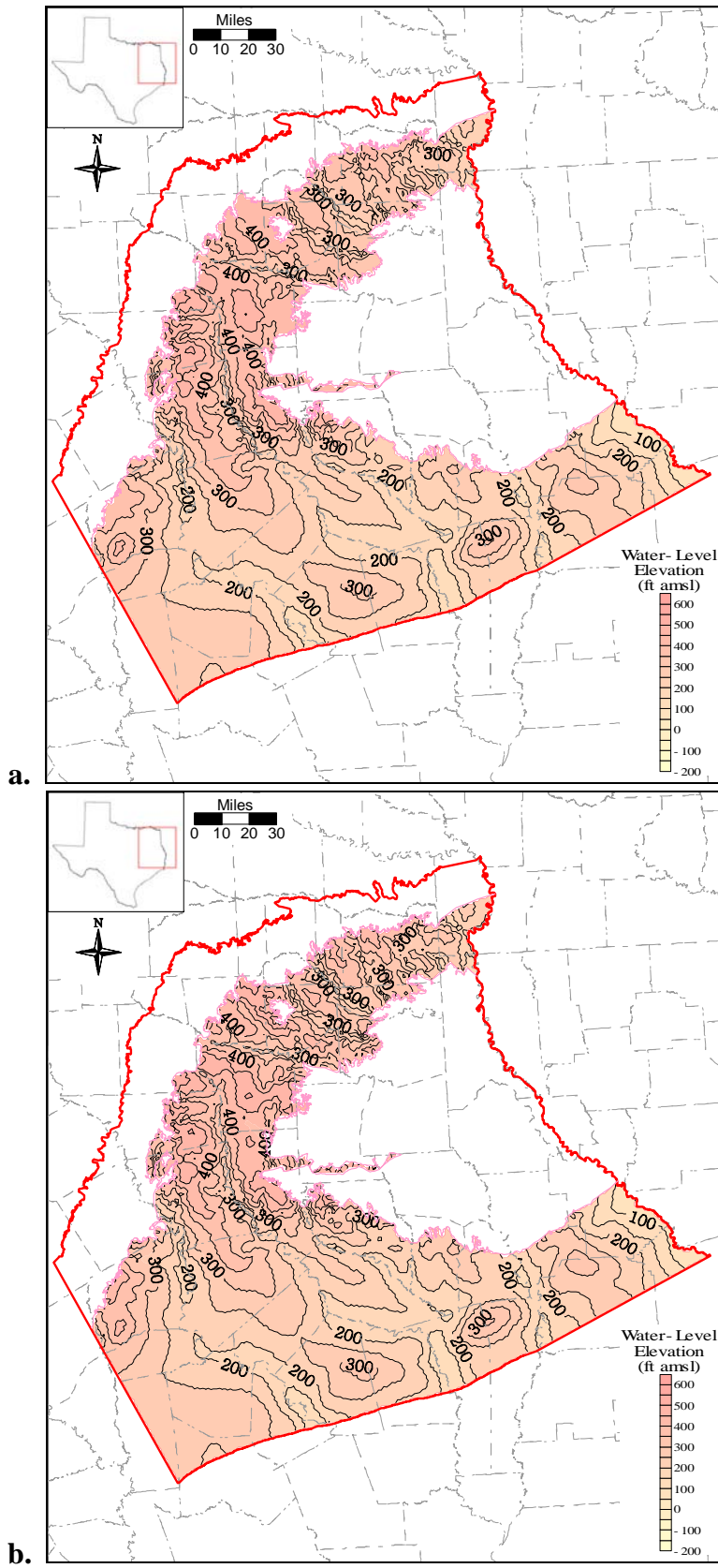


Figure 10.2.1 Simulated 2000 (a) and 2050 (b) heads surfaces for Layer 1 (Queen City).

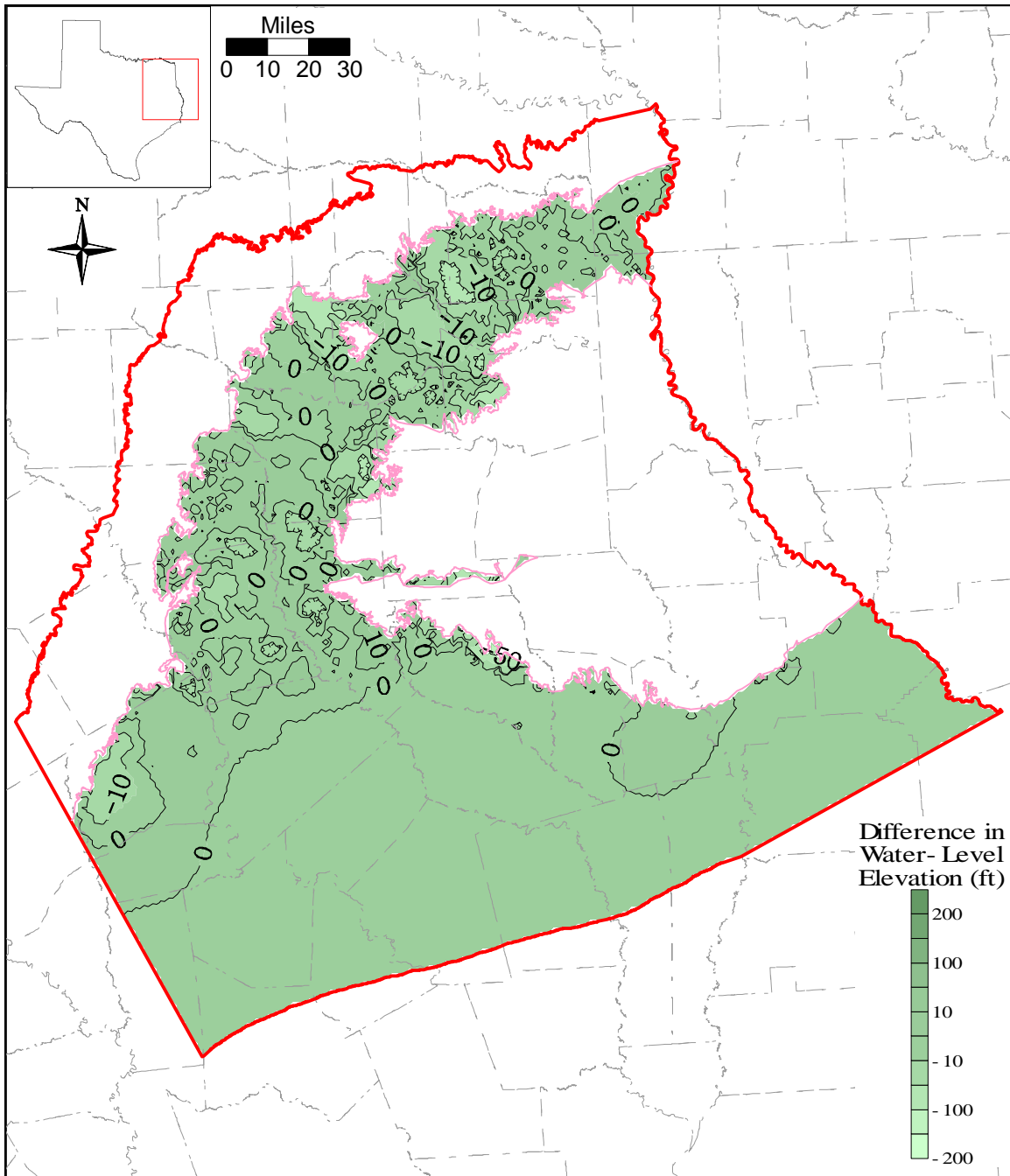


Figure 10.2.2 Difference between 2000 and 2050 simulated head surfaces for Layer 1 (Queen City).

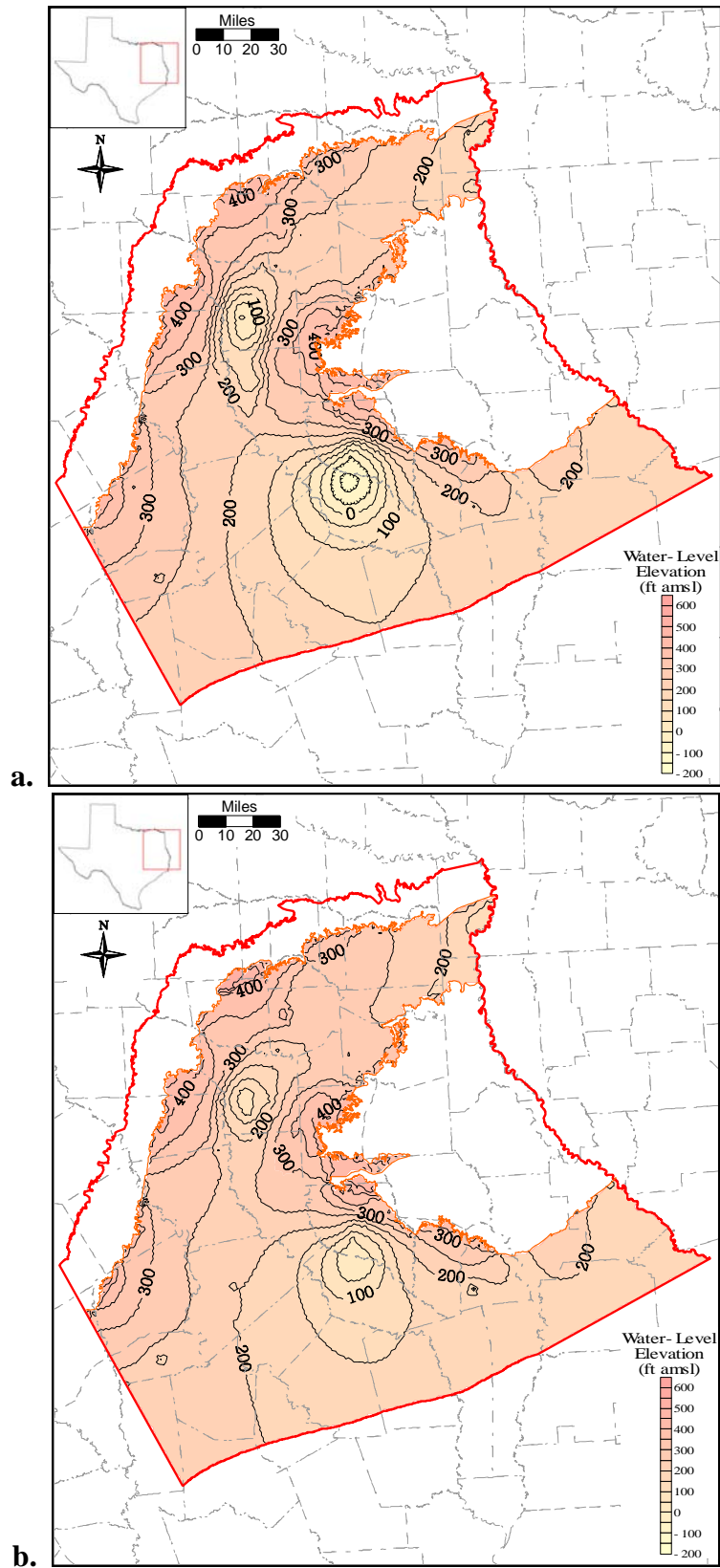


Figure 10.2.3 Simulated 2000 (a) and 2050 (b) heads surfaces for Layer 3 (Carrizo).

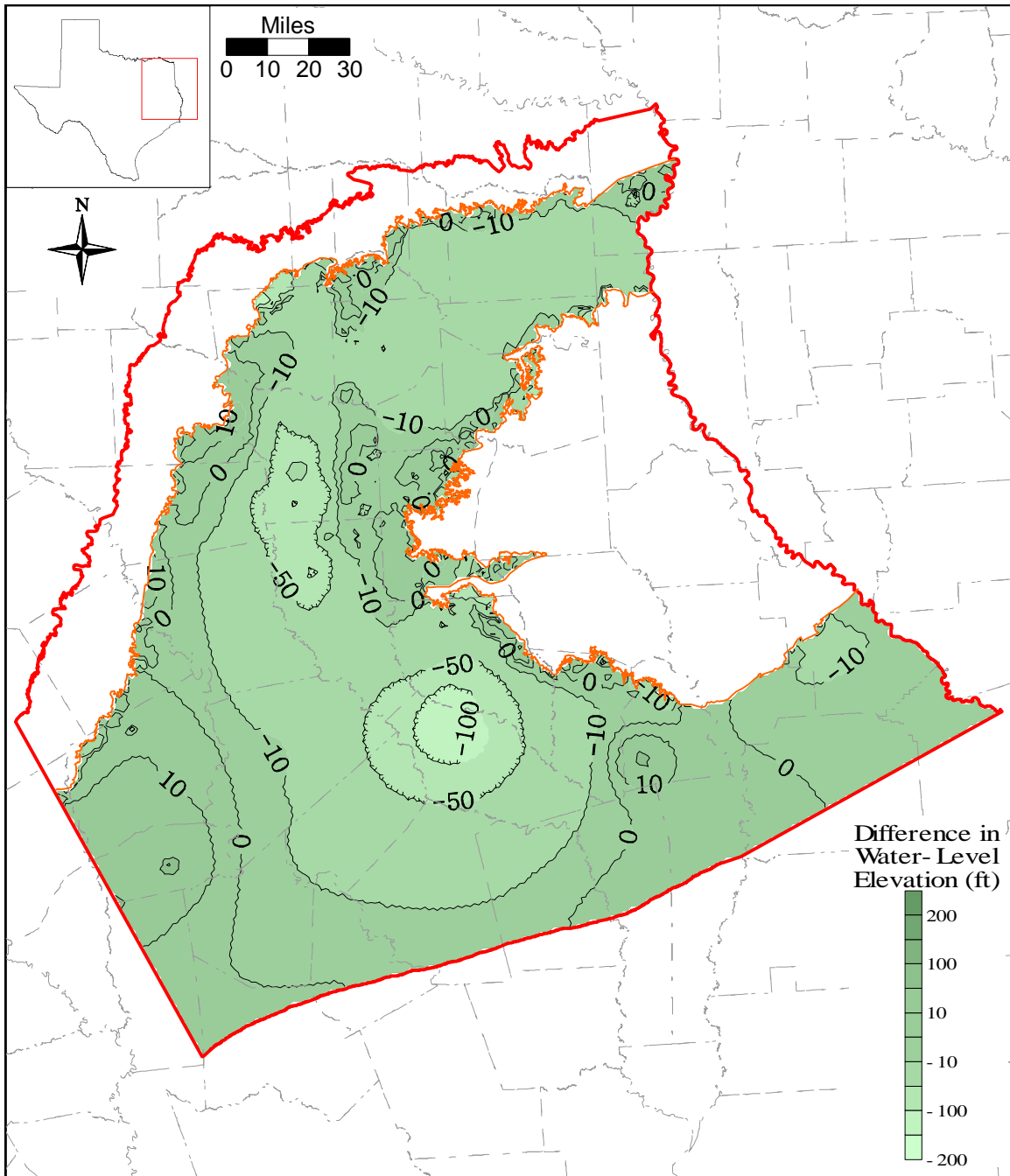


Figure 10.2.4 Difference between 2000 and 2050 simulated head surfaces for Layer 3 (Carrizo).

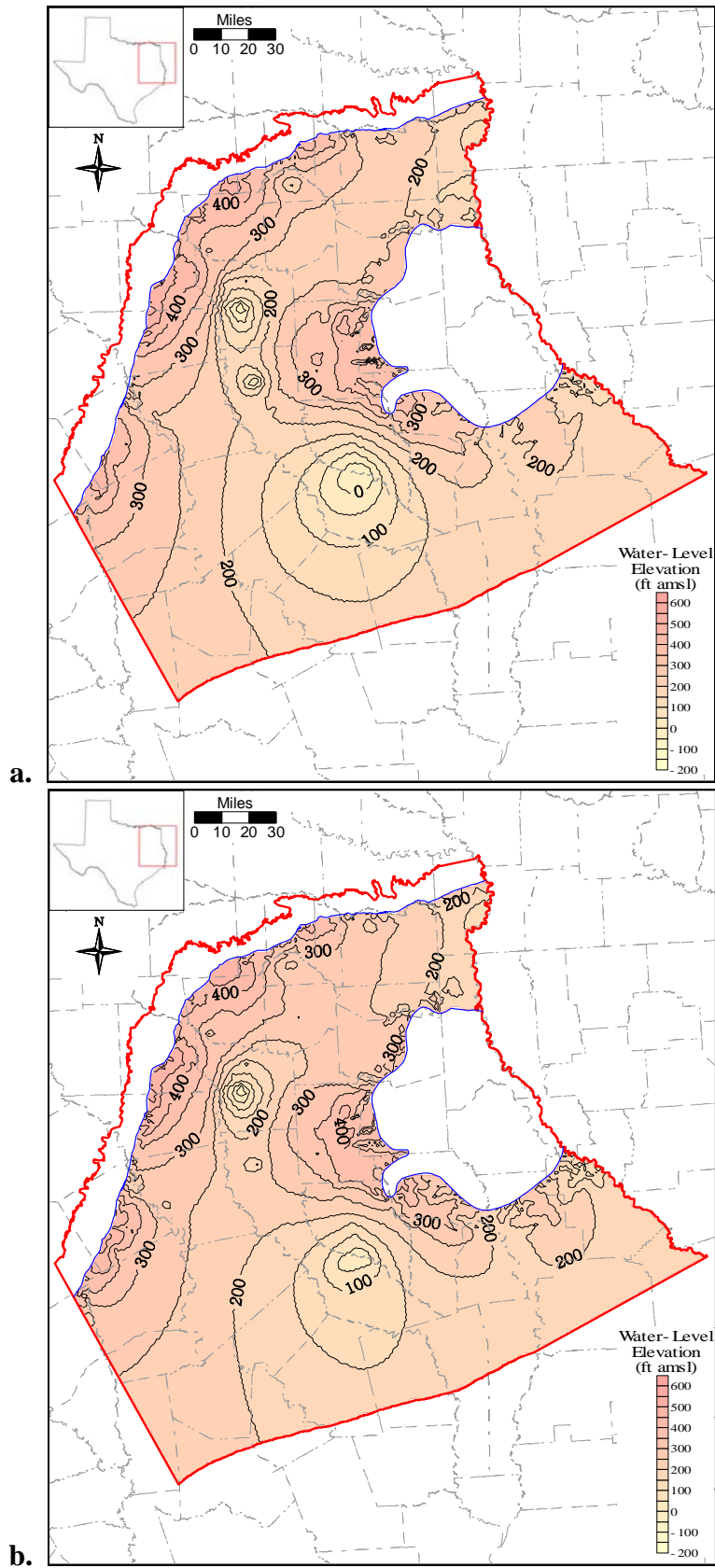


Figure 10.2.5 Simulated 2000 (a) and 2050 (b) heads surfaces for Layer 4 (upper Wilcox).

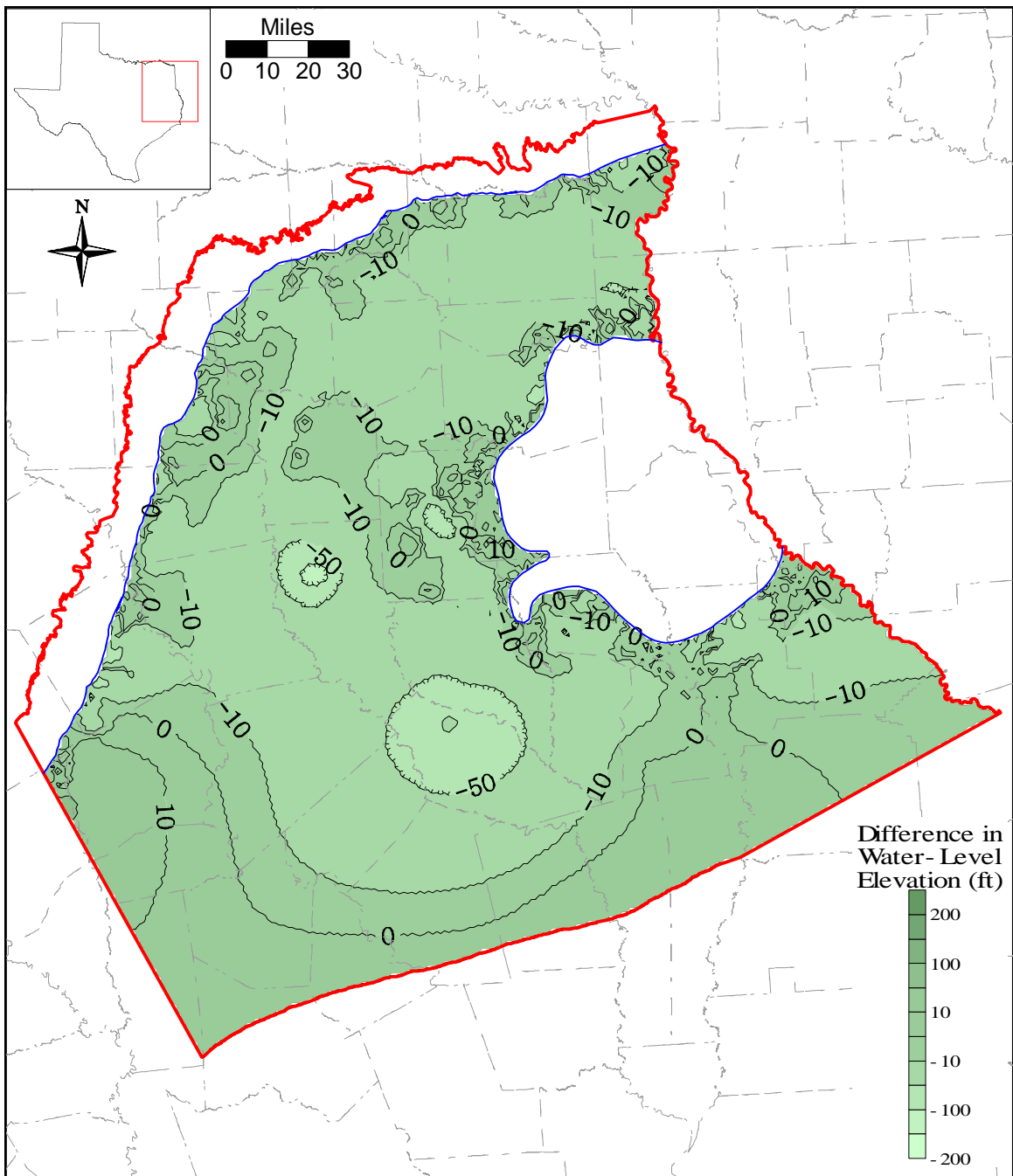


Figure 10.2.6 Difference between 2000 and 2050 simulated head surfaces for Layer 4 (upper Wilcox).

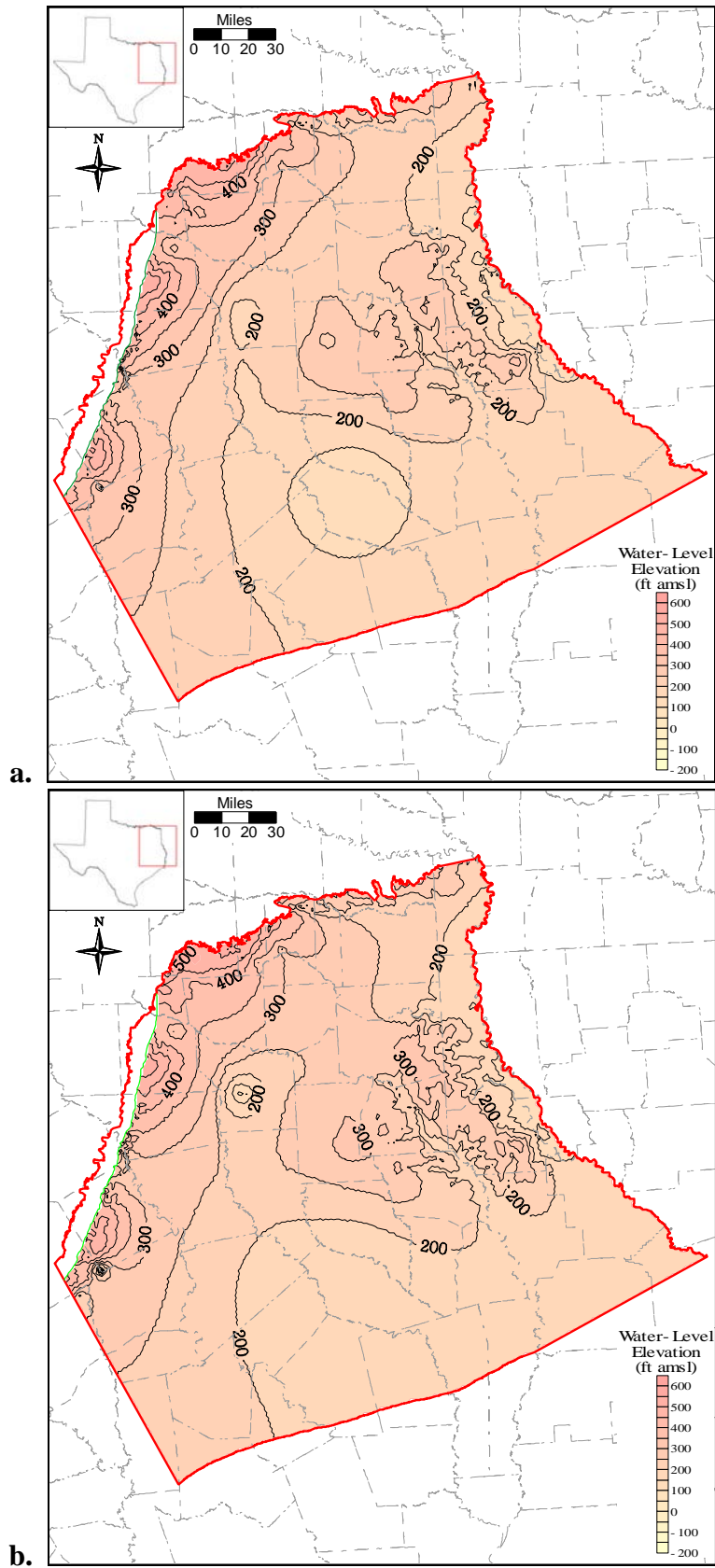


Figure 10.2.7 Simulated 2000 (a) and 2050 (b) heads surfaces for Layer 5 (middle Wilcox).

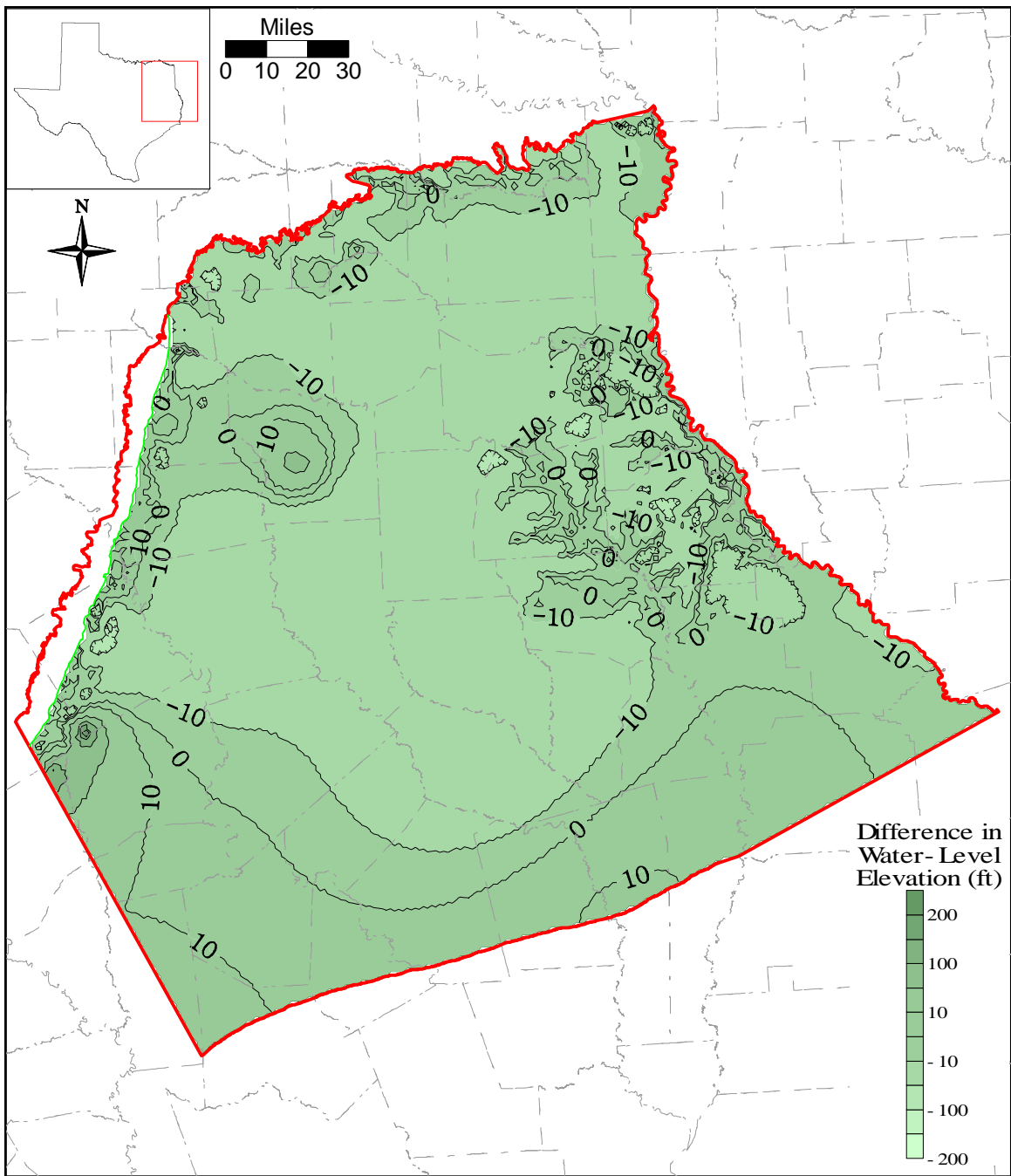


Figure 10.2.8 Difference between 2000 and 2050 simulated head surfaces for Layer 5 (middle Wilcox).

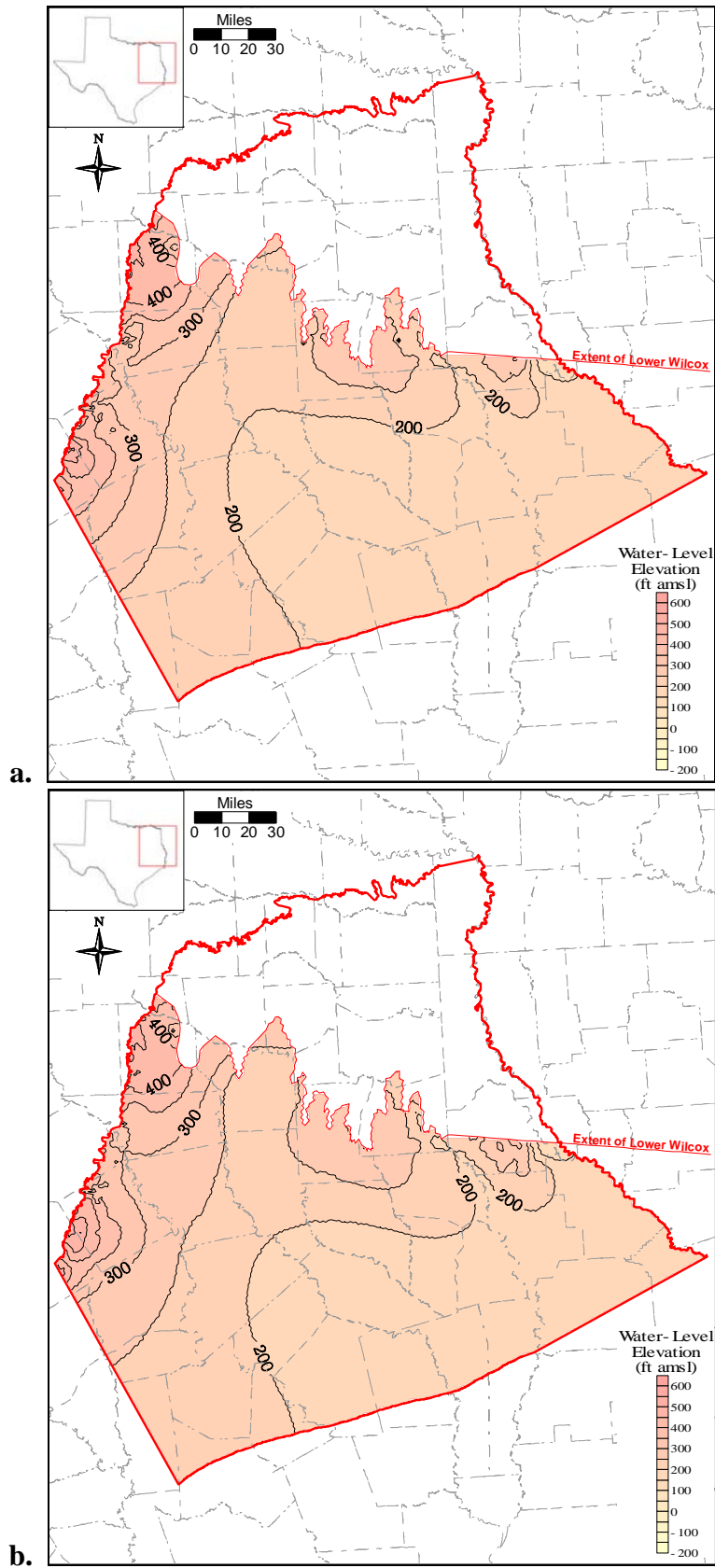


Figure 10.2.9 Simulated 2000 (a) and 2050 (b) heads surfaces for Layer 6 (lower Wilcox).

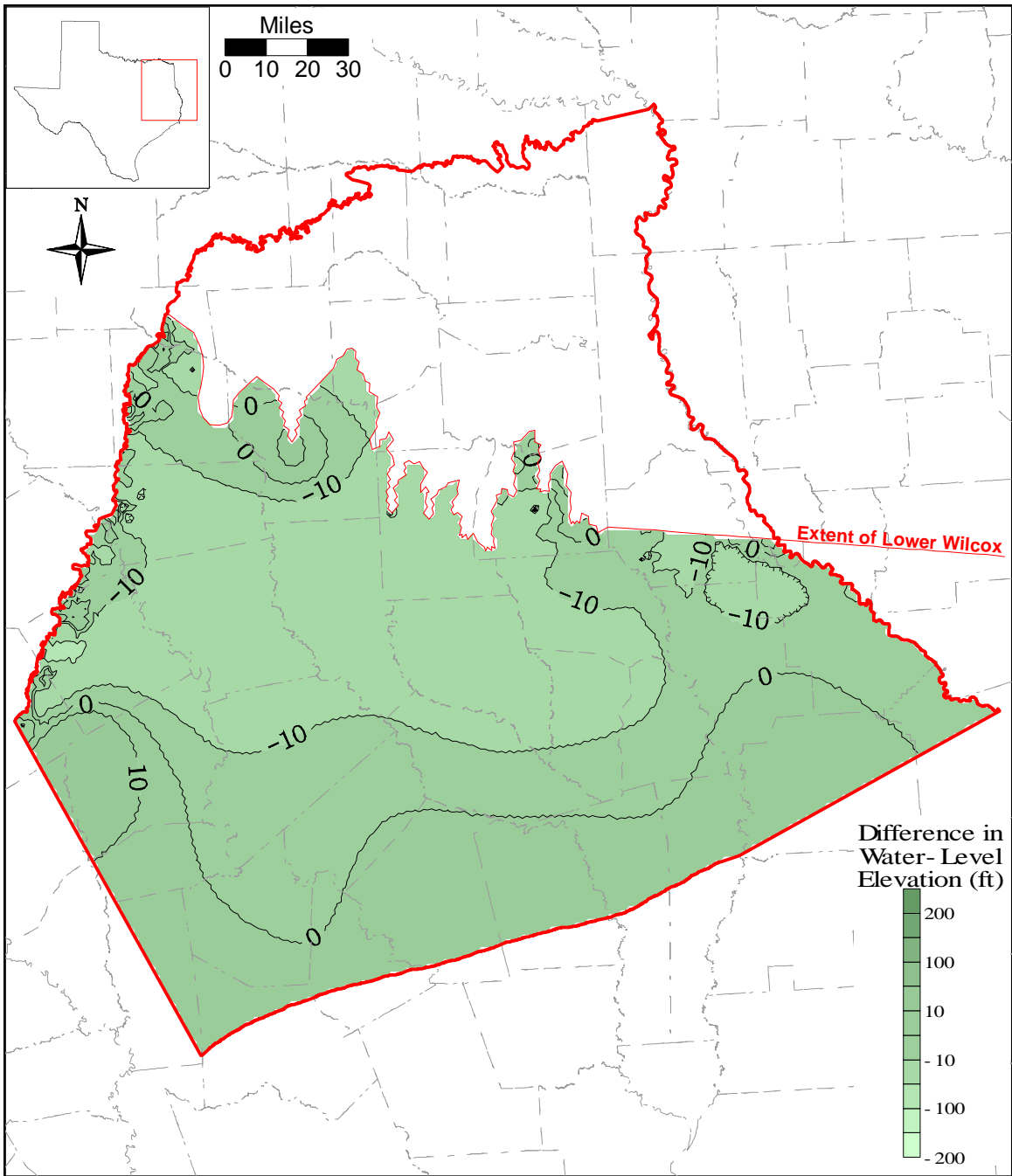


Figure 10.2.10 Difference between 2000 and 2050 simulated head surfaces for Layer 6 (lower Wilcox).

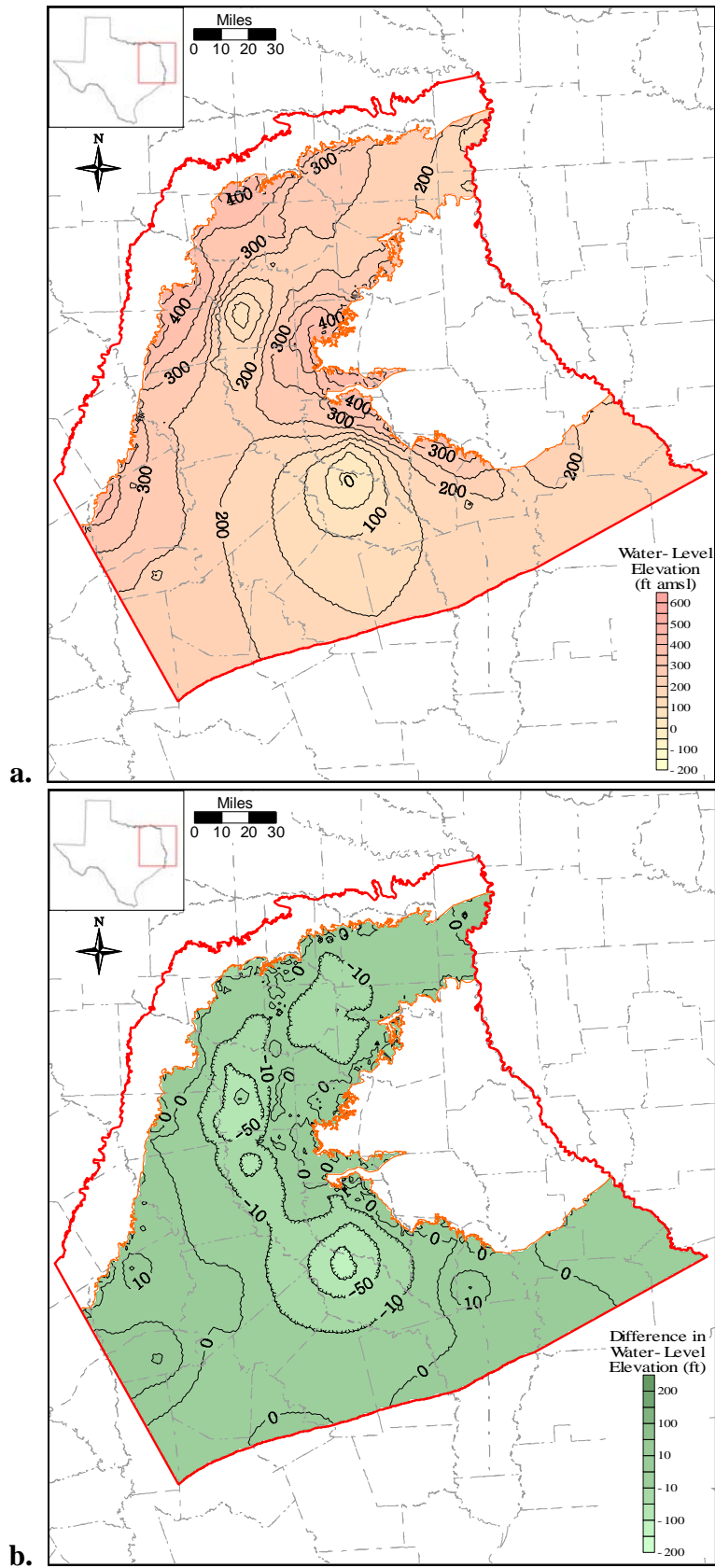


Figure 10.2.11 Simulated 2010 head surface (a) and drawdown from 2000 (b), Layer 3 (Carrizo).

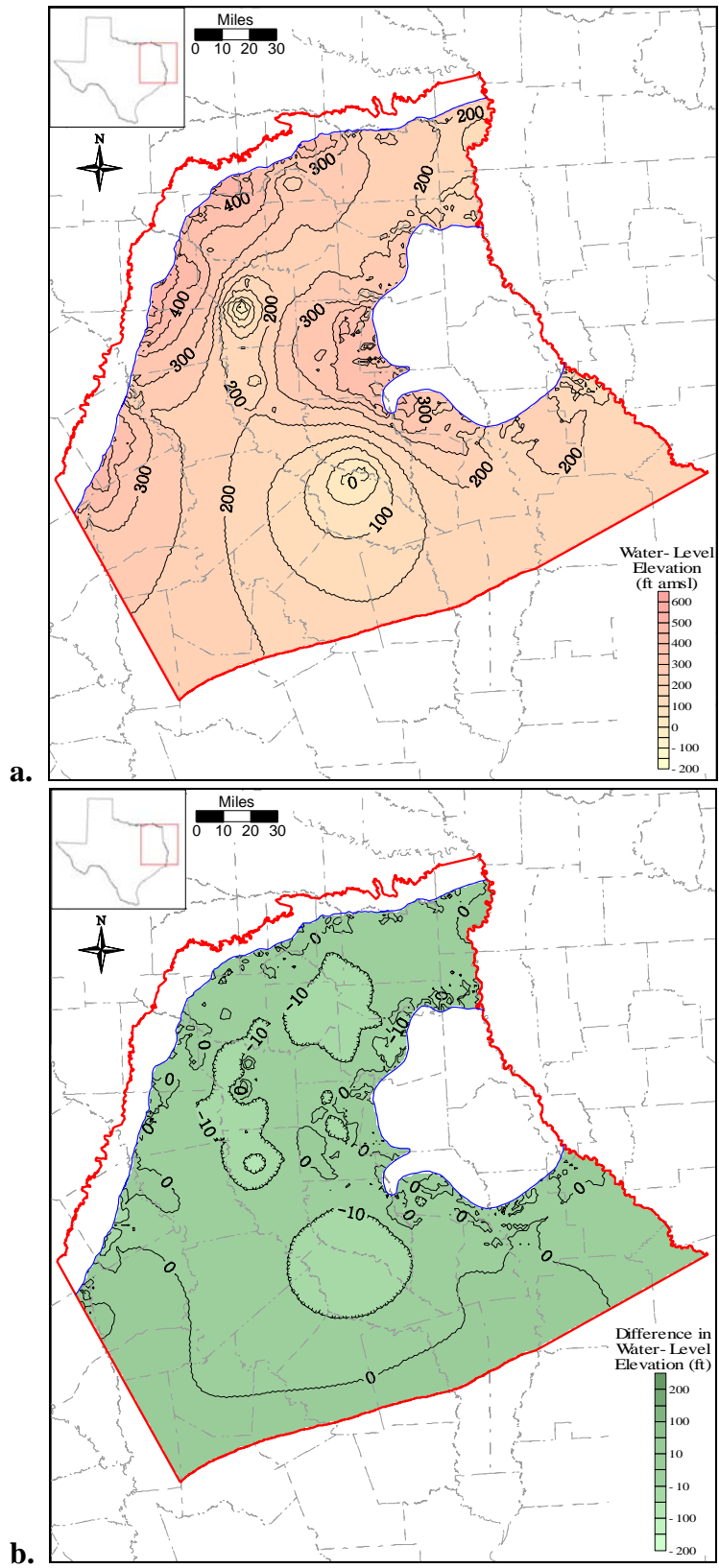


Figure 10.2.12 Simulated 2010 head surface (a) and drawdown from 2000 (b), Layer 4 (upper Wilcox).

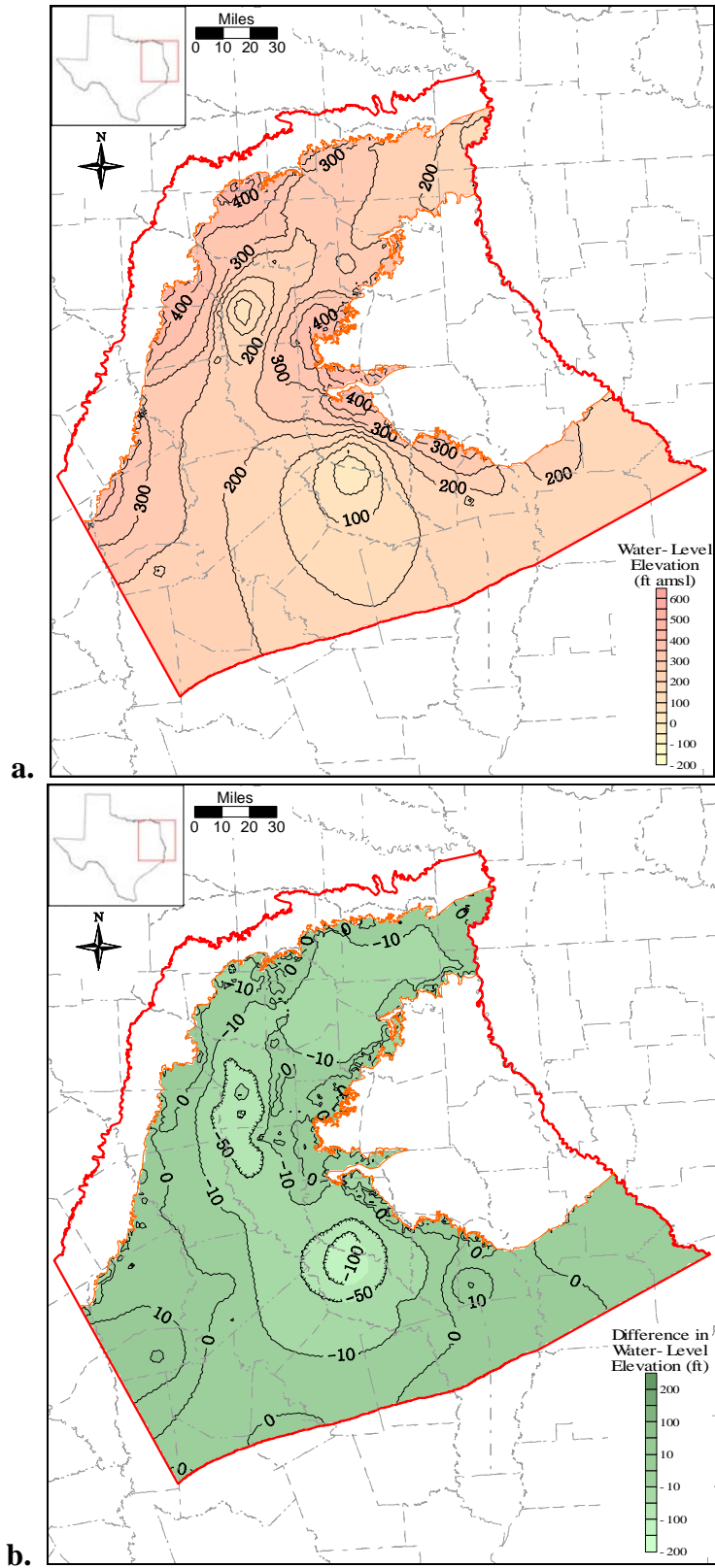


Figure 10.2.13 Simulated 2020 head surface (a) and drawdown from 2000 (b), Layer 3 (Carrizo).

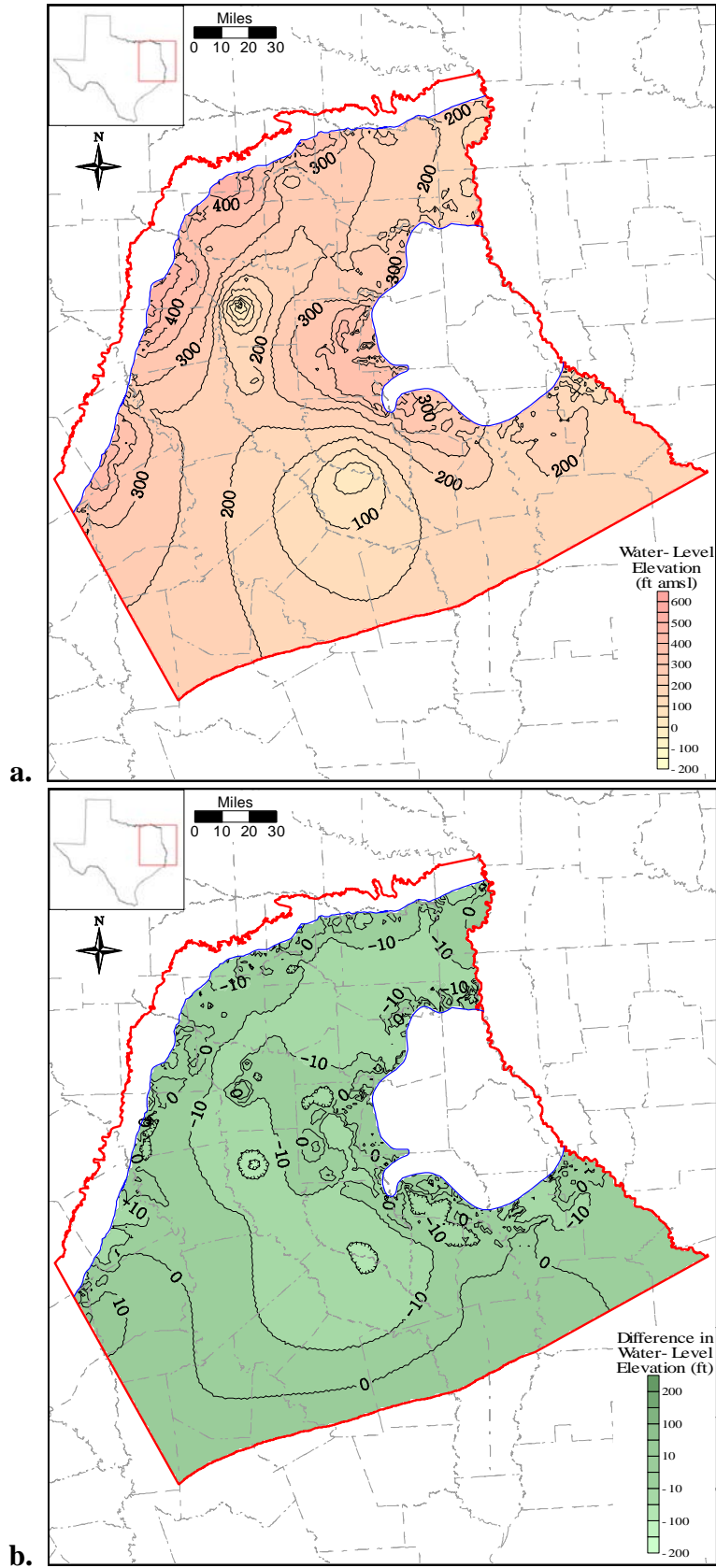


Figure 10.2.14 Simulated 2020 head surface (a) and drawdown from 2000 (b), Layer 4 (upper Wilcox).

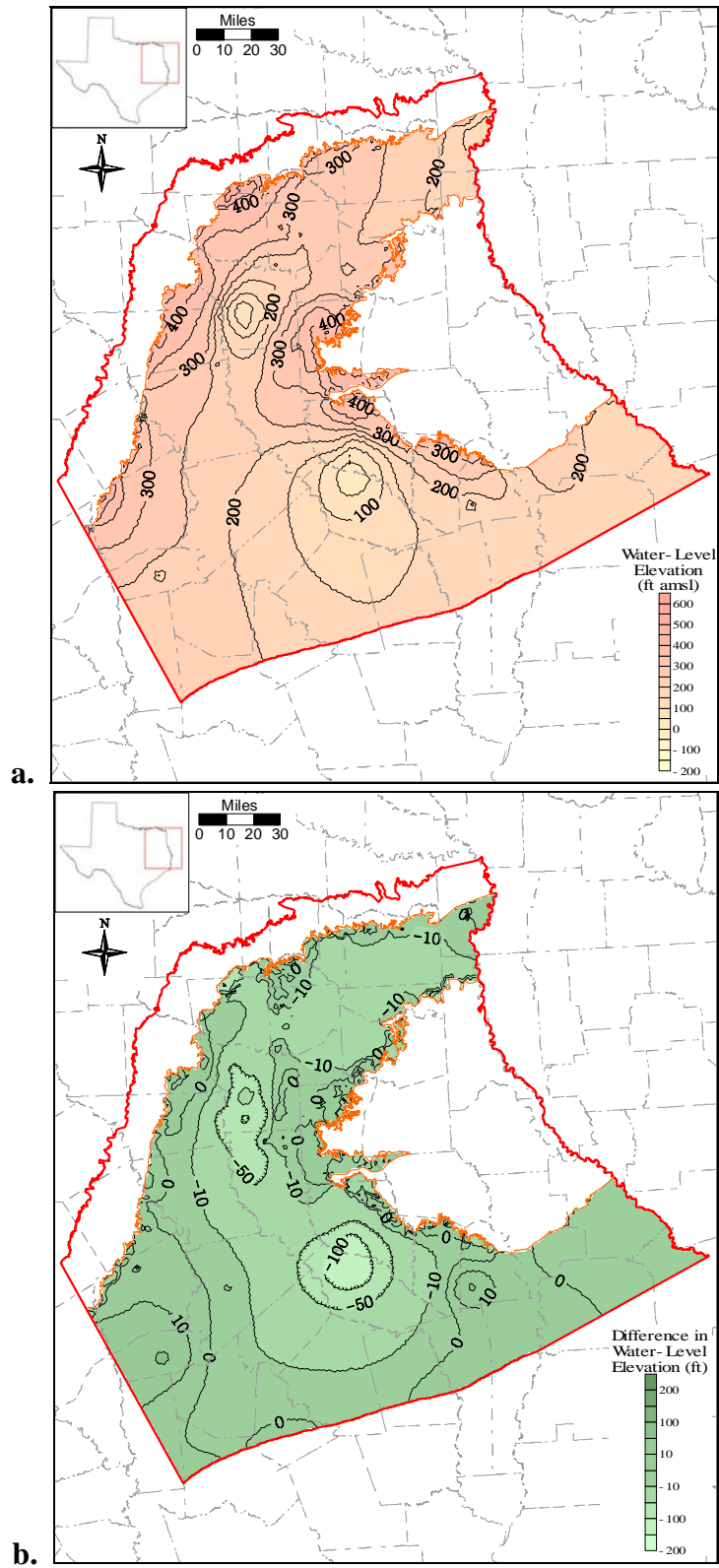


Figure 10.2.15 Simulated 2030 head surface (a) and drawdown from 2000 (b), Layer 3 (Carrizo).

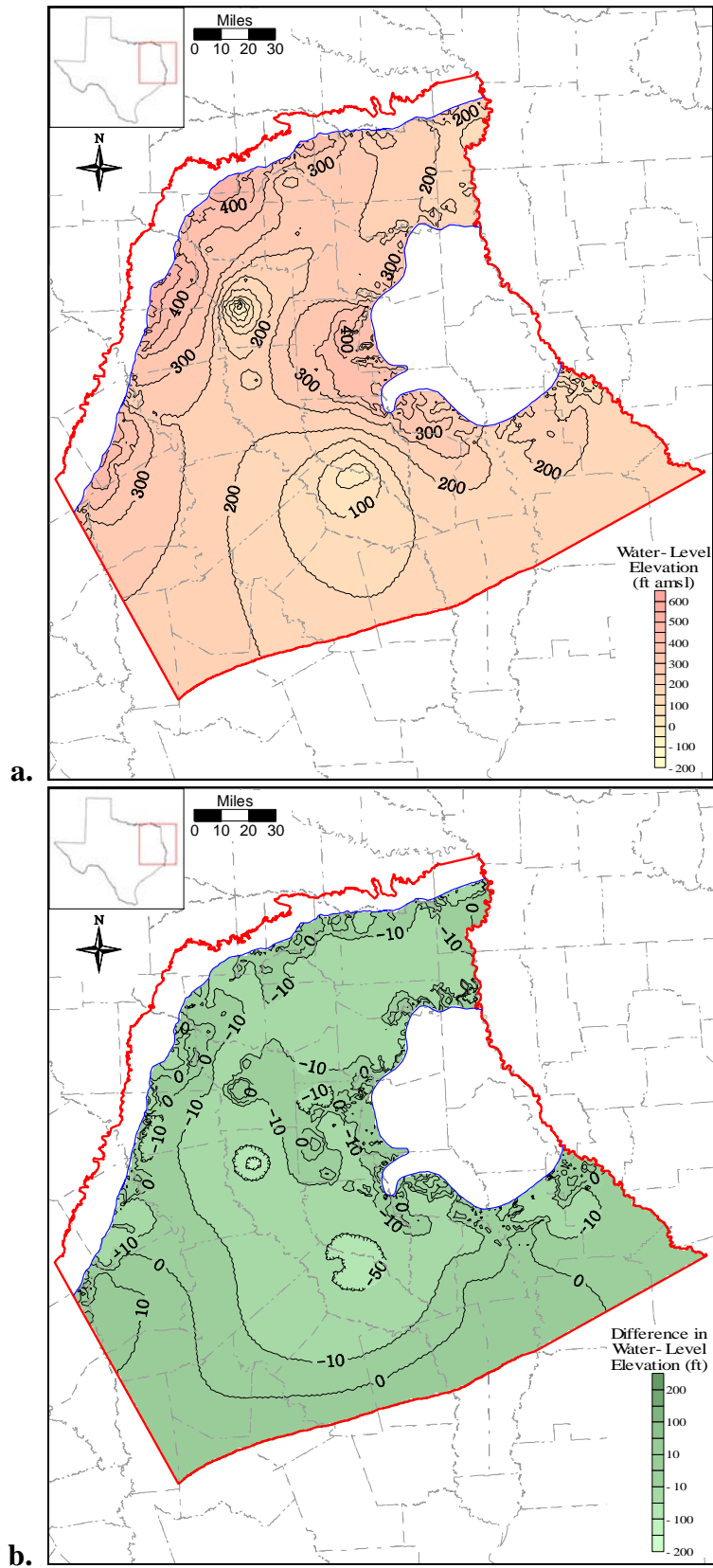


Figure 10.2.16 Simulated 2030 head surface (a) and drawdown from 2000 (b), Layer 4 (upper Wilcox).

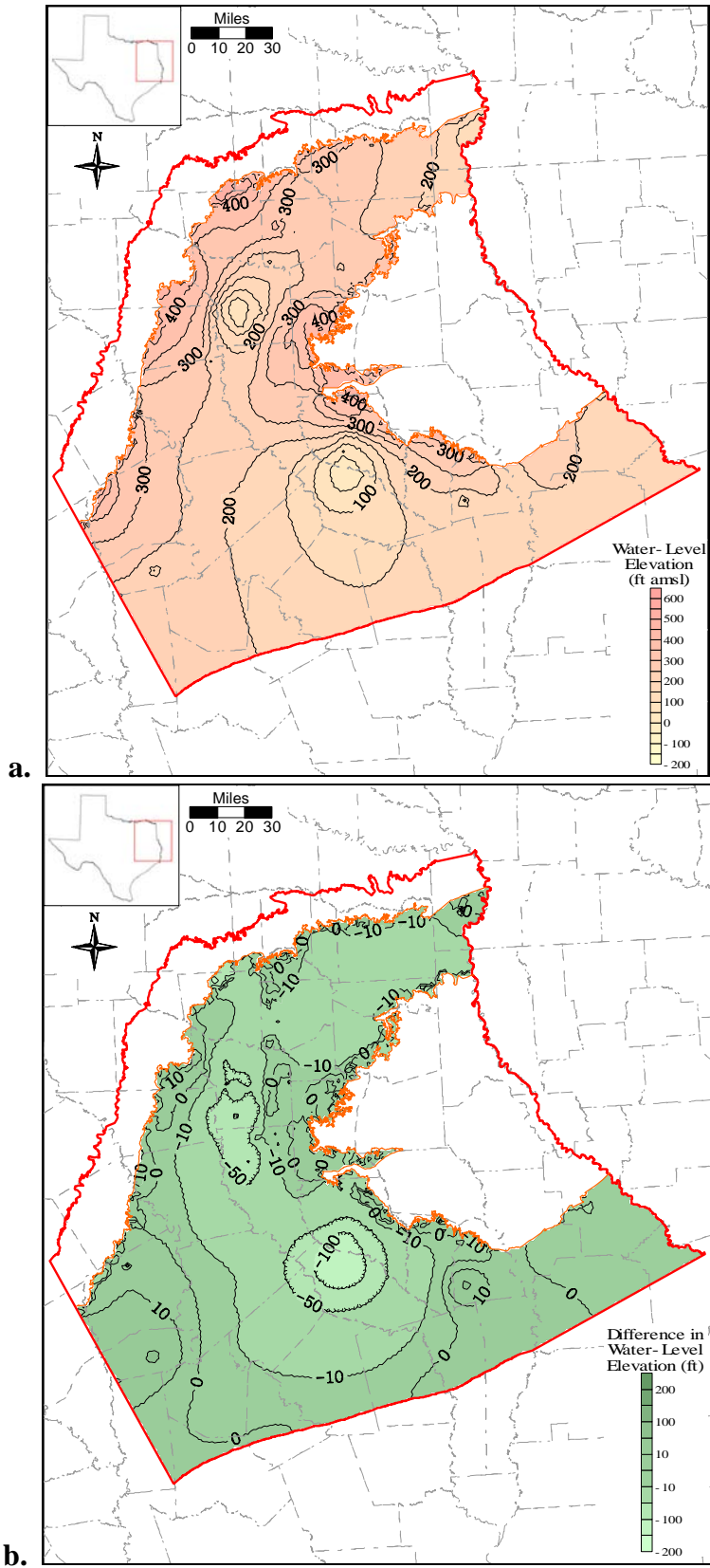


Figure 10.2.17 Simulated 2040 head surface (a) and drawdown from 2000 (b), Layer 3 (Carrizo).

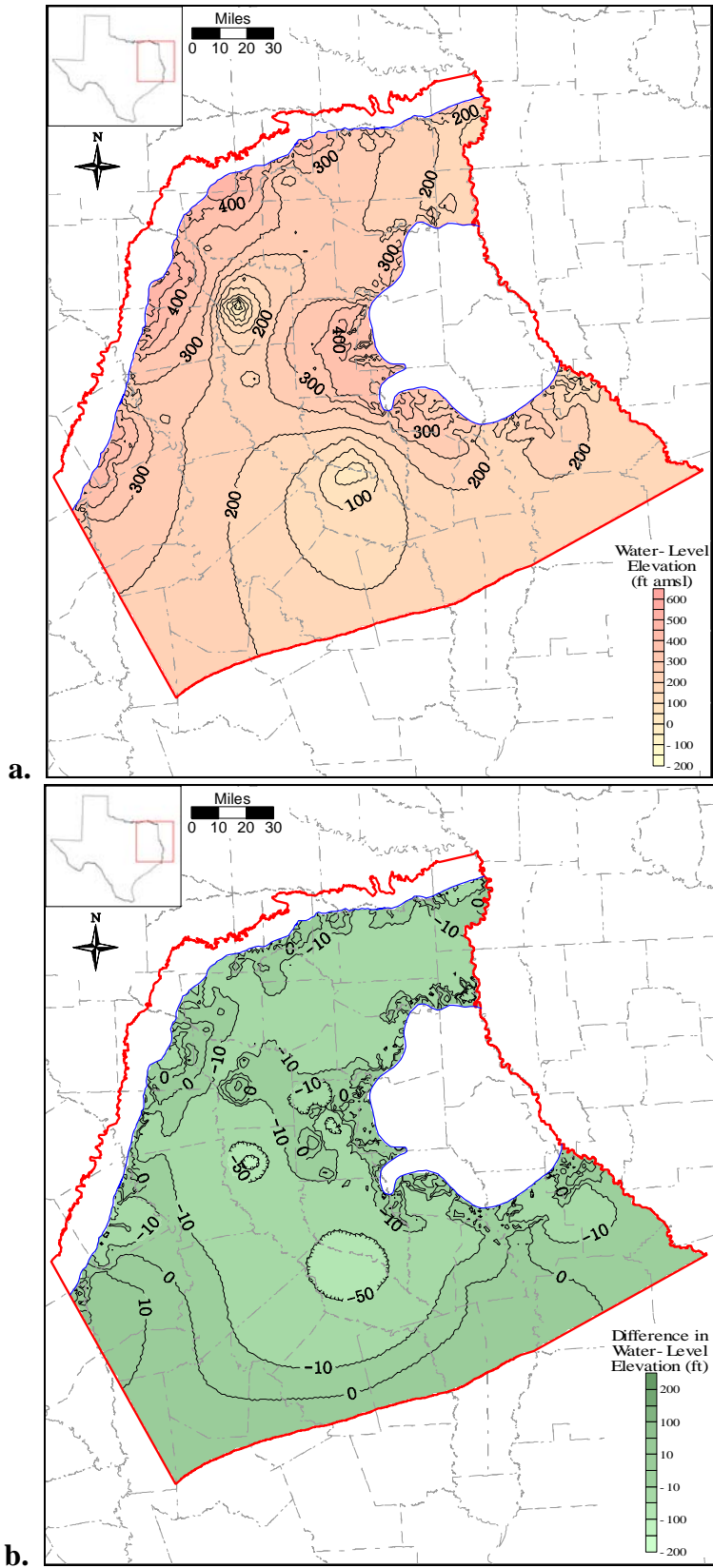


Figure 10.2.18 Simulated 2040 head surface (a) and drawdown from 2000 (b), Layer 4 (upper Wilcox).

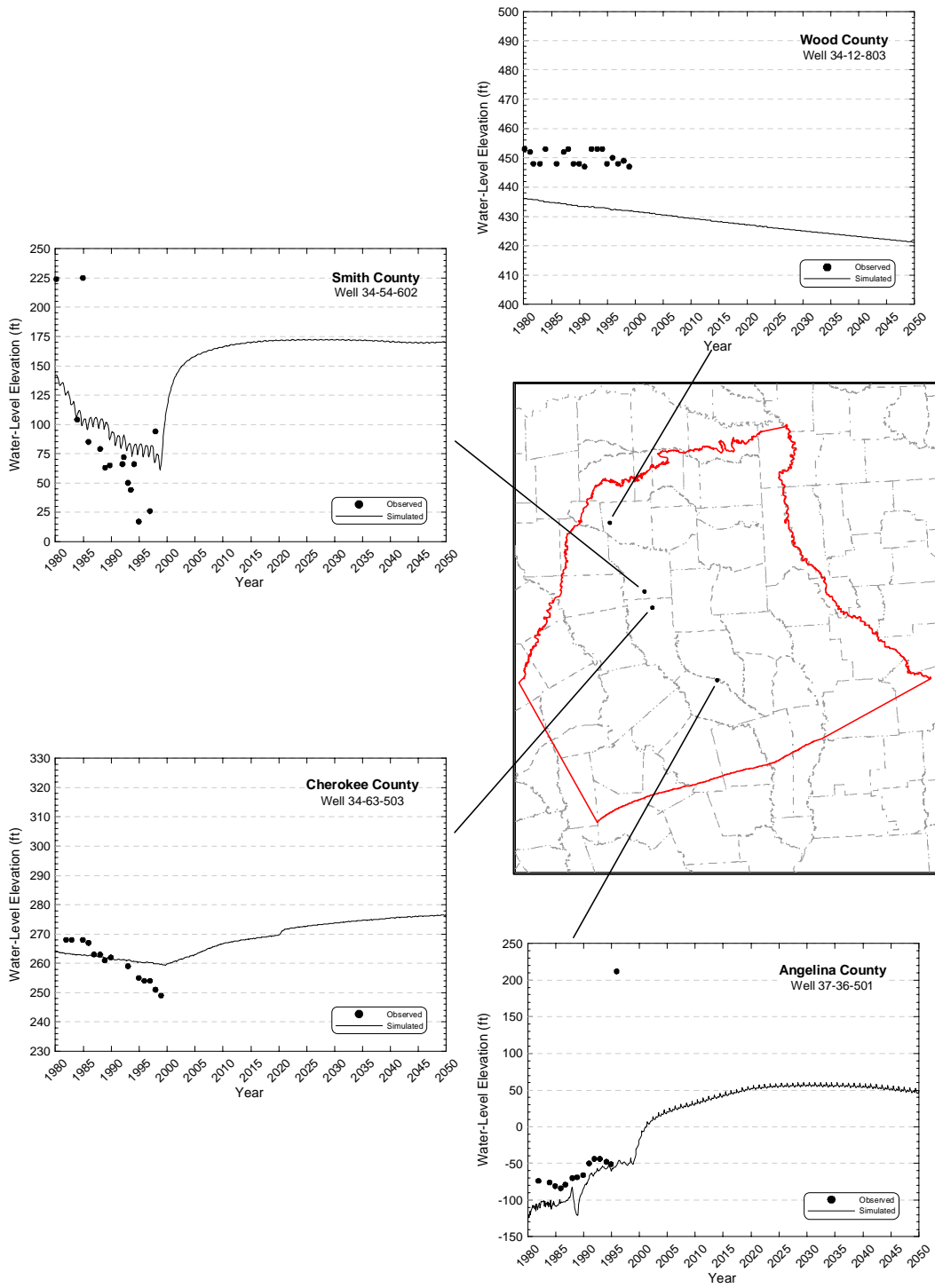


Figure 10.2.19 Selected hydrographs from predictive simulation to 2050, Layer 3 (Carrizo).

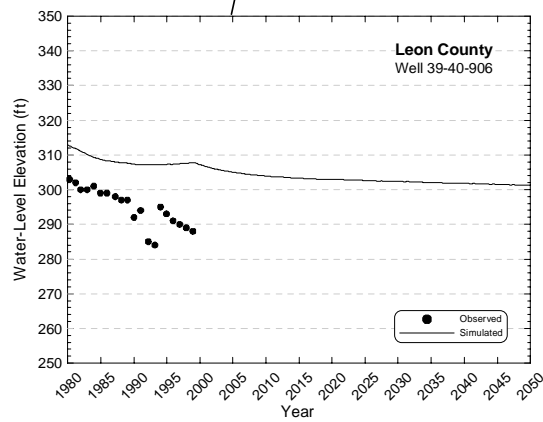
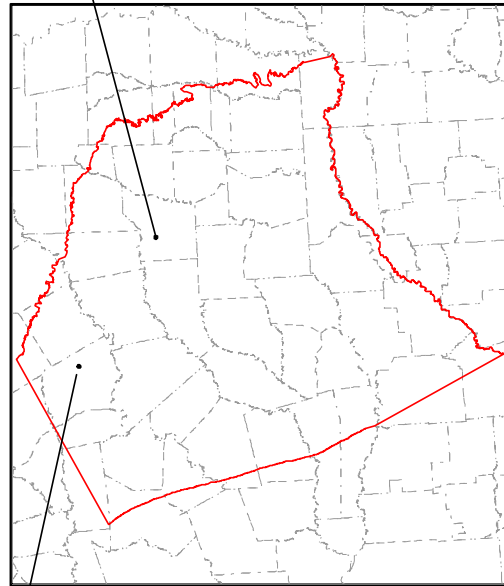
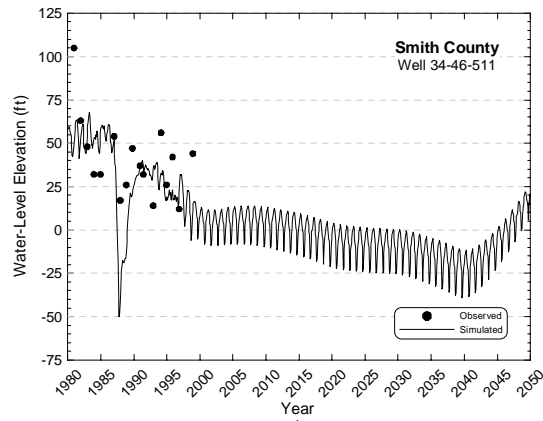


Figure 10.2.20 Selected hydrographs from predictive simulation to 2050, Layer 4 (upper Wilcox).

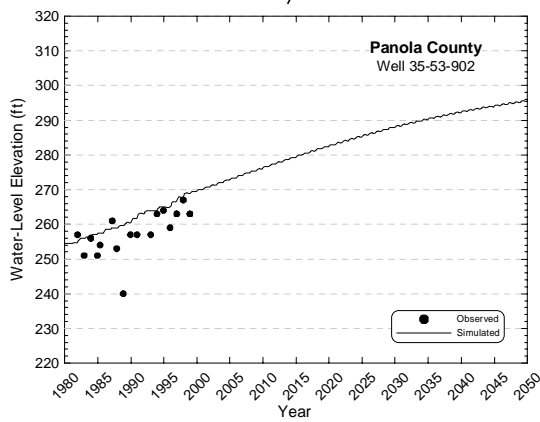
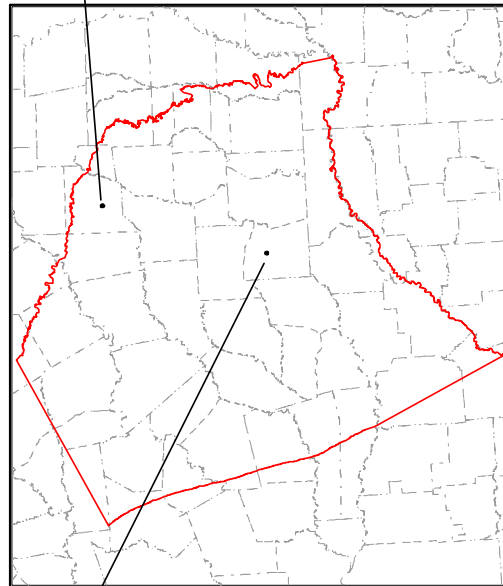
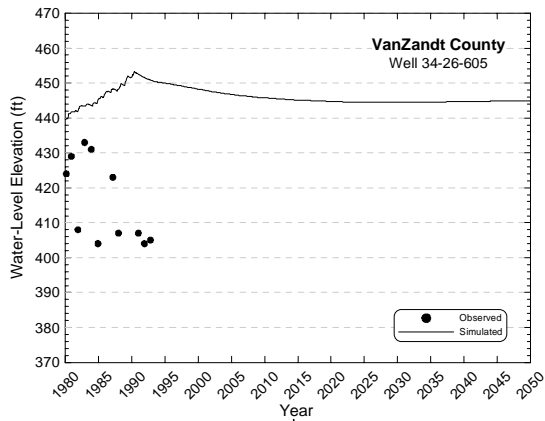


Figure 10.2.21 Selected hydrographs from predictive simulation to 2050, Layer 5 (middle Wilcox).

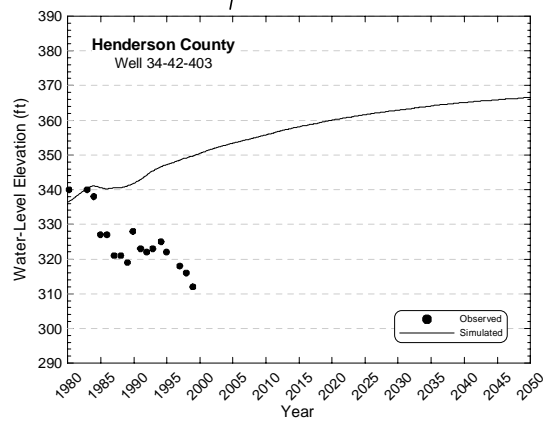
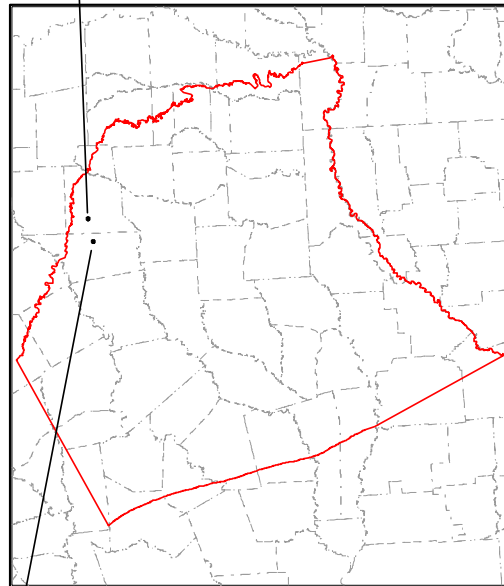
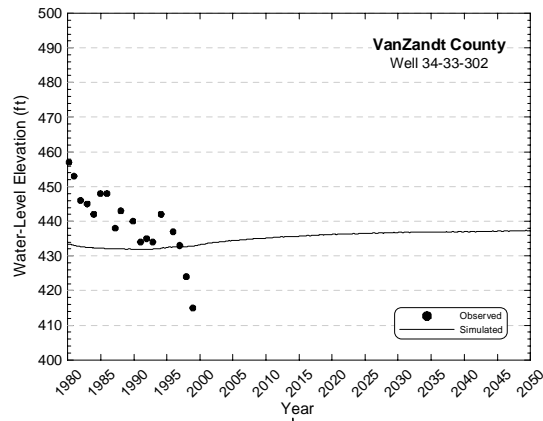


Figure 10.2.22 Selected hydrographs from predictive simulation to 2050, Layer 6 (lower Wilcox).

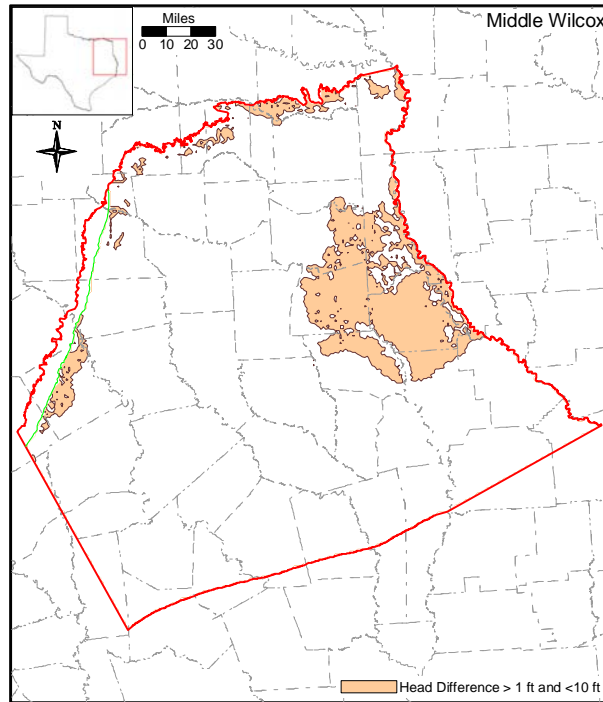
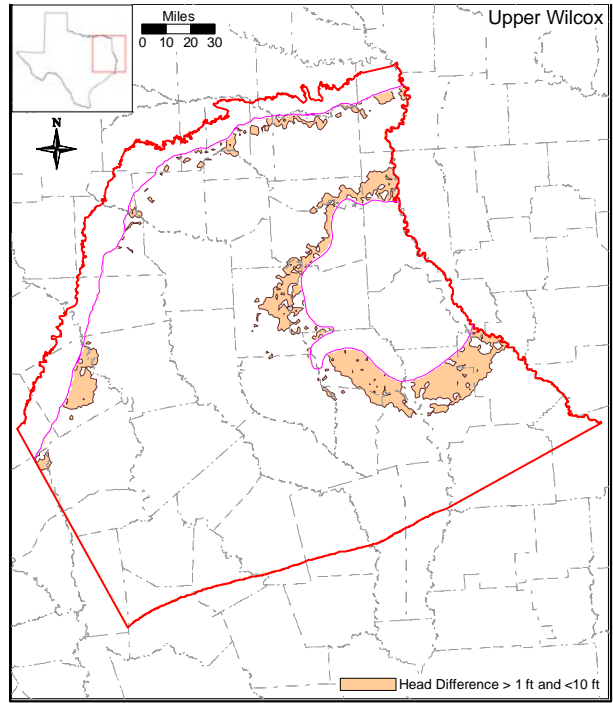
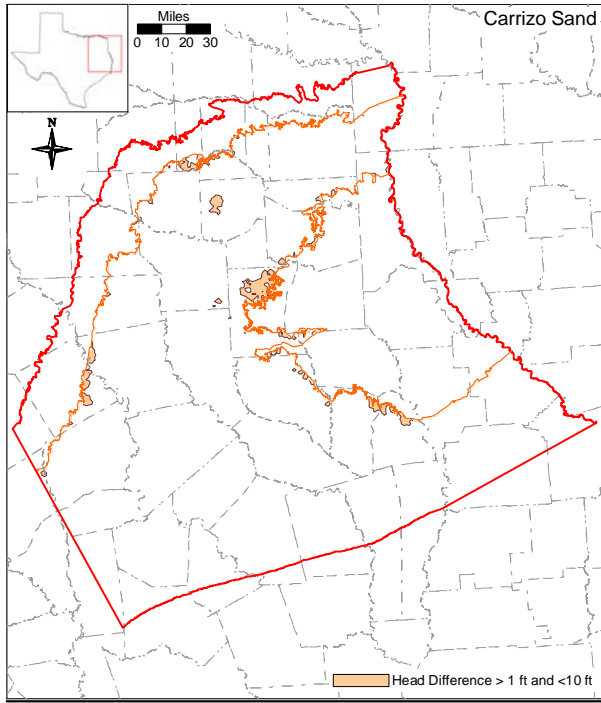


Figure 10.2.23 Simulated difference in head surfaces between the average condition 2050 simulation and the DOR 2050 simulation.

10.3 Predictive Simulation Water Budget

Table 10.3.1 shows the water budget for the predictive simulations. The table shows the water budget for the final year of each of the predictive simulations. Because the simulations ended in March (defined by the DOR), these balances are from March of the previous year to March of the given year. For example, the water budget for 2010 extends from March 2009 to March 2010. This accounts for the difference in mass balance between that in 1989 in the transient calibration (Table 9.2.3) and that for 1990 in Table 10.3.1. In general, the predictive simulation water budget shows similar trends and variations to that of the calibration/verification simulations. Table 10.3.1 shows an overall increase in pumpage from 1990 to 2050 by about 22,000 acre-ft/yr. However, the model shows an overall trend of water-level increase in the confined section. As with the calibration/verification simulations, the amount of leakance from the streams and from the reservoir can vary significantly through the predictive period. In all years shown in the table, the streams are gaining more water than they are losing. This is likely due to the DOR which has decreased the amount of flow in the streams to the point where the losing streams are not contributing as significantly to the aquifer. Also, comparing the 2050 run with average recharge with the DOR years shows the difference between average and drought condition recharge is approximately 1,000,000 AFY, or almost half of the average recharge. Groundwater evapotranspiration is also higher in the 2050 DOR simulation than in the 2050 average condition simulation.

Table 10.3.1 Water budget for predictive simulations. All rates reported in acre-ft/yr.

Year	Layer	GHBs	Reservoirs	Wells	ET	Top	Bottom	Recharge	Streams	Storage
1990	1	24,206	-17,888	-9,407	-176,757	0	-30,320	983,608	-129,799	-643,666
	2	0	-1,142	-663	-61,678	30,320	-40,904	250,299	-69,677	-106,558
	3	0	-2,722	-48,685	-43,220	40,904	-34,650	140,983	-29,403	-23,213
	4	0	-937	-43,862	-62,370	34,650	-23,027	467,050	4,072	-375,586
	5	0	41,390	-31,220	-71,461	23,027	-10,987	558,201	157,902	-666,875
	6	0	191,506	-6,230	-10,420	10,987	0	44,008	3,931	-233,783
	Sum		24,206	210,209	-140,068	-425,906	139,887	-139,887	2,444,149	-62,973
2000	1	21,827	-31,705	-13,077	-384,707	0	-30,573	743,951	-374,864	68,976
	2	0	-260	-756	-121,001	30,573	-42,172	181,594	-85,669	37,691
	3	0	-3,814	-48,158	-55,632	42,172	-30,912	89,770	-36,318	42,887
	4	0	-111,795	-38,661	-108,174	30,912	-22,027	335,803	-88,218	2,159
	5	0	-101,474	-39,868	-103,468	22,027	-9,229	444,656	-76,654	-136,006
	6	0	-15,778	-7,431	-17,512	9,229	0	35,351	-13,651	9,792
	Sum		21,827	-264,825	-147,951	-790,494	134,913	-134,913	1,831,124	-675,374
2010	1	19,723	-17,842	-17,025	-672,141	0	-28,014	626,227	-321,068	410,127
	2	0	-749	-617	-217,076	28,014	-37,949	184,523	-60,052	103,902
	3	0	-1,646	-29,707	-95,873	37,949	-38,450	89,396	-26,429	85,044
	4	0	-8,509	-45,772	-202,548	38,450	-25,822	285,072	-98,336	57,452
	5	0	-12,658	-46,078	-179,256	25,822	-6,532	304,350	-102,732	17,061
	6	0	4,165	-8,189	-22,338	6,532	0	23,302	-5,342	1,866
	Sum		19,723	-37,240	-147,388	-1,389,233	136,766	-136,766	1,512,870	-613,959
2020	1	18,610	-18,657	-17,956	-710,035	0	-27,414	630,882	-321,929	446,487
	2	0	-769	-632	-224,809	27,414	-37,449	184,969	-57,944	109,214
	3	0	-1,597	-29,059	-91,244	37,449	-36,597	90,343	-25,198	55,893
	4	0	-9,341	-45,902	-209,576	36,597	-26,167	280,353	-99,712	73,734
	5	0	-13,865	-46,400	-198,760	26,167	-6,292	303,379	-113,285	49,035
	6	0	3,512	-8,261	-23,765	6,292	0	23,229	-6,009	4,998
	Sum		18,610	-40,718	-148,211	-1,458,188	133,919	-133,919	1,513,155	-624,077
2030	1	17,808	-19,448	-19,189	-740,417	0	-27,650	638,113	-324,046	474,832
	2	0	-797	-655	-230,235	27,650	-37,678	183,433	-57,010	134,036
	3	0	-1,557	-30,182	-89,980	37,678	-35,048	93,564	-24,438	56,822
	4	0	-11,512	-47,184	-218,358	35,048	-25,651	272,298	-102,167	97,997
	5	0	-14,812	-46,615	-221,166	25,651	-5,893	303,797	-123,856	82,887
	6	0	3,044	-8,200	-24,960	5,893	0	23,040	-6,453	7,632
	Sum		17,808	-45,082	-152,026	-1,525,115	131,921	-131,921	1,514,244	-637,972
2040	1	17,263	-20,161	-20,428	-773,076	0	-27,566	644,140	-326,648	506,638
	2	0	-811	-674	-234,142	27,566	-38,309	183,534	-56,544	119,377
	3	0	-1,525	-31,345	-91,534	38,309	-34,236	91,794	-24,376	52,905
	4	0	-12,016	-48,838	-225,619	34,236	-24,822	268,146	-105,279	114,178
	5	0	-15,673	-47,486	-245,690	24,822	-5,607	304,276	-132,293	117,632
	6	0	2,746	-8,499	-26,050	5,607	0	23,046	-6,976	10,122
	Sum		17,263	-47,441	-157,271	-1,596,111	130,541	-130,541	1,514,936	-652,115
2050	1	16,946	-20,789	-21,867	-801,316	0	-28,595	647,445	-328,754	537,054
	2	0	-814	-698	-239,089	28,595	-39,912	183,152	-56,176	124,939
	3	0	-1,496	-33,145	-92,717	39,912	-32,548	94,187	-24,265	50,061
	4	0	-12,417	-49,620	-234,460	32,548	-23,874	263,481	-107,753	132,082
	5	0	-16,486	-47,940	-266,317	23,874	-5,446	303,680	-139,166	147,782
	6	0	2,555	-8,689	-26,963	5,446	0	23,046	-7,493	12,093
	Sum		16,946	-49,447	-161,959	-1,660,862	130,374	-130,374	1,514,992	-663,607
2050*	1	16,845	-31,132	-21,867	-522,404	0	-28,819	1,128,537	-356,746	-184,420
	2	0	-1,049	-698	-163,391	28,819	-39,946	278,946	-60,559	-42,129
	3	0	-2,179	-33,152	-70,189	39,946	-32,798	130,356	-25,359	-6,637
	4	0	-25,617	-49,620	-179,598	32,798	-24,350	421,602	-105,041	-70,190
	5	0	-27,427	-47,940	-208,075	24,350	-5,667	567,626	-161,333	-141,551
	6	0	1,245	-8,689	-23,882	5,667	0	54,651	-13,950	-15,048
	Sum		16,845	-86,159	-161,967	-1,167,539	131,581	-131,581	2,581,719	-722,987

*Does not include DOR.

11.0 LIMITATIONS OF THE MODEL

A model can be defined as a representation of reality that attempts to explain the behavior of some aspect of it, but is always less complex than the real system it represents (Domenico, 1972). As a result, limitations are intrinsic to models. Model limitations can be grouped into several categories including: (1) limitations in the data supporting a model, (2) limitations in the implementation of a model which may include assumptions inherent to the model application, and (3) limitations regarding model applicability. The limitations of this modeling study are discussed in the following consistent with the grouping provided above.

11.1 Limitations of Supporting Data

Developing the supporting database for a regional model at this scale and with this large a number of grid cells is a challenge. An adequate database was available from published sources for estimation of the structural surfaces for the Carrizo-Wilcox aquifer at the scale of the model. Because the model is at a regional scale, structural data will not have every bend and discontinuity found at a local scale.

Our discussion will now focus on the parameters which were found to be important in the sensitivity analyses and the quality of the targets used to assess calibration and verification. For the steady-state model, the primary parameters controlling model behavior are recharge and the hydraulic conductivity of the Wilcox. For the transient model, the primary parameters controlling model behavior are pumping, vertical hydraulic conductivity of the Reklaw, and horizontal hydraulic conductivity of the Wilcox and Carrizo. Recharge in the Carrizo-Wilcox aquifer has been studied by many investigators. Scanlon et al. (2002) provide a good summary of the available recharge estimates in the study area. Estimates of recharge for the Carrizo-Wilcox vary from less than an inch per year to up to five inches per year. The Northern Carrizo-Wilcox steady-state GAM provides a good means for estimating viable recharge estimates for the aquifer. However, because of the correlation between recharge and vertical conductance of the formations, recharge cannot be uniquely determined. The vertical conductance of the modeled aquifers can only be estimated regionally by models such as this GAM. The conundrum is that in the steady-state model, the vertical conductance of the aquifers is inversely related to recharge which means that unique determination of these two parameters is not

possible. To take advantage of this, we estimated recharge with a forward model (SWAT), and considered the spatial recharge distribution to be fixed for the most part, although we adjusted the overall magnitude during calibration. Estimates of recharge are important to the GAM modeling process because they provide a means of constraining the vertical conductance terms in the model especially when calibrating to steady-state and transient conditions. Studies should be continued into the nature of recharge in the Carrizo-Wilcox aquifer.

For the transient model, the most important parameter through the calibration process was the vertical conductivity of the Carrizo-Wilcox aquifer and the Reklaw Formation. When we completed calibration, the sensitivity analysis indicated that the most important parameters at the final calibration state were pumping and the horizontal hydraulic conductivities of the Carrizo and Wilcox layers. The pumping estimates were derived through a detailed process (see Appendices B and C). However, there are potential uncertainties in terms of the pumping volume and pumping allocation to the different layers. Industrial, agricultural, and rural pumping data are reported to the TWDB on a voluntary basis. The allocation of pumping to the different model layers is done by approximation and by correlation to the nearest wells, where no specific well information is available. Because the northern Carrizo-Wilcox aquifer is most heavily developed in the confined portion of the aquifer, errors in pumping rates have a significant impact on simulated water levels. Not unlike the situation with recharge and vertical conductance in the steady-state model, horizontal hydraulic conductivity and pumping are correlated parameters and unique determination of them is not possible. We modified horizontal conductivities for the Carrizo and upper Wilcox layers in certain areas as well as vertical conductivities of the confining Reklaw, though we could not find good evidence in the available hydrogeologic data for the adjustment.

The model also lacks horizontal hydraulic conductivity data for the Queen City and the Wilcox Group. This is especially true in the downdip confined portions of the aquifer, where there is limited data. Hydraulic conductivity data for the Carrizo is also lacking in the deeper portions of the aquifer. The model was sensitive to the Carrizo and Wilcox hydraulic conductivity. With improved control on hydraulic conductivity data in the confined portions of the aquifer, estimates of vertical conductance in the aquifer system would be better constrained.

The primary type of calibration target is hydraulic head. There is a general lack of heads representative of the predevelopment for all model layers. However, we believe the steady-state model is important for constraining the model calibration and accept the uncertainty in predevelopment conditions. Head calibration targets for the transient (historical model) are also lacking in some portions of the Wilcox and the Carrizo for the confined portions of the model. The model calibration could be improved with more head targets in these areas.

The other type of calibration target used was stream gain/loss estimates. There are limited stream gain/loss estimates in the model area. There were also a limited number of stream gages in the outcrop that were amenable to estimation of losses or gains through the study region. Because the MODFLOW stream routing package does not model runoff, direct comparison to stream gages is problematic. It would be beneficial if publicly available surface water models were developed for the outcrop regions in the study area. These would provide better estimates of the hydrography of the area and could be coupled with MODFLOW.

11.2 Limiting Assumptions

There are several assumptions that are key to the model regarding construction, calibration, and prediction. These are briefly discussed below with a discussion of the potential limitations of the assumption.

We modeled the lower boundary of the model as a no-flow boundary at the base of the Wilcox Group. This assumption is consistent with other regional models in the area and is probably a good assumption for the model in the overall sense. However, as the model moves to the outcrop, the no-flow nature of the base of the lower Wilcox creates some problems with recharge rates where the lower Wilcox is thin. This is not considered a significant limitation to the model since it causes only limited-area edge effects.

The lateral model boundaries were also modeled as no-flow boundaries. The western model boundary is the drainage divide between the Trinity and Brazos rivers and probably does not limit the model's performance in the west. We used a no-flow boundary because we assumed that the boundary provided a conservative reflective boundary as long as pumping west of the boundary was equal to or less than pumping east of the boundary. We reviewed the Central Carrizo-Wilcox GAM transient heads and concluded that drawdowns were not

significant enough to use a transient boundary condition for the historical period. The east boundary is the Red River and it is felt that any uncertainty in characterizing this boundary as no flow would be negligible with respect to simulated heads within Texas counties.

Another assumption used in our model is that the recharge estimated from SWAT was applicable to the region. As discussed earlier, modifications to the SWAT output were required for the Northern Carrizo-Wilcox GAM. We believe that the model provided preliminary regional estimates of recharge in the model region using physical models and parameters representative of the area. We did not model the interflow zone in SWAT. We used MODFLOW to reject recharge to the stream networks, which has its limitations due to the averaging of topography on a 1 by 1-mile grid scale. The steady-state simulation in MODFLOW encountered difficulties when ET approached or exceeded recharge, for which we had to make adjustments. This problem did not occur in the transient simulations.

In the predictive simulations, we assumed (in accordance with TWDB's GAM requirements) that the pumping estimates available from the Regional Water Planning Group database tables were representative of the future demands. In the model, the overall pumpage increased, but relative pumpage in different layers changed between the transient and predictive simulations, particularly between the Queen City and Carrizo-Wilcox, as discussed in Sections 4.7, 9.1 and 10. The apparent discrepancy causes drastic changes in water-level in the model predictions. Because the Queen City was not part of this GAM study, the potential problem with the pumpage allocation could not be resolved. However, this is being addressed in the GAM study for the Queen City and Sparta Aquifer.

Finally, our pumping demand estimates are based upon drought-of-record conditions. As a result, pumping does not increase at the end of each predictive simulation when the drought of record occurs. It is expected that we would see greater water level declines in the aquifer system as a whole if the pumping and climate (recharge) were impacted as a result of the drought of record.

11.3 Limits for Model Applicability

The model was developed on a regional scale and is only capable of predicting aquifer conditions at the regional scale. The model is applicable for assessing regional aquifer conditions resulting from groundwater development over a fifty-year time period.

The model itself was developed at a grid scale of one square mile. The model is not capable of being used in its current state to predict aquifer responses at specific points such as a particular well at a particular municipality. The aquifer is accurate at the scale of tens of miles which is adequate for understanding groundwater availability at the scale of the northern Carrizo-Wilcox aquifer.

The model is ideal for refinement for more local scale issues related to specific water resource questions. Questions regarding local drawdown to a well should be based upon analytical solutions to the diffusion equation or a refined numerical model. The GAM provides water levels representative of large volumes of aquifer (e.g., 5,280 ft X 5,280 ft X aquifer thickness in feet). The model was built to determine how regional water levels will respond to water resource development in an area smaller than a county and larger than a square mile.

The GAM model provides a first-order approach to coupling surface water to groundwater which is adequate for the GAM model purposes and for the scale of application. However, this model does not provide a rigorous solution to surface water modeling in the region and should not be used as a surface water modeling tool in isolation.

The GAM model does not simulate transport of solutes and cannot address explicitly water quality issues. The model also did not delineate specific regions within individual aquifer layers having potentially poor quality water not suitable as a groundwater resource. Only a preliminary assessment of water quality is given in the report.

12.0 FUTURE IMPROVEMENTS

To use models to predict future conditions requires a commitment to improve the model as new data becomes available or when modeling assumptions or implementation issues change. This GAM model is no different. Through the modeling process one generally learns what can be done to improve the model's performance or what data would help better constrain the model calibration. Future improvements to the model will be discussed below.

12.1 Supporting Data

Several types of data could be collected to better support the GAM model development process. These include recharge studies, surface water/groundwater studies and basic addition of stream gages, and water level monitoring in the confined portion of the Carrizo-Wilcox aquifer.

Estimates of recharge are important to the GAM modeling process because they provide a means of constraining the vertical hydraulic conductivity of the aquifer system when calibrating to steady-state and transient conditions. Studies should be continued into the nature of recharge in the Carrizo-Wilcox aquifer.

Surface water/groundwater interaction requires a good coverage of stream gages in the model outcrop areas, preferably immediately upstream and downstream of the outcrop areas. The model predicts that stream-aquifer interaction is significant in the model region. It would be beneficial if publicly available surface water models were developed for the outcrop regions in the study area. These would provide better estimates of the hydrography of the area and could be coupled with MODFLOW in future model improvement.

Additional water-level monitoring in the Wilcox Group and in deeper downdip portions of the Carrizo Formation is important for future model development. There are a limited number of Wilcox water-level measurements in the deeper downdip portions of the aquifer. Although the Wilcox may be non-potable in portions of the confined section, it is still advantageous to monitor water levels in these deep sections to improve aquifer understanding and to incorporate those additional data into the model. It is also important to increase water-level monitoring in areas that are potential areas of future development but which are currently not greatly developed. If monitoring begins prior to increased development, the GAM can be calibrated against the aquifer response to improve model predictive capability in those regions.

Currently, horizontal hydraulic conductivity data are limited for the Queen City Formation and the lower part of the Wilcox Group in the model area. This is especially true in some portions of the downdip confined section of the aquifer. Hydraulic conductivity data for the Carrizo is also lacking in the deeper, confined portions of the aquifer. Any additional hydraulic conductivity estimates and storativity estimates from pump tests will further help parameterize future improvements to this model.

12.2 Future Model Improvements

The lateral model boundaries were modeled as no-flow boundaries. We used a no-flow boundary along the western boundary because we assumed that the boundary provided a conservative reflective boundary as long as pumping east of the boundary was equal to or less than pumping west of the boundary. The applicability of this assumption along the western boundary should be reviewed with the finalization of the Central and Northern Carrizo-Wilcox GAMs. If a review of the final Central and Northern Carrizo-Wilcox GAM results indicates that the western boundary should be transiently applied as a head-dependent flow boundary, these changes can be made when the Queen City-Sparta aquifers are added to the model in the future.

Additional improvement of the model includes focus on refining the spatial hydraulic conductivities distribution for calibration and evaluation of the spatial recharge distribution in areas that indicate large variations. On the modeling side, the numerical problems during steady-state MODFLOW simulations in case of high ET rates relative to recharge rate needs to be examined for consistency with the transient behavior of the model.

The GAM model indicated the importance of pumping to the transient and predictive model results. The pumping data base developed based on the TWDB technical guidance as described in Appendices B and C needs to be improved. This requires identifying possible inconsistencies between different data sources and potential data gaps. Furthermore, the allocation of pumping to the different layers needs to be verified to improve consistency between the historical pumping data through 1999 and predictive pumping data starting in 2000.

13.0 CONCLUSIONS

This report documents a three-dimensional groundwater model developed for the northern Carrizo-Wilcox aquifer to the GAM standards defined by the TWDB. This regional scale model was developed using MODFLOW with the stream-routing package to simulate stream-aquifer interaction and the reservoir package to model groundwater interaction with lakes and reservoirs. The model divides the Carrizo-Wilcox aquifer into four layers: the Carrizo, and the upper, middle, and lower Wilcox. The Reklaw Formation and the Queen City Sand are also modeled as individual model layers.

The purpose of this GAM is to provide predictions of groundwater availability through the year 2050 based on current projections of groundwater demands during drought-of-record conditions. This GAM provides an integrated tool for the assessment of water management strategies to directly benefit state planners, Regional Water Planning Groups (RWPGs), and Groundwater Conservation Districts (GCDs).

This GAM has been developed using a modeling protocol which is standard to the groundwater model industry. This protocol includes: (1) the development of a conceptual model for groundwater flow in the aquifer, (2) model design, (3) model calibration, (4) model verification, (5) sensitivity analysis, (6) model prediction, and (7) reporting.

The model has been calibrated to predevelopment conditions (prior to significant resource use) which are considered to be at steady state. The steady-state model reproduces the predevelopment aquifer heads well and within the uncertainty in the head estimates. The median recharge rate estimated for the steady-state model was 0.93 inches per year. In the predevelopment model, recharge accounted for approximately 93% of the aquifer inflow and streams and ET discharged approximately 68% and 28% of the aquifer outflow, respectively. Approximately 3% of the aquifer inflowing water passed from the outcrop through to the confined aquifer and exited vertically through the GHBs in the southern part of the model. A sensitivity analysis was performed to determine which parameters had the most influence on aquifer performance and calibration. The two most sensitive parameters for the steady-state model were recharge, and to a lesser extent, horizontal hydraulic conductivities of the aquifer units and vertical conductivity of the confining stratum.

The model was also satisfactorily calibrated to transient aquifer conditions from 1980 through December 1989. The model did a good job of reproducing aquifer heads and available estimates of aquifer-stream interaction. The transient-calibrated model was verified by simulating to aquifer conditions from 1990 through December 1999. Again, the model satisfactorily simulated observed conditions. Regionally, the model reproduces model heads to within head target errors. A sensitivity analysis was performed on the transient model. The two most sensitive parameters for the transient model were pumping and the horizontal hydraulic conductivity of the Carrizo and Wilcox layers.

The net recharge to the aquifer (e.g., recharge minus ET) for the long-term average in the transient model is 0.93 inches per year, based on an average recharge of 2.59 inches/yr. This compares to a net recharge of 0.65 inches/yr for steady-state model, based on a total recharge of 0.93 inches/yr. The increased recharge amount during transient conditions may constitute rejected recharge during predevelopment conditions.

Model predictions were performed to estimate aquifer conditions for the next 50 years based upon projected pumping demands under drought-of-record (DOR) conditions as developed by the Regional Water Planning Groups. The model indicated a noticeable rebound of the cones of depression in the confined section. Predictive pumping data indicated some reallocation of pumping to different aquifer layers in some counties during the transition from the historical period to the predictive period, which accounts for much of the simulated responses in the hydraulic head surfaces. The simulations incorporating the DOR conditions at the end of the predictive periods show relatively small head declines that are limited to the outcrop and shallow confining section of the Carrizo-Wilcox aquifer. This is due to the fact that the DOR only considers climatic conditions (e.g., recharge), but not the potential increase in pumping.

This model, like all models, has limitations and can be improved. The GAM reproduced the steady-state (predevelopment) and transient (historical) conditions of the aquifer within the given calibration measures. More importantly, this calibrated GAM provides a documented, publicly-available tool for the assessment of future groundwater availability on a regional scale in the northern Carrizo-Wilcox aquifer.

14.0 ACKNOWLEDGEMENTS

The Northern Carrizo-Wilcox GAM was developed with the participation of a group of stakeholders representing varied interests within the model region. Interaction with these stakeholders was performed through a series of Stakeholder Advisory Forums (SAF) held across the model region. In these meetings, stakeholders were solicited for data and were provided updates on a regular basis beginning in spring 2001. The model described in this report has benefited from the stakeholders involvement and interest. In addition, we would like to specifically thank those members of the SAF who have hosted meetings across the model region.

We would also like to thank the TWDB GAM staff led by Robert Mace for their support during this modeling exercise. We also would like to thank Sanjeev Kalaswad who has managed our contract with professionalism. The GAM has benefited significantly from input from the TWDB staff during the scheduled technical review meetings as well as additional meetings held to address key technical challenges, and from the detailed review comments provided by TWDB staff on the Draft Final Report.

We greatly appreciate the interest and hospitality of the various SAF groups in the Northern Carrizo-Wilcox GAM region who provided meeting rooms for the SAF meetings and offered input during the GAM development and valuable comments on the draft report. Our senior external experts, Dr. Graham Fogg from the University of California, Davis, and Dr. Steven Gorelik from Stanford University shared valuable insights into various aspects of numerical modeling and provided crucial review and support during the development of the Northern Carrizo-Wilcox GAM. We would also like to thank Jeannie Gibbs of INTERA for her efforts in compiling and organizing the tremendous amount of data collected for this study and her GIS support. Finally, we would like to thank Judy Ratto of INTERA for her efforts above and beyond the call of duty in developing this report.

15.0 REFERENCES

- Alexander, W.H., and D.E. White, 1966. Ground-water resources of Atascosa and Frio Counties, Texas. Texas Water Development Board, Report 32.
- Anders, R.B., 1967. Ground-water resources of Sabine and San Augustine Counties, Texas. Texas Water Development Board, Report 37.
- Anderson, M.P., and W.W. Woessner, 1992. Applied Groundwater Modeling. Academic Press, San Diego, CA, 381 p.
- Ashworth, J.B., and J. Hopkins, 1995. Aquifers of Texas. Texas Water Development Board, Report 345.
- Ayers, W.B., Jr., and A.H. Lewis, 1985. The Wilcox Group and Carrizo Sand (Paleogene) in East-Central Texas: Depositional systems and deep-basin lignite: The University of Texas at Austin, Bureau of Economic Geology Special Publication, 19p., 30 pls.
- Baker, E.T., Jr., and C.R. Follett, 1974. Ground-water resources of Grimes County, Texas. Texas Water Development Board, Report 186.
- Bebout, D.G., B.R. Weise, A.R. Gregory, and M.B. Edwards, 1982. Wilcox sandstone reservoirs in the deep subsurface along the Texas Gulf Coast: their potential for production of geopressured geothermal energy: The University of Texas at Austin, Bureau of Economic Geology Report of Investigations No. 117, 125 p.
- Borrelli, J., C.B. Fedler, and J.M. Gregory, 1998. Mean crop consumptive use and free-water evaporation for Texas. Report for TWDB Grant 95-483-137. Feb. 1, 1998.
- Broom, M.E., 1968. Ground-water resources of Wood County, Texas. Texas Water Development Board, Report 79.
- Broom, M.E., 1969. Ground-water resources of Gregg and Upshur Counties, Texas. Texas Water Development Board, Report 101.
- Broom, M.E., 1971. Ground-water resources of Cass and Marion Counties, Texas. Texas Water Development Board, Report 135.

- Broom, M.E., and B.N. Myers, 1966. Ground-water resources of Harrison County, Texas. Texas Water Development Board, Report 27.
- Broom, M.E., W.H. Alexander, Jr., and B.N. Myers, 1965. Ground-water resources of Camp, Franklin, Morris and Titus Counties, Texas. Texas Water Commission, Bulletin 6517.
- Brune, G., 1975. Major and historical springs of Texas. Texas Water Development Board, report 189.
- Brune, G., 1981. Springs of Texas, Volume I. Branch-Smith, Inc.
- Bureau of Economic Geology (BEG), 1996. River Basin Map of Texas. Bureau of Economic Geology, The University of Texas at Austin.
- Chiang, W.-H., and W. Kinzelbach, 1998. Processing Modflow- A simulation system for modeling groundwater flow and pollution: software manual, 325 p.
- de Marsily, G., 1986. Quantitative Hydrogeology, Groundwater Hydrology for Engineers. Academic Press, Orlando, FL, p. 440.
- Dillard, J.W., 1963. Availability and quality of ground water in Smith County, Texas. Texas Water Commission, Bulletin 6302.
- Domenico, P.A., 1972. Concepts and Models in Groundwater Hydrology. McGraw-Hill, New York.
- Domenico, P.A. and F.W. Schwartz, 1990. Physical and Chemical Hydrology: John Wiley & Sons, New York, 824 p.
- Deussen, A., 1914. Geology and Under Ground Waters of the Southeastern Part of the Texas Coastal Plain. USGS Water Supply Paper 335.
- Duffin, G.L., and G.R. Elder, 1979. Variations in specific yield in the outcrop of the Carrizo Sand in South Texas as estimated by seismic refraction. Texas Department of Water Resources, Report 229.
- Dutton, A.R., 1990. Vadose-zone recharge and weathering in an Eocene sand deposit, East Texas, U.S.A. Journal of Hydrology, v. 114, p. 93 – 108.

- Dutton, A.R., 1999. Groundwater availability in the Carrizo-Wilcox aquifer in Central Texas – numerical simulations of 2000 through 2050 withdrawal projections. The University of Texas at Austin, Bureau of Economic Geology, Report of Investigations No. 256.
- Edwards, D.C., and T.B. McKee, 1997. Characteristics of 20th Century drought in the United States at multiple time scales. Climatology Report Number 97-2, Colorado State University, Fort Collins, Colorado.
- Fenske, J.P., S.A. Leake, and D.E. Prudic, 1996. Documentation of a computer program (RESI) to simulate leakage from reservoirs using the modular finite-difference ground-water flow model (MODFLOW). U.S. Geological Survey, Open-File Report 96-364.
- Fisher, W.L., 1969. Facies characterization of Gulf Coast basin delta systems, with some Holocene analogues. Transactions – Gulf Coast Association of Geological Sciences, Volume XIX, p. 239 – 261.
- Fisher, W.L., and J.H. McGowen, 1967. Depositional systems in the Wilcox Group of Texas and their relationship to occurrence of oil and gas. Transactions-Gulf Coast Association of Geological Societies, Vol. XVII.
- Fogg, G.E., 1986. Groundwater flow and sand-body interconnectedness in a thick, multiple-aquifer system: Water Resources Research, v. 22, no. 5, p. 679-694.
- Fogg, G.E., 1989. Stochastic analysis of aquifer interconnectedness: Wilcox Group, Trawick area, East Texas: The University of Texas at Austin, Bureau of Economic Geology, Report of Investigations No. 189, 68 p.
- Fogg, G.E., and W.R. Kaiser, 1986. Regional hydrogeologic considerations for deep-basin lignite development in Texas, *in* Kaiser, W. R., and others, Geology and ground-water hydrology of deep-basin lignite in the Wilcox Group of East Texas: The University of Texas at Austin, Bureau of Economic Geology Special Publication, p. 57-59.
- Fogg, G.E., and C.W. Kreitler, 1982. Ground-water hydraulics and hydrochemical facies in Eocene aquifers of the East Texas Basin: The University of Texas at Austin, Bureau of Economic Geology Report of Investigations No. 127, 75 p.

- Fogg, G.E., S.J. Seni, and C.W. Kreitler, 1983. Three-dimensional ground-water modeling in depositional systems, Wilcox Group, Oakwood salt dome area, east Texas. The University of Texas at Austin, Bureau of Economic Geology Report of Investigations No. 133, 55 p.
- Follett, C.R., 1981. Ground-water resources of Bastrop County, Texas. Texas Water Development Board, Report 109.
- Freeze, R.A., 1969. The mechanism of natural ground-water recharge and discharge. 1. One-dimensional, vertical, unsteady, unsaturated flow above a recharging or discharging ground-water flow system: *Water Resources Research*, Vol. 5, No. 1, p. 153-171.
- Freeze, R.A., 1971. Three-dimensional, transient, saturated-unsaturated flow in a groundwater basin: *Water Resources Research*, Vol. 7, No. 2, p. 347-366.
- Freeze, R.A., 1975. A stochastic-conceptual analysis of one-dimensional ground-water flow in nonuniform homogeneous media: *Water resources Research*, Vol. 11, No. 5, p. 679-694.
- Freeze, R.A., and J.A. Cherry, 1979. *Groundwater*: Prentice-Hall, Inc., New Jersey, 604 p.
- Galloway, W.E., X. Liu, D. Travis-Neuberger, and L. Xue, 1994. References high-resolution correlation cross sections, Paleogene section, Texas Coastal Plain. The University of Texas at Austin, Bureau of Economic Geology.
- Garza, S., 1975. Simulated effects of the proposed Tennessee Colony Reservoir on ground-water conditions in the Carrizo-Wilcox aquifer and Trinity River alluvium, Texas. IAHS Publication No. 117, p. 597-605.
- Grubb, H.F., 1997. Summary of hydrology of the regional aquifer systems, Gulf Coastal Plain, south-central United States. U.S. Geological Survey, Professional Paper 1416-A.
- Guevara, E.H., and R. Garcia, 1972. Depositional systems and oil-gas reservoirs in the Queen City Formation (Eocene), Texas. *Gulf Coast Association of Geological Societies, Transactions*, v. 22, p. 1-22.
- Gutjahr, A.L., L.W. Gelhar, A.A. Bakr, and J.R. MacMillan, 1978. Stochastic analysis of spatial variability in subsurface flows -2, Evaluation and application. *Water Resources Research*, v. 14, no. 5, p. 953-959.

- Hamlin, H.S., 1988. Depositional and ground-water flow systems of the Carrizo-Upper Wilcox, South Texas. The University of Texas at Austin, Bureau of Economic Geology, Report of Investigations No. 175.
- Harbaugh, A.W., and M.G. McDonald, 1996. User's documentation for MODFLOW-96, an update to the U.S. Geological Survey modular finite-difference ground-water flow model: U.S. Geological Survey Open-File Report 96-485, 56 p.
- Harden and Associates, Inc., 2000. Brazos G Regional Water Planning Area, Carrizo-Wilcox ground water flow model and simulations results.
- Hayes, M., 2001. Drought Indices. National Drought Mitigation Center, Available online at <http://enso.unl.edu/ndmc/enigma/indices.htm>.
- HDR Engineering, Inc., 2000. Preliminary feasibility options to deliver ALCOA/CPS groundwater to Bexar County. Technical report prepared for San Antonio Water Systems.
- Helm, D.C., 1976. One-dimensional simulation of aquifer system compaction near Pixley, California - 2, Stress-dependent parameters, Water Resources Research, Vol. 12, No. 3, p. 375-391.
- Henry, C.D., J.M. Basciano, and T.W. Duex, 1980. Hydrology and water quality of the Eocene Wilcox Group; significance for lignite development in East Texas: The University of Texas at Austin, Bureau of Economic Geology Geological Circular 80-3,9p.
- Hibbs, B.J., and J.M. Sharp, Jr., 1991. Evaluation of underflow and the potential for instream flow depletion of the lower Colorado River by high capacity wells in adjoining alluvial systems : final report for the Lower Colorado River Authority, Water Resources Division, 126p.
- Isaaks, E.H., and R.M. Srivastava, 1989. An Introduction to Applied Geostatistics. Oxford University Press, New York.
- Kaiser, W.R., 1974. Texas lignite: near-surface and deep-basin resources: The University of Texas at Austin, Bureau of Economic Geology Report of Investigations No. 79, 70 p.

- Kaiser, W.R., 1978. Depositional systems in the Wilcox Group (Eocene) of east-central Texas and the occurrence of lignite, *in* Kaiser, W.R., ed., Proceedings, 1976 Gulf Coast Lignite Conference: geology, utilization, and environmental aspects. The University of Texas at Austin, Bureau of Economic Geology, Report of Investigations No. 90.
- Kaiser, W.R., 1990. The Wilcox Group (Paleocene-Eocene) in the Sabine Uplift area, Texas: Depositional systems and deep-basin lignite: The University of Texas at Austin, Bureau of Economic Geology Special Publication, 20p.
- Kaiser, W.R., J.E. Johnston, and W.N. Bach, 1978. Sand-body geometry and the occurrence of lignite in the Eocene of Texas. The University of Texas at Austin, Bureau of Economic Geology, Geological Circular 78-4, 19 p.
- Kaiser, W.R., M.L. Ambrose, W.B. Ayers, Jr., P.E. Blanchard, G.F. Collins, G.E. Fogg, D.L. Gower, C.L. Ho, C.S. Holland, M.L.W. Jackson, C.M. Jones, A.H. Lewis, G.L. Macpherson, C.A. Mahan, A.H. Mullin, D.A. Prouty, S.J. Tewalt, and S.W. Tweedy, 1986. Geology and ground-water hydrology of deep-basin lignite in the Wilcox Group of East Texas: The University of Texas at Austin, Bureau of Economic Geology Special Publication, 182 p.
- Klemt, W.B., G.L. Duffin, and G.R. Elder, 1976. Ground-water resources of the Carrizo aquifer in the Winter Garden area of Texas, Volume 1: Texas Water Development Board, Report 210.
- Kuiper, L.K., 1985. Documentation of a numerical code for the simulation of variable density ground-water flow in three dimensions. U.S. Geological Survey, Water-Resources Investigations Report 84-4302.
- LBG-Guyton Associates and HDR Engineering Inc., 1998. Interaction between ground water and surface water in the Carrizo-Wilcox aquifer.
- Ludwig, A.H., 1972. Water resources of Hempstead, Lafayette, Little River, Miller, and Nevada Counties, Arkansas. U.S. Geological Survey Water-Supply Paper 1998.
- Mace, R.E., R.C. Smyth, L. Xu, and J. Liang, 2000a. Transmissivity, hydraulic conductivity, and storativity of the Carrizo-Wilcox Aquifer in Texas, The University of Texas at

- Austin, Bureau of Economic Geology Final Report submitted to the Texas Water Development Report, 76p.
- Mace, R.E., A.H. Chowdhury, R. Anaya, and S.-C. Way, 2000b. Groundwater availability of the Middle Trinity aquifer in the Hill Country area of Texas – Numerical simulations through 2050: Texas Water Development Board Report, 174p.
- Maidment, D.R., 1992. Handbook of Hydrology. McGraw-Hill, Inc.
- McDonald, M.G., and A.W. Harbaugh, 1988. A modular three-dimensional finite-difference ground-water flow model. U.S. Geological Survey, Techniques of Water-Resources Investigations, book 6, chapter A1.
- McKee, T.B., N.J. Doesken, and J. Kleist, 1993. The relationship of drought frequency and duration to time scales. Preprints, 8th Conference on Applied Climatology, 17-22 January, Anaheim, CA, pp. 179-184.
- Newcome, R., Jr., L.V. Page, and R. Sloss, 1963. Water resources of Natchitoches Parish, Louisiana. State of Louisiana Dept. of Conservation Geological Survey and Dept. of Public Works, Water Resources Bulletin No. 4.
- Opfel, W.J., and G.R. Elder, 1978. Results of an infiltration study on the Carrizo Sand outcrop in Atascosa County, Texas. Texas Department of Water Resources, LP-61.
- Page, L.V., and H.G. May, 1964. Water resources of Bossier and Caddo Parishes, Louisiana. State of Louisiana Dept. of Conservation Geological Survey and Dept. of Public Works, Water Resources Bulletin No. 5.
- Page, L.V., R. Newcome, Jr., and G.D. Graeff, Jr., 1963. Water resources of Sabine Parish, Louisiana. State of Louisiana Dept. of Conservation Geological Survey and Dept. of Public Works, Water Resources Bulletin No. 3.
- Payne, J.N., 1975. Geohydrologic significance of lithofacies of the Carrizo Sand of Arkansas, Louisiana, and Texas and the Meridian Sand of Mississippi: U.S. Geological Survey Professional Paper, P 0569-D, 11p.
- Peckham, R.C., 1965. Availability and Quality of Ground Water in Leon County, Texas. Texas Water Commission, Bulletin 6513.

- Popkin, B.P., 1971. Ground-Water Resources of Montgomery County, Texas Water Development Board, Report 136.
- Prudic, D.E., 1988. Documentation of a computer program to simulate stream-aquifer relations using a modular, finite-difference, ground-water flow model, U.S. Geological Survey, Open-File Report 88-729, Carson City, Nevada.
- Prudic, D.E., 1991. Estimates of hydraulic conductivity from aquifer-test analyses and specific capacity data, gulf coast regional aquifer systems, south-central United States., U.S. Geological Survey, Water- Resources Investigation Report 90-4121, Austin, Texas.
- Rettman, P.L., 1984. Ground-water resources of Limestone County, Texas. USGS Open-File Report 84-713.
- Ritchey, J.D., and J.O. Rumbaugh, 1996. Subsurface fluid flow (ground-water and vadose zone) modeling. ASTM Special Technical Publication 1288.
- Ryder, P.D., 1988. Hydrogeology and predevelopment flow in the Texas Gulf Coast aquifer systems. USGS Water-Resources Investigations Report 87-4248.
- Ryder, P.D., and A.F. Ardis, 1991. Hydrology of the Texas Gulf Coast aquifer systems. U.S. Geological Survey, Open-File Report 91-64.
- Sandeen, W.M., 1968. Ground-water resources of San Jacinto County, Texas. Texas Water Development Board, Report 80.
- Sandeen, W.M., 1987. Ground-water resources of Rusk County, Texas. Texas Water Development Board, Report 297.
- Scanlon, B.R., A. Dutton, and M. Sophocleus, 2002. Groundwater recharge in Texas.
- Slade, R.M., Jr., J.T. Bentley, and D. Michaud, 2002. Results of streamflow gain-loss studies in Texas, with emphasis on gains from and losses to major and minor aquifers, Texas, 2000. U.S. Geological Survey, Open-File Report 02-068.
- Tarver, G.E., 1966. Ground-water resources of Houston County, Texas. Texas Water Development Board, Report 18.
- Tarver, G.R., 1968a. Ground-water resources of Polk County, Texas. Texas Water Development Board, Report 82.

- Tarver, G.R., 1968b. Ground-water resources of Tyler County, Texas. Texas Water Development Board, Report 74.
- Texas Water Development Board (TWBD), 1972. Survey of the subsurface saline water of Texas, Report 157.
- Texas Water Development Board (TWBD), 1997. Water for Texas, A consensus-based update to the State Water Plan, Volume II, Technical Planning Appendix, August 1997, Document No. GP-6-2.
- Texas Water Development Board (TWBD), 2002. Water for Texas – 2002. Document No. GP-7-1.
- Texas Water Development Board (TWBD), unpublished. East-Texas Model.
- Theis, C. V., 1940. The source of water derived from wells - essential factors controlling the response of an aquifer to development: Civil Engineering, American Society of Civil Engineers, p. 277-280.
- Thompson, G.L., 1972. Ground-water resources of Navarro County, Texas: Texas Water Development Board Report 160, 63p.
- Thorkildsen, D., and R.D. Price, 1991. Ground-water resources of the Carrizo-Wilcox aquifer in the central Texas region: Texas Water Development Board Report 332, 59p.
- Thorkildsen, D., R. Quincy, and R. Preston, 1989. A digital model of the Carrizo-Wilcox aquifer within the Colorado River Basin of Texas. Texas Water Development Board, LP-208.
- Turner, S.F., T.W. Robinson, and W.N. White, revised by D.E. Outlaw, W.O. George, and others, 1960. Geology and ground-water resources of the Winter Garden District Texas, 1948. USGS Water-Supply Paper 1481.
- Warren, J.E., and H.S. Price, 1961. Flow in heterogeneous porous media, Society of Petroleum Engineers Journal, Vol. 1, p. 153-169.
- Wesselman, J.G., 1967. Ground-water resources of Jasper and Newton Counties, Texas. Texas Water Development Board, Report 59.
- White, D.E., 1973. Ground-water resources of Rains and Van Zandt Counties, Texas. Texas Water Development Board, Report 169.

- William F. Guyton & Associates, 1970. Ground-water conditions in Angelina and Nacogdoches Counties, Texas. Texas Water Development Board, Report 110.
- William F. Guyton & Associates, 1972. Ground-water conditions in Anderson, Cherokee, Freestone, and Henderson Counties, Texas. Texas Water Development Board, Report 150.
- Williams, T.A., and A.K. Williamson, 1989. Estimating water-table altitudes for regional ground-water flow modeling. U.S. Gulf Coast: National Water Well Association, Ground Water, v. 27, no. 3, p. 333-340.
- Williamson, A.K., H.F. Grubb, and J.S. Weiss, 1990. Ground-water flow in the Gulf Coast aquifer systems, South Central United States – A preliminary analysis. U.S. Geological Survey, Water-Resources Investigations Report 89-4071.
- Wilson, T.A., and R.L. Hossman, 1988. Geophysical well-log data base for the Gulf Coast aquifer systems, south-central United States. U.S. Geological Survey, Open-File Report 87-677.
- Winslow, A.G., 1950. Geology and Ground-water resources of Walker County, Texas. Texas Board of Water Engineers, Bulletin 5003.

APPENDIX A

Brief Summary of the Development of the Carrizo-Wilcox Aquifer in Each County and List of Reviewed Reports

Anderson County, Texas

Little information related to the historical development of the Carrizo Sand and the Wilcox Group in Anderson County was found during the literature review. The Carrizo Sand and the sands of the Wilcox Group are considered to be separate aquifers in this county, with the Wilcox aquifer being the most important water-bearing formation (William F. Guyton & Associates, 1972). Deussen (1914) states that pressures in the lower Eocene sand were sufficient to drive water to the ground surface only in low lying areas along streams in this county. Fourteen wells completed in the Carrizo Sand only, the Wilcox Group only, and in both the Carrizo Sand and the Wilcox Group were found to flow between 1960 and 1970 (William F. Guyton & Associates, 1972). Flows in some of the wells were as high as 200 to 500 gpm.

The earliest date given on the TWDB website¹ for completion of a well to the Carrizo Sand in Anderson County is 1927. The earliest water-level measurements are from 1938. Only two wells were completed in the Carrizo Sand at the time of the first water-level measurement. Based on an evaluation of maximum measured water levels regardless of time, the early measurements in the Carrizo Sand appear to reflect pumping effects. Therefore, the earliest measurement is not considered to be representative of predevelopment conditions.

The earliest date given on the TWDB website for completion of a well to the Wilcox Group in Anderson County is 1929. The first water-level measurement was taken in this well also in 1929. Deussen (1914) lists two wells completed to the Wilcox Group in the late 1800s. These wells are not included in the data provided on the TWDB website. Since the first water-level measurement was taken at the time the first well was drilled, that measurement is considered to be representative of predevelopment conditions.

Fogg and Kreidler (1982) observed a local high in the water-level elevation in both the Carrizo Sand and the Wilcox Group in north central Anderson County near a topographic high. They attribute this high to “high topography supplying the downward-driving force and to disruption of overlying aquitards by faults associated with Concord Dome.”

¹ <http://rio.twdb.state.tx.us/publications/reports/GroundWaterReports/GWDatabaseReports/GWdatabaserpt.htm>

Angelina County, Texas

Little information related to the historical development of the Carrizo Sand and the Wilcox Group in Angelina County was found during the literature review. Unless stated otherwise, the following discussion comes from William F. Guyton & Associates (1970). The Carrizo Sand and the sands of the Wilcox Group are considered to be separate aquifers in this county, with the Carrizo aquifer being the most productive. Of the total amount of water removed from the Carrizo Sand and the sands of the Wilcox group in the county, the percentage obtained from the Wilcox is very low (less than 1 percent in 1968). The Carrizo aquifer has been developed extensively in this county since the late 1930s by the city of Lufkin and by the Southland Paper Mills located north-northeast of Lufkin near the border between Angelina and Nacogdoches Counties. Suitable groundwater wells did not operate near Lufkin until 1935 when a test well was drilled to the Carrizo aquifer (White et al., 1941). Scalapino (1963) states that the areas of largest development of water from the Carrizo Sand are the Lufkin area, which includes water used by the cities of Lufkin and Nacogdoches and by the Southland Paper Mills, and the Winter Garden Area located in the southern Carrizo-Wilcox GAM. Flowing wells were observed in southern Nacogdoches County and northern Angelina County in the 1940s, but by 1961 most of those wells had stopped flowing (Baker et al., 1963). Extensive pumpage from the Carrizo since 1939 has resulted in drawdowns of up to 500 ft at pumping centers. Deussen (1914) states that several wells in the northwestern portion of the county flowed; one located near the city of Platt and the other located west of the city of Lufkin.

The earliest dates given on the TWDB website for wells completed to the Carrizo Sand in Angelina County are 1922 and 1935. The earliest water-level measurements are from 1939 (nine measurements). About two wells were completed to the Carrizo Sand prior to the time of these measurements which correspond to times when additional wells were drilled. Therefore, the earliest water-level measurements are considered to represent predevelopment conditions.

The earliest date given on the TWDB website for a well completed to the Wilcox Group in Angelina County is 1941. The earliest water-level measurement is from 1941. This early measurement reflected the effects of pumpage and was not considered representative of predevelopment conditions.

Bowie County, Texas

Information regarding historical development of the Wilcox Group in Bowie County could not be found during the literature search. The Wilcox Group outcrops in the lower third to half of the county. The Carrizo Sand is not found in Bowie County. The earliest completion date given on the TWDB website is 1910 for wells completed in the sands of the Wilcox Group. The earliest water-level measurement was made in 1973 based on the data on the TWDB website. As a result, all water-level measurements for the Wilcox in Bowie County appeared to be effected by pumpage and are not considered representative of predevelopment conditions.

Caddo Parish, Louisiana

Little information related to the historical development of the Carrizo Sand and the Wilcox Group in Caddo Parish was found during the literature review. Unless stated otherwise, the following discussion comes from Page and May (1964). The Carrizo Sand and the sands of the Wilcox Group are considered to be separate aquifers in this parish. The Wilcox aquifer is the principal source of groundwater in Caddo Parish. Of the total amount of groundwater removed from the Carrizo aquifer and the Wilcox aquifer in the parish, the percentage obtained from the Carrizo is very low. The cities of Shreveport and Bossier City used water from the Wilcox aquifer until surface-water supplies were developed from 1926-1928. Some pumpage for industrial purposes was reported for 1941. In 1962, the dominate users of groundwater from the Wilcox aquifer were municipalities and rural residences.

The first well completed to the Wilcox aquifer in Caddo Parish was drilled in 1900 (LaDOT, website²). About 11 additional wells were drilled from 1910 to 1920. The earliest available water levels are one measurement in 1921 and one measurement in 1923 (LaDOT, website). Since several wells had been completed to and pumping from the Wilcox aquifer at the time of the earliest water level measurements, those measurements are not considered to be representative of predevelopment conditions.

² <http://www2.dotd.state.la.us/wells/wells.html>

Camp County, Texas

Little information related to the historical development of the Carrizo Sand and the Wilcox Group in Camp County was found during the literature review. Broom et al. (1965) state that the sands of the Wilcox Group, the Carrizo Sand, the Reklaw Formation, and the Queen City Sand are hydraulically connected and act as a single aquifer which they refer to as the Cypress aquifer. No flowing wells are reported in Broom et al. (1965). No general decline in water levels for shallow wells (less than 60 ft deep) has been observed (Broom et al., 1965). Broom et al. (1965) state, “Water levels in the heavily-pumped deeper wells show average declines of 3.5 to 15.7 feet per year for various periods of record.”

The earliest completion date given on the TWDB website for a well completed in the Cypress aquifer in Camp County is 1896. Several additional wells were drilled in the early 1900s. The first water-level measurements were taken in 1934. About eight wells were completed to the Cypress aquifer at the time of these measurements. As a result, the early measurements are not considered to be representative of predevelopment conditions.

Cass County, Texas

Little information related to the historical development of the Carrizo Sand and the Wilcox Group in Cass County was found during the literature review. Broom (1971) states that the sands of the Wilcox Group, the Carrizo Sand, the Reklaw Formation, and the Queen City Sand are hydraulically connected and act as a single aquifer which he refers to as the Cypress aquifer. Several wells completed in the Cypress aquifer were found to flow in 1967/1968 (Broom, 1971). Broom (1971) states the following regarding water-level changes in Cass County,

“Available data indicate that water levels in the artesian section of the [Cypress] aquifer have declined considerably in areas where the aquifer is heavily pumped. In the Bryans Mill area, water levels have declined as much as 86 feet since 1961. In the Atlanta area, water levels have declines as much as 100 feet since 1936, and in parts of the Rodessa oil field, water levels have declined as much as 109 feet since about 1964. Elsewhere in the report area [Cass and Marion Counties], water levels show no appreciable changed during the period of record.”

The earliest completion date given on the TWDB website for a well in the Cypress aquifer in Cass County is 1901. The first water-level measurements, taken in 1936, appear to reflect pumpage effects. Therefore, the earliest measurements are not considered to be representative of predevelopment conditions.

Cherokee County, Texas

Little information related to the historical development of the Carrizo Sand and the Wilcox Group in Cherokee County was found during the literature review. The Carrizo Sand and the sands of the Wilcox Group are considered to be separate aquifers in this county, with the Wilcox aquifer being the most important water-bearing formation (William F. Guyton & Associates, 1972). The area where the lower Eocene reservoir flows in Cherokee county is "...confined entirely to the valleys..." (Deussen, 1914). No wells completed in either the Carrizo Sand or the Wilcox Group were found to flow by William F. Guyton & Associates (1972).

The earliest date given on the TWDB website for a well completed to the Carrizo Sand in Cherokee County is 1900. The earliest water-level measurements are from 1929 (1 measurement) and 1936 (13 measurements). These early measurements reflect the effects of pumping and are not considered representative of predevelopment conditions.

The earliest date given on the TWDB website for wells completed to the Wilcox Group in Cherokee County is 1935. The earliest water-level measurement is not until 1954. Because all of the available water-level data for the Wilcox Group, including the earliest measurements, reflect the effects of pumpage, none of the water-level measurements were considered to be representative of predevelopment conditions.

DeSoto Parish, Louisiana

No information related to historical development of the Carrizo Sand and Wilcox Group in DeSoto Parish was found during the literature review. The first wells completed to the Wilcox aquifer in this parish were drilled in 1900 (LaDOT, website). The earliest available water levels are one measurement in 1927 and one measurement in 1938 (LaDOT, website). At the time of the first water-level measurement, approximately 20 wells were completed to the Wilcox. Since many wells had been completed to the Wilcox at the time of the earliest water level

measurements, those measurements are not considered to be representative of predevelopment conditions.

Franklin County, Texas

Little information related to the historical development of the Carrizo Sand and the Wilcox Group in Franklin County was found during the literature review. Broom et al. (1965) state that the sands of the Wilcox Group, the Carrizo Sand, the Reklaw Formation, and the Queen City Sand are hydraulically connected and act as a single aquifer which they refer to as the Cypress aquifer. Five wells completed to the Cypress aquifer in Franklin County were found to flow in 1942 and 1963 (Broom et al., 1965). No general decline in water levels for shallow wells (less than 60 ft deep) has been observed (Broom et al., 1965). Broom et al. (1965) state, “Water levels in the heavily-pumped deeper wells show average declines of 3.5 to 15.7 feet per year for various periods of record.”

The earliest completion data given on the TWDB website for a well completed in the Cypress aquifer in Franklin County is 1875. Several additional wells were drilled in the early 1900s. The first water-level measurements were taken in 1942. Since over ten wells had been pumping from the Cypress aquifer prior to this time, the earliest water-level measurements are not considered to be representative of predevelopment conditions.

Freestone County, Texas

Little information related to the historical development of the Carrizo Sand and the Wilcox Group in Freestone County was found during the literature review. The Carrizo Sand and the sands of the Wilcox Group are considered to be separate aquifers in this county, with the Wilcox aquifer being the most important water-bearing formation (William F. Guyton & Associates, 1972). Deussen (1914) states that flowing wells in the Wilcox Formation, which includes the then undistinguished Carrizo Sand, are uncommon since the Wilcox crops out over the entire county. Several wells completed in the Wilcox Group with flows less than 15 gpm were reported in William F. Guyton & Associates (1972).

The earliest date given on the TWDB website for a well completed to the Carrizo Aquifer in Freestone County is 1896. The earliest water-level measurement, on the other hand, is from a 1936 measurement. A total of three wells were completed to the Carrizo aquifer at the time of

this measurement. Since only a few wells had been pumping from the Carrizo prior to the earliest water-level measurement, that measurement is considered to be fairly representative of predevelopment conditions.

The earliest date given on the TWDB website for a well completed to the Wilcox aquifer in Freestone County is 1896. At the time of the earliest water-level measurement in 1935, over 90 wells were completed to the Wilcox aquifer. Consequently, this first water-level measurement is not considered to be representative of predevelopment conditions.

Gregg County, Texas

Little information related to historical development of the Carrizo Sand and Wilcox Group in Gregg County was found during the literature review. Unless stated otherwise, the following discussion of development of the Carrizo Sand and Wilcox Group in Gregg County comes from Broom (1969). The Carrizo Sand and the sands of the Wilcox Group are considered hydraulically connected and a single aquifer in this county, with the Carrizo Sand being the principal water source. Duessen (1914) observed two flowing wells in the Sabine River bottoms. Little development of the waters in the Carrizo-Wilcox aquifer occurred in this county until the discovery of the East Texas oil field in 1930-1931. Numerous processes related to the oil industry and the increased population in the area of the oil field created an immediate demand for water. The water needs were met by completing wells to the Carrizo-Wilcox aquifer. By the mid-1950s, the dominate municipality in the area began deriving its water from a Carrizo-Wilcox field in Smith County.

The data on the TWDB website and in the county report (Broom, 1969) indicate that the first wells drilled to the Carrizo-Wilcox aquifer were completed in 1931 and the first water-level measurements were also taken in 1931. Therefore, the early water-level data for this county is considered to be representative of predevelopment conditions.

Grimes County, Texas

As of 1974, no water wells were completed to the Carrizo Sand or the sands of the Wilcox Group in Grimes County (Baker and Follett, 1974)

Harrison County, Texas

Little information related to the historical development of the Carrizo Sand and the Wilcox Group in Harrison County was found during the literature review. Unless otherwise stated, the following information was taken from Broom and Myers (1966). The sands of the Wilcox Group, the Carrizo Sand, the Reklaw Formation, and the Queen City Sand are hydraulically connected and act as a single aquifer which they refer to as the Cypress aquifer. Deussen (1914) discusses the presence of several flowing wells in the county. Nine wells completed to the Cypress aquifer in Harrison County were found to flow in 1964. Broom and Myers (1966) state that, "Prior to 1949, relatively large amounts of groundwater for municipal and industrial use were pumped by wells in and near Marshall." For shallow wells completed to the water table, the decline in water level between the late 1930s and 1964 was negligible. The decline in water level in the artesian portion of the aquifer was approximately 15 feet per year near the city of Marshall (located near the center of the county) prior the 1949, which is when the city switched to surface water for its public supply, but only 2 feet per year near the city of Hallsville (located in the west-southwest portion of the county). Because the average annual rainfall in Harrison is high, little need exists for irrigation. The largest uses of groundwater from the Cypress aquifer during 1964 were for industrial and domestic purposes.

The earliest completion dates given on the TWDB website for a well in the Cypress aquifer in Harrison County is 1871. Several additional wells were drilled in the early 1900s. The first water-level measurements were taken in 1936. By this time, 25 wells had been pumping from the Cypress Aquifer in this county. Consequently, the earliest water-level data available for Harrison County is not considered to be representative of predevelopment conditions.

Henderson County, Texas

Little information related to historical development of the Carrizo Sand and Wilcox Group in Henderson County was found during the literature review. The Carrizo Sand and the sands of the Wilcox Group are considered to be separate aquifers in this county, with the Wilcox aquifer being the most important water-bearing formation (William F. Guyton & Associates, 1972). Deussen (1914) states, "The sands of the Wilcox formation...should not be expected to yield flows except in the valleys of the eastern half of the county." William F. Guyton &

Associates (1972) report that five wells completed to the Carrizo Sand and the Wilcox Group flowed at one time.

The earliest date given on the TWDB website for a well completed to the Carrizo aquifer in Henderson County is 1870. The earliest water-level measurement was taken in 1936. Ten wells had been completed to the Carrizo Sand by the time the first water-level measurement was taken. As a result, that measurement is not considered to be representative of predevelopment conditions.

The earliest date given on the TWDB website for a well completed to the Wilcox aquifer in Henderson County is 1880. The earliest water-level measurement was taken in 1900. Since only one well had been pumping prior to the first water-level measurement, that measurement is considered to be representative of predevelopment conditions in the Wilcox aquifer in Henderson County.

Hopkins County, Texas

Information regarding historical development of the Wilcox Group in Hopkins County could not be found during the literature search. The Wilcox Group outcrops in the lower third to half of the county. Only one well, drilled in 1972, is completed to the Carrizo Sand (TWDB, website). The earliest completion date given on the TWDB website is 1948 for wells completed in the sands of the Wilcox Group. The earliest water-level measurement was made in 1973 based on the data on the TWDB website. As a result, all water-level measurements for the Wilcox in Hopkins County appeared to be effected by pumpage and are not considered representative of predevelopment conditions.

Houston County, Texas

Little information related to the historical development of the Carrizo Sand and the Wilcox Group in Houston County was found during the literature review. Unless stated otherwise, the following discussion comes from Tarver (1966). The Carrizo Sand and the sands of the Wilcox Group are considered to be separate aquifers in this county, with the Carrizo aquifer being the most productive. As of 1966, only one well was completed to sands of the Wilcox Group. In general, little to no fresh water is available from the Wilcox Group in Houston County based on analysis of electric logs. Several normal faults are present in the subsurface in

this county. However, they are not considered to significantly interfere with groundwater movement in the Carrizo Sand. Groundwater is primarily used in the county by municipalities and industries, and for domestic, stock, and irrigation purposes. The majority of this groundwater is removed from the Sparta Sand, with minor amounts removed from the Yegua Formation and the Queen City Sand. All three of these aquifers overlie the Carrizo Sand. Only a few wells withdraw water from the Carrizo Sand.

According to data on the TWDB website and in Tarver (1966), the first wells completed to the Carrizo Sand in Houston County were drilled in 1930. The first available water-level data are one measurement from 1961 and two other measurements from 1963. Due to the extended period between the time the first well was drilled and the time of the first water-level measurements, none of the water-level data for Houston County is considered to be representative of predevelopment conditions.

Jasper County, Texas

The Carrizo Sand and Wilcox Group are not sources of fresh to slightly saline water in Jasper County (Wesselman, 1967).

Leon County, Texas

Essentially no information related to the historical development of the Carrizo Sand and the Wilcox Group in Leon County was found during the literature review. Unless stated otherwise, the following discussion comes from Peckham (1965). The Carrizo Sand and the sands of the Wilcox Group are hydraulically connected and considered to function as a single aquifer in this county. The data presented in Peckham (1965) are from field work conducted in 1958 and 1959. The little historical data evaluated by Peckham (1965) suggests little to no decline in water levels in this county. All water obtained for municipal purposes, with the exception of one city, comes from the Carrizo-Wilcox aquifer. Carrizo-Wilcox waters are also used for irrigation, industrial, domestic, and livestock purposes. The industrial use of groundwater from the Carrizo Wilcox was quite small in 1958-1959. Most of the development of the Carrizo-Wilcox aquifer has occurred in the northern portion of the county. Because good quality water can be obtained from shallower sources, little development of the Carrizo-Wilcox aquifer has occurred in the southern portion of the county.

According to data on the TWDB website and in Peckham (1965), the first wells in Leon County were drilled in the mid and late 1930s. The first available water-level data are one measurement from 1937 and another measurement from 1949. The water-level measurement from 1937 is considered to be representative of predevelopment conditions.

Limestone County, Texas

Unless stated otherwise, the following discussion of development of the Carrizo Sand and Wilcox Group in Limestone County comes from Rettman (1984; 1987). The Carrizo Sand is not present and the Wilcox Group is a major aquifer in this county. In this county, the Wilcox Group can be divided into three distinct members; the Calvert Bluff Formation, the Simsboro Formation, and the Hooper Formation from top to bottom. Rettman (1984) states, "...the Wilcox is considered a hydraulic unit...[with] no apparent regional barriers to water moving from one unit to another." Deussen (1914) reports that a couple of shallow Wilcox wells flow near the city of Groesbeck. Rettman (1987) lists two Wilcox wells that were flowing in 1982.

The first use of groundwater from the Wilcox Group for municipal supply appears to have been by the city of Mexia in 1925. The city discontinued using groundwater in 1962. The cities of Tehuacana and Thornton began using groundwater from the Wilcox in 1940. Groundwater from the Wilcox in this county was used by the city of Kosse from 1939 to 1978. Between 1955 and 1980, the use of groundwater for industrial purposes peaked in 1965, the use of groundwater for domestic and livestock purposes has gradually increased each year, and the use of groundwater for public supply peaked in 1960 and significantly decreased thereafter. Little groundwater is used for irrigation purposes in this county due to the generally high annual precipitation. Overall, the use of groundwater in this county generally declined between 1955 and 1980. This discussion of groundwater use in Limestone County was taken from Rettman (1984).

The earliest completion date given on the TWDB website for Limestone County is 1885 for wells in the Wilcox Group. The earliest water-level measurement for the Wilcox Group is from a single value measured in 1938. By this time, five wells had been completed to and pumping from the Wilcox Aquifer. As a result, the earliest water-level measurement may not be representative of predevelopment conditions.

Madison County, Texas

Information regarding historical development of the Carrizo Sand and Wilcox Group in Madison County could not be found during the literature search. Data on the TWDB website indicate that a few wells (five) are completed to the Carrizo Sand in this county but that there are no wells completed to the Wilcox Group. One well was completed in 1937, three were completed in the 1950s, and the fifth well was completed in 1986. The first water-level measurement was made in 1957 (TWDB, website). Three wells were completed to the Carrizo Sand at the time of this measurement, which is considered to be fairly representative of predevelopment conditions.

Marion County, Texas

Little information related to historical development of the Carrizo Sand and Wilcox Group in Marion County was found during the literature review. Broom (1971) states that the sands of the Wilcox Group, the Carrizo Sand, the Reklaw Formation, and the Queen City Sand are hydraulically connected and act as a single aquifer which he refers to as the Cypress aquifer. Deussen (1914) states that wells completed to the Lower Eocene Aquifer will flow only in low lying areas and in river bottoms. One well completed in the Cypress aquifer was found to flow in 1968 (Broom, 1971).

The earliest completion date given on the TWDB website for a well in the Cypress aquifer in Marion County is 1914. A well completed in 1887 is listed in Deussen (1914). The first water-level measurements were taken in 1942. By that time, ten wells in Marion County were completed to the Cypress Aquifer. As a results, the earliest water-level measurement for this county is not considered to be representative of predevelopment conditions.

Miller County, Arkansas

Little information related to the historical development of the Carrizo Sand and the Wilcox Group in Miller County was found during the literature review. Unless stated otherwise, the following discussion comes from Ludwig (1972). The Carrizo Sand and the sands of the Wilcox Group are considered to be separate aquifers in this county. Moderate yields of groundwater are obtained from the Carrizo aquifer in this county. The Wilcox aquifer yields only small quantities of water in only the northern portion of Miller County. The Wilcox is a

minor aquifer in this county because of its "...lenticularity and fine-grained texture of the water-bearing sand beds." The Wilcox aquifer is not used by municipalities in this county. The Wilcox aquifer supplies water for small-capacity domestic and stock wells. Few wells tapping the Carrizo aquifer are found in Miller County. The only municipality using groundwater from the Carrizo aquifer is the city of Fouke. In general, "...development of the [Carrizo] aquifer for water supplies is negligible."

The first wells completed to the Wilcox aquifer in Miller County were drilled in 1899 (USGS, website³). The earliest water-level measurement was also made in 1899 (USGS, website). This first measurement is considered to be representative of predevelopment conditions.

Montgomery County, Texas

The Carrizo Sand and Wilcox Group are not sources of fresh to slightly saline water in Montgomery County (Popkin, 1971).

Morris County, Texas

Little information related to historical development of the Carrizo Sand and Wilcox Group in Morris County was found during the literature review. Broom et al. (1965) state that the sands of the Wilcox Group, the Carrizo Sand, the Reklaw Formation, and the Queen City Sand are hydraulically connected and act as a single aquifer which they refer to as the Cypress aquifer. Two wells completed to the Cypress aquifer in Morris County were found to flow in 1963 (Broom et al., 1965). No general decline in water levels for shallow wells (less than 60 ft deep) has been observed (Broom et al., 1965). Broom et al. (1965) state, "Water levels in the heavily-pumped deeper wells show average declines of 3.5 to 15.7 feet per year for various periods of record."

The earliest completion date given on the TWDB website for a well in the Cypress aquifer in Morris County is 1916. By the time the first water-level measurements were taken in 1935, 15 wells were completed to the Cypress Aquifer in this county. Consequently, the earliest

³ <http://water.usgs.gov/ar/nwis>

water-level data available for Morris County is not considered to be representative of predevelopment conditions.

Nacogdoches County, Texas

Little information related to historical development of the Carrizo Sand and Wilcox Group in Nacogdoches County was found during the literature review. Unless stated otherwise, the following discussion of development of the Carrizo Sand and Wilcox Group in Nacogdoches County comes from William F. Guyton & Associates (1970). The Carrizo Sand and the sands of the Wilcox Group are considered to be separate aquifers in this county, with the Carrizo aquifer being the most productive. Of the total amount of water removed from the Carrizo Sand and the sands of the Wilcox group in the county, only a small percentage is obtained from the Wilcox (about 5 percent in 1968). Flowing wells were observed in southern Nacogdoches County and northern Angelina County in the 1940s, but by 1961 most of those wells had stopped flowing (Baker et al., 1963). The Carrizo aquifer has been developed extensively in the county by the city of Nacogdoches and by the Southland Paper Mills located south of Nacogdoches near the border between Angelina and Nacogdoches Counties. Scalapino (1963) states that the areas of largest development of water from the Carrizo Sand are the Lufkin area, which includes water used by the cities of Lufkin and Nacogdoches and by the Southland Paper Mills, and the Winter Garden Area located in the southern Carrizo-Wilcox GAM. Extensive pumpage from the Carrizo since 1939 has resulted in drawdowns of up to 500 ft at pumping centers. Decline in Carrizo water levels in the outcrop has been much less (approximately 20 to 25 ft). Deussen (1914) states that the Lower Eocene aquifer yields flowing wells over much of Nacogdoches County.

The earliest completion dates given in the TWDB database for Nacogdoches County are 1890 for wells completed in the Carrizo Sand and 1886 for wells completed in the Wilcox Group. The earliest water-level measurements are from 1936 for both units. Since neither aquifer was extensively developed until the late 1930's, these early water-level measurements may be representative of predevelopment conditions.

Natchitoches Parish, Louisiana

Little information related to the historical development of the Carrizo Sand and the Wilcox Group in Natchitoches Parish was found during the literature review. Unless stated otherwise, the following discussion comes from Newcome et al. (1963). The Carrizo Sand and the sands of the Wilcox Group are considered to be separate aquifers in this parish. Relative to the Wilcox aquifer, the Carrizo aquifer is the principal source of groundwater in this parish. The majority of wells completed to the Wilcox aquifer are used for domestic and farm purposes. In general, yield from the Wilcox aquifer is low (less than 25 to 200 gpm). Some of the early wells completed to the Carrizo flowed to surface in the flood plain of the Red River. The Carrizo aquifer is the main source of water for the city of Natchitoches since 1944. With the exception of the municipal use by the city of Natchitoches, groundwater from the Carrizo aquifer is primarily used for domestic and farm purposes in this parish. Since the city of Natchitoches is the largest user of groundwater from the Wilcox and Carrizo aquifers, declines in water levels have been greatest near the city. The decline has been approximately 35 ft in the Carrizo aquifer and 65 ft in the Wilcox aquifer.

The first wells completed to the Carrizo aquifer in Natchitoches Parish were drilled in 1940 (LaDOT, website). The earliest available water levels are also from 1940 (LaDOT, website). Since the first water-level measurements were close to the time of well completion, those early measurements are considered to be representative of predevelopment conditions.

The first well completed to the Wilcox aquifer in Natchitoches Parish was drilled in 1906 (LaDOT, website). Two additional wells were drilled in 1915 and 1920. The earliest available water levels are one measurement in 1920 and one measurement in 1921 (LaDOT, website). Since few wells had been completed to and pumping from the Wilcox aquifer at the time of the earliest water level measurements, those measurements are considered to be representative of predevelopment conditions.

Newton County, Texas

The Carrizo Sand and Wilcox Group are not sources of fresh to slightly saline water in Newton County (Wesselman, 1967).

Panola County, Texas

Information regarding historical development of the Wilcox Group in Panola County could not be found during the literature search. The Wilcox Group outcrops across this entire county. The Carrizo Sand is not found in Panola County. The earliest completion date given on the TWDB website is 1924 for wells completed in the sands of the Wilcox Group. The earliest water-level measurements were made in 1936 (one measurement) and 1942 (one measurement). Because about six wells were completed to the Wilcox Group at the time of the first water-level measurement, this early water level is not considered to be representative of predevelopment conditions.

Polk County, Texas

The Carrizo Sand and Wilcox Group are not sources of fresh to slightly saline water in Polk County (Tarver, 1968a).

Rains County, Texas

Little information related to historical development of the Carrizo Sand and Wilcox Group in Rains County was found during the literature review. Unless stated otherwise, the following discussion of development of the Carrizo Sand and Wilcox Group in Rains County comes from William F. Guyton & Associates (1970). The Carrizo Sand and the sands of the Wilcox Group are considered hydraulically connected and a single aquifer in this county, with the Wilcox being the principal water source. Groundwaters of the Carrizo-Wilcox aquifer are pumped for both municipal and industrial purposes. Historically, very little groundwater has been used for irrigation in this county. Domestic and stock wells completed in the Carrizo-Wilcox are found through out the county.

Wells were completed to the Carrizo-Wilcox aquifer in Rains County as early as 1870. Approximately six Carrizo-Wilcox wells were in use by 1900. The drilling of wells essentially stopped in the early 1900s according to William F. Guyton & Associates (1970) and the data on the TWDB website. The first well recorded as completed to the Carrizo-Wilcox in the 1900s was drilled in 1934. The earliest available water levels are one 1948 measurement given in William F. Guyton & Associates (1970) and another measurement in 1958 given on the TWDB website. According to the data on the TWDB website, only four wells were completed to the

Carrizo-Wilcox aquifer at the time the first water-level measurement was recorded. Therefore, these earliest measurements might be representative of predevelopment conditions.

Rusk County, Texas

Little information related to historical development of the Carrizo Sand and Wilcox Group in Rusk County was found during the literature review. Unless stated otherwise, the following discussion of development of the Carrizo Sand and Wilcox Group in Rusk County comes from Sandeen(1987). The Carrizo Sand and the sands of the Wilcox Group are considered to be separate aquifers in this county, with the Wilcox aquifer being the most significant hydrologic unit. Little development of the waters in the Carrizo and Wilcox aquifers occurred in this county until the discovery of the East Texas oil field in 1930. Numerous processes related to the oil industry created an immediate demand for water. The water needs were met by wells completed to the Carrizo and Wilcox aquifers. Most water for municipal use was obtained from surface bodies. In 1947, groundwater was used for industrial, public supply, and oilfield purposes.

Almost all of the groundwater used in Rusk County in 1980 was withdrawn from the Wilcox aquifer. In 1960 and 1970, the major users of groundwater were industries and municipalities. By 1980, the use of groundwater by industries had significantly reduced but the use by municipalities had significantly increased. In addition, the use of groundwater for mining purposes began around 1980. The largest municipal user is the city of Henderson. Total withdrawal of groundwater increased 14 percent from 1960 to 1970 and 53 percent from 1970 to 1980. The greatest long-term declines in water levels have been observed near the area of the East Texas Oil Field and near the city of Henderson. One of the wells near Henderson shows a 135-ft decline in water level from 1935 to 1981. Another well shows a 43-ft increase in water level from 1947 to 1979.

The earliest date given on the TWDB website for a well completed to the Carrizo Sand in Rusk County is 1860. The earliest water-level measurements are from 1931 (1 measurement) and 1936 (over 30 measurements). By the time of the first measurement in 1931, about 21 wells were completed to the Carrizo Sand. As a result, the earliest measurement most likely reflects the effects of pumping and is not considered representative of predevelopment conditions.

The earliest date given on the TWDB website for wells completed to the Wilcox Group in Cherokee County is 1866. The earliest water-level measurement was taken in 1931. By the time of this first measurement, about 15 wells were completed to the Wilcox Group. Because it is likely that all of the available water-level data for the Wilcox Group, including the earliest measurements, reflect the effects of pumpage, none of the water-level measurements were considered to be representative of predevelopment conditions.

Sabine County, Texas

Little information related to historical development of the Carrizo Sand and Wilcox Group in Sabine County was found during the literature review. Unless stated otherwise, the following discussion of development of the Carrizo Sand and Wilcox Group in Sabine County comes from Anders(1967). The Carrizo Sand and the sands of the Wilcox Group are considered to be one hydrologic unit in this county, with the Wilcox Group being the most important especially in the southern part of the county. Groundwater is used primarily by municipalities and for rural, domestic, and livestock purposes. Very little groundwater is used for industrial or irrigation purposes. Some groundwater is lost to uncontrolled flowing wells.

The earliest date given on the TWDB website for a well completed to the Carrizo-Wilcox Aquifer in Sabine County is 1870. The earliest water-level measurements are from 1942 (1 measurement) and 1957(1 measurement). By the time of the first measurement in 1942, about six wells were completed to the Carrizo Sand and, by the second measurement, seven additional wells had been drilled. As a result, the earliest measurement most likely reflects the effects of pumping and is not considered representative of predevelopment conditions.

Sabine Parish, Louisiana

Little information related to the historical development of the Carrizo Sand and the Wilcox Group in Sabine Parish was found during the literature review. Unless stated otherwise, the following discussion comes from Page et al. (1963). The Carrizo Sand and the sands of the Wilcox Group are considered to be separate aquifers in this parish. The Carrizo Sand is not a significant aquifer in Sabine Parish because it has "...been faulted out in much of its normal outcrop area...". In addition, it is difficult to distinguish the sands of the Carrizo with sands of the underlying Wilcox Group. The Wilcox aquifer is "... the most extensively tapped source of

groundwater in Sabine Parish.” The largest users of groundwater from the Wilcox aquifer are the towns of Many and Pleasant Hill. Between 1931 and 1959, water levels in the Many well field have declined about 69 ft. The majority of the wells tapping the Wilcox aquifer are used for domestic and small farm purposes.

The first wells completed to the Wilcox aquifer in Sabine Parish were drilled in 1900 (LaDOT, website). The earliest water-level measurement was made in 1931 (LaDOT, website). By the time of the first water-level measurement, over 30 wells were completed to the Wilcox aquifer. Since many wells had been completed to and pumping from the Wilcox aquifer at the time of the earliest water-level measurement, that measurement is not considered to be representative of predevelopment conditions.

San Augustine County, Texas

Little information related to historical development of the Carrizo Sand and Wilcox Group in San Augustine County was found during the literature review. Unless stated otherwise, the following discussion of development of the Carrizo Sand and Wilcox Group in San Augustine County comes from Anders(1967). The Carrizo Sand and the sands of the Wilcox Group are considered to be one hydrologic unit in this county, with the Wilcox Group being the most important especially in the southern part of the county. Groundwater is used primarily by municipalities and for rural, domestic, and livestock purposes. Very little groundwater is used for industrial or irrigation purposes. Some groundwater is lost to uncontrolled flowing wells.

The earliest date given on the TWDB website for a well completed to the Carrizo-Wilcox Aquifer in Sabine County is 1890. The earliest water-level measurements are from 1907 (1 measurement) and 1942 (1 measurement). By the time of the first measurement in 1942, about three wells were completed to the Carrizo Sand and, by the second measurement, 12 additional wells had been drilled. Since only a few wells had been pumping from the aquifer prior to the first water-level measurement, that measurement is considered to be representative of predevelopment conditions.

San Jacinto County, Texas

The Carrizo Sand and Wilcox Group are not sources of fresh to slightly saline water in San Jacinto County (Sandeem, 1968)

Shelby County, Texas

Information regarding historical development of the Wilcox Group in Shelby County could not be found during the literature search. The Wilcox Group outcrops across this entire county. The Carrizo Sand is not found in Shelby County. The earliest completion date given on the TWDB website is 1907 for wells completed in the sands of the Wilcox Group. The earliest water-level measurement was made in 1966. Because over 15 wells were completed to the Wilcox Group at the time of the first water-level measurement, this early water level is not considered to be representative of predevelopment conditions.

Smith County, Texas

Little information related to historical development of the Carrizo Sand and Wilcox Group in Smith County was found during the literature review. Unless stated otherwise, the following discussion of development of the Carrizo Sand and Wilcox Group in Smith County comes from Dillard (1963). The Carrizo Sand and the sands of the Wilcox Group are considered hydraulically connected and a single aquifer in this county. Groundwater from the Carrizo-Wilcox aquifer in this county is used for municipal, industrial, domestic, and agricultural purposes. In 1961, the municipalities were the largest users of groundwater, followed by industries and domestic supplies. Pumping of Carrizo-Wilcox waters for agricultural purposes in 1961 was negligible. Preston and Moore (1991) indicate that water levels in the Tyler area have decreased up to 500 ft since before World War II. Several wells in Smith County were observed to flow during the field work conducted for the county report. Deussen (1914) states that pressures in the lower Eocene sand were sufficient to drive water to the ground surface only in the valleys are river bottoms.

The first wells completed to the Carrizo-Wilcox aquifer in Smith County were drilled in 1930 (TWDB, website). The earliest available water levels are two measurements in 1940 and two measurements in 1952 (TWDB, website). According to the data on the TWDB website, about six wells were completed to the Carrizo-Wilcox aquifer at the time of the first water-level measurement. The earliest measurements are considered to be somewhat representative of predevelopment conditions.

Titus County, Texas

Little information related to historical development of the Carrizo Sand and Wilcox Group in Titus County was found during the literature review. Broom et al. (1965) state that the sands of the Wilcox Group, the Carrizo Sand, the Reklaw Formation, and the Queen City Sand are hydraulically connected and act as a single aquifer which they refer to as the Cypress aquifer. Three wells completed to the Cypress aquifer in Titus County were found to flow from 1 to 5 gpm in 1963 (Broom et al., 1965). No general decline in water levels for shallow wells (less than 60 ft deep) has been observed (Broom et al., 1965). Broom et al. (1965) state, “Water levels in the heavily-pumped deeper wells show average declines of 3.5 to 15.7 feet per year for various periods of record.”

The earliest completion date given on the TWDB website for a well in the Cypress aquifer in Titus County is 1860. Several additional wells were completed in the early 1900s. The first water-level measurements were taken in 1942. Since numerous wells were pumping from the Carrizo-Wilcox aquifer prior to the time that the first water-level measurement was taken, that first measurement is most likely not representative of predevelopment conditions.

Trinity County, Texas

Information on the Carrizo Sand and sands of the Wilcox Group could not be found during the literature search. The TWDB website does not contain any water-level data for either the Carrizo Sand or the Wilcox Group. Based on this information, it is assumed that the Carrizo Sand and the sands of the Wilcox Group are not used to supply groundwater in Trinity County.

Tyler County, Texas

The Carrizo Sand and Wilcox Group are not sources of fresh to slightly saline water in Tyler County (Tarver, 1968b).

Upshur County, Texas

Little information related to historical development of the Carrizo Sand and Wilcox Group in Upshur County was found during the literature review. Unless stated otherwise, the following discussion of development of the Carrizo Sand and Wilcox Group in Upshur County comes from Broom (1969). The Carrizo Sand and the sands of the Wilcox Group are considered

hydraulically connected and a single aquifer in this county, with the Carrizo Sand being the principal water source. Little development of the waters in the Carrizo-Wilcox aquifer occurred in this county until the discovery of the East Texas oil field in 1930-1931. Numerous processes related to the oil industry and the increased population in the area of the oil field created an immediate demand for water. The water needs were met by completing wells to the Carrizo-Wilcox aquifer. By the mid-1950s, the dominate municipality in the area began deriving its water from a surface-water sources.

The data on the TWDB website and in the county report (Broom, 1969) indicate that the first two wells drilled to the Carrizo-Wilcox aquifer were completed in 1924 and 1937. By 1950, six additional wells had been drilled to the Carrizo-Wilcox aquifer. The earliest water-level data available in Upshur County consists of one 1937 measurement, two 1940 measurements, and one 1941 measurement. The earliest water-level measurement for this county is probably fairly representative of predevelopment conditions.

Van Zandt County, Texas

Little information related to historical development of the Carrizo Sand and Wilcox Group in Van Zandt County was found during the literature review. Unless stated otherwise, the following discussion of development of the Carrizo Sand and Wilcox Group in Van Zandt County comes from William F. Guyton & Associates (1970). The Carrizo Sand and the sands of the Wilcox Group are considered hydraulically connected and a single aquifer in this county, with the Wilcox being the principal water source. Groundwaters of the Carrizo-Wilcox aquifer are pumped for both municipal and industrial purposes. The highest concentration of municipal and industrial pumpage has historically occurred in the Grand Saline area. Between 1936 and 1969, water levels in this area have declined as much as 105 ft. Historically, very little groundwater has been used for irrigation in this county. Domestic and stock wells completed in the Carrizo-Wilcox are found through out the county.

Approximately 34 wells were completed to the Carrizo-Wilcox aquifer between 1870 and 1920 (William F. Guyton & Associates, 1970). Neither the county report (William F. Guyton & Associates, 1970) nor the TWDB website indicate drilling to the Carrizo-Wilcox aquifer during the 1920s. Wells began to be completed again to the Carrizo-Wilcox aquifer in 1930. The first three recorded water levels for wells completed to the Carrizo-Wilcox aquifer were measured in

1936, 1949, and 1953 according to both the county report (William F. Guyton & Associates, 1970) and the TWDB website. Consequently, numerous wells had been in operation prior to the time that the first water levels were measured. Therefore, the earliest water-level data for this county is most likely not representative of predevelopment conditions.

Walker County, Texas

According to Winslow (1950) the Carrizo Sand and the sands of the Wilcox Group are not sources of freshwater in Walker County.

Wood County, Texas

Little information related to historical development of the Carrizo Sand and Wilcox Group in Wood County was found during the literature review. Unless stated otherwise, the following discussion of development of the Carrizo Sand and Wilcox Group in Wood County comes from Broom (1968). The Carrizo Sand and the sands of the Wilcox Group are considered to function as a single aquifer in this county due to their similar properties and hydraulic connection. Deussen (1914) states that wells completed into the Lower Eocene Aquifer will flow only in the Sabine River bottoms. Broom (1968) lists 14 wells completed in either the Carrizo Sand, Wilcox Group, or both, that flowed in 1963 or 1965.

The earliest date given on the TWDB website for a well completed in the Carrizo-Wilcox aquifer in Wood County is 1880. Several additional wells were completed in the early 1900s. A significant increase in groundwater pumpage for municipal purposes occurred between 1955 and 1965. Evaluations of water level declines in some shallow wells in the county indicate no significant changes in water levels between 1942 and 1965. Declines of 0.7 to 31.2 feet per year were observed in several municipal and industrial wells between 1960 and 1965. The first water-level measurements were taken in this county in 1942. Since numerous wells were pumping from the Carrizo-Wilcox aquifer prior to the time that the first water-level measurement was taken, that first measurement is most likely not representative of predevelopment conditions.

Reviewed Reports

- Anders, R.B., 1967. Ground-Water Resources of Sabine and San Augustine Counties, Texas. Texas Water Development Board, Report 37.
- Baker, E.T., Jr., and C.R. Follett, 1974. Ground-Water Resources of Grimes County, Texas. Texas Water Development Board, Report 186.
- Baker, B.B., J.W. Dillard, V.L. Souders, and R.C. Peckham, 1963. Reconnaissance Investigation of the Ground-Water Resources of the Sabine River Basin, Texas. Texas Water Commission, Bulletin 6307.
- Baker, B.B., R.C. Peckham, J.W. Dillard, and V.L. Souders, 1963. Reconnaissance Investigation of the Ground-Water Resources of the Neches River Basin, Texas. Texas Water Commission, Bulletin 6308
- Bennett, R.R., 1942. Ground-Water Resources in the Vicinity of Palestine, Texas. USGS Open-File Report.
- Broom, M.E., 1968. Ground-Water Resources of Wood County, Texas. Texas Water Development Board, Report 79.
- Broom, M.E., 1969. Ground-Water Resources of Gregg and Upshur Counties, Texas. Texas Water Development Board, Report 101
- Broom, M.E., 1971. Ground-Water Resources of Cass and Marion Counties, Texas. Texas Water Development Board, Report 135.
- Broom, M.E., and B.N. Myers, 1966. Ground-Water Resources of Harrison County, Texas. Texas Water Development Board, Report 27.
- Broom, M.E., W.H. Alexander, Jr., and B.N. Myers, 1965. Ground-Water Resources of Camp, Franklin, Morris and Titus Counties, Texas. Texas Water Commission, Bulletin 6517.
- Deussen, A., 1914. Geology and Underground Water of the Southeastern Part of the Texas Coastal Plain. USGS Water-Supply Paper 335.
- Dillard, J.W., 1963. Availability and Quality of Ground Water in Smith County, Texas. Texas Water Commission, Bulletin 6302.

- Fogg, G.E., and C.W. Kreitler, 1982. Ground-water hydraulics and hydrochemical facies in Eocene aquifers of the East Texas Basin. Bureau of Economic Geology. Report of Investigations No. 127.
- Ludwig, A.H., 1972. Water Resources of Hempstead, Lafayette, Little River, Miller, and Nevada Counties, Arkansas. U.S. Geological Survey Water-Supply Paper 1998.
- Newcome, R., Jr., L.V. Page, and R. Sloss, 1963. Water Resources of Natchitoches Parish, Louisiana. State of Louisiana Dept. of Conservation Geological Survey and Dept. of Public Works, Water Resources Bulletin No. 4.
- Page, L.V., R.Newcome, Jr., and G.D. Graeff, Jr., 1963. Water Resources of Sabine Parish, Louisiana. State of Louisiana Dept. of Conservation Geological Survey and Dept. of Public Works, Water Resources Bulletin No. 3.
- Page, L.V., and H.G. May., 1964. Water Resources of Bossier and Caddo Parishes, Louisiana. State of Louisiana Dept. of Conservation Geological Survey and Dept. of Public Works, Water Resources Bulletin No. 5.
- Peckham, R.C., 1965. Availability and Quality of Ground Water in Leon County, Texas. Texas Water Commission, Bulletin 6513.
- Preston, R.D., and S.W. Moore, 1991. Evaluation of Ground-Water Resources In the Vicinity of the Cities of Henderson, Jacksonville, Kilgore, Lufkin, Nacogdoches, Rusk, and Tyler in East Texas. Texas Water Development Board, Report 327.
- Popkin, B.P., 1971. Ground-Water Resources of Montgomery County, Texas Water Development Board, Report 136
- Rettman, P.L., 1984. Ground-Water Resources of Limestone County, Texas. USGS Open-File Report 84-713
- Rettman, P.L., 1987. Ground-Water Resources of Limestone County, Texas. Texas Water Development Board, Report 299.
- Sandeen, W.M., 1968. Ground-Water Resources of San Jacinto County, Texas. Texas Water Development Board, Report 80.

- Sandeen, W.M., 1987. Ground-Water Resources of Rusk County, Texas. Texas Water Development Board, Report 297.
- Scalapino, R.A., 1963. Ground-Water Conditions in the Carrizo Sand in Texas. Presented at Annual Meeting of Geological Society of America, November 12, 1962, Houston, Texas.
- Sundstrom, R.W., W.W. Hastings, W.L. Broadhurst, 1948. Public Water Supplies in Eastern Texas. USGS Water-Supply Paper 1047.
- Tarver, G.E., 1966. Ground-Water Resources of Houston County, Texas. Texas Water Development Board, Report 18.
- Tarver, G.R., 1968a. Ground-Water Resources of Polk County, Texas. Texas Water Development Board, Report 82.
- Tarver, G.R., 1968b. Ground-Water Resources of Tyler County, Texas. Texas Water Development Board, Report 74.
- Wesselman, J.G., 1967. Ground-Water Resources of Jasper and Newton Counties, Texas. Texas Water Development Board, Report 59.
- White, D.E., 1973. Ground-Water Resources of Rains and Van Zandt Counties, Texas. Texas Water Development Board, Report 169.
- White, W.N., A.N. Sayre, and J.F. Heuser, 1941. Geology and Ground-Water Resources of the Lufkin Area, Texas. USGS Water-Supply Paper 849-A.
- William F. Guyton & Associates, 1970. Ground-Water Conditions in Angelina and Nacogdoches Counties, Texas. Texas Water Development Board, Report 110.
- William F. Guyton & Associates, 1972. Ground-Water Conditions in Anderson, Cherokee, Freestone, and Henderson Counties, Texas. Texas Water Development Board, Report 150.
- Winslow, A.G., 1950. Geology and Ground-Water Resources of Walker County, Texas. Texas Board of Water Engineers, Bulletin 5003.

APPENDIX B

Standard Operating Procedures (SOPs) for Processing Historical Pumpage Data TWDB Groundwater Availability Modeling (GAM) Projects

**Standard Operating Procedures (SOPs)
for Processing Historical Pumpage Data
TWDB Groundwater Availability Modeling (GAM) Projects**

TABLE OF CONTENTS

1. Groundwater Use Source Data	1
1.1 Pumpage by Major Aquifer 1980-1997	1
1.2 RawDataMUN_WaterUseSurvey	1
1.3 RawDataMFG_WaterUseSurvey.....	1
1.4 RuralDomestic_Master_Post1980_021502.xls	1
2. Initial Processing.....	1
2.1. Completion of monthly pumpage estimates for MUN, MFG, PWR, and MIN uses.....	1
2.2 Predicting historical pumpage for 1981-83 and 1997-1999.....	2
2.3 Selecting pumpage within the model domain.....	3
2.4 Preparing a county-basin Arcview shapefile and associating model grid cells with a county-basin	4
3. Matching Pumpage to Specific Wells.....	5
3.1 Create All Wells Table.....	5
3.2 Linking water use data to the state well database.....	6
3.3 Locating unmatched pumpage 1	6
3.4 Locating unmatched pumpage 2	6
3.5 Locating unmatched pumpage 3	6
3.6 Locating unmatched pumpage 4.....	6
3.7 Count wells matched.....	7
3.8 Apportion water use between matched wells	7
3.9 Calculate additional fields	7

3.10 Append out-of-state data	7
3.11 Summarize well-specific matching completeness	8
4. Spatial Allocation of Groundwater Pumpage to the Model Grid	8
4.1 Spatial allocation of well-specific groundwater pumpage	8
4.2 Spatial allocation of irrigation groundwater pumpage.....	9
4.3 Spatial allocation of livestock groundwater pumpage	12
4.4 Spatial allocation of rural domestic (C-O) groundwater pumpage.....	14
4.5 Vertical distribution of groundwater pumpage (all uses).....	16
5. Temporal Distribution of Rural Domestic, Livestock, and Irrigation Groundwater Use	19
5.1. Temporal distribution of livestock pumpage.....	20
5.2 Temporal distribution of irrigation (IRR) pumpage	20
5.3 Temporal distribution of rural domestic (C-O) pumpage	21
6. Summarize Pumpage Information	22
6.1 Summary queries	22
6.2 Join pumpage queries to Arcview shapefile	25
Appendix 1. Vertical Distribution Avenue Script	26
Appendix 2. Script to Return Land Surface Elevation for a Well from a DEM Grid	31

1. Groundwater use source data - Groundwater use data is derived from three tables provided by the Texas Water Development Board (TWDB) in a MS Access 97 database and one spreadsheet provided in MS Excel format:
 - 1.1. **PumpagebyMajorAquifer1980-1997** – This table contains water use summaries, in acre-feet/year) from each major aquifer, county, and basin for the years 1980 and 1984-1997 for the water use categories:
 - IRR – irrigation
 - STK – livestock
 - MIN - mineral extraction
 - MFG – manufacturing
 - PWR – power generation
 - MUN – municipal water supply, and
 - C-O – county-other (rural domestic) use.
 - 1.2. **RawDataMUN_WaterUseSurvey** – This table contains reported annual and monthly self-generated groundwater use totals, in gallons, from each municipal water user for the years 1980-1999. Monthly totals are missing in many cases. The data originate from the annual water use surveys. The county, basin, and major aquifer of origin are reported, as well as the water user group ID, alphanumeric code of the water user, and line 1 of the address of the water user. The number of wells from which the water was pumped is reported in most cases.
 - 1.3. **RawDataMFG_WaterUseSurvey** – This table contains reported annual and monthly self-generated groundwater use totals, in gallons, from each manufacturing, power generation, or mining water user for the years 1980-1999. Monthly totals are missing in many cases. The data originate from the annual water use surveys. The county, basin, and major aquifer of origin are reported, as well as the water user group ID, alphanumeric code of the water user, and line 1 of the address of the water user. The number of wells from which the water was pumped is reported in most cases.
 - 1.4. **RuralDomestic_Master_Post1980_021502.xls** – This Excel spreadsheet contains summaries of annual rural domestic water use, by county-basin, from 1980 to 1997.
2. Initial Processing
 - 2.1. Completion of Monthly Pumpage Estimates for MUN, MFG, PWR, and MIN Uses - In the tables **RawDataMUN_WaterUseSurvey** and **RawDataMFG_WaterUseSurvey**, monthly pumpage estimates are reported for the majority, but not all, of the water users. For other users, only the annual total pumpage is reported. It is necessary to estimate the

monthly pumpage totals for some water users via the following procedure.

- 2.1.1. First, export the tables **RawDataMFG_WaterUseSurvey** and **RawDataMUN_WaterUseSurvey** to Microsoft Excel. Append the records from the latter file to the former. Delete records with reported annual total water use (in gallons) of “0”.
 - 2.1.2. In Excel, calculate the monthly fractions of annual total water use for each record for which monthly pumpage was reported. As an example, a monthly distribution factor of 1/12, or 0.0833, would result from a uniform annual distribution.
 - 2.1.3. Calculate the average monthly distribution factor for each county-basin and water use category. Statistically review these average monthly fractions for outliers. Generally, monthly distribution factors fall within the range 0.035 to 0.15.
 - 2.1.4. Next, for those water use records that contain an annual total water use but no monthly value, calculate estimated monthly water use values by multiplying annual total pumpage by the average monthly distribution factor for the same water use category (MUN, MFG, PWR, MIN) in the county-basin within which it was located. If the monthly distribution factor for its county basin and water use category was an outlier, usually due to the fact that only one or two water users were located in the county-basin, use the monthly distribution factor from the nearest adjacent county-basin. (Note: For Louisiana and Arkansas parishes/counties, for which no monthly values are available, use the values from the nearest Texas counties.)
 - 2.1.5. Add an additional field, “Monthly Calculated” to the spreadsheet, with “N” entered in those records containing original, reported monthly pumpage values, and “Y” for those records with calculated monthly pumpage values.
 - 2.1.6. Finally, re-import the Excel spreadsheet into the Access database as a table **MUN+MFG_WaterUseSurvey**.
- 2.2. Predicting historical pumpage for 1981-83 and 1997-1999 - In the table **PumpagebyMajorAquifer1980-1997**, groundwater use summaries were reported for the years 1980 and 1984-1997 for the categories MIN, MFG, PWR, STK, IRR, and MUN (actually MUN + C-O) for each major aquifer and county-basin. Water use summaries for the years 1981-1983 and 1998-1999 were not reported. In the spreadsheet **RuralDomestic_Master_Post1980_021502.xls**, water use is not reported for 1998 and 1999. The groundwater use for these years must be obtained by interpolation from existing data.
- 2.2.1. First, import the tables **PumpagebyMajorAquifer1980-1997** and **RuralDomestic_Master_Post1980_021502.xls** into SAS datasets.
 - 2.2.2. Import into a SAS dataset the weather parameters “average annual temperature” and “total annual precipitation” for 1980-1999 from National Weather Service cooperative weather stations. Delete those stations that have valid measurements in less than 16 of the 20 years. Also, delete data from any stations that do not have

valid measurements for at least 4 of the 5 years 1981, 1982, 1983, 1998, and 1999.

2.2.3. In Arcview, identify the weather station (with valid data for at least 16 of the 20 years) closest to each county-basin. Create a look-up table in SAS to link each county-basin with the closest weather station.

2.2.4. In SAS, apply linear regression in Proc REG with stepwise selection, to regress annual pumpage (dependent variable) vs. 1) year, 2) average annual temperature and 3) total annual precipitation from the nearest weather station, for each county-basin, major aquifer, and water use category, for the years 1980 and 1984-97. Select the best valid regression equation based on the statistic Mallows' Cp, which balances the improvement in regression fit as independent variables are added to the regression with the increasing uncertainty in the resulting dependent variable estimates. Transformations (e.g., natural logarithms) of the independent variables may yield a better regression equation. There should be a regression equation for each county-basin, and water use category.

2.2.5. Using the regression equations and weather data for the years 1981, 1982, 1983, 1998, and 1999, in SAS, calculate predicted pumping for these years each county-basin and water use category. If predicted values are less than zero, a value of zero is entered. Append the predicted water use for these five years to the reported water use for 1980 and 1984-1997. Export this table, then import it into the Access database as **PumpagebyMajorAquifer1980-1999**.

2.2.6. In general, this regression procedure is appropriate for pumpage changes that might be expected based on gradual annual changes (e.g., population) or year-to-year weather variability. It may not make good predictions when pumpage changes rapidly for non-weather-related factors. Review and inspect the regression-based pumpage estimates for 1981-83 and 1998-99 versus the TWBD-provided pumpage estimates for 1984-1997. Carefully inspect all between-year pumpage differences of more than 20%. Subjectively, if the predicted pumpage estimates do not make sense, replace the regression-based estimate with the TWDB pumpage estimate for the previous year.

2.2.7. Add a new column "Annual Source" to the table, and enter in it "Reported" for those years for which annual water use was reported, and "Regression" or "Previous Year" for those years for which pumpage sums were predicted from regression or previous years.

2.3. (OPTIONAL) Selecting Pumpage within the model domain – The tables contain pumpage estimates for the entire state, or the entire aquifer of interest. Ultimately, pumpage originating within the model domain will be made during attribution of data to model grid cells. To speed the analysis, it may be beneficial to create a subset of data for pumpage that will encompass the model domain, with a buffer. **WARNING:** Pumpage sometimes originates (e.g., wells exist) in a different geographic area from where water is used and reported. Be careful that this procedure does not exclude any reported pumpage!

- 2.3.1. Once the model domain has been identified by the modelers, it is overlain on the county GIS layer in Arcview, and all counties containing, or very near to, any part of the model domain are selected.
 - 2.3.2. Next, in MS Access, a new field “Domain?” is added to the table **Reference_Countyname_number_FIPS**. A value of “Y” is entered in this field for records of counties within the model domain.
 - 2.3.3. Using this table, in a select query with other tables or queries joined by county name, number, or FIPS (federal information processing system) code, one can specify “Domain='Y’ as a condition to limit queries to those counties within the model domain.
- 2.4. Preparing a County-basin Arcview Shapefile and Associating Model Grid Cells with a County-Basin – Much of the reported pumpage is spatially divided into county-basin units, which consist of the area in the same county and river basin. Many counties are split between two or more river basins, thus, county-basins are smaller than counties.
- 2.4.1. To create a county-basin Arcview shapefile, in Arcview, load GIS shapefiles of counties and river basins in GAM projection. Intersect these two layers using the Geoprocessing Wizard to create a new shapefile **countybasins.shp**.
 - 2.4.2. Associate each model grid cell with the county-basin it falls primarily within. This will be useful when we need to determine monthly distribution factors and water user group IDs (WUG IDs) for non-well-specific pumpage categories (IRR, STK, C-O). These monthly distribution factors are estimated as averages within a county-basin. **Note:** The primary county-basin is not used to spatially distribute pumpage among grid cells because it is inexact. A grid cell may be part of multiple county-basins. For spatial distribution purposes, this grid cell should be split by county-basin – then later aggregated.
 - 2.4.2.1. Load the model grid shapefile in GAM projection. Union this shapefile with countybasins.shp using the Geoprocessing Wizard. Add a numeric field “fr_grdarea” to the attribute table, and use the field calculator function to enter its values ($fr_grdarea = shape.returnarea/27878400$). Here, 27878400 is the area, in square feet, of each grid cell. Export the table as a dbf file.
 - 2.4.2.2. Import the dbf file into MS Access as a new table - **Table1**. Our goal is to identify, for each grid cell, the county-basin with which it is primarily associated.
 - 2.4.2.3. Select by query the records with no value for the field “CountyBasin.” Delete these records, as they are grid cells over Mexico or the ocean.
 - 2.4.2.4. Run a make table query, sorting the table1 records by grid_id (ascending) and fr_grd_area (descending) to create a new table, **Table2**.
 - 2.4.2.5. Copy **Table2**, and paste only the table structure as a new table –

Grid_countybasin.

2.4.2.6. In design view, make the field “grid_id” a primary key in the table **Grid_countybasin**.

2.4.2.7. Run an append query, to append all fields of the records from table 2 to **Grid_countybasin**. When the warning window comes up, say yes to proceed with the query. This appends only the first record for each grid_id to **Grid_countybasin**, leaving one record for each grid cell with the county basin with the largest value of “fr_grdarea”. The resulting table should have one record for each grid cell in the model grid, and the county-basin name for that model grid cell.

3. Matching Pumpage to Specific Wells

Historical groundwater use from the categories MUN, MIN, MFG, and PWR is to be matched with specific wells from which it was pumped. Reported groundwater use for these uses, from the annual water use surveys, is contained in the table **MUN+MFG_WaterUseSurvey**. For MUN, MFG, MIN, and PWR, water use is reported for each year from 1980 to 1999. These tables report total annual use and, in most cases, monthly use, for each water user. The water user is identified by a unique alphanumeric code “alphanum.” The tables also list the county and river basin, as well as their water user group ID, their regional water planning group, their water use category, the major aquifer from which the groundwater was pumped, and the number of wells from which the water was pumped. These tables do not indicate the specific location of the wells, well elevation, well depth, a specific aquifer name, or other information needed for groundwater modeling. This information must be retrieved from other sources. The primary source of well information is the state well database maintained by the TWDB. Secondary sources include well data found in the TNRCC public water supply database, and the USGS site inventory. A final source is the follow-up survey provided by the TWDB in October 2001.

3.1. Create **All_wells** table –

3.1.1. Download the state well database as a table **wellda.txt** for the entire state (under the menu “all counties combined”) from the TWDB web site <http://www.twdb.state.tx.us/publications/reports/GroundWaterReports/GWDatabaseReports/GWdatabaserpt.htm>. Import this table into MS Access as a new table **All_Wells**.

3.1.2. The TNRCC public water supply database includes data for some wells that are not found in the TWDB state well database. Retrieve this database from the TNRCC. Create a query to link the required well data, and append the well data to **All_wells**, exercising care to match fields appropriately.

3.1.3. The USGS site inventory <http://waterdata.usgs.gov/tx/nwis/inventory> contains data for wells that may not be found from other sources. Run a query for the state of Texas with site type = ‘ground water’ to download the well data and append it to **All_wells**. Be careful to match fields appropriately.

- 3.1.4. Delete any oil, gas, geothermal, or observation wells, anodes, drains, or springs after a query of the attribute table on the fields “GW_type_cd” or “Site_use1_cd”.
- 3.2. Linking water use data to the state well database – Using a make-table query to create a new table **MUN+MFG_linkedwithwellinfo**, all fields from the water use survey are merged with all fields from the state well database by joining the field “alphanum,” in the table **MUN+MFG_WaterUseSurvey**, to the field “user code econ,” in the state well database table **All_wells**. In many cases, several different wells may have the same “user code econ,” making a one-to-many match (this is expected, since one city may own multiple wells). Add a field “Location Source” to the table **MUN+MFG_linkedwithwellinfo**. For the pumpage records with one or more matched well, enter the text “state well database” in this field.
- 3.3. Locating unmatched pumpage 1 – Identify the pumpage records without a matching well using a **Find Unmatched** query. Check the field “alphanum” in unmatched pumpage records of the table **MUN+MFG_WaterUseSurvey**, and “user_code_econ” in the table **All_Wells** for obvious errors that prevent automatic matching, and correct any found and repeat the steps to make the table above. Next, manually search the **All Wells** table for wells in the same county and basin, for which the user name field “owner_1” matches the field “line1” in **MUN+MFG_WaterUseSurvey**. When a match is found, add a field to the well table, and copy the “alphanum” field from the water use survey, to facilitate match-merging. Next, match this new field in the well database to “alphanum” of the water use survey, and append these matched records to the table **MUN+MFG_linkedwithwellinfo**. Enter “state well database manual match” for the field “Location Source” for these new appended records.
- 3.4. Locating unmatched pumpage 2 – For those pumpage records not matched via the above procedures, open the TNRCC public water supply database and attempt to manually match the water user to specific wells based on the county, aquifer_id, and owner name - “A1Name.” When a match is found, add a field to the well table, copy the “alphanum” field from the water use survey, perform a match-merging query, and update these new matched records to the table **MUN+MFG_linkedwithwellinfo**. Enter “TNRCC PWS database” for the field “Location Source” for these new appended records.
- 3.5. Locating unmatched pumpage 3 - For those pumpage records, if any, still not matched in the above procedures, manually search the TWDB follow-up survey data. When a match is found, this data must be manually copied to the table **MUN+MFG_linkedwithwellinfo** because the table format is substantially different. Enter “TWDB followup survey” for the field “Location Source” for these new appended records.
- 3.6. Locating unmatched pumpage 4 - For those pumpage records, if any, still not matched in the above procedures, it may be possible to identify an approximate well location via the EPA’s Envirofacts facility database. In an internet browser, go to http://www.epa.gov/enviro/html/fii/fii_query_java.html and perform a facility information query using a characteristic part of the facility name in the query field “facility site name.” If a single facility of matching name is located in the same county,

copy the facility latitude and longitude, in degrees, minutes, seconds into the appropriate fields of the table **MUN+MFG_linkedwithwellinfo**. Enter “facility centroid” in the field “Location Source” if Envirofacts lists that as the source of the latitude and longitude, or “facility zip code centroid” if Envirofacts lists that as the source of the latitude and longitude. Note that the median size of a zip code in Texas is approximately 5.5 square miles. Thus, pumpage located based on a zip code centroid may be very uncertain, especially in rural areas, and should be used with caution. However, it was felt that having an approximate location was better than leaving them out of the model. Note: Because this step is labor-intensive, it may be acceptable to perform this procedure for only the “major” water users, as indicated by volume used.

3.7. Count wells matched - Count the number of wells matched to each pumpage record via a crosstab query on **MUN+MFG_linkedwithwellinfo**.

3.8. Apportion water use between matched wells –

3.8.1. For that water use matched to more than one well, compare the number of matched wells to the number of wells reported as used in the water use survey. If the number of matched wells exceeds the number reportedly used, inspect the well data, including the county, basin, aquifer_id, well_type, drill_date, and other fields to see if some of the wells can be excluded from consideration as the source form which the water was reportedly pumped. If so, remove that well from the table.

3.8.2. Next, we need to apportion the reported pumpage among the wells matched. Since we don’t have data indicating otherwise, pumpage will be divided equally between wells. Create a new query that 1) adds a column “Num Wells Matched” indicating the number of wells matched (based on the aforementioned crosstab query) to the table **MUN+MFG_linkedwithwellinfo**, and 2) if one or more wells are matched, divides the reported pumpage in the fields “annual total in gallons” and “jan” – “dec” by the number of wells matched. Add another field “Corrected for Numwells” with a value of “Y” if the original pumpage sum for the water user was divided by two or more wells, and “N” otherwise.

3.8.3. Quality control check – In a query, summarize total annual water use by county-basin-year in the table **MUN+MFG_linkedwithwellinfo**. Make sure that these match the corresponding totals from the original table **MUN+MFG_WaterUseSurvey**. If not, correct the situation, which may occur by double-matching some water use records to wells.

3.9. Calculate Additional Fields - In a new make-table query, create the table **Well-specific_pumpage** based on **MUN+MFG_linkedwithwellinfo**, calculate latitude and longitude as decimal degrees from degrees-minutes-seconds in new fields “lat_dd” and “long_dd.” Also in the same query, calculate water use in acre-feet from gallons in new fields “Annual total in acre-ft”, “JAN in acre-ft”, “FEB in acre-ft”,.....,”DEC in acre-ft.”

3.10. Append Out-of-State Data - Append the well-specific Louisiana and Arkansas water use, in acre-ft, from LADEQ and USGS, to the table **Well-specific_pumpage**.

- 3.11. Summarize well-specific matching completeness – Perform queries to calculate the sum of matched water use by county-basin-year, and the total water use (matched and unmatched) by county-basin-year. Based on these queries, calculate the volumetric percent completeness of matching by county, basin, and year. Completeness should be high (e.g., >80%) to facilitate accurate accounting for water use in the model.
4. Spatial Allocation of Groundwater Pumpage to the Model Grid - The model grid is comprised of an equal-spaced grid with a size of one mile by one mile. The grid has 3 dimensions- row, column, and model layer. Each cell of the model grid is labeled with a 7-digit integer “grid_id”. The first digit represents the model layer. Digits 2 through 4 represent the row number. Digits 5 through 7 represent the column. The model grid is represented in a MS Access table linked to an Arcview shapefile via the field “grid_id”.
 - 4.1. Spatial allocation of well-specific groundwater pumpage from the categories MUN, MFG, MIN, and PWR
 - 4.1.1. Distribute pumpage into grid cells
 - 4.1.1.1. In MS Access, verify that all records in the table **Well-specific_pumpage** have x,y coordinates in decimal degrees.
 - 4.1.1.2. In Access, add a new autonumbered, long integer field “Unique ID” to the table **Well-specific_pumpage**.
 - 4.1.1.3. In Arcview, enable the Database Access extension. Add a new table **PtSrcTbl** to an ArcView project via SQL connect, including only the fields “unique_id”, “well_depth”, “lat_dd”, and “long_dd”. To perform an SQL connect, select the “SQL connect” menu item under the Project menu. Then navigate to the correct database and select the table **Well-specific_pumpage**.
 - 4.1.1.4. Add **PtSrcTbl** as an event theme named **Wellpts** to a view based on lat/long coordinates. To do this, from the view menu, select the “add event theme” menu item, and choose long_dd for x field and lat_dd for y field in the dialog. Re-project the view to GAM projection using the View->Properties dialog box according to GAM Technical Memo 01-01 (rev A), then save it as a shapefile **Wellpts.shp**. Load **Wellpts.shp** and the model grid, also as a shapefile in GAM projection, into a new view.
 - 4.1.1.5. Spatially join the model Grid table to the **WellPts** table. To do this make the “shape” fields of each table active, and with the **WellPts** table active, choose “join” from the table menu. This will join the 1 mile grid cell records to all of the **WellPts** records that are contained with that grid cell.
 - 4.1.1.6. Migrate the GridId to the **WellPts** table. Do this by first adding a new 7-digit, no decimal, field to the **WellPts** table called “Grid_Id”. Then, with the new field active, using the field calculator button make the new field equal to the “GridId” field from the joined table.

- 4.1.1.7. Delete those pumpage records outside the model domain with a “Grid_ID” of “0”.
- 4.1.1.8. Vertical Distribution: Follow procedures outlined in sections 4.5.
- 4.1.2. Import the Arcview attribute table **Wellpts.dbf** to the MS Access database. Change the data type for the fields “Unique ID” and “Grid_ID” back to long integer if they were converted to double length real numbers during the import operation.
- 4.1.3. Run an update query to update the empty values of “Grid ID” in the table **Well-specific_pumpage** with the “Grid_ID” values from the table **Wellpts**, using an inner join on the field “Unique ID.”
- 4.1.4. The table **Well-specific_pumpage** now has only the grid_id of the upper model, i.e., the first digit is 1. The actual vertical distribution data is in the fields “per1” to “perx” where x is the number of vertical layers (L) in the model. Copy the table x-1 times in an append query, incrementing the first digit of the grid id, to create a record for each model layer. There now should be L times the original number of records in the table. For example, for the northwestmost grid cells of a model with four layers, the following grid id’s should now exist: 1001001, 2001001, 3001001, and 4001001; whereas only 1001001 was in the original table.
- 4.1.5. Calculate for each year the actual pumpage for each record as the product of the pumpage for a given year multiplied by the percent of pumpage from that model layer (from the fields “per1” – “per4”, for a model with 4 layers).
- 4.1.6. Create a new summary query **gridsum_well_specific** to summarize the pumpage for each grid_id and year from the table **Well-specific_pumpage**.
- 4.2. Spatial allocation of irrigation groundwater pumpage – Irrigation pumpage is distributed between the USGS MRLC land use types 61 (orchard/vineyard), 82 (row crops), and 83 (small grains) within each county-basin based on area. The distribution is further weighted based on proximity to the irrigated farmlands mapped from the 1989 or 1994 irrigated farmlands survey. The weighting factor is the natural logarithm of distance in miles to an irrigated polygon. However, this weighting factor is manually constrained to be between 0.5 and 2, in order to limit the effect of weighting to a factor of 4. All grid cells further than roughly 7.4 miles from an irrigated polygon will have a weight of 0.5, while all grid cells nearer than 1.6 miles from an irrigated polygon will have a weight of 2.
 - 4.2.1. Create shapefile for MRLC land use categories 61, 82, and 83.
 - 4.2.1.1. In ArcView, load MRLC grid. Resample grid with a larger grid size to make the file more manageable (use x4 factor and set the analysis extent to the model domain). Select, in the new resampled grid, values 61, 82, and 83, and convert to shapefile. Call it “mrlc_irrigated.shp.”
 - 4.2.2. Create “distance grids” for the irrigated farmlands 89 and 94 shapefiles. These

will be grid files that contain the distance from each grid cell to the nearest irrigated farmlands polygon.

- 4.2.2.1. Add “irr_farms89.shp” to a view, and make it active. With Spatial Analyst extension activated, select “find distance” from the analysis menu. Choose a grid cell size of 1 mile, and set the extent to the model domain. This will generate a grid of distance values to the nearest irrigated farm. Repeat for “irr_farms94.shp.” Call them “dist_irryy.”
- 4.2.3. Using the Geoprocessing Wizard, intersect county-basin boundaries with “mrlc_irrigated.shp” to create “mrlc_cb.shp.” Create a unique id “cb_irr_id” so that, if necessary, these unique polygons can be queried.
- 4.2.4. Intersect “mrlc_cb.shp” with the 1 mi. sq. grid cells.
 - 4.2.4.1. Select only the 1 mile grid cells that are above the aquifer of concern’s extents (The county-basin irrigation pumpage totals are aquifer specific, so the pumpage should only be distributed where the proper underlying aquifer is present).
 - 4.2.4.2. It is also necessary to distribute across the entire county-basin area where the underlying aquifer is present, and not limited to the model domain in counties partly within the model domain. Therefore, if a county-basin is intersected by the model domain boundary, the pumpage total must be distributed across the entire county-basin so that only the proper percentage gets distributed inside the model domain. To insure that this happens, select the county-basins on the perimeter that get intersected by the model domain boundaries. With the Geoprocessing Wizard, intersect these county-basins with the subsurface aquifer boundaries, the resulting file will be county-basins above the aquifer. Clip out the areas that reside inside the model domain (Union with model domain and delete that which is inside). What is left, (county-basins above aquifer of concern and outside of model domain) can be dissolved into one polygon and merged with the 1 mile grid cells. Give this new polygon a grid_id of “9999999” (later when pumpage values are summed by grid id the “9999999” values will fall out).
 - 4.2.4.3. Add the new record “9999999” to the selected set from 4.3.4.1. Using Geoprocessing Wizard, intersect the selected 1 mile grid cells with the “mrlc_cb.shp” file. The result will be all of the irrigated land with the proper grid_id and county-basin name. Call it “mrlc_cb_grid.shp”.
 - 4.2.4.4. Add field “un_area_gd” and calculate the polygons’ areas in sq. miles using the field calculator (“un_area_gd” = [shape].returnarea/27878400).
- 4.2.5. Determine weighting factor for each polygon based on area and proximity with irrigated farms.
 - 4.2.5.1. Add fields “dist_irr89”, “dist_fact89”, “ardisfac89”, “sumcbfac89”,

“w_ar_dis89”.

- 4.2.5.2. Populate the distance to irrigated farmland field (“dist_irr89”) using the values from the “dist_irr89” grid file.
 - 4.2.5.3. Calculate the distance to irrigated farms factor using the field calculator (“dist_fact89”= $1/(1+[dist_irr89]).ln + 0.0001$). Select all values that are greater than 2 and change them to 2, and select all values that are less than 0.5 and change to 0.5 so that the range is 0.5 – 2.
 - 4.2.5.4. Calculate the area-distance factor using the field calculator (“ardisfac89” = “un_area_gd” * “dist_fact89”).
 - 4.2.5.5. Create a summary table by county-basin that summarizes the “ardisfac89” field. Link the summary table back up by county-basin and migrate the summed values into “sumcbfac89”.
 - 4.2.5.6. Calculate the distribution weighting factor for area of irrigated land (mrlc land use) and distance to irrigated farmland (farmland survey) using the field calculator (“w_ar_dis89” = “ardisfac89” / “sumcbfac89”). This is basically the fraction of the total county-basin pumpage that will be distributed to a specific polygon.
 - 4.2.5.7. Repeat section 4.3.5 for irrigated farmland 94.
- 4.2.6. Calculate unique pumpage values for 1 mile grid cells.
- 4.2.6.1. Create 20 new fields (1 for each year: “pmp_80” – “pmp_99”).
 - 4.2.6.2. Using SQL Connect, query the Access table **PumpagebyMajorAquifer1980-1999** for all years.
 - 4.2.6.3. Query the records (by the year column) for each year and specific aquifer (by aquifer code column) and export each query as a separate *.dbf file. “Pump_by_cb_yyyy_aquifer.dbf.” These tables will have a column for each use category, and can therefore also be used in livestock calculations for the same aquifer of concern.
 - 4.2.6.4. Join the table “pump_by_cb_1980_cw.dbf” to the attribute table “mrlc_cb_grid.shp” by countybasin. (make certain that all countybasin names are spelled the same).
 - 4.2.6.5. Calculate “pmp_80” using the field Calculator ($pmp_80 = w_ar_dis89 * irrigation$). Irrigation is the column of the joined table “pump_by_cb_1980” that contains the countybasin annual pumpage totals for irrigation use. Use “w_ar_dis89” for years 80-89 and use “w_ar_dis94” for years 90-99.
 - 4.2.6.6. Repeat 4.2.6.4 – 4.2.6.5 for all years.

- 4.2.7. Summarize all unique pumpage totals by grid cell id.
 - 4.2.7.1. Summarize all the “pump_unyy” fields by grid cell id, by using the summarize button and adding “pmp_80” (sum) through “pmp_99” (sum) in the dialog box. Name this summary file **area_irr_pumpbygrid_80_99**. (i.e. **sw_irr_pumpbygrid_80_99.dbf**).
 - 4.2.8. Vertical Distribution: Follow procedures outlined in sections 4.5.
 - 4.2.9. Import irrigation pumpage table back into MS Access database as a table **area_irrigation_total**, e.g., **sw_irrigation_total**
 - 4.2.9.1. In MS Access, import the attribute table for the Arcview shape file **grid_irr_yy.dbf** as a dbase file. This table should include one record for each possible Grid_ID, and at least the fields “Grid_ID”, “year”, and “pumpy_IRR.”
 - 4.2.10. The table **area_irrigation_total** now has only the grid_id of the upper model, i.e., the first digit is 1. The actual vertical distribution data is in the fields “per1” to “perx” where x is the number of vertical layers in the model. Copy the table x-1 times in an append query, incrementing the first digit of the grid id, to create a record for each model layer. There now should be L times the original number of records in the table. For example, for the northwestmost grid cells of a model with four layers, the following grid id’s should now exist: 1001001, 2001001, 3001001, and 4001001; whereas only 1001001 was in the original table.
 - 4.2.11. Calculate for each year the actual pumpage for each record as the product of the pumpage for a given year multiplied by the percent of pumpage from that model layer (from the fields “per1” – “per4”, for a model with 4 layers).
 - 4.2.12. Create a new summary query **Irrigation_annual_area** to summarize the pumpage for each grid_id and year from the table **area_irrigation_total**.
- 4.3. Spatial allocation of livestock groundwater pumpage – Livestock groundwater use within each county-basin is distributed evenly to all rangeland, Anderson Level II land use codes 31 (herbaceous rangeland), 32 (shrub and brush rangeland), and 33 (mixed rangeland) of the USGS 1:250,000 land use land cover data set (http://edcwww.cr.usgs.gov/glis/hyper/guide/1_250_lulc).
 - 4.3.1. Determine rangeland within each county-basin
 - 4.3.1.1. In Arcview, create a rangeland-only land use shapefile by loading the USGS land use shapefiles by quadrangle, merging them as required to cover the model domain, selecting the land use codes 31, 32, and 33 in a query, then saving the theme as a new shapefile **Rangeland.shp**.

- 4.3.1.2. Using the Geoprocessing Wizard, intersect the Rangeland shapefile with the County-basin shapefile (make sure to use entire county basin areas, and not the “clipped to domain” version) to make a new intersection shapefile **range_countybasin.shp**.
- 4.3.1.3. Calculate the unique area (in square miles) of the new intersected polygons “area_un1” using the field calculator ($\text{area_un1} = \text{shape.returnarea} / 27878400$).
- 4.3.1.4. Summarize the unique area by county-basin (total area of rangeland within county-basin) using the summary button.
- 4.3.1.5. Link the summary table back to the range_countybasin shape file and migrate it into a new field “rg_cb_tot” using the field calculator.
- 4.3.1.6. Determine weighted area factor “w_area1” for each polygon using the field calculator ($\text{w_area1} = (\text{area_un1} / \text{rg_cb_tot})$). W_area1 is, for each rangeland polygon, the fraction of the total rangeland area within the county-basin.
- 4.3.2. Intersect the rangeland/countybasin polygons with the Model Grid and set up for unique pumpage calculations.
 - 4.3.2.1. Using the Geoprocessing Wizard, intersect the shapefiles range_countybasin and Model Grid to create a new shape file **rng_cb_mg.shp**.
 - 4.3.2.2. Calculate the unique area of “intersected” polygons (area_un_grid) using the field calculator ($\text{area_un_grid} = \text{shape.returnarea} / 27878400$). Double check that no values are greater than 1.
 - 4.3.2.3. Determine the weighted area factor ($\text{w_area_grid} = (\text{area_un_grid} / \text{area_un1})$).
- 4.3.3. Calculate unique pumpage “pump_un_yy” for the intersected polygons for every year (80-99).
 - 4.3.3.1. Add the fields “pump_un80” – “pump_un99” to the **rng_cb_mg** attribute table.
 - 4.3.3.2. Using SQL Connect, query the Access table **PumpagebyMajorAquifer1980-1999** for all years.
 - 4.3.3.3. Query the records (by the year column) for each year, and specific aquifer (by aquifer code column) and export each query as a separate .dbf file. “Pump_by_cb_yyyy_aquifer.dbf.” These tables will have a column for each use category, and can therefore be used in the irrigation calculations for the same aquifer of concern.
 - 4.3.3.4. Join the table “pump_by_cb_1980.dbf” to the attribute table “rng_cb_mg” by countybasin. (make certain that all countybasin names are spelled the same).

- 4.3.3.5. Calculate “pump_un80” using the field Calculator ($\text{pump_un80} = \text{w_area_grid} * (\text{w_area_1} * \text{livestock})$). (livestock is the column of the joined table “pump_by_cb_1980” that contains the countybasin annual pumpage totals for livestock use).
 - 4.3.3.6. Repeat 4.3.3.4 – 4.3.3.5 for all years.
 - 4.3.4. Summarize all unique pumpage totals by grid cell id.
 - 4.3.4.1. Summarize all the “pump_unyy” fields by grid cell id, by using the summarize button and adding “pump_un_80” (sum) through “pump_un_99” (sum) in the dialog box. Name this summary file “area_stk_pumpbygrid_80_99.” (i.e. sw_stk_pumpbygrid_80_90.dbf).
 - 4.3.5. Vertical Distribution: Follow procedures outlined in sections 4.5.
 - 4.3.6. Import livestock pumpage summary table back into MS Access database as a table **area_livestock_total**, e.g. **sw_livestock_total**.
 - 4.3.7. The table **area_livestock_total** now has only the grid_id of the upper model, i.e., the first digit is 1. The actual vertical distribution data is in the fields “per1” to “perx” where x is the number of vertical layers in the model. Copy the table x-1 times in an append query, incrementing the first digit of the grid id, to create a record for each model layer. There now should be L times the original number of records in the table. For example, for the northwestmost grid cells of a model with four layers, the following grid id’s should now exist: 1001001, 2001001, 3001001, and 4001001; whereas only 1001001 was in the original table.
 - 4.3.8. Calculate for each year the actual pumpage for each record as the product of the pumpage for a given year multiplied by the percent of pumpage from that model layer (from the fields “per1” – “per4”, for a model with 4 layers).
 - 4.3.9. Create a new summary query **Livestock_annual_area** to summarize the pumpage for each grid_id and year from the table **area_irrigation_total**.
- 4.4. Spatial allocation of rural domestic (C-O) groundwater pumpage.
 - 4.4.1. Calculate the Population in each 1 mile grid cell.
 - 4.4.1.1. In Arcview, load the 1990 block-level census population shapefile.
 - 4.4.1.2. Load Arcview polygon shapefiles for cities. Select census blocks that fall within city boundaries and delete those records so that rural domestic pumpage does not get distributed to cities. (Note: we’re assuming that city boundaries are good surrogates for the extent of the area served by public water supply systems, whose pumpage is reported under the category “MUN”).

Repeat this process for the reservoir areas.

- 4.4.1.3. Calculate the area of census blocks in sq. miles in a new field “blk_area” using the Field Calculator function ($\text{blk_area} = \text{shape.returnarea} / 27878400$).
 - 4.4.1.4. Load the model grid, model domain, and county-basins shapefile. Select all county-basins that are intersected by the model domain boundary. Union the selected county-basins with the model domain boundary. In the resulting shapefile, delete the polygons that are inside the model domain, leaving only areas of the county-basins that are outside of the model domain. Dissolve these polygons into one and merge with the model grid shapefile. Give this new record a grid_id of 9999999. (Adding this new area will insure that, when the county-basin total populations are calculated, the population outside of the model domain will be included).
 - 4.4.1.5. In the Geoprocessing Wizard, intersect the census block shapefile with the model grid shapefile to create a new shape file **intrsect90.shp**. (Note: Because the model grid size is 1 square mile, no intersected polygon (inside the model domain) should be larger than 1 square mile. Make sure that this is the case before proceeding).
 - 4.4.1.6. Calculate the unique area of all intersected polygons in square miles as a new field “area_un1” using the Field Calculator function ($\text{area_un1} = \text{shape.returnarea} / 27878400$). (so that one grid cell has an area of 1).
 - 4.4.1.7. Add a new numeric field “pop_un1” – the unique Population of the intersected polygons. Using the Field Calculator, calculate its value as ($\text{POP_un1} = \text{pop90} * \text{area_un1} / \text{blk_area}$) where pop90 is the block Population from the census file.
 - 4.4.1.8. Sum the field “pop_un1” by grid_id using the Field Summarize function to calculate the total population within each grid cell. Join this summary table to the original grid table by grid_id and copy value into new field “pop_90”.
 - 4.4.1.9. Repeat steps 4.5.1.1 – 4.5.1.8 (no need to repeat step 4.5.1.4, just use the grid file that was used for previous iteration).
- 4.4.2. Calculate the rural domestic pumpage for each 1 mile grid cell.
- 4.4.2.1. Intersect the county-basins shapefile with the model grid (which now has census populations for 1990 and 2000) to create a new shapefile **grid_cb_pop**.
 - 4.4.2.2. Create new field “area_un2” and calculate unique area using field calculator (“area_un2” = $[\text{shape}].\text{returnarea}/27878400$)
 - 4.4.2.3. Create two new fields “pop_un90” and “pop_un00”. Calculate using the field calculator (“pop_unyy” = $\text{“area_un2”}/\text{“pop_yy”}$)

- 4.4.2.4. Using SQL Connect, query the Access table **PumpagebyMajorAquifer1980-1999** for all years.
 - 4.4.2.5. Query the records (by the year column) for each year (because Rural Domestic pumpage data is not aquifer specific, there is no need to query by aquifer) and export each query as a separate .dbf file. “Pump_by_cb_yyyy.dbf.”
 - 4.4.2.6. Join table “pump_by_cb_1980.dbf” to grid_cb_pop.dbf by county-basin.
 - 4.4.2.7. Add field “pmp80.” Using field calculator, calculate “pmp80” (pmp80=CO*pop_un90/cb_pop90).
 - 4.4.2.8. Repeat steps 4.4.2.6 – 4.4.2.7 for each year. Use pop90 for years 1980-1989 and use pop00 for years 1990-1999.
 - 4.4.2.9. As a quality control check, sum the values of “rdom_pump” for each county-basin and make sure it matches the total for the county-basin from the Access table.
 - 4.4.2.10. Summarize pmp80 through pmp99 by grid id. Link summary back to model grid file and migrate pumpage values.
- 4.4.3. Vertical Distribution: Follow procedures outlined in section 4.5.
 - 4.4.4. Import the rural domestic pumpage table into the MS Access database as a table **area_rurdom_total**, e.g., **sw_rurdom_total**.
 - 4.4.5. The table **area_rurdom_total** now has only the grid_id of the upper model, i.e., the first digit is 1. The actual vertical distribution data is in the fields “per1” to “perx” where x is the number of vertical layers in the model. Copy the table x-1 times in an append query, incrementing the first digit of the grid id, to create a record for each model layer. There now should be L times the original number of records in the table. For example, for the northwestmost grid cells of a model with four layers, the following grid id’s should now exist: 1001001, 2001001, 3001001, and 4001001; whereas only 1001001 was in the original table.
 - 4.4.6. Calculate for each year the actual pumpage for each record as the product of the pumpage for a given year multiplied by the percent of pumpage from that model layer (from the fields “per1” – “per4”, for a model with 4 layers).
 - 4.4.7. Create a new summary query **Rurdom_annual_area** to summarize the pumpage for each grid_id and year from the table **area_rurdom_total**.
- 4.5. Vertical Distribution of groundwater pumpage. *Note: These procedures are for all use categories, and this section is referenced multiple times. Take care, and perform only

the operations that apply to that particular use.

- 4.5.1. Assign default well depths to model grid cells – Most, but not all, well-specific pumpage from the categories MUN, MFG, PWR, and MIN are associated with a reported well depth, screened interval, land surface elevation, which are used to attribute the pumpage to a specific vertical model layer. For those wells whose depth, screened interval, or land surface elevation is unknown, and for the non-well-specific pumpage in the categories C-O, STK, and IRR, it is necessary to interpolate these depths/elevations to assign the pumpage to a specific model layer. In this procedure, the approach is to interpolate on the basis of the depths of nearby (<10 miles) wells. On average, municipal, industrial, and irrigation water wells tend to be deeper than rural domestic or livestock wells. Thus, if there are nearby wells in the same water use category, the interpolation is based on these wells. In the absence of nearby wells of the same use category, the interpolation is based on nearby wells of any water use category. **The procedures outlined in section 4.5.1 cover all use categories, and therefore, only need to be done once per model area.*
- 4.5.1.1. In Arcview, using SQL Connect, query the MS Access database table **All_wells** for all wells in the major aquifer of concern (based on the field “aqfr_id_1”). Save this query as a table **AQ_wells**, where **AQ** is a 2-character code representing the aquifer of interest.
- 4.5.1.2. Load these wells in a View as an event theme, using the fields lat_dd as y-coordinate and long_dd as x-coordinate. Convert the event theme to GAM projection as per GAM Technical Memo 1-01, then save this theme as a shape file.
- 4.5.1.3. Query the shape file’s attribute table for all domestic water wells (water_use_1 = “domestic”).
- 4.5.1.4. Using Arcview Spatial Analyst, under the Analyst, Properties menu, set analysis extent and grid size to be equal to the GAM model grid.
- 4.5.1.5. Next, under the Surface menu, interpolate a grid with values of interpolated well depth, via the inverse distance weighting method, within a fixed radius of 10 miles, with a power of 2.
- 4.5.1.6. Repeat steps 4.5.1.3 – 4.5.1.5 to create an interpolated well depth grid for each of the other water use categories MUN, MFG, PWR, MIN, STK, and IRR, as well as a well depth grid for all water use categories combined.
- 4.5.1.7. When a depth was not reported for a well, these grid values can be used as an estimated well depth. A new text field “depth source” is added to the well table to indicate that the well depth was estimated by interpolation, not reported. This allows a hydrogeologist or modeler to review these wells to make sure they fall in the proper model layer. When a well depth is checked and corrected manually, a value of “manual” is entered in the field “depth source”. Valid values of depth source include “reported”, “interpolated”, or

“manual”.

- 4.5.2. Assign default screened intervals to wells – For wells with no reported screened interval, calculate the well screened interval. The lower boundary is the well depth, while the upper boundary of the screened interval is calculated as the well depth minus an estimated screen length. The default screen lengths will be estimated from other wells in the same aquifer for which the screened interval is known.
- 4.5.2.1. An Excel file *Screened_Interval.xls* is provided by the modelers. It contains the land surface elevation and depths to the top and bottom of the screen for each well. The screened interval is calculated as the difference between the top and bottom depths. This file is loaded in Arcview and joined to the *AQ_Wells* table by state well number. Next, under the Surface menu, interpolate a grid with values of interpolated screened interval, via the inverse distance weighting method, within a fixed radius of 10 miles, with a power of 2.
- 4.5.2.2. When a screened interval is not reported for a well, these grid values can be used to estimate the upper depth of the screened interval, assuming that the well depth is the bottom of the interval. A new text field “screen_source” is added to the well table to indicate that the well depth was estimated by interpolation, not reported. Valid values of screen source include “reported” or “interpolated”, or “manual”.
- 4.5.3. Assign land surface elevations to wells – For wells without a reported land surface elevation (in the field “elev of lsd”) a land surface elevation must be estimated. For this purpose, a 30-meter digital elevation model (DEM) grid is added to an Arcview project with the well data table. The Arcview script “getgridvalue” in Appendix 2 is run to return the value of the land surface elevation for the well.
- 4.5.4. Estimate the screened interval for non-well-specific pumpage - For the non-well-specific uses STK, IRR, and C-O, in order to distribute the pumpage vertically, each model grid cell may be treated as a well. Using the centroids of the model grid cells as if they were wells, copy the interpolated values of well depth, screened interval, and land surface elevation to each grid cell as described above.
- 4.5.5. Convert depths to elevations - In order to compare to model layers, which are reported as elevation (feet above mean sea level), it is necessary to convert the depths of the top and bottom of screened intervals to elevations. To do this, subtract the depths from the land surface elevation, in feet above mean sea level.
- 4.5.6. Determine vertical distribution of pumpage totals by comparing the elevations of the top and bottom of the well screened interval to model layer elevations. (For point source water use categories, this will be done for each specific well. For non-point source this will be done for each 1 mile grid cell).
- 4.5.7. Spatially join the flow layer structure (model grid cells with tops of aquifer elevations) to the wells. (for non-point source join by grid id).

- 4.5.8. Run vertical distribution avenue script on points (see appendix for code). This script will place a “pumpage percentage” in the flow layer percentage columns (per1 – per6). This value is actually the percentage of the total length of the screened interval that resides in each flow layer (possible 0 – 100).
- 4.5.9. Once script is successfully run, a series of QA checks must be run, and in certain cases percentage values must be altered manually. Field “calc_code” will be given a specific code for each case of manual alteration.
 - 4.5.9.1. Query records that have a value of “99999” for every layer elevation (i.e. layer doesn’t exist at that location). Set calc_code to “N”.
 - 4.5.9.2. Query records whose top of screen elevation is shallower than the top of the shallowest existing layer. (i.e. (top of layer 2 = 999999 and per2 > 0)). The script automatically puts a value in per2 if the top of screen is shallower than layer 3, but if layer 2 doesn’t exist there then per2 should be zero and the value should be shifted down. In this case, calc_code should be set to “S3”. This will tell someone that the screen is shallower than the shallowest layer which is layer 3.
 - 4.5.9.3. Query records whose depth is deeper than the bottom layer. (i.e. depth < bottom layer). Put the remainder of the pumpage that was lost below into the bottom layer and set calc_code to “D”.
 - 4.5.9.4. Query records whose screened interval spans layer 1 or 2 and enters layer 3 (Carrizo). (i.e. per3 > 0 and per2 > 0). It is assumed that if the screened interval reaches the Carrizo then all of the water is being taken from that layer and not the above layers of inferior quality. Set per1 and per2 to zero and add their values to per3. Set calc_code to “C”.
 - 4.5.9.5. Query records whose reported top of screen elevation is less than the bottom of screen elevation. Manually set the appropriate layer percentage to 100%. Set calc_code to “E”.
 - 4.5.9.6. Query records whose top of screen elevation exactly equals one of the layer top elevations. This is very rare, but if it happens, the percentage value must be manually entered. Set calc_code to “=”.
 - 4.5.9.7. Query records whose total percentage is less than 100% by less than .5%. Due to a program glitch values of 99.5% get rounded to 100% and the rest is left out. Manually set percentage value to 100%. Set calc_code to “R”.
 - 4.5.9.8. Query all other records (records that don’t have a calc_code value and whose tot_per = 100%). Set calc_code to “NP” for no problems.

5. Temporal Distribution of Rural Domestic, Livestock, and Irrigation Groundwater Use

5.1. Temporal distribution of livestock pumpage - Because we have only annual total groundwater pumpage estimates for STK, we need to derive monthly pumpage estimates. According to TWDB GAM Technical Memo 01-06, annual total livestock pumpage may be distributed uniformly to months since the water needs of livestock are not likely to vary significantly over the course of a year.

5.1.1. In the MS Access database, create a new table called Monthly Factors with the fields "countyname", "basinname", "countynumber", "basinnumber", "data_cat", "year", and "month". The table should include a record for every county-basin within the model domain, water use category "data_cat", year (1980-1999), and month (1-12), as well as an additional annual total record (month="0") for each county-basin, year, and water use category. Add 2 new fields "mfraction" and "Monthly distribution factor source" to the new table. The former is the numeric monthly distribution factor, while the latter is a text field indicating the source of the distribution factor. For all monthly livestock water use records (data_cat=STK, month in 1-12), enter an mfactor of "0.0833" (1/12) and a monthly distribution factor source of "Tech Memo 01-06". For all annual total water use records (data_cat=STK, month =0), enter an mfactor of "1" and a monthly distribution factor source of "NA".

5.2. Temporal distribution of irrigation (IRR) pumpage - Because we have only annual total groundwater pumpage estimates for IRR, we need to derive monthly pumpage estimates. Monthly distribution factors will be derived separately for rice-farming counties and non-rice-farming counties.

5.2.1. Temporal distribution of groundwater used for non-rice irrigation –

5.2.1.1. Record monthly crop evapotranspiration (ET), or total water demand, for each of the Texas Crop Reporting Districts (TCRDs) that occur within the model domain, from the report "Mean Crop Consumptive Use and Free-Water Evaporation for Texas" by J. Borrelli, C.B. Fedler, and J.M. Gregory, Feb. 1, 1998 (TWDB Grant No. 95-483-137). Use these values for all years.

5.2.1.2. Next, determine monthly precipitation (P) for the period 1980-1999 for the locale within each of the TCRDs that occur within the model domain.

5.2.1.3. Determine the monthly water deficit for each month of the two periods 1980-1989 and 1990-1999 by subtracting the P values from the ET values for each TCRD. Replace negative values with zero. Sum all water deficit values by month for each of the two periods, and divide by the number of months in each period to obtain an average non-rice monthly distribution factor for each month for the two periods 1980-89 and 1990-99.

5.2.2. Temporal distribution of groundwater used for rice irrigation –

5.2.2.1. First, identify the counties within the model area where rice is irrigated, using the 1989 and 1994 irrigation reports. Include only those counties in this analysis.

- 5.2.2.2. Next, using monthly pump power usage records provided by rice farmers, calculate monthly distribution factors for total annual power usage. Average all distribution factors within a county to get an average rice irrigation distribution factor.
- 5.2.3. Develop composite irrigation monthly distribution factors for each county and year based on the monthly factors for rice and non-rice irrigation, and the fraction of irrigation for rice in that county.
- 5.2.3.1. The TWDB irrigation survey data files Irr1989.xls and Irr1994.xls contain reported irrigation water use estimates for each crop and county. From these tables, calculate the fraction of irrigation water for rice in each county for the 1980s (based on 1989) and the 1990's (based on 1994).
- 5.2.3.2. Calculate the composite monthly distribution factor (MF_{comp}) for irrigation for each county as:
- $$MF_{comp} = MF_{rice} * X + MF_{non-rice} * (1 - X)$$
- where X is the fraction of water used for rice, and MF_{rice} and $MF_{non-rice}$ are the monthly distribution factors for rice and non-rice crops determined in steps 5.2.1 and 5.2.2, above.
- 5.2.4. For the county-basins where rice is not irrigated, enter the monthly distribution factors from step 5.2.3, above, in the table **Monthly Factors** for each year, county, basin, using "data_cat"="IRR", and "Monthly Distribution Factor Source"="ET/P Water Deficit Analysis."
- 5.2.5. For the county-basins where rice is irrigated, enter the monthly distribution factors from step 5.2.3, above, in the table **Monthly Factors** for each year, county, basin, using "data_cat"="IRR", and "Monthly Distribution Factor Source"="ET/P + Power Usage Analysis."
- 5.3. Temporal distribution of rural domestic (C-O) pumpage - Because we have only annual total groundwater pumpage estimates for C-O, we need to derive monthly pumpage estimates. According to TWDB GAM Technical Memo 01-06, annual rural domestic pumpage may be distributed based on the average monthly distribution of all municipal water use within the same county-basin.
- 5.3.1. In a MS Access query based on the table **RawDataMUN_linkedwithwellinfo**, calculate the sum of the fields "Annual total in gallons", "jan", "feb", ".....", "dec" for each county, basin, and year.
- 5.3.2. Next, calculate "mfraction," the fraction of the annual total for each month, by dividing the columns "sum of jan", "sum of feb", ".....", "sum of dec" by the "sum of annual total in gallons.". Transpose this table via a query to make a table with the following fields: "countyname", "basinname", "year", "month", "mfraction", "data_cat," and "monthly distribution factor source." A value of "C-O" should be

entered in the field “data_cat”, and the value of “monthly distribution factor source”=“this county-basin mun.”

5.3.3. The values of “mfraction” are statistically reviewed for outliers. Generally, monthly distribution factors fall within the range 0.035 to 0.15. Higher or lower values can be found when there is little municipal water use in a county-basin. In this case, substitute the values of “mfraction” from an adjacent county-basin, preferably from within the same county. Update the field “monthly distribution factor source” with the name of the county-basin used as a source.

5.3.4. For Louisiana and Arkansas parishes and counties, use the monthly distribution factors of the nearest Texas county-basin.

5.3.5. Add an annual total record for each county-basin-year, with “data_cat”=“C-O”, “month”=“0”, “mfraction”=“1”, and “monthly distribution factor source”=“NA.”

5.3.6. Using an append query, append these records to the table **Monthly Factors**.

6. Summarize Pumpage Information

6.1. Summary Queries

6.1.1. Queries for livestock - Create a new select query **MMMY_STK** to calculate pumpage for the month and year of interest by multiplying the monthly factor for that month, year, and water use category, in the table **Monthly Factors**, by each entry in the imported table **Livestock_annual_CGC**. For any specified month (MMM) and year (YY), the SQL for the query **MMMY_STK** is:

```
SELECT Livestock_annual_CGC.GRID_ID, Livestock_annual_CGC.DATA_CAT,  
Livestock_annual_CGC.Year, Livestock_annual_CGC.MODEL, [MONTHLY  
FACTORS].MONTH, [SumPumpageAF]*[mfraction] AS PumpageAF
```

```
FROM Livestock_annual_CGC LEFT JOIN [MONTHLY FACTORS] ON  
(Livestock_annual_CGC.Year = [MONTHLY FACTORS].YEAR) AND  
(Livestock_annual_CGC.DATA_CAT = [MONTHLY FACTORS].DATA_CAT)  
AND (Livestock_annual_CGC.basinum = [MONTHLY FACTORS].basinum)  
AND (Livestock_annual_CGC.CountyNumber = [MONTHLY  
FACTORS].countynum)
```

```
WHERE (((Livestock_annual_CGC.DATA_CAT)="STK") AND  
((Livestock_annual_CGC.Year)=1980) AND  
((Livestock_annual_CGC.MODEL)="CGC") AND (([MONTHLY  
FACTORS].MONTH)=1))
```

```
ORDER BY [SumPumpageAF]*[mfraction];
```

6.1.2. Queries for irrigation – Create a new select query **MMMY_IRR** to calculate pumpage for the month and year of interest by multiplying the monthly factor for

that month, year, and water use category, in the table **Monthly Factors**, by each entry in the imported table **Irrigation_annual_CGC**. For any specified month (MMM) and year(YY), the SQL for the query **MMMYY_IRR** is:

```
SELECT Irrigation_annual_CGC.GRID_ID, Irrigation_annual_CGC.DATA_CAT,  
Irrigation_annual_CGC.Year, Irrigation_annual_CGC.MODEL, [MONTHLY  
FACTORS].MONTH, [SumPumpageAF]*[mfraction] AS PumpageAF
```

```
FROM Irrigation_annual_CGC LEFT JOIN [MONTHLY FACTORS] ON  
(Irrigation_annual_CGC.basinum = [MONTHLY FACTORS].basinum) AND  
(Irrigation_annual_CGC.CountyNumber = [MONTHLY FACTORS].countynum)  
AND (Irrigation_annual_CGC.Year = [MONTHLY FACTORS].YEAR) AND  
(Irrigation_annual_CGC.DATA_CAT = [MONTHLY FACTORS].DATA_CAT)
```

```
WHERE (((Irrigation_annual_CGC.DATA_CAT)="IRR") AND  
((Irrigation_annual_CGC.Year)=1980) AND  
((Irrigation_annual_CGC.MODEL)="CGC") AND (([MONTHLY  
FACTORS].MONTH)=1))
```

```
ORDER BY [SumPumpageAF]*[mfraction];
```

- 6.1.3. Queries to summarize rural domestic (county-other) - Create a new select query **MMMYY_C-O** to calculate pumpage for the month and year of interest by multiplying the monthly factor for that month, year, and water use category, in the table **Monthly Factors**, by each entry in the imported table **Rurdom_annual_CGC**. For any selected month (MMM) and year(YY), the SQL for the query **MMMYY_C-O** is:

```
SELECT Rurdom_annual_CGC.GRID_ID, Rurdom_annual_CGC.DATA_CAT,  
Rurdom_annual_CGC.Year, Rurdom_annual_CGC.MODEL, [MONTHLY  
FACTORS].MONTH, [SumPumpageAF]*[mfraction] AS PumpageAF
```

```
FROM Rurdom_annual_CGC LEFT JOIN [MONTHLY FACTORS] ON  
(Rurdom_annual_CGC.DATA_CAT = [MONTHLY FACTORS].DATA_CAT)  
AND (Rurdom_annual_CGC.Year = [MONTHLY FACTORS].YEAR) AND  
(Rurdom_annual_CGC.CountyNumber = [MONTHLY FACTORS].countynum)  
AND (Rurdom_annual_CGC.basinum = [MONTHLY FACTORS].basinum)
```

```
WHERE (((Rurdom_annual_CGC.DATA_CAT)="C-O") AND  
((Rurdom_annual_CGC.Year)=1980) AND  
((Rurdom_annual_CGC.MODEL)="CGC") AND (([MONTHLY  
FACTORS].MONTH)=1))
```

```
ORDER BY [SumPumpageAF]*[mfraction];
```

- 6.1.4. Query to summarize well-specific pumpage - Create a new select query in MS Access **MMMYYWell-SpecificSum** to summarize the well-specific pumpage from all wells within a grid cell for the desired month or year. For any specified month

and year, the SQL query for well-specific pumpage would be:

```
SELECT CGC_gridsum_well_specific.GRID_ID, "WS" AS DATA_CAT,
CGC_gridsum_well_specific.year, CGC_gridsum_well_specific.Model,
CGC_gridsum_well_specific.month,
CGC_gridsum_well_specific.SumPumpage_af AS PumpageAF

FROM CGC_gridsum_well_specific

WHERE (((CGC_gridsum_well_specific.year)=[Enter year]) AND
((CGC_gridsum_well_specific.Model)="CGC") AND
((CGC_gridsum_well_specific.month)=[Enter month]))

ORDER BY CGC_gridsum_well_specific.SumPumpage_af;
```

6.1.5. In order to ensure that each grid cell is included in the final summary queries, even if there is no pumpage from the cell, we must create a full grid with values of zero.

6.1.5.1. Create a new table **Zero_grid_annual** in a make-table query based on the table **grid_lkup_area** with one record for each grid cell and year. For instance, a model with 212 rows, 180 columns, and 6 layers, for 20 years would be create a table with 212 x 180 x 6 x 20= 4,579,200 records. In the make-table query, add a field “SumPumpageAF” with a value of zero for each record.

6.1.5.2. Create a new query **MMMYZ_ZeroGrid** to provide zero values for each grid cell for each month. You can use any of the monthly factors, as all results will equal zero. As an example, the SQL query for January 1980 would be:

```
SELECT Zero_Grid_Annual.GRID_ID, Zero_Grid_Annual.DATA_CAT,
Zero_Grid_Annual.Year, Zero_Grid_Annual.MODEL, [MONTHLY
FACTORS].MONTH, Zero_Grid_Annual.SumPumpageAF

FROM Zero_Grid_Annual LEFT JOIN [MONTHLY FACTORS] ON
(Zero_Grid_Annual.basinum = [MONTHLY FACTORS].basinum) AND
(Zero_Grid_Annual.CountyNumber = [MONTHLY FACTORS].countynum)
AND (Zero_Grid_Annual.Year = [MONTHLY FACTORS].YEAR)

WHERE (((Zero_Grid_Annual.Year)=[Enter year]) AND (([MONTHLY
FACTORS].MONTH)=[Enter month]) AND (([MONTHLY
FACTORS].DATA_CAT)="IRR"))

ORDER BY Zero_Grid_Annual.GRID_ID;
```

6.1.6. In Access, create a new union query **MMMYZ_UnionofPumpage** to combine the domestic, livestock, rural domestic, and well-specific pumpage sums, as well as the

zero value, for each grid cell. As an example, the SQL for any given year and month is:

```
SELECT * FROM [MMMY_C-O] UNION ALL SELECT * FROM  
[MMMY_IRR] UNION ALL SELECT * FROM [MMMY_STK]  
UNION ALL SELECT * FROM [MMMY_ZeroGrid] UNION ALL  
SELECT * FROM [MMMYWell-specificSum];
```

- 6.1.7. Create a new select query **SumPumpageGrid_MMMYY** to summarize all pumpage by grid cell, grouping by grid_id, month, and year the pumpage from the above union query. As an example, the SQL for January 1980 is:

```
SELECT MMYUnionofPumpage.GRID_ID,  
MMYUnionofPumpage.Year, MMYUnionofPumpage.MONTH,  
Sum(MMYUnionofPumpage.PumpageAF) AS SumOfPumpageAF,  
Sum([PumpageAF]*[MGDfromAF]) AS PumpageMGD  
  
FROM MMYUnionofPumpage LEFT JOIN UnitConversion ON  
MMYUnionofPumpage.MONTH = UnitConversion.Month  
  
GROUP BY MMYUnionofPumpage.GRID_ID,  
MMYUnionofPumpage.Year, MMYUnionofPumpage.MONTH  
  
ORDER BY MMYUnionofPumpage.GRID_ID;
```

- 6.2. Join pumpage queries to Arcview shapefile if visual display of the results for a month or year is desired.

- 6.2.1. In Arcview, import the MS Access query **SumPumpageGrid_MMMYY**, and join it to the model grid cells in the Arcview shapefile based on the field "Grid_ID."
- 6.2.2. In Arcview, import the MS Access queries **MMMY_STK**, **MMMY_IRR**, **MMMY_C-O**, and **Well-specificpumpage**. Link these tables to the model grid cells in the Arcview shapefile based on the field "Grid_ID" and, for well-specific pumpage, "year." Selection of a grid cell in Arcview will then also select the records in each of these tables that pump from the grid cell selected.

Appendix 1 - Vertical Distribution Avenue Script

```
theView = Av.GetActiveDoc
theTheme = theView.findTheme("wells")
theFtab = theTheme.GetFtab

'get elevation values for layers
theLay1Field = theFtab.findField("top_young")
theLay2Field = theFtab.findField("top_reklaw")
theLay3Field = theFtab.findField("top_carriz")
theLay4Field = theFtab.findField("top_uwilco")
theLay5Field = theFtab.findField("top_mwilco")
theLay6Field = theFtab.findField("top_lwilco")
theBottomField = theFtab.findField("bas_lwilco")

'get percentfield holders
thePer1Field = theFtab.findField("per1")
thePer2Field = theFtab.findField("per2")
thePer3Field = theFtab.findField("per3")
thePer4Field = theFtab.findField("per4")
thePer5Field = theFtab.findField("per5")
thePer6Field = theFtab.findField("per6")
theTotPerField = theFtab.findField("tot_per")

'get well values
theScreenField = theFtab.findField("Screen")
theDepthField = theFtab.findField("depth")

theSel = theFtab.GetSelection

for each rec in theSel
  ct = 0
  totPerVal = 0
  cumPerVal = 0
  theDepthVal = theFtab.ReturnValue(theDepthfield,rec)
  theScreenVal = theFtab.ReturnValue(theScreenfield,rec)
  screenLengthVal = (theScreenVal - theDepthVal).abs

  theLay1Val = theFtab.ReturnValue(theLay1field,rec)
  theLay2Val = theFtab.ReturnValue(theLay2field,rec)
  theLay3Val = theFtab.ReturnValue(theLay3field,rec)
  theLay4Val = theFtab.ReturnValue(theLay4field,rec)
  theLay5Val = theFtab.ReturnValue(theLay5field,rec)
  theLay6Val = theFtab.ReturnValue(theLay6field,rec)
  theBotVal = theFtab.ReturnValue(theBottomField,rec)

  if ((theScreenVal < theLay1Val ) And (theScreenVal > theLay2Val)) then
    if (theDepthVal < theLay2Val) then
      per1 = (((theLay2Val - theScreenVal) / screenLengthVal) * 100).abs
      theFtab.SetValue(thePer1field,rec,per1)
      cumPerVal = cumPerVal + per1
    else
      per1 = (100 - cumPerVal)
      cumPerVal = cumPerVal + per1
```

```
        theFtab.SetValue(thePer1field,rec,per1)
    end
else
    per1 = 0
    theFtab.SetValue(thePer1field,rec,per1)
end
'-----layer 2
if (cumperval.round = 100) then
    'continue
    ct=ct+1
    per2 = 0
    theFtab.SetValue(thePer2field,rec,per2)
else
    if ((theScreenVal < theLay2Val ) And (theScreenVal > theLay3Val)) then
        if (theDepthVal < theLay3Val) then
            per2 = (((theScreenVal - theLay3Val) / screenLengthVal) * 100).abs
            cumPerVal = cumPerVal + per2
            theFtab.SetValue(thePer2field,rec,per2)
        else
            per2 = (100 - cumPerVal)
            cumPerVal = cumPerVal + per2
            theFtab.SetValue(thePer2field,rec,per2)
        end
    end
else
    if (cumPerVal > 0) then 'if continuing
        if (theDepthVal < theLay3Val) then
            per2 = (((theLay3Val - theLay2Val) / screenLengthVal) * 100).abs
            cumPerVal = cumPerVal + per2
            theFtab.SetValue(thePer2field,rec,per2)
        else
            per2 = (((theDepthVal - theLay2Val) / screenLengthVal) * 100).abs
            cumPerVal = cumPerVal + per2
            theFtab.SetValue(thePer2field,rec,per2)
        end
    end
else
    per2 = 0
    theFtab.SetValue(thePer2field,rec,per2)
end
end
end
'-----layer 3
if (cumperval.round = 100) then
    'continue
    ct=ct+1
    per3 = 0
    theFtab.SetValue(thePer3field,rec,per3)
else
    if ((theScreenVal < theLay3Val ) And (theScreenVal > theLay4Val)) then
        if (theDepthVal < theLay4Val) then
            per3 = (((theScreenVal - theLay4Val) / screenLengthVal) * 100).abs
            cumPerVal = cumPerVal + per3
            theFtab.SetValue(thePer3field,rec,per3)
        else
            per3 = (100 - cumPerVal)
            cumPerVal = cumPerVal + per3
            theFtab.SetValue(thePer3field,rec,per3)
        end
    end
end
```

```

end
else
if (cumPerVal > 0) then 'if continuing
if (theDepthVal < theLay4Val) then
per3 = (((theLay4Val - theLay3Val) / screenLengthVal) * 100).abs
cumPerVal = cumPerVal + per3
theFtab.SetValue(thePer3field,rec,per3)
else
per3 = (((theDepthVal - theLay3Val) / screenLengthVal) * 100).abs
cumPerVal = cumPerVal + per3
theFtab.SetValue(thePer3field,rec,per3)
end
else
per3 = 0
theFtab.SetValue(thePer3field,rec,per3)
end
end
end
'-----layer 4
if (cumperval.round = 100) then
'continue
ct=ct+1
per4 = 0
theFtab.SetValue(thePer4field,rec,per4)
else
if ((theScreenVal < theLay4Val ) And (theScreenVal > theLay5Val)) then
if (theDepthVal < theLay5Val) then
per4 = (((theScreenVal - theLay5Val) / screenLengthVal) * 100).abs
cumPerVal = cumPerVal + per4
theFtab.SetValue(thePer4field,rec,per4)
else
per4 = (100 - cumPerVal)
cumPerVal = cumPerVal + per4
theFtab.SetValue(thePer4field,rec,per4)
end
else
if (cumPerVal > 0) then 'if continuing
if (theDepthVal < theLay5Val) then
per4 = (((theLay5Val - theLay4Val) / screenLengthVal) * 100).abs
cumPerVal = cumPerVal + per4
theFtab.SetValue(thePer4field,rec,per4)
else
per4 = (((theDepthVal - theLay4Val) / screenLengthVal) * 100).abs
cumPerVal = cumPerVal + per4
theFtab.SetValue(thePer4field,rec,per4)
end
else
per4 = 0
theFtab.SetValue(thePer4field,rec,per4)
end
end
end
'-----layer 5
if (cumperval.round = 100) then
'continue
ct = ct+1

```

```

per5 = 0
theFtab.SetValue(thePer5field,rec,per5)
else
if ((theScreenVal < theLay5Val ) And (theScreenVal > theLay6Val)) then
if (theDepthVal < theLay6Val) then
per5 = (((theScreenVal - theLay6Val) / screenLengthVal) * 100).abs
cumPerVal = cumPerVal + per5
theFtab.SetValue(thePer5field,rec,per5)
else
per5 = (100 - cumPerVal)
cumPerVal = cumPerVal + per5
theFtab.SetValue(thePer5field,rec,per5)
end
else
if (cumPerVal > 0) then 'if continuing
if (theDepthVal < theLay6Val) then
per5 = (((theLay6Val - theLay5Val) / screenLengthVal) * 100).abs
cumPerVal = cumPerVal + per5
theFtab.SetValue(thePer5field,rec,per5)
else
per5 = (((theDepthVal - theLay5Val) / screenLengthVal) * 100).abs
cumPerVal = cumPerVal + per5
theFtab.SetValue(thePer5field,rec,per5)
end
else
per5 = 0
theFtab.SetValue(thePer5field,rec,per5)
end
end
end
'-----layer 6
if (cumPerVal.round = 100) then
'continue
ct = ct+1
per6 = 0
theFtab.SetValue(thePer6field,rec,per6)
else
if ((theScreenVal < theLay6Val ) And (theScreenVal > theBotVal)) then
if (theDepthVal < theBotVal) then
per6 = (((theScreenVal - theBotVal) / screenLengthVal) * 100).abs
cumPerVal = cumPerVal + per6
theFtab.SetValue(thePer6field,rec,per6)
else
per6 = (100 - cumPerVal)
cumPerVal = cumPerVal + per6
theFtab.SetValue(thePer6field,rec,per6)
end
else
if (cumPerVal > 0) then 'if continuing
if (theDepthVal < theBotVal) then
per6 = (((theBotVal - theLay6Val) / screenLengthVal) * 100).abs
cumPerVal = cumPerVal + per6
theFtab.SetValue(thePer6field,rec,per6)
else
per6 = (((theDepthVal - theLay6Val) / screenLengthVal) * 100).abs
cumPerVal = cumPerVal + per6

```

```
        theFtab.SetValue(thePer6field,rec,per6)
    end
else
    per6 = 0
    theFtab.SetValue(thePer6field,rec,per6)
end
end
end
theFtab.SetValue(theTotPerField,rec,cumPerVal)
end 'end for loop
```

Appendix 2 – Arcview script to return land surface elevation for a well from a DEM grid

```
'-----  
' Name: getgridvalue.ave  
' Date: 991004  
'  
' Description: Moves copies values from a grid to a  
' feature theme. The values from the grid are placed  
' in a user defined field. If the feature theme isn't  
' a point theme, then the feature gets the grid value  
' from the value under it's centroid point.  
'  
' Requires: Spatial Analyst  
'  
' Author: Originally written by Mikael Elmquist (mikael@swegis.com), but later  
' modified by Jeremy Davies (jeremy.davies@noaa.gov)  
'-----  
  
theView = av.GetActiveDoc  
theThemes={ }  
  
'-----  
' Choose in theme  
'-----  
themeList = theView.GetThemes  
rep = 0  
stupid = 0  
while (rep = 0)  
  theTheme = MsgBox.ChoiceAsString(themeList,"Select theme that shall get values from the grid  
  theme. ","GetGridValue")  
  if (theTheme = NIL) then  
    exit  
  end  
  if (theTheme.Is(Ftheme).Not) then  
    stupid = stupid+1  
    if (stupid = 4) then  
      msgBox.Info("Dear ArcView GIS user. Try to select a valid theme","Problem?")  
    end  
    msgBox.Error("Not a valid theme","Error")  
  else  
    rep = 1  
    theFtab = theTheme.GetFtab  
  end  
end  
rep = 0  
stupid = 0  
  
theThemes={ }  
if (theFtab.CanEdit) then  
  theFtab.SetEditable(true)
```

```
if ((theFtab.CanAddFields).Not) then
  MsgBox.Info("Can't add fields to the table."+NL+"Check write permission.", "Can't add grid values")
  exit
end
else
  MsgBox.Info("Can't modify the feature table."+NL+"Check write permission.", "Can't add grid values")
  exit
end

'-----
'Choose grid theme
'-----

for each TargetTheme in theView.GetThemes
  if (TargetTheme.Is(Gtheme)) then
    theThemes.Add(TargetTheme)
  end
end
theGtheme = MsgBox.ChoiceAsString(theThemes, "Select grid that shall assign values to the point
theme.", "GetGridValue")
if (theGtheme = Nil) then
  exit
end
theGrid = theGtheme.Clone.GetGrid.Clone
thePrj = Prj.MakeNull

'-----
' Add the new field
'-----

'enter name of new field name and parameters
newField = MsgBox.Input( "Enter new field name:", "Value", "" )
fieldsize = MsgBox.Input( "Enter new field width:", "Value", "10" )
precision = MsgBox.Input( "Enter number of decimals places in new field:", "Value", "4" )

gridvalueField = Field.Make (newField,#FIELD_DECIMAL,fieldsize.asNumber,precision.asNumber)
theShapeField = theFtab.FindField("shape")
theFtab.AddFields({ gridvalueField})

'-----
' Copy values
'-----
av.ShowMsg("Calculating values")
av.SetStatus(0)
sstatus = theFtab.GetNumRecords.Clone
for each aRec in theFtab
  av.SetStatus(aRec/sstatus*100)
  theValue = theGrid.CellValue(theFtab.returnValue(theShapeField,aRec).ReturnCenter,thePrj)
  av.SetStatus(aRec/sstatus*100)
  if (theValue<>Nil) then
    theFtab.SetValue(gridvalueField,aRec,theValue)
  end
end
```

end

'-----
'Reset arcview
'-----

theFtab.Flush
theFtab.Refresh
theFTab.SetEditable(False)
av.purgeobjects
av.ClearStatus
av.ClearMsg

APPENDIX C

Standard Operating Procedures (SOPs) for Processing Predictive Pumpage Data TWDB Groundwater Availability Modeling (GAM) Projects

**Standard Operating Procedures (SOPs)
for Processing Predictive Pumpage Data
TWDB Groundwater Availability Modeling (GAM) Projects**

TABLE OF CONTENTS

1. Background.....	1
2. Groundwater Use Source Data	1
3. Initial Processing.....	1
3.1. Create a sub-set of data for the modeled aquifer and geographic area	2
3.2. Split water use between surface and ground water.....	2
3.3. Interpolate pumpage estimates for all years 2000-2050	2
4. Spatially distribute well-specific pumpage	2
4.1. Identify locations of new wells.....	2
4.2. Matching Predictive to Historical Locations by Alphanum.....	2
4.3. Create new tables for each well-specific water use category	3
5. Spatially distribute non-well-specific pumpage	3
5.1. Calculate the fraction of groundwater pumpage for “C-O” use from each grid cell within a county-basin from 1999	4
5.2. Calculate the fraction of groundwater pumpage for “IRR” use from each grid cell within a county-basin from 1999	4
5.3. Calculate the fraction of groundwater pumpage for “STK” use from each grid cell within a county-basin from 1999	4
5.4. Note.....	5
6. Monthly Distribution of Annual Pumpage Totals.	5
7. Summarize Pumpage Information to Create Model Input Files.....	5
8. Handling Non-Texas Pumpage.....	5

1. Background – These procedures were developed to further implement the guidance provided by the Texas Water Development Board (TWDB) in their Technical Memorandum 02-01 “Development of Predictive Pumpage Data Set for GAM.” The information in that technical memorandum will not be repeated here, and readers should first consult that document.
2. Groundwater Use Source Data - To the extent possible, procedures for predictive pumpage distribution among model grid cells mimicked the procedures for historical pumpage data. Predicted future groundwater use estimates are derived from one spreadsheet (**GAMPredictivePumpage_2002SWP.xls**) provided by the Texas Water Development Board (TWDB), as well as the previously developed historical pumpage datasets. This spreadsheet contains water use estimates from the state water plans for each water user group for the years 2000, 2010, 2020, 2030, 2040, and 2050. Water user groups are generally assigned for each water user category (IRR, STK, MIN, MFG, PWR, MUN, and C-O) in each county-basin. However, individual municipal water supplies within a county-basin are assigned identified as separate water user groups. The water use categories are listed below:

- IRR – irrigation
- STK – livestock
- MIN - mineral extraction
- MFG – manufacturing
- PWR – power generation
- MUN – municipal water supply, and
- C-O – county-other (rural domestic) use.

Historical groundwater use records from the categories MIN, MFG, PWR, and MUN are available for each specific water user, each assigned an alphanumeric water user code (aka “alphanum”) in historical water use data tables. Specific locations and wells from which this groundwater was pumped were identified in historical pumpage records. These are known as “well-specific” water use categories. However, the particular locations of historical groundwater pumpage were generally not known for the use categories IRR, STK, and C-O. These categories are known as “non-well-specific” water use categories. This pumpage was distributed spatially based on population density, land use, and other factors.

The spreadsheet **GAMPredictivePumpage_2002SWP.xls** was downloaded from the TWDB web site. The spreadsheet file was then imported into a new Microsoft Access database file **Predictive Pumpage**.

3. Initial Processing

- 3.1. Create a sub-set of data for the modeled aquifer and geographic area – The table

Predictive Pumpage_2002SWP was queried for water use in the aquifer of interest based on the aquifer’s major aquifer code, as well as the code “99.” Other records were deleted. Next, the table was queried for those records within source county ID’s found in the modeling domain. Records for water pumpage outside the model domain were deleted.

- 3.2. Split water use between surface and ground water – Some records contain an aggregate of surface and ground water use, as indicated by a value of “04” in the field “SO_TYPE_ID_NEW.” A new field “PERCENT GROUNDWATER” was added to the table and assigned a value from 0 to 1 based on information in the field “ADDTL COMMENTS.”
- 3.3. Interpolate pumpage estimates for all years 2000-2050 – The table **Predictive Pumpage_2002SWP** only contains water use estimates for the years 2000, 2010, 2020, 2030, 2040, and 2050. Water use estimates for the intervening years are calculated by linear interpolation. This can be calculated in a query as for example:

$$\text{Pumpage}_{2001} = \text{Pumpage}_{2000} + \text{modulus}(2001,10)*[(\text{Pumpage}_{2010}-\text{Pumpage}_{2000})/10]$$

4. Spatially distribute well-specific pumpage –

- 4.1. Identify locations of new wells – If the field “Possible_New_Wells” contained a flag “NW”, it was necessary to identify the location of the new wells. The Regional Water Plan was consulted to identify the location of the new wells (a map showing the projected locations of the new wells was available). Using Arcview, the latitude and longitude of the well(s) were estimated and copied into a new field “KD_comment.” This latitude and longitude were used to identify the model grid_id(s) from which the well was expected to pump. These grid_id’s were copied into a new field “grid_id” in the predictive pumpage table.
- 4.2. Matching Predictive to Historical Locations by “Alphanum” - We assumed that a water user would tend to pump water in the future from the same locations from which they had pumped groundwater historically. A specific water user can best be identified in the TWDB predictive pumpage data using the field “WUG_Prime_Alpha”, or, if the water was purchased, the field “Seller Alpha.”
 - 4.2.1. A new field “Source_Alpha” was created and populated with the value from the field “WUG_Prime_Alpha” or, if available, the value from the field “Seller Alpha.”
 - 4.2.2. In many cases, no value of alpha_num was provided in the table for a well-specific WUG_ID, typically for MIN, MFG, and PWR. Therefore, the value(s) of “alphanum” associated with that WUG_ID in the historical pumpage table was copied to the predictive pumpage table.

In the case that multiple values of “alphanum” were identified for a given “WUG_ID” in the historical data, we first made replicate copies of the record in the predictive pumpage table for each value of alphanum, copied each alphanum into

the field “Source_Alpha”, and entered in the field “percent groundwater” the fraction of pumpage for each alphanum for the period 1995-1999 from the historical table. An explanation was entered in the field “KD_comment.”

- 4.2.3. The value of “Source_Alpha” was matched manually to the field “alphanum” in the historical pumpage datasets, and the model grid_id identified for this water user in historical pumpage distribution was manually copied to the field “Grid_ID” in the predictive pumpage table.

In many cases, more than one grid was associated with a given “alphanum”. The predictive pumpage for each alphanum was distributed among multiple Grid ID’s in an identical manner as the average for the period 1995-1999. Additional copies of predictive pumpage records were added to equal the number of grid_id’s, and a field “grid_frac” was added to the predictive pumpage table, and assigned a value from 0 to 1, calculated as the average of the 1995-1999 fraction of pumpage from that grid_id for that alphanum in the historical pumpage dataset. The values of grid_frac summed to 1 for each “source_alpha.”

4.3. Create new tables for each well-specific water use category –

- 4.3.1. Create a new table or query for the water use category MUN containing a value of MUN pumpage for each grid_id for each year from 2000 to 2050. The pumpage for each record is calculated as the total pumpage for the year of interest multiplied by the fields “grid_frac” and “percent groundwater.”
- 4.3.2. Create a new table or query for the water use category MFG containing a value of MFG pumpage for each grid_id for each year from 2000 to 2050. The pumpage for each record is calculated as the total pumpage for the year of interest multiplied by the fields “grid_frac” and “percent groundwater.”
- 4.3.3. Create a new table or query for the water use category MIN containing a value of MIN pumpage for each grid_id for each year from 2000 to 2050. The pumpage for each record is calculated as the total pumpage for the year of interest multiplied by the fields “grid_frac” and “percent groundwater.”
- 4.3.4. Create a new table or query for the water use category PWR containing a value of PWR pumpage for each grid_id for each year from 2000 to 2050. The pumpage for each record is calculated as the total pumpage for the year of interest multiplied by the fields “grid_frac” and “percent groundwater.”

5. Spatially distribute non-well-specific pumpage – We assume that groundwater pumpage in the future would be distributed within each county-basin in a similar way that it has been done in the recent past. While we do not discount the impact of changes in population and land use due to urban growth, sprawl, and other factors, we cannot reliably predict the spatial locations of these changes.

- 5.1. Calculate the fraction of groundwater pumpage for “C-O” use from each grid cell within

- a county-basin from 1999.
- 5.1.1. Run a query to summarize “C-O” groundwater pumpage in 1999 for each county-basin within the model domain.
 - 5.1.2. For each `grid_id` within each county-basin, divide the “C-O” pumpage value for the year 1999 by the total “C-O” pumpage for that county-basin. Save this as a new field “`Fr_pumpage`” for each `grid_id`.
 - 5.1.3. As a quality check, sum the values of “`Fr_pumpage`” for C-O by county-basin to ensure they sum to 1.
 - 5.1.4. Create a new table or query for the water use category “C-O” containing a value of C-O pumpage for each `grid_id` for each year from 2000 to 2050. The pumpage for each record is calculated as the total pumpage for the year of interest (from the TWDB-provided table **GAMPredictivePumpage_2002SWP.xls**, with interpolated values for intervening years) multiplied by the fields “percent groundwater” (from the same table) and the field “`Fr_pumpage`” from the previous three steps.
- 5.2. Calculate the fraction of groundwater pumpage for “IRR” use from each grid cell within a county-basin from 1999.
- 5.2.1. Run a query to summarize “IRR” groundwater pumpage in 1999 for each county-basin within the model domain.
 - 5.2.2. For each `grid_id` within each county-basin, divide the “IRR” pumpage value for the year 1999 by the total “IRR” pumpage for that county-basin. Save this as a new field “`Fr_pumpage`” for each `grid_id`.
 - 5.2.3. As a quality check, sum the values of “`Fr_pumpage`” for IRR by county-basin to ensure they sum to 1.
 - 5.2.4. Create a new table or query for the water use category “IRR” containing a value of IRR pumpage for each `grid_id` for each year from 2000 to 2050. The pumpage for each record is calculated as the total pumpage for the year of interest (from the TWDB-provided table **GAMPredictivePumpage_2002SWP.xls**, with interpolated values for intervening years) multiplied by the fields “percent groundwater” (from the same table) and the field “`Fr_pumpage`” from the previous three steps.
- 5.3. Calculate the fraction of groundwater pumpage for “STK” use from each grid cell within a county-basin from 1999.
- 5.3.1. Run a query to summarize “STK” groundwater pumpage in 1999 for each county-basin within the model domain.
 - 5.3.2. For each `grid_id` within each county-basin, divide the “STK” pumpage value for the year 1999 by the total “STK” pumpage for that county-basin. Save this as a new field “`Fr_pumpage`” for each `grid_id`.

- 5.3.3. As a quality check, sum the values of “Fr_pumpage” for STK by county-basin to ensure they sum to 1.
- 5.3.4. Create a new table or query for the water use category “STK” containing a value of STK pumpage for each grid_id for each year from 2000 to 2050. The pumpage for each record is calculated as the total pumpage for the year of interest (from the TWDB-provided table **GAMPredictivePumpage_2002SWP.xls**, with interpolated values for intervening years) multiplied by the fields “percent groundwater” (from the same table) and the field “Fr_pumpage” from the previous three steps.
- 5.4. Note: The result of this step should be three tables (or queries), one each for C-O, IRR, and STK. Each should contain, at a minimum, the fields “Grid_ID”, “county_name”, “basin_name”, “year”, “data_cat”, and “pumpage.”
6. Monthly Distribution of Annual Pumpage Totals - We assume that the historical average of monthly water use distribution is a valid predictor of future monthly distribution.

Monthly factors are calculated for each county-basin and data_cat as the average of mfraction for the period 1995-1999 (in the historical pumpage table “MONTHLY FACTORS”) in a new table **PredictiveMonthlyFactors**. There should be a monthly factor for each combination of the seven water use categories and county-basin. If no monthly factor can be calculated because there was no historical pumpage, then the monthly factor for that data_cat in the nearest other county-basin should be used.
7. Summarize Pumpage Information to Create Model Input Files - Summary queries for a given year and/or month should be performed as described in the SOP for historical pumpage data.
8. Handling Non-Texas Pumpage – Predictions of future pumpage for portions of the model domain outside of Texas are not available from the Texas Regional Water Plans. In this case, we will assume that the average pumpage for the period 1995-1999 is the best estimate of future pumpage for the water use categories MFG, MIN, PWR, STK, and IRR. Because population projections are available, however, we can project future water use for MUN and C-O based on the 1990 water use for each county or parish and the ratio of projected future county/parish population to its 1990 population.
 - 8.1. Download from the respective state census data center or the U.S. census bureau population estimates from each county or parish through 2050. Linearly interpolate values for intervening years if necessary.
 - 8.2. For each year from 2000 to 2050, calculate the ratio of projected population for each year to that in 2000 for each county or parish.
 - 8.3. Multiply the historical pumpage value from C-O or MUN out-of-Texas records in 1999 by the factor to obtain a projected pumpage estimate for that year.

APPENDIX D1

Tabulated Groundwater Withdrawal Estimates for the Carrizo-Wilcox for 1980, 1990, 2000, 2010, 2020, 2030, 2040, and 2050

Table D1.1
Rate of groundwater withdrawal (acre-feet per year) from flow layer 1 of the
Carrizo-Wilcox aquifer for counties within the study area

<u>County</u>	<u>1980</u>	<u>1990</u>	<u>2000</u>	<u>2010</u>	<u>2020</u>	<u>2030</u>	<u>2040</u>	<u>2050</u>
Anderson	1,198	1,876	2,663	2,723	2,753	2,789	2,781	2,842
Angelina	16,322	13,746	2,309	2,144	2,151	2,257	2,287	2,419
Bienville, LA	-	-	669	669	669	669	669	669
Bossier, LA	-	-	1,634	1,728	1,817	1,901	1,981	2,056
Bowie	-	-	-	-	-	-	-	-
Caddo, LA	9	545	7	7	7	7	8	8
Camp	31	42	60	70	71	71	71	72
Cass	1,124	1,305	291	302	309	317	355	361
Cherokee	1,255	1,732	2,484	908	973	1,027	1,077	1,121
De Soto, LA	-	-	-	-	-	-	-	-
Franklin	-	-	-	-	-	-	-	-
Freestone	24	21	22	21	20	20	20	20
Gregg	382	356	173	238	237	249	259	267
Grimes	383	733	411	437	465	498	475	538
Harrison	242	370	304	304	344	354	351	350
Henderson	533	911	661	673	673	667	655	672
Hopkins	-	-	-	-	-	-	-	-
Houston	1,581	1,726	703	767	765	766	770	772
Leon	451	683	1,070	1,094	1,121	1,150	1,181	1,217
Limestone	-	-	-	-	-	-	-	-
Madison	815	944	326	324	318	313	305	297
Marion	398	477	339	363	390	419	450	486
Miller, AR	-	363	10	10	10	10	10	10
Morris	315	325	39	39	37	37	36	34
Nacogdoches	1,658	1,620	785	793	805	516	813	818
Natchitoches, LA	613	458	929	948	975	1,008	1,050	1,098
Navarro	-	-	-	-	-	-	-	-
Panola	-	-	-	-	-	-	-	-
Rains	-	-	-	-	-	-	-	-
Red River, LA	-	-	699	724	777	858	968	1,107
Robertson	-	2	24	23	21	21	21	21
Rusk	55	65	68	69	74	80	80	85
Sabine, LA	961	1,141	1,842	1,977	2,122	2,281	2,452	2,635
Sabine, TX	792	1,045	1,025	1,094	1,158	1,272	1,340	1,369
San Augustine	6,089	4,468	253	250	246	249	247	249
Shelby	-	-	-	-	-	-	-	-
Smith	4,502	6,605	8,431	8,643	9,470	121	122	122
Titus	23	23	19	25	26	29	30	30
Trinity	1,819	1,816	-	-	-	-	-	-
Upshur	1,144	1,547	1,315	1,401	1,402	1,413	1,378	1,381
Van Zandt	176	224	214	221	250	260	262	262
Wood	756	1,163	1,345	1,476	1,539	1,645	1,722	1,890
Total	43,651	46,332	31,124	30,465	31,995	23,274	24,226	25,278

Table D1.2
Rate of groundwater withdrawal (acre-feet per year) from flow layer 2 of the
Carrizo-Wilcox aquifer for counties within the study area

<u>County</u>	<u>1980</u>	<u>1990</u>	<u>2000</u>	<u>2010</u>	<u>2020</u>	<u>2030</u>	<u>2040</u>	<u>2050</u>
Anderson	317	431	611	623	629	636	634	646
Angelina	8	9	4	4	4	4	4	4
Bienville, LA	-	-	-	-	-	-	-	-
Bossier, LA	1	1	1	1	1	1	1	1
Bowie	-	-	-	-	-	-	-	-
Caddo, LA	11	7	6	7	7	7	8	9
Camp	23	28	51	56	56	57	57	57
Cass	375	488	407	111	113	116	127	129
Cherokee	658	955	1,364	550	584	611	637	599
De Soto, LA	-	-	-	-	-	-	-	-
Franklin	1	4	-	-	-	-	-	-
Freestone	35	37	44	43	41	40	40	40
Gregg	224	202	69	113	112	116	119	121
Grimes	-	-	-	-	-	-	-	-
Harrison	442	605	424	425	474	484	487	485
Henderson	155	223	230	234	236	236	233	236
Hopkins	-	-	-	-	-	-	-	-
Houston	34	37	22	23	22	22	23	23
Leon	167	259	520	526	534	542	550	560
Limestone	-	-	-	-	-	-	-	-
Madison	3	3	205	205	205	205	205	205
Marion	70	107	63	65	66	69	68	69
Miller, AR	-	23	44	44	44	44	44	44
Morris	295	312	38	38	36	36	34	33
Nacogdoches	816	1,017	1,089	1,098	1,101	1,020	1,113	1,126
Natchitoches, LA	54	68	91	94	98	103	108	115
Navarro	-	-	-	-	-	-	-	-
Panola	-	-	-	-	-	-	-	-
Rains	-	-	-	-	-	-	-	-
Red River, LA	-	-	-	-	-	-	-	-
Robertson	-	-	-	-	-	-	-	-
Rusk	97	119	124	127	135	145	146	154
Sabine, LA	-	-	-	-	-	-	-	-
Sabine, TX	-	-	-	-	-	-	-	-
San Augustine	78	68	40	40	39	39	39	39
Shelby	-	-	-	-	-	-	-	-
Smith	457	633	829	847	928	1,027	1,137	1,250
Titus	37	54	38	54	57	63	67	69
Trinity	-	-	-	-	-	-	-	-
Upshur	690	687	365	393	394	403	406	408
Van Zandt	24	34	31	32	36	37	37	37
Wood	244	310	320	350	365	389	407	445
Total	5,316	6,721	7,030	6,103	6,317	6,452	6,731	6,904

Table D1.3
Rate of groundwater withdrawal (acre-feet per year) from flow layer 3 of the
Carrizo-Wilcox aquifer for counties within the study area

<u>County</u>	<u>1980</u>	<u>1990</u>	<u>2000</u>	<u>2010</u>	<u>2020</u>	<u>2030</u>	<u>2040</u>	<u>2050</u>
Anderson	713	1,021	1,098	1,110	1,112	1,119	1,114	1,127
Angelina	5,592	5,786	3,257	2,185	2,224	2,553	2,711	3,047
Bienville, LA	-	-	-	-	-	-	-	-
Bossier, LA	-	-	-	-	-	-	-	-
Bowie	-	-	-	-	-	-	-	-
Caddo, LA	92	40	25	25	26	27	28	30
Camp	191	230	309	380	385	391	394	396
Cass	210	271	58	59	60	61	65	66
Cherokee	2,144	2,027	2,221	828	868	974	1,018	1,105
De Soto, LA	-	-	-	-	-	-	-	-
Franklin	26	29	7	7	7	8	9	5
Freestone	43	31	54	54	54	54	54	54
Gregg	10	8	56	56	56	56	56	56
Grimes	-	-	331	340	351	366	394	429
Harrison	540	726	462	486	527	546	576	592
Henderson	332	520	460	469	472	370	362	472
Hopkins	-	-	-	-	-	-	-	-
Houston	295	16	704	665	670	676	680	682
Leon	395	606	2,170	1,827	1,342	1,246	1,222	1,253
Limestone	-	-	-	-	-	-	-	-
Madison	68	154	1,202	1,158	1,125	1,091	1,041	998
Marion	115	117	71	73	74	76	77	77
Miller, AR	-	525	931	931	931	931	931	931
Morris	304	103	9	9	9	9	8	8
Nacogdoches	5,087	5,669	2,751	2,601	2,734	2,929	3,135	3,421
Natchitoches, LA	28	30	35	35	36	36	36	37
Navarro	-	-	-	-	-	-	-	-
Panola	-	-	-	-	-	-	-	-
Rains	-	-	-	-	-	-	-	-
Red River, LA	-	-	-	-	-	-	-	-
Robertson	11	13	255	248	244	239	235	231
Rusk	495	591	473	441	472	511	515	544
Sabine, LA	-	-	-	-	-	-	-	-
Sabine, TX	-	-	-	-	-	-	-	-
San Augustine	176	193	123	123	123	124	125	126
Shelby	1	1	-	-	-	-	-	-
Smith	1,178	1,267	1,533	1,578	1,716	1,882	2,064	2,257
Titus	71	88	69	91	94	104	109	111
Trinity	-	-	-	-	-	-	-	-
Upshur	854	760	598	630	628	644	653	667
Van Zandt	82	144	130	136	168	166	168	168
Wood	1,267	1,049	718	764	810	867	909	988
Total	20,320	22,015	20,110	17,309	17,318	18,056	18,689	19,878

Table D1.4
Rate of groundwater withdrawal (acre-feet per year) from flow layer 4 of the
Carrizo-Wilcox aquifer for counties within the study area

<u>County</u>	<u>1980</u>	<u>1990</u>	<u>2000</u>	<u>2010</u>	<u>2020</u>	<u>2030</u>	<u>2040</u>	<u>2050</u>
Anderson	992	1,269	2,173	2,127	2,065	2,052	2,021	2,048
Angelina	601	649	12,237	11,841	10,698	11,298	11,992	13,208
Bienville, LA	-	-	-	-	-	-	-	-
Bossier, LA	11	5	8	8	8	8	8	8
Bowie	1	3	-	-	-	-	-	-
Caddo, LA	592	195	464	473	490	517	554	600
Camp	675	879	814	1,025	1,041	1,059	1,070	1,077
Cass	459	513	276	571	266	263	261	258
Cherokee	3,033	3,039	2,536	2,007	1,990	1,940	2,078	2,215
De Soto, LA	-	-	-	-	-	-	-	-
Franklin	119	160	75	76	76	77	80	80
Freestone	410	448	510	495	474	467	470	469
Gregg	1,770	1,515	1,072	1,213	1,216	1,272	1,320	1,363
Grimes	-	-	-	-	-	-	-	-
Harrison	586	744	559	593	640	655	674	683
Henderson	711	1,106	934	942	938	935	929	944
Hopkins	45	49	33	42	41	45	50	54
Houston	2	2	11	11	11	11	11	11
Leon	1,021	1,440	2,145	2,172	2,200	2,296	2,386	2,510
Limestone	18	33	117	118	120	125	130	136
Madison	4	10	-	-	-	-	-	-
Marion	257	246	153	156	160	162	164	165
Miller, AR	-	1,122	1,945	1,945	1,945	1,945	1,945	1,945
Morris	452	6,681	26	26	25	25	24	23
Nacogdoches	779	958	2,122	2,020	2,097	2,229	2,367	2,563
Natchitoches, LA	289	350	574	592	619	652	692	739
Navarro	-	-	-	-	-	-	-	-
Panola	19	20	11	11	11	10	10	10
Rains	-	-	-	-	-	-	-	-
Red River, LA	-	-	-	-	-	-	-	-
Robertson	198	200	7,777	7,615	7,550	7,372	7,206	7,047
Rusk	3,276	3,884	3,849	3,270	3,347	3,540	3,589	3,733
Sabine, LA	-	-	-	-	-	-	-	-
Sabine, TX	-	-	-	-	-	-	-	-
San Augustine	266	267	141	142	142	145	145	146
Shelby	1,220	1,358	1,289	1,482	1,238	1,001	1,582	1,819
Smith	4,338	2,868	5,130	5,642	6,031	6,075	6,544	5,222
Titus	272	363	309	396	410	448	466	477
Trinity	-	-	-	-	-	-	-	-
Upshur	807	939	843	890	894	913	605	965
Van Zandt	504	715	1,021	1,099	1,284	1,318	1,376	1,445
Wood	1,465	1,007	1,507	1,618	1,761	1,911	2,061	2,273
Total	25,192	33,037	50,661	50,618	49,788	50,766	52,810	54,236

Table D1.5
Rate of groundwater withdrawal (acre-feet per year) from flow layer 5 of the
Carrizo-Wilcox aquifer for counties within the study area

<u>County</u>	<u>1980</u>	<u>1990</u>	<u>2000</u>	<u>2010</u>	<u>2020</u>	<u>2030</u>	<u>2040</u>	<u>2050</u>
Anderson	209	20	179	188	196	202	215	226
Angelina	-	-	-	-	-	-	-	-
Bienville, LA	-	-	-	-	-	-	-	-
Bossier, LA	107	67	80	83	86	88	90	92
Bowie	1,082	1,274	643	681	681	681	681	681
Caddo, LA	3,389	2,405	2,858	2,932	3,084	3,313	3,619	4,003
Camp	477	527	301	299	302	307	314	322
Cass	1,090	1,064	57	56	55	53	52	52
Cherokee	3	37	108	28	30	32	34	37
De Soto, LA	1,290	1,053	226	226	226	226	226	226
Franklin	654	714	1,675	1,581	1,535	1,476	1,500	1,562
Freestone	382	1,143	509	523	507	497	499	499
Gregg	431	282	465	448	433	435	439	442
Grimes	-	-	-	-	-	-	-	-
Harrison	1,433	1,729	1,341	1,358	1,481	1,518	1,559	1,584
Henderson	1,031	1,105	883	863	859	867	877	899
Hopkins	657	959	790	910	909	941	1,003	1,037
Houston	-	-	-	-	-	-	-	-
Leon	-	-	-	-	-	-	-	-
Limestone	107	805	6,919	7,611	7,622	7,643	7,666	7,694
Madison	-	-	-	-	-	-	-	-
Marion	80	96	151	125	113	108	105	119
Miller, AR	24	6,736	4,234	4,236	4,238	4,238	4,240	4,242
Morris	575	395	590	593	582	576	564	560
Nacogdoches	358	360	391	395	395	420	435	453
Natchitoches, LA	137	112	155	155	156	157	157	159
Navarro	10	16	-	-	-	-	-	-
Panola	3,067	4,172	2,005	1,960	1,890	1,962	1,963	1,960
Rains	297	465	368	389	408	276	293	311
Red River, LA	23	76	174	174	175	176	177	179
Robertson	173	50	6,450	6,295	6,212	6,055	5,917	5,781
Rusk	3,241	3,249	3,464	3,123	2,798	2,601	2,512	2,464
Sabine, LA	-	-	-	-	-	-	-	-
Sabine, TX	-	-	-	-	-	-	-	-
San Augustine	-	-	-	-	-	-	-	-
Shelby	1,740	1,794	1,984	2,262	1,852	2,102	2,386	2,750
Smith	1,073	653	2,261	2,486	2,655	2,669	2,839	2,243
Titus	989	1,229	2,698	2,743	2,731	2,784	2,817	2,846
Trinity	-	-	-	-	-	-	-	-
Upshur	85	110	106	110	109	110	110	110
Van Zandt	2,132	1,919	1,477	1,622	2,219	2,049	2,119	2,195
Wood	368	622	704	767	797	848	886	967
Total	26,714	35,238	44,246	45,222	45,336	45,410	46,294	46,695

Table D1.6
Rate of groundwater withdrawal (acre-feet per year) from flow layer 6 of the
Carrizo-Wilcox aquifer for counties within the study area

<u>County</u>	<u>1980</u>	<u>1990</u>	<u>2000</u>	<u>2010</u>	<u>2020</u>	<u>2030</u>	<u>2040</u>	<u>2050</u>
Anderson	64	84	16	17	17	18	18	19
Angelina	-	-	-	-	-	-	-	-
Bienville, LA	-	-	-	-	-	-	-	-
Bossier, LA	9	2	5	5	5	5	5	5
Bowie	841	914	224	1,264	1,265	1,267	1,271	1,276
Caddo, LA	930	614	619	634	664	711	772	849
Camp	-	5	7	7	7	7	7	7
Cass	645	656	202	340	335	330	325	309
Cherokee	-	-	-	-	-	-	-	-
De Soto, LA	615	327	5	5	5	5	5	5
Franklin	307	428	275	276	276	276	278	278
Freestone	1,514	1,657	1,881	1,903	1,931	1,975	2,001	2,025
Gregg	-	-	356	372	387	409	432	459
Grimes	-	-	-	-	-	-	-	-
Harrison	406	318	398	506	557	591	599	620
Henderson	1,373	1,797	2,002	1,741	1,740	1,747	1,751	1,768
Hopkins	1,430	1,970	989	1,092	1,092	1,106	1,140	1,155
Houston	-	-	-	-	-	-	-	-
Leon	-	-	-	-	-	-	-	-
Limestone	243	339	1,441	1,448	1,472	1,516	1,564	1,623
Madison	-	-	-	-	-	-	-	-
Marion	2	-	-	-	-	-	-	-
Miller, AR	2	11	21	22	22	22	23	23
Morris	4	5	16	16	16	16	16	16
Nacogdoches	-	-	1	1	1	1	1	1
Natchitoches, LA	-	-	-	-	-	-	-	-
Navarro	57	99	12	12	12	12	12	12
Panola	401	446	1,861	1,608	1,360	2,180	2,205	2,178
Rains	90	153	-	-	-	-	-	-
Red River, LA	1	23	59	59	59	59	59	59
Robertson	-	-	-	-	-	-	-	-
Rusk	74	4	995	895	794	760	756	760
Sabine, LA	-	-	-	-	-	-	-	-
Sabine, TX	-	-	-	-	-	-	-	-
San Augustine	-	-	-	-	-	-	-	-
Shelby	21	29	156	152	149	149	150	154
Smith	-	-	-	-	-	-	-	-
Titus	108	138	60	60	60	61	61	61
Trinity	-	-	-	-	-	-	-	-
Upshur	-	-	-	-	-	-	-	-
Van Zandt	1,638	2,017	1,731	1,758	2,073	2,091	2,299	2,428
Wood	1	2	1,129	1,129	1,129	1,129	1,129	1,129
Total	10,776	12,038	14,461	15,322	15,428	16,443	16,879	17,219

Table D1.7

Rate of groundwater withdrawal (acre-feet per year) from flow layer 1 of the Carrizo-Wilcox Aquifer for counties within the study area

Municipal and Industrial*

<u>County</u>	<u>1980</u>	<u>1990</u>	<u>2000</u>	<u>2010</u>	<u>2020</u>	<u>2030</u>	<u>2040</u>	<u>2050</u>
Anderson	-	-	-	-	-	-	-	-
Angelina	13,317	9,705	524	344	350	404	429	484
Bienville, LA	-	-	669	669	669	669	669	669
Bossier, LA	-	-	1,634	1,728	1,817	1,901	1,981	2,056
Bowie	-	-	-	-	-	-	-	-
Caddo, LA	-	540	-	-	-	-	-	-
Camp	-	-	-	-	-	-	-	-
Cass	-	-	-	-	-	-	-	-
Cherokee	-	-	-	-	-	-	-	-
De Soto, LA	-	-	-	-	-	-	-	-
Franklin	-	-	-	-	-	-	-	-
Freestone	-	-	-	-	-	-	-	-
Gregg	-	-	-	-	-	-	-	-
Grimes	-	-	-	-	-	-	-	-
Harrison	-	-	-	-	-	-	-	-
Henderson	5	6	-	-	-	-	-	-
Hopkins	-	-	-	-	-	-	-	-
Houston	-	-	2	3	3	4	5	5
Leon	-	-	-	-	-	-	-	-
Limestone	-	-	-	-	-	-	-	-
Madison	-	-	-	-	-	-	-	-
Marion	-	-	-	-	-	-	-	-
Miller, AR	-	360	-	-	-	-	-	-
Morris	-	-	-	-	-	-	-	-
Nacogdoches	1,145	815	-	-	-	-	-	-
Natchitoches, LA	-	-	285	301	324	352	387	428
Navarro	-	-	-	-	-	-	-	-
Panola	-	-	-	-	-	-	-	-
Rains	-	-	-	-	-	-	-	-
Red River, LA	-	-	699	724	777	858	968	1,107
Robertson	-	1	-	-	-	-	-	-
Rusk	-	-	-	-	-	-	-	-
Sabine, LA	-	569	979	1,055	1,137	1,227	1,324	1,428
Sabine, TX	-	-	786	843	895	946	996	1,045
San Augustine	5,723	4,075	-	-	-	-	-	-
Shelby	-	-	-	-	-	-	-	-
Smith	-	-	-	-	-	-	-	-
Titus	-	-	-	-	-	-	-	-
Trinity	1,145	815	-	-	-	-	-	-
Upshur	-	-	-	-	-	-	-	-
Van Zandt	-	-	-	-	-	-	-	-
Wood	-	-	-	-	-	-	-	-
Total	21,335	16,886	5,578	5,667	5,972	6,361	6,759	7,222

*industrial includes manufacturing, mining, and power generation

Table D1.7 (Continued...)
Rate of groundwater withdrawal (acre-feet per year) from flow layer 1 of the Carrizo-Wilcox Aquifer for counties within the study area

County – Other (Non-reported Domestic)

<u>County</u>	<u>1980</u>	<u>1990</u>	<u>2000</u>	<u>2010</u>	<u>2020</u>	<u>2030</u>	<u>2040</u>	<u>2050</u>
Anderson	1,179	1,752	2,623	2,683	2,713	2,749	2,741	2,802
Angelina	3,005	4,041	1,785	1,800	1,801	1,853	1,858	1,935
Bienville, LA	-	-	-	-	-	-	-	-
Bossier, LA	-	-	-	-	-	-	-	-
Bowie	-	-	-	-	-	-	-	-
Caddo, LA	4	3	3	3	3	3	4	4
Camp	24	26	29	39	40	40	40	41
Cass	1,114	1,281	287	298	305	313	351	357
Cherokee	1,255	1,624	2,331	755	820	874	924	968
De Soto, LA	-	-	-	-	-	-	-	-
Franklin	-	-	-	-	-	-	-	-
Freestone	23	20	20	19	18	18	18	18
Gregg	382	356	173	238	237	249	259	267
Grimes	383	733	411	437	465	498	475	538
Harrison	242	370	303	303	343	353	350	349
Henderson	490	843	628	640	640	634	622	639
Hopkins	-	-	-	-	-	-	-	-
Houston	1,539	1,661	627	688	687	686	688	692
Leon	315	474	339	363	390	419	450	486
Limestone	-	-	-	-	-	-	-	-
Madison	810	939	170	168	162	157	149	141
Marion	398	477	339	363	390	419	450	486
Miller, AR	-	-	-	-	-	-	-	-
Morris	308	314	39	39	37	37	36	34
Nacogdoches	495	790	763	771	784	495	793	796
Natchitoches, LA	17	38	50	53	57	62	69	76
Navarro	-	-	-	-	-	-	-	-
Panola	-	-	-	-	-	-	-	-
Rains	-	-	-	-	-	-	-	-
Red River, LA	-	-	-	-	-	-	-	-
Robertson	-	1	24	23	21	21	21	21
Rusk	55	65	68	69	74	80	80	85
Sabine, LA	844	2	749	808	871	940	1,014	1,093
Sabine, TX	725	960	149	155	162	171	177	143
San Augustine	343	368	213	210	206	208	206	208
Shelby	-	-	-	-	-	-	-	-
Smith	4,463	6,560	8,332	8,544	9,371	22	23	23
Titus	20	19	12	18	19	22	23	23
Trinity	674	1,001	-	-	-	-	-	-
Upshur	1,137	1,535	1,289	1,375	1,376	1,387	1,352	1,355
Van Zandt	175	222	214	221	250	260	262	262
Wood	739	1,139	1,326	1,457	1,520	1,626	1,703	1,871
Total	21,158	27,614	23,296	22,540	23,762	14,596	15,138	15,713

Table D1.7 (Continued...)
Rate of groundwater withdrawal (acre-feet per year) from flow layer 1 of the Carrizo-Wilcox Aquifer for counties within the study area

Livestock

<u>County</u>	<u>1980</u>	<u>1990</u>	<u>2000</u>	<u>2010</u>	<u>2020</u>	<u>2030</u>	<u>2040</u>	<u>2050</u>
Anderson	19	124	40	40	40	40	40	40
Angelina	-	-	-	-	-	-	-	-
Bienville, LA	-	-	-	-	-	-	-	-
Bossier, LA	-	-	-	-	-	-	-	-
Bowie	-	-	-	-	-	-	-	-
Caddo, LA	2	2	2	2	2	2	2	2
Camp	7	7	20	20	20	20	20	20
Cass	10	24	4	4	4	4	4	4
Cherokee	-	108	153	153	153	153	153	153
De Soto, LA	-	-	-	-	-	-	-	-
Franklin	-	-	-	-	-	-	-	-
Freestone	1	1	2	2	2	2	2	2
Gregg	-	-	-	-	-	-	-	-
Grimes	-	-	-	-	-	-	-	-
Harrison	-	-	-	-	-	-	-	-
Henderson	38	62	33	33	33	33	33	33
Hopkins	-	-	-	-	-	-	-	-
Houston	42	65	64	66	65	66	66	64
Leon	136	209	731	731	731	731	731	731
Limestone	-	-	-	-	-	-	-	-
Madison	2	2	156	156	156	156	156	156
Marion	-	-	-	-	-	-	-	-
Miller, AR	-	1	6	6	6	6	6	6
Morris	7	11	-	-	-	-	-	-
Nacogdoches	18	15	20	20	19	19	18	20
Natchitoches, LA	298	-	109	109	109	109	109	109
Navarro	-	-	-	-	-	-	-	-
Panola	-	-	-	-	-	-	-	-
Rains	-	-	-	-	-	-	-	-
Red River, LA	-	-	-	-	-	-	-	-
Robertson	-	-	-	-	-	-	-	-
Rusk	-	-	-	-	-	-	-	-
Sabine, LA	117	569	113	113	113	113	113	113
Sabine, TX	67	85	90	96	101	155	167	181
San Augustine	23	25	33	33	33	34	34	34
Shelby	-	-	-	-	-	-	-	-
Smith	39	45	98	98	98	98	98	98
Titus	3	4	7	7	7	7	7	7
Trinity	-	-	-	-	-	-	-	-
Upshur	7	12	26	26	26	26	26	26
Van Zandt	1	2	-	-	-	-	-	-
Wood	17	23	17	17	17	17	17	17
Total	854	1,396	1,724	1,732	1,735	1,791	1,802	1,816

Table D1.7 (Continued...)
Rate of groundwater withdrawal (acre-feet per year) from flow layer 1 of the Carrizo-Wilcox Aquifer for counties within the study area

Irrigation

<u>County</u>	<u>1980</u>	<u>1990</u>	<u>2000</u>	<u>2010</u>	<u>2020</u>	<u>2030</u>	<u>2040</u>	<u>2050</u>
Anderson	-	-	-	-	-	-	-	-
Angelina	-	-	-	-	-	-	-	-
Bienville, LA	-	-	-	-	-	-	-	-
Bossier, LA	-	-	-	-	-	-	-	-
Bowie	-	-	-	-	-	-	-	-
Caddo, LA	3	-	2	2	2	2	2	2
Camp	-	9	11	11	11	11	11	11
Cass	-	-	-	-	-	-	-	-
Cherokee	-	-	-	-	-	-	-	-
De Soto, LA	-	-	-	-	-	-	-	-
Franklin	-	-	-	-	-	-	-	-
Freestone	-	-	-	-	-	-	-	-
Gregg	-	-	-	-	-	-	-	-
Grimes	-	-	-	-	-	-	-	-
Harrison	-	-	1	1	1	1	1	1
Henderson	-	-	-	-	-	-	-	-
Hopkins	-	-	-	-	-	-	-	-
Houston	-	-	10	10	10	10	11	11
Leon	-	-	-	-	-	-	-	-
Limestone	-	-	-	-	-	-	-	-
Madison	3	3	-	-	-	-	-	-
Marion	-	-	-	-	-	-	-	-
Miller, AR	-	2	4	4	4	4	4	4
Morris	-	-	-	-	-	-	-	-
Nacogdoches	-	-	2	2	2	2	2	2
Natchitoches, LA	298	420	485	485	485	485	485	485
Navarro	-	-	-	-	-	-	-	-
Panola	-	-	-	-	-	-	-	-
Rains	-	-	-	-	-	-	-	-
Red River, LA	-	-	-	-	-	-	-	-
Robertson	-	-	-	-	-	-	-	-
Rusk	-	-	-	-	-	-	-	-
Sabine, LA	-	1	1	1	1	1	1	1
Sabine, TX	-	-	-	-	-	-	-	-
San Augustine	-	-	7	7	7	7	7	7
Shelby	-	-	-	-	-	-	-	-
Smith	-	-	1	1	1	1	1	1
Titus	-	-	-	-	-	-	-	-
Trinity	-	-	-	-	-	-	-	-
Upshur	-	-	-	-	-	-	-	-
Van Zandt	-	-	-	-	-	-	-	-
Wood	-	1	2	2	2	2	2	2
Total	304	436	526	526	526	526	527	527

Table D1.8
Rate of groundwater withdrawal (acre-feet per year) from flow layer 2 of the
Carrizo-Wilcox Aquifer for counties within the study area

Municipal and Industrial*

<u>County</u>	<u>1980</u>	<u>1990</u>	<u>2000</u>	<u>2010</u>	<u>2020</u>	<u>2030</u>	<u>2040</u>	<u>2050</u>
Anderson	-	-	-	-	-	-	-	-
Angelina	-	-	-	-	-	-	-	-
Bienville, LA	-	-	-	-	-	-	-	-
Bossier, LA	-	-	-	-	-	-	-	-
Bowie	-	-	-	-	-	-	-	-
Caddo, LA	-	-	-	-	-	-	-	-
Camp	-	-	-	-	-	-	-	-
Cass	-	-	-	-	-	-	-	-
Cherokee	-	-	-	-	-	-	-	-
De Soto, LA	-	-	-	-	-	-	-	-
Franklin	-	-	-	-	-	-	-	-
Freestone	-	-	-	-	-	-	-	-
Gregg	-	-	-	-	-	-	-	-
Grimes	-	-	-	-	-	-	-	-
Harrison	-	-	-	-	-	-	-	-
Henderson	49	55	104	106	108	109	108	108
Hopkins	-	-	-	-	-	-	-	-
Houston	-	-	-	-	-	-	-	-
Leon	-	-	-	-	-	-	-	-
Limestone	-	-	-	-	-	-	-	-
Madison	-	-	-	-	-	-	-	-
Marion	-	-	-	-	-	-	-	-
Miller, AR	-	-	-	-	-	-	-	-
Morris	-	-	-	-	-	-	-	-
Nacogdoches	-	-	-	-	-	-	-	-
Natchitoches, LA	-	-	-	-	-	-	-	-
Navarro	-	-	-	-	-	-	-	-
Panola	-	-	-	-	-	-	-	-
Rains	-	-	-	-	-	-	-	-
Red River, LA	-	-	-	-	-	-	-	-
Robertson	-	-	-	-	-	-	-	-
Rusk	-	-	-	-	-	-	-	-
Sabine, LA	-	-	-	-	-	-	-	-
Sabine, TX	-	-	-	-	-	-	-	-
San Augustine	-	-	-	-	-	-	-	-
Shelby	-	-	-	-	-	-	-	-
Smith	-	-	-	-	-	-	-	-
Titus	-	-	-	-	-	-	-	-
Trinity	-	-	-	-	-	-	-	-
Upshur	312	166	-	-	-	-	-	-
Van Zandt	-	-	-	-	-	-	-	-
Wood	-	-	-	-	-	-	-	-
Total	361	221	104	106	108	109	108	108

*industrial includes manufacturing, mining, and power generation

Table D1.8 (Continued...)
Rate of groundwater withdrawal (acre-feet per year) from flow layer 2 of the Carrizo-Wilcox Aquifer for counties within the study area

County – Other (Non-reported Domestic)

<u>County</u>	<u>1980</u>	<u>1990</u>	<u>2000</u>	<u>2010</u>	<u>2020</u>	<u>2030</u>	<u>2040</u>	<u>2050</u>
Anderson	270	338	507	519	525	532	530	542
Angelina	8	9	4	4	4	4	4	4
Bienville, LA	-	-	-	-	-	-	-	-
Bossier, LA	-	-	-	-	-	-	-	-
Bowie	-	-	-	-	-	-	-	-
Caddo, LA	9	5	4	5	5	5	6	7
Camp	11	13	15	20	20	21	21	21
Cass	362	456	402	106	108	111	122	124
Cherokee	653	831	1,192	386	420	447	473	435
De Soto, LA	-	-	-	-	-	-	-	-
Franklin	1	4	-	-	-	-	-	-
Freestone	23	28	29	28	26	25	25	25
Gregg	224	202	69	113	112	116	119	121
Grimes	-	-	-	-	-	-	-	-
Harrison	433	602	423	423	472	482	485	483
Henderson	82	130	98	100	100	99	97	100
Hopkins	-	-	-	-	-	-	-	-
Houston	32	34	13	14	14	14	14	14
Leon	81	129	88	94	102	110	118	128
Limestone	-	-	-	-	-	-	-	-
Madison	-	-	-	-	-	-	-	-
Marion	70	107	63	65	66	69	68	69
Miller, AR	-	-	-	-	-	-	-	-
Morris	290	305	38	38	36	36	34	33
Nacogdoches	677	895	864	873	888	801	898	902
Natchitoches, LA	14	36	48	51	55	60	65	72
Navarro	-	-	-	-	-	-	-	-
Panola	-	-	-	-	-	-	-	-
Rains	-	-	-	-	-	-	-	-
Red River, LA	-	-	-	-	-	-	-	-
Robertson	-	-	-	-	-	-	-	-
Rusk	86	110	115	117	125	135	136	144
Sabine, LA	-	-	-	-	-	-	-	-
Sabine, TX	-	-	-	-	-	-	-	-
San Augustine	75	65	35	35	34	34	34	34
Shelby	-	-	-	-	-	-	-	-
Smith	444	619	792	810	891	990	1,100	1,213
Titus	35	51	33	49	52	58	62	64
Trinity	-	-	-	-	-	-	-	-
Upshur	376	517	356	384	385	394	397	399
Van Zandt	22	32	30	31	35	36	36	36
Wood	230	290	304	334	349	373	391	429
Total	4,508	5,808	5,522	4,599	4,824	4,952	5,235	5,399

Table D1.8 (Continued...)
Rate of groundwater withdrawal (acre-feet per year) from flow layer 2 of the Carrizo-Wilcox Aquifer for counties within the study area

Livestock

<u>County</u>	<u>1980</u>	<u>1990</u>	<u>2000</u>	<u>2010</u>	<u>2020</u>	<u>2030</u>	<u>2040</u>	<u>2050</u>
Anderson	47	92	97	97	97	97	97	97
Angelina	-	-	-	-	-	-	-	-
Bienville, LA	-	-	-	-	-	-	-	-
Bossier, LA	1	1	1	1	1	1	1	1
Bowie	-	-	-	-	-	-	-	-
Caddo, LA	2	2	2	2	2	2	2	2
Camp	12	12	32	32	32	32	32	32
Cass	13	32	5	5	5	5	5	5
Cherokee	1	115	163	163	163	163	163	163
De Soto, LA	-	-	-	-	-	-	-	-
Franklin	-	-	-	-	-	-	-	-
Freestone	12	9	15	15	15	15	15	15
Gregg	-	-	-	-	-	-	-	-
Grimes	-	-	-	-	-	-	-	-
Harrison	9	3	1	2	2	2	2	2
Henderson	24	38	28	28	28	28	28	28
Hopkins	-	-	-	-	-	-	-	-
Houston	2	3	2	2	2	2	2	2
Leon	86	130	432	432	432	432	432	432
Limestone	-	-	-	-	-	-	-	-
Madison	2	2	205	205	205	205	205	205
Marion	-	-	-	-	-	-	-	-
Miller, AR	-	2	8	8	8	8	8	8
Morris	5	7	-	-	-	-	-	-
Nacogdoches	139	112	151	151	139	145	141	150
Natchitoches, LA	17	-	6	6	6	6	6	6
Navarro	-	-	-	-	-	-	-	-
Panola	-	-	-	-	-	-	-	-
Rains	-	-	-	-	-	-	-	-
Red River, LA	-	-	-	-	-	-	-	-
Robertson	-	-	-	-	-	-	-	-
Rusk	11	9	9	10	10	10	10	10
Sabine, LA	-	-	-	-	-	-	-	-
Sabine, TX	-	-	-	-	-	-	-	-
San Augustine	3	3	5	5	5	5	5	5
Shelby	-	-	-	-	-	-	-	-
Smith	12	14	35	35	35	35	35	35
Titus	2	3	5	5	5	5	5	5
Trinity	-	-	-	-	-	-	-	-
Upshur	2	4	9	9	9	9	9	9
Van Zandt	2	2	1	1	1	1	1	1
Wood	14	19	14	14	14	14	14	14
Total	418	614	1,226	1,228	1,216	1,222	1,218	1,227

Table D1.8 (Continued...)
Rate of groundwater withdrawal (acre-feet per year) from flow layer 2 of the Carrizo-Wilcox Aquifer for counties within the study area

Irrigation

<u>County</u>	<u>1980</u>	<u>1990</u>	<u>2000</u>	<u>2010</u>	<u>2020</u>	<u>2030</u>	<u>2040</u>	<u>2050</u>
Anderson	-	1	7	7	7	7	7	7
Angelina	-	-	-	-	-	-	-	-
Bienville, LA	-	-	-	-	-	-	-	-
Bossier, LA	-	-	-	-	-	-	-	-
Bowie	-	-	-	-	-	-	-	-
Caddo, LA	-	-	-	-	-	-	-	-
Camp	-	3	4	4	4	4	4	4
Cass	-	-	-	-	-	-	-	-
Cherokee	4	9	9	1	1	1	1	1
De Soto, LA	-	-	-	-	-	-	-	-
Franklin	-	-	-	-	-	-	-	-
Freestone	-	-	-	-	-	-	-	-
Gregg	-	-	-	-	-	-	-	-
Grimes	-	-	-	-	-	-	-	-
Harrison	-	-	-	-	-	-	-	-
Henderson	-	-	-	-	-	-	-	-
Hopkins	-	-	-	-	-	-	-	-
Houston	-	-	7	7	6	6	7	7
Leon	-	-	-	-	-	-	-	-
Limestone	-	-	-	-	-	-	-	-
Madison	1	1	-	-	-	-	-	-
Marion	-	-	-	-	-	-	-	-
Miller, AR	-	21	36	36	36	36	36	36
Morris	-	-	-	-	-	-	-	-
Nacogdoches	-	10	74	74	74	74	74	74
Natchitoches, LA	23	32	37	37	37	37	37	37
Navarro	-	-	-	-	-	-	-	-
Panola	-	-	-	-	-	-	-	-
Rains	-	-	-	-	-	-	-	-
Red River, LA	-	-	-	-	-	-	-	-
Robertson	-	-	-	-	-	-	-	-
Rusk	-	-	-	-	-	-	-	-
Sabine, LA	-	-	-	-	-	-	-	-
Sabine, TX	-	-	-	-	-	-	-	-
San Augustine	-	-	-	-	-	-	-	-
Shelby	-	-	-	-	-	-	-	-
Smith	1	-	2	2	2	2	2	2
Titus	-	-	-	-	-	-	-	-
Trinity	-	-	-	-	-	-	-	-
Upshur	-	-	-	-	-	-	-	-
Van Zandt	-	-	-	-	-	-	-	-
Wood	-	1	2	2	2	2	2	2
Total	29	78	178	170	169	169	170	170

Table D1.9
Rate of groundwater withdrawal (acre-feet per year) from flow layer 3 of the
Carrizo-Wilcox Aquifer for counties within the study area

Municipal and Industrial*

<u>County</u>	<u>1980</u>	<u>1990</u>	<u>2000</u>	<u>2010</u>	<u>2020</u>	<u>2030</u>	<u>2040</u>	<u>2050</u>
Anderson	421	515	323	319	314	311	308	305
Angelina	5,592	5,786	3,257	2,185	2,224	2,553	2,711	3,047
Bienville, LA	-	-	-	-	-	-	-	-
Bossier, LA	-	-	-	-	-	-	-	-
Bowie	-	-	-	-	-	-	-	-
Caddo, LA	53	27	-	-	-	-	-	-
Camp	-	-	-	-	-	-	-	-
Cass	-	-	-	-	-	-	-	-
Cherokee	1,920	1,712	970	620	649	746	782	862
De Soto, LA	-	-	-	-	-	-	-	-
Franklin	-	-	-	-	-	-	-	-
Freestone	-	-	-	-	-	-	-	-
Gregg	-	-	-	-	-	-	-	-
Grimes	-	-	331	340	351	366	394	429
Harrison	89	119	27	36	36	36	36	36
Henderson	102	116	156	160	163	164	161	163
Hopkins	-	-	-	-	-	-	-	-
Houston	281	-	687	648	653	659	663	665
Leon	61	73	1,392	1,031	526	410	364	369
Limestone	-	-	-	-	-	-	-	-
Madison	66	150	1,163	1,119	1,086	1,052	1,002	959
Marion	-	-	-	-	-	-	-	-
Miller, AR	-	-	-	-	-	-	-	-
Morris	242	26	-	-	-	-	-	-
Nacogdoches	4,360	4,708	1,420	1,262	1,391	1,570	1,781	2,057
Natchitoches, LA	-	-	-	-	-	-	-	-
Navarro	-	-	-	-	-	-	-	-
Panola	-	-	-	-	-	-	-	-
Rains	-	-	-	-	-	-	-	-
Red River, LA	-	-	-	-	-	-	-	-
Robertson	-	-	-	-	-	-	-	-
Rusk	111	114	-	-	-	-	-	-
Sabine, LA	-	-	-	-	-	-	-	-
Sabine, TX	-	-	-	-	-	-	-	-
San Augustine	18	1	9	10	10	11	11	12
Shelby	-	-	-	-	-	-	-	-
Smith	347	83	14	14	14	14	14	14
Titus	-	-	-	-	-	-	-	-
Trinity	-	-	-	-	-	-	-	-
Upshur	490	388	287	298	296	309	326	340
Van Zandt	-	-	-	-	-	-	-	-
Wood	1,037	704	388	406	438	472	498	541
Total	15,190	14,522	10,424	8,448	8,151	8,673	9,051	9,799

*industrial includes manufacturing, mining, and power generation

Table D1.9 (Continued...)
Rate of groundwater withdrawal (acre-feet per year) from flow layer 3 of the Carrizo-Wilcox Aquifer for counties within the study area

County – Other (Non-reported Domestic)

<u>County</u>	<u>1980</u>	<u>1990</u>	<u>2000</u>	<u>2010</u>	<u>2020</u>	<u>2030</u>	<u>2040</u>	<u>2050</u>
Anderson	256	456	684	700	707	717	715	731
Angelina	-	-	-	-	-	-	-	-
Bienville, LA	-	-	-	-	-	-	-	-
Bossier, LA	-	-	-	-	-	-	-	-
Bowie	-	-	-	-	-	-	-	-
Caddo, LA	16	11	10	10	11	12	13	15
Camp	160	183	206	277	282	288	291	293
Cass	179	199	45	46	47	48	52	53
Cherokee	213	267	383	124	135	144	152	159
De Soto, LA	-	-	-	-	-	-	-	-
Franklin	23	25	2	2	2	3	4	4
Freestone	-	-	-	-	-	-	-	-
Gregg	-	-	-	-	-	-	-	-
Grimes	-	-	-	-	-	-	-	-
Harrison	414	591	325	324	350	352	364	363
Henderson	213	376	286	291	291	188	183	291
Hopkins	-	-	-	-	-	-	-	-
Houston	13	15	6	6	6	6	6	6
Leon	202	342	239	257	277	297	319	345
Limestone	-	-	-	-	-	-	-	-
Madison	1	1	-	-	-	-	-	-
Marion	113	115	68	70	71	73	74	74
Miller, AR	-	-	-	-	-	-	-	-
Morris	59	73	9	9	9	9	8	8
Nacogdoches	615	814	786	794	808	819	817	820
Natchitoches, LA	1	2	3	3	4	4	4	5
Navarro	-	-	-	-	-	-	-	-
Panola	-	-	-	-	-	-	-	-
Rains	-	-	-	-	-	-	-	-
Red River, LA	-	-	-	-	-	-	-	-
Robertson	-	2	51	48	45	44	44	44
Rusk	384	476	469	437	468	507	511	540
Sabine, LA	-	-	-	-	-	-	-	-
Sabine, TX	-	-	-	-	-	-	-	-
San Augustine	127	159	77	76	75	75	75	75
Shelby	1	1	-	-	-	-	-	-
Smith	811	1,164	1,461	1,506	1,644	1,810	1,992	2,185
Titus	60	76	47	69	72	82	87	89
Trinity	-	-	-	-	-	-	-	-
Upshur	364	371	311	332	332	335	327	327
Van Zandt	82	144	130	136	168	166	168	168
Wood	230	299	284	312	326	349	365	401
Total	4,537	6,162	5,882	5,829	6,130	6,328	6,571	6,996

Table D1.9 (Continued...)
Rate of groundwater withdrawal (acre-feet per year) from flow layer 3 of the Carrizo-Wilcox Aquifer for counties within the study area

Livestock

<u>County</u>	<u>1980</u>	<u>1990</u>	<u>2000</u>	<u>2010</u>	<u>2020</u>	<u>2030</u>	<u>2040</u>	<u>2050</u>
Anderson	36	46	74	74	74	74	74	74
Angelina	-	-	-	-	-	-	-	-
Bienville, LA	-	-	-	-	-	-	-	-
Bossier, LA	-	-	-	-	-	-	-	-
Bowie	-	-	-	-	-	-	-	-
Caddo, LA	1	1	1	1	1	1	1	1
Camp	31	31	83	83	83	83	83	83
Cass	31	72	13	13	13	13	13	13
Cherokee	-	25	35	35	35	35	35	35
De Soto, LA	-	-	-	-	-	-	-	-
Franklin	3	4	4	4	4	4	4	-
Freestone	43	31	54	54	54	54	54	54
Gregg	10	8	56	56	56	56	56	56
Grimes	-	-	-	-	-	-	-	-
Harrison	37	12	103	119	134	151	169	186
Henderson	17	28	18	18	18	18	18	18
Hopkins	-	-	-	-	-	-	-	-
Houston	1	1	1	1	1	1	1	1
Leon	132	191	539	539	539	539	539	539
Limestone	-	-	-	-	-	-	-	-
Madison	-	1	39	39	39	39	39	39
Marion	2	2	3	3	3	3	3	3
Miller, AR	-	10	45	45	45	45	45	45
Morris	3	4	-	-	-	-	-	-
Nacogdoches	112	90	122	122	112	117	114	121
Natchitoches, LA	10	4	4	4	4	4	4	4
Navarro	-	-	-	-	-	-	-	-
Panola	-	-	-	-	-	-	-	-
Rains	-	-	-	-	-	-	-	-
Red River, LA	-	-	-	-	-	-	-	-
Robertson	11	11	54	54	54	54	54	54
Rusk	-	-	-	-	-	-	-	-
Sabine, LA	-	-	-	-	-	-	-	-
Sabine, TX	-	-	-	-	-	-	-	-
San Augustine	31	33	29	29	30	30	31	31
Shelby	-	-	-	-	-	-	-	-
Smith	17	19	48	48	48	48	48	48
Titus	11	12	22	22	22	22	22	22
Trinity	-	-	-	-	-	-	-	-
Upshur	-	-	-	-	-	-	-	-
Van Zandt	-	-	-	-	-	-	-	-
Wood	-	-	-	-	-	-	-	-
Total	539	636	1,347	1,363	1,369	1,391	1,407	1,427

Table D1.9 (Continued...)
Rate of groundwater withdrawal (acre-feet per year) from flow layer 3 of the Carrizo-Wilcox Aquifer for counties within the study area

Irrigation

<u>County</u>	<u>1980</u>	<u>1990</u>	<u>2000</u>	<u>2010</u>	<u>2020</u>	<u>2030</u>	<u>2040</u>	<u>2050</u>
Anderson	-	4	17	17	17	17	17	17
Angelina	-	-	-	-	-	-	-	-
Bienville, LA	-	-	-	-	-	-	-	-
Bossier, LA	-	-	-	-	-	-	-	-
Bowie	-	-	-	-	-	-	-	-
Caddo, LA	22	1	14	14	14	14	14	14
Camp	-	16	20	20	20	20	20	20
Cass	-	-	-	-	-	-	-	-
Cherokee	11	23	833	49	49	49	49	49
De Soto, LA	-	-	-	-	-	-	-	-
Franklin	-	-	1	1	1	1	1	1
Freestone	-	-	-	-	-	-	-	-
Gregg	-	-	-	-	-	-	-	-
Grimes	-	-	-	-	-	-	-	-
Harrison	-	4	7	7	7	7	7	7
Henderson	-	-	-	-	-	-	-	-
Hopkins	-	-	-	-	-	-	-	-
Houston	-	-	10	10	10	10	10	10
Leon	-	-	-	-	-	-	-	-
Limestone	-	-	-	-	-	-	-	-
Madison	1	2	-	-	-	-	-	-
Marion	-	-	-	-	-	-	-	-
Miller, AR	-	515	886	886	886	886	886	886
Morris	-	-	-	-	-	-	-	-
Nacogdoches	-	57	423	423	423	423	423	423
Natchitoches, LA	17	24	28	28	28	28	28	28
Navarro	-	-	-	-	-	-	-	-
Panola	-	-	-	-	-	-	-	-
Rains	-	-	-	-	-	-	-	-
Red River, LA	-	-	-	-	-	-	-	-
Robertson	-	-	150	146	145	141	137	133
Rusk	-	1	4	4	4	4	4	4
Sabine, LA	-	-	-	-	-	-	-	-
Sabine, TX	-	-	-	-	-	-	-	-
San Augustine	-	-	8	8	8	8	8	8
Shelby	-	-	-	-	-	-	-	-
Smith	3	1	10	10	10	10	10	10
Titus	-	-	-	-	-	-	-	-
Trinity	-	-	-	-	-	-	-	-
Upshur	-	1	-	-	-	-	-	-
Van Zandt	-	-	-	-	-	-	-	-
Wood	-	46	46	46	46	46	46	46
Total	54	695	2,457	1,669	1,668	1,664	1,660	1,656

Table D1.10
Rate of groundwater withdrawal (acre-feet per year) from flow layer 4 of the
Carrizo-Wilcox Aquifer for counties within the study area

Municipal and Industrial*

<u>County</u>	<u>1980</u>	<u>1990</u>	<u>2000</u>	<u>2010</u>	<u>2020</u>	<u>2030</u>	<u>2040</u>	<u>2050</u>
Anderson	344	173	461	378	298	264	238	228
Angelina	601	649	12,237	11,841	10,698	11,298	11,992	13,208
Bienville, LA	-	-	-	-	-	-	-	-
Bossier, LA	-	-	-	-	-	-	-	-
Bowie	-	-	-	-	-	-	-	-
Caddo, LA	196	148	235	243	258	282	314	354
Camp	236	259	35	35	36	37	39	41
Cass	166	154	185	479	174	170	165	162
Cherokee	2,842	2,771	2,171	1,841	1,816	1,830	1,892	2,023
De Soto, LA	-	-	-	-	-	-	-	-
Franklin	-	-	-	-	-	-	-	-
Freestone	-	-	-	-	-	-	-	-
Gregg	449	214	269	274	281	290	299	309
Grimes	-	-	-	-	-	-	-	-
Harrison	87	83	80	107	107	107	107	107
Henderson	69	170	151	152	148	149	150	155
Hopkins	-	-	-	-	-	-	-	-
Houston	-	-	-	-	-	-	-	-
Leon	644	888	1,475	1,482	1,489	1,562	1,628	1,723
Limestone	-	-	-	-	-	-	-	-
Madison	4	10	-	-	-	-	-	-
Marion	-	-	-	-	-	-	-	-
Miller, AR	-	-	-	-	-	-	-	-
Morris	221	6,412	-	-	-	-	-	-
Nacogdoches	308	358	1,073	967	1,048	1,169	1,311	1,497
Natchitoches, LA	-	113	233	246	265	288	317	350
Navarro	-	-	-	-	-	-	-	-
Panola	-	-	-	-	-	-	-	-
Rains	-	-	-	-	-	-	-	-
Red River, LA	-	-	-	-	-	-	-	-
Robertson	-	-	42	51	61	72	84	98
Rusk	774	944	1,032	758	676	684	692	710
Sabine, LA	-	-	-	-	-	-	-	-
Sabine, TX	-	-	-	-	-	-	-	-
San Augustine	100	95	18	19	20	22	22	23
Shelby	23	52	-	-	-	-	-	-
Smith	3,927	2,364	4,444	4,934	5,272	5,256	5,660	4,267
Titus	-	-	-	-	-	-	-	-
Trinity	-	-	-	-	-	-	-	-
Upshur	486	493	370	395	399	416	450	480
Van Zandt	-	-	511	560	605	663	715	782
Wood	1,206	532	1,010	1,081	1,205	1,323	1,450	1,611
Total	12,683	16,882	26,032	25,843	24,856	25,882	27,525	28,128

*industrial includes manufacturing, mining, and power generation

Table D1.10 (Continued...)
Rate of groundwater withdrawal (acre-feet per year) from flow layer 4 of the Carrizo-Wilcox Aquifer for counties within the study area

County – Other (Non-reported Domestic)

<u>County</u>	<u>1980</u>	<u>1990</u>	<u>2000</u>	<u>2010</u>	<u>2020</u>	<u>2030</u>	<u>2040</u>	<u>2050</u>
Anderson	612	1,043	1,570	1,607	1,625	1,646	1,641	1,678
Angelina	-	-	-	-	-	-	-	-
Bienville, LA	-	-	-	-	-	-	-	-
Bossier, LA	-	-	-	-	-	-	-	-
Bowie	1	3	-	-	-	-	-	-
Caddo, LA	53	36	33	34	36	39	44	50
Camp	390	540	610	821	836	853	862	867
Cass	272	319	73	74	74	75	78	78
Cherokee	180	199	286	93	101	107	113	119
De Soto, LA	-	-	-	-	-	-	-	-
Franklin	75	93	8	9	9	10	13	13
Freestone	269	339	344	329	308	301	304	303
Gregg	1,288	1,273	615	751	747	794	833	866
Grimes	-	-	-	-	-	-	-	-
Harrison	440	637	386	384	423	428	437	436
Henderson	556	832	712	719	719	715	708	718
Hopkins	42	45	31	40	39	43	48	52
Houston	2	2	1	1	1	1	1	1
Leon	242	372	267	287	308	331	355	384
Limestone	14	28	68	69	71	76	81	87
Madison	-	-	-	-	-	-	-	-
Marion	243	232	137	140	144	146	148	149
Miller, AR	-	1	1	1	1	1	1	1
Morris	221	255	23	23	22	22	21	20
Nacogdoches	348	435	420	424	431	437	436	438
Natchitoches, LA	29	70	95	100	108	118	129	143
Navarro	-	-	-	-	-	-	-	-
Panola	18	19	9	9	9	8	8	8
Rains	-	-	-	-	-	-	-	-
Red River, LA	-	-	-	-	-	-	-	-
Robertson	4	9	202	190	177	172	172	172
Rusk	2,153	2,626	2,474	2,165	2,320	2,509	2,545	2,673
Sabine, LA	-	-	-	-	-	-	-	-
Sabine, TX	-	-	-	-	-	-	-	-
San Augustine	143	147	46	46	45	45	45	45
Shelby	913	1,000	540	571	556	163	561	575
Smith	365	468	576	598	649	709	774	845
Titus	210	292	183	270	284	322	340	351
Trinity	-	-	-	-	-	-	-	-
Upshur	303	397	348	370	370	372	30	360
Van Zandt	352	530	447	476	616	592	598	600
Wood	232	348	400	440	459	491	514	565
Total	9,970	12,590	10,905	11,041	11,488	11,526	11,840	12,597

Table D1.10 (Continued...)
Rate of groundwater withdrawal (acre-feet per year) from flow layer 4 of the Carrizo-Wilcox Aquifer for counties within the study area

Livestock

<u>County</u>	<u>1980</u>	<u>1990</u>	<u>2000</u>	<u>2010</u>	<u>2020</u>	<u>2030</u>	<u>2040</u>	<u>2050</u>
Anderson	36	41	74	74	74	74	74	74
Angelina	-	-	-	-	-	-	-	-
Bienville, LA	-	-	-	-	-	-	-	-
Bossier, LA	2	2	2	2	2	2	2	2
Bowie	-	-	-	-	-	-	-	-
Caddo, LA	8	8	8	8	8	8	8	8
Camp	49	49	131	131	131	131	131	131
Cass	21	40	18	18	18	18	18	18
Cherokee	1	52	73	73	73	3	73	73
De Soto, LA	-	-	-	-	-	-	-	-
Franklin	44	66	62	62	62	62	62	62
Freestone	141	99	165	165	165	165	165	165
Gregg	33	28	188	188	188	188	188	188
Grimes	-	-	-	-	-	-	-	-
Harrison	59	21	87	96	104	114	124	134
Henderson	63	99	71	71	71	71	71	71
Hopkins	3	4	2	2	2	2	2	2
Houston	-	-	-	-	-	-	-	-
Leon	135	180	403	403	403	403	403	403
Limestone	4	5	49	49	49	49	49	49
Madison	-	-	-	-	-	-	-	-
Marion	14	14	16	16	16	16	16	16
Miller, AR	-	6	27	27	27	27	27	27
Morris	10	14	3	3	3	3	3	3
Nacogdoches	123	99	134	134	123	128	125	133
Natchitoches, LA	142	-	53	53	53	53	53	53
Navarro	-	-	-	-	-	-	-	-
Panola	1	1	2	2	2	2	2	2
Rains	-	-	-	-	-	-	-	-
Red River, LA	-	-	-	-	-	-	-	-
Robertson	181	178	905	905	905	905	905	905
Rusk	349	295	288	292	296	292	297	295
Sabine, LA	-	-	-	-	-	-	-	-
Sabine, TX	-	-	-	-	-	-	-	-
San Augustine	23	25	22	22	22	23	23	23
Shelby	284	298	738	900	670	823	1,003	1,223
Smith	27	31	55	55	55	55	55	55
Titus	62	71	126	126	126	126	126	126
Trinity	-	-	-	-	-	-	-	-
Upshur	18	49	125	125	125	125	125	125
Van Zandt	152	185	63	63	63	63	63	63
Wood	27	36	22	22	22	22	22	22
Total	2,012	1,996	3,912	4,087	3,858	3,953	4,215	4,451

Table D1.10 (Continued...)
Rate of groundwater withdrawal (acre-feet per year) from flow layer 4 of the Carrizo-Wilcox Aquifer for counties within the study area

Irrigation

<u>County</u>	<u>1980</u>	<u>1990</u>	<u>2000</u>	<u>2010</u>	<u>2020</u>	<u>2030</u>	<u>2040</u>	<u>2050</u>
Anderson	-	12	68	68	68	68	68	68
Angelina	-	-	-	-	-	-	-	-
Bienville, LA	-	-	-	-	-	-	-	-
Bossier, LA	9	3	6	6	6	6	6	6
Bowie	-	-	-	-	-	-	-	-
Caddo, LA	335	3	188	188	188	188	188	188
Camp	-	31	38	38	38	38	38	38
Cass	-	-	-	-	-	-	-	-
Cherokee	10	17	6	-	-	-	-	-
De Soto, LA	-	-	-	-	-	-	-	-
Franklin	-	1	5	5	5	5	5	5
Freestone	-	10	1	1	1	1	1	1
Gregg	-	-	-	-	-	-	-	-
Grimes	-	-	-	-	-	-	-	-
Harrison	-	3	6	6	6	6	6	6
Henderson	23	5	-	-	-	-	-	-
Hopkins	-	-	-	-	-	-	-	-
Houston	-	-	10	10	10	10	10	10
Leon	-	-	-	-	-	-	-	-
Limestone	-	-	-	-	-	-	-	-
Madison	-	-	-	-	-	-	-	-
Marion	-	-	-	-	-	-	-	-
Miller, AR	-	1,115	1,917	1,917	1,917	1,917	1,917	1,917
Morris	-	-	-	-	-	-	-	-
Nacogdoches	-	66	495	495	495	495	495	495
Natchitoches, LA	118	167	193	193	193	193	193	193
Navarro	-	-	-	-	-	-	-	-
Panola	-	-	-	-	-	-	-	-
Rains	-	-	-	-	-	-	-	-
Red River, LA	-	-	-	-	-	-	-	-
Robertson	13	13	6,628	6,469	6,407	6,223	6,045	5,872
Rusk	-	19	55	55	55	55	55	55
Sabine, LA	-	-	-	-	-	-	-	-
Sabine, TX	-	-	-	-	-	-	-	-
San Augustine	-	-	55	55	55	55	55	55
Shelby	-	8	11	11	12	15	18	21
Smith	19	5	55	55	55	55	55	55
Titus	-	-	-	-	-	-	-	-
Trinity	-	-	-	-	-	-	-	-
Upshur	-	-	-	-	-	-	-	-
Van Zandt	-	-	-	-	-	-	-	-
Wood	-	91	75	75	75	75	75	75
Total	527	1,569	9,812	9,647	9,586	9,405	9,230	9,060

Table D1.11
Rate of groundwater withdrawal (acre-feet per year) from flow layer 5 of the
Carrizo-Wilcox Aquifer for counties within the study area

Municipal and Industrial*

<u>County</u>	<u>1980</u>	<u>1990</u>	<u>2000</u>	<u>2010</u>	<u>2020</u>	<u>2030</u>	<u>2040</u>	<u>2050</u>
Anderson	192	-	130	139	146	152	165	176
Angelina	-	-	-	-	-	-	-	-
Bienville, LA	-	-	-	-	-	-	-	-
Bossier, LA	-	-	-	-	-	-	-	-
Bowie	23	26	25	25	25	25	25	25
Caddo, LA	943	1,030	1,115	1,149	1,219	1,324	1,465	1,641
Camp	469	514	273	271	274	279	286	294
Cass	1,070	1,033	46	45	44	42	41	41
Cherokee	3	4	60	13	14	15	16	18
De Soto, LA	422	835	96	96	96	96	96	96
Franklin	459	401	1,479	1,384	1,338	1,278	1,297	1,359
Freestone	101	809	179	204	204	199	199	200
Gregg	317	150	382	352	337	335	335	334
Grimes	-	-	-	-	-	-	-	-
Harrison	313	265	52	47	45	39	42	43
Henderson	542	486	324	303	299	308	319	339
Hopkins	78	76	-	-	-	-	-	-
Houston	-	-	-	-	-	-	-	-
Leon	-	-	-	-	-	-	-	-
Limestone	-	646	6,200	6,889	6,889	6,889	6,889	6,889
Madison	-	-	-	-	-	-	-	-
Marion	-	-	91	63	50	44	40	54
Miller, AR	-	4,248	9	10	11	11	12	13
Morris	477	291	409	412	401	395	383	379
Nacogdoches	275	271	256	259	262	284	301	316
Natchitoches, LA	-	-	-	-	-	-	-	-
Navarro	-	-	-	-	-	-	-	-
Panola	1,007	1,691	357	331	291	401	402	399
Rains	-	-	-	-	-	-	-	-
Red River, LA	-	-	-	-	-	-	-	-
Robertson	-	-	-	-	-	-	-	-
Rusk	2,887	2,850	3,086	2,789	2,450	2,241	2,144	2,092
Sabine, LA	-	-	-	-	-	-	-	-
Sabine, TX	-	-	-	-	-	-	-	-
San Augustine	-	-	-	-	-	-	-	-
Shelby	427	369	305	304	303	311	317	328
Smith	1,057	634	2,239	2,460	2,627	2,639	2,807	2,208
Titus	135	213	1,876	1,771	1,735	1,722	1,724	1,735
Trinity	-	-	-	-	-	-	-	-
Upshur	39	38	6	7	6	7	7	7
Van Zandt	1,213	643	569	611	648	699	741	800
Wood	-	-	-	-	-	-	-	-
Total	12,449	17,523	19,564	19,934	19,714	19,735	20,053	19,786

*industrial includes manufacturing, mining, and power generation

Table D1.11 (Continued...)
Rate of groundwater withdrawal (acre-feet per year) from flow layer 5 of the Carrizo-Wilcox Aquifer for counties within the study area

County – Other (Non-reported Domestic)

<u>County</u>	<u>1980</u>	<u>1990</u>	<u>2000</u>	<u>2010</u>	<u>2020</u>	<u>2030</u>	<u>2040</u>	<u>2050</u>
Anderson	11	11	15	15	16	16	16	16
Angelina	-	-	-	-	-	-	-	-
Bienville, LA	-	-	-	-	-	-	-	-
Bossier, LA	47	40	38	41	44	46	48	50
Bowie	963	1,141	76	76	76	76	76	76
Caddo, LA	1,556	1,324	1,222	1,262	1,344	1,468	1,633	1,841
Camp	-	-	-	-	-	-	-	-
Cass	16	26	6	6	6	6	6	6
Cherokee	-	33	48	15	16	17	18	19
De Soto, LA	659	201	-	-	-	-	-	-
Franklin	74	130	11	12	12	13	18	18
Freestone	205	274	253	242	226	221	223	222
Gregg	110	128	62	75	75	79	83	87
Grimes	-	-	-	-	-	-	-	-
Harrison	1,074	1,405	933	933	1,034	1,053	1,065	1,062
Henderson	371	490	469	470	470	469	468	470
Hopkins	245	342	521	641	640	672	734	768
Houston	-	-	-	-	-	-	-	-
Leon	-	-	-	-	-	-	-	-
Limestone	72	121	297	300	311	332	355	383
Madison	-	-	-	-	-	-	-	-
Marion	74	90	53	55	56	57	58	58
Miller, AR	11	12	12	13	14	14	15	16
Morris	49	51	-	-	-	-	-	-
Nacogdoches	44	51	49	50	51	52	51	52
Natchitoches, LA	3	6	8	8	9	10	10	12
Navarro	10	16	-	-	-	-	-	-
Panola	1,621	1,951	945	926	896	858	858	858
Rains	238	366	368	389	408	276	293	311
Red River, LA	9	7	9	9	10	11	12	14
Robertson	14	24	534	503	469	455	456	455
Rusk	183	238	212	166	178	193	197	205
Sabine, LA	-	-	-	-	-	-	-	-
Sabine, TX	-	-	-	-	-	-	-	-
San Augustine	-	-	-	-	-	-	-	-
Shelby	856	943	501	522	509	515	513	526
Smith	13	19	22	23	25	27	29	32
Titus	608	726	316	466	490	556	587	605
Trinity	-	-	-	-	-	-	-	-
Upshur	38	52	49	52	52	52	52	52
Van Zandt	733	1,051	637	739	1,290	1,059	1,073	1,082
Wood	311	520	642	705	735	786	824	905
Total	10,218	11,789	8,308	8,714	9,462	9,389	9,771	10,201

Table D1.11 (Continued...)
Rate of groundwater withdrawal (acre-feet per year) from flow layer 5 of the Carrizo-Wilcox Aquifer for counties within the study area

Livestock

County	1980	1990	2000	2010	2020	2030	2040	2050
Anderson	5	5	9	9	9	9	9	9
Angelina	-	-	-	-	-	-	-	-
Bienville, LA	-	-	-	-	-	-	-	-
Bossier, LA	11	11	12	12	12	12	12	12
Bowie	96	107	542	580	580	580	580	580
Caddo, LA	37	36	39	39	39	39	39	39
Camp	8	8	22	22	22	22	22	22
Cass	4	5	5	5	5	5	5	5
Cherokee	-	-	-	-	-	-	-	-
De Soto, LA	192	3	111	111	111	111	111	111
Franklin	121	183	179	179	179	179	179	179
Freestone	76	54	75	75	75	75	75	75
Gregg	4	4	21	21	21	21	21	21
Grimes	-	-	-	-	-	-	-	-
Harrison	46	20	340	362	386	410	436	463
Henderson	76	120	90	90	90	90	90	90
Hopkins	334	541	269	269	269	269	269	269
Houston	-	-	-	-	-	-	-	-
Leon	-	-	-	-	-	-	-	-
Limestone	35	38	422	422	422	422	422	422
Madison	-	-	-	-	-	-	-	-
Marion	6	6	7	7	7	7	7	7
Miller, AR	13	61	61	61	61	61	61	61
Morris	49	53	181	181	181	181	181	181
Nacogdoches	39	32	45	45	41	43	42	44
Natchitoches, LA	60	-	22	22	22	22	22	22
Navarro	-	-	-	-	-	-	-	-
Panola	439	530	703	703	703	703	703	703
Rains	59	99	-	-	-	-	-	-
Red River, LA	10	8	10	10	10	10	10	10
Robertson	149	16	745	745	745	745	745	745
Rusk	171	155	149	151	153	150	154	150
Sabine, LA	-	-	-	-	-	-	-	-
Sabine, TX	-	-	-	-	-	-	-	-
San Augustine	-	-	-	-	-	-	-	-
Shelby	457	479	1,170	1,427	1,030	1,264	1,541	1,878
Smith	-	-	-	-	-	-	-	-
Titus	246	290	506	506	506	506	506	506
Trinity	-	-	-	-	-	-	-	-
Upshur	8	20	51	51	51	51	51	51
Van Zandt	186	225	51	52	61	71	85	93
Wood	57	79	59	59	59	59	59	59
Total	2,994	3,188	5,896	6,216	5,850	6,117	6,437	6,807

Table D1.11 (Continued...)
Rate of groundwater withdrawal (acre-feet per year) from flow layer 5 of the Carrizo-Wilcox Aquifer for counties within the study area

Irrigation

<u>County</u>	<u>1980</u>	<u>1990</u>	<u>2000</u>	<u>2010</u>	<u>2020</u>	<u>2030</u>	<u>2040</u>	<u>2050</u>
Anderson	1	4	25	25	25	25	25	25
Angelina	-	-	-	-	-	-	-	-
Bienville, LA	-	-	-	-	-	-	-	-
Bossier, LA	49	16	30	30	30	30	30	30
Bowie	-	-	-	-	-	-	-	-
Caddo, LA	853	15	482	482	482	482	482	482
Camp	-	5	6	6	6	6	6	6
Cass	-	-	-	-	-	-	-	-
Cherokee	-	-	-	-	-	-	-	-
De Soto, LA	17	14	19	19	19	19	19	19
Franklin	-	-	6	6	6	6	6	6
Freestone	-	6	2	2	2	2	2	2
Gregg	-	-	-	-	-	-	-	-
Grimes	-	-	-	-	-	-	-	-
Harrison	-	39	16	16	16	16	16	16
Henderson	42	9	-	-	-	-	-	-
Hopkins	-	-	-	-	-	-	-	-
Houston	-	-	-	-	-	-	-	-
Leon	-	-	-	-	-	-	-	-
Limestone	-	-	-	-	-	-	-	-
Madison	-	-	-	-	-	-	-	-
Marion	-	-	-	-	-	-	-	-
Miller, AR	-	2,415	4,152	4,152	4,152	4,152	4,152	4,152
Morris	-	-	-	-	-	-	-	-
Nacogdoches	-	6	41	41	41	41	41	41
Natchitoches, LA	74	106	125	125	125	125	125	125
Navarro	-	-	-	-	-	-	-	-
Panola	-	-	-	-	-	-	-	-
Rains	-	-	-	-	-	-	-	-
Red River, LA	4	61	155	155	155	155	155	155
Robertson	10	10	5,171	5,047	4,998	4,855	4,716	4,581
Rusk	-	6	17	17	17	17	17	17
Sabine, LA	-	-	-	-	-	-	-	-
Sabine, TX	-	-	-	-	-	-	-	-
San Augustine	-	-	-	-	-	-	-	-
Shelby	-	3	8	9	10	12	15	18
Smith	3	-	-	3	3	3	3	3
Titus	-	-	-	-	-	-	-	-
Trinity	-	-	-	-	-	-	-	-
Upshur	-	-	-	-	-	-	-	-
Van Zandt	-	-	220	220	220	220	220	220
Wood	-	23	3	3	3	3	3	3
Total	1,053	2,738	10,478	10,358	10,310	10,169	10,033	9,901

Table D1.12
Rate of groundwater withdrawal (acre-feet per year) from flow layer 6 of the
Carrizo-Wilcox Aquifer for counties within the study area

Municipal and Industrial*

<u>County</u>	<u>1980</u>	<u>1990</u>	<u>2000</u>	<u>2010</u>	<u>2020</u>	<u>2030</u>	<u>2040</u>	<u>2050</u>
Anderson	61	81	4	5	5	6	6	7
Angelina	-	-	-	-	-	-	-	-
Bienville, LA	-	-	-	-	-	-	-	-
Bossier, LA	-	-	-	-	-	-	-	-
Bowie	95	57	74	74	75	77	81	86
Caddo, LA	92	116	4	4	4	5	5	6
Camp	-	-	-	-	-	-	-	-
Cass	645	656	202	340	335	330	325	309
Cherokee	-	-	-	-	-	-	-	-
De Soto, LA	587	316	-	-	-	-	-	-
Franklin	-	-	3	3	3	3	3	3
Freestone	982	1,021	1,169	1,212	1,269	1,324	1,346	1,371
Gregg	-	-	356	372	387	409	432	459
Grimes	-	-	-	-	-	-	-	-
Harrison	366	298	331	435	482	512	516	532
Henderson	606	667	927	666	665	672	676	693
Hopkins	134	88	102	108	112	119	126	134
Houston	-	-	-	-	-	-	-	-
Leon	-	-	-	-	-	-	-	-
Limestone	-	-	-	-	-	-	-	-
Madison	-	-	-	-	-	-	-	-
Marion	2	-	-	-	-	-	-	-
Miller, AR	-	-	-	-	-	-	-	-
Morris	-	-	-	-	-	-	-	-
Nacogdoches	-	-	-	-	-	-	-	-
Natchitoches, LA	-	-	-	-	-	-	-	-
Navarro	-	-	-	-	-	-	-	-
Panola	138	127	1,438	1,185	937	1,757	1,782	1,755
Rains	-	-	-	-	-	-	-	-
Red River, LA	-	-	-	-	-	-	-	-
Robertson	-	-	-	-	-	-	-	-
Rusk	74	4	995	895	794	760	756	760
Sabine, LA	-	-	-	-	-	-	-	-
Sabine, TX	-	-	-	-	-	-	-	-
San Augustine	-	-	-	-	-	-	-	-
Shelby	16	24	153	149	146	146	147	151
Smith	-	-	-	-	-	-	-	-
Titus	-	-	-	-	-	-	-	-
Trinity	-	-	-	-	-	-	-	-
Upshur	-	-	-	-	-	-	-	-
Van Zandt	738	723	1,451	1,412	1,362	1,455	1,564	1,639
Wood	-	-	1,128	1,128	1,128	1,128	1,128	1,128
Total	4,536	4,178	8,337	7,988	7,704	8,703	8,893	9,033

*industrial includes manufacturing, mining, and power generation

Table D1.12 (Continued...)
Rate of groundwater withdrawal (acre-feet per year) from flow layer 6 of the Carrizo-Wilcox Aquifer for counties within the study area

County – Other (Non-reported Domestic)

<u>County</u>	<u>1980</u>	<u>1990</u>	<u>2000</u>	<u>2010</u>	<u>2020</u>	<u>2030</u>	<u>2040</u>	<u>2050</u>
Anderson	2	2	3	3	3	3	3	3
Angelina	-	-	-	-	-	-	-	-
Bienville, LA	-	-	-	-	-	-	-	-
Bossier, LA	-	-	-	-	-	-	-	-
Bowie	557	646	43	43	43	43	43	43
Caddo, LA	548	488	449	464	494	540	601	677
Camp	-	-	-	-	-	-	-	-
Cass	-	-	-	-	-	-	-	-
Cherokee	-	-	-	-	-	-	-	-
De Soto, LA	24	9	-	-	-	-	-	-
Franklin	135	167	4	5	5	5	7	7
Freestone	328	480	485	464	435	424	428	427
Gregg	-	-	-	-	-	-	-	-
Grimes	-	-	-	-	-	-	-	-
Harrison	-	-	-	-	-	-	-	-
Henderson	569	860	872	872	872	872	872	872
Hopkins	141	183	548	645	641	648	675	682
Houston	-	-	-	-	-	-	-	-
Leon	-	-	-	-	-	-	-	-
Limestone	175	263	631	638	662	706	754	813
Madison	-	-	-	-	-	-	-	-
Marion	-	-	-	-	-	-	-	-
Miller, AR	2	4	4	5	5	5	6	6
Morris	-	1	-	-	-	-	-	-
Nacogdoches	-	-	-	-	-	-	-	-
Natchitoches, LA	-	-	-	-	-	-	-	-
Navarro	42	84	-	-	-	-	-	-
Panola	-	-	-	-	-	-	-	-
Rains	-	-	-	-	-	-	-	-
Red River, LA	-	-	-	-	-	-	-	-
Robertson	-	-	-	-	-	-	-	-
Rusk	-	-	-	-	-	-	-	-
Sabine, LA	-	-	-	-	-	-	-	-
Sabine, TX	-	-	-	-	-	-	-	-
San Augustine	-	-	-	-	-	-	-	-
Shelby	5	5	3	3	3	3	3	3
Smith	-	-	-	-	-	-	-	-
Titus	79	103	1	1	1	2	2	2
Trinity	-	-	-	-	-	-	-	-
Upshur	-	-	-	-	-	-	-	-
Van Zandt	630	967	231	286	589	448	454	459
Wood	-	-	-	-	-	-	-	-
Total	3,237	4,262	3,274	3,429	3,753	3,699	3,848	3,994

Table D1.12 (Continued...)

Rate of groundwater withdrawal (acre-feet per year) from flow layer 6 of the Carrizo-Wilcox Aquifer for counties within the study area

Livestock

<u>County</u>	<u>1980</u>	<u>1990</u>	<u>2000</u>	<u>2010</u>	<u>2020</u>	<u>2030</u>	<u>2040</u>	<u>2050</u>
Anderson	1	1	2	2	2	2	2	2
Angelina	-	-	-	-	-	-	-	-
Bienville, LA	-	-	-	-	-	-	-	-
Bossier, LA	-	-	-	-	-	-	-	-
Bowie	189	211	107	1,147	1,147	1,147	1,147	1,147
Caddo, LA	3	3	3	3	3	3	3	3
Camp	-	-	-	-	-	-	-	-
Cass	-	-	-	-	-	-	-	-
Cherokee	-	-	-	-	-	-	-	-
De Soto, LA	2	-	1	1	1	1	1	1
Franklin	172	261	268	268	268	268	268	268
Freestone	204	148	224	224	224	224	224	224
Gregg	-	-	-	-	-	-	-	-
Grimes	-	-	-	-	-	-	-	-
Harrison	40	16	66	70	74	78	82	87
Henderson	166	263	203	203	203	203	203	203
Hopkins	1,155	1,699	339	339	339	339	339	339
Houston	-	-	-	-	-	-	-	-
Leon	-	-	-	-	-	-	-	-
Limestone	68	76	810	810	810	810	810	810
Madison	-	-	-	-	-	-	-	-
Marion	-	-	-	-	-	-	-	-
Miller, AR	-	1	7	7	7	7	7	7
Morris	4	4	16	16	16	16	16	16
Nacogdoches	-	-	-	-	-	-	-	-
Natchitoches, LA	-	-	-	-	-	-	-	-
Navarro	15	15	12	12	12	12	12	12
Panola	263	319	423	423	423	423	423	423
Rains	90	153	-	-	-	-	-	-
Red River, LA	-	-	-	-	-	-	-	-
Robertson	-	-	-	-	-	-	-	-
Rusk	-	-	-	-	-	-	-	-
Sabine, LA	-	-	-	-	-	-	-	-
Sabine, TX	-	-	-	-	-	-	-	-
San Augustine	-	-	-	-	-	-	-	-
Shelby	-	-	-	-	-	-	-	-
Smith	-	-	-	-	-	-	-	-
Titus	29	35	59	59	59	59	59	59
Trinity	-	-	-	-	-	-	-	-
Upshur	-	-	-	-	-	-	-	-
Van Zandt	270	327	49	60	122	188	281	330
Wood	1	2	1	1	1	1	1	1
Total	2,672	3,534	2,590	3,645	3,711	3,781	3,878	3,932

Table D1.12 (Continued...)
Rate of groundwater withdrawal (acre-feet per year) from flow layer 6 of the Carrizo-Wilcox Aquifer for counties within the study area

Irrigation

<u>County</u>	<u>1980</u>	<u>1990</u>	<u>2000</u>	<u>2010</u>	<u>2020</u>	<u>2030</u>	<u>2040</u>	<u>2050</u>
Anderson	-	-	7	7	7	7	7	7
Angelina	-	-	-	-	-	-	-	-
Bienville, LA	-	-	-	-	-	-	-	-
Bossier, LA	9	2	5	5	5	5	5	5
Bowie	-	-	-	-	-	-	-	-
Caddo, LA	287	7	163	163	163	163	163	163
Camp	-	5	7	7	7	7	7	7
Cass	-	-	-	-	-	-	-	-
Cherokee	-	-	-	-	-	-	-	-
De Soto, LA	2	2	4	4	4	4	4	4
Franklin	-	-	-	-	-	-	-	-
Freestone	-	8	3	3	3	3	3	3
Gregg	-	-	-	-	-	-	-	-
Grimes	-	-	-	-	-	-	-	-
Harrison	-	4	1	1	1	1	1	1
Henderson	32	7	-	-	-	-	-	-
Hopkins	-	-	-	-	-	-	-	-
Houston	-	-	-	-	-	-	-	-
Leon	-	-	-	-	-	-	-	-
Limestone	-	-	-	-	-	-	-	-
Madison	-	-	-	-	-	-	-	-
Marion	-	-	-	-	-	-	-	-
Miller, AR	-	6	10	10	10	10	10	10
Morris	-	-	-	-	-	-	-	-
Nacogdoches	-	-	1	1	1	1	1	1
Natchitoches, LA	-	-	-	-	-	-	-	-
Navarro	-	-	-	-	-	-	-	-
Panola	-	-	-	-	-	-	-	-
Rains	-	-	-	-	-	-	-	-
Red River, LA	1	23	59	59	59	59	59	59
Robertson	-	-	-	-	-	-	-	-
Rusk	-	-	-	-	-	-	-	-
Sabine, LA	-	-	-	-	-	-	-	-
Sabine, TX	-	-	-	-	-	-	-	-
San Augustine	-	-	-	-	-	-	-	-
Shelby	-	-	-	-	-	-	-	-
Smith	-	-	-	-	-	-	-	-
Titus	-	-	-	-	-	-	-	-
Trinity	-	-	-	-	-	-	-	-
Upshur	-	-	-	-	-	-	-	-
Van Zandt	-	-	-	-	-	-	-	-
Wood	-	-	-	-	-	-	-	-
Total	331	64	260	260	260	260	260	260

APPENDIX D2

Post Plots of Groundwater Withdrawal Estimates for the Carrizo-Wilcox for 1980, 1990, 2000, 2010, 2020, 2030, 2040, and 2050

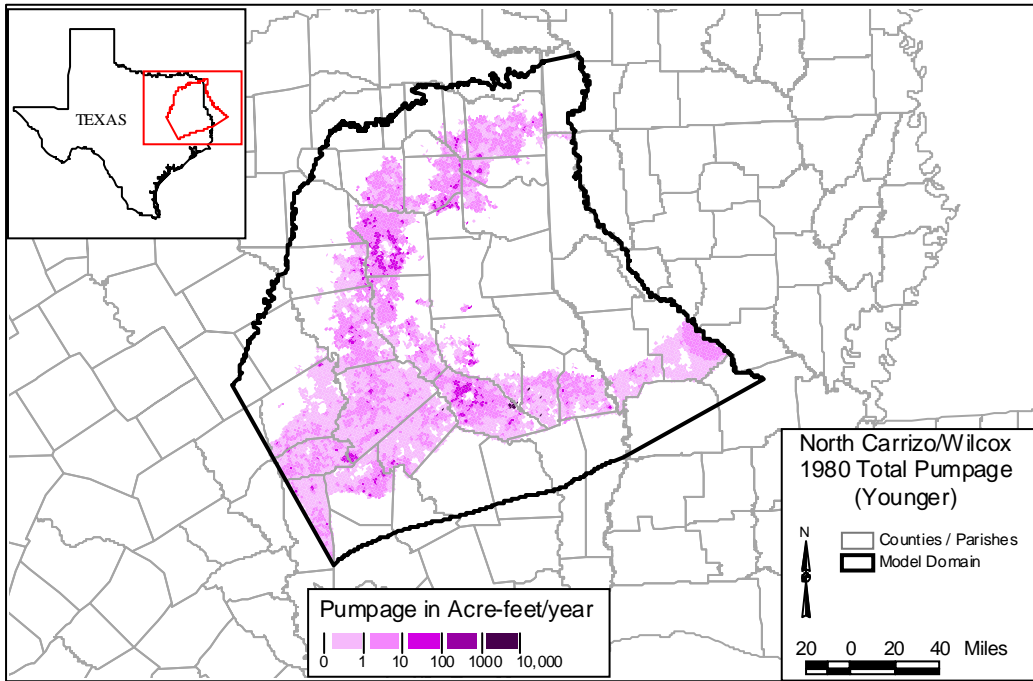


Figure D.2.1 Younger (Layer 1) Pumpage, 1980 (AFY)

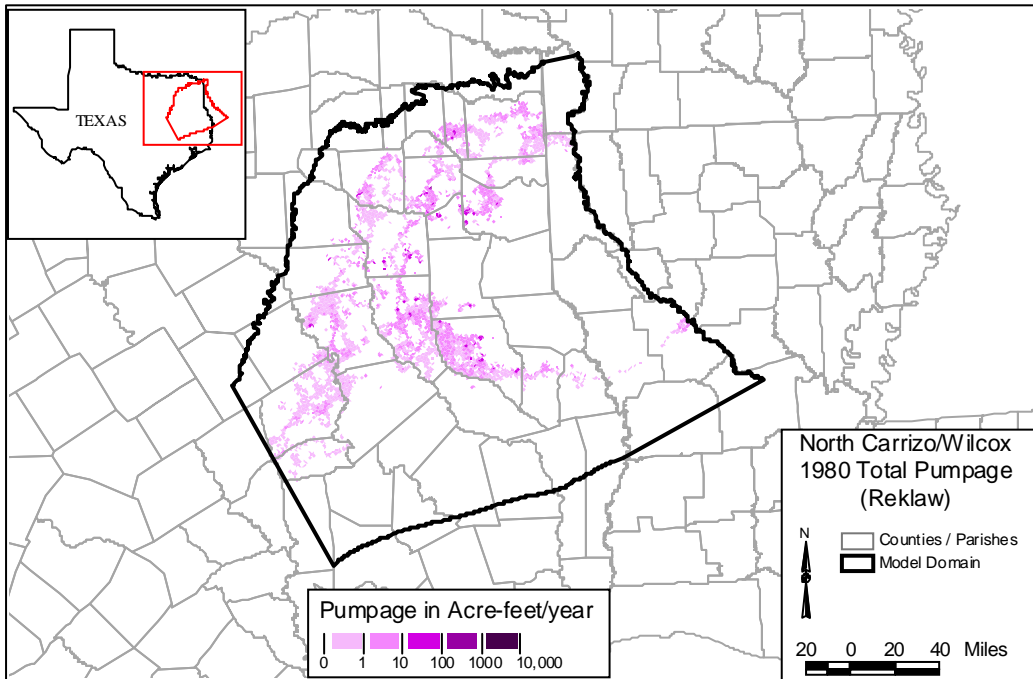


Figure D.2.2 Reklaw (Layer 2) Pumpage, 1980 (AFY)

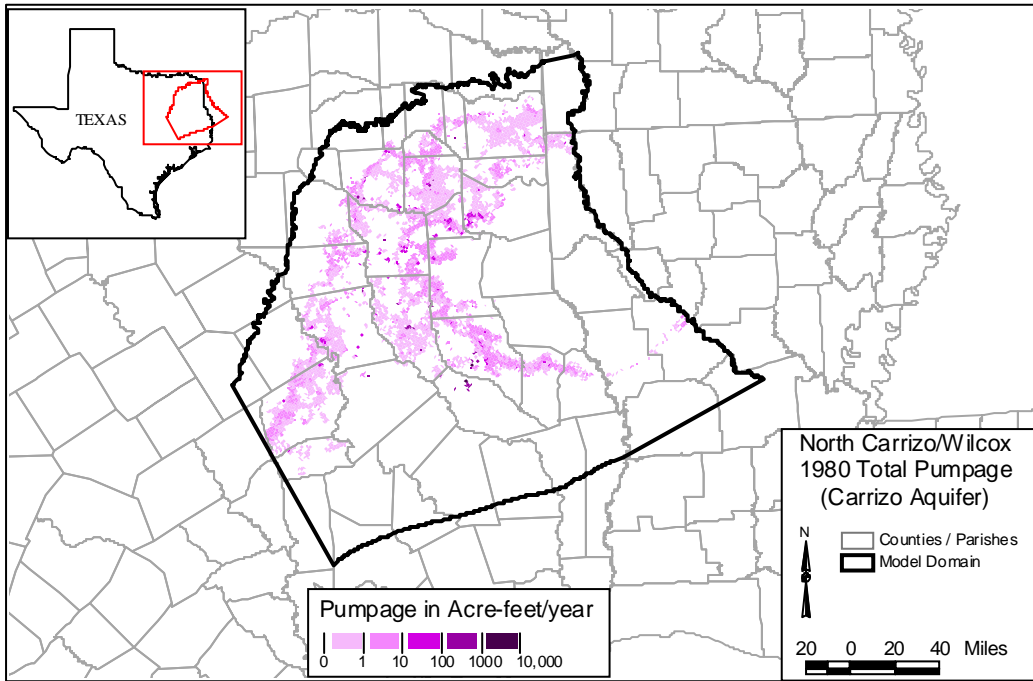


Figure D.2.3 Carrizo (Layer 3) Pumpage, 1980 (AFY)

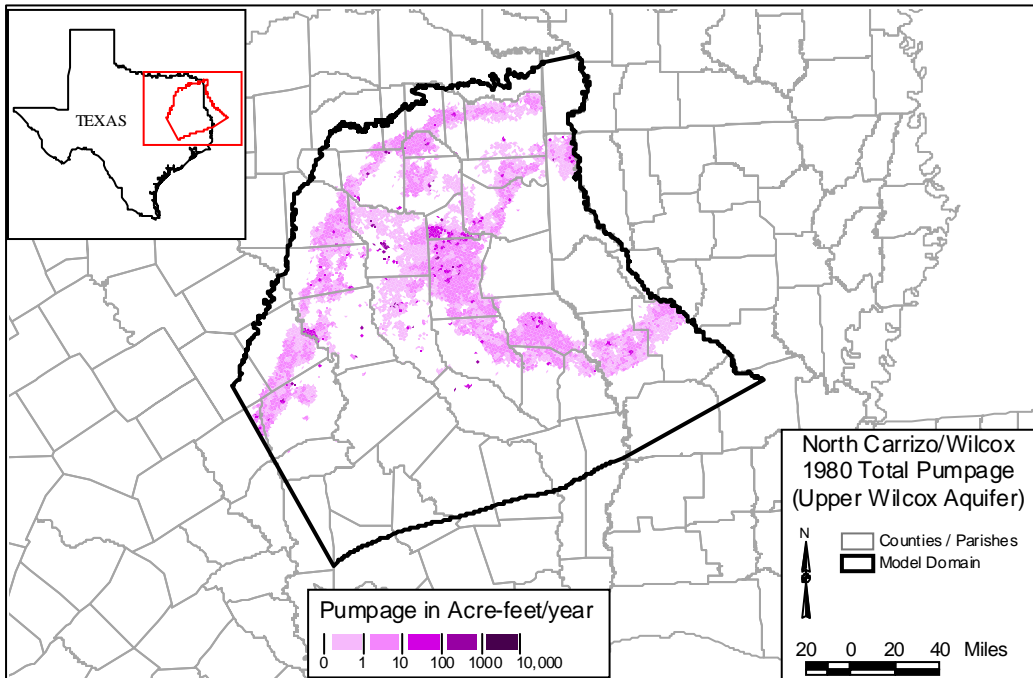


Figure D.2.4 Upper Wilcox (Layer 4) Pumpage, 1980 (AFY)

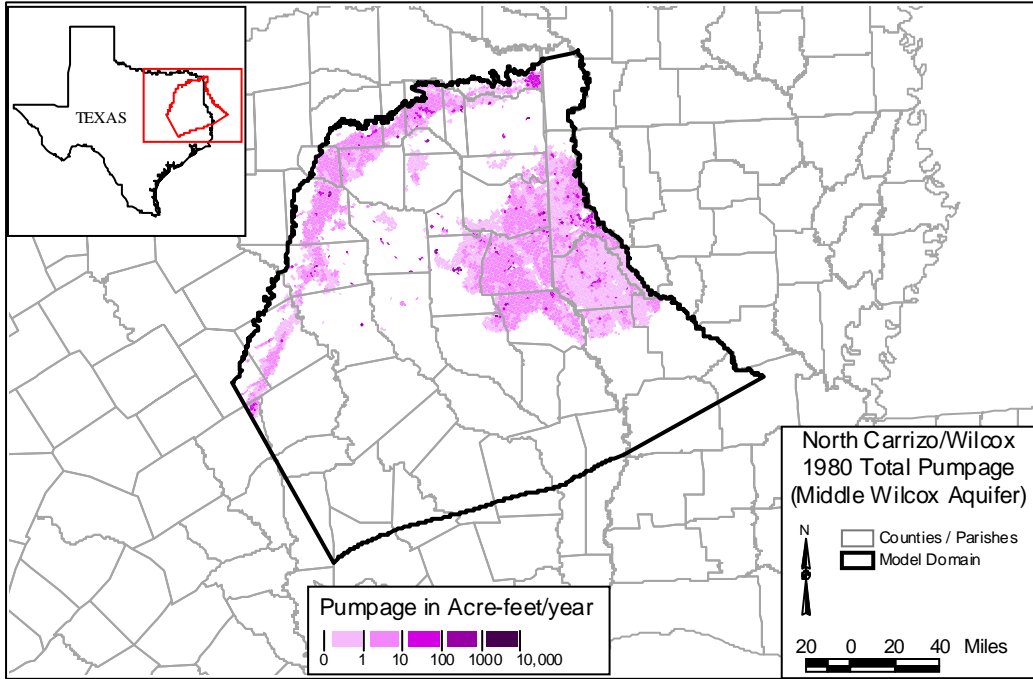


Figure D.2.5 Middle Wilcox (Layer 5) Pumpage, 1980 (AFY)

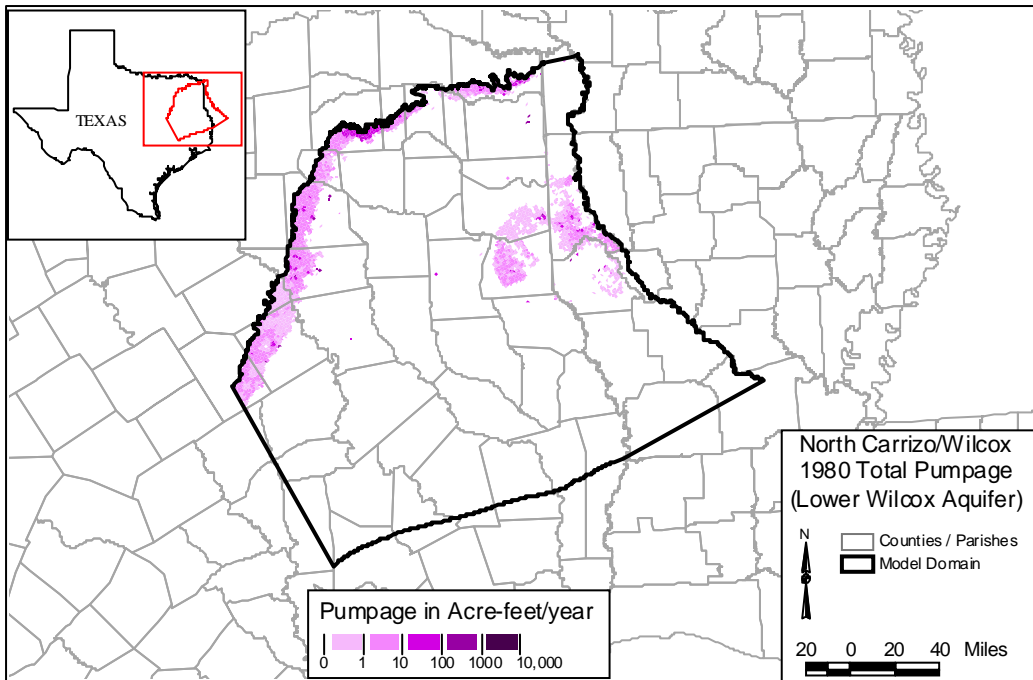


Figure D.2.6 Lower Wilcox (Layer 6) Pumpage, 1980 (AFY)

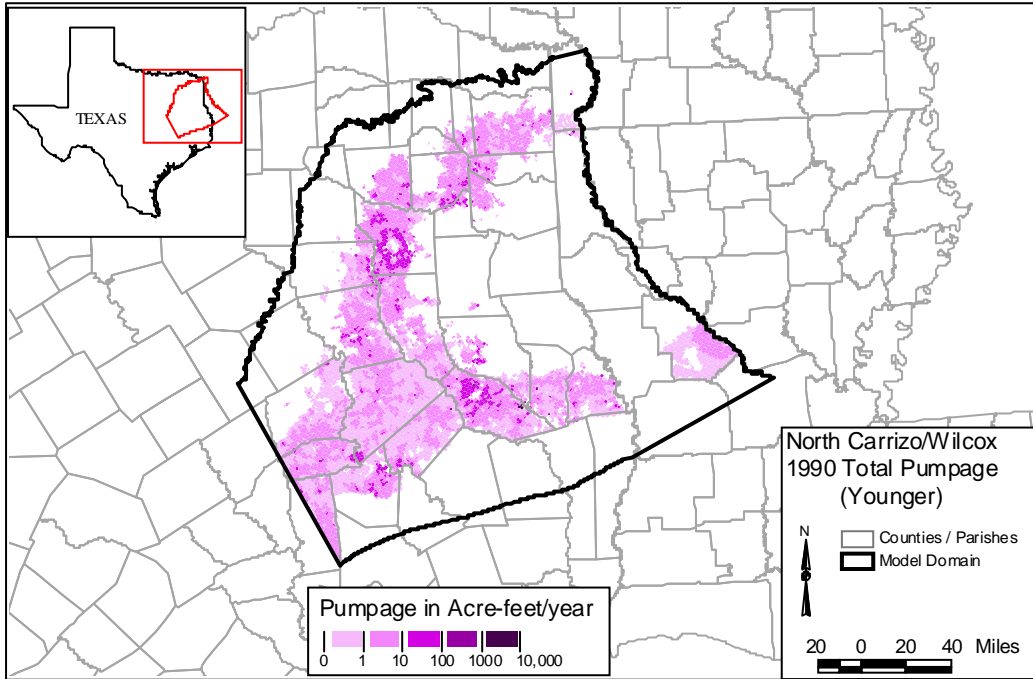


Figure D.2.7 Younger (Layer 1) Pumpage, 1990 (AFY)

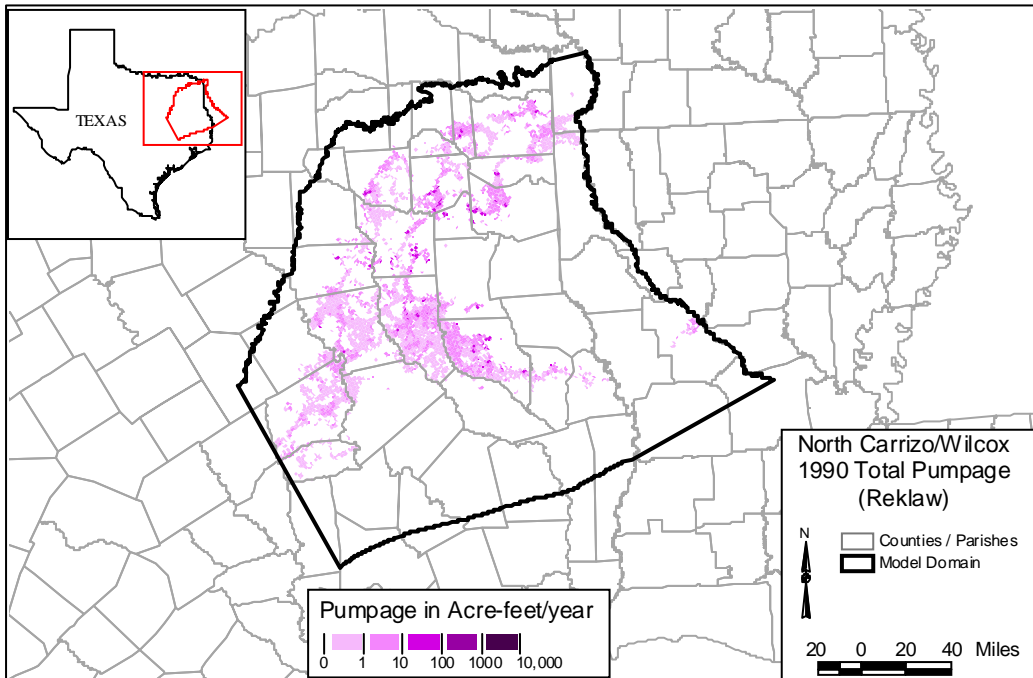


Figure D.2.8 Reklaw (Layer 2) Pumpage, 1990 (AFY)

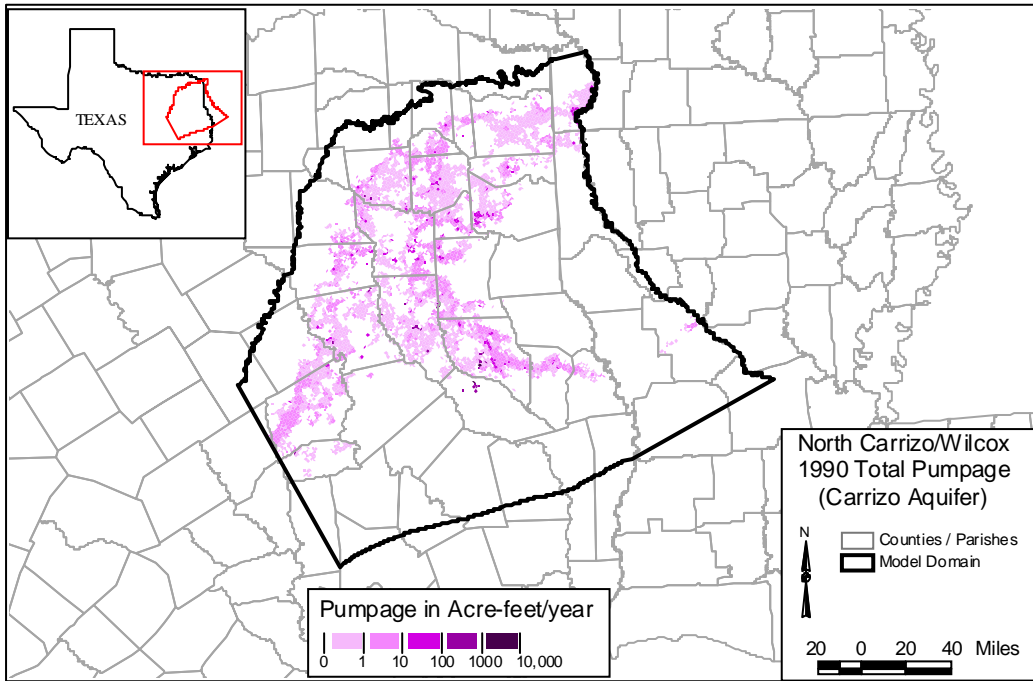


Figure D.2.9 Carrizo (Layer 3) Pumpage, 1990 (AFY)

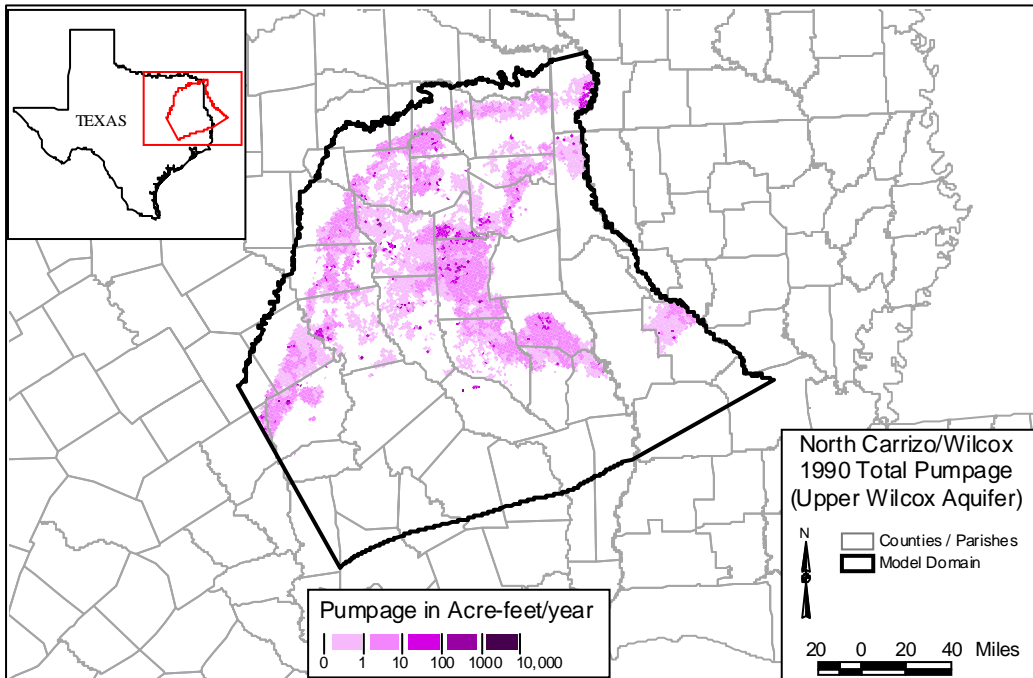


Figure D.2.10 Upper Wilcox (Layer 4) Pumpage, 1990 (AFY)

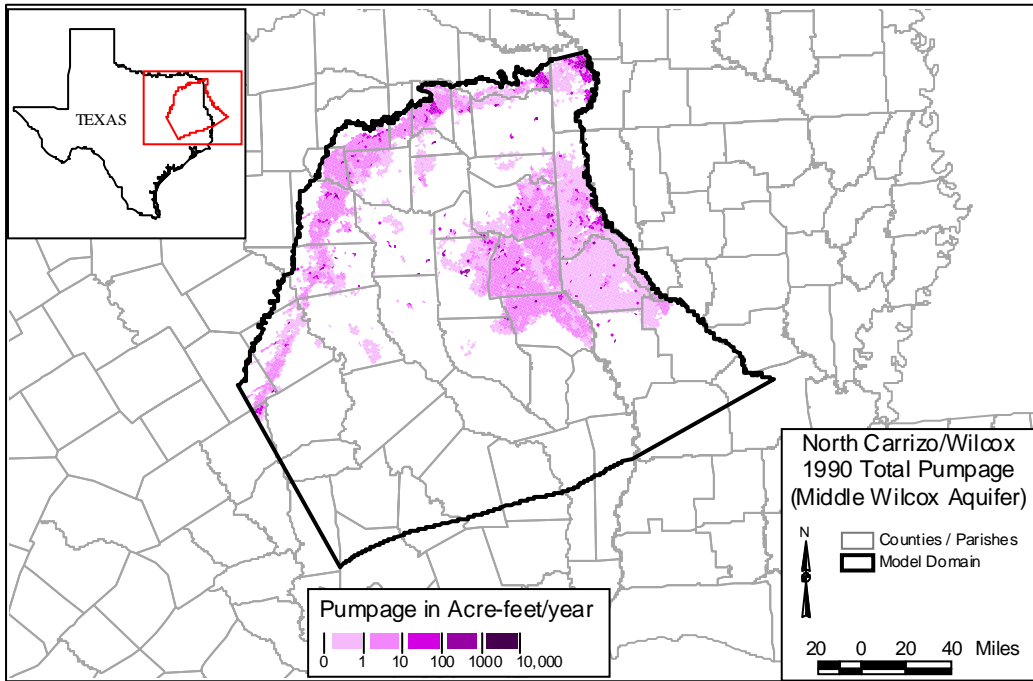


Figure D.2.11 Middle Wilcox (Layer 5) Pumpage, 1990 (AFY)

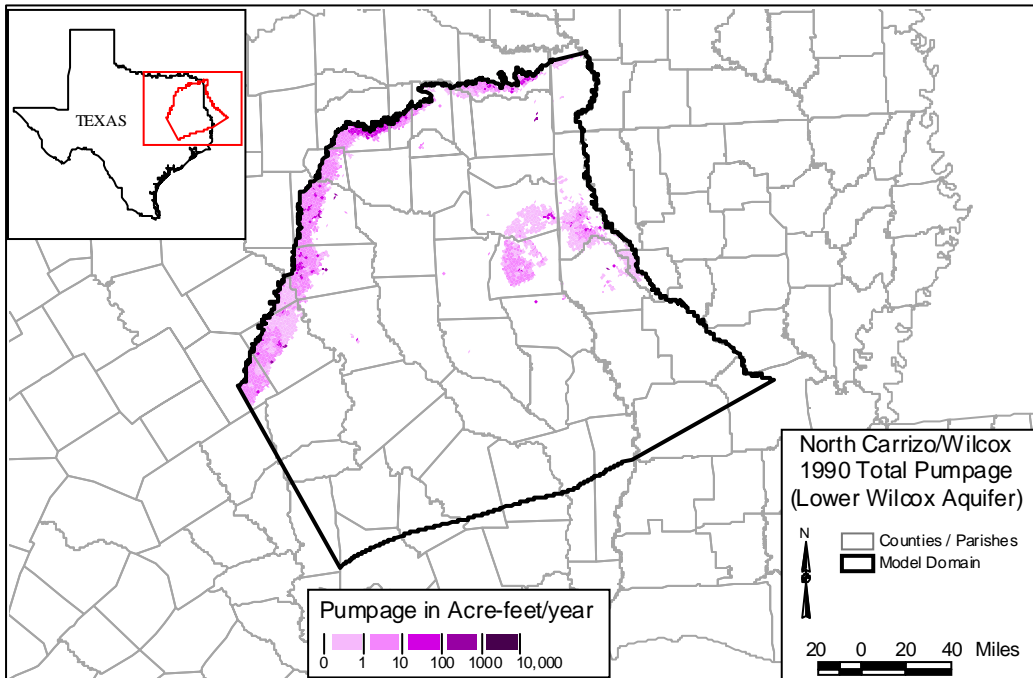


Figure D.2.12 Lower Wilcox (Layer 6) Pumpage, 1990 (AFY)

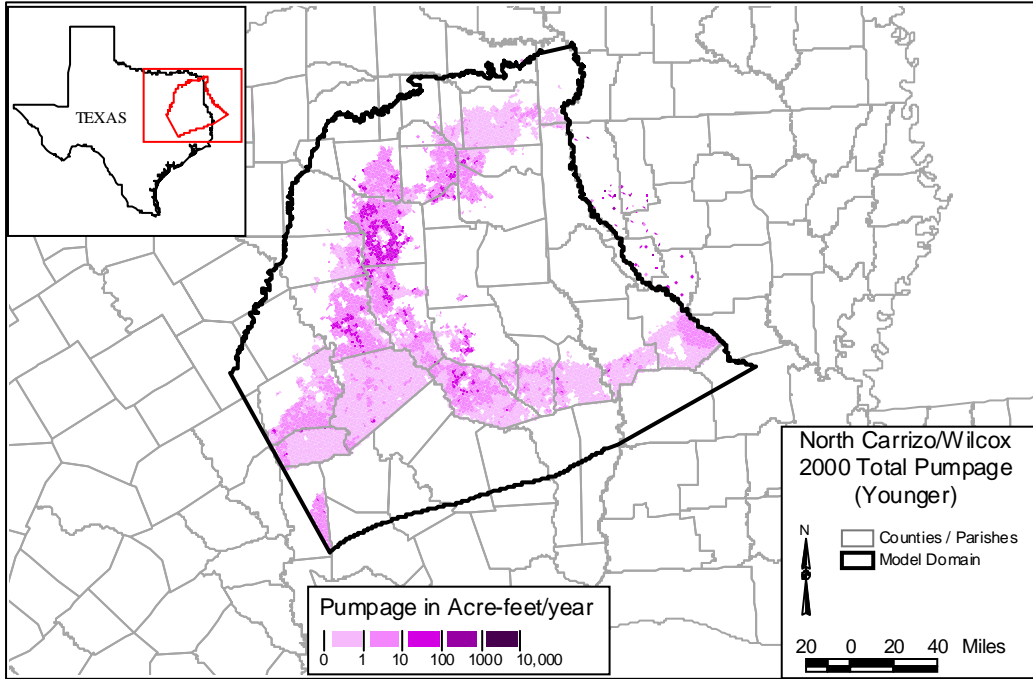


Figure D.2.13 Younger (Layer 1) Pumpage, 2000 (AFY)

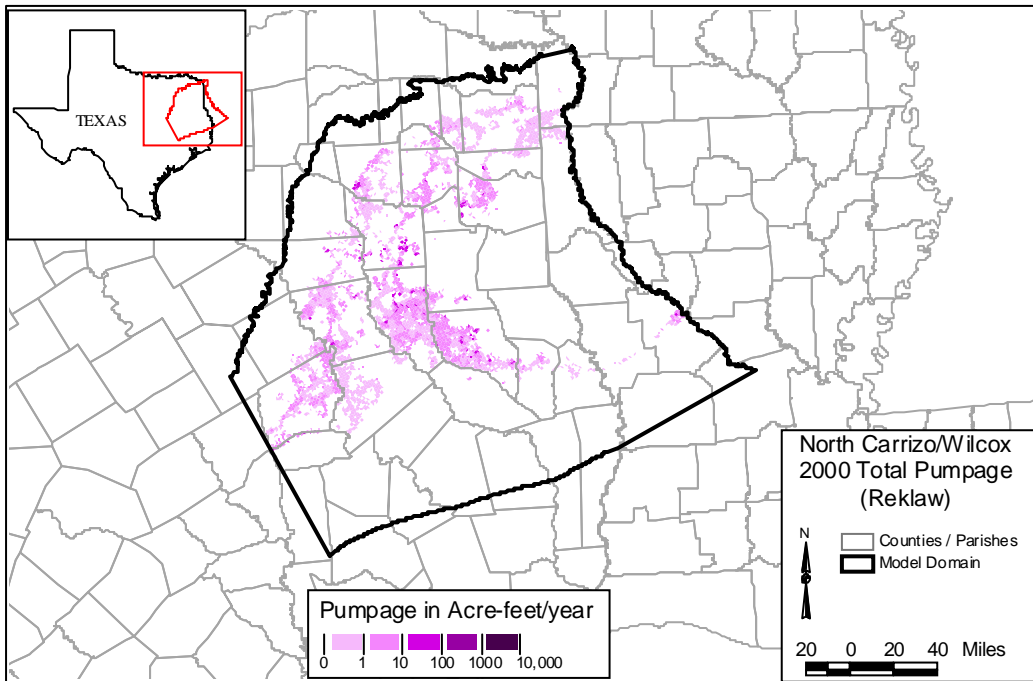


Figure D.2.14 Reklaw (Layer 2) Pumpage, 2000 (AFY)

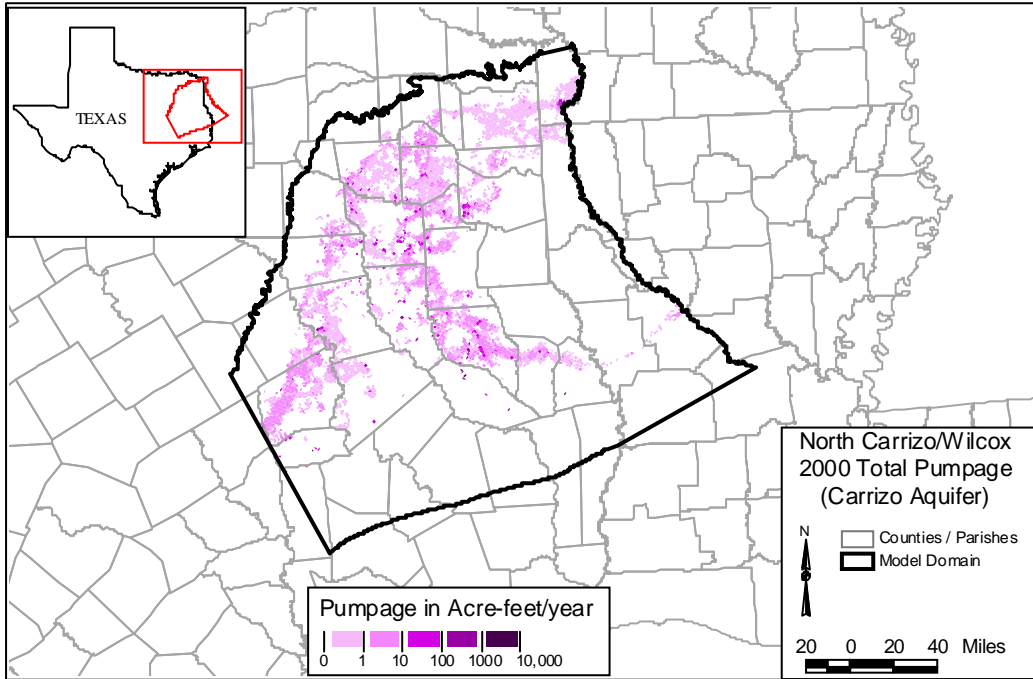


Figure D.2.15 Carrizo (Layer 3) Pumpage, 2000 (AFY)

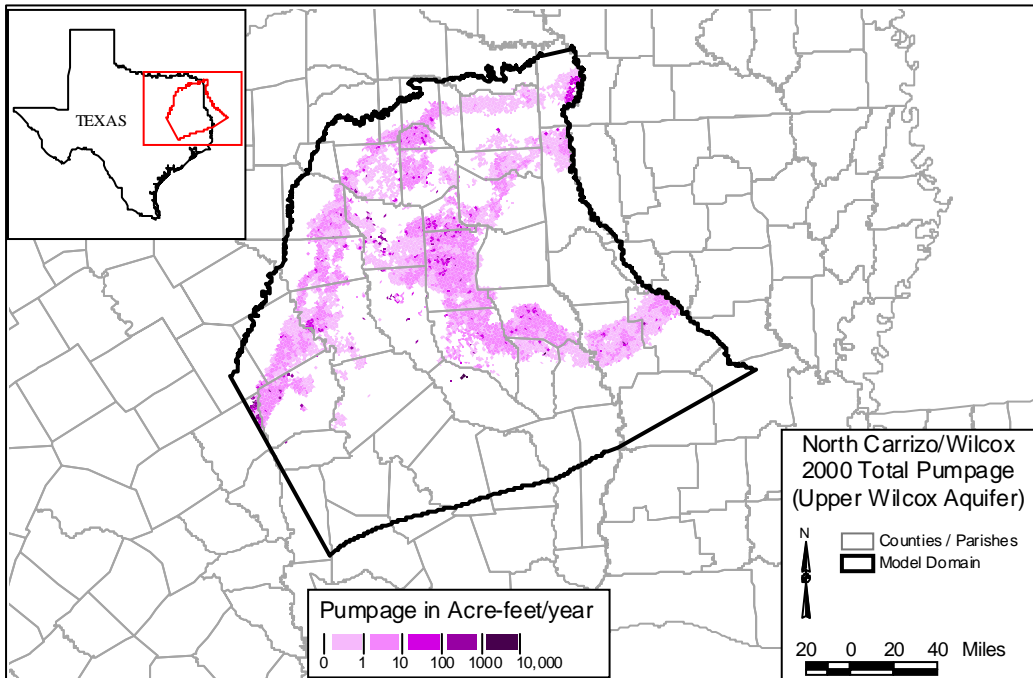


Figure D.2.16 Upper Wilcox (Layer 4) Pumpage, 2000 (AFY)

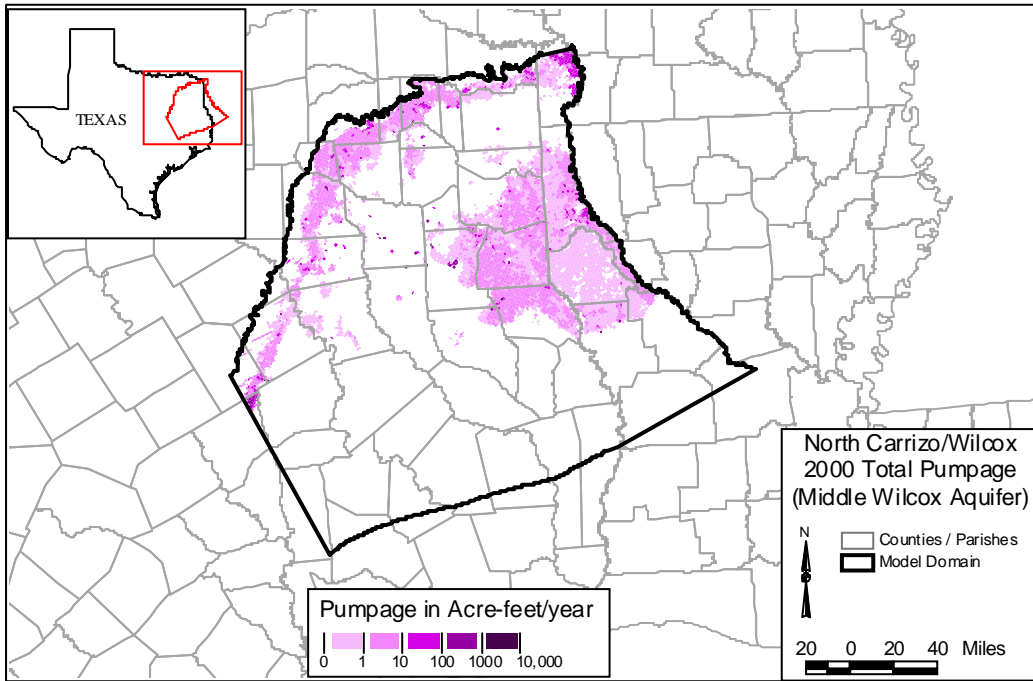


Figure D.2.17 Middle Wilcox (Layer 5) Pumpage, 2000 (AFY)

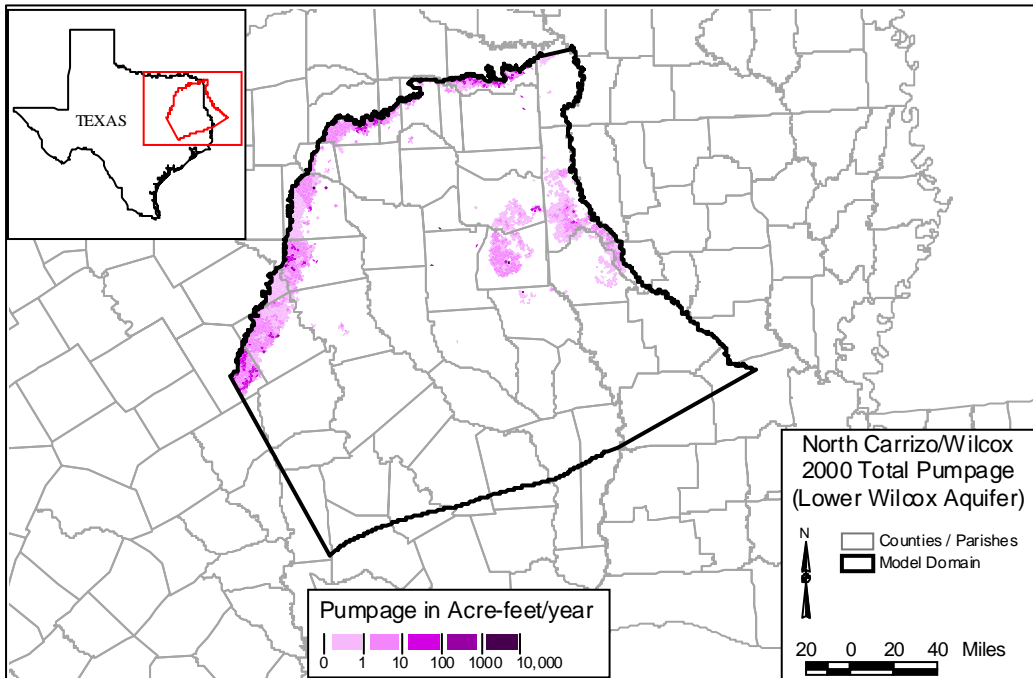


Figure D.2.18 Lower Wilcox (Layer 6) Pumpage, 2000 (AFY)

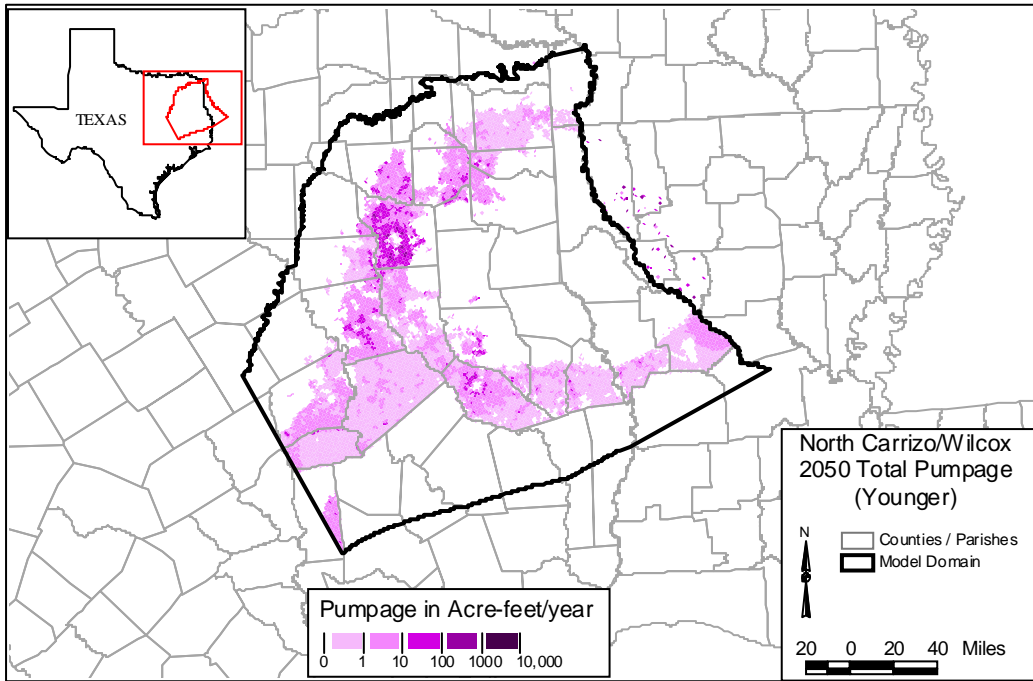


Figure D.2.19 Younger (Layer 1) Pumpage, 2000 (AFY)

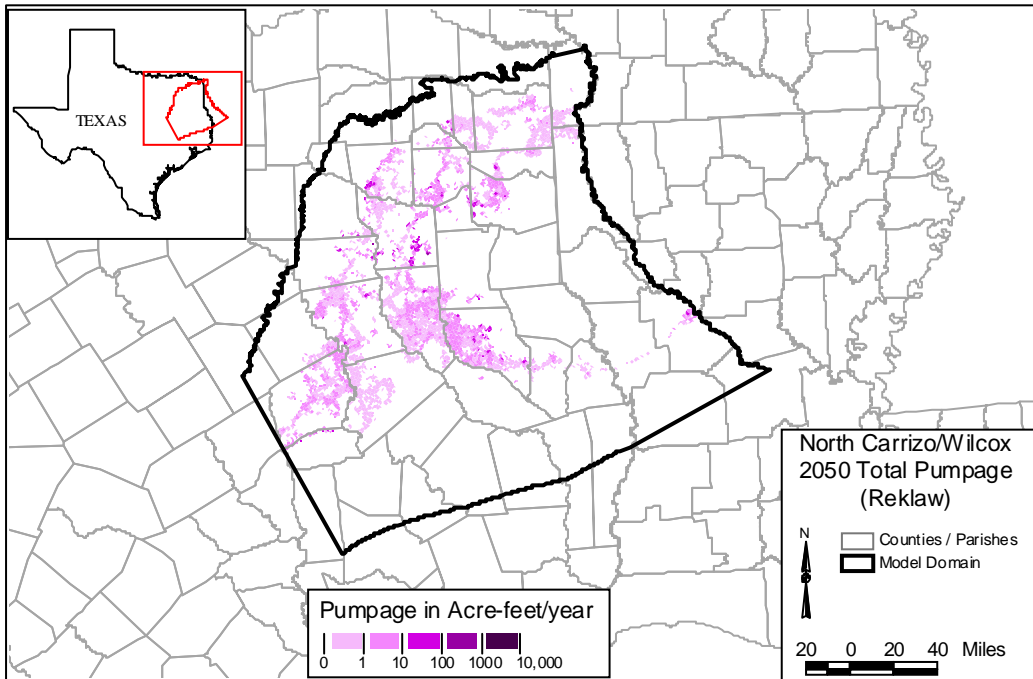


Figure D.2.20 Reklaw (Layer 2) Pumpage, 2050 (AFY)

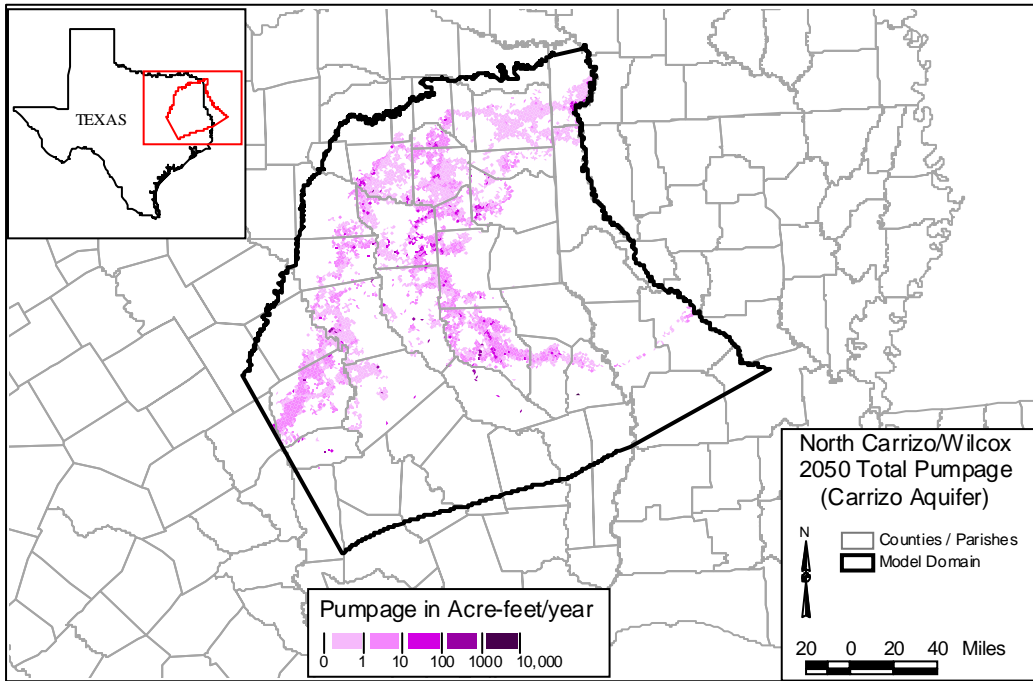


Figure D.2.21 Carrizo (Layer 3) Pumpage, 2050 (AFY)

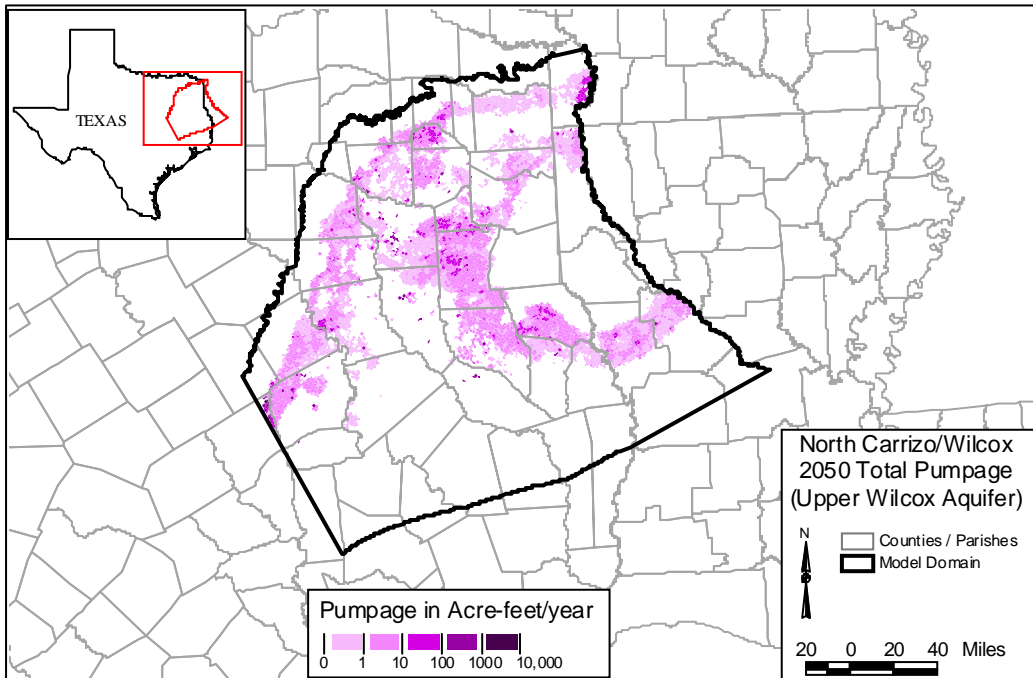


Figure D.2.22 Upper Wilcox (Layer 4) Pumpage, 2050 (AFY)

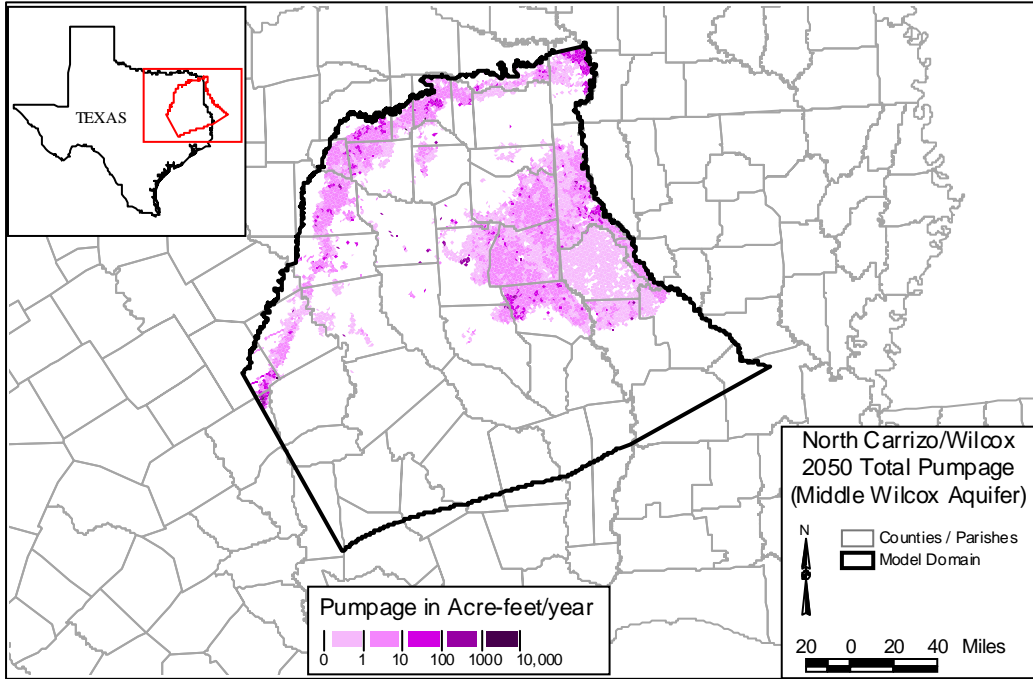


Figure D.2.23 Middle Wilcox (Layer 5) Pumpage, 2050 (AFY)

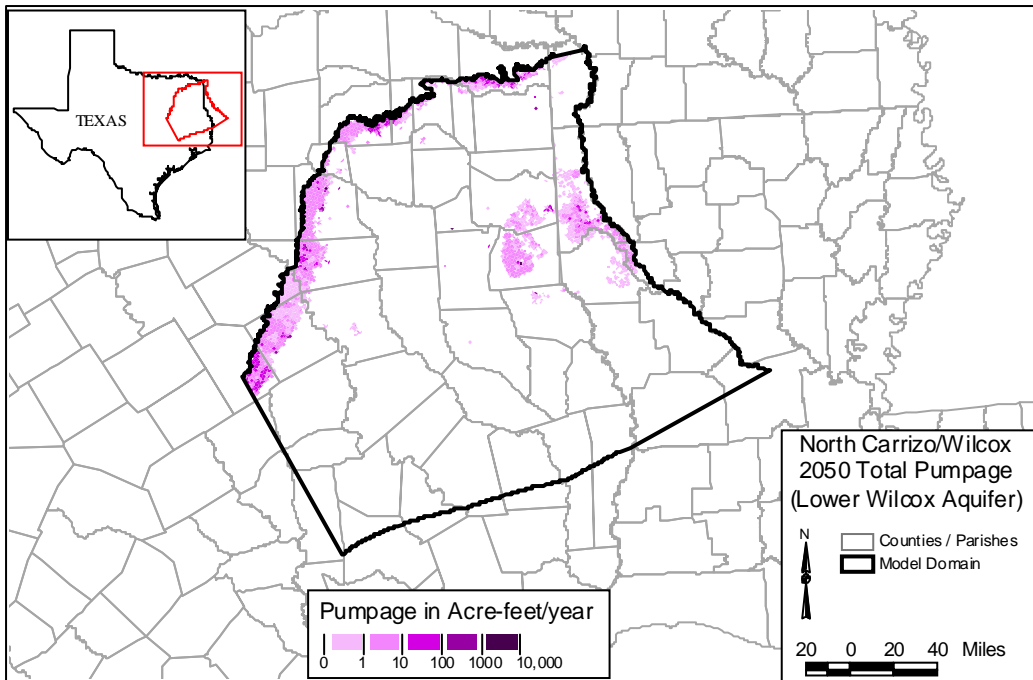
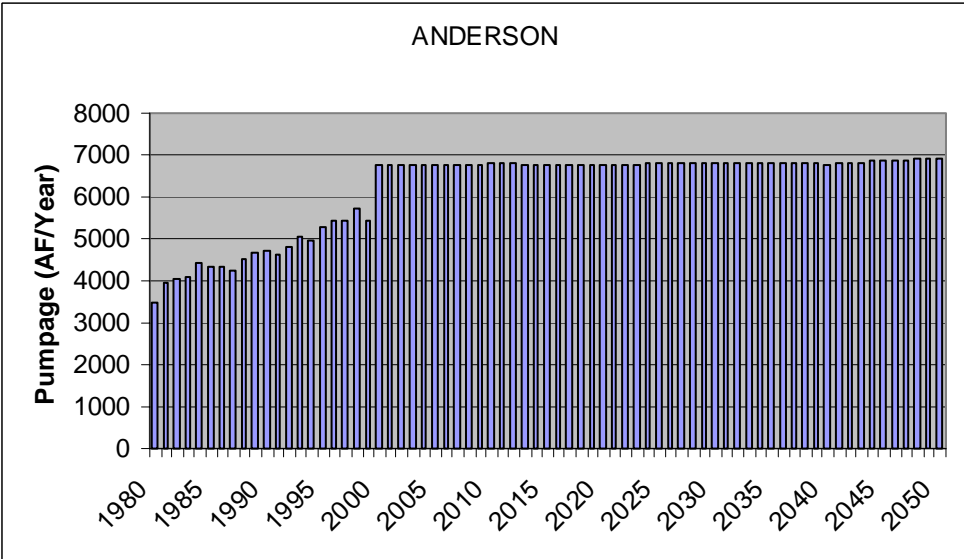
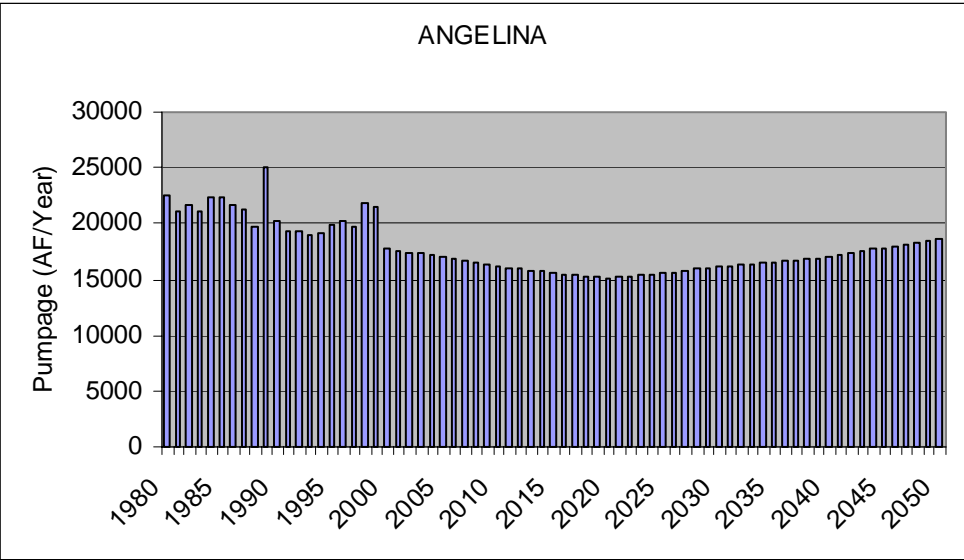
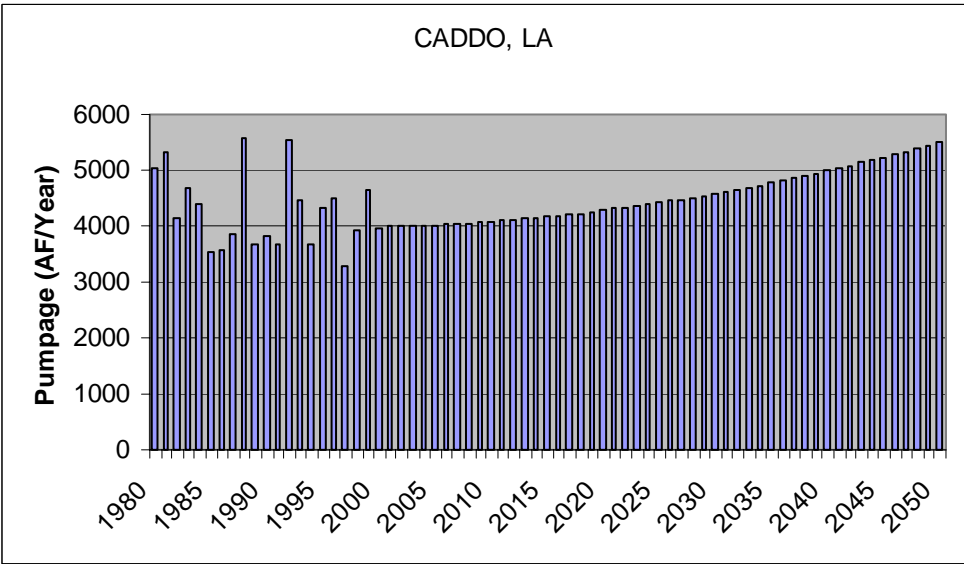
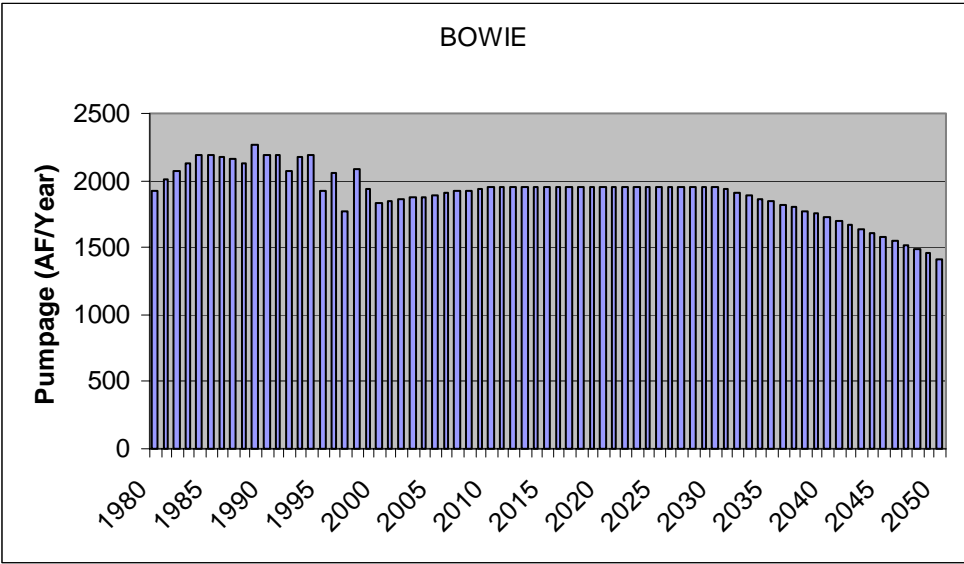


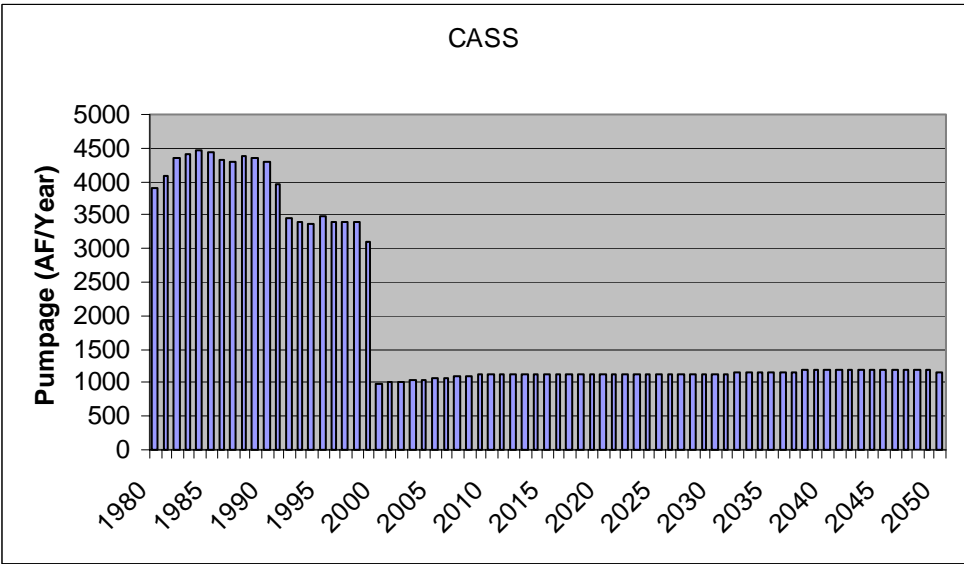
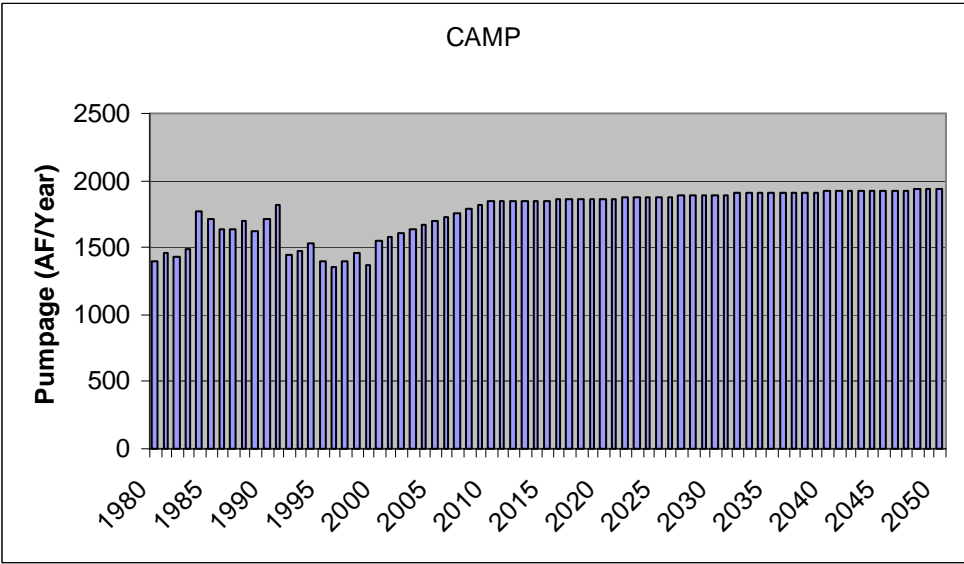
Figure D.2.24 Lower Wilcox (Layer 6) Pumpage, 2050 (AFY)

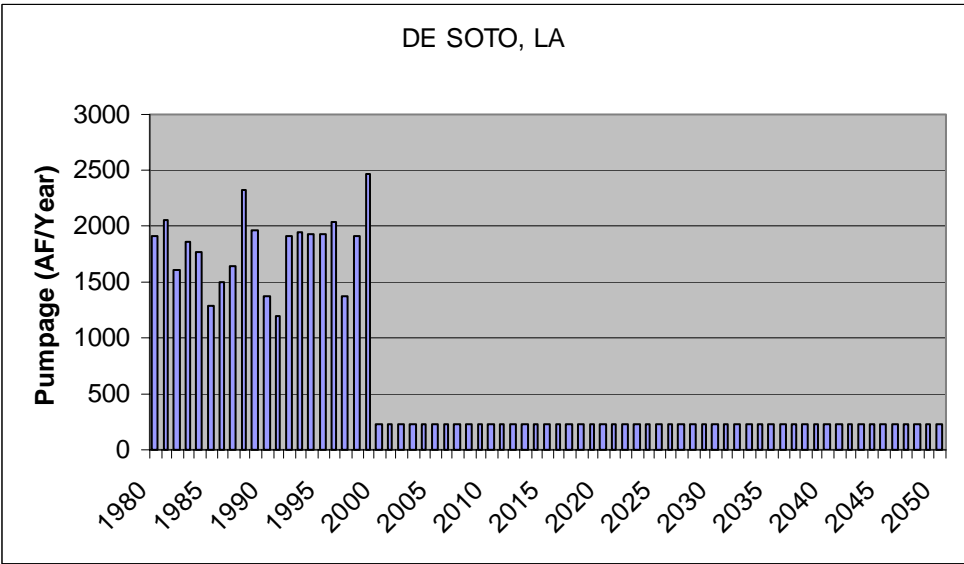
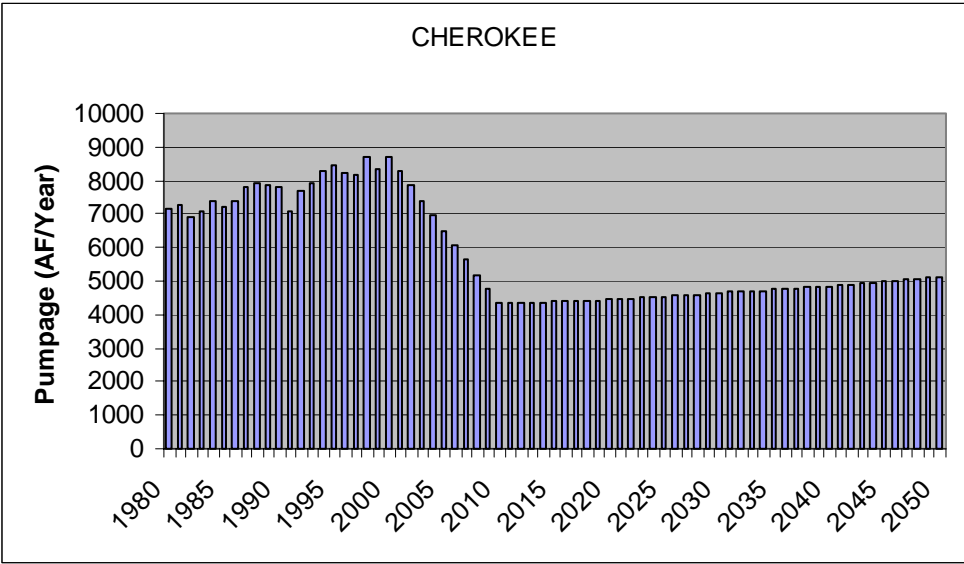
APPENDIX D3

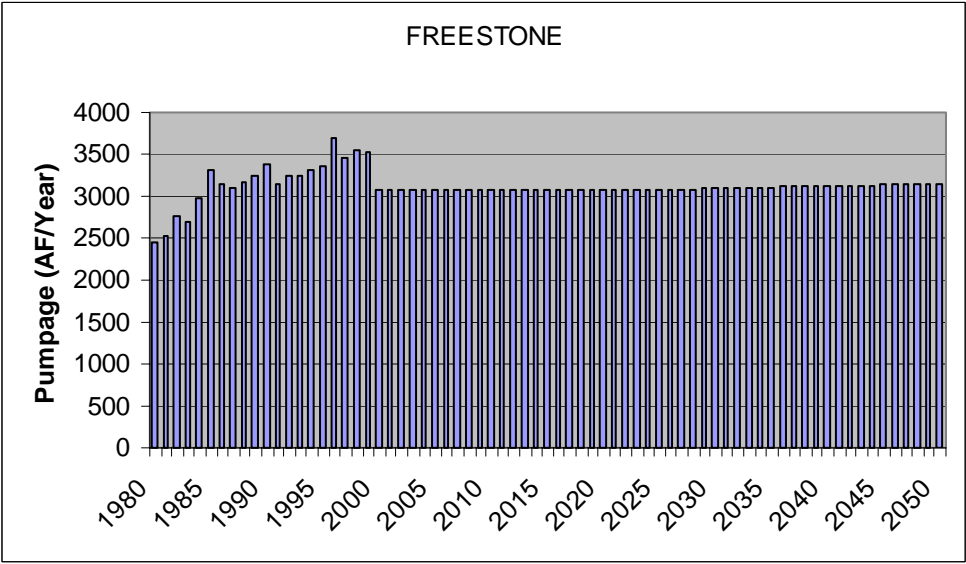
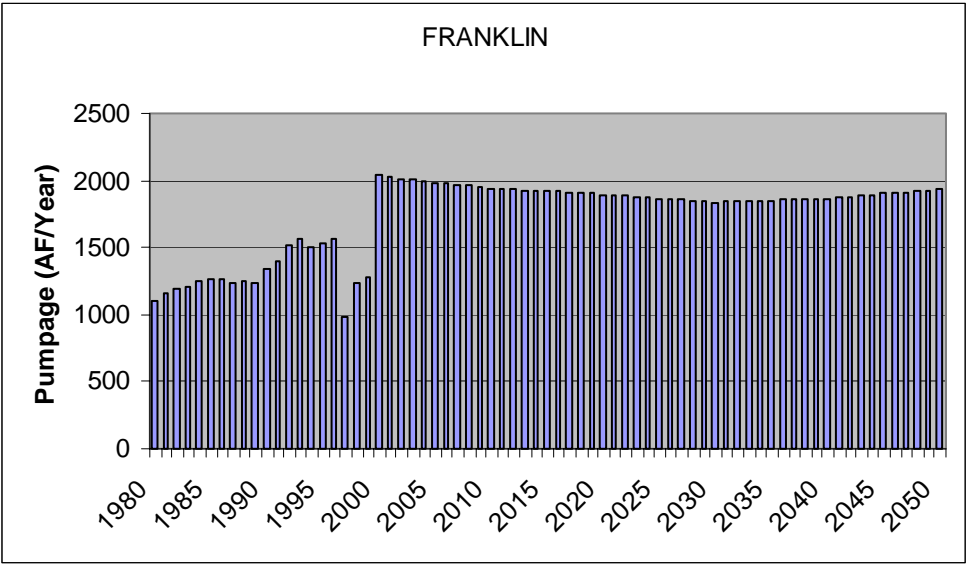
**Carrizo-Wilcox Groundwater
Withdrawal Distributions by County**

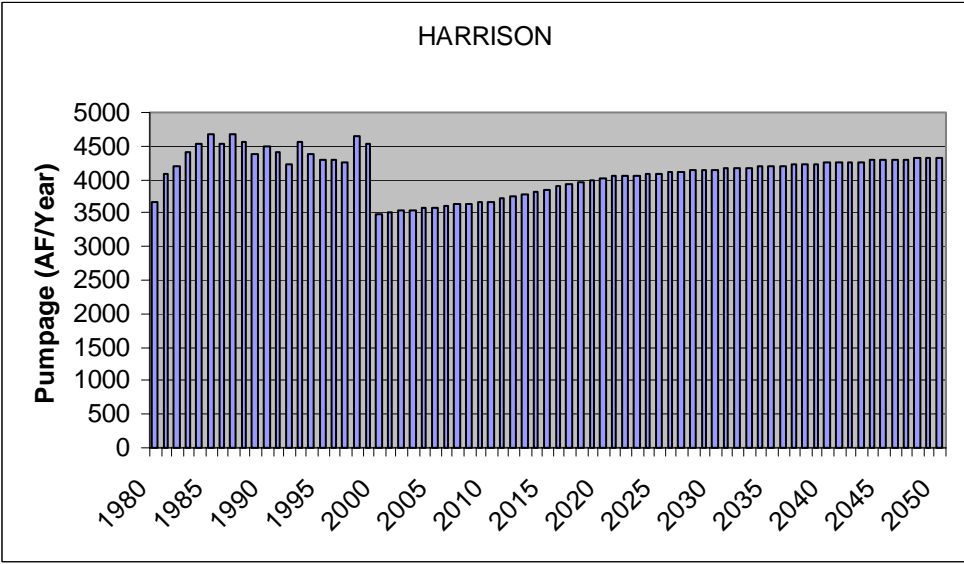
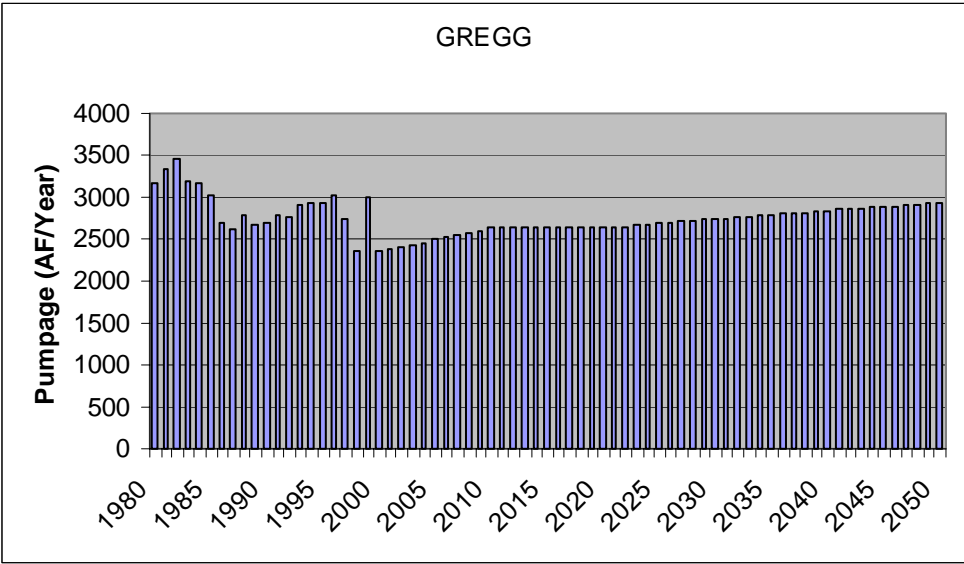


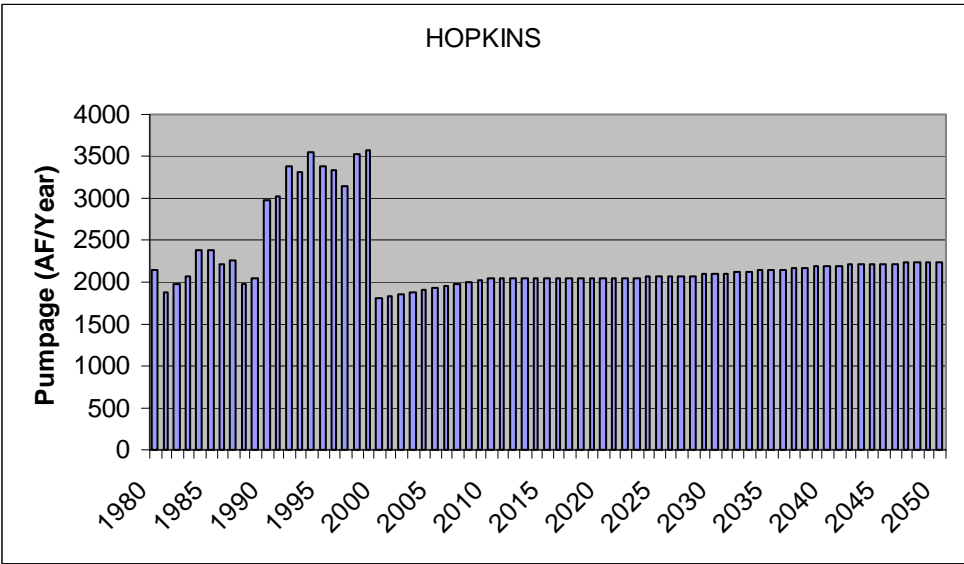
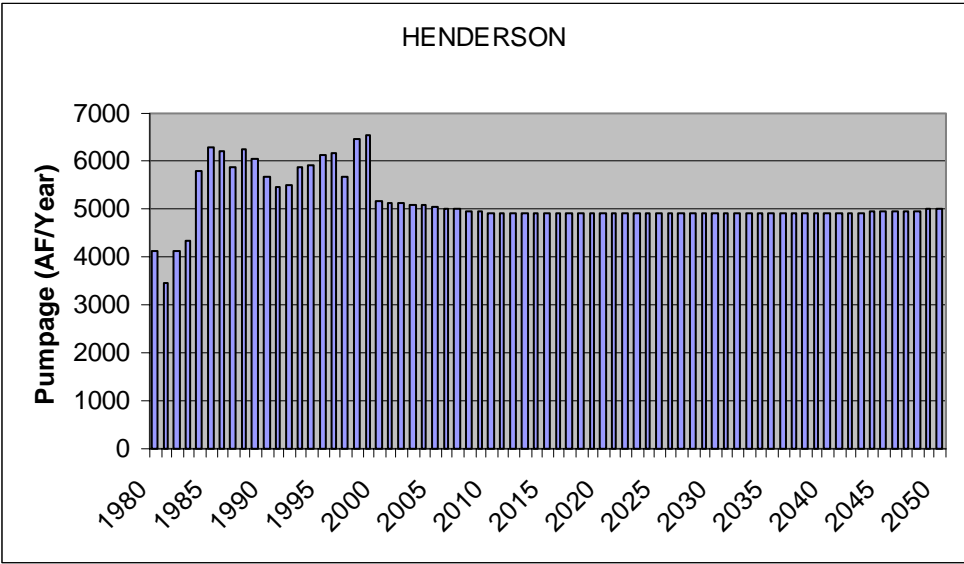


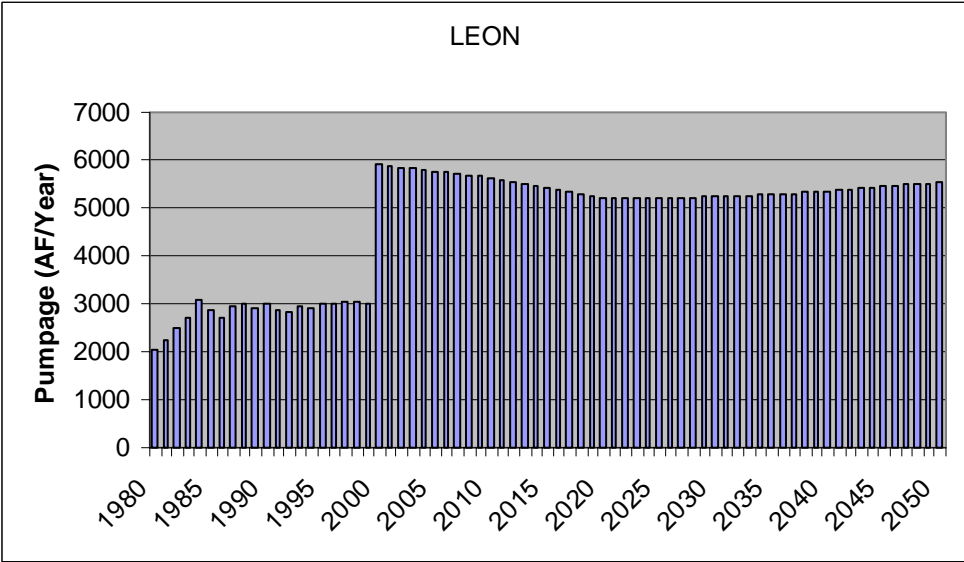
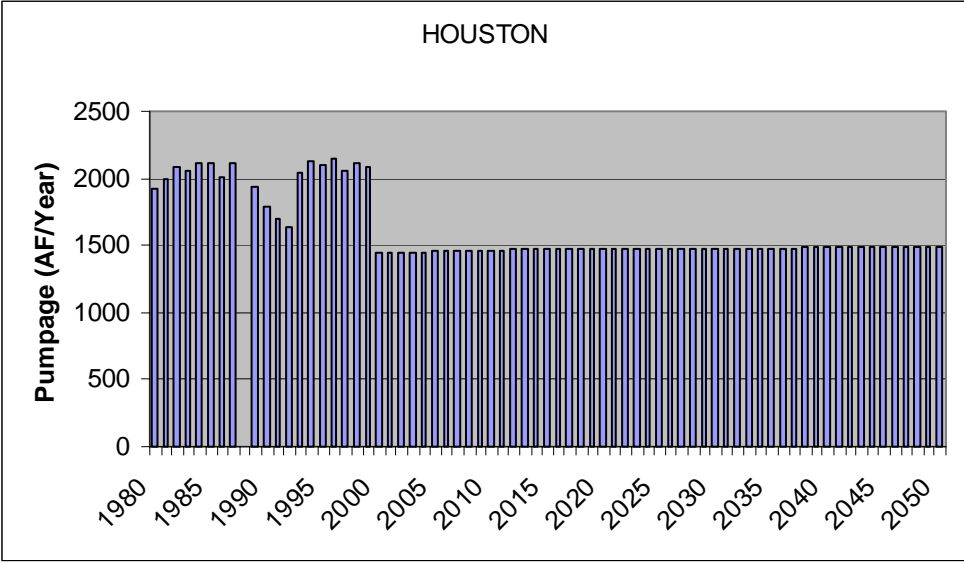


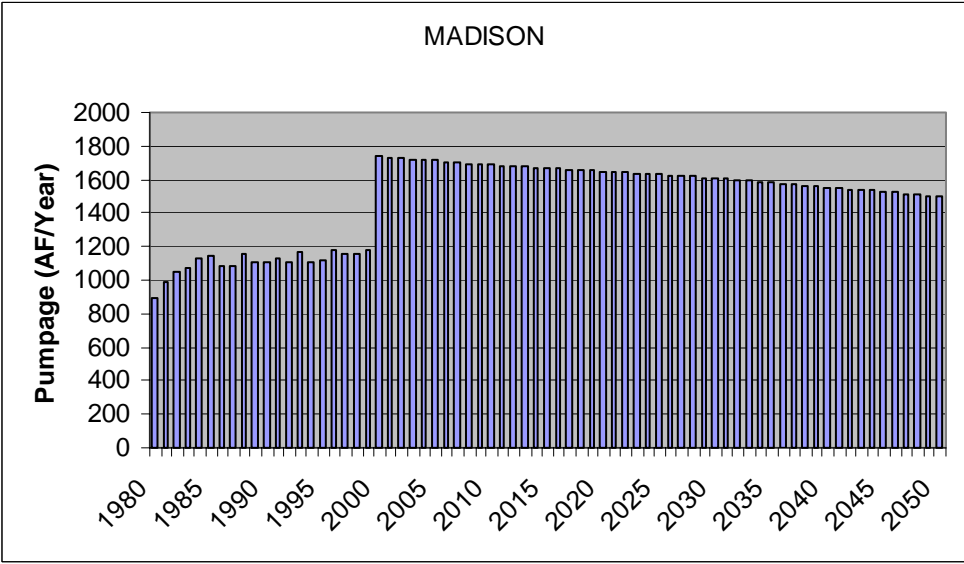
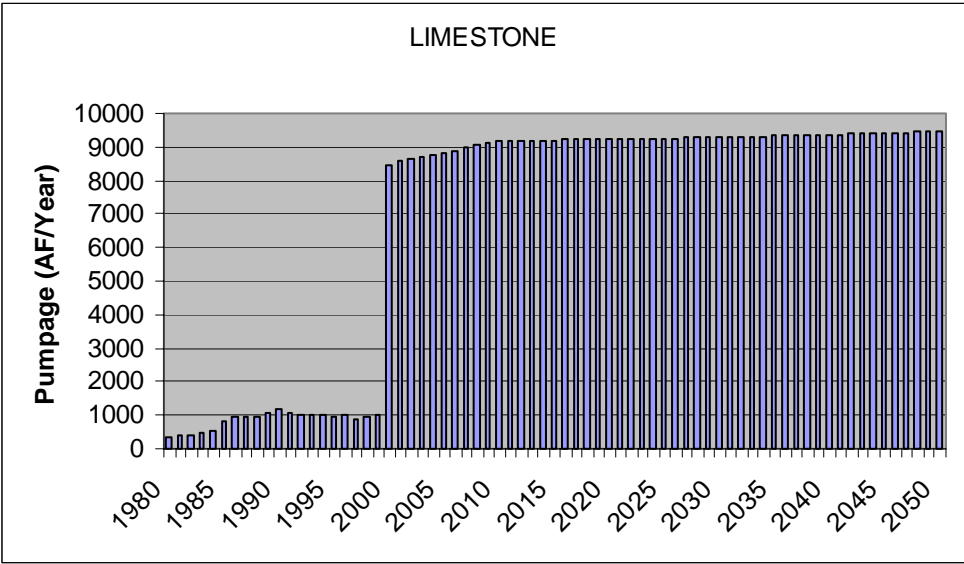


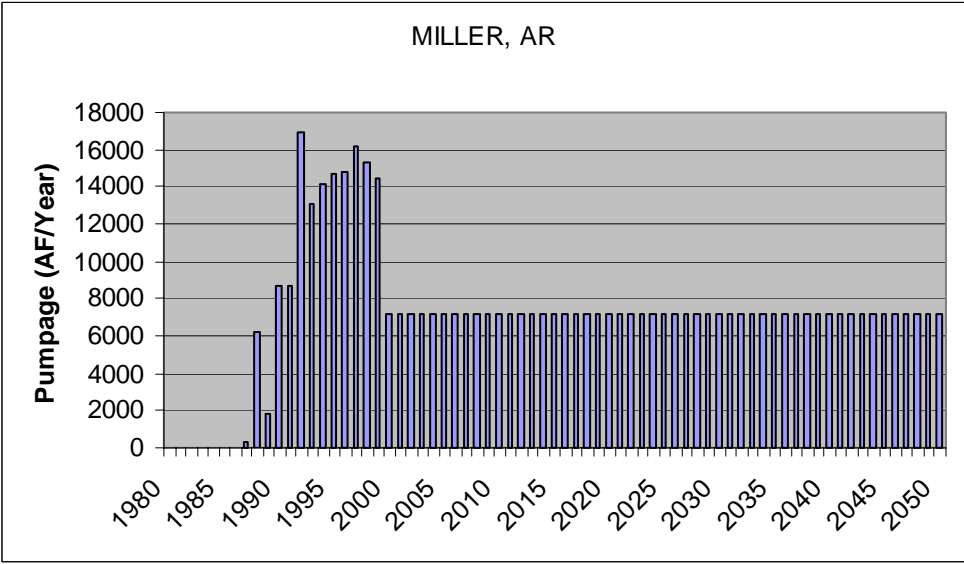
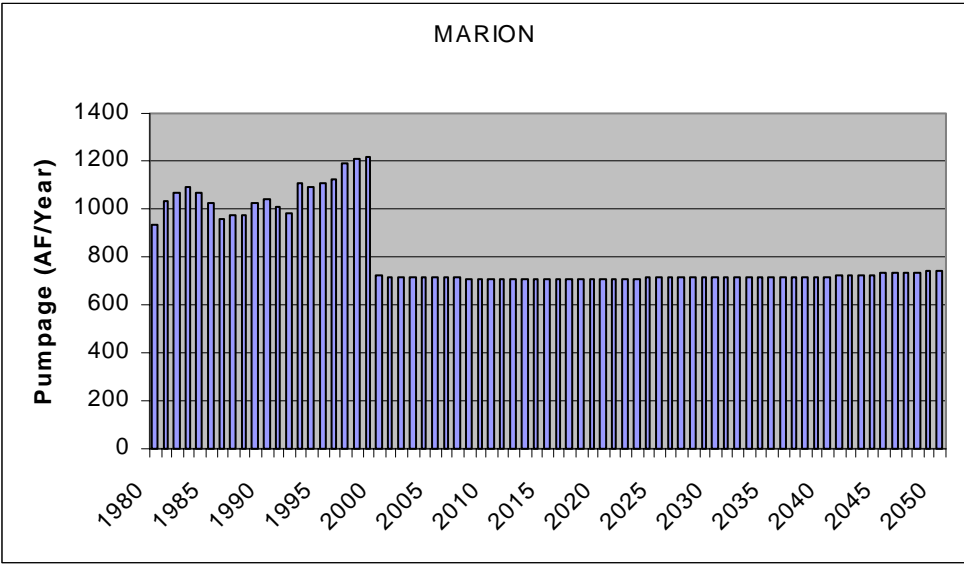


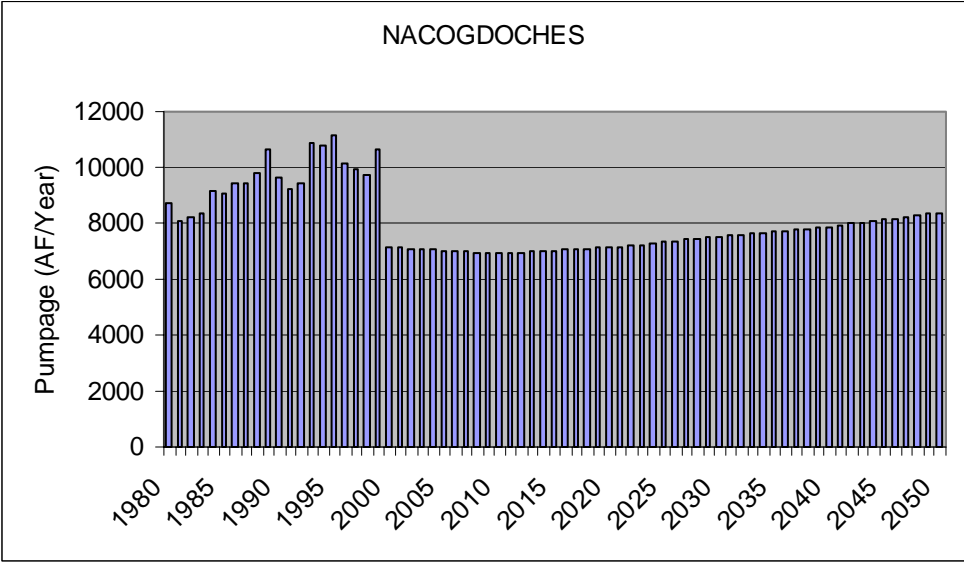
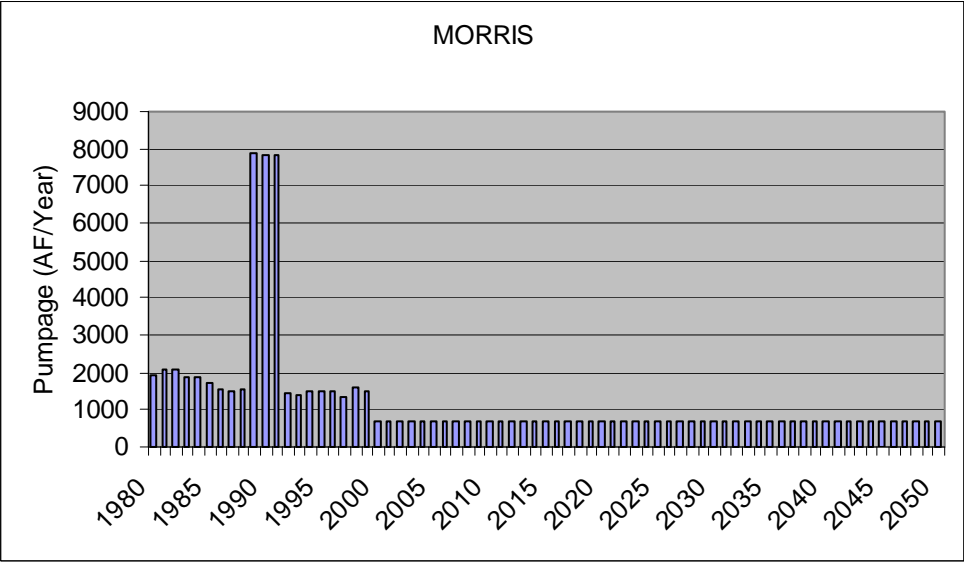


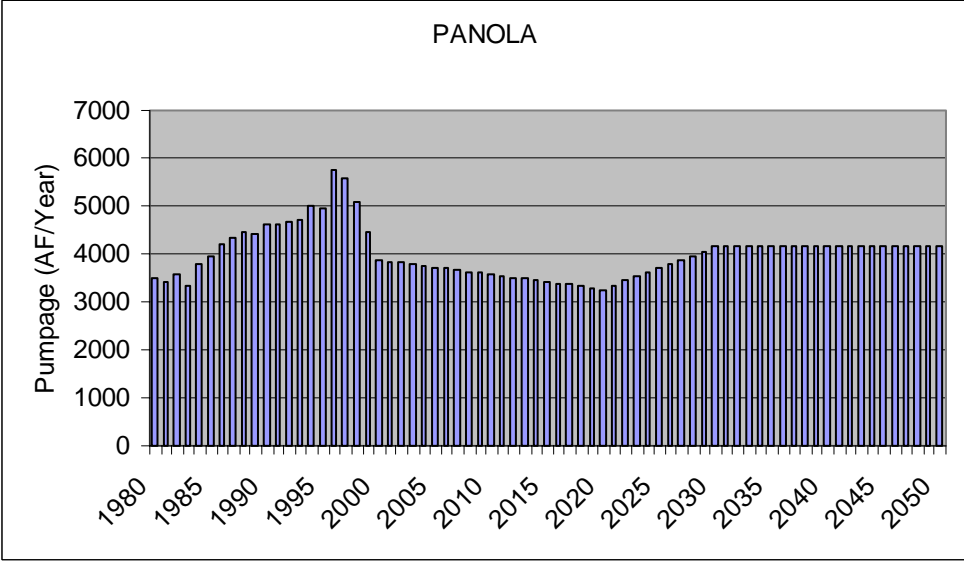
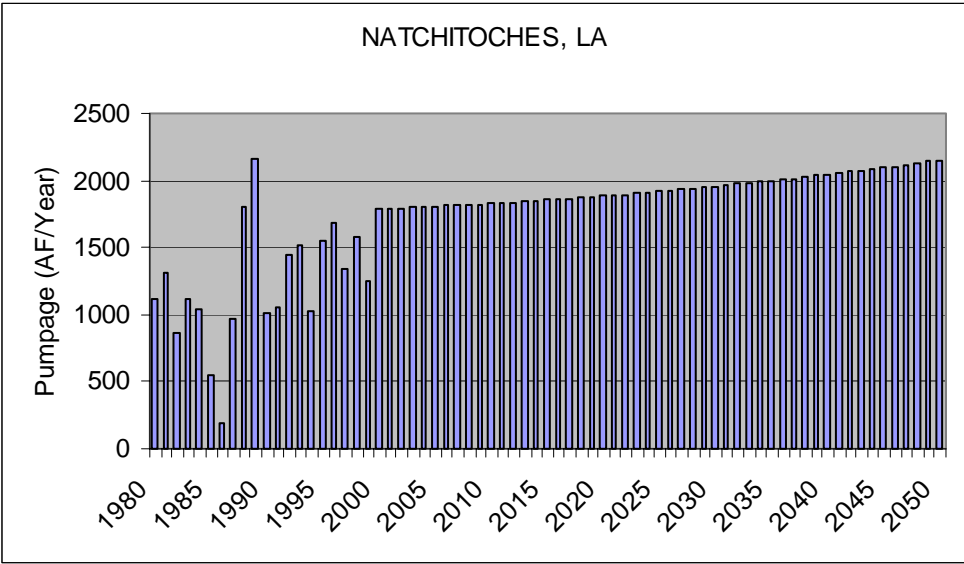


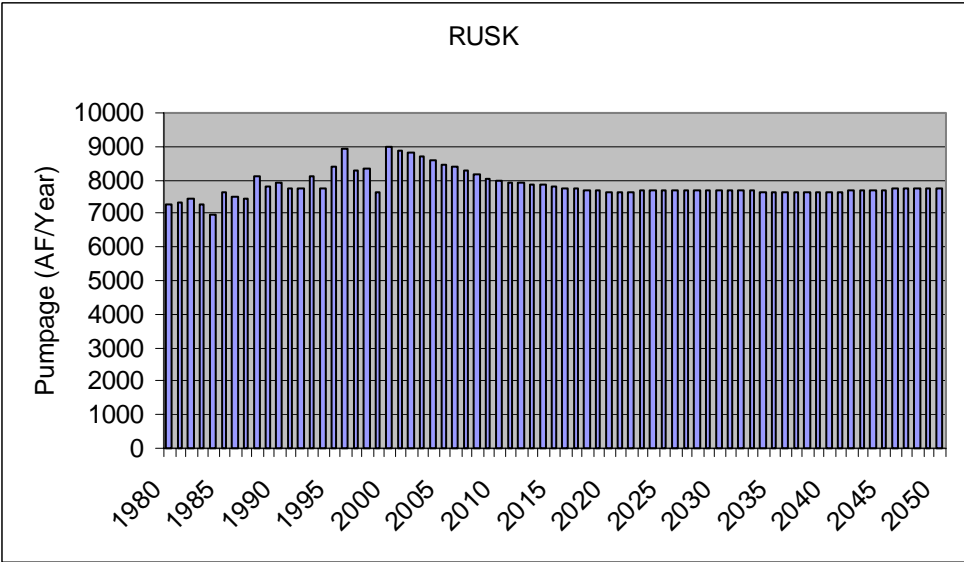
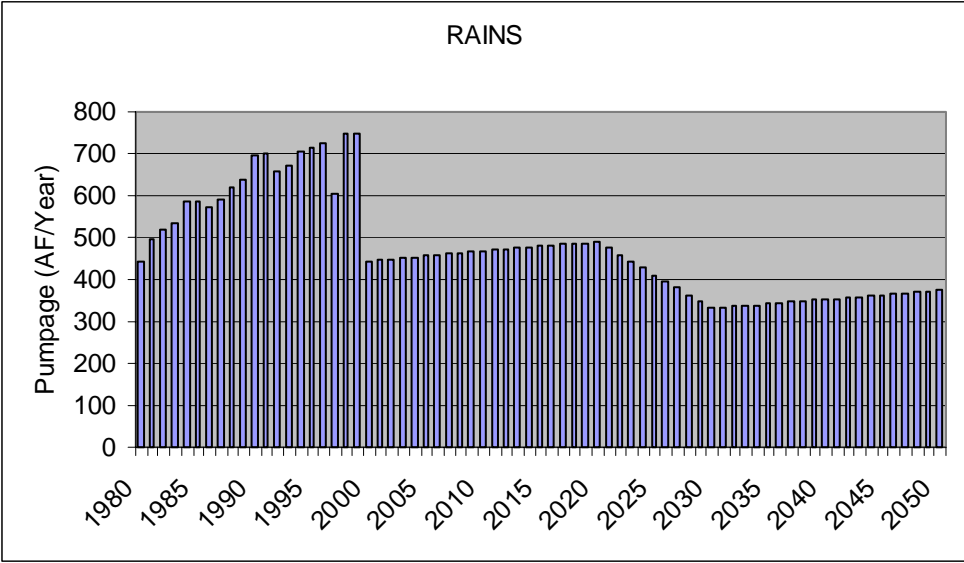


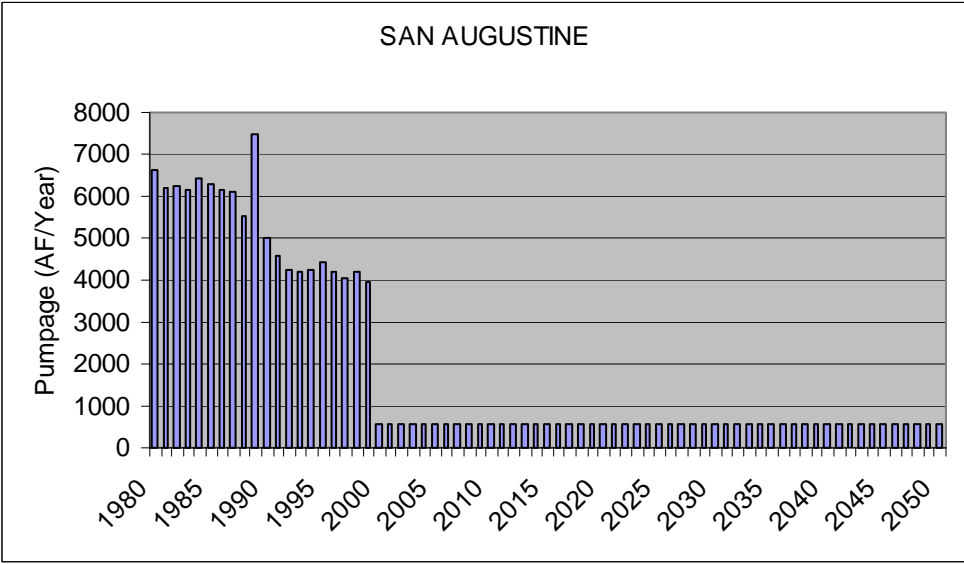
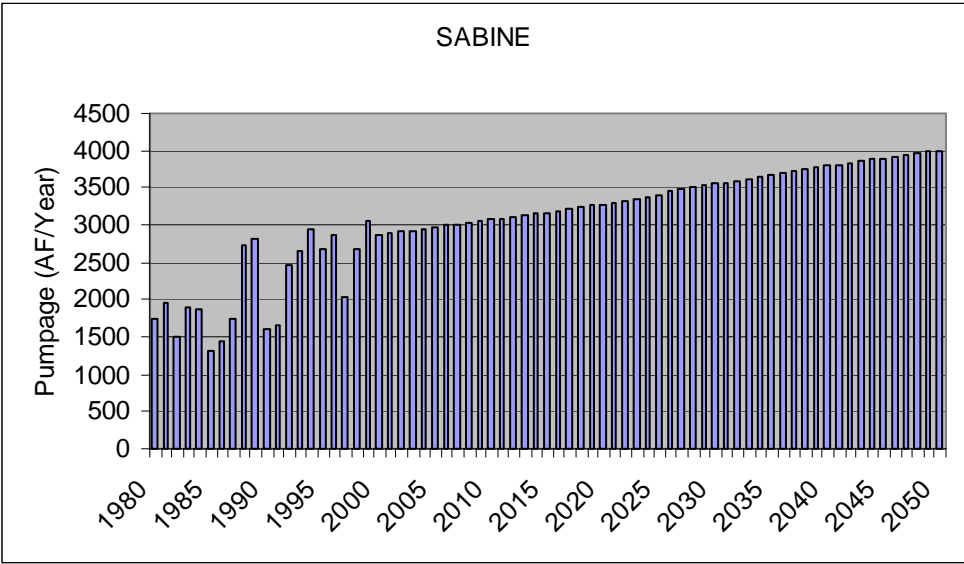


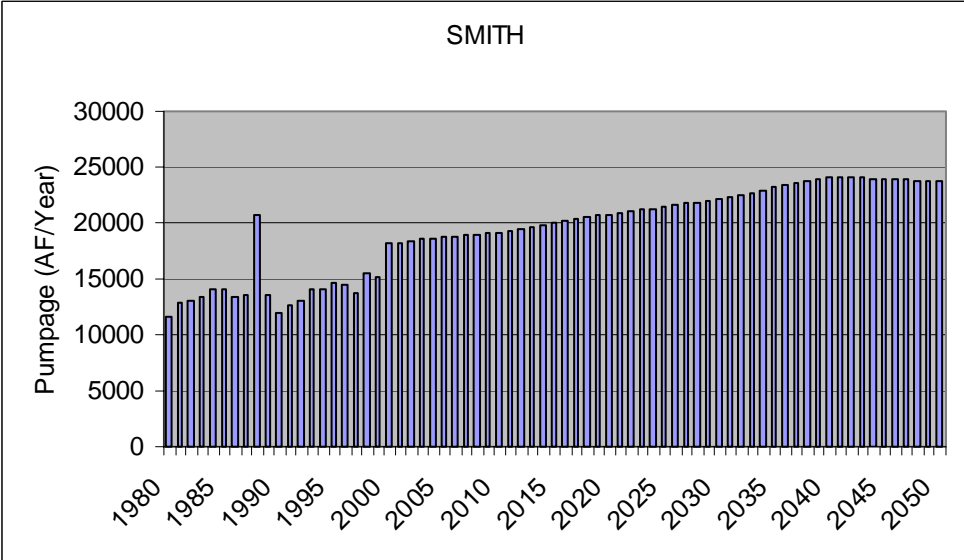
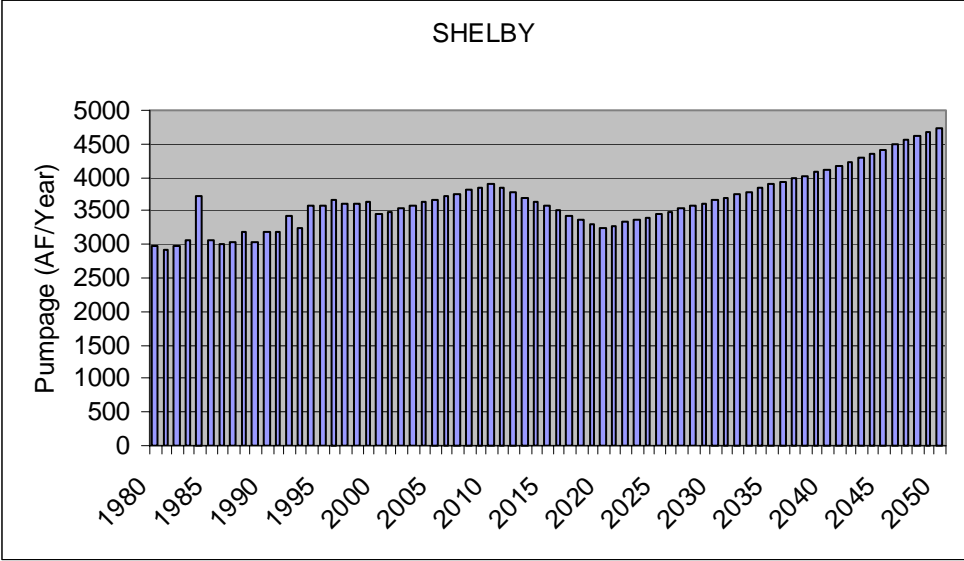


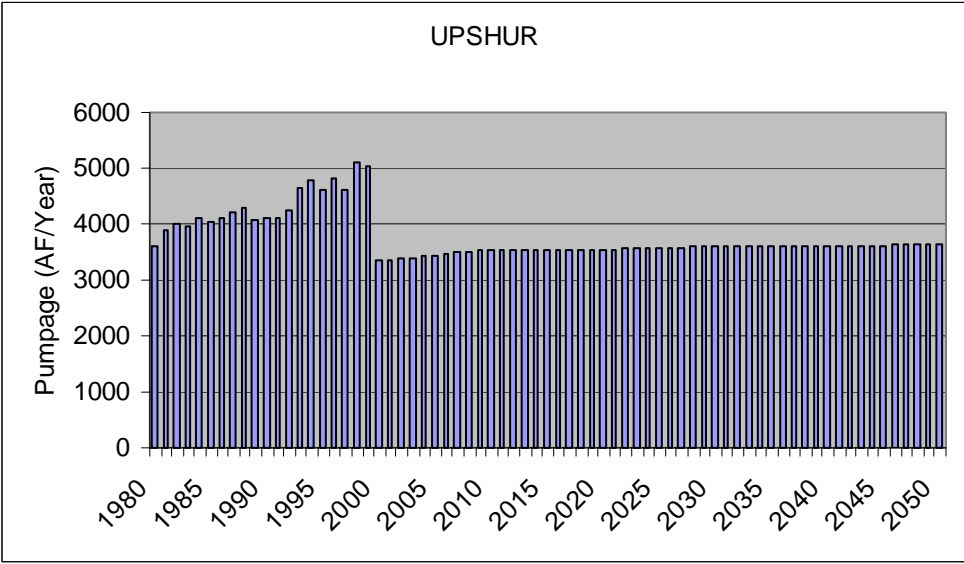
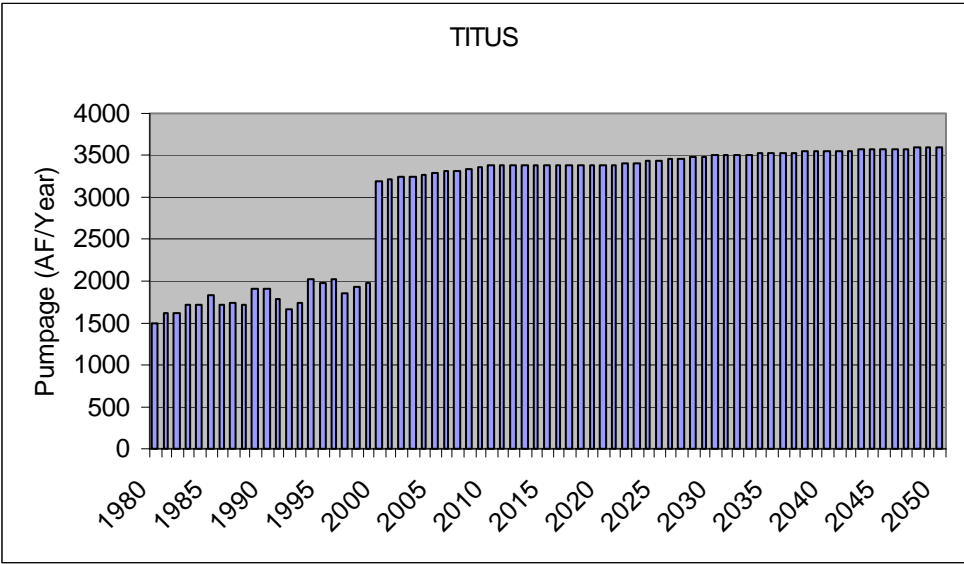


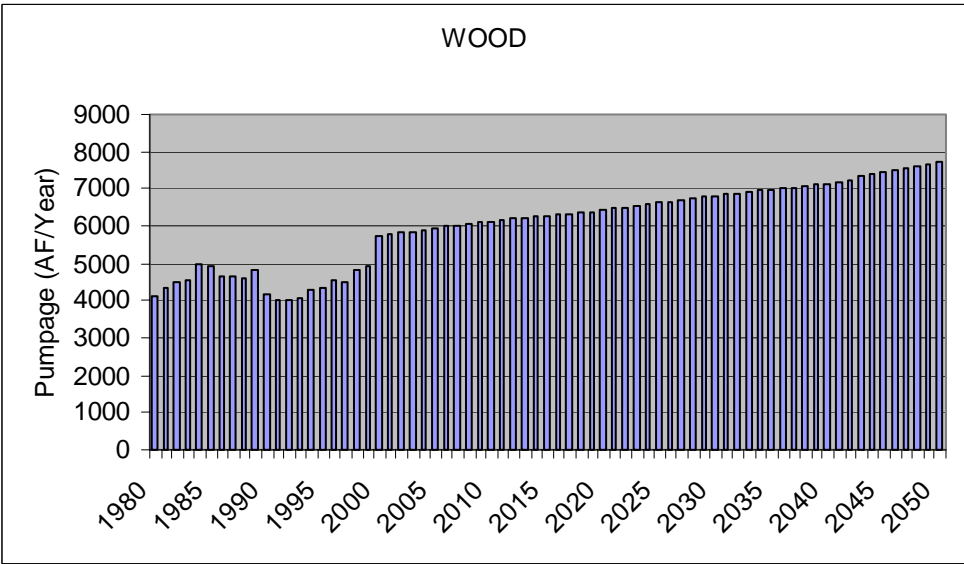
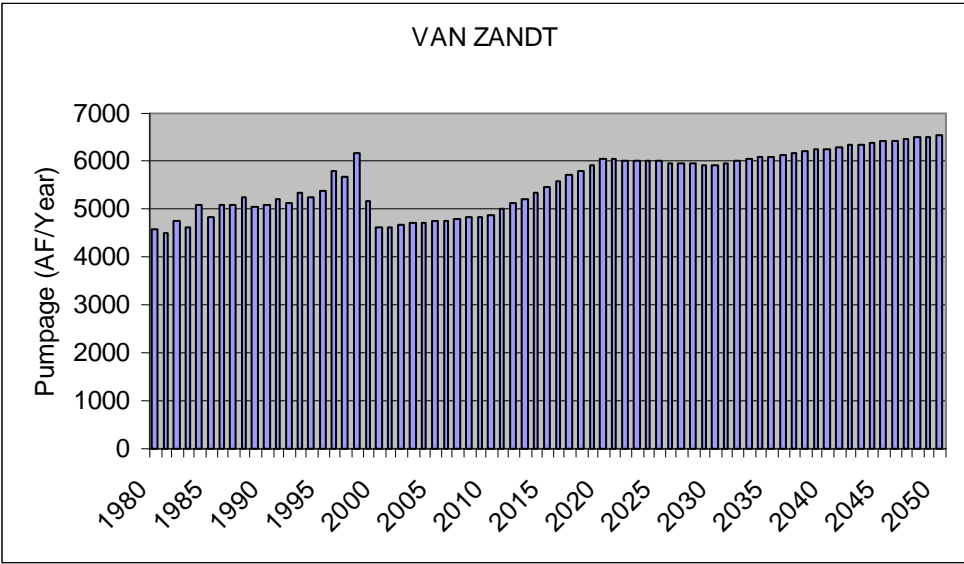












APPENDIX E

Using SWAT with MODFLOW in a Decoupled Environment

Appendix E Using SWAT with MODFLOW in a Decoupled Environment

Background:

Our goal is to use the recharge/evapotranspiration estimates from a SWAT simulation to estimate recharge/evapotranspiration inputs to a MODFLOW simulation. We do not want to do any iteration and are not allowed real-time updating between the two.

The following is a general description of how these physical processes are implemented in the two models.

Recharge/Evapotranspiration in MODFLOW:

In MODFLOW, recharge is input in length/time units. This rate of water is added directly to the uppermost active layer during each stress period. The rate can be varied spatially for each grid block, and temporally for each stress period.

In MODFLOW, evapotranspiration removes water directly from the uppermost saturated layer. When the water table is at or above a specified elevation (called the “ET surface”), water is removed at the specified maximum rate. If the water table is below the ET surface, but above a specified extinction depth, then water is removed at a rate that decreases linearly from a maximum at the ET surface to zero at the extinction depth. Below the extinction depth, no water is removed. Figure E.1 illustrates this approach.

Recharge/Evapotranspiration in SWAT:

In SWAT, basically

$$\text{Change in Soil Water} = \text{Infiltration} - \text{Evapotranspiration} - \text{Recharge}$$

where

$$\text{Infiltration} = \text{Precipitation} - \text{Runoff}$$

A running soil water balance is calculated during the simulation. Precipitation is separated into infiltration and runoff using the SCS Curve Number method. Evapotranspiration requires more complex calculations. The following is a summary of how evapotranspiration is calculated in SWAT (skipping some of the minor details):

First, a potential (or more correctly, “reference”) evapotranspiration (Figure E.2), $E_{t,0}$, is calculated, typically using some flavor of the Penman approach. This reference evapotranspiration is that which would occur for some reference grass with no soil water

limitation. Three separate steps are required to estimate an actual evapotranspiration (Figure E.3) from this potential evapotranspiration.

Step 1: Account for vegetative differences -- since not all vegetation is reference grass, differences in growing cycles, size, and water use are accounted for by correlating the maximum daily transpiration with the leaf area index (LAI) of the plant, i.e.

$$E_{t,max} = \frac{(LAI)(E_{t,0})}{3.0} \quad 0 < LAI < 3.0$$

$$E_{t,max} = E_{t,0} \quad LAI > 3.0$$

The LAI changes with plant type, growth cycle, growing conditions, etc.

Step 2: Account for decreasing potential with increasing root zone depth -- root density is assumed to be greatest near the soil surface, and decreases with depth. With default SWAT parameters, about 50% of the water uptake occurs in the top 6% of the root zone.

Step 3: Account for soil water limitation -- plants cannot remove water from the soil if the soil water content is at the plant wilting point. So the $E_{t,max}$ that is calculated in Step 1 has to be limited by soil water.

Without writing down all of the equations, we just note that

$$E_{t,actual} = f(E_{t,max}, depth, soil\ moisture)$$

Note that this explanation applies to the unsaturated zone only. SWAT does allow for calculation of groundwater transpiration (called “revap” in SWAT). However, SWAT has a very crude implementation of groundwater modeling, so the relative height of the water table is unlikely to be consistent. Therefore, we do not calculate groundwater evapotranspiration in SWAT.

The Approach

So if we apply the recharge from SWAT directly MODFLOW, we neglect groundwater transpiration. The greatest error will occur when SWAT is predicting dry soil conditions and MODFLOW is predicting a near-surface water table (i.e. within the root zone). When these conditions occur, SWAT will underpredict actual ET.

What we will do to rectify this is to apply the “unused” ET (that is, the difference between maximum ET and actual ET) as ET in MODFLOW. In MODFLOW, we set

$$\text{Recharge} = \text{Recharge from SWAT}$$

$$ET = (E_{t,max} - E_{t,actual}) \text{ from SWAT}$$

The four main scenarios are discussed below:

Scenario 1: Infiltration > Evapotranspiration, water table below extinction depth

This scenario should be fine, with no MODFLOW ET (since the water table is below the extinction depth), but with recharge being estimated by SWAT. The SWAT estimate does not include groundwater ET of course, but with the water table below the extinction depth, there should be no groundwater ET.

Scenario 2: Infiltration > Evapotranspiration, water table above extinction depth

In this scenario, MODFLOW starts to draw water from the water table based on the difference between the maximum transpiration and the actual transpiration estimated by SWAT. However, the MODFLOW ET shouldn't have much impact in this case because with infiltration occurring, soil moisture should be high, $E_{t,actual}$ will be similar to $E_{t,max}$ and the difference will be near zero.

Scenario 3: Infiltration < Evapotranspiration, water table below extinction depth

In this scenario, there will be no recharge, and MODFLOW will have shut down ET.

Scenario 4: Infiltration < Evapotranspiration, water table above extinction depth

In this scenario, SWAT will have set recharge to zero, and will not remove water from the soil profile below the wilting point. SWAT will not account for the fact that the groundwater evapotranspiration should be occurring. However, the ET in MODFLOW will be pulling water off of the water table at a rate near $E_{t,max}$ (since $E_{t,actual}$ will be small due to low soil moisture) which is a good estimate for this situation.

Figure E.4 shows an example of preliminary SWAT results from a deciduous forest area for the year 1975 in the northern model region. Note that actual evapotranspiration is primarily due to soil evaporation in the winter months. In the spring and summer, transpiration begins to dominate the ET, and when soil water is high, actual transpiration is similar to maximum potential transpiration. Note that in late summer, the precipitation is inconsistent and soil water is decreasing, so the difference between maximum and actual transpiration is significant on some days.

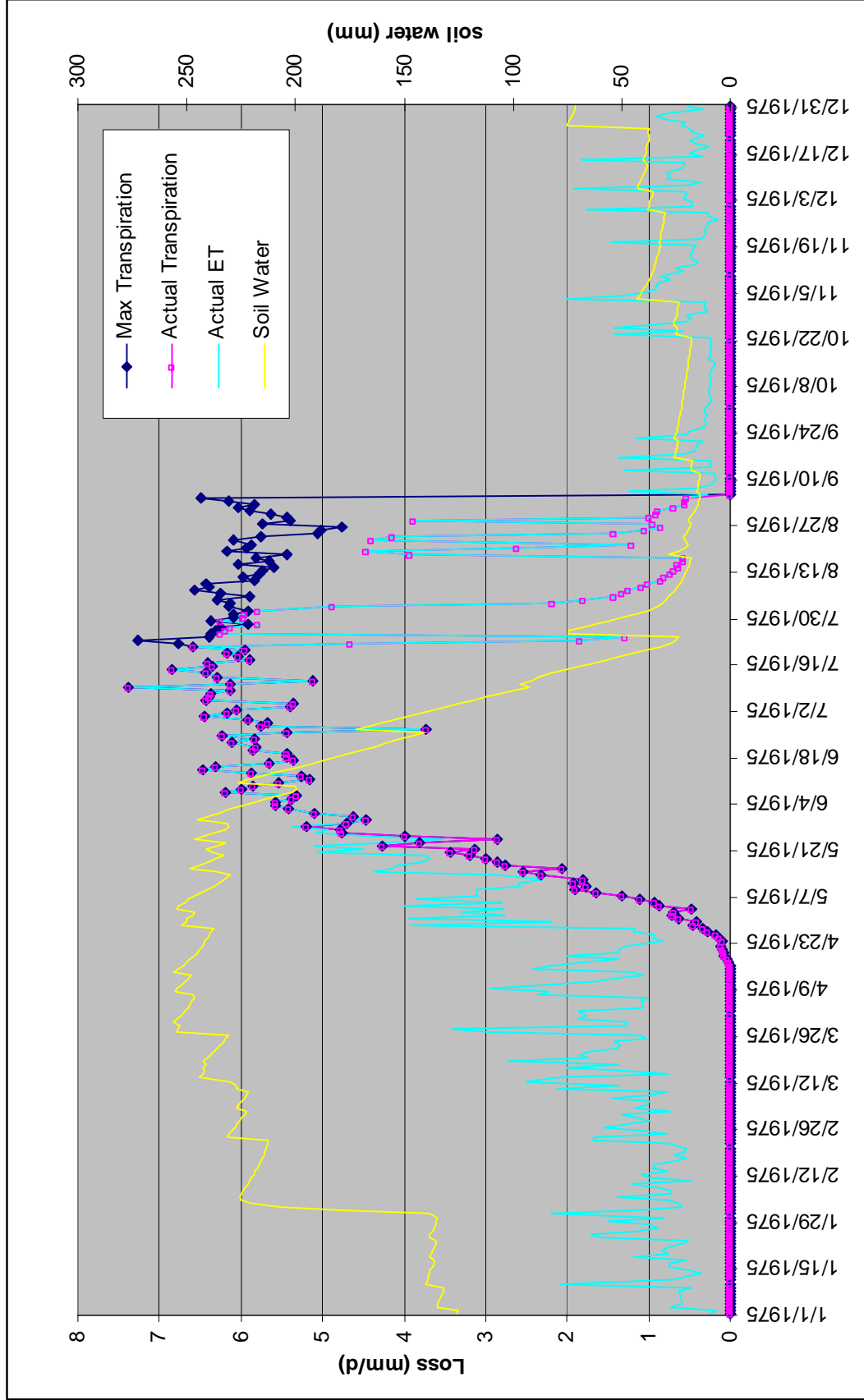


Figure E.1 Example SWAT results

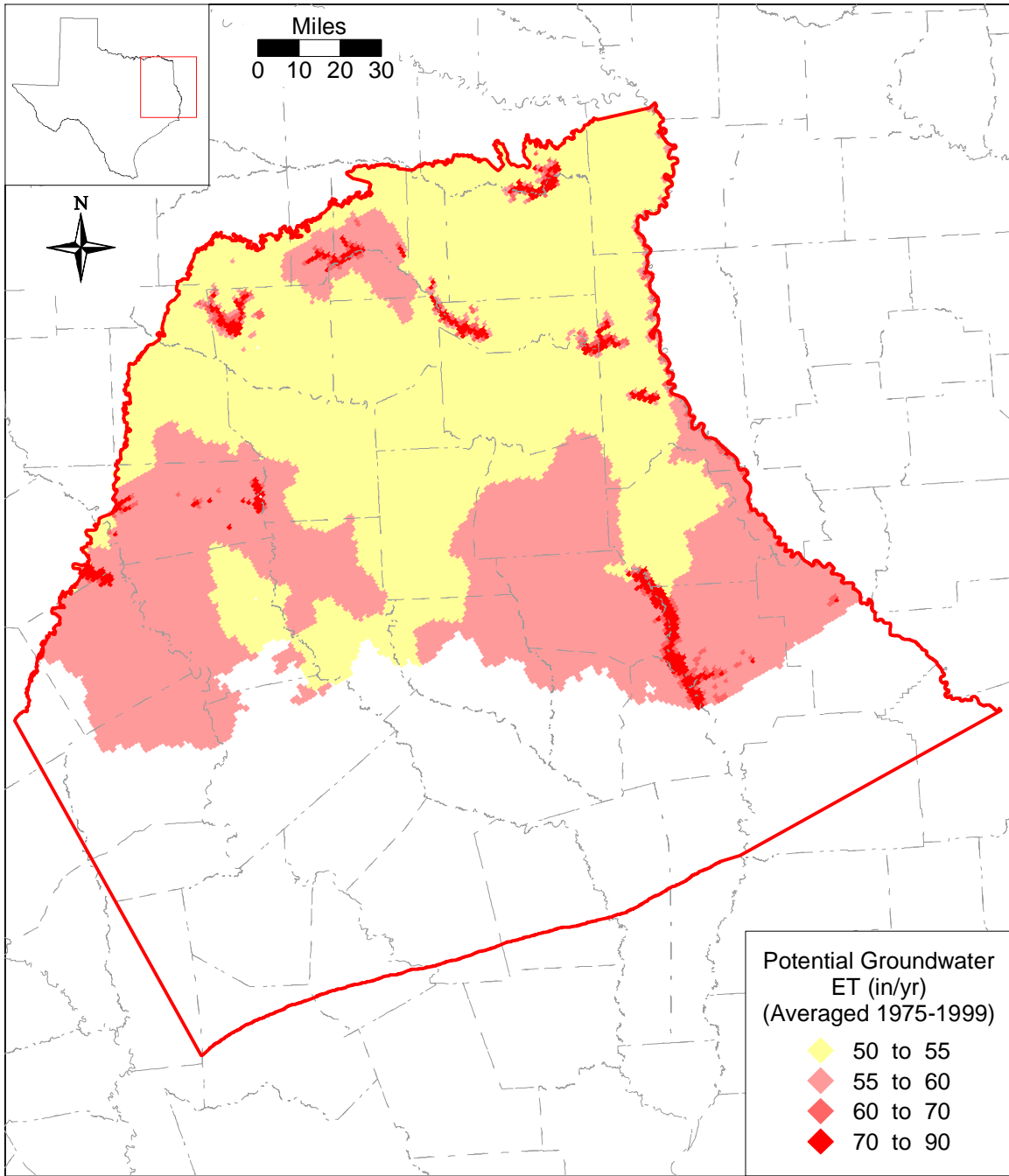


Figure E.2 Potential ET averaged over 1975 – 1999.

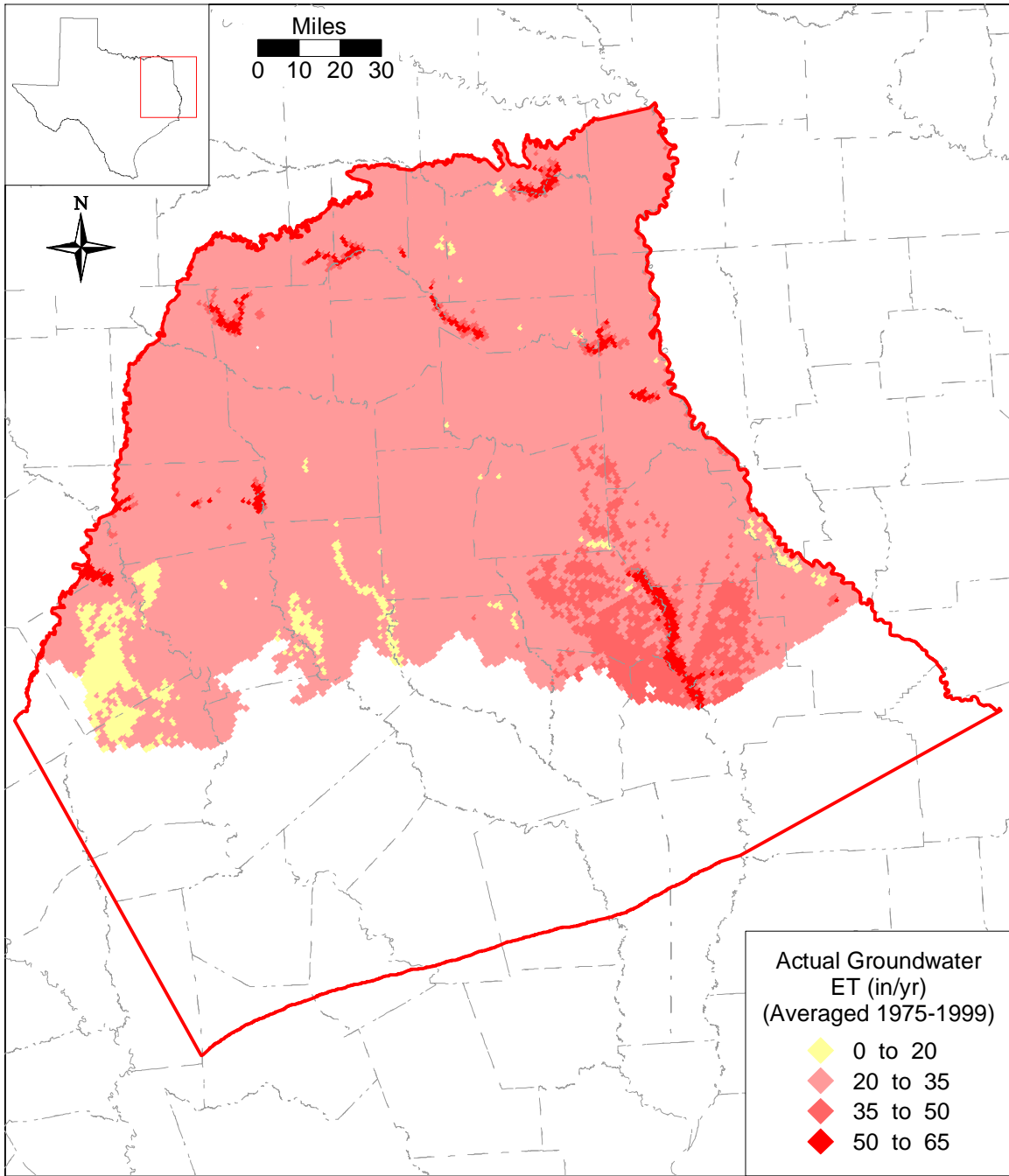


Figure E.3 Actual ET (vadose zone) averaged over 1975 – 1999.

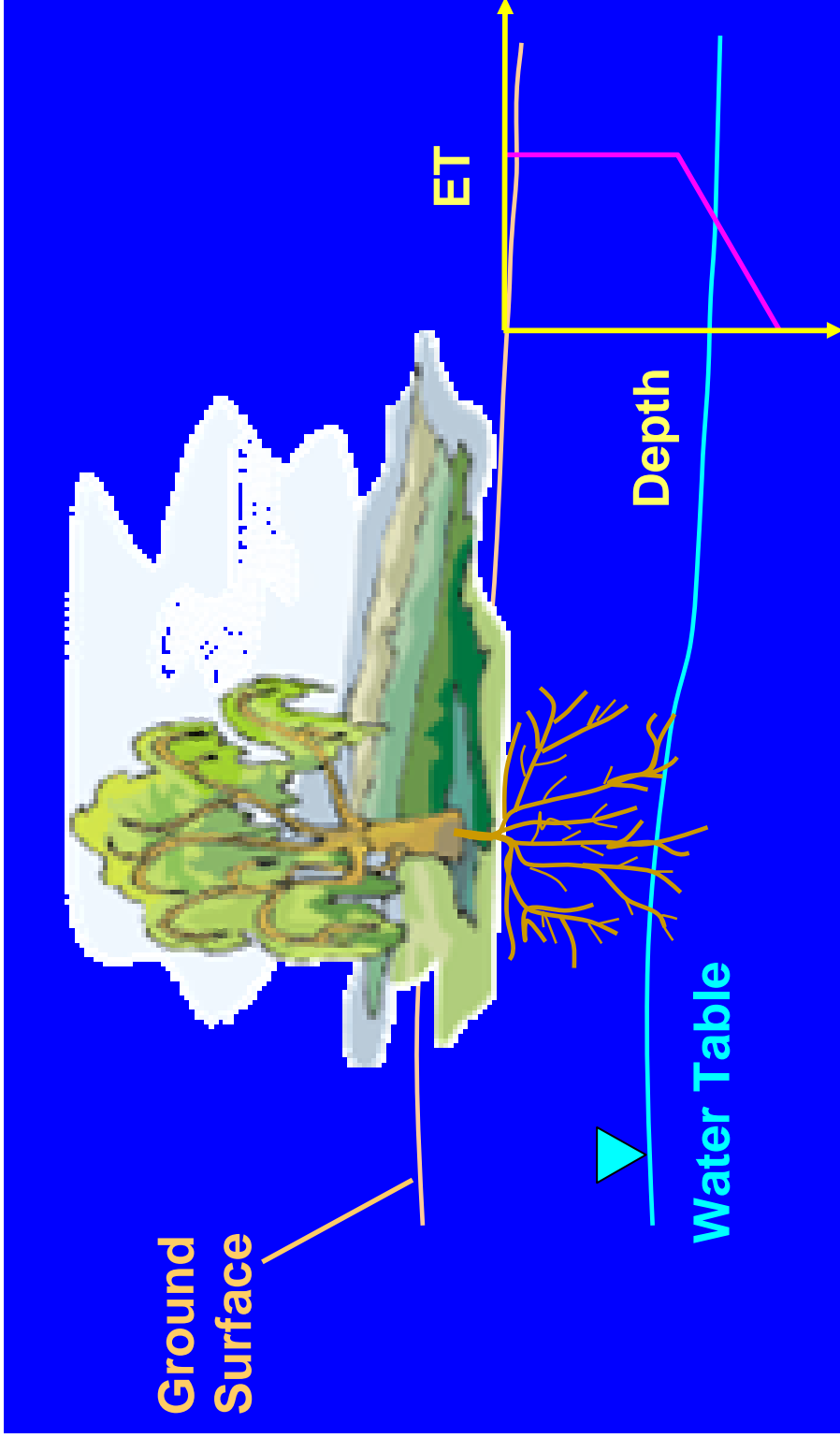


Figure E.4 MODFLOW approach to groundwater evapotranspiration

APPENDIX F
Water Quality

Appendix F

Water Quality

Groundwater in the northern Carrizo-Wilcox aquifer was evaluated for its quality as a drinking water supply, for irrigation of crops, and for industrial purposes, by comparing the measured chemical and physical properties of the water to screening levels. Water quality measurements were retrieved for the entire available historical record, from about 1920 through 2001, from databases maintained by the Texas Water Development Board, the U.S. Geological Survey, and the Texas Commission on Environmental Quality's Public Water System. The percentages of wells in the aquifer with one or more measurements exceeding individual screening levels are illustrated in Table F.1. Table F.2 indicates the percentage of wells in the northern Carrizo-Wilcox aquifer from each county that exceeded at least one screening level for drinking water, irrigation, or industrial uses.

Concentration levels of selected constituents were evaluated for well data from the identified databases. They are presented in Figures F.1 through F.7 for nitrate nitrogen, lead, iron, sodium hazard, total dissolved solids, hardness, and silica, respectively. Each column in the figures reflects the highest observed measurement in a single well. The height of the column, and its color, represent the magnitude of the concentration. A general discussion of drinking, irrigation, and industrial water quality within the northern Carrizo-Wilcox GAM area is presented below.

Drinking Water Quality - Screening levels for drinking water supply are based on the maximum contaminant levels (MCLs) established in National Primary Drinking Water Regulations and National Secondary Drinking Water Regulations. National Primary Drinking Water Regulations are legally enforceable standards that apply to public water systems to protect human health from contaminants in drinking water. National Secondary Drinking Water Regulations are non-enforceable guidelines for drinking water contaminants that may cause aesthetic effects (taste, color, odor, foaming), cosmetic effects (skin or tooth discoloration), and technical effects (e.g., corrosivity, expensive water treatment, plumbing fixture staining, scaling, and sediment).

Total dissolved solids (TDS) is a measure of water saltiness, the sum of concentrations of all dissolved ions (such as sodium, calcium, magnesium, potassium, chloride, sulfate, carbonates) plus silica. Some dissolved solids, such as calcium, give water a pleasant taste, but most, including chloride and sulfate, make water taste salty, bitter, or metallic. Dissolved solids can also increase its corrosiveness. TDS levels have exceeded secondary MCLs, the maximum contaminant level of National Secondary Drinking Water Regulations, in almost 30% of the wells in the northern Carrizo-Wilcox aquifer.

Elevated levels of iron and manganese adversely impact water quality in approximately 20% of the wells in the northern Carrizo-Wilcox aquifer. Water containing iron in excess of 0.3 mg/L and manganese in excess of 0.05 mg/L may cause reddish-brown or blackish-gray stains on laundry, utensils, and plumbing fixtures, as well as color, taste and odor problems.

High concentrations of nitrate nitrogen can cause serious illness in infants younger than 6 months old. Nitrate nitrogen levels that exceed the primary MCL of 10 mg/L were detected in about 6% of the wells.

Fluoride is a naturally-occurring element found in most rocks. At very low concentrations, fluoride is a beneficial nutrient. At a concentration of 1 mg/L, fluoride helps to prevent dental cavities. However, at concentrations above 2 mg/L, fluoride can stain children's teeth. At concentrations above 4 mg/L, fluoride can cause a type of bone disease.

Overall, approximately 6% of the wells in the northern Carrizo-Wilcox aquifer are deemed to have unsuitable drinking water quality for health reasons, and approximately 40% of the wells have water that may be unpalatable for drinking, cause stains to teeth, plumbing fixtures, and laundry, or cause scaling or corrosion in plumbing without prior treatment.

Irrigation Water Quality - The utility of groundwater for crop irrigation was evaluated based on the concentrations of boron, chloride, and total dissolved solids, as well as the salinity hazard, the sodium hazard, and the sodium absorption ratio. Various soils and plants differ in their tolerance of salts. This tolerance is also affected by the abundance of rainfall and frequency of irrigation. In the absence of consensus standards for water quality for irrigation, we attempted to identify thresholds that would be unsuitable for long-term use on most types of plants and soils.

Boron may cause toxicity to many plants at levels above 2 mg/L (van der Leeden et al., 1990). Most crops cannot tolerate chloride levels above 1000 mg/L for an extended period of time (Tanji, 1990). Salinity, as measured by total dissolved solids (TDS) or electrical conductivity, can also be toxic to plants by making plants unable to take up water. James et al. (1982) consider TDS levels above 2100 unsuitable for most irrigation. The salinity hazard classification system of the U.S. Salinity Laboratory (1954) indicates that waters with electrical conductivity over 750 micromhos present a high salinity hazard, and those with electrical conductivity over 2250 micromhos present a very high salinity hazard. Irrigation water containing large amounts of sodium cause a breakdown in the physical structure of soil such that movement of water through the soil is restricted. The sodium absorption ratio (SAR) is an indication of the sodium hazard to soils. An SAR of greater than 18 is generally considered unsuitable for continuous use in irrigation, but the sodium hazard depends on both the SAR and water salinity. The sodium hazard was calculated based on the classification system developed by the U.S. Salinity Laboratory (1954).

Overall, approximately 23% of the wells in the northern Carrizo-Wilcox aquifer are deemed to have unsuitable water quality for irrigation of many types of crops.

Industrial Water Quality - The quality of water for most industrial purposes is indicated by the content of dissolved solids, as well as its corrosivity and tendency to form scale and sediment in boilers and cooling systems. Some constituents responsible for scaling are hardness (calcium and magnesium), silica, and iron. Water temperature and pH also have a direct effect on how quickly and severely these constituents cause scaling or corrosion. pH values below 6.5 may enhance corrosion, while pH values above 8.5 will contribute to scaling and sediment. Waters with a silica concentration of 40 mg/L or higher are considered unsuitable for use in most steam boilers. Waters with a hardness of 180 mg/L (as calcium carbonate) or higher are considered very hard, and are unsuitable for many industrial purposes because water softening becomes uneconomical.

Overall, approximately 38% of the wells in the northern Carrizo-Wilcox aquifer are deemed to have unsuitable water quality for many industrial purposes without substantial pre-treatment, such as water softening.

Literature Cited

- James, D.W., R.J. Hanks, and J.H. Jurinak. 1982. *Modern Irrigated Soils*. John Wiley and Sons, New York.
- Shafer, G.H. 1968. *Ground-water Resources of Nueces and San Patricio Counties, Texas*. Report 73. Texas Water Development Board, Austin, Texas
- Tanji, K.K. 1990. *Agricultural Salinity Assessment and Management*. American Society of Civil Engineers. *Manuals and Reports on Engineering Practice Number 71*.
- U.S. Salinity Laboratory Staff. 1954. *Diagnosis and Improvement of Saline and Alkali Soils*. U.S. Department of Agriculture, Agricultural. Handbook 60.
- Van der Leeden, F., F.L. Troise, and D.K. Todd. 1990. *The Water Encyclopedia*. Lewis Publishers.

Table F.1 Occurrence and levels of some commonly-measured groundwater quality constituents in the northern Carrizo-Wilcox aquifer.

Constituent	Number Of Wells	Screening Level (Mg/L)	Type	Percent Of Wells Exceeding Screening Level*
Nitrate Nitrogen	2502	10	1° MCL	6.2%
Lead	388	0.015	1° MCL	2.1%
Beryllium	255	0.004	1° MCL	0.8%
Alpha Activity, pCi/L	245	15	1° MCL	0.8%
Cadmium	385	0.005	1° MCL	0.8%
Beta Activity, pCi/L	246	50	1° MCL	0.4%
Fluoride	2681	4	1° MCL	0.3%
Barium	391	2	1° MCL	0.3%
Selenium	432	0.05	1° MCL	0.2%
Arsenic	392	0.01	1° MCL	0.0%
Copper	387	1.3	1° MCL	0.0%
Antimony	256	0.006	1° MCL	0.0%
Chromium	390	0.1	1° MCL	0.0%
Mercury	237	0.002	1° MCL	0.0%
Nitrite Nitrogen	241	1	1° MCL	0.0%
Thallium	210	0.002	1° MCL	0.0%
Total Dissolved Solids	2977	500	2° MCL	29%
Iron	961	0.3	2° MCL	19%
Manganese	575	0.05	2° MCL	18%
Chloride	3225	250	2° MCL	8.5%
Fluoride	2681	2	2° MCL	2.6%
Sulfate	3065	250	2° MCL	2.4%
Aluminum	286	0.2	2° MCL	2.4%
Zinc	387	5	2° MCL	0.0%
Copper	387	1.0	2° MCL	0.0%
Silver	254	0.1	2° MCL	0.0%
Salinity Hazard	2464	Very High (Sp. Cond. >2250)	Irrigation	3.2%
		High Or Very High (Sp. Cond. > 750)	Irrigation	35%
Sodium (Alkali) Hazard	2858	Very High (SAR>26)	Irrigation	24%
		High Or Very High (SAR>18)	Irrigation	33%
Boron	425	2	Irrigation	1.9%
Total Dissolved Solids	2977	2100	Irrigation	1.4%
Chloride	3225	1000	Irrigation	1.0%
PH	2512	<6.5 OR >8.5	Industrial	30%
Hardness	3312	180	Industrial	11%
Silica	2241	40	Industrial	10%

* percentage of wells with one or more measurements of the parameter that exceeded the screening level.

Table F.2 County-level water quality in the northern Carrizo-Wilcox aquifer.

County Name	RWPG	% of Wells Exceeding One or More Screening Levels				
		Wells Sampled	1° MCL	2° MCL	Irrigation	Industrial
Anderson	I	119	3.5%	40%	39%	37%
Angelina	I	46	0.0%	91%	91%	89%
Bowie	D	28	19%	39%	11%	68%
Brazos	G	17	6.3%	47%	88%	25%
Caddo (LA)		219	2.3%	30%	4.1%	12%
Camp	D	43	9.5%	16%	9.5%	17%
Cass	D	101	14%	33%	17%	30%
Cherokee	I	105	5.3%	47%	52%	47%
De Soto (LA)		139	2.8%	64%	24%	37%
Franklin	D	43	27%	33%	4.8%	40%
Freestone	C	236	7.5%	33%	9.7%	52%
Gregg	D	75	1.5%	51%	76%	32%
Harrison	D	166	4.2%	30%	18%	27%
Henderson	C/I	209	6.3%	28%	5.3%	31%
Hopkins	D	28	18%	57%	7.1%	64%
Houston	I	25	0.0%	32%	72%	28%
Leon	H	44	0.0%	32%	16%	26%
Limestone	G	73	1.4%	45%	5.7%	43%
Madison	H	6	0.0%	33%	80%	40%
Marion	D	31	0.0%	57%	61%	32%
Miller (AR)		1	0.0%	100%	0.0%	100%
Morris	D	54	21%	18%	11%	22%
Nacogdoches	I	160	4.0%	46%	19%	46%
Natchitoches (LA)		82	1.5%	57%	23%	37%
Navarro	C	13	50%	50%	10%	92%
Panola	I	92	1.1%	48%	36%	64%
Rains	D	26	24%	58%	12%	54%
Red River (LA)		57	0.0%	53%	8.8%	22%
Robertson	G	157	4.7%	25%	18%	42%
Rusk	I	126	4.1%	66%	52%	66%
Sabine	I	32	17%	46%	38%	19%
Sabine (LA)		70	3.4%	76%	30%	36%
San Augustine	I	62	23%	29%	17%	16%
Shelby	I	97	5.2%	59%	54%	62%
Smith	D/I	170	0.6%	36%	20%	33%
Titus	D	75	26%	26%	8.5%	28%
Upshur	D	74	2.9%	45%	24%	36%
Van Zandt	D	150	5.1%	23%	6.9%	27%
Wood	D	117	4.8%	34%	14%	31%
All		3368	6.2%	41%	23%	38%

Figure F.1 Maximum observed nitrate nitrogen levels.

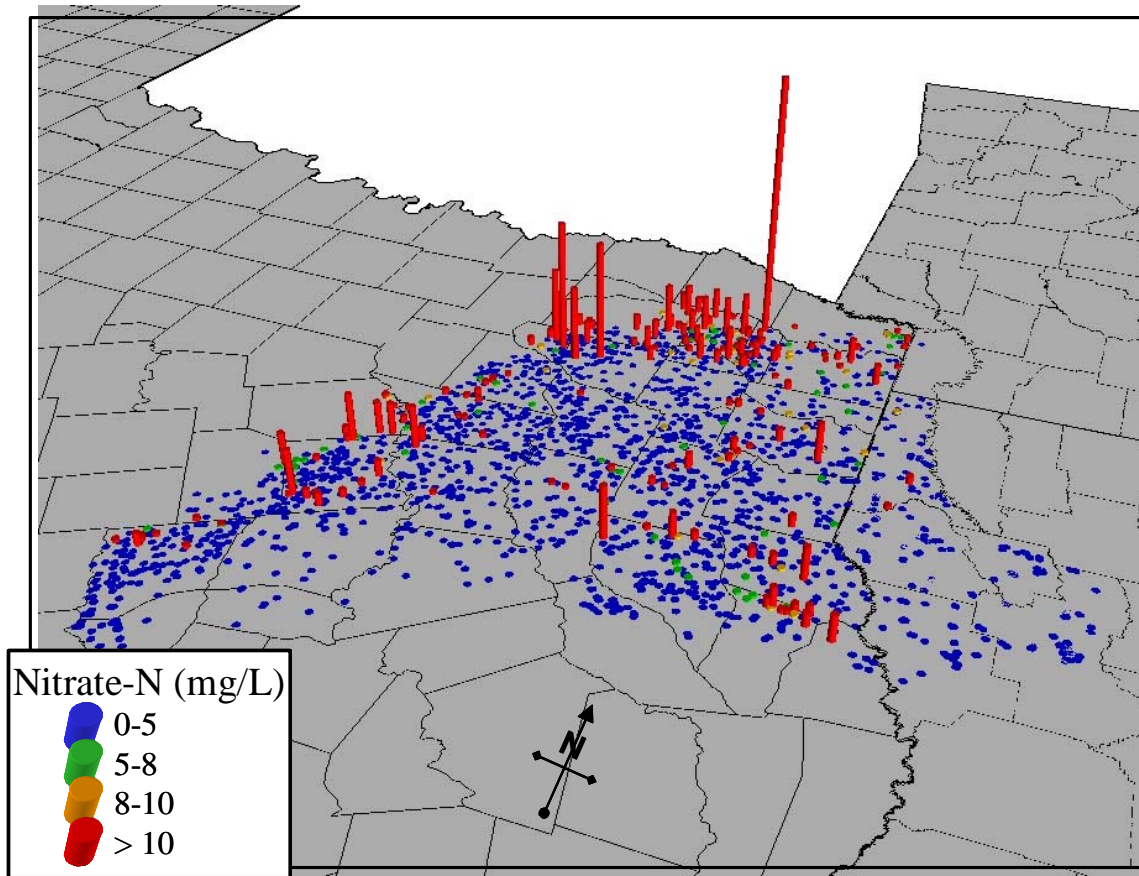


Figure F.2 Maximum observed lead levels.

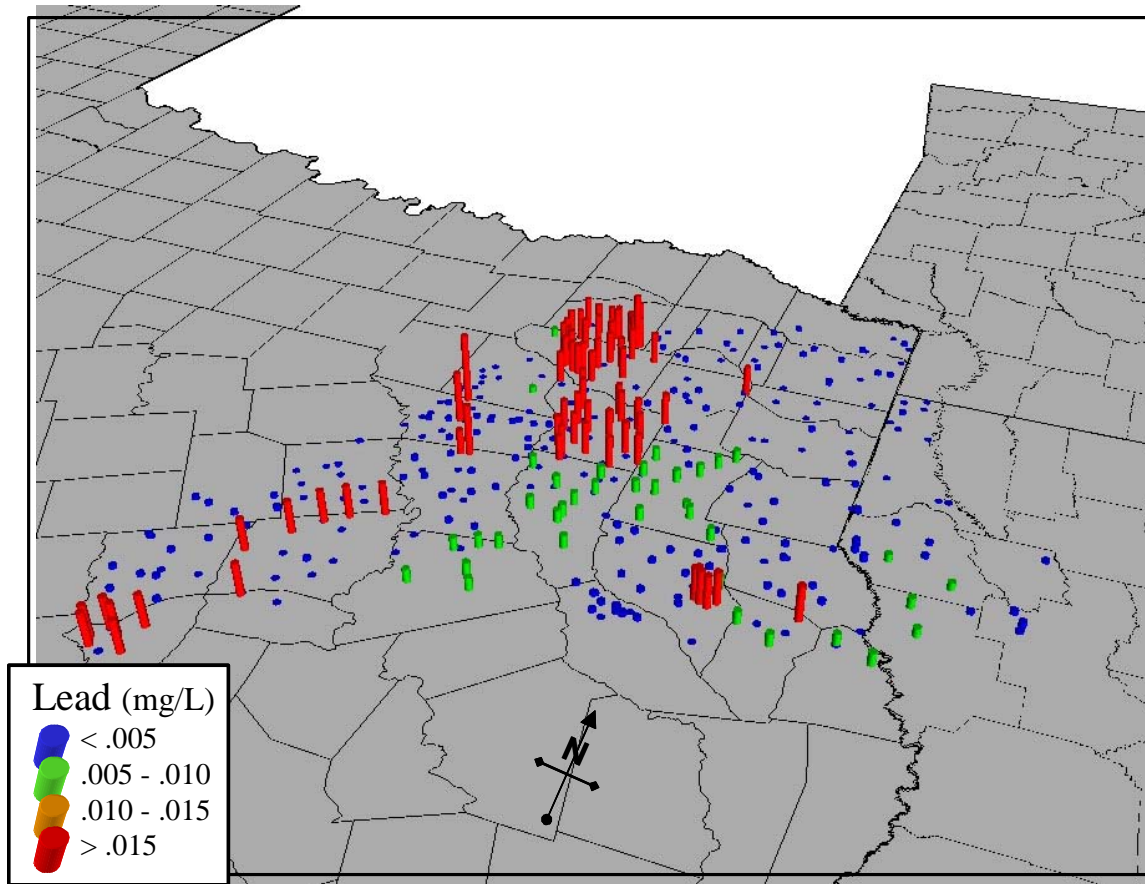


Figure F.3 Maximum observed iron levels.

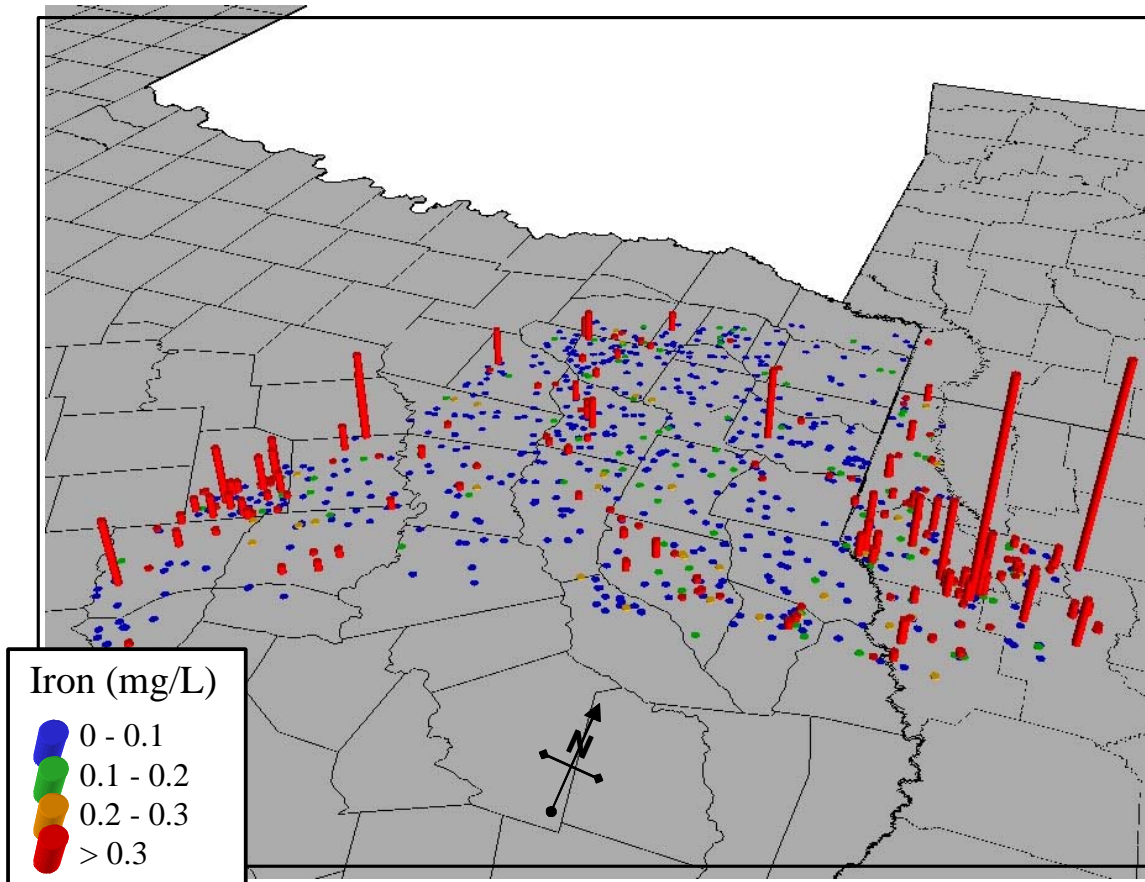


Figure F.4 Maximum observed sodium hazard levels.

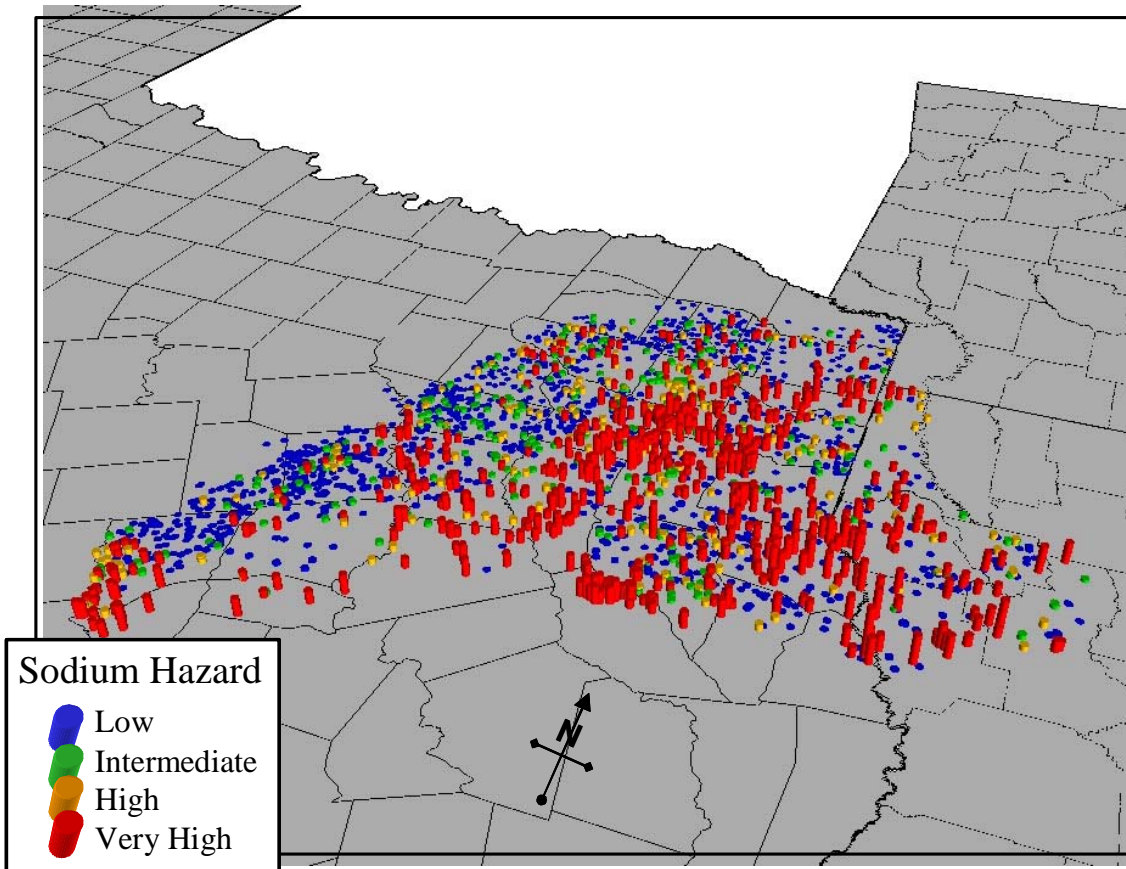


Figure F.5 Maximum observed total dissolved solids (TDS) levels.

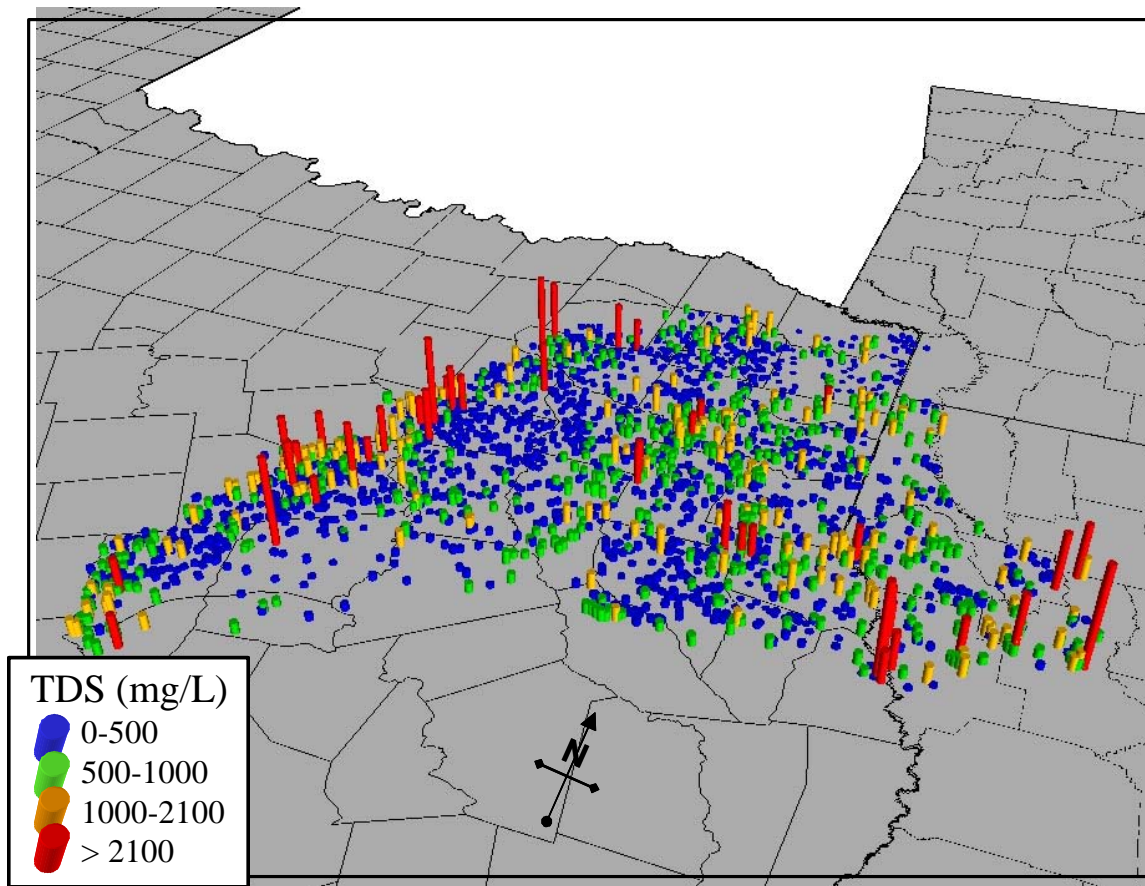


Figure F.6 Maximum observed hardness levels.

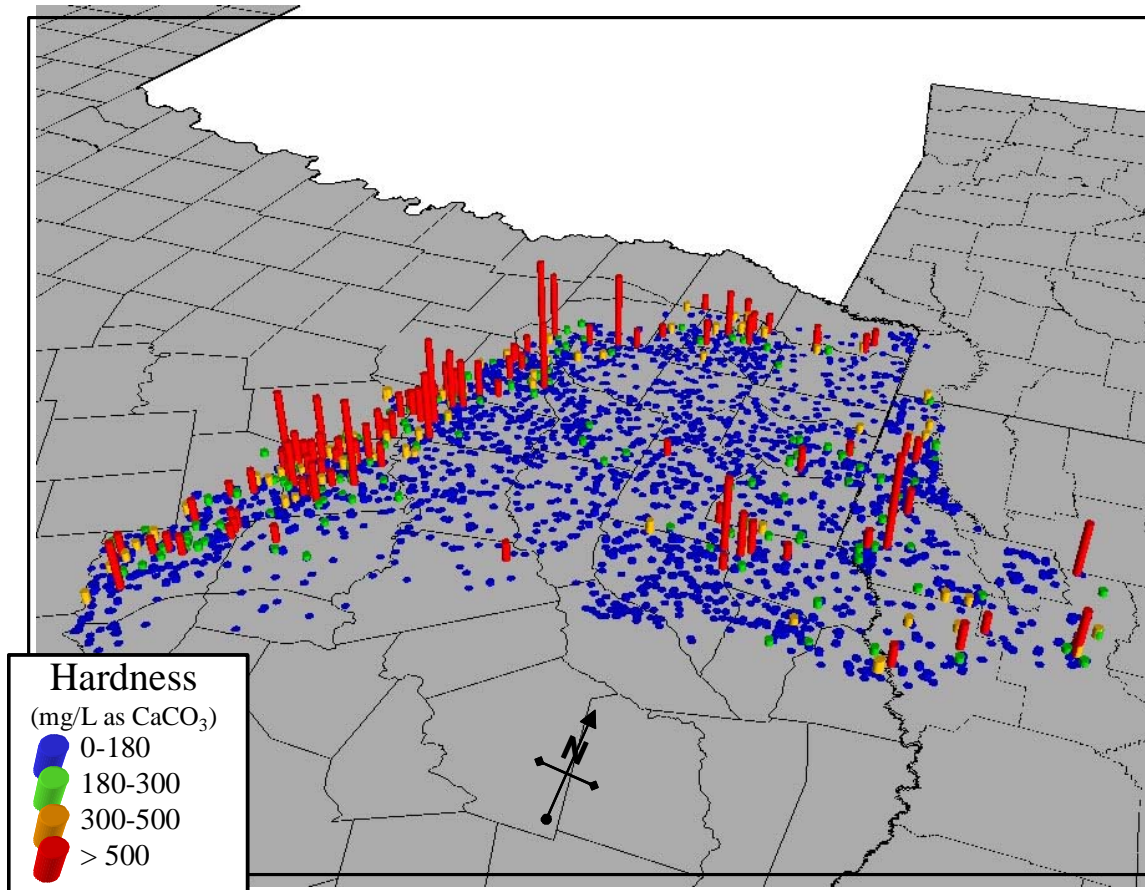
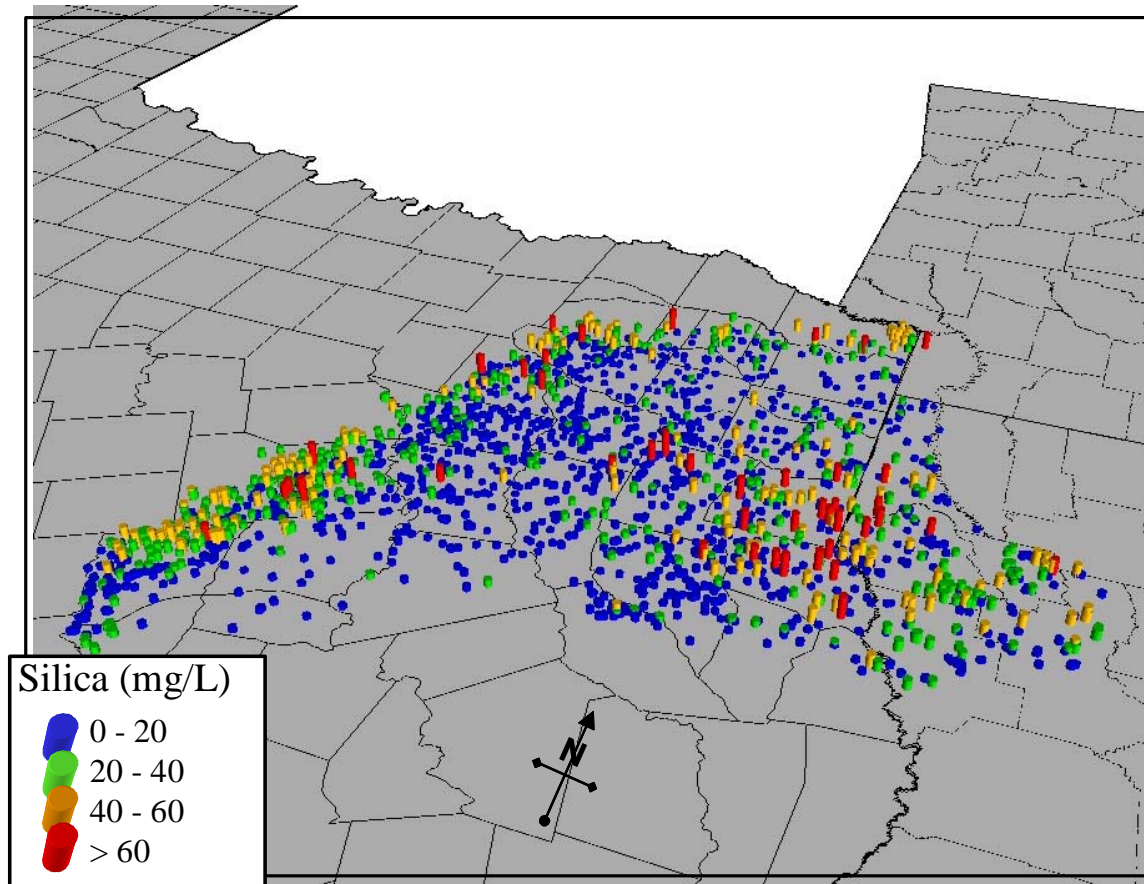


Figure F.7 Maximum observed silica levels.



APPENDIX G

Draft report Comments and Responses

Appendix G

Responses to Texas Water Development Board Comments on the September 2002 Draft Report

TEXAS WATER DEVELOPMENT BOARD Review of the Draft Final Report: Contract No. 2001-483-377 " Groundwater Availability Model for the Northern Carrizo-Wilcox Aquifer"

ADMINISTRATIVE AND TECHNICAL COMMENTS ON DRAFT REPORT

(Note: The Para Lines referred to below are the line numbers in the paragraph of the section and not the line number from the top of the page.)

General Comments:

1. Please consider using higher resolution graphics. Many of the graphics are pixelated.
Completed.
2. Please include an authorship list.
Completed.
3. Please include the following figures:
 - representative stream flow hydrographs for the major streams in the study area
Completed. See Figure 9.2.3.
 - spring-flow hydrographs, if available
None were available.
 - map of rural population density
Completed. See Figure 4.7.1.
 - map of estimated recharge rates, factors or coefficients.
Calibrated recharge rates for the steady-state model are shown in Figure 8.1.6. Calibrated recharge rates for the transient model averaged over 1980-1999 are shown in Figure 9.2.20 .

Table of Contents:

1. Page i, Section 4.4.3: Change number of subsection to 4.4.4.
Completed.
2. Page i, Section 4.4.4: Change number of subsection to 4.4.5.
Completed.
3. Page ii, Section 8.1.2: Change number of subsection to 8.1.3.
Completed.
4. Page ii, Section 8.1.3: Change number of subsection to 8.1.4.
Completed.

Abstract:

1. Please add a short summary of the main findings of the study including the predictions for the next 50 years. The limitations of the study, and areas that need improving for similar future studies, should be listed.
Completed.

Section 1: Introduction

1. Section 1.0, Page 1-3: Please add information on Region D's water needs and supply plans, similar to that of Region I.
Completed.

Section 2: Study Area

1. Section 2.2, Page 2-14, Para 3, Para Line 4: Reference Mexia-Talco fault zone to a figure. *Reference to the Mexia-Talco fault zone was removed from this sentence since this section is not dealing with structure. The Mexia-Talco fault zone is shown on Figure 4.2.1 under Section 4.2, Structure.*
2. Section 2.2, Page 2-18, Para 6, Para Line 5: Are the lower and upper Wilcox formations formal stratigraphic units? If they are, please capitalize lower and upper.
This division is informal; upper and lower will not be capitalized.
3. Section 2.2, Page 2-21, Para 7, Para Line 7: Please correct the spelling of "Fischer and McGowan". The correct spelling is Fisher and McGowen.
Completed.
5. Section 2.2, Page 2-21, Para 7, Para Line 18: Please correct the spelling of McGowan. The correct spelling is McGowen.
Completed.

Section 3: Previous Investigations

1. Section 3.0, Page 3-1, Para 3, Para Line 2: "Oakwood Dome". Please describe the general location of this feature or show on a map.
Completed.
2. Section 3.0, Page 3-4, Para 8, Para Line 5: Please add "Formation" at the end of "Newby".
Completed.
3. Section 3.0, Page 3-4, Para 8, Para Line 7: Please verify year "1985". It is cited as "1988" in Table 3.1.
Completed.

Section 4: Hydrogeologic Setting

1. Section 4.0: Hydrogeologic Setting. Please include a sub-section on the water-quality work done for the project.
Completed. Added as Section 4.8.
2. Section 4.2, Page 4-13, Para 4, Para Line 10: Please delete "certain", and give examples (with locations) of where the Reklaw is relatively thin.
Deleted sentence. False points were added in areas where data were sparse and kriging created artifacts.

3. Section 4.2, Page 4-21, Para 5, Para Line 10: Please show the Trinity River on the maps if it is being used extensively as a reference feature.
Completed. The Trinity River is shown and labeled on Figures 2.2 and 2.13.
4. Section 4.2, Page 4-21, Para 5, Para Lines 12, 13: The observation “indicating a more east-west trend in the deeper section.” is not clear. Please clarify.
Deleted “indicating a more east-west trend in the deeper section.”
5. Section 4.3, Page 4-21, Para 1, Para Lines 2 and 7: Please correct the reference to Mace et al. Cited as “2000a” in References.
Completed.
6. Section 4.3, Page 4-22, Para 3, Para Line 2: Please correct the reference to Mace et al. Cited as “2000a” in References.
Completed.
7. Section 4.3.1, Page 4-23, Para 2, Para Line 3: Please clarify that the aquifer code is the TWDB aquifer code.
This section was rewritten to clarify the methodology used for processing the hydraulic conductivity database. TWDB is included with “aquifer code” where it is mentioned in the new text.
8. Section 4.3.1, Page 4-23, Para 2, Para Line 5: Is it 4,108 or 5,108 (1,680 + 3,430 - 2)? Please check all other numbers accordingly, later in the paragraph.
This section was rewritten to clarify the methodology used for processing the hydraulic conductivity database.
9. Section 4.3.2, Page 4-25, Para 2, Para Line 1: Please correct the reference to Mace et al. Cited as “2000a” in References.
This section was rewritten to clarify the methodology used for processing the hydraulic conductivity database. The citation is no longer included in this section.
10. Section 4.3.2, Page 4-25, Para 2, Para Line 6: Please explain what CDF stands for.
This section was rewritten to clarify the methodology used for processing the hydraulic conductivity database. CDF is defined.
11. Section 4.3.3: Spatial Distribution of Hydraulic Property Data. Please explain how K was kriged. The distribution does not look like a simple-kriged distribution.
Log hydraulic conductivities were kriged in Surfer 7.02 using ordinary kriging.
12. Section 4.3.3: Spatial Distribution of Hydraulic Property Data. Please include a discussion on horizontal anisotropy.
Completed.
13. Section 4.3.3, Page 4-27, Para 4, Para Lines 6, 7: Please check the accuracy of the statement that the Carrizo sand decreases in thickness southward. On page 4-21 it is stated that the thickness of the unit increases to the southeast.
These sentences were rewritten. The Carrizo thickens significantly only to the southwest.
14. Section 4.3.4, Page 4-38, Para 5, Para Line 2: McGown and Fisher (1976) is not in the Reference list. Is it Fisher and McGowen (1976)?
Completed.
15. Section 4.4.3, Page 4-55, Para 3, Para Line 12, 13: Possible contradiction to the statement that flow is upward. Earlier in the para, on line 5, it states that flow is downward.
The last two sentences of this paragraph have been removed to eliminate this inconsistency.
16. Section 4.4.3, Page 4-58, Para 2, Para Line 6: Please clarify if all water levels were used if they met “any” criterion or “all” criteria.
Completed; water levels were used if any of the criteria were met.
17. Section 4.5, Page 4-86: Recharge. Please discuss possible temporal variations in recharge.
Completed.

18. Section 4.5, Page 4-87, Para 2, Para Lines 7, 8: Please explain why the Wilcox Group has good potential for recharge.

Completed.

19. Section 4.5, Page 4-87, Para 3, Para Line 7: Atascosa County is not in the study area. Please mention this.

Completed.

20. Section 4.6, Page 4-93, Para 4: Table 4.6.2 shows springs in the study area. Have these springs been assigned as drains in the model? If so, what are the simulated discharges at these springs?

As noted in Section 6.3.3, springs with significant flow rates were in or very near modeled stream segments and were, therefore, not included as drains.

21. Section 4.6, Page 4-93, Para 4, Para Line 4: Please clarify if the spring survey was a field survey or a literature survey.

Completed; it was a literature survey.

Section 5: Conceptual Model of Groundwater Flow in the Aquifer

1. No comments.

Section 6: Model Design

1. Section 6.3.4, Page 6-9, Para 4, Lines 8, 9: "This rooting depth is passed through to MODFLOW as the extinction depth required by the MODFLOW recharge package." Do the authors mean MODFLOW ET package?

Completed; "Recharge package" was changed to "ET package".

2. Section 6.3.2, Page 6-5, Para 1, Para Line 7: Please check reference of "Williamson et al. (1989). Is cited as "Williamson et al., 1990" in the References section.

Completed.

3. Section 6.3.3, Page 6-6, Para 3, Para Line 8: Lowercase "Alluvium".

Completed.

4. Section 6.4.1, Page 6-10, Para 2, Para Line 3: Please check and correct the year in "Gutjahr et al., 1967". It is cited as 1978 in the References section.

Completed.

5. Section 6.4.1, Page 6-11, Para 3, Para Line 2: Correct the reference to Mace et al. Cited as "2000a" in References.

Completed.

6. Section 6.4.1, Page 6-13, Para 8, Para Line 10: Please explain why a percent sand study was not done for the Queen City Sand.

Completed. Because the Queen City Formation was not in the scope of the Carrizo-Wilcox GAM and because it was added to act as a boundary condition for the Carrizo-Wilcox GAM, we did not consider a detailed study of the Queen City Formation necessary.

7. Section 6.4.2, Page 6-14, Para 2, Para Line 3: Please correct the typo "Mace at al (200)." Should be "Mace et al. (2000a)".

Completed.

Section 7: Modeling Approach

1. Section 7.2, Page 7-5, Para 3, Para Line 3: Please check and correct the reference of "(Williamson et al., 1989)". It is cited as "1990" in the References section

Completed.

Section 8: Steady-State Model

1. Section 8.1.2, Page 8-1: Please include maps showing extinction depth and final ET rate (ET max). Please also append the potential ET map and actual ET map obtained from the SWAT in Appendix E. SWAT model (into one or more CDs) used to estimate recharge and ET should also be submitted.

Maps showing steady-state ET extinction depth and calibrated ET max were added as Figures 8.1.7 and 8.1.8. Maps showing average potential ET and average actual ET in SWAT were included as Figures E.2 and E.3 in Appendix E. The SWAT data is included on CD.

2. Section 8.1.2, Page 8-1, Para 1, Para Line 7: Please explain why spatial Kh distribution for Layer 1 was considered preliminary.

Because the Queen City Formation (Layer 1) was not in the scope of the Carrizo-Wilcox GAM and because it was added to act as a boundary condition for the Carrizo-Wilcox GAM, we did not consider a detailed study of the Queen City Formation necessary .

3. Section 8.1.2, Page 8-2, Para 4, Para Line 4: Reference to “Figure 8.1.4” is incorrect. Please change to “Figure 8.1.5.”

Completed.

4. Section 8.1.3, Page 8-3, Para 1, Para Line 4: Please check and correct the reference of “(Williamson et al., 1989)”. It is cited as “1990” in the References section.

Completed.

5. Section 8.2, Page 8-12: Simulation Results. Please include MAE and ME along with RMS.

Completed. ME and MAE were added to Table 8.2.1.

6. Section 8.2.1, Page 8-14, Para 8, Lines 2, 3: Please include actual values to replace the XXX and YYYs.

Completed.

7. Section 8.2.2, Page 8-14: Streams. Please include an assessment of how well the simulated stream baseflow matches the measured streamflow.

Completed. Simulated stream baseflow was compared to available gain/loss estimates.

8. Section 8.2.2, Page 8-14, Para 1, Para Line 3: Please clarify if “These are” are losses.

Completed.

9. Section 8.3, Page 8-28, Para 1: Please renumber the equations. Should be “8.3.1, 8.3.2 and 8.3.3”, and change in the text where applicable.

Completed.

Section 9: Transient Model

1. Section 9.1, Page 9-1, Para 3, Para Line 3: Specific storage value is not in the same units as that in 6.4.2. Please correct.

Completed.

2. Section 9.1, Page 9-2, Para 3, Para Line 4: Please correct the reference to Mace et al. Cited as “2000a” in References.

Completed.

3. Section 9.2, Page 9-4: Simulation Results. Please include MAE and ME along with RMS.

Completed. ME and MAE were added to Table 9.2.1.

4. Section 9.2.1, Page 9-4, Para 1, Para Line 5: Please explain why a hydraulic head contour map was not produced for the Queen City.

Because the Queen City Formation was not in the scope of the Carrizo-Wilcox GAM and because it was added to act as a boundary condition for the Carrizo-Wilcox GAM, we did not consider a detailed study of the Queen City Formation necessary .

5. Section 9.2.3, Page 9-8, Para 1, Para Line 8: Please change “Figure 9.2.5” to “Figure 9.2.25”.

Completed.

6. Section 9.3, Page 9-44, Para 6, Para Line 3: Please change “Figures 9.3.9” to “Figure 9.3.9”.

Completed.

Section 10: Model Predictive Simulations

1. No comments.

Section 11: Limitations of the Model

1. Section 11.1, Page 11-2, Para 3, Para Line 6: Please explain why the pumping data must be considered uncertain, or reference another section if it has been discussed there.

Completed. An expanded discussion has been added to Section 11.

2. Section 11.2, Page 11-3, Para 2, Para Line 5: Please explain why this is not considered a significant limitation of the model.

Completed.

3. Section 11.2, Page 11-4, Para 4, Para Line 9: Please explain when and where the adjustments have to be examined in more detail.

We examined the problem that MODFLOW encountered when ET approached or exceeded recharge under steady-state conditions and determined that the problem is probably inherent to MODFLOW in cases where depth to groundwater is shallow.

Section 12: Future Improvements

1. Section 12.1, Page 12-1, Para 4, Para Line 6: Please explain the kind of monitoring required.

Completed.

2. General: Are any pumping-data improvements necessary?

Completed.

Section 13: Conclusions

1. Section 13.0, Page 13-1, Para 1, Para Line 6: Please change “Queen City Clay Formation” to “Queen City Sand”

Completed.

2. General: Please expand the discussion of the predictive results with at least some specific highlights of the results and areas.

Completed.

3. General: Please mention the regional scale of the model.

Completed.

Section 14: Acknowledgements

1. No comments.

Section 15: References

1. Page 15-1: Alexander and White, 1966 should appear before Anders, 1967.
Completed.
2. Page 15-4: Grubb, 1997 should appear before Guevara and Garcia, 1972.
Completed.
3. Page 15-7: Page and May, 1964 should appear before Page, Newcome and Graeff, 1963.
Completed.

Figures:

Section 1: Introduction

1. No comments.

Section 2: Study Area

1. Figure 2.2, Page 2-3: Please simplify the map. Include only large streams. Keep only major roadways.
Completed.
2. Figure 2.3, Page 2-4: Please change the title to "Areal extent of the major aquifers in the study area." The figure also shows the downdip part of the aquifer in Texas.
Completed.
3. Figure 2.5, Page 2-7: Please add the Lake Country Groundwater Conservation District (Wood County) to the map. The district is yet to be confirmed. Also, the following districts were confirmed at the 11/05/02 elections: Bluebonnet GCD, Brazos Valley GCD and the Mid-East Texas GCD.
Completed.
4. Figure 2.6, Page 2-8: Please enlarge map. Remove the subtitle in the legend box and simplify scale. Lakes in legend box are not shown on the map.
Completed.
5. Figure 2.7, Page 2-9: Label large towns for reference?
Completed.
6. Figure 2.8, Page 2-11: Please correct the title to "Average pan evaporation rate, in inches per year, in the study area." Describe in the legend what the grid blocks are.
Completed.
7. Figure 2.9, Page 2-12: Please add a number to the precipitation gage symbol in the legend box to match the map. In the title, change "available for" to "in".
Completed.
8. Figure 2.10, Page 2-13: Oregon Climate Services is not listed in the References. Please list.
Completed. See page 2-11.
9. Figure 2.11a, Page 2-15: Ellis County is not within or close to the study area. Is this graph appropriate?
Since this figure was designed to show regional trends in precipitation, we feel that showing the gage in Ellis County is appropriate.

10. Figure 2.12, Page 2-17: Please label the Trinity River on the map since it is referred to in the text and used to describe the stratigraphy. In the table below the map, add River to Trinity at both locations. In the stratigraphy table, correct the spelling of Quarternary (should be Quaternary). In legend box, add A and A' to the cross section line and change "trace" to "line". Show Sabine Uplift, East Texas Basin, Houston Embayment and Mexia-Talia Fault on the map?
The structural features were not added because they made the figure too confusing. Structural features are shown on Figure 4.2.1. All other comments completed.
11. Figure 2.13, Page 2-19: Please correct the spellings of "Claibourne" and "Recklaw". Should be "Claiborne" and "Reklaw", respectively. Also, please add a comma after "Kaiser et al."
Completed.
12. Figure 2.14, Page 2-20: The cross-sections are hard to read. Can they be enlarged? Also, in the title, please add that the cross-section lines are shown in Figure 2.12.
Completed.

Section 3: Previous Investigations

1. Figure 3.1, Page 3-3: In the title, please add "Carrizo-Wilcox" after "Northern". Check the references to Harden and Associates and Thorkildsen. They are listed as 2001, and Thorkildsen et al., 1989, respectively, in the Reference section.
Completed. The Thorkildsen reference was corrected to Thorkildsen and Price. The Harden and Associates reference was corrected in Section 15.

Section 4: Hydrogeologic Setting

1. Figure 4.1.1, Page 4-3: Please correct the spellings of "Claibourne" and "Recklaw" to "Claiborne" and "Reklaw", respectively.
Completed.
2. Figure 4.2.1, Page 4-4: Please add an explanation for the arrows (e.g., regional dip of the geological units) in the legend.
Completed.
3. Figure 4.2.2 to 4.2.8, Pages 4-6 to 4-12: On all the maps, please note the contour interval used. Also, give complete reference (e.g., with year) for all sources of data listed under "Data Sources". Remove any outcrop symbols in the legend box not shown on the map. On Figure 4.2.8, add a space between "map" and "of" in the title.
Completed. Contour interval was added to the figure titles. Complete references for all data sources are included in Table 4.2.1.
4. Figures 4.2.9 to 4.2.15, Pages 4-14 to 4-20: On all the maps, please note the contour interval used. On Figure 4.2.15, correct the title by removing "younger" and lowercasing "Formation."
Completed. Contour interval was added to the figure titles.
5. Figure 4.3.1, Page 4-26: What is CDF? Please spell out. Also, use smaller font for the horizontal axis.
Completed.
6. Figure 4.3.2, Page 4-28: Please use smaller font for the horizontal axis.
Completed.

7. Figures 4.3.3 to 4.3.7, Pages 4-29 to 4-34: Please use comma separators for the numbers in the variograms.
Because these are insets, they will be left as is.
8. Figure 4.3.8, Page 4-37: Please label the figures as (a) and (b) and reference them as such in the title, instead of “top” and “bottom”. Also in the title, change “maximum sand thickness of the upper Wilcox and hydraulic conductivity (Log K)” to “maximum sand thickness and hydraulic conductivity (Log K) of the upper Wilcox.”
Completed.
9. Figure 4.3.9, Page 4-39: Please add contour interval used. Check reference of “Fisher and McGowen, 1976”. It is listed as “1967” in the References section.
Completed. Contour interval was added to the figure title.
10. Figure 4.4.1, Page 4-42: Please correct the spelling of “seperate” at both locations.
Completed.
11. Figure 4.4.2, Page 4-44: Please change the title. It only mentions the Carrizo Sand and the Wilcox Group, but the map shows other aquifers.
Completed.
12. Figure 4.4.6, Page 4-54: Please add comma separators to numbers on the axes.
Completed.
13. Figure 4.4.7, Page 4-56: Why is data for the Cypress aquifer included in the map?
The Cypress aquifer is discussed on page 4-41 and is included here for completeness.
14. Figure 4.4.8, Page 4-57: Please add comma separators to numbers on the axes. Again, explain why data for the Cypress aquifer is included?
Completed. The Cypress aquifer is discussed on page 4-41 and is included here for completeness.
15. Figures 4.4.9a to 4.4.9e, Pages 4-59 to 4-63: Please add contour interval to all maps in this series and the unit of elevation, in the legend.
Completed.
16. Figures 4.4.10a to 4.4.10d, Pages 4-65 to 4-68: Please add contour interval to all maps in this series and the unit of elevation, in the legend.
Completed.
17. Figures 4.4.11a to 4.4.11d, Pages 4-69 to 4-72: Please add contour interval to all maps in this series and the unit of elevation, in the legend.
Completed.
18. Figures 4.4.16a to 4.4.19b, Pages 4-78 to 4-85: Please add contour interval to all maps in this series and the unit of elevation, in the legend. Also, make a note that (-) values mean decline and (+) values mean rise.
Completed.
19. Figure 4.5.1, Page 4-90: Please make a note that reservoir numbers are listed in Table 4.5.2 and the reservoir characteristics described there.
Completed.
20. Figure 4.6.1, Page 4-94: Please check reference year of Slade, Bentley and Michaud. It is listed as 2002 in the References section, and in the figure title. Make a note in the legend that the survey numbers are listed in Table 4.6.1, and details are provided in this table.
Completed.

21. Figure 4.6.2, Page 4-96: Please make a note in the legend that the spring numbers are listed in Table 4.6.2 and details about the springs are provided in this table.
Completed.
22. Figures 4.7.1 to 4.7.6, Pages 4-107 to 4-109: Please remove the subtitles in the legend box. Change the title to read "XXXX (Layer Y) pumpage (AFY), 1990."
Completed.

Section 5: Conceptual Model of Groundwater Flow in the Aquifer

1. Figure 5.1, Page 5-5: In the cross-section, correct Es to Esb. Please show offsets on the faults.
Completed.

Section 6: Model Design

1. Figure 6.2.1, Page 6-15: Please redesign the map to make the county names legible. Are rivers and lakes necessary on this map?
Completed.
2. Figure 6.3.1 to 6.3.6, Pages 6-16 to 6-21: Please include a box to show active cells in the legend.
Inactive cells are shown in the legend. All other cells are active.

Section 7: Modeling Approach

1. No comments.

Section 8: Steady-State Model

1. Figures 8.1.1 to 8.1.4, Pages 8-6 to 8-9: Please use either Kh in the title and legend box, or horizontal hydraulic conductivity in both places.
Completed.
2. Figure 8.1.5, Page 8-10: Please explain what Kh and Kv stand for.
Completed.
3. Figures 8.2.1a to 8.2.5, Pages 8-18 to 8-26: In the legend box explain that the symbols are residuals and the blue lines hydraulic head contours. Provide contour intervals and units of measurements. Also, in Figure 8.2.1a, delete "and" in the title between "residuals" and "for".
Completed.
4. Figure 8.2.6, Page 8-27: Use comma separators for numbers.
Completed.
5. Figures 8.3.1 to 8.3.10, Pages 8-31 to 8-35: Explain what Kv, Kh, and K stand for wherever applicable on these figures. Please assign negative signs to all fraction values left of 0. Please also include +/- 10 % in these sensitivity plots.
The sensitivity titles in the legends of these figures have been included in the text with each sensitivity definition in Section 8.3. There was not enough room on the figures to fully define Kv, Kh, and K on each figure. The sensitivities are listed as positive fractions instead of +/- percent so that the values on the figures correlate to the equations listed in the text. The sensitivities at 0.9 and 1.1 are at +/- 10% .

Section 9: Transient Model

1. Figures 9.2.1 to 9.2.5, Pages 9-11 to 9-15: Please provide units of measurement and contour intervals on all maps. Relocate numbers that overlie each other.
Completed.
2. Figures 9.2.6 to 9.2.9, Pages 9-16 to 9-19: Please provide units of measurement and contour intervals on all maps. Relocate numbers that overlie each other. Explain what (-) and (+) values mean.
Completed. Explanation of positive/negative residuals is included in the text.
3. Figures 9.2.12 to 9.2.15, Pages 9-22 to 9-25: Please provide units of measurement and contour intervals on all maps. Relocate numbers that overlie each other.
Completed.
4. Figures 9.2.16a to 9.2.19, Pages 9-26 to 9-36: Please indicate (either in map title or legend) points/lines that are simulated heads and points/lines that are measured heads.
Completed.
5. Figure 9.2.23, Page 9-40: Please redesign the graphs so that two different data sets are visible.
Completed.
6. Figure 9.2.24, Page 9-41: Correct the reference of Slade et al. in both figure and title. Should be Slade et al., 2002.
Completed.
7. Figures 9.3.1 to 9.3.10, Pages 9-46 to 9-50: Please explain what K_v , K_h and K denote in these figures. Assign negative signs to all fraction values left of 0. Please also include $\pm 10\%$ in these sensitivity plots.
The sensitivity titles in the legends of these figures have been included in the text with each sensitivity definition in Section 9.3. There was not enough room on the figures to fully define K_v , K_h , and K on each figure. The sensitivities are listed as positive fractions instead of \pm percent so that the values on the figures correlate to the equations listed in the text. The sensitivities for $\pm 10\%$ were not performed because the sensitivities are almost linear and additional sensitivities at $\pm 10\%$ would not add significant additional information to the plots. Since these sensitivities can be estimated from the $\pm 25\%$ sensitivities presented, the TWDB has agreed that the additional runs are not needed .

Section 10: Model Predictive Simulations

1. Figure 10.1.1, Page 10-5: Years 1952 and 1956 have been repeated on the horizontal axis. Change to 1953 and 1957, respectively.
Completed.
2. Figures 10.2.1 to 10.2.18, Pages 10-11 to 10-28: Identify each figure on a 2-figure page with (a) and (b) and change title accordingly (delete "top" and "bottom" in the title). Add contour intervals to all figures.
Completed. Contour interval was not included since the contour intervals are variable on the difference plots. Contour lines are labeled and scale bars are included for each figure.

Section 11: Limitations of the Model

1. No comments.

Section 12: Future Improvements

1. No comments.

Section 13: Conclusions

1. No comments.

Section 14: Acknowledgements

1. No comments.

Section 15: References

1. No comments.

Tables:

Section 1: Introduction

1. No comments.

Section 2: Study Area

1. No comments.

Section 3: Previous Investigations

1. Table 3.1, Page 3-1: Please check the reference for Thorkildsen (1991). It is not listed in the References. Also, check and correct reference for R.W. Harden and Associates (2000) which is listed as (2001) in the References section.
The reference for Thorkildsen (1991) was corrected in Table 3.1. The reference for Harden and Associates was corrected in the Section 15.

Section 4: Hydrogeologic Setting

1. Table 4.2.1, Page 4-5: Please check and correct the reference for Wilson and Hosman (1987) at both locations. It is cited as (1988) in the References section.
Completed.
2. Table 4.3.1, Page 4-24: Please explain in note what K and T denote.
Completed.
3. Table 4.3.2, Page 4-41: Please check and correct references for Thorkildsen, and Harden and Associates.
The reference for Thorkildsen et al. was corrected in Table 4.3.2. The reference for Harden and Associates was corrected in the Section 15.

4. Table 4.4.1, Page 4-52: Duessen (1914) is not listed in the References section. *This reference was added to Section 15.*
5. Table 4.5.1, Page 4-88: Please check and correct the following references: Harden and Associates (2000) and Thorkildsen et al. (1989). Also, the following two are not in the References section: Thompson (1972) and Guyton and Associates (1998). *The references for Harden (2000), Thorkildsen et al. (1991), and Guyton & Assoc. and HDR (1998) were corrected in Table 4.5.1. The reference for Thompson (1972) was added to Section 15.*
6. Table 4.5.2, Page 4-91: Is there no information available for Clear Lake, Eastman Lakes, and Trinidad Lake? *There was no information available for these lakes. This was so noted in the table.*
7. Table 4.6.2, Pages 4-97 to 4-100: Please change Gunnar Brune, 1975 and 1981, to Brune, 1975 and 1981 everywhere in the table. *Completed.*

Section 5: Conceptual Model of Groundwater Flow in the Aquifer

1. No comments.

Section 6: Model Design

1. No comments.

Section 7: Modeling Approach

1. No comments.

Section 8: Steady-State Model

1. Table 8.1.1, Page 8-5: Table shows horizontal hydraulic conductivity and anisotropy ratio. Please insert a column to show calibrated vertical hydraulic conductivity that was used to calculate the anisotropy ratio. *Completed.*
2. Table 8.2.1, Page 8-16: Please add a note that RMS = Root Mean Square. *Completed.*

Section 9: Transient Model

1. Table 9.2.1, Page 9-9: Please add a note that RMS = Root Mean Square. *Completed.*
2. Table 9.2.2, Page 9-10: Please expand "Reser." and "Rech." in the column headings. It is unclear what they denote. *Completed.*

Section 10: Model Predictive Simulations

1. Table 10.3.1, Page 10-35: Please change title to "Water Budget (AFY) for Predictive Simulations." Also, explain in note what 2050* is (i.e., how is it different from 2050). *Completed.*

Section 11: Limitations of the Model

1. No comments.

Section 12: Future Improvements

1. No comments.

Section 13: Conclusions

1. No comments.

Section 14: Acknowledgements

1. No comments.

Section 15: References

1. No comments.

Appendices:

General Comment:

1. Please include in the appendix all of the transient plots comparing simulated to measured for the model. The reader should also be able to identify where these plots spatially relate to.
In Figures 9.2.16 to 9.2.19 there are 55 hydrographs shown with location information. We selected these hydrographs to be representative of the regional heads within the model and thus of the full set of hydrographs used for calibration and verification over the model region. The scatterplots shown in Figures 9.2.10 and 9.2.11 contain all target values for the calibration and verification periods. During discussions with the TWDB it was agreed that the 55 hydrographs presented are sufficient to represent the entire dataset. All hydrograph data is included in the data model.

Appendix A: Brief Summary of the development of the Carrizo-Wilcox Aquifer in Each County and List of Reviewed Reports

1. Please change "William F Guyton & Associations (1970)" to "William F. Guyton & Associates (1970)" everywhere that it is used in this appendix.
Completed.
2. Page A-25: Newcome et al. Please add "1963" to the reference.
Completed.

Appendix B: Standard Operating Procedures (SOPs) for Processing Historical Pumpage Data TWDB Groundwater Availability Modeling (GAM) Projects

1. No comments.

Appendix C: Standard Operating Procedures (SOPs) for Processing Predictive Pumpage Data TWDB Groundwater Availability Modeling (GAM) Projects

1. No comments.

Appendix D1: Tabulated Groundwater Withdrawal Estimates for the Carrizo-Wilcox for 1980, 1990, 2000, 2010, 2020, 2030, 2040 and 2050

1. No comments.

Appendix D2: Post Plots of Groundwater Withdrawal Estimates for the Carrizo-Wilcox for 1980, 1990, 2000, 2010, 2020, 2030, 2040 and 2050

1. No comments.

Appendix D3: Carrizo-Wilcox Groundwater Withdrawal Distributions by County

1. No comments.

Appendix E: Using SWAT with MODFLOW in a Decoupled Environment

1. No comments.

Stakeholder Comment:

1. First, when we did our first water plan for Region I, we had planned to use the TWDB's in house GAM for the Carrizo-Wilcox. Unfortunately the numbers were so large, indicating that we had a lot more ground water in the Carrizo and associated aquifers than our water users had be led to believe existed. So we did not use the GAM in our first plan. Of particular concern is the Nacogdoches Lufkin area where the level of the aquifer has dropped significantly over time due to pretty heavy pumping yet the model didn't seem (if I remember correctly) to show this. Your new model (the one you showed today) does seem to show this, but only after you went back in and changed some of the parameters (the Kv values on some of the layers) and the cause-effect relationship of why the changes worked could not be given. It appears that there are properties of the aquifer that affect water availability which are not adequately represented in the model. Is this fixable or are we going to be required to use this model for our next plan knowing it has problems?

Vertical hydraulic conductivity (Kv) is not measurable on a model grid scale and is, therefore, a calibrated parameter. For the transient calibration, the Kv of the Reklaw was important for reproducing the observed cone of depression in the Carrizo-Wilcox aquifer. In the Nacogdoches County area, the simulated drawdown was actually greater than the observed drawdown and Kv of the Reklaw was increased to limit the simulated head decline in the area. On the other hand, in the Smith County area, Kv of the Reklaw was reduced to achieve the observed drawdown. The cones of depression are produced by groundwater withdrawals; consequently, accurate pumpage data are required to constrain the calibrated hydraulic parameters, particularly those parameters for which no measurements exist and have to be inferred from model calibrations.

Second, one of the problems with the early model is that it showed a lot of water in the geologic layers above the Carrizo (the Queen City and Reklaw). This water is generally of low quality (high Fe, I think) and low yield, only able to support small production wells. I don't think your new model showed this water as being available but then you used this water in the adjustment of the Kv discussed above (at least that's what I understood). What is really happening here?"

The volume of water that the Queen City can contribute as cross-formational flow to the Carrizo-Wilcox is strongly affected by the Kv of the Reklaw, which was adjusted during calibration to reproduce observed water levels, and accounted for in the Northern Carrizo-Wilcox GAM. However, the potential impact of leakage of low-quality water from the Queen City above the Reklaw into Carrizo-Wilcox is not explicitly modeled in this GAM (e.g., no transport calculations were performed). On the other hand, the calculated flow in this GAM indicates that because of the relatively low permeability of the Reklaw the actual travel time of water from the Queen City into the Carrizo is typically greater than the historical period (ie. 1900 – 2000) and would not be noticed in the water quality data.

(Note: TWDB will address the policy portion of this comment regarding use of the GAM for planning purposes. The entire comment are being included for the sake of completeness.)

EDITORIAL COMMENTS ON DRAFT REPORT

Table of Contents:

1. Page ix, Figure 10.2.2: Please complete the parenthesis after Queen City.
Completed.
2. Page ix, Figure 10.2.5: Please complete the parenthesis after upper Wilcox.
Completed.
3. Page ix, Figure 10.2.7: Please complete the parenthesis after middle Wilcox.
Completed.

Abstract:

1. No comments.

Sections 1 to 15:

General Comments:

1. If there are only two authors, list both authors instead of et al. Use et al. only if more than two authors.
Completed.
2. Use "**Northern Carrizo-Wilcox GAM**" throughout the report instead of "north" or "northeastern".
Completed.
3. Replace TNRCC with TCEQ (Texas Commission on Environmental Quality) everywhere in the report.
Completed.
4. Use comma separators for numbers on all figures and tables (except years, of course), and in the text.
Completed.
5. If two or more rivers, counties or geological units are listed, keep the "rivers", "counties", etc. lowercase (e.g., Walker and Grimes counties, Sabine and Neches rivers, Wilcox and Queen City formations).
Completed.

Section 1: Introduction

1. Section 1.0, Page 1-1, Para 4, Para Line 1: Please delete "This" at the beginning of the sentence and replace with "The".
Completed.
2. Section 1.0, Page 1-2, Para 4, Para Line 10: Please change "development of the model grid, development of the model" to "developing a model grid and model".
Completed.

Section 2: Study Area

1. Section 2.0, Page 2-1, Para 1, Para Line 3: Please delete “River” from “Rio Grande River”.
Completed.
2. Section 2.0, Page 2-1, Para 3, Para Line 6: Insert “the” between “as model”.
Completed.

Section 3: Previous Investigations

1. No comments.

Section 4: Hydrogeologic Setting

1. Section 4.2, Page 4-21, Para 6, Para Line 6: Please change the spelling of “later”. Should be “latter”.
Completed.
2. Section 4.3.5, Page 4-40, Para 2, Para Line 7: Please correct the spelling of “Clairborne” to “Claiborne”.
Completed.
3. Section 4.4, Page 4-41, Para 2, Para Line 6: Please change “Broom and Alexander, 1965” to “Broom et al., 1965”.
Completed.
4. Section 4.4.3, Page 4-55: Please change subsection number to “4.4.4”.
Completed.
5. Section 4.4.4, Page 4-64: Please change subsection number to “4.4.5”.
Completed.

Section 5: Conceptual Model of Groundwater Flow in the Aquifer

1. Section 5.0, Page 5-1, Para 2, Para Line 9: Please replace “gulf coast” with “Gulf of Mexico”.
Completed.
2. Section 5.0, Page 5-2, Para 5, Para Line 2: Please delete “ evapotranspiration” and the parentheses around “ET”.
Completed.

Section 6: Model Design

1. Section 6.3.4, Page 6-7, Para 1, Para Line 8: Please replace “evapotranspiration (ET)” with “ET”. It has already been defined.
Completed.

Section 7: Modeling Approach

1. General: Change the tense in the entire section from future tense (we will perform) to past tense (we performed).
Completed.

Section 8: Steady-State Model

1. Section 8.1, Page 8-1: Please add a brief description of the subsections that follow.
Completed.
2. Section 8.1.2, Page 8-3: Please change subsection number to 8.1.3.
Completed.
3. Section 8.1.2, Page 8-3, Para 2, Para Lines 1, 5, 8: Please replace “evapotranspiration” with “ET” on all these lines.
Completed.
4. Section 8.1.3, Page 8-3: Please change subsection number to 8.1.4.
Completed.
5. Section 8.2.3, Page 8-14, Para 1, Para Line 4: Please correct the spelling of “decending”.
Completed.

Section 9: Transient Model

1. Section 9.2, Page 9-4: Please include a short sentence or two describing the subsections that follow.
Completed.
2. Section 9.2.1, Page 9-5, Para 5, Para Line 5: Please change “measure” to “measured”.
Completed.
3. Section 9.2.1, Page 9-5, Para 5, Para Line 7: Please change “decrease” to “decreases”.
Completed.
4. Section 9.2.1, Page 9-6, Para 7, Para Line 7: Please change “measure” to “measured”.
Completed.
5. Section 9.2.1, Page 9-6, Para 7, Para Line 13: Please change “increase” to “increased”.
Completed.

Section 10: Model Predictive Simulations

1. Section 10.1, Page 10-1, Para 1, Para Line 3: Please change “recurrent” to “recurring”.
Completed.
2. Section 10.1, Page 10-3, Para 6, Para Line 18: Uppercase “county”.
Completed.
3. Section 10.3, Page 10-34, Para 2, Para Line 3: Uppercase “formation”.
This paragraph was removed.

Section 11: Limitations of the Model

1. Section 11.1, Page 11-2, Para 3, Para Line 2: Please delete “s” from “Formations”.

Completed.

Section 12: Future Improvements

1. Section 12.2, Page 12-2, Para 1, Para Lines 5 to 7: Sentence is unclear. Please rewrite.

Completed.

Section 13: Conclusions

1. No comments.

Section 14: Acknowledgements

1. No comments.

Section 15: References

1. General: For consistency, please add a comma everywhere between the last author’s initials and the year of publication, or remove the comma where present.

Completed.

2. Page 15-5: Isaaks and Srivastava, 1989. Please add a space between “University” and Press”.

Completed.

3. Page 15-6: Kaiser, Johnston and Bach, 1978. Please correct typo in “Beological”.

Completed.

Figures:

1. No comments.

Tables:

1. No comments.

Appendices:

Appendix A:

1. Please change “hydraulic connected” to “hydraulically connected” everywhere it appears in the text of the appendix.

Completed.

2. Page A-11: Limestone County, Texas, Line 2. Change “Rettman 1994” to “Rettman 1984”.

Completed.

3. The following authors (Baker, et al., 1963; Bennett, 1942; Sundstrom et al., 1948; White, 1973) in the Reviewed Reports list are not referenced in the text of the appendix. Please include in the text or remove from the list of references.
The Reviewed Reports list includes all reports reviewed for information about development of the Carrizo-Wilcox aquifer, not just those referenced in the county summaries.

Appendix B:

1. No comments.

Appendix C:

1. No comments.

Appendix D1:

1. No comments.

Appendix D2:

1. No comments.

Appendix D3:

1. No comments.

Appendix E:

1. No comments.

COMMENTS ON THE DRAFT MODEL

1. Section 8: Steady-state model as provided fails to converge in PM 5.3.0 using MODFLOW version provided by the consultants. When we used the SIP solver, output.dat file flags "failed to converge at the end of time step 1". If we used PCG2 or SSOR, the steady-state model converges but the simulated heads generated don't match those included in the report. Because of this problem, additional review comments may be provided by the TWDB once the consultants have provided a workable steady-state model.
The TWDB successfully ran the steady-state model after retrieving the files from the data model CDs a second time. We suspect that the files may have been corrupted when originally retrieved from the data model CDs.
2. Section 9.0: Transient model 1980-1999 runs and produces the general distribution of the simulated heads as reported. In the simulated heads, we observed that some active cells around the outcrop areas go dry that were not accounted for in the report. These cells are active with ibound values of 1 and simulated head values of 999 indicative of dry cells. Please include the simulated heads more representative of the simulation runs. Please provide an explanation on the occurrences of these dry cells.
Some cells around the edges of the outcrops do go dry during the simulation. This is to be expected since many of the edge cells are thin (down to a thickness of 20 ft) and the water table could be below the base of these cells. Since the rewetting option was used, cells are allowed to dewater and resaturate. Dry cells were added to Figures 9.2.1 – 9.2.5 (end of calibration period) and 9.2.12 – 9.2.15 (end of verification period).
3. Section 9.0: Transient model. Please provide the bore hole file and the observation well file for the transient model so that we can review the RMS values.
Completed.
4. Please include a detailed water budget for:
 - steady-state
Please see Table 8.2.2.
 - beginning of calibration period
Please see Table 9.2.3.
 - the drought of the calibration period
Completed. Added to Table 9.2.3.
 - end of the calibration period
Please see Table 9.2.3.
 - end of the verification period
Please see Table 9.2.3.
 - end of 2000, 2010, 2020, 2030, 2040, and 2050.
Please see Table 10.3.1.

COMMENTS ON DRAFT DATA STRUCTURE

Did we get all of the data files we requested? NO
Is the data organized in the way we requested? YES

Introduction:

It is imperative that we receive enough source data to completely rebuild the groundwater model from scratch and reproduce all report figures and tables should it be necessary. In other words, if a new model grid resolution and/or orientation was needed, there should be sufficient data to create a new model for the study area. Moreover, there should be enough data to regenerate any or all of the intermediate derivative data with updated information. This source and intermediate derivative data should be organized under the SRCDATA folder/directory according to the guidelines set forth in Attachments 1 & 2 of the RFP. An empty directory tree structure was provided to facilitate the organization of the project data. The empty directory tree structure is available for download in zip format at http://www.twdb.state.tx.us/gam/resources/gam_tree.zip.

It is also required that all **final** model parameter and variable/stress data be delivered in a database format that can easily be referenced to each and every model grid cell. In other words, there should be enough cell-referenced data to regenerate all or update any individual cell value of the required MODFLOW or PMWIN input files. The file format of these databases may be in Excel 97, Access 97, or in an ESRI GIS format compatible with ArcView 3.2 or ArcInfo 7.21. Each sheet, table, or coverage should be attributed with the appropriate model grid cell-reference information as set forth in Attachments 1 & 2 of the RFP. These data sets should be organized under the GRDDATA folder directory and with in the appropriate sub-folders/directories. The GRDDATA OUTPUT folder and its sub-folders/directories may be omitted or left empty.

Finally, the actual MODFLOW 96 and PMWIN 5.0 formatted files for both INPUT and OUTPUT must be organized as set forth in Attachments 1 & 2 of the RFP. Separate folders/directories must be used for 1) the calibrated steady-state model files; 2) the calibrated transient model files; 3) the verification transient model files; 4) and each of the decadal transient predictive model simulation run files.

Review Summary:

The data provided by the CZWX_n contractor is missing some required data sets as listed in sections below. Listing files are needed within each folder/directory listing all file names or groups of file names and their contents

Descriptors were added.

The contractor did follow the requirements as set forth in Attachments 1 & 2 of the RFP for the most part. However, a few of the metadata files had incorrect spatial reference information or missing altogether. Furthermore, the SWAT model and all data used within the SWAT model must be provided in a separate folder/directory tree structure if used to calculate parameters for the ET, streamflow-routing, and/or recharge packages of MODFLOW.

Metadata was examined and augmented where necessary. SWAT data added in a separate directory.

DRIVE:\CZWX_n\grddata\input\hydraul

Unable to evaluate data because Access file format not compatible with Access97. Must make Access database file compatible with Access97 as stated in Attachments 1 and 2 of RFP.

Access database files converted to Access97.

DRIVE:\CZWX_n\grddata\input\bnd

Unable to evaluate data because Access file format not compatible with Access97. Must make Access database file compatible with Access97 as stated in Attachments 1 and 2 of RFP.

Access97 tables added.

DRIVE:\CZWX_n\grddata\input\stress\ststate\drns

Unable to evaluate data because Access file format not compatible with Access97. Must make Access database file compatible with Access97 as stated in Attachments 1 and 2 of RFP.

N/A.

DRIVE:\CZWX_n\grddata\input\stress\ststate\levt

Unable to evaluate data because Access file format not compatible with Access97. Must make Access database file compatible with Access97 as stated in Attachments 1 and 2 of RFP.

Access97 tables added.

DRIVE:\CZWX_n\grddata\input\stress\ststate\rech

Unable to evaluate data because Access file format not compatible with Access97. Must make Access database file compatible with Access97 as stated in Attachments 1 and 2 of RFP.

Access database files converted to Access97.

DRIVE:\CZWX_n\grddata\input\stress\ststate\res

Unable to evaluate data because Access file format not compatible with Access97. Must make Access database file compatible with Access97 as stated in Attachments 1 and 2 of RFP.

N/A.

DRIVE:\CZWX_n\grddata\input\stress\ststate\strm

Unable to evaluate data because Access file format not compatible with Access97. Must make Access database file compatible with Access97 as stated in Attachments 1 and 2 of RFP.

N/A.

DRIVE:\CZWX_n\grddata\input\storage

Unable to evaluate data because Access file format not compatible with Access97. Must make Access database file compatible with Access97 as stated in Attachments 1 and 2 of RFP.

Access97 tables added.

DRIVE:\CZWX_n\grddata\input\stress\ststate\well

Unable to evaluate data because Access file format not compatible with Access97. Must make Access database file compatible with Access97 as stated in Attachments 1 and 2 of RFP.

Access97 tables added.

DRIVE:\CZWX_n\grddata\input\stress\trans\drns

Unable to evaluate data because Access file format not compatible with Access97. Must make Access database file compatible with Access97 as stated in Attachments 1 and 2 of RFP.

N/A.

DRIVE:\CZWX_n\grddata\input\stress\trans\levt

Unable to evaluate data because Access file format not compatible with Access97. Must make Access database file compatible with Access97 as stated in Attachments 1 and 2 of RFP.

Access97 tables added.

DRIVE:\CZWX_n\grddata\input\stress\trans\rech

Unable to evaluate data because Access file format not compatible with Access97. Must make Access database file compatible with Access97 as stated in Attachments 1 and 2 of RFP.

Access97 tables added.

DRIVE:\CZWX_n\grddata\input\stress\trans\res

Unable to evaluate data because Access file format not compatible with Access97. Must make Access database file compatible with Access97 as stated in Attachments 1 and 2 of RFP.

Access97 tables added.

DRIVE:\CZWX_n\grddata\input\stress\trans\strm

Unable to evaluate data because Access file format not compatible with Access97. Must make Access database file compatible with Access97 as stated in Attachments 1 and 2 of RFP.

Access97 tables added.

DRIVE:\CZWX_n\grddata\input\stress\trans\well

Unable to evaluate data because Access file format not compatible with Access97. Must make Access database file compatible with Access97 as stated in Attachments 1 and 2 of RFP.

Access97 tables added.

DRIVE:\CZWX_n\grddata\input\struct

Unable to evaluate data because Access file format not compatible with Access97. Must make Access database file compatible with Access97 as stated in Attachments 1 and 2 of RFP.

Access database files converted to Access97.

DRIVE:\CZWX_n\modflow\modfl_96\input\ststate

These files are acceptable.

DRIVE:\CZWX_n\modflow\modfl_96\input\trans

These files are acceptable.

DRIVE:\CZWX_n\modflow\pmwin_50\input\ststate

These files are acceptable except for missing calibration borehole file.

Borehole and observation files added.

DRIVE:\CZWX_n\modflow\pmwin_50\input\trans

These files are acceptable except for missing calibration borehole file.

Borehole and observation files added.

DRIVE:\CZWX_n\modflow\pmwin_50\refdx

These files are acceptable.

DRIVE:\CZWX_n\scrdata\bndy

Need a listing file listing name of each file or grouped set of files and their contents or purpose.

Completed.

Aquifers coverage has incorrect spatial reference in metadata file.

Aquifers coverage was moved to \subhyd with corrected referencing.

DRIVE:\CZWX_n\scrdata\clim

Need a listing file listing name of each file or grouped set of files and their contents or purpose.

Completed.

The evaporation coverage needs a completed metadata file.

Spatial information added.

The monthly precipitation Access database must be compatible with Access97.

Access database files converted to Access97.

Redundant metadata files for precipitation raster data.

Redundant files removed.

DRIVE:\CZWX_n\scrdata\cnsv

Need a listing file listing name of each file or grouped set of files and their contents or purpose.

Completed.

The ecological regions coverages for Arkansas and Louisiana have incorrect projection information in metadata file.

Metadata corrected.

DRIVE:\CZWX_n\scrdata\geol

Need a listing file listing name of each file or grouped set of files and their contents or purpose.

Completed.

The outcrop delineations coverages need at least one metadata file or readme document describing the metadata and purpose of the coverages.

Completed.

Must make Access database file compatible with Access97 as stated in Attachments 1 and 2 of RFP.

Access database files converted to Access97.

No cross-sections used in study? If yes, cross-sections must be provided under this folder.

N/A.

DRIVE:\CZWX_n\scrdata\geom

Need a listing file listing name of each file or grouped set of files and their contents or purpose.

Completed.

The DEM needs a completed metadata file.

Completed.

The DEM needs a completed metadata file and must be in units of feet rather than meters.

Completed.

A physiography coverage is required by RFP.

USGS coverage added.

DRIVE:\CZWX_n\scrdata\geop

NO DATA FOUND – geophysical data should go here if used in study.

N/A.

DRIVE:\CZWX_n\scrdata\soil

Need a listing file listing name of each file or grouped set of files and their contents or purpose.

Completed.

The runoff raster data for Texas needs a metadata file as well as for remaining soil coverages.

Runoff data not used in final model and was subsequently removed. Metadata added for soil coverages.

DRIVE:\CZWX_n\scrdata\subhyd

Need a listing file listing name of each file or grouped set of files and their contents or purpose.

Completed.

Unable to evaluate data because Access file format not compatible with Access97. Must make Access database file compatible with Access97 as stated in Attachments 1 and 2 of RFP.

Access database files converted to Access97.

The binary Surfer grid files should be converted into ESRI, Access97, or ASCII format.

Completed.

Need source and intermediate derivative coverages used to spatially distribute pumpage data here.

Pumping datasets added.

Need source and intermediate derivative coverages used to spatially distribute water level data here.

Water level data added.

Need source and intermediate derivative coverages used to spatially distribute conductivity data here.

Hydraulic conductivity data added.

Need source and intermediate derivative coverages used to spatially distribute specific yield and porosity if available.

N/A.

Need point coverage of calibration target boreholes and hydrographs.

Target location coverage added.

DRIVE:\CZWX_n\scrdata\surhyd

Need a listing file listing name of each file or grouped set of files and their contents or purpose.

Completed.

Must make Access database file compatible with Access97 as stated in Attachments 1 and 2 of RFP.

Access database files converted to Access97.

DRIVE:\CZWX_n\scrdata\tran

Need a listing file listing name of each file or grouped set of files and their contents or purpose otherwise, these files are acceptable.

Completed.